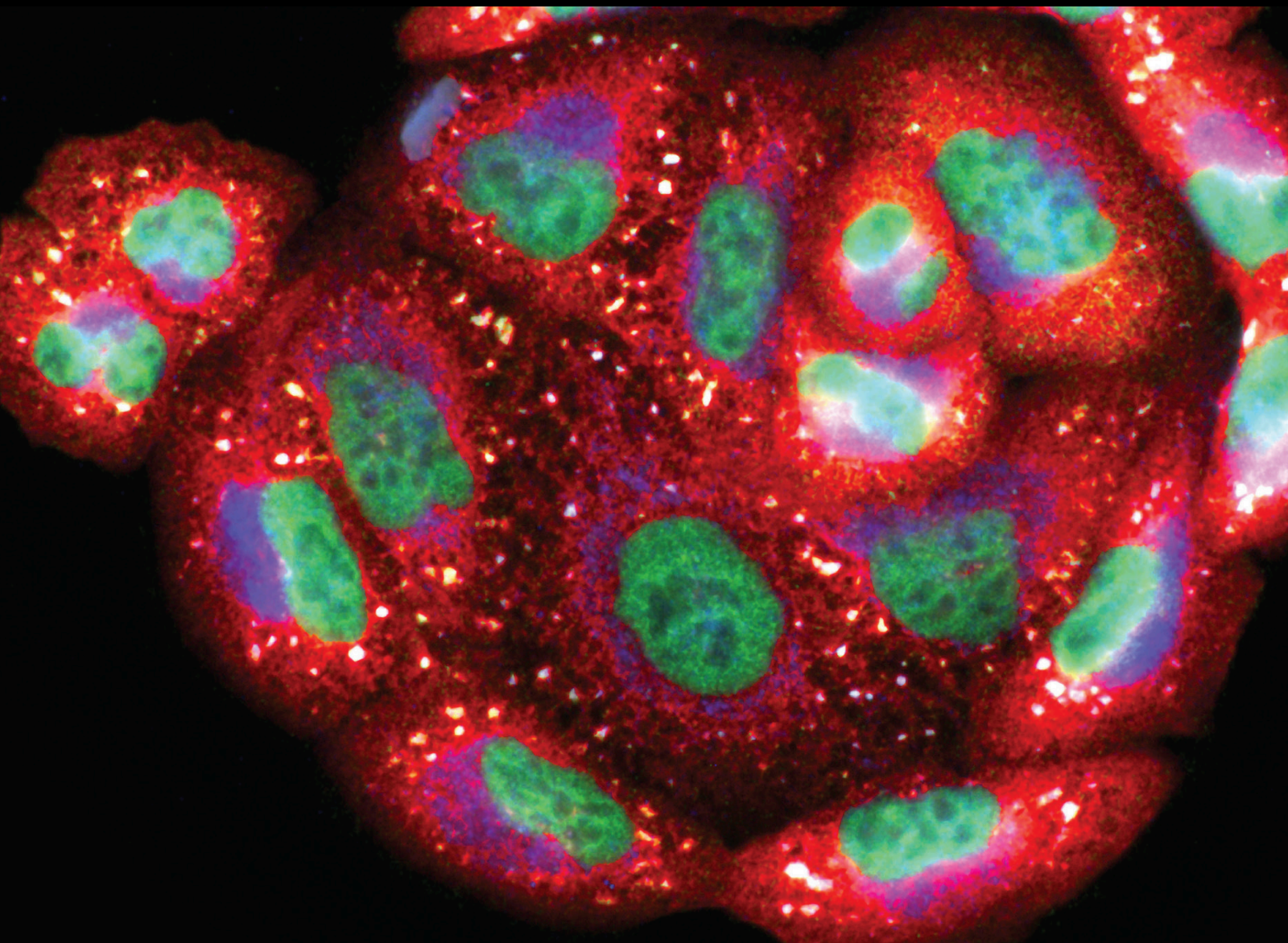


Novel Approaches for Diagnosing and Management of Cardiovascular Disorders Mediated by Oxidative Stress

Lead Guest Editor: Adrian Doroszko

Guest Editors: Aneta Radziwon-Balicka and Robert P. Skomro





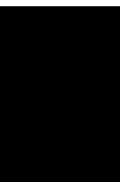
**Novel Approaches for Diagnosing and
Management of Cardiovascular Disorders
Mediated by Oxidative Stress**

Oxidative Medicine and Cellular Longevity

**Novel Approaches for Diagnosing
and Management of Cardiovascular
Disorders Mediated by Oxidative Stress**

Lead Guest Editor: Adrian Doroszko

Guest Editors: Aneta Radziwon-Balicka and Robert
P. Skomro



Copyright © 2020 Hindawi Limited. All rights reserved.

This is a special issue published in "Oxidative Medicine and Cellular Longevity" All articles are open access articles distributed under the Creative Commons Attribution License, which permits unrestricted use, distribution, and reproduction in any medium, provided the original work is properly cited.

Chief Editor

Jeannette Vasquez-Vivar, USA

Editorial Board

Ivanov Alexander, Russia
Fabio Altieri, Italy
Fernanda Amicarelli, Italy
José P. Andrade, Portugal
Cristina Angeloni, Italy
Antonio Ayala, Spain
Elena Azzini, Italy
Peter Backx, Canada
Damian Bailey, United Kingdom
Sander Bekeschus, Germany
Ji C. Bihl, USA
Consuelo Borrás, Spain
Nady Braidy, Australia
Ralf Braun, Austria
Laura Bravo, Spain
Amadou Camara, USA
Gianluca Carnevale, Italy
Roberto Carnevale, Italy
Angel Catalá, Argentina
Giulio Ceolotto, Italy
Shao-Yu Chen, USA
Ferdinando Chiaradonna, Italy
Zhao Zhong Chong, USA
Alin Ciobica, Romania
Ana Cipak Gasparovic, Croatia
Giuseppe Cirillo, Italy
Maria R. Ciriolo, Italy
Massimo Collino, Italy
Graziamaria Corbi, Italy
Manuela Corte-Real, Portugal
Mark Crabtree, United Kingdom
Manuela Curcio, Italy
Andreas Daiber, Germany
Felipe Dal Pizzol, Brazil
Francesca Danesi, Italy
Domenico D'Arca, Italy
Sergio Davinelli, USA
Claudio De Lucia, Italy
Yolanda de Pablo, Sweden
Sonia de Pascual-Teresa, Spain
Cinzia Domenicotti, Italy
Joël R. Drevet, France
Grégory Durand, France
Javier Egea, Spain



Ersin Fadillioglu, Turkey
Ioannis G. Fatouros, Greece
Qingping Feng, Canada
Gianna Ferretti, Italy
Giuseppe Filomeni, Italy
Swaran J. S. Flora, India
Teresa I. Fortoul, Mexico
Rodrigo Franco, USA
Joaquin Gadea, Spain
Juan Gambini, Spain
José Luís García-Giménez, Spain
Gerardo García-Rivas, Mexico
Janusz Gebicki, Australia
Alexandros Georgakilas, Greece
Husam Ghanim, USA
Rajeshwary Ghosh, USA
Eloisa Gitto, Italy
Daniela Giustarini, Italy
Saeid Golbidi, Canada
Aldrin V. Gomes, USA
Tilman Grune, Germany
Nicoletta Guaragnella, Italy
Solomon Habtemariam, United Kingdom
Eva-Maria Hanschmann, Germany
Tim Hofer, Norway
John D. Horowitz, Australia
Silvana Hrelia, Italy
Stephan Immenschuh, Germany
Maria Isagulians, Latvia
Luigi Iuliano, Italy
FRANCO J. L, Brazil
Vladimir Jakovljevic, Serbia
Marianna Jung, USA
Peeter Karihtala, Finland
Eric E. Kelley, USA
Kum Kum Khanna, Australia
Neelam Khaper, Canada
Thomas Kietzmann, Finland
Demetrios Kouretas, Greece
Andrey V. Kozlov, Austria
Jean-Claude Lavoie, Canada
Simon Lees, Canada
Christopher Horst Lillig, Germany
Paloma B. Liton, USA

Ana Lloret, Spain
Lorenzo Loffredo, Italy
Daniel Lopez-Malo, Spain
Antonello Lorenzini, Italy
Nageswara Madamanchi, USA
Kenneth Maiese, USA
Marco Malaguti, Italy
Tullia Maraldi, Italy
Reiko Matsui, USA
Juan C. Mayo, Spain
Steven McAnulty, USA
Antonio Desmond McCarthy, Argentina
Bruno Meloni, Australia
Pedro Mena, Italy
V́ctor M. Mendoza-Núñez, Mexico
Maria U. Moreno, Spain
Trevor A. Mori, Australia
Ryuichi Morishita, Japan
Fabiana Morroni, Italy
Luciana Mosca, Italy
Ange Mouithys-Mickalad, Belgium
Iordanis Mourouzis, Greece
Danina Muntean, Romania
Colin Murdoch, United Kingdom
Pablo Muriel, Mexico
Ryoji Nagai, Japan
David Nieman, USA
Hassan Obied, Australia
Julio J. Ochoa, Spain
Pál Pacher, USA
Pasquale Pagliaro, Italy
Valentina Pallottini, Italy
Rosalba Parenti, Italy
Vassilis Paschalis, Greece
Visweswara Rao Pasupuleti, Malaysia
Daniela Pellegrino, Italy
Ilaria Peluso, Italy
Claudia Penna, Italy
Serafina Perrone, Italy
Tiziana Persichini, Italy
Shazib Pervaiz, Singapore
Vincent Pialoux, France
Ada Popolo, Italy
José L. Quiles, Spain
Walid Rachidi, France
Zsolt Radak, Hungary
Namakkal Soorappan Rajasekaran, USA






Sid D. Ray, USA
Hamid Reza Rezvani, France
Alessandra Ricelli, Italy
Paola Rizzo, Italy
Francisco J. Romero, Spain
Joan Roselló-Catafau, Spain
H. P. Vasantha Rupasinghe, Canada
Gabriele Saretzki, United Kingdom
Luciano Saso, Italy
Nadja Schroder, Brazil
Sebastiano Sciarretta, Italy
Ratanesh K. Seth, USA
Honglian Shi, USA
Cinzia Signorini, Italy
Mithun Sinha, USA
Carla Tatone, Italy
Frank Thévenod, Germany
Shane Thomas, Australia
Carlo Gabriele Tocchetti, Italy
Angela Trovato Salinaro, Italy
Paolo Tucci, Italy
Rosa Tundis, Italy
Giuseppe Valacchi, Italy
Daniele Vergara, Italy
Victor M. Victor, Spain
László Virág, Hungary
Natalie Ward, Australia
Philip Wenzel, Germany
Georg T. Wondrak, USA
Michal Wozniak, Poland
Sho-ichi Yamagishi, Japan
Liang-Jun Yan, USA
Guillermo Zalba, Spain
Mario Zoratti, Italy

Contents


Novel Approaches for Diagnosing and Management of Cardiovascular Disorders Mediated by Oxidative Stress

Adrian Doroszko , Aneta Radziwon-Balicka, and Robert Skomro 
Editorial (3 pages), Article ID 7096727, Volume 2020 (2020)



Redox-Active Drug, MnTE-2-PyP5+, Prevents and Treats Cardiac Arrhythmias Preserving Heart Contractile Function

Andrezza M. Barbosa, José F. Sarmiento-Neto , José E. R. Menezes Filho, Itamar C. G. Jesus, Diego S. Souza, Valério M. N. Vasconcelos, Fagner D. L. Gomes, Aline Lara, Juliana S. S. Araújo, Sandra S. Mattos, Carla M. L. Vasconcelos , Silvia Guatimosim, Jader S. Cruz, Ines Batinic-Haberle, Demetrius A. M. Araújo , Júlio S. Rebouças , and Enéas R. Gomes 
Research Article (15 pages), Article ID 4850697, Volume 2020 (2020)




Semicarbazide-Sensitive Amine Oxidase Increases in Calcific Aortic Valve Stenosis and Contributes to Valvular Interstitial Cell Calcification

Nathalie Mercier, Sven-Christian Pawelzik, John Pirault, Miguel Carracedo, Oscar Persson, Bastien Wollensack, Anders Franco-Cereceda, and Magnus Bäck 
Research Article (9 pages), Article ID 5197376, Volume 2020 (2020)




lncRNA MALAT1 Suppression Protects Endothelium against oxLDL-Induced Inflammation via Inhibiting Expression of MiR-181b Target Gene TOX

Liuqing Wang, Yinliang Qi, Yi Wang, Haitao Tang, Zhenzhen Li, Yuan Wang, Songtao Tang , and Huaqing Zhu 
Research Article (11 pages), Article ID 8245810, Volume 2019 (2019)



LOX-1, the Common Therapeutic Target in Hypercholesterolemia: A New Perspective of Antiatherosclerotic Action of Aegeline

Abhilasha Singh , Ashok Kumar Srinivasan, Lakshmi Narasimhan Chakrapani , and Periandavan Kalaiselvi 
Research Article (11 pages), Article ID 8285730, Volume 2019 (2019)

Can Lipoic Acid Attenuate Cardiovascular Disturbances Induced by Ethanol and Disulfiram Administration Separately or Jointly in Rats?

Anna Bilska-Wilkosz , Magdalena Kotańska , Magdalena Górny, Barbara Filipek , and Małgorzata Iciek
Research Article (10 pages), Article ID 1974982, Volume 2019 (2019)

Activation of TGR5 Partially Alleviates High Glucose-Induced Cardiomyocyte Injury by Inhibition of Inflammatory Responses and Oxidative Stress

Li Deng, Xuxin Chen, Yi Zhong, Xing Wen, Ying Cai, Jiafu Li , Zhongcai Fan, and Jian Feng 
Research Article (11 pages), Article ID 6372786, Volume 2019 (2019)





Cardiovascular Risk Factors and Haematological Indexes of Inflammation in Paralympic Athletes with Different Motor Impairments

Marco Bernardi , Anna Lucia Fedullo, Barbara Di Giacinto, Maria Rosaria Squeo, Paola Aiello, Donatella Dante, Silvio Romano , Ludovico Magaouda, Iliaria Peluso , Maura Palmery , and Antonio Spataro
Research Article (11 pages), Article ID 6798140, Volume 2019 (2019)


5 α ,6 α -Epoxyphytosterols and 5 α ,6 α -Epoxycholesterol Increase Oxidative Stress in Rats on Low-Cholesterol Diet

Tomasz Wielkoszyński , Jolanta Zalejska-Fiolka , Joanna K. Strzelczyk , Aleksander J. Owczarek , Armand Cholewka , Aneta Krawczyk, and Agata Stanek 
Research Article (8 pages), Article ID 1983975, Volume 2019 (2019)




Early Oxidative Stress Response in Patients with Severe Aortic Stenosis Undergoing Transcatheter and Surgical Aortic Valve Replacement: A Transatlantic Study

Michael Mahmoudi, Juan Guillermo Gormaz, Marcia Erazo , Michael Howard, Cristian Baeza, Martin Feelisch, Nick Curzen, Bartosz Olechowski , Bernadette Fernandez, Magdalena Minnion, Monika Mikus-Lelinska, Mía Meiss, Laurie Lau, Nicolas Valls, Abraham I. J. Gajardo , Amy Rivotta, Rodrigo Carrasco, Gabriel Cavada, Maria Jesus Vergara, and Gabriel Maluenda 
Research Article (8 pages), Article ID 6217837, Volume 2019 (2019)







miR-200a Attenuated Doxorubicin-Induced Cardiotoxicity through Upregulation of Nrf2 in Mice

Xiaoping Hu, Huagang Liu, Zhiwei Wang , Zhipeng Hu, and Luo Cheng Li
Research Article (13 pages), Article ID 1512326, Volume 2019 (2019)

Sitagliptin-Dependent Differences in the Intensity of Oxidative Stress in Rat Livers Subjected to Ischemia and Reperfusion

Małgorzata Trocha, Małgorzata Krzystek-Korpacka , Anna Merwid-Ląd, Beata Nowak, Małgorzata Pieśniewska, Piotr Dziegiel, Agnieszka Gomulkiwicz, Przemysław Kowalski, Dorota Diakowska , Adam Szelać, and Tomasz Sozański 
Research Article (10 pages), Article ID 2738605, Volume 2019 (2019)

Malondialdehyde and Uric Acid as Predictors of Adverse Outcome in Patients with Chronic Heart Failure







Ewa Romuk , Celina Wojciechowska , Wojciech Jacheć , Aleksandra Zemła-Woszek , Alina Momot , Marta Buczkowska , and Piotr Rozentryt
Research Article (15 pages), Article ID 9246138, Volume 2019 (2019)

Stimulation of Na⁺/K⁺-ATPase with an Antibody against Its 4th Extracellular Region Attenuates Angiotensin II-Induced H9c2 Cardiomyocyte Hypertrophy via an AMPK/SIRT3/PPAR γ Signaling Pathway

Siping Xiong, Hai-Jian Sun , Lei Cao, Mengyuan Zhu, Teng Teng Liu, Zhiyuan Wu, and Jin-Song Bian 
Research Article (16 pages), Article ID 4616034, Volume 2019 (2019)




Contents

Decreased Lipid Profile and Oxidative Stress in Healthy Subjects Who Underwent Whole-Body Cryotherapy in Closed Cryochamber with Subsequent Kinesiotherapy

Agata Stanek , Ewa Romuk , Tomasz Wielkoszyński , Stanisław Bartuś , Grzegorz Cieślar , and Armand Cholewka 

Research Article (10 pages), Article ID 7524878, Volume 2019 (2019)

Metabolites of the Nitric Oxide (NO) Pathway Are Altered and Indicative of Reduced NO and Arginine Bioavailability in Patients with Cardiometabolic Diseases Complicated with Chronic Wounds of Lower Extremities: Targeted Metabolomics Approach (LC-MS/MS)

Małgorzata Krzystek-Korpacka , Jerzy Wiśniewski, Mariusz G. Fleszar , Iwona Bednarz-Misa , Agnieszka Bronowicka-Szydełko, Małgorzata Gacka, Leszek Masłowski, Krzysztof Kędzior, Wojciech Witkiewicz, and Andrzej Gamian

Research Article (13 pages), Article ID 5965721, Volume 2019 (2019)

Editorial

Novel Approaches for Diagnosing and Management of Cardiovascular Disorders Mediated by Oxidative Stress

Adrian Doroszko ¹, **Aneta Radziwon-Balicka**,² and **Robert Skomro** ³

¹Department of Internal Medicine, Occupational Diseases and Hypertension, Wrocław Medical University, Wrocław, Poland

²Department of Clinical Experimental Research, Glostrup Research Institute, Rigshospitalet, Glostrup, Denmark

³Division of Respirology, Critical Care and Sleep Medicine, Department of Medicine, University of Saskatchewan, Saskatoon, Canada

Correspondence should be addressed to Adrian Doroszko; adrian.doroszko@umed.wroc.pl

Received 4 April 2020; Accepted 4 April 2020; Published 20 April 2020

Copyright © 2020 Adrian Doroszko et al. This is an open access article distributed under the Creative Commons Attribution License, which permits unrestricted use, distribution, and reproduction in any medium, provided the original work is properly cited.

The cardiovascular disease is one of the major healthcare problems of the world population, and understanding its determinants is essential for designing effective interventions.

Reactive oxygen species (ROS) are toxic, highly reactive, and unstable compounds formed during a variety of physiological and pathological biochemical reactions. ROS are produced in all viable cells, and strong evidence suggests an important role of ROS in the development and progression of cardiovascular disease. Nevertheless, the precise mechanisms contributing to the cardiovascular system injury due to increased oxidative stress are still under investigation. Recent experimental studies suggest that ROS plays a causational role in the development of systolic dysfunction following myocardial infarction (MI), the brain ischemia-reperfusion injury in the course of stroke and in cardiometabolic disorders. Endothelium plays a crucial role in regulation of vascular tone, and endothelial dysfunction (ED) is an important risk factor of cardiovascular disease. The mechanisms involved in decreased vasodilative activity of endothelial cells include decreased bioavailability of nitric oxide, oxidative stress, and disorders in the metabolism of prostanoids. The decreased bioavailability of nitric oxide (NO), as well as increased oxidative stress, plays a crucial role in contributing to the decrease of endothelial vasodilative properties. According to several experimental studies, increased peroxynitrite (ONOO⁻) formation correlates with the development of neurological deficits following ischemic stroke and the cardiac ischemia-reperfusion injury in the course of coronary artery disease and develop-

ment of peripheral atherosclerotic lesions. Therefore, increased ONOO⁻ production followed by ONOO⁻-dependent protein modifications should be considered as one of the molecular mechanisms contributing vascular injury. The peroxynitrite-dependent modifications of proteins have been shown in many cardiovascular disorders; however, its molecular consequences still remain unknown.

Sufficient synthesis and bioavailability of nitric oxide is crucial for proper functioning of vascular endothelium. Consequently, NO deficiency is prerequisite for and a hallmark of endothelial dysfunction, a pathology preceding the development of cardiovascular disease (CVD). CVD and its main risk factors, such as obesity, hypertension, and type 2 diabetes mellitus (T2DM), are, in turn, among the key factors negatively affecting proper wound healing. Recently, a decreased nitric oxide bioavailability as expressed by an elevation in serum ADMA and decrease in serum L-arginine have been reported in patients with chronic wounds. Detrimental effects of diminished NO bioavailability on cardiovascular health and wound healing are well documented and have led to an outburst of novel treatment strategies aiming at its increase. Therefore, in a study by M. Krzystek-Korpacka et al., a wider panel of the L-arginine/ADMA/NO pathway metabolites using a targeted metabolomics approach was used in order to determine their status and clinical relevance in patients with chronic wounds of various etiologies. The authors demonstrate that patients with chronic wounds in the course of cardiometabolic disorders have reduced bioavailability of NO and its substrate, arginine, resulting from

ADMA and SDMA accumulation rather than from arginine deficiency. Citrulline was decreased in patients with cardio-metabolic diseases in general, but the presence of chronic wounds is associated with its elevation, reflecting degree of ADMA and SDMA accumulation and inversely related to NO and arginine bioavailability.

E. Romuk and colleagues have evaluated a wide range of oxidative stress markers and their impact on mortality and morbidity in patients with chronic heart failure. Malondialdehyde, a marker of lipid peroxidation, and serum uric acid level were strongly associated with worse prognosis in this group of subjects. The authors postulate that validation of elevated malonyldialdehyde and uric acid levels as independent predictors of outcome could have a potentially significant value for risk stratification of chronic HF patients.

Oxidized-LDL-induced inflammation, as a mediator atherosclerosis in malignancies, was investigated by L. Wang et al. Thymocyte selection-associated high mobility group box (TOX), which was reported to be regulated by lncRNA, has been closely related to the immune cell-associated proliferative diseases, such as cancer. Human metastasis-associated lung adenocarcinoma transcript 1 (MALAT1), an 8.7kb lncRNA, has been demonstrated to be overexpressed in several cancers, but the roles of MALAT1 in the pathogenesis of CVDs are still not well defined. In this study, the authors evaluated the crosstalk between MALAT1 and TOX through investigating whether the regulatory mechanism was associated with the miRNA network. The authors demonstrate that suppression of MALAT1 may attenuate inflammation in oxLDL-incubated endothelial cells by upregulating miR-181b and inhibiting the expression of TOX, which is closely related to the inhibition of the MAPK signaling pathway that attenuate the pathogenesis of atherosclerosis.

Lectin-like oxidized-LDL receptor-1 (LOX-1) is the major receptor for oxidized low-density lipoprotein (oxLDL), and targeting LOX-1 may provide a novel diagnostic strategy towards hypercholesterolemia and vascular diseases. In a study by A. Singh et al., the aegeline was shown to be effective in reducing the lipid abnormalities in aged hypercholesterolemic rats when compared to atorvastatin by targeting LOX-1 and had a pronounced effect in downregulating the expression of oxidized-LDL. Interestingly, T. Wielkoszynski et al. showed that $5\alpha,6\alpha$ -epoxy-phytosterols and $5\alpha,6\alpha$ -epoxy-cholesterol similarly impair the redox state in rats by increasing the production of free oxygen radicals and free radical-mediated lipid modification, as well as by affecting the mechanisms of nonenzymatic antioxidant defense and the activity of antioxidant enzymes.

A. Stanek et al. in an original study estimated the impact of whole-body cryotherapy (WBC) and subsequent kinesiotherapy on oxidative stress and lipid profile when performed in a closed cryochamber on healthy subjects. Until now, WBC has been used mainly in sports medicine and in the treatment of locomotor system diseases. In the available literature, there has been only one study, which estimated the influence of WBC on lipid profile parameters in healthy subjects, but WBC procedures were not connected with a subsequent session of kinesiotherapy, and the authors only estimated lipid profile parameters. As results from this study,

a significant decrease of oxidative stress markers and total cholesterol as well as LDL and a significant increase of total antioxidant capacity were observed following WBC treatment. The activity of plasma SOD-Mn and erythrocyte total SOD increased significantly in the WBC group. On the other hand, M. Bernardi with colleagues investigated the cardiovascular risk factors and hematological indexes of inflammation in Paralympic Athletes with different motor impairment. Interestingly, Paralympic Athletes with lower limb amputation had a higher cardiometabolic risk, whereas Paralympic Athletes with spinal cord injury had a higher platelet-derived cardiovascular risk.

Vascular smooth muscle cells (VSMCs) are the center of the calcification process. Many studies have confirmed that HAP crystals cause damage to VSMCs and induce cell phenotype transformation, which in turn promote vascular calcification. For example, exogenous calcifying nanoparticles, which are nanosized complexes of calcium phosphate mineral and proteins, are taken up by aortic smooth muscle cells *in vitro*, thereby decreasing cell viability, accumulating apoptotic bodies at mineralization sites, and accelerating vascular calcification. Interestingly, S. Xiong et al. have shown that stimulation of Na/K-ATPase with an antibody against its 4 extracellular region attenuates angiotensin II-induced H9c2 cardiomyocyte hypertrophy via an AMPK/SIRT3/PPAR γ signaling pathway. In this study, the effects of the differences in the morphological characteristics of nano-HAP on rat aortic smooth muscle cell (A7R5) injury and its phenotypic transformation were investigated to provide a basis for the determination of the effects of the physicochemical properties of crystals on cellular toxicity and vascular calcification. The extent of cell damage was closely related to the morphological characteristics of the crystals. More calcium deposits on the cell surface, more expressions of osteogenic protein (BMP-2, Runx2, OCN, and ALP), and a stronger osteogenic transformation ability were observed in the crystal with a high cell cytotoxicity than in the other crystals with a low cytotoxicity, thus increasing the risk of vascular calcification.

A very interesting study on calcific aortic valve stenosis (CAVS) was performed by N. Mercier and colleagues. Oxidative stress could be one potential mechanism that increases valve calcification and CAVS disease burden. Semicarbazide-sensitive amine oxidase (SSAO), also known as vascular adhesion protein-1 (VAP-1), is a mediator of tissue oxidative stress and a contributor to atherosclerotic plaque development. Furthermore, serum levels of SSAO are higher in patients with severe CAVS compared with patients presenting moderate CAVS and are significantly correlated with CAVS severity as assessed by echocardiography. The study by N. Mercier et al. is the first report showing a gradual and significant increase in SSAO mRNA, protein, and activity in human aortic valves divided into healthy, intermediate, and calcified tissue. The SSAO upregulation with valve calcification was independent of the cardiovascular and CAVS risk factors obesity, diabetes, and smoking. Furthermore, a significant correlation of SSAO expression with pathways of oxidative stress was also revealed. The results of this study indicate a link between SSAO, oxidative stress, and aortic valve calcification and point to SSAO inhibition

as a putative therapeutic approach to be explored for the prevention of valve calcification and CAVS progression.

With respect to aortic stenosis therapeutic strategy (classical surgical valve replacement, SAVR vs. transcatheter valve replacement, TAVR), M. Mahmoudi and colleagues compared the early oxidative stress response in the blood of patients undergoing TAVR with a group of patients undergoing SAVR by applying established biochemical readouts of cellular and extracellular redox status. As compared to patients undergoing SAVR, patients undergoing TAVR did not show significant changes in biomarkers of oxidative stress despite having greater comorbidities and impaired baseline antioxidant defenses. TAVR was associated with an improvement in the antioxidant capacity of plasma.

This special issue provides also some new data on novel therapeutic targets as well as some unknown, additional pleiotropic effects of drugs already used in clinical practice.

High glucose-induced cardiomyocyte injury is the leading cause of diabetic cardiomyopathy, which is associated with the induction of inflammatory responses and oxidative stress. A member of the G protein-coupled receptor family, G protein-coupled bile acid receptor 1 (GPBAR1; also known as TGR5), plays an important role in the regulation of glucose metabolism and has been recently identified as a drug target in type 2 diabetes. TGR5 is activated by bile acids and mediates the endocrine effects of bile acids on energy balance, inflammation, and digestion and regulates insulin secretion to maintain glucose homeostasis. The TGR5 ligand (oleanolic acid) shows significant blood glucose-lowering and weight-losing effects in diabetic animal models. L. Deng and colleagues have shown that activation of TGR5 partially alleviates high glucose-induced cardiomyocyte injury by inhibition of inflammatory responses and oxidative stress and postulate that activation of TGR5 has cardioprotective effects against HG-induced cardiomyocyte injury by suppressing inflammation and apoptosis partially through inhibiting the NF- κ B pathway and activating the Nrf2 pathway. Therefore, the authors postulate that TGR5 could be a pharmacological target for the treatment of diabetic cardiomyopathy.

M. Trocha et al. analyzed the antidiabetic SGLT-2 inhibitor-dependent differences in the intensity of oxidative stress in rat livers subjected to ischemia-reperfusion injury. Among the many phenomena occurring in the IR, there is an excessive production of free radicals and the development of oxidative stress. A body of evidence has gathered concerning protective effect of new drugs on hepatic cells during IR, providing rationale for new therapeutic strategies. Among others, glucose-lowering activity of incretins and hence indirectly of sitagliptin, STG, translates into reduced oxidative stress, condition fueled by hyperglycemia (21). Moreover, STG has been found to be an efficient scavenger of reactive oxygen species (ROS), directly reducing superoxide generation in various organs. In this study, a protective effect of SGLT-2 inhibitor on the rat liver, especially its antioxidant properties, was revealed under IR conditions. Also, despite the small degree of steatosis, the aminotransferase activity analysis does not suggest any hepatotoxic action of STG. Contrarily, even a slight protective effect of this drug was seen, especially in IR conditions.

Interestingly, A. Bilaska-Wilkosz et al. demonstrated that lipoic acid (LA) may exert beneficial effects on ethanol-induced cardiotoxicity. The administration of ethanol, linoleic acid, and disulfiram separately or jointly affected the aldehyde dehydrogenase activity in the rat liver indicating that LA is an inhibitor of aldehyde dehydrogenase. This study for the first time demonstrated that LA could partially attenuate the cardiac arrhythmia (extrasystoles and atrioventricular blocks) induced by EtOH and reduced the EtOH-induced mortality of animals, which supports a potential of LA for use in acute EtOH-intoxication and suggests that further experiments are necessary to elucidate the mechanism of action of LA as an antidote to EtOH poisoning.

Another original paper, by A. Barbosa et al., points out that the redox-active drug, MnTE-2-PyP5+, prevents and treats cardiac arrhythmias preserving the cardiac systolic function.

The death of cancer survivors was mainly attributed to cardiac factors, which emphasizes the need for pharmacological strategies offering protection against cardiotoxicity caused by anticancer drugs. Doxorubicin (DOX), an anthracycline chemotherapeutic, has been widely used for the treatment of both solid and hematologic malignancies, but its therapeutic use is limited by its dose-dependent cardiotoxicity, resulting in the cardiomyocyte loss, mitochondrial dysfunction, myofibrillar degeneration, and congestive heart failure with poor prognosis. In the study by X. Hu et al., the authors demonstrate that miR-200a supplementation, by activating Nrf2, could reduce cardiac injury, improve cardiac function, and attenuate DOX-related oxidative stress and cell apoptosis. miR-200a also protected the hearts from DOX-induced chronic damage and may thus, according to the authors, represent a new cardioprotective strategy against DOX-induced cardiotoxicity.

Conflicts of Interest

The editors declare that they have no conflicts of interest regarding the publication of this special issue.

Acknowledgments

We would like to thank all the authors who contributed to this special issue, as well as the numerous reviewers who reviewed each and every paper in a timely manner and provided their intellectual input to improve the quality of papers published. Finally, we want to acknowledge the Editorial Board of Oxidative Medicine and Cellular Longevity for giving us this opportunity to publish this special issue.

*Adrian Doroszko
Aneta Radziwon-Balicka
Robert Skomro*

Research Article

Redox-Active Drug, MnTE-2-PyP⁵⁺, Prevents and Treats Cardiac Arrhythmias Preserving Heart Contractile Function

Andrezza M. Barbosa,^{1,2} José F. Sarmiento-Neto ,³ José E. R. Menezes Filho,⁴ Itamar C. G. Jesus,⁵ Diego S. Souza,⁴ Valério M. N. Vasconcelos,¹ Fagner D. L. Gomes,¹ Aline Lara,¹ Juliana S. S. Araújo,^{2,6} Sandra S. Mattos,² Carla M. L. Vasconcelos ,⁴ Silvia Guatimosim,⁵ Jader S. Cruz,⁷ Ines Batinic-Haberle,⁸ Demetrius A. M. Araújo ,¹ Júlio S. Rebouças ,³ and Enéas R. Gomes ^{1,2}

¹Department of Biotechnology, Federal University of Paraíba, Joao Pessoa, Brazil

²Heart Circle, Recife, Brazil

³Department of Chemistry, Federal University of Paraíba, Joao Pessoa, Brazil

⁴Department of Physiology, Federal University of Sergipe, Aracaju, Brazil

⁵Department of Physiology and Biophysics, Federal University of Minas Gerais, Belo Horizonte, Brazil

⁶Department of Public Health, Federal University of Paraíba, Joao Pessoa, Brazil

⁷Department of Biochemistry and Immunology, Federal University of Minas Gerais, Belo Horizonte, Brazil

⁸Department of Radiation Oncology, Duke University School of Medicine, Durham, NC 27710, USA

Correspondence should be addressed to Enéas R. Gomes; eneasricardo@yahoo.com.br

Received 12 July 2019; Accepted 11 January 2020; Published 21 March 2020

Guest Editor: Adrian Doroszko

Copyright © 2020 Andrezza M. Barbosa et al. This is an open access article distributed under the Creative Commons Attribution License, which permits unrestricted use, distribution, and reproduction in any medium, provided the original work is properly cited.

Background. Cardiomyopathies remain among the leading causes of death worldwide, despite all efforts and important advances in the development of cardiovascular therapeutics, demonstrating the need for new solutions. Herein, we describe the effects of the redox-active therapeutic Mn(III) meso-tetrakis(*N*-ethylpyridinium-2-yl)porphyrin, AEOL10113, BMX-010 (MnTE-2-PyP⁵⁺), on rat heart as an entry to new strategies to circumvent cardiomyopathies. **Methods.** Wistar rats weighing 250-300 g were used in both *in vitro* and *in vivo* experiments, to analyze intracellular Ca²⁺ dynamics, L-type Ca²⁺ currents, Ca²⁺ spark frequency, intracellular reactive oxygen species (ROS) levels, and cardiomyocyte and cardiac contractility, in control and MnTE-2-PyP⁵⁺-treated cells, hearts, or animals. Cells and hearts were treated with 20 μM MnTE-2-PyP⁵⁺ and animals with 1 mg/kg, i.p. daily. Additionally, we performed electrocardiographic and echocardiographic analysis. **Results.** Using isolated rat cardiomyocytes, we observed that MnTE-2-PyP⁵⁺ reduced intracellular Ca²⁺ transient amplitude, without altering cell contractility. Whereas MnTE-2-PyP⁵⁺ did not alter basal ROS levels, it was efficient in modulating cardiomyocyte redox state under stress conditions; MnTE-2-PyP⁵⁺ reduced Ca²⁺ spark frequency and increased sarcoplasmic reticulum (SR) Ca²⁺ load. Accordingly, analysis of isolated perfused rat hearts showed that MnTE-2-PyP⁵⁺ preserves cardiac function, increases SR Ca²⁺ load, and reduces arrhythmia index, indicating an antiarrhythmic effect. *In vivo* experiments showed that MnTE-2-PyP⁵⁺ treatment increased Ca²⁺ transient, preserved cardiac ejection fraction, and reduced arrhythmia index and duration. MnTE-2-PyP⁵⁺ was effective both to prevent and to treat cardiac arrhythmias. **Conclusion.** MnTE-2-PyP⁵⁺ prevents and treats cardiac arrhythmias in rats. In contrast to most antiarrhythmic drugs, MnTE-2-PyP⁵⁺ preserves cardiac contractile function, arising, thus, as a prospective therapeutic for improvement of cardiac arrhythmia treatment.

1. Introduction

Therapeutic improvements, lifestyle modifications, and wider adoption of evidence-based medicine have resulted in a remarkable 30–35% decline in cardiovascular mortality [1]. However, despite all efforts and advances in developing cardiovascular therapeutics, cardiomyopathies are still a major public health problem and the main causes of death around the world [2, 3].

Since the first observation that Ca^{2+} was required for cardiac contraction and pacemaker activity, the role of Ca^{2+} as a signaling ion in the heart has been progressively dissected and better understood at molecular level, and it is clear that abnormalities in Ca^{2+} homeostasis play a pivotal role in the pathogenesis of many cardiovascular diseases, including cardiac arrhythmias [4]. Inherited gene alteration and acquired defects of multiple Ca^{2+} -handling proteins can contribute to the pathogenesis of arrhythmias in different categories of heart disease [4]. However, drug therapy is available only for some of these conditions and is often only partially effective [5].

Ca^{2+} handling within cardiomyocytes is widely recognized as a potential target for the treatment of cardiac disease. Whereas the role of Ca^{2+} channels in cardiac muscle contraction has long been elucidated [6], the biophysical and genetic identities of various voltage-gated Ca^{2+} channels were disclosed [7, 8], contributing along the way to several classes of antagonists being described, which comprise now part of the formulary for the treatment of cardiac diseases including arrhythmias [4].

Accordingly, Ca^{2+} channel blockers are able to decrease the automaticity of ectopic foci in the heart and can be used in many arrhythmias [4]. Overall, it is thought that reduced L-type calcium currents ($I_{\text{Ca,L}}$) result in less Ca^{2+} overload on the myocyte, reducing tendency to ectopy, which can trigger arrhythmias [4]. Additionally, cardiotonic glycosides or digitalis are positive inotropes used in clinical practice for the treatment of heart failure that also behave as endogenous ligands for Na^+/K^+ ATPase. An increase in intracellular Ca^{2+} content mediates their positive inotropic effect but has also been suggested as a trigger of life-threatening arrhythmias [9].

In many tissues, including the heart, reactive oxygen/nitrogen species (ROS/RNS) are often derived from mitochondria, NADPH oxidase, or uncoupled-nitric oxide synthase (NOS) and are kept under tight homeostatic control [10, 11]. In the cardiovascular system, ROS/RNS has been shown to play an important role in regulation of K^+ , Na^+ , L-type Ca^{2+} channels (in plasmatic membrane), and ryanodine receptor (RyR2) in sarcoplasmic reticulum membrane [12–14]. Mn-porphyrin-based compounds have been widely recognized as potent redox-active therapeutics, being able to modulate ROS/RNS in several animal models of oxidative stress [15–18]. Mn(III) *meso*-tetrakis(*N*-ethylpyridinium-2-yl) porphyrin (MnTE-2-PyP⁵⁺), also known as AEOL10113 or BMX-010, is currently under phase I/II clinical trials in Canada and the USA [15], and preclinical toxicological studies in conscious telemetered male cynomolgus monkeys showed that administration of MnTE-2-PyP⁵⁺ at a

dose of 1 mg/kg/day led to no statistically significant changes in heart rate or arterial blood pressure [19].

The pharmacokinetic studies on MnTE-2-PyP⁵⁺ show a good distribution of this compound into the heart [20, 21]. Such data prompted us to investigate MnTE-2-PyP⁵⁺ as a redox-active experimental therapeutic for cardiomyopathy, with particular focus on reducing Ca^{2+} stress and preserving cardiac contractile function. We demonstrate that MnTE-2-PyP⁵⁺ exerts protective effects in rat hearts, by modulating Ca^{2+} dynamics, reducing arrhythmia score, and preserving contractile function of the heart. Additionally, MnTE-2-PyP⁵⁺ was effective in preventing and treating cardiac arrhythmias *in vivo*.

2. Methods

2.1. Animals. All experiments were performed using rats of both sexes (*Rattus norvegicus*, 200–250 g). Animals were maintained at the Federal University of Paraiba (UFPB), Brazil, in accordance with NIH guidelines for the care and use of animals. Experiments were performed according to approved animal protocols from the Institutional Animal Care and Use Committee at UFPB (CEUA Protocol 016/2017). All animals were euthanized by decapitation.

2.2. MnTE-2-PyP⁵⁺ Synthesis. MnTE-2-PyP⁵⁺ was synthesized and characterized as described elsewhere [22–25]. Concentrations of MnTE-2-PyP⁵⁺ stock solutions were determined spectrophotometrically ($\log \epsilon_{454\text{nm}} = 5.14$) [22–24]. Moreover, MnTE-2-PyP⁵⁺ is extremely stable toward demetallation, even in strong concentrated acids (e.g., 98% sulfuric acid) [26–28], or in the presence of strong chelating agents, such as EDTA [26–29]. For both *in vitro* and *in vivo* experiments, MnTE-2-PyP⁵⁺ was diluted in 0.9% NaCl sterile solution.

2.3. Cardiomyocyte Isolation and Ca^{2+} Recordings. Ventricular rat cardiomyocytes were isolated and stored until they were used as previously described [30]. Intracellular Ca^{2+} analysis was performed with Fluo-4 AM (10 μM ; Invitrogen, Eugene, OR)-loaded cardiomyocytes. The cells were stained for 30 min and then washed to remove the excess dye. Cells were electrically stimulated at 1 Hz to produce steady-state conditions. The images were recorded in a Zeiss LSM 510META confocal microscope. As an indicator of the SR Ca^{2+} load, 10 mM caffeine stimulation (in a Ca^{2+} - and Na^+ -free solution) and the amplitude of the Ca^{2+} transient evoked were recorded [31]. Preconditioning pulses (1 Hz) were used in the cells before caffeine was applied. Ca^{2+} spark frequencies were recorded in resting ventricular myocytes. The Ca^{2+} level was reported as F/F_0 (or as $\Delta F/F_0$), where F_0 is the resting Ca^{2+} fluorescence.

2.4. ROS Recordings. Isolated cardiomyocytes were incubated with 10 μM dihydroethidium (DHE, Molecular Probes, Eugene, OR) for 30 min at 37°C and were subsequently washed with an extracellular solution to remove the excess dye. Images were acquired with a Zeiss LSM 510 META confocal microscope. Images were analyzed in ImageJ software.

2.5. Measurement of L-Type Ca^{2+} Current. Whole-cell voltage-clamp recordings were done at 22–25°C using an EPC-9.2 patch-clamp amplifier (HEKA Electronics, Rheinland-Pfalz, Germany) as described previously [32, 33]. L-type Ca^{2+} current ($I_{Ca,L}$) measurement was done using internal solution as follows (in mM): 5 NaCl, 120 CsCl, 20 TEACl, 5 EGTA, and 10 HEPES and pH 7.2 (adjusted using CsOH 1.0 M). External solution composition was as follows (in mM): 5.4 KCl, 140 NaCl, 1.8 $CaCl_2$, 1 $MgCl_2$, 10 HEPES, and 10 glucose and pH 7.2 (adjusted with NaOH 1.0 M). To measure the effect of MnTE-2-PyP⁵⁺ on $I_{Ca,L}$ density, we used a holding potential of –80 mV. Next, to inactivate both voltage-gated Na^+ channels and T-type Ca^{2+} channels, a pre-step of 50 ms to –40 mV was applied. Then, the membrane potential was swapped to 0 mV for 300 ms. This protocol was used before, during, and after washing off each concentration of MnTE-2-PyP⁵⁺.

2.6. Measurement of LV Myocyte Shortening. Cellular contractility was evaluated as previously described [34]. Briefly, isolated myocytes were placed in a chamber mounted on the stage of an inverted microscope (Eclipse TS 100; Nikon, Japan). The chamber was perfused with Tyrode's solution (in mM): 150 NaCl, 5.4 KCl, 0.5 $MgCl_2$, 1.8 $CaCl_2$, 10 HEPES, and 10 glucose and pH set at 7.4. All experiments were performed at room temperature. Myocytes were stimulated to contract at 1 Hz with 4 ms square pulse. Shortening was measured using a video-edge detection acquisition system (IonOptix, Milton, MA, USA). Sarcomeric shortening was expressed as a percentage of diastolic LV myocyte length. Five consecutive myocyte contractions were averaged before analysis. Cell shortening, maximal rates of contraction and relaxation, and times to 10% contraction and relaxation were determined for all groups.

2.7. Atrial Contractility. The left atrium was mounted in an organ chamber and maintained in modified Krebs–Henseleit solution (KHS) containing (in mM) 120 NaCl, 5.4 KCl, 1.2 $MgCl_2$, 1.25 $CaCl_2$, 11 glucose, 27 $NaHCO_3$, and 2 NaH_2PO_4 (pH 7.4), oxygenated with carbogen mixture (95% O_2 and 5% CO_2) and maintained at 29 ± 0.1°C. The atrium was electrically stimulated (1 Hz, 80 V, 1.5 ms, SD9 stimulator, Grass). Tissue was placed under 5 mN tension, and an isometric force transducer (HP FTA 10-1 Sunborn) was used to record the contraction force. After 30 min of stabilization, MnTE-2-PyP⁵⁺ was added cumulatively to the bath (1, 3, 10, 30, 100, and 300 μ M).

2.8. Sarcoplasmic Reticular Ca^{2+} Load. The heart was quickly removed, placed in a Krebs–Henseleit solution continuously bubbled with 95% O_2 and 5% CO_2 , and the left atrium was dissected. The left atrium was tied with an isometric force transducer (Grass FT03) which was mounted vertically on a micromanipulator. Stimulation (STIMULATOR SD9 GRASS) was with pulses of 0.5 ms duration at a suprathreshold voltage, and frequency of stimulation was 1 Hz for a 30 min equilibration period. Steady level and postrest contractions following 20 s of pause in stimulation were observed in caffeine-treated (10 mM) or caffeine-treated containing

20 μ M MnTE-2-PyP⁵⁺. Measurements were made on the last contraction before the pause and on the first contraction after the rest interval.

2.9. Langendorff Preparation-Perfused Hearts. Animals were euthanized 10–15 min after intraperitoneal injection of 1000 IU heparin/kg. The heart was dissected and perfused through a 1.0 ± 0.3 cm aortic stump with Krebs–Henseleit solution (KHS) containing (in mM) NaCl, 120; KCl, 5.4; $MgCl_2$, 1.2; $CaCl_2$, 1.25; glucose, 11; $NaHCO_3$, 27; and NaH_2PO_4 , 2 (pH 7.4). The perfusion fluid was maintained at 34 ± 1°C with a pressure of 10 ml/min in constant oxygenation (5% CO_2 and 95% O_2). Electrical activity was recorded utilizing three platinum electrodes (Ag/AgCl, in NaCl 1 M electrolytic solution) placed inside the chamber close to the heart for sensing electrical signals. Hearts were perfused for an initial 20 min period with KHS. After equilibration, the hearts were perfused for 12 min with KHS, 12 min with KHS+20 μ M MnTE-2-PyP⁵⁺, and last 30 min period with KHS. The high-calcium model was used to determine cardiac arrhythmias. Therefore, after a 20 min stabilization, hearts were perfused for 25 min with normal perfusion KHS at 34°C, started 25 min with high calcium (HC) (3.3 mM) and 25 min with HC+20 μ M MnTE-2-PyP⁵⁺.

2.10. In Vitro Arrhythmia. *In vitro* arrhythmia was determined in an isolated heart as described previously [35]. Hearts were subjected to perfusion with KHS containing 1.25 mM of calcium (control group) at 34°C during 20 min. After stabilization, the hearts were subjected to perfusion with 3.3 mM high calcium (HC group) or with high calcium in the presence of 20 μ M MnTE-2-PyP⁵⁺ during 25 min. Arrhythmia scores were determinate as previously described [36]. Therefore, to quantify the arrhythmias, 25 min of experiment was divided into 3 min intervals and the arrhythmia scores were added at the end.

2.11. Measurement of Left Ventricular Pressure. Left intraventricular pressure was measured using a water-filled balloon introduced into the cavity of the left ventricle with a constant diastolic pressure of 15 mmHg by adjusting the volume of the balloon, connected to a pressure transducer (FE221, Bridge Amp, ADInstruments, Australia) coupled to an amplifier (PowerLab 8/35, ADInstruments). Ventricular pressures were processed using a dedicated software (LabChart 8 Pro, ADInstruments).

2.12. In Vivo MnTE-2-PyP⁵⁺ Safety. To test the *in vivo* safety of MnTE-2-PyP⁵⁺, animals were randomized into two groups: (1) control 0.9% saline (1 ml/kg/day, i.p.) and (2) MnTE-2-PyP⁵⁺ (1 mg/kg/day, i.p.), which were treated for 15 days. The dose regimen for MnTE-2-PyP⁵⁺ administration was chosen based on rat model experiments carried out previously by our group [17, 37, 38].

2.13. In Vivo ECG Measurements. The animals were anesthetized with ketamine (80 mg/kg, i.p.); surface ECG measurements were conducted using subdermal electrodes placed in the DII lead arrangement connected to a cardiograph, amplified and digitalized (PowerLab 4/35 ADInstruments,

USA). ECG signals were recorded for 15 min, then animals received an injection of caffeine (120 mg/kg, i.p.) and epinephrine (2 mg/kg, i.p.). Data were analyzed in LabChart 8 (ADInstruments, USA) and arrhythmic score measured as described previously [36].

2.14. In Vivo Arrhythmia Susceptibility. The animals were injected with dexamethasone (4 mg/kg, i.p.) for 7 days to predispose to arrhythmia. In the prevention protocol, animals received MnTE-2-PyP⁵⁺ (1 mg/kg/day, i.p.) during the 7 days of dexamethasone administration. In the treatment protocol, the animals received only dexamethasone until day 5 and MnTE-2-PyP⁵⁺ (1 mg/kg/day, i.p.) and dexamethasone (4 mg/kg, i.p.) in days 6 and 7. Rats were randomized into four experimental groups: 1: control; 2: dexamethasone; 3: dexamethasone+MnP (treatment); and 4: dexamethasone +MnP (prevention).

2.15. M-Mode Echocardiography. Cardiac function under noninvasive conditions was assessed by two-dimensional guided M-mode echocardiography of halothane-anesthetized mice as previously described [39]. Briefly, animals were positioned on supine position with front paws wide open and trichotomized. Transthoracic echocardiography was performed using a SonoSite M-Turbo Ultrasound System B (USA) equipped with a 14 MHz linear transducer.

2.16. Statistical Analysis. Data are presented as mean \pm SEM. Sample comparisons were performed using Student's *t*-test for two-group analysis or one-way ANOVA followed by post hoc analysis for multiple comparisons. In all statistical tests, a *p* < 0.05 was used as a measure of statistical significance.

3. Results

3.1. MnTE-2-PyP⁵⁺ Reduces Ca²⁺ Signaling Preserving Cardiomyocyte Contractility. To investigate whether MnTE-2-PyP⁵⁺ modulates Ca²⁺ signaling in the heart, we performed Ca²⁺ transient analysis in isolated cardiomyocytes loaded with Fluo-4/AM (5 μ M), incubated for 90 min with crescent concentrations of MnTE-2-PyP⁵⁺ (2–200 μ M), and observed a significant reduction in peak Ca²⁺ transient in a concentration-dependent manner (Figure 1(a)). However, the kinetics of Ca²⁺ decay was altered only for T90 at 200 μ M concentration (Figures 1(b) and 1(c)). Considering that 20 μ M MnTE-2-PyP⁵⁺ concentration reduced approximately by 50% the peak Ca²⁺ transient, we chose this concentration to continue the experiments. To further understand the MnTE-2-PyP⁵⁺ effect on cardiac myocytes, we performed a time course analysis of Ca²⁺ transient from 5 to 15 min. Once again, MnTE-2-PyP⁵⁺ promoted a significant decrease in peak Ca²⁺ transient, observed after 15 min of incubation (Figure 1(d)), without causing alterations in the kinetics of Ca²⁺ decay (Figures 1(e) and 1(f)). Additionally, we observed that MnTE-2-PyP⁵⁺ did not change the basal Fluo-4 fluorescence (Supplementary videos 1–4).

Considering that MnTE-2-PyP⁵⁺ is a superoxide dismutase (SOD) mimetic (currently recognized as a broad redox modulator) [17, 18], we used dihydroethidium (DHE), a fluorescent, cell-permeable, reactive oxygen species (ROS)

indicator, to evaluate MnTE-2-PyP⁵⁺ effect on cardiomyocyte ROS levels. MnTE-2-PyP⁵⁺ did not change the basal levels of ROS. However, as its well-known that MnTE-2-PyP⁵⁺, physiologically, has antioxidant activity under oxidative stress conditions, we used isoproterenol (ISO) as a cell stressor. As expected, ISO induced an increase in DHE fluorescence that was prevented by MnTE-2-PyP⁵⁺ (Figures 2(a) and 2(b)), indicating that MnTE-2-PyP⁵⁺ is efficient in modulating cardiomyocyte redox state under stress conditions. Nevertheless, as MnTE-2-PyP⁵⁺ did not change basal ROS levels in cardiomyocytes, this result suggests that the observed reduction in Ca²⁺ transient induced by MnTE-2-PyP⁵⁺ is likely independent of its antioxidant effect.

As L-type Ca²⁺ channels (LTCC) and ryanodine receptors (RyR) are critical for normal Ca²⁺ signaling, we investigated the MnTE-2-PyP⁵⁺ effects on L-type Ca²⁺ current (*I*_{Ca,L}) using whole-cell voltage-clamp recordings. Figures 2(d)–2(f) show that MnTE-2-PyP⁵⁺ induced a significant reduction in *I*_{Ca,L} current density, compatible with the reduction in the peak Ca²⁺ transient. Additionally, we measured Ca²⁺ spark frequency, and interestingly, MnTE-2-PyP⁵⁺ reduced basal spark frequency (Figure 2(c)) and prevented the increase in Ca²⁺ spark frequency induced by ISO (Figure 2(c)).

As we observed all these alterations in pivotal components of excitation-contraction coupling (ECC) and considering the importance of Ca²⁺ ion for cellular contraction, we next analyzed the MnTE-2-PyP⁵⁺ effects on cardiomyocyte contractility. Remarkably, despite the reduction in *I*_{Ca,L} and in peak Ca²⁺ transient, no changes in fractional shortening, systolic length, or diastolic length of MnTE-2-PyP⁵⁺-treated cardiomyocytes were observed, which is in direct contrast to the LTCC blocker verapamil-treated group (Figures 3(a)–3(d)). This result is noteworthy, because it indicates that although MnTE-2-PyP⁵⁺ decreases Ca²⁺ transient, it preserves cardiomyocyte contractility.

3.2. MnTE-2-PyP⁵⁺ Preserves Heart Contractility Reducing Arrhythmia Index. Based on effects observed in isolated cardiomyocytes, we decided to investigate MnTE-2-PyP⁵⁺ actions on heart contractility. First, using isolated left atria preparation, it was observed that MnTE-2-PyP⁵⁺ did not evoke alterations in contraction force, dT/dt(+), and dT/dt(-) (Figures 3(e)–3(g)), corroborating the data obtained in isolated cardiomyocytes and indicating that MnTE-2-PyP⁵⁺ preserves cardiomyocyte contractility, also in tissue analysis. Furthermore, in Langendorff-perfused hearts, MnTE-2-PyP⁵⁺ did not change the left ventricular developed pressure (LVDP) (Figure 3(h)). Additionally, we verified that systole, diastole, and cardiac cycle duration were not modified by MnTE-2-PyP⁵⁺ (Supplementary Fig. S1A–C). Overall, these data show that although MnTE-2-PyP⁵⁺ acutely reduces Ca²⁺ signaling in isolated cardiomyocytes, it preserves heart contractility.

As we observed alterations in Ca²⁺ spark frequency in isolated cardiomyocytes, we also tested if MnTE-2-PyP⁵⁺ altered SR Ca²⁺ content in isolated atria. Consistent with isolated cell data, MnTE-2-PyP⁵⁺ increased the SR Ca²⁺ load in approximately 66%, which helps to explain the maintenance of the cardiac contractility (Supplementary Figs. S1D and E).

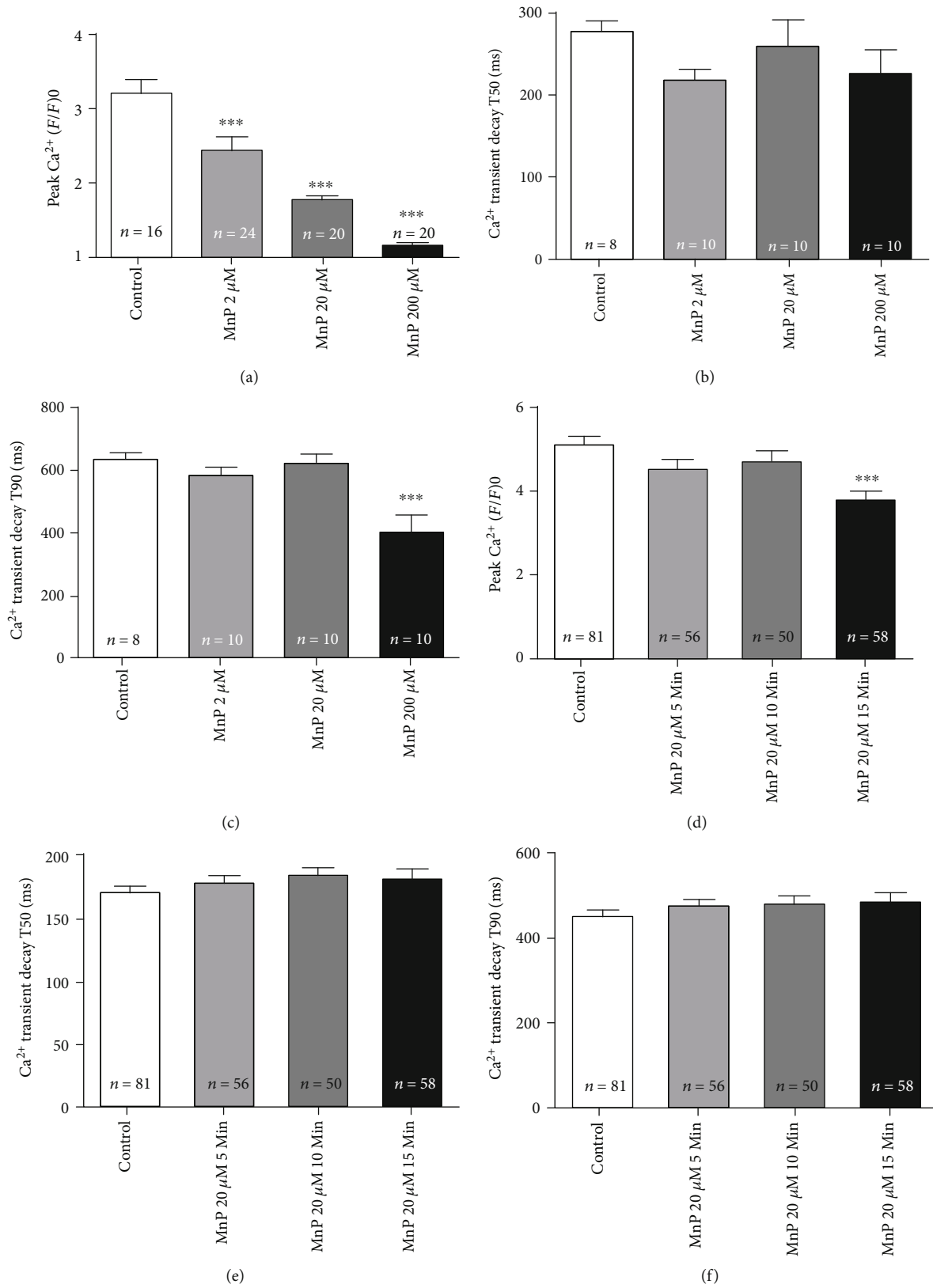


FIGURE 1: MnTE-2-PyP⁵⁺ reduces Ca²⁺ transients in cardiac myocytes. Concentration effect of MnTE-2-PyP⁵⁺ on Ca²⁺ transients. (a) Significant reduction in peak Ca²⁺ transient amplitude in isolated cardiomyocytes treated with MnTE-2-PyP⁵⁺. Ca²⁺ transient kinetics of decay in ms for (b) T50 or (c) T90. (d, e) Time course effect of MnTE-2-PyP⁵⁺ 20 μM on Ca²⁺ transients. (d) Significant reduction in peak Ca²⁺ transient amplitude in MnTE-2-PyP⁵⁺-treated cardiomyocytes for 15 min. (e, f) Ca²⁺ transient kinetics of decay in ms for (e) T50 or (f) T90; n = at least 10 cells per animal and 3 animals per group. *p < 0.05; **p < 0.01; ***p < 0.001. MnP = MnTE-2-PyP⁵⁺.

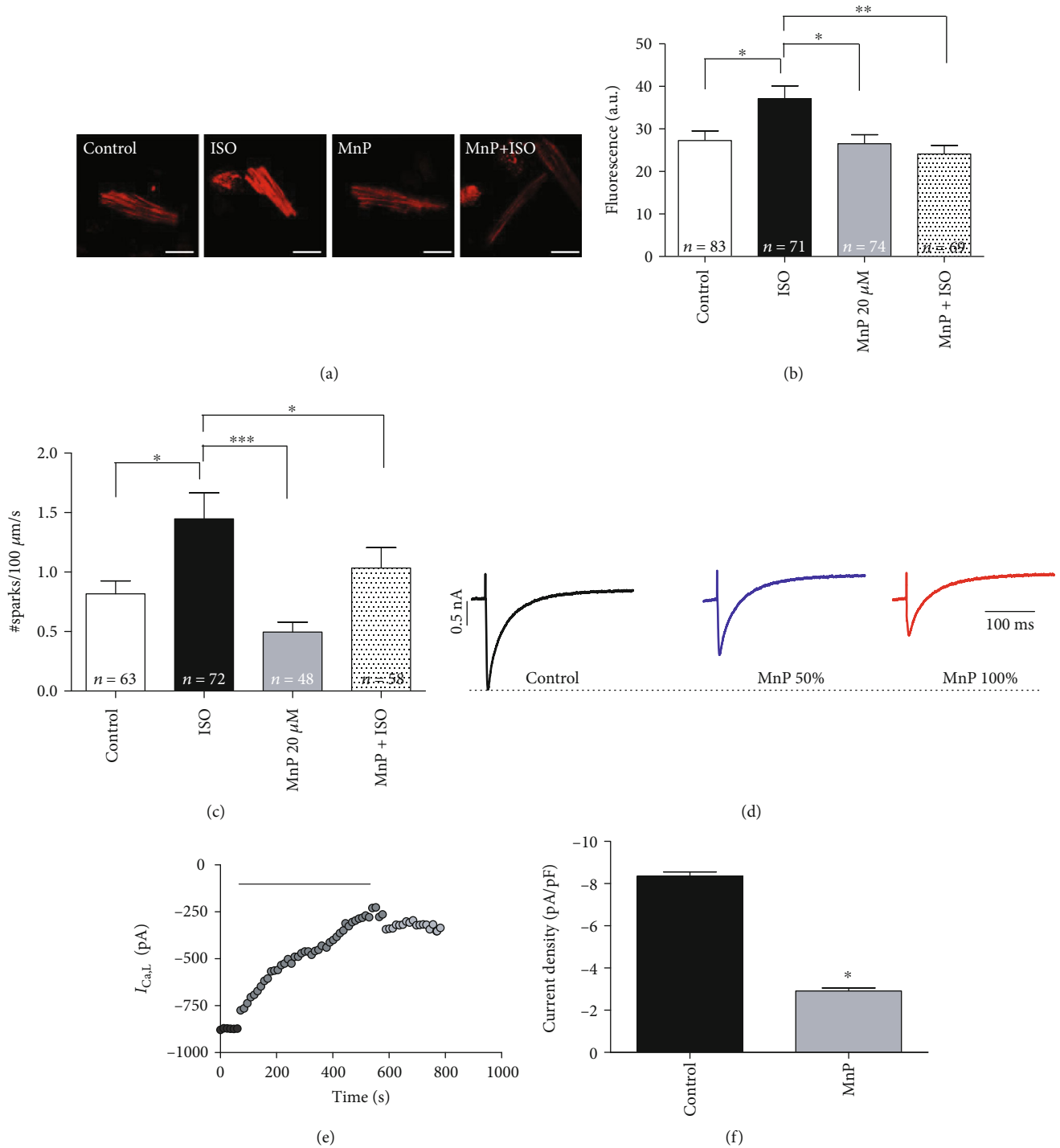


FIGURE 2: MnTE-2-PyP⁵⁺ reduces Ca²⁺ currents independent of antioxidant activity. (a) Representative images of DHE-stained cells. Scale bar = 10 μm . (b) Bar graph showing that MnTE-2-PyP⁵⁺ does not change basal ROS levels but prevents ISO-induced ROS increase. (c) MnTE-2-PyP⁵⁺ prevents ISO-induced increase in Ca²⁺ spark frequency. (d) Representative traces of $I_{\text{Ca,L}}$. (e) Time course of $I_{\text{Ca,L}}$ current. (f) Bar graph showing $I_{\text{Ca,L}}$ density reduction by MnTE-2-PyP⁵⁺. $n =$ at least 10 cells per animal and 3 animals per group. * $p \leq 0.05$; ** $p \leq 0.01$; *** $p \leq 0.001$. MnP = MnTE-2-PyP⁵⁺.

Considering the involvement of Ca²⁺ ions in triggering cardiac arrhythmias, we used Langendorff-perfused hearts to test whether MnTE-2-PyP⁵⁺ could alter the electrical activity of the heart. Electrocardiographic (ECG) recordings were used to analyze ECG intervals and segments. The results

showed that heart rate and QRS complex length were not modified by MnTE-2-PyP⁵⁺ (Figures 4(a)–4(c)). However, QTcV was significantly shortened and PRi increased (Figures 4(d) and 4(e)). Additionally, to investigate if MnTE-2-PyP⁵⁺ could target cardiac arrhythmias, isolated

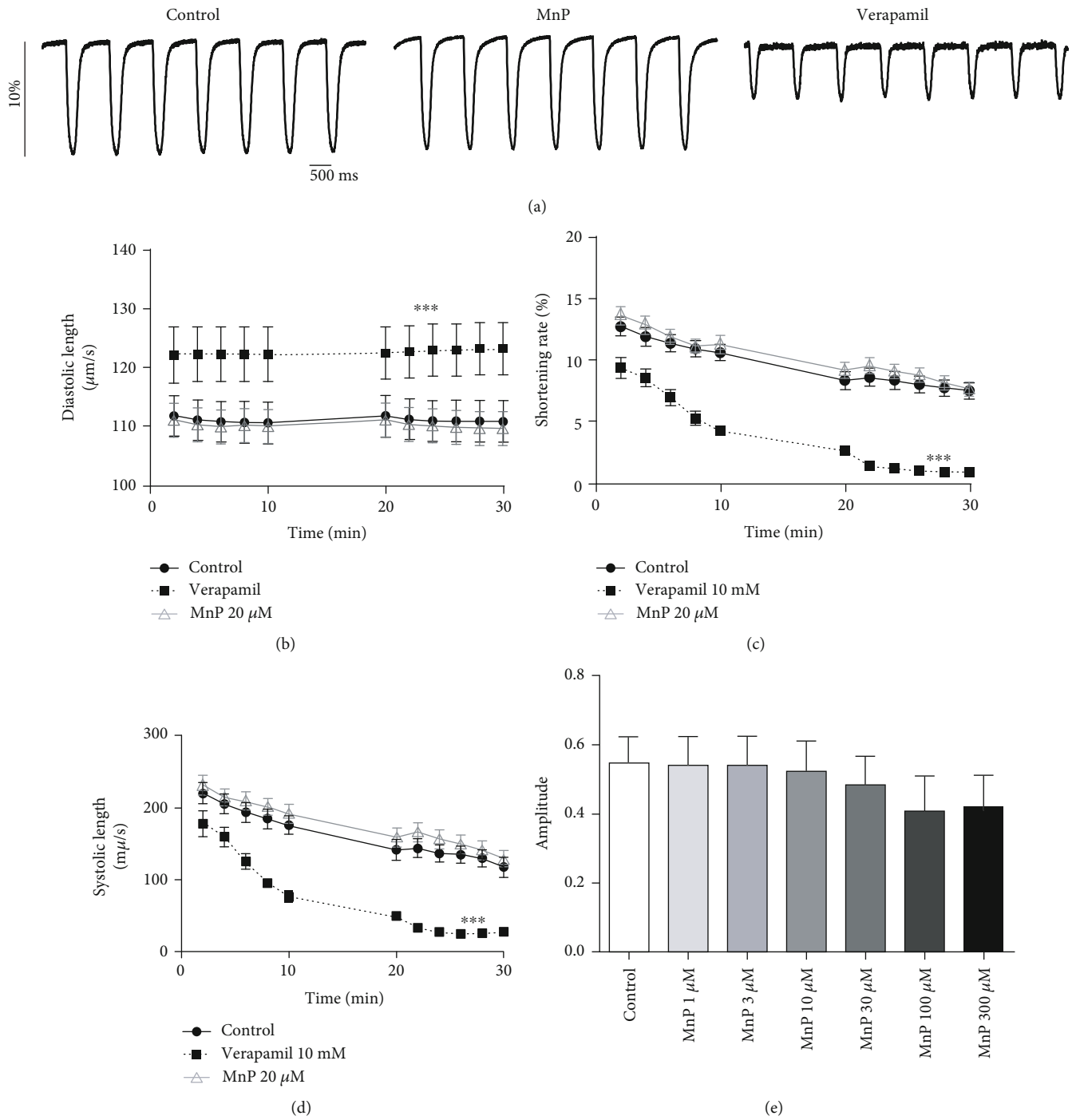


FIGURE 3: Continued.

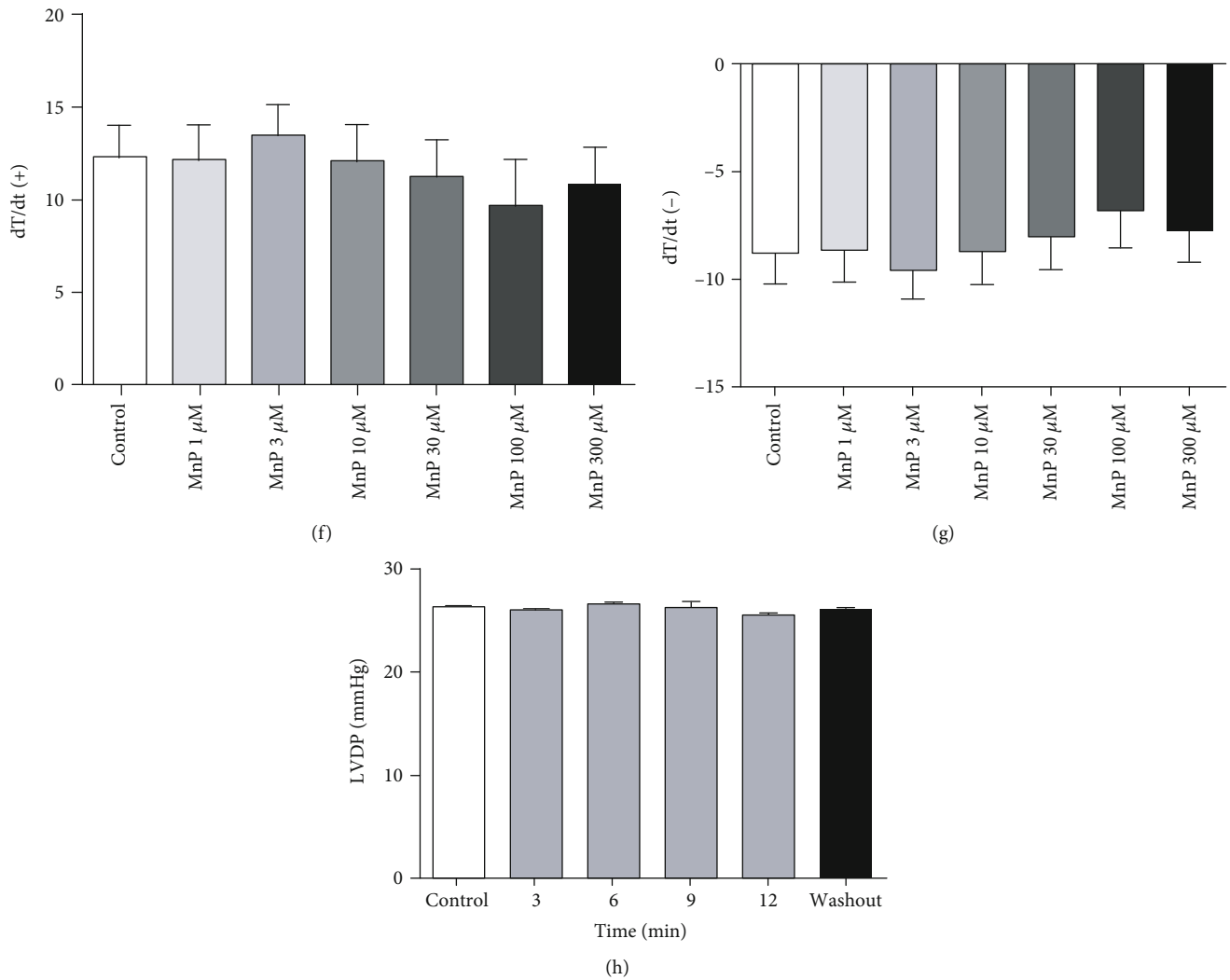


FIGURE 3: MnTE-2-PyP⁵⁺ preserves cardiomyocyte and atria contractility. (a) Representative traces of isolated ventricular cardiomyocyte contractility. Time course of (b) diastolic length, (c) shortening rate, and (d) systolic length in MnTE-2-PyP⁵⁺-treated cardiomyocytes. Concentration effect of MnTE-2-PyP⁵⁺ on isolated perfused hearts' (e) amplitude of contraction, (f) dT/dt(+), and (g) dT/dt(-). (h) Bar graph showing time course effect of MnTE-2-PyP⁵⁺ on LVDP. LVDP=left ventricular diastolic pressure. (b–d) n =at least 10 cells per animal and 5 animals per group. (e–h) n =5 animals per group. * p ≤0.05; ** p ≤0.01; *** p ≤0.001. MnP=MnTE-2-PyP⁵⁺.

hearts were perfused with high calcium (HC) to induce cardiac arrhythmias. Figure 4(f) shows normal ECG traces in control situation (top panel) and induced arrhythmias in HC-perfused heart (bottom panel). As shown in Figure 4(g), HC perfusion significantly increased the arrhythmia scores and MnTE-2-PyP⁵⁺ decreased HC-induced cardiac arrhythmias. Furthermore, most of the arrhythmias evidenced in control situation were of lower severity, such as ventricular premature beats (VPB, Figure 4(h)). In contrast, HC-perfused hearts presented ventricular fibrillation (VF), the most severe type of arrhythmia. Remarkably, MnTE-2-PyP⁵⁺ prevented the incidence of the most severe arrhythmia events (Figure 4(h)).

3.3. MnTE-2-PyP⁵⁺ Increases Ca²⁺ Transient and Preserves Heart Function In Vivo. Based on our *in vitro* results, we visualized MnTE-2-PyP⁵⁺ as a potential lead for therapeutic approaches for some cardiac arrhythmias. Thus, we designed

in vivo experiments in rats to investigate the effect of MnTE-2-PyP⁵⁺ on the heart. Animals were treated daily with 1 mg/kg MnTE-2-PyP⁵⁺ (i.p. injections) for 15 days. First, we tested MnTE-2-PyP⁵⁺ effects on Ca²⁺ transient. Cardiomyocytes from MnTE-2-PyP⁵⁺-treated rats presented increased peak Ca²⁺ transient and T90 time for Ca²⁺ decay, different from what we observed in acutely treated isolated myocytes (Figures 5(a)–5(c)). Additionally, as we verified an increase in SR load *in vitro*, we decided to investigate the SR load in cardiomyocytes isolated from treated animals. In agreement with *in vitro* experiments, MnTE-2-PyP⁵⁺ treatment increased SR Ca²⁺ load by approximately 14% (Figure 5(d)).

Additionally, heart weight/body weight (HW/BW) and heart weight/tibia length (HW/TL) ratios were evaluated as markers of cardiac hypertrophy in MnTE-2-PyP⁵⁺-treated animals. As shown in Figures 5(e) and 5(f), these parameters did not differ from those of the control group. Next, by

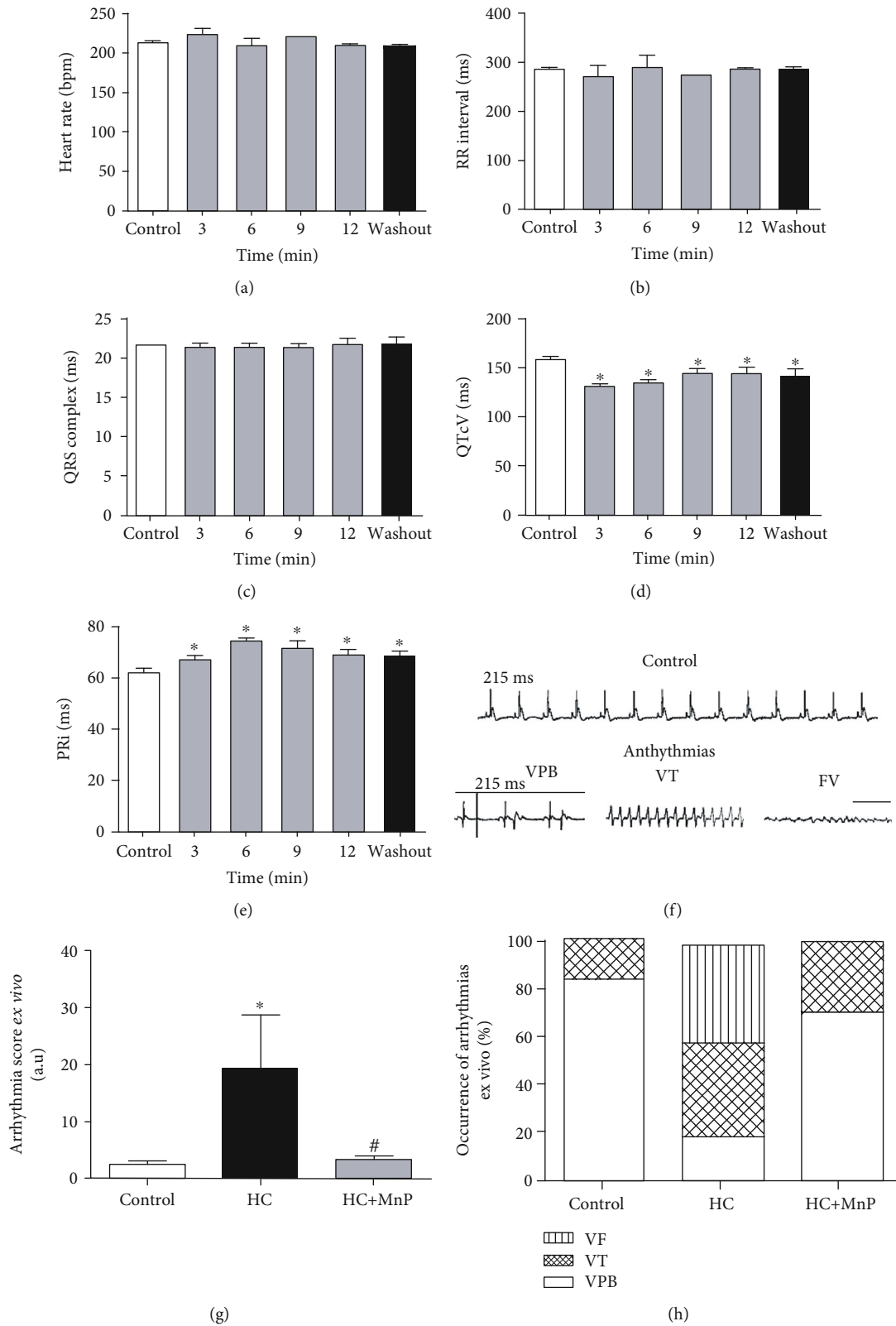


FIGURE 4: MnTE-2-PyP⁵⁺ preserves cardiac electrical activity and prevents high calcium-induced arrhythmias. Bar graphs showing (a) significant increase in PR interval, (b) RR interval, (c) QRS complex duration, (d) significant reduction in adjusted QT duration, and (e) heart rate. (f) Representative electrocardiographic traces. Bar graphs showing MnTE-2-PyP⁵⁺ preventive effect on (g) arrhythmia score and (h) severity. *n* = 5 animals per group. **p* ≤ 0.05; ***p* ≤ 0.01; ****p* ≤ 0.001. #*p* ≤ 0.05 compared to control. Mn = MnTE-2-PyP⁵⁺.

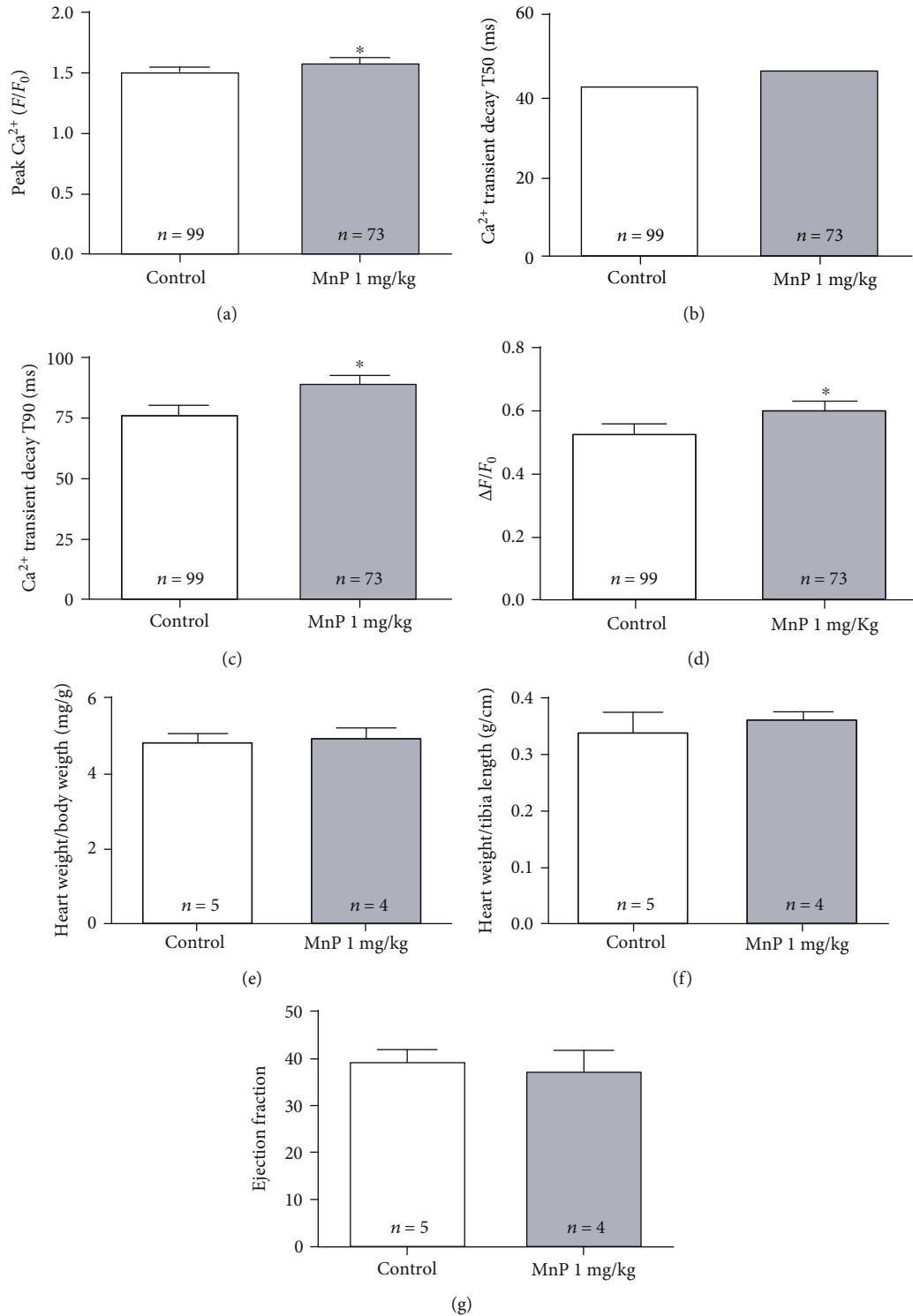


FIGURE 5: MnTE-2-PyP⁵⁺ (1 mg/kg/day, i.p., 15 days) increases Ca^{2+} transients *in vivo* and preserves cardiac mass and function. (a–c) Effect of MnTE-2-PyP⁵⁺ on Ca^{2+} transients. (a) Significant increase in peak Ca^{2+} transient amplitude in cardiomyocytes from animals treated with MnTE-2-PyP⁵⁺. Ca^{2+} transient kinetics of decay in ms for (b) T50 or (c) T90. (d) SR load is increased in cells from MnTE-2-PyP⁵⁺-treated animals. MnTE-2-PyP⁵⁺ preserves cardiac mass when measured by (e) heart weight/body weight or (f) heart weight/tibia length. (g) Bar graph of echocardiographic measurement of ejection fraction showing that MnTE-2-PyP⁵⁺ preserves systolic function *in vivo*. (a–d) n =number of cells (at least 5 animals per group). (e–g) n =number of animals. * $p \leq 0.05$; ** $p \leq 0.01$; *** $p \leq 0.001$. MnP = MnTE-2-PyP⁵⁺. VF = ventricular fibrillation; VT = ventricular tachycardia; VPB = ventricular premature beat; HC = high calcium; MnP = MnTE-2-PyP⁵⁺. MnTE-2-PyP⁵⁺ 20 μM per 25 minutes was used in all experiments.

echocardiographic analysis, we verified that MnTE-2-PyP⁵⁺-treated animals had no difference in ejection fraction (EF) when compared to control (Figure 5(g)), indicating that MnTE-2-PyP⁵⁺ preserves cardiac contractility *in vivo*. Taken together, these results indicate that MnTE-2-PyP⁵⁺ administered at 1 mg/kg/day i.p. does not alter normal heart function *in vivo*.

3.4. MnTE-2-PyP⁵⁺ Effectively Prevents and Treats Cardiac Arrhythmias *In Vivo*. Considering the robust effects of MnTE-2-PyP⁵⁺ in preventing cardiac arrhythmias in isolated hearts, we assessed its antiarrhythmic property *in vivo*. By using a dexamethasone-induced arrhythmia model, we tested both preventive and therapeutic actions of MnTE-2-PyP⁵⁺. Figure 6(a) shows representative ECG traces along with the type of the recorded arrhythmias: isolated VPB, sustained VPB, and VT. Remarkably, in both prevention and treatment protocols, MnTE-2-PyP⁵⁺ was completely effective to reduce both arrhythmia score and duration (Figures 6(b) and 6(c)), restoring the control profile. When we analyzed the severity of ventricular arrhythmias, we observed that MnTE-2-PyP⁵⁺ prevented the occurrence of ventricular tachycardia (VT) (Figure 6(d)). However, although MnTE-2-PyP⁵⁺ reduced the duration of arrhythmias, it was not able to reverse the relative occurrence of VT (Figure 6(d)).

To better view the multiple actions of MnTE-2-PyP⁵⁺, Figure 7 presents a schematic summary of the main effects of MnTE-2-PyP⁵⁺ both *in vitro* and *in vivo*.

To better view the multiple actions of MnTE-2-PyP⁵⁺, Figure 7 presents a schematic summary of the main effects of MnTE-2-PyP⁵⁺ both *in vitro* and *in vivo*.

4. Discussion

Cardiac arrhythmias are important causes of sudden death; thus, proper treatment of these conditions is of utmost importance. Indeed, over the last two decades, there has been a great deal of progress in arrhythmia management. However, most antiarrhythmic drugs proved ineffective or dangerous in patients with ventricular arrhythmias [40], demonstrating the need for new therapeutic strategies.

Although the mainstay of treatment for catecholaminergic polymorphic ventricular tachycardia (CPVT) has been β -blockade, there has also been early evidence that blocking $I_{Ca,L}$ with the LTCC blocker verapamil prevents ventricular arrhythmias [41]. Overall, it is thought that reduced $I_{Ca,L}$ results in less Ca^{2+} overload of the myocyte, reducing predisposition to ectopy that can trigger arrhythmias [4]. In agreement with these findings, our study shows that acute administration of MnTE-2-PyP⁵⁺ to isolated cardiomyocytes reduced the peak Ca^{2+} transient in these cells, in association with reduced $I_{Ca,L}$. Additionally, acute administration of MnTE-2-PyP⁵⁺ in isolated hearts resulted in reduction in arrhythmia index, severity, and duration of arrhythmias, demonstrating, for the first time, that MnTE-2-PyP⁵⁺ represents a new lead molecule for the treatment of cardiac arrhythmias.

Additionally, while *in vitro* acute use of MnTE-2-PyP⁵⁺ reduced Ca^{2+} transient in cardiomyocytes, *in vivo* 15-day

use of MnTE-2-PyP⁵⁺ in healthy rats did not change Ca^{2+} transient in cardiomyocytes. Although these results may at first seem inconsistent, when we consider that MnTE-2-PyP⁵⁺ reduced Ca^{2+} spark rate and increased SR load, chronically, these two effects combined may account for the final increased Ca^{2+} transient observed *in vivo*. Additionally, as we and others [15, 17, 18] demonstrated that under stress conditions MnTE-2-PyP⁵⁺ prevents oxidative stress, this effect can also contribute, chronically, to cellular restoration of basal transient kinetics. Accordingly, Almeida et al. [42] demonstrated that aldosterone-treated cardiomyocytes presented increased $I_{Ca,L}$ and Ca^{2+} transient and that Angiotensin-(1-7) restored basal $I_{Ca,L}$ albeit with a great increase in Ca^{2+} transient. Further investigation demonstrated that this alteration in Ca^{2+} transient was caused by reduction in Ca^{2+} spark frequency and consequent increased SR load. MnTE-2-PyP⁵⁺ apparently works via a similar mechanism by improving Ca^{2+} transient in the long term. In addition, the systemic antioxidant effect of MnTE-2-PyP⁵⁺ must be considered in the cardiovascular health *in vivo*.

By reducing peripheral vasoconstriction and LV afterload, calcium channel blockers were thought to have a potential role in the management of chronic heart failure (HF). However, first-generation dihydropyridine and nondihydropyridine calcium channel blockers also have myocardial depressant activity [43]. Several clinical trials have demonstrated either no clinical benefit or even worse outcomes in patients with HF treated with these drugs [44–48]. Despite their greater selectivity for calcium channels in vascular smooth muscle cells, second-generation calcium channel blockers, dihydropyridine derivatives such as amlodipine and felodipine, have failed to demonstrate any functional or survival benefit in patients with HF [49–53]. Together, these data show that although calcium channel blockers have an important role in the management of cardiac arrhythmias, they are of limited use, especially in patients with HF.

Although the use of calcium channel blockers for arrhythmia treatment is often plagued by myocardial depressant activity, here, we demonstrated that MnTE-2-PyP⁵⁺ prevents and treats cardiac arrhythmias while preserving contractility at both cardiomyocyte and heart levels. These combined effects respond to a large gap in arrhythmia treatments, especially in patients with HF.

It is worth noting that our study demonstrates that MnTE-2-PyP⁵⁺ preserves cardiomyocyte and heart contractility and exerts antiarrhythmic effects both *in vitro* and *in vivo*, representing, thus, a potentially new strategy to treat cardiac arrhythmias in patients with contractile dysfunctions. In addition, although reduction in peak calcium transients is usually related to reduction in cardiac contractility, modulation of proteins involved in calcium handling or contractile machinery can alter this relationship. In this way, Vanzelli et al [54]. demonstrated that heart failure mice treated with carvedilol had an improvement in cardiac fractional shortening instead of no alterations in peak calcium transients. Although we did not analyze these mechanisms directly, we speculate that MnTE-2-PyP⁵⁺ effect may be somewhat related to the mechanism described by Vanzelli et al [54].; further investigations are obviously

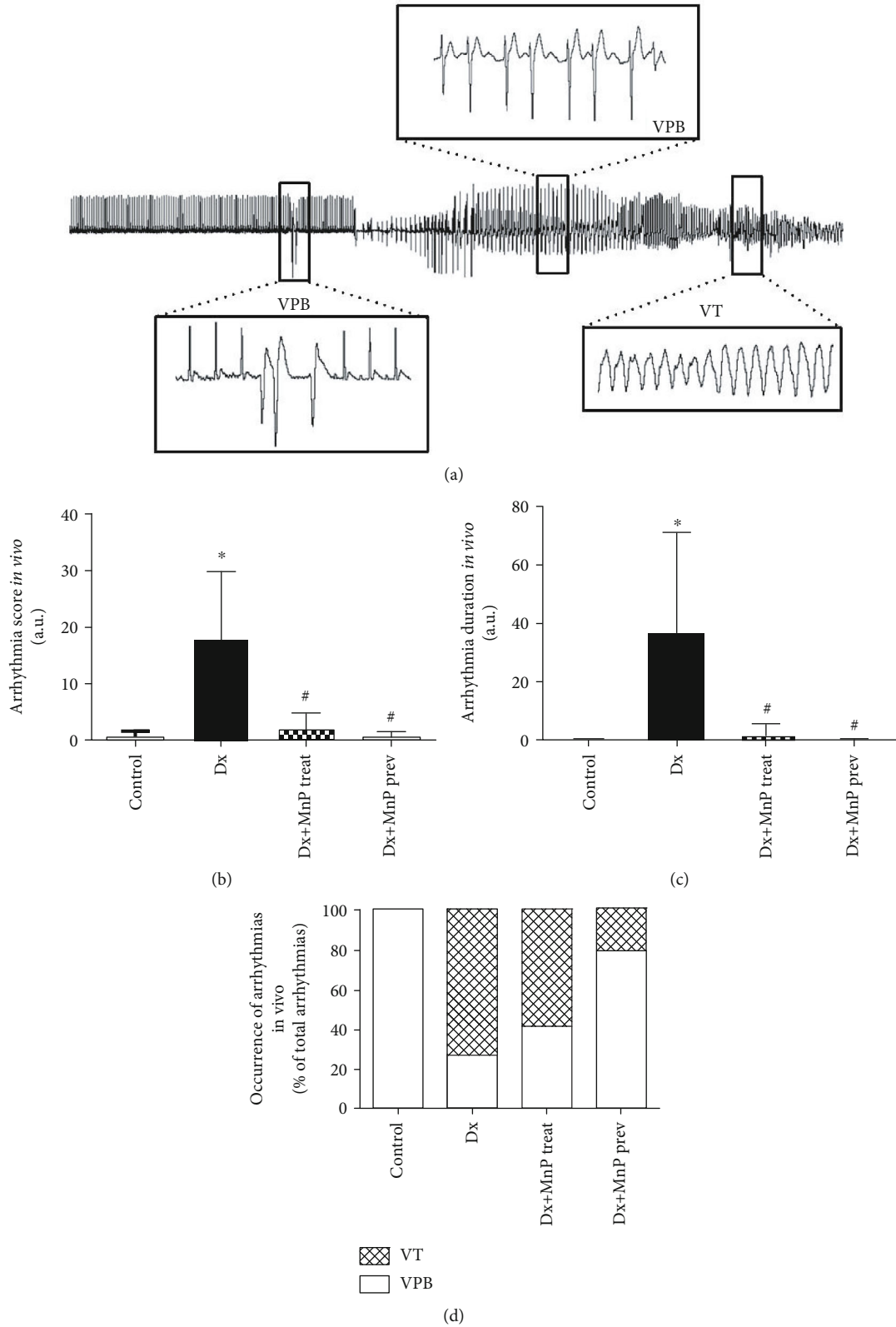


FIGURE 6: MnTE-2-PyP⁵⁺ effectively prevents and treats cardiac arrhythmias. (a) Representative images of electrocardiogram records, cardiac arrhythmias are highlighted. Bar graphs showing that MnTE-2-PyP⁵⁺ reduces (b) arrhythmia score and (c) duration. (d) Bar graph showing protective effect of MnTE-2-PyP⁵⁺ on severity of arrhythmias. $n = 5$ animals per group. Dx = dexamethasone (4 mg/kg, i.p., 7 days); Dx+MnP treat = dexamethasone+MnP treatment (MnTE-2-PyP⁵⁺, 1 mg/kg/day, i.p., during the last 2 days of Dx); Dx+MnP prev = dexamethasone+MnP prevention (MnTE-2-PyP⁵⁺, 1 mg/kg/day, i.p., during the 7 days of Dx). * $p \leq 0.05$; ** $p \leq 0.01$; *** $p \leq 0.001$. # $p \leq 0.05$ compared to control. VT = ventricular tachycardia; VPB = ventricular premature beat. Mn = MnTE-2-PyP⁵⁺.

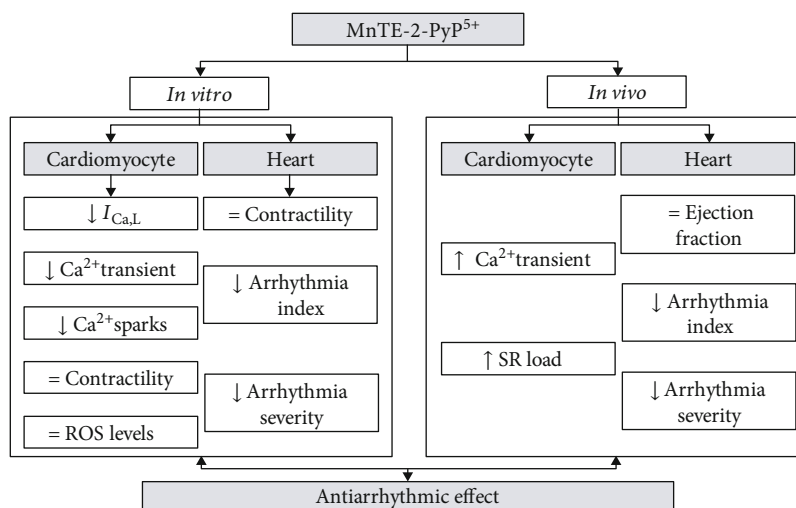


FIGURE 7: Schematic summarization of the main effects of MnTE-2-PyP⁵⁺ both in vitro and in vivo and the consequent antiarrhythmic effect. I_{Ca,L} = L-type calcium current; ROS = reactive oxygen species; SR = sarcoplasmic reticulum.

needed to disclose the actual MnTE-2-PyP⁵⁺ mechanism(s) of action.

Finally, it is important to highlight that the use of Mn porphyrin-based SOD mimics for cardiovascular treatments is in its infancy. A first report [55] was very recently published on the ability of an analogous Mn porphyrin, MnTnBuOE-2-PyP⁵⁺ (BMX-001) [28], to suppress aortic valve sclerosis in mice and human models. We showed herein that the prototypical Mn-porphyrin MnTE-2-PyP⁵⁺ represents a simple, promising redox-active therapeutic for preventing and treating cardiac arrhythmias, preserving heart contractile function. Taken together, the data strengthen the therapeutic potential of Mn porphyrins in a quite unexplored field of cardiac applications.

Data Availability

Part of this manuscript is under patent registration. Because of that the authors do not present a data availability statement.

Conflicts of Interest

The authors declare that I.B.H. is a consultant with and holds equities in BioMimetix JV LLC. I.B.H. and Duke University have patent rights and have licensed technologies to BioMimetix JV LLC.

Acknowledgments

This work was supported by CNPq, FINEP, and FAPEMIG. A.M.B. and J.F.S.N. acknowledge CAPES (Brazil) for Ph.D. fellowships.

Supplementary Materials

Supplementary 1. Supplementary figure 1: (A-C) duration time for systole, diastole, and cardiac cycle, calculated in electrocardiograms recorded in isolated hearts, and (D)

representative traces of the left atrium contraction. Steady level and postrest contractions following 20 s of pause in stimulation were observed in caffeine-treated (10 mM) or caffeine-treated containing 20 μM MnTE-2-PyP⁵⁺.

Supplementary 2. Supplementary figure 1: (E) the bar graph of contraction force average for each group. Measurements were made on the last contraction before the pause and on the first contraction after the rest interval. Supplementary videos 1-4: representative videos of Fluo-4 AM (10 μM; Invitrogen, Eugene, OR)-loaded cardiomyocytes, under field stimulation (1 Hz), recorded in a Zeiss Axio Observer A1 fluorescent microscope.

References


- [1] D. Mozaffarian, E. J. Benjamin, A. S. Go et al., "Heart disease and stroke statistics—2015 update," *Circulation*, vol. 131, no. 4, pp. e29–322, 2015.
- [2] A. S. Go, D. Mozaffarian, V. L. Roger et al., "Heart disease and stroke statistics—2014 update: a report from the American Heart Association," *Circulation*, vol. 129, no. 3, 2014.
- [3] J. M. Gonzalez-Rosa, V. Martin, M. Peralta, M. Torres, and N. Mercader, "Extensive scar formation and regression during heart regeneration after cryoinjury in zebrafish," *Development*, vol. 138, no. 9, pp. 1663–1674, 2011.
- [4] A. P. Landstrom, D. Dobrev, and X. H. T. Wehrens, "Calcium signaling and cardiac arrhythmias," *Circulation Research*, vol. 120, no. 12, pp. 1969–1993, 2017.
- [5] S. Nattel, "Allele-specific gene silencing: another step in the inexorable advance of gene therapy for cardiac arrhythmia management," *Circulation Research*, vol. 121, no. 5, pp. 480–482, 2017.
- [6] H. A. Fozzard, "Cardiac sodium and calcium channels: a history of excitatory currents," *Cardiovascular Research*, vol. 55, no. 1, pp. 1–8, 2002.
- [7] B. Nilius, P. Hess, J. B. Lansman, and R. W. Tsien, "A novel type of cardiac calcium channel in ventricular cells," *Nature*, vol. 316, no. 6027, pp. 443–446, 1985.

- [8] B. M. Curtis and W. A. Catterall, "Purification of the calcium antagonist receptor of the voltage-sensitive calcium channel from skeletal muscle transverse tubules," *Biochemistry*, vol. 23, no. 10, pp. 2113–2118, 1984.
- [9] L. A. Gonano and M. V. Petroff, "Subcellular mechanisms underlying digitalis-induced arrhythmias: role of calcium/calmodulin-dependent kinase ii (camkii) in the transition from an inotropic to an arrhythmogenic effect," *Heart, Lung & Circulation*, vol. 23, no. 12, pp. 1118–1124, 2014.
- [10] A. A. Sovari, C. A. Rutledge, E. M. Jeong et al., "Mitochondria oxidative stress, connexin43 remodeling, and sudden arrhythmic death," *Circulation: Arrhythmia and Electrophysiology*, vol. 6, no. 3, pp. 623–631, 2013.
- [11] T. Munzel, G. G. Camici, C. Maack, N. R. Bonetti, V. Fuster, and J. C. Kovacic, "Impact of oxidative stress on the heart and vasculature: part 2 of a 3-part series," *Journal of the American College of Cardiology*, vol. 70, no. 2, pp. 212–229, 2017.
- [12] D. M. Bers and S. Morotti, "Ca²⁺ current facilitation is camkii-dependent and has arrhythmogenic consequences," *Frontiers in Pharmacology*, vol. 5, p. 144, 2014.
- [13] J. Mustroph, L. S. Maier, and S. Wagner, "Camkii regulation of cardiac k channels," *Frontiers in Pharmacology*, vol. 5, p. 20, 2014.
- [14] A. Sierra, Z. Zhu, N. Sapay et al., "Regulation of cardiac atp-sensitive potassium channel surface expression by calcium/calmodulin-dependent protein kinase ii," *The Journal of Biological Chemistry*, vol. 288, no. 3, pp. 1568–1581, 2013.
- [15] I. Batinić-Haberle, J. S. Rebouças, and I. Spasojević, *Redox-active therapeutics*, Springer International Publishing, 2016.
- [16] I. Batinić-Haberle and M. E. Tome, "Thiol regulation by mn porphyrins, commonly known as sod mimics," *Redox Biology*, vol. 25, article 101139, 2019.
- [17] I. Batinić-Haberle, J. S. Rebouças, and I. Spasojevic, "Superoxide dismutase mimics: chemistry, pharmacology, and therapeutic potential," *Antioxidants & Redox Signaling*, vol. 13, no. 6, pp. 877–918, 2010.
- [18] I. Batinić-Haberle, A. Tovmasyan, and I. Spasojevic, "Mn porphyrin-based redox-active drugs: differential effects as cancer therapeutics and protectors of normal tissue against oxidative injury," *Antioxidants & Redox Signaling*, vol. 29, no. 16, pp. 1691–1724, 2018.
- [19] S. C. Gad, D. W. Sullivan Jr., J. D. Crapo, and C. B. Spainhour, "A nonclinical safety assessment of mnte-2-pyp, a manganese porphyrin," *International Journal of Toxicology*, vol. 32, no. 4, pp. 274–287, 2013.
- [20] I. Spasojevic, Y. Chen, T. J. Noel et al., "Pharmacokinetics of the potent redox-modulating manganese porphyrin, mnte-2-pyp⁵⁺, in plasma and major organs of b6c3f1 mice," *Free Radical Biology & Medicine*, vol. 45, no. 7, pp. 943–949, 2008.
- [21] T. Weitner, I. Kos, H. Sheng et al., "Comprehensive pharmacokinetic studies and oral bioavailability of two mn porphyrin-based sod mimics, mnte-2-pyp⁵⁺ and mntnhex-2-pyp⁵⁺," *Free Radical Biology & Medicine*, vol. 58, pp. 73–80, 2013.
- [22] I. Batinić-Haberle, I. Spasojević, P. Hambright, L. Benov, A. L. Crumbliss, and I. Fridovich, "Relationship among redox potentials, proton dissociation constants of pyrrolic nitrogens, and in vivo and in vitro superoxide dismutating activities of manganese(iii) and iron(iii) water-soluble porphyrins," *Inorganic Chemistry*, vol. 38, no. 18, pp. 4011–4022, 1999.
- [23] J. S. Rebouças, I. Spasojevic, and I. Batinić-Haberle, "Quality of potent mn porphyrin-based sod mimics and peroxynitrite scavengers for pre-clinical mechanistic/therapeutic purposes," *Journal of Pharmaceutical and Biomedical Analysis*, vol. 48, no. 3, pp. 1046–1049, 2008.
- [24] J. S. Rebouças, I. Kos, Z. Vujaskovic, and I. Batinić-Haberle, "Determination of residual manganese in mn porphyrin-based superoxide dismutase (sod) and peroxynitrite reductase mimics," *Journal of Pharmaceutical and Biomedical Analysis*, vol. 50, no. 5, pp. 1088–1091, 2009.
- [25] V. H. Pinto, D. Carvalhoda-Silva, J. L. Santos et al., "Thermal stability of the prototypical mn porphyrin-based superoxide dismutase mimic and potent oxidative-stress redox modulator mn(iii) meso-tetrakis(N-ethylpyridinium-2-yl)porphyrin chloride, mnte-2-pyp⁵⁺," *Journal of Pharmaceutical and Biomedical Analysis*, vol. 73, pp. 29–34, 2013.
- [26] I. Batinić-Haberle, L. Benov, I. Spasojevic, and I. Fridovich, "The ortho effect makes manganese(iii) meso-tetrakis(N-methylpyridinium-2-yl)porphyrin a powerful and potentially useful superoxide dismutase mimic," *Journal of Biological Chemistry*, vol. 273, no. 38, pp. 24521–24528, 1998.
- [27] I. Batinić-Haberle, I. Spasojević, R. D. Stevens et al., "New class of potent catalysts of o₂-dismutation. Mn(iii) ortho-methoxyethylpyridyl- and di-ortho-methoxyethylimidazolylporphyrins," *Dalton Transactions*, no. 11, pp. 1696–1702, 2004.
- [28] I. Batinić-Haberle, I. Spasojević, R. D. Stevens et al., "New peg-ylated mn(iii) porphyrins approaching catalytic activity of sod enzyme," *Dalton Transactions*, no. 4, pp. 617–624, 2006.
- [29] I. Batinić-Haberle, "Manganese porphyrins and related compounds as mimics of superoxide dismutase," *Methods in Enzymology*, vol. 349, pp. 223–233, 2002.
- [30] S. Guatimosim, E. A. Sobie, J. dos Santos Cruz, L. A. Martin, and W. J. Lederer, "Molecular identification of a ttx-sensitive Ca²⁺ current," *American Journal of Physiology-Cell Physiology*, vol. 280, no. 5, pp. C1327–C1339, 2001.
- [31] F. A. Oliveira, S. Guatimosim, C. H. Castro et al., "Abolition of reperfusion-induced arrhythmias in hearts from thiamine-deficient rats," *American Journal of Physiology-Heart and Circulatory Physiology*, vol. 293, no. 1, pp. H394–H401, 2007.
- [32] A. Lara, D. D. Damasceno, R. Pires et al., "Dysautonomia due to reduced cholinergic neurotransmission causes cardiac remodeling and heart failure," *Molecular and Cellular Biology*, vol. 30, no. 7, pp. 1746–1756, 2010.
- [33] A. N. S. Gondim, A. Lara, A. Santos-Miranda et al., "(-)-Terpinen-4-ol changes intracellular Ca²⁺ handling and induces pacing disturbance in rat hearts," *European Journal of Pharmacology*, vol. 807, pp. 56–63, 2017.
- [34] D. Roman-Campos, H. L. L. Duarte, P. A. Sales Jr. et al., "Changes in cellular contractility and cytokines profile during *trypanosoma cruzi* infection in mice," *Basic Research in Cardiology*, vol. 104, no. 3, pp. 238–246, 2009.
- [35] G. Zhou, S. Chen, G. Chen et al., "Procedural arrhythmia termination and long-term single-procedure clinical outcome in patients with non-paroxysmal atrial fibrillation," *Journal of Cardiovascular Electrophysiology*, vol. 24, no. 10, pp. 1092–1100, 2013.
- [36] M. J. Curtis and M. J. Walker, "Quantification of arrhythmias using scoring systems: an examination of seven scores in an in vivo model of regional myocardial ischaemia," *Cardiovascular Research*, vol. 22, no. 9, pp. 656–665, 1988.

- [37] B. Gauter-Fleckenstein, K. Fleckenstein, K. Owzar, C. Jiang, I. Batinic-Haberle, and Z. Vujaskovic, "Comparison of two mn porphyrin-based mimics of superoxide dismutase in pulmonary radioprotection," *Free Radical Biology and Medicine*, vol. 44, no. 6, pp. 982–989, 2008.
- [38] B. Gauter-Fleckenstein, K. Fleckenstein, K. Owzar et al., "Early and late administration of mnte-2-pyp⁵⁺ in mitigation and treatment of radiation-induced lung damage," *Free Radical Biology and Medicine*, vol. 48, no. 8, pp. 1034–1043, 2010.
- [39] J. B. Bartholomeu, A. S. Vanzelli, N. P. Rolim et al., "Intracellular mechanisms of specific β -adrenoceptor antagonists involved in improved cardiac function and survival in a genetic model of heart failure," *Journal of Molecular and Cellular Cardiology*, vol. 45, no. 2, pp. 240–249, 2008.
- [40] T. F. Lüscher, "Progress in the management of arrhythmias: risk scores, ablation, and anticoagulation," *European Heart Journal*, vol. 39, no. 6, pp. 421–424, 2018.
- [41] R. Rosso, J. M. Kalman, O. Rogowski et al., "Calcium channel blockers and beta-blockers versus beta-blockers alone for preventing exercise-induced arrhythmias in catecholaminergic polymorphic ventricular tachycardia," *Heart Rhythm*, vol. 4, no. 9, pp. 1149–1154, 2007.
- [42] P. W. M. de Almeida, R. de Freitas Lima, E. R. de Moraes Gomes et al., "Functional cross-talk between aldosterone and angiotensin-(1-7) in ventricular myocytes," *Hypertension*, vol. 61, no. 2, pp. 425–430, 2013.
- [43] C. W. Yancy, M. Jessup, B. Bozkurt et al., "2013 ACCF/AHA guideline for the management of heart failure," *Circulation*, vol. 128, no. 16, pp. e240–e327, 2013.
- [44] B. He, A. Shiau, K. Y. Choi, H. Zalkin, and J. M. Smith, "Genes of the *Escherichia coli* pur regulon are negatively controlled by a repressor-operator interaction," *Journal of Bacteriology*, vol. 172, no. 8, pp. 4555–4562, 1990.
- [45] R. E. Goldstein, S. J. Boccuzzi, D. Cruess, and S. Nattel, "Diltiazem increases late-onset congestive heart failure in postinfarction patients with early reduction in ejection fraction. The adverse experience committee; and the multicenter diltiazem postinfarction research group," *Circulation*, vol. 83, no. 1, pp. 52–60, 1991.
- [46] The Multicenter Diltiazem Postinfarction Trial Research Group, "The effect of diltiazem on mortality and reinfarction after myocardial infarction," *New England Journal of Medicine*, vol. 319, no. 7, pp. 385–392, 1988.
- [47] H. R. Figulla, F. Gietzen, U. Zeymer et al., "Diltiazem improves cardiac function and exercise capacity in patients with idiopathic dilated cardiomyopathy. Results of the diltiazem in dilated cardiomyopathy trial," *Circulation*, vol. 94, no. 3, pp. 346–352, 1996.
- [48] U. Elkayam, J. Amin, A. Mehra, J. Vasquez, L. Weber, and S. H. Rahimtoola, "A prospective, randomized, double-blind, cross-over study to compare the efficacy and safety of chronic nifedipine therapy with that of isosorbide dinitrate and their combination in the treatment of chronic congestive heart failure," *Circulation*, vol. 82, no. 6, pp. 1954–1961, 1990.
- [49] M. Packer, C. M. O'Connor, J. K. Ghali et al., "Effect of amlodipine on morbidity and mortality in severe chronic heart failure. Prospective randomized amlodipine survival evaluation study group," *New England Journal of Medicine*, vol. 335, no. 15, pp. 1107–1114, 1996.
- [50] J. N. Cohn, S. Ziesche, R. Smith et al., "Effect of the calcium antagonist felodipine as supplementary vasodilator therapy in patients with chronic heart failure treated with enalapril: V-heft iii. Vasodilator-heart failure trial (v-heft) study group," *Circulation*, vol. 96, no. 3, pp. 856–863, 1997.
- [51] J. E. Udelson, C. A. DeAbate, M. Berk et al., "Effects of amlodipine on exercise tolerance, quality of life, and left ventricular function in patients with heart failure from left ventricular systolic dysfunction," *American Heart Journal*, vol. 139, no. 3, pp. 503–510, 2000.
- [52] S. Thackray, K. Witte, A. L. Clark, and J. G. Cleland, "Clinical trials update: Optime-CHF, Praise-2, All-Hat," *European Journal of Heart Failure*, vol. 2, no. 2, pp. 209–212, 2000.
- [53] W. A. Littler and D. J. Sheridan, "Placebo controlled trial of felodipine in patients with mild to moderate heart failure. UK study group," *Heart*, vol. 73, no. 5, pp. 428–433, 1995.
- [54] A. S. Vanzelli, A. Medeiros, N. Rolim et al., "Integrative effect of carvedilol and aerobic exercise training therapies on improving cardiac contractility and remodeling in heart failure mice," *PLoS One*, vol. 8, no. 5, article e62452, 2013.
- [55] W. Anselmo, E. Branchetti, J. B. Grau et al., "Porphyrin-Based SOD Mimic MnTnBuOE-2-PyP⁵⁺ inhibits mechanisms of aortic valve remodeling in human and murine models of aortic valve sclerosis," *Journal of the American Heart Association*, vol. 7, no. 20, article e007861, 2018.

Research Article

Semicarbazide-Sensitive Amine Oxidase Increases in Calcific Aortic Valve Stenosis and Contributes to Valvular Interstitial Cell Calcification

Nathalie Mercier,^{1,2} Sven-Christian Pawelzik,^{3,4} John Pirault,^{1,2} Miguel Carracedo,^{3,4} Oscar Persson,^{3,4} Bastien Wollensack,^{1,2} Anders Franco-Cereceda,^{4,5} and Magnus Bäck^{1,2,3,4} 

¹Inserm UMR_S 1116, Vandoeuvre-Lès-Nancy, France

²Université de Lorraine, Vandoeuvre-Lès-Nancy, France

³Translational Cardiology, Department of Medicine, Solna, Karolinska Institutet, Stockholm, Sweden

⁴Theme Heart and Vessels, Division of Valvular and Coronary Disease, Karolinska University Hospital, Stockholm, Sweden

⁵Department of Molecular Medicine and Surgery, Karolinska Institutet, Stockholm, Sweden

Correspondence should be addressed to Magnus Bäck; magnus.back@ki.se

Received 12 July 2019; Revised 21 October 2019; Accepted 26 November 2019; Published 14 January 2020

Guest Editor: Aneta Radziwon-Balicka

Copyright © 2020 Nathalie Mercier et al. This is an open access article distributed under the Creative Commons Attribution License, which permits unrestricted use, distribution, and reproduction in any medium, provided the original work is properly cited.

Introduction. Calcific aortic valve stenosis (CAVS) is a common disease associated with aging. Oxidative stress participates in the valve calcification process in CAVS. Semicarbazide-sensitive amine oxidase (SSAO), also referred to as vascular adhesion protein 1 (VAP-1), transforms primary amines into aldehydes, generating hydrogen peroxide and ammonia. SSAO is expressed in calcified aortic valves, but its role in valve calcification has remained largely unexplored. The aims of this study were to characterize the expression and the activity of SSAO during aortic valve calcification and to establish the effects of SSAO inhibition on human valvular interstitial cell (VIC) calcification. **Methods.** Human aortic valves from $n = 80$ patients were used for mRNA extraction and expression analysis, Western blot, SSAO activity determination, immunohistochemistry, and the isolation of primary VIC cultures. **Results.** SSAO mRNA, protein, and activity were increased with increasing calcification within human aortic valves and localized in the vicinity of the calcified zones. The valvular SSAO upregulation was consistent after stratification of the subjects according to cardiovascular and CAVS risk factors associated with increased oxidative stress: body mass index, diabetes, and smoking. SSAO mRNA levels were significantly associated with poly(ADP-ribose) polymerase 1 (PARP1) in calcified tissue. Calcification of VIC was inhibited in the presence of the specific SSAO inhibitor LJP1586. **Conclusion.** The association of SSAO expression and activity with valvular calcification and oxidative stress as well as the decreased VIC calcification by SSAO inhibition points to SSAO as a possible marker and therapeutic target to be further explored in CAVS.

1. Introduction

Calcification of the aortic valve can evolve into calcific aortic valve stenosis (CAVS), which, if untreated, leads to heart failure. In the absence of a medical treatment, current options for severe symptomatic CAVS are limited to surgical or catheter-based prosthetic valve implantation. Oxidative

stress could be one potential mechanism that increases valve calcification and CAVS disease burden [1, 2]. Valvular oxidative stress predominates around calcifying foci and enhances progression of CAVS. Acute H₂O₂-induced oxidative stress and the resulting higher reactive oxygen species (ROS) levels induce osteoblastic differentiation of human valvular interstitial cells (VIC), which are the main structural cells of the

aortic valve [3]. These processes highly resemble those observed in atherosclerosis, in which, for example, vascular peroxidase 1, an enzyme generating H_2O_2 , has been implicated in Ox-LDL-induced calcification of vascular smooth muscle cells [4].

Although the endogenous substrate is unknown, semicarbazide-sensitive amine oxidase (SSAO), also known as vascular adhesion protein-1 (VAP-1), is a mediator of tissue oxidative stress and a contributor to atherosclerotic plaque development [5]. The SSAO enzyme generates aldehydes, hydrogen peroxide (H_2O_2), and ammonia (NH_3) from primary amines or amine groups within proteins. SSAO expression has been detected in human aortic valves, with significant upregulation in CAVS compared with noncalcified valves [6]. Furthermore, serum levels of SSAO are higher in patients with severe CAVS compared with patients presenting moderate CAVS and are significantly correlated with CAVS severity as assessed by echocardiography [7]. SSAO has been implicated in the differentiation of several cell types, such as chondrocytes and adipocytes [8–10], but its effects on VIC have not previously been investigated.

SSAO serves as a cardiovascular risk factor in particular for obese patients [11]. SSAO predicts an increased 9-year absolute risk of major cardiovascular events and cardiovascular mortality in subjects aged >50 years. Moreover, serum SSAO activity increases in types I and II diabetic patients compared with a nondiabetic control group [12]. Also, nicotine-enhanced oxidative stress through SSAO has been reported to contribute to the adverse effects of smoking [13]. Since obesity, diabetes, and smoking are also major risk factors for the incidence of CAVS [14–16], SSAO emerges as a common risk factor for atherosclerotic vascular disease and CAVS.

Taken together, the above observations converge to the hypothesis that oxidative stress through SSAO could be implicated in CAVS and could represent a novel target to develop anticalcification therapies. The aims of the present study were therefore (1) to determine the SSAO expression and activity in relation to the degree of calcification in human aortic valves, (2) to establish whether cardiovascular risk factors affect SSAO upregulation during valve calcification, and (3) to identify potential correlations between SSAO and other oxidative stress pathways. Finally, we aimed (4) to determine the role of SSAO in valve calcification by evaluating the potential of SSAO inhibition to inhibit human VIC calcification.

2. Material and Methods

2.1. Human Aortic Valves. Human aortic valves were obtained from 80 patients undergoing aortic valve replacement surgery at the Karolinska University Hospital in Stockholm, Sweden. The study was approved by the local ethics committee (2012/1633), and all patients gave informed consent.

2.2. Sample Collection and Macroscopic Dissection. Immediately after surgical removal, the valves were immersed in either RNA Later (Qiagen) and stored at 4°C until transport to the laboratory. For Western blot and SSAO activity determinations, valves were collected in phenol red-free DMEM

supplemented with 10% fetal bovine serum (FBS), dissected, and stored at -80°C. Adjacent pieces were embedded in paraffin for histological analysis. Macroscopic dissection was performed dividing each valve into healthy, thickened, or calcified regions as previously described [17–19].

2.3. Valve mRNA Expression. Total RNA from aortic valves was isolated using the RNeasy Lipid Tissue Mini kit (Qiagen, Hilden, Germany). Quantification and the quality of RNA were assessed using a NanoDrop (Thermo Scientific, Waltham, MA, USA) and a 2100 Bioanalyzer (Agilent, Santa Clara, CA, USA), respectively. Valve gene expression data was obtained using Gene Chip Affymetrix human transcriptome 2.0 (HTA 2.0 arrays, Santa Clara, CA, USA) and normalized with a signal space transformation-robust multi-chip analysis (SST-RMA) using Expression Console (Affymetrix, Santa Clara, CA, USA) [18].

2.4. Western Blot and SSAO Activity Homogenates. Tissue specimens of human aortic valves were weighed and crushed in liquid nitrogen using a BioPulverizer (Biospec). The samples were suspended in 20 μ l of 1 mM NaH_2PO_4/Na_2HPO_4 , pH 7.4 (NaPi buffer) containing 250 mM sucrose per mg of tissue. The tissue homogenates were centrifuged at 600xg for 5 minutes at 4°C, and the supernatants were stored at -80°C until use. The protein concentration was determined using DC Protein Assay (Bio-Rad, Bovine Gamma Globulin, S60) according to the manufacturer's protocol. Absorbance was read at 750 nm with FLUOstar® OPTIMA (BMG) 413-0149.

2.5. SSAO Activity. SSAO activity was analyzed by measurement of H_2O_2 production by a fluorimetric method adapted from Matsumoto et al. [20], using benzylamine as a substrate. Tissue homogenates (20 μ g of protein/well) were preincubated in duplicate in the absence or presence of the SSAO inhibitor semicarbazide (250 μ M, Sigma) for 15 minutes at 37°C in a total reaction volume of 50 μ l containing 40 mM NaPi buffer, 1 mM pargyline (Sigma), 1 IU/ml HRP, and 80 nM Amplex Red (Molecular Probes). Then, the SSAO substrate benzylamine (500 μ M, Sigma) was added. Incubation was carried out for 1 h at 37°C. H_2O_2 was used as the standard curve to determine the quantity generated in each condition. The fluorescence intensity was measured with a FLUOstar OPTIMA (413-0149) fluorescence microplate reader using excitation at 563 nm and fluorescence detection at 587 nm. To get the SSAO specific activity, the quantity of hydrogen peroxide detected with benzylamine in the presence of semicarbazide was subtracted from the hydrogen peroxide generated from the benzylamine in the absence of semicarbazide.

2.6. Western Blot. Tissue homogenates (10 μ g) were denatured in loading buffer (Laemmli Sample Buffer, BioRad) for 5 min at 95°C and loaded on an acrylamide SDS/PAGE gel (Bio-Rad) in a Mini-PROTEAN Tetra Cell (Bio-Rad). Resolved protein was subsequently transferred to a nitrocellulose membrane (Bio-Rad) with a Mini Trans-Blot Module. The membranes were blocked for 1 h at room temperature (RT) in 0.1% Tween 20 in TBS buffer (10 mM Tris-Base and 15 mM NaCl, pH 7.5) containing 5% nonfat dry milk and incubated with primary antibodies (rabbit anti-SSAO,

clone H43, and anti β -actin, Santa Cruz Biotechnology, Dallas, TX, USA) in blocking solution. After several washes, the membrane was incubated with an appropriate horseradish peroxidase- (HRP-) coupled secondary antibody (anti-mouse or anti-rabbit IgG, GE Healthcare, Chicago, IL, USA) in blocking solution for 1 h at RT. Following washes, the protein bands were visualized using the Chemiluminescence Kit (Immun-Star™ WesternC™ Chemiluminescence Kit, Bio-Rad) on a Fujifilm Luminescent Image Analyzer LAS4000 system. The image analysis was performed with the Multi Gauge v3.0 program.

2.7. Histology and Immunohistochemistry. Aortic valve sections derived from 4 patients were deparaffinized in toluene, hydrated in ethanol at decreasing concentrations (100%, 95%, and 50%), and rinsed in distilled water before histochemical detection of calcification using alizarin red. For immunohistochemistry, deparaffinized sections were incubated in TBS-T 0.05%/3% H₂O₂ to block endogenous peroxidases. Nonspecific sites were blocked in TBS-T 0.05%/5% BSA (bovine serum albumin). The sections were then incubated with a primary anti-SSAO antibody (H-43, Santa Cruz Biotechnology, sc-28642) overnight at 4°C. After several washes in TBS-T 0.05%, sections were incubated with biotinylated donkey anti-rabbit secondary antibody (Jackson ImmunoResearch) for one hour at RT, followed by Streptavidin/HRP solution (Thermo Fisher Scientific, Waltham, MA, USA) for 10 min and DAB (3,3'-diaminobenzidine) (Vector Laboratories, SK-4100). Finally, some of the sections were counter-stained with haematoxylin (Vector Laboratories, H-3404) for one min and observed under an Eclipse Ci-S, 403116 microscope (Nikon).

2.8. VIC Isolation. Human aortic valves from $n = 9$ patients were digested for 16 h using an enzymatic cocktail containing collagenase I and dispase II as previously described [18]. Isolated VIC were seeded onto polystyrene tissue culture containers and cultured in DMEM supplemented with 10% FBS, 100 units/ml penicillin, 100 μ g/ml streptomycin, 1 mM sodium pyruvate, 10 mM HEPES, and 2 mM L-glutamine. Culture medium was changed every other day. Cells were used for experiments between passages 1 and 3. Cell culture reagents were purchased from Gibco, plastics were from Corning as previously described [18].

2.9. VIC Calcification. For measurement of *in vitro* calcification, VIC were seeded in a 96-well plate and incubated with standard medium or osteogenic medium containing 2.8 mM inorganic phosphate (Pi). Cells were treated with the specific SSAO inhibitor LJP1586 (1 μ M). Medium was changed every other day for eight to nine days. At the last medium change, 10 nM IRDye 800CW BoneTag Optical Probe (LI-COR, Bad Homburg, Germany) was added to all media, and VIC were incubated for another 24 h. Cells were washed three times with PBS, the plate was subsequently scanned on an Odyssey CLx near-infrared (NIR) fluorescence imager, and the obtained images were quantified using Image Studio Software Version 5.2 (LI-COR, Bad Homburg, Germany).

2.10. VIC TaqMan Real-Time PCR. Reverse transcription of mRNA isolated from VIC was performed using the High Capacity RNA-to-cDNA Kit (Thermo Fisher Scientific, Waltham, MA, USA) as previously described [21]. Quantitative real-time PCR was performed on a Quant7 Fast Real-Time PCR system (Thermo Fisher Scientific, Waltham, MA, USA) using TaqMan Assay-on-Demand Hs00907290_m1 (Thermo Fisher Scientific, Waltham, MA, USA) for SSAO. The relative mRNA expression of the target gene was quantified by the Δ Ct method using TaqMan Assay-on-Demand Hs99999905_m1 for GAPDH as endogenous control.

2.11. Statistical Analysis. Results are expressed as mean \pm SD. Statistical significance was assessed with one- or two-way ANOVA for repeated measurements followed by Holm-Sidak post hoc test for multiple comparisons. For comparisons of SSAO mRNA levels between different subgroups after stratification according to BMI, diabetes, and smoking, a two-way ANOVA was used taking into consideration the stratification groups and type of tissue (healthy, intermediate, and calcified tissue). Correlations were established using Spearman's correlations. Statistical significance was assigned at $P < 0.05$. To correct univariate analyses for multiple testing, we imposed a Bonferroni-corrected significance threshold of 0.007 (i.e., 0.05/7 univariate analyses). Statistical analyses were performed using SigmaPlot 12.5 (Systat Software Inc., USA).

3. Results

3.1. SSAO Expression, Activity, and Localization in Human Valves. The levels of SSAO mRNA from human aortic valves derived from $n = 55$ patients with CAVS are shown in Figure 1(a). The SSAO mRNA expression was significantly and gradually upregulated in intermediately and fully calcified parts compared with healthy parts of the aortic valves (Figure 1(a)). SSAO protein levels measured in valves from $n = 7$ CAVS patients followed the same pattern of expression (Figure 1(b)). SSAO activity was significantly increased in calcified parts of $n = 9$ human aortic valves (Figure 1(c)). Immunohistochemical analysis revealed SSAO staining in valves derived from $n = 4$ CAVS patients (Figure 1(d)), with the most prominent signal in proximity to the alizarin red-stained calcified valves areas (Figure 1(e), left panels).

3.2. Valvular SSAO mRNA Expression in Relation to Obesity, Diabetes, and Smoking. Out of the $n = 55$ CAVS patients donating aortic valves for mRNA determinations, 9 patients were of normal weight (BMI: 18.5-25 kg/m²), 33 patients were overweight (BMI: 25-30 kg/m²), and 13 were obese (BMI: >30 kg/m²). Fourteen patients had type 2 diabetes and none had type 1 diabetes. There was one current smoker, 29 patients were former smokers, and 25 patients had never smoked. Stratification of patients based on BMI (Figure 2(a)), prevalent type 2 diabetes (Figure 2(b)), and smoking (Figure 2(c)) revealed that while the significant changes for the type of tissue (healthy, intermediate, and calcified tissue) were retained, no statistically significant differences in SSAO expression were detected between the different subgroups.

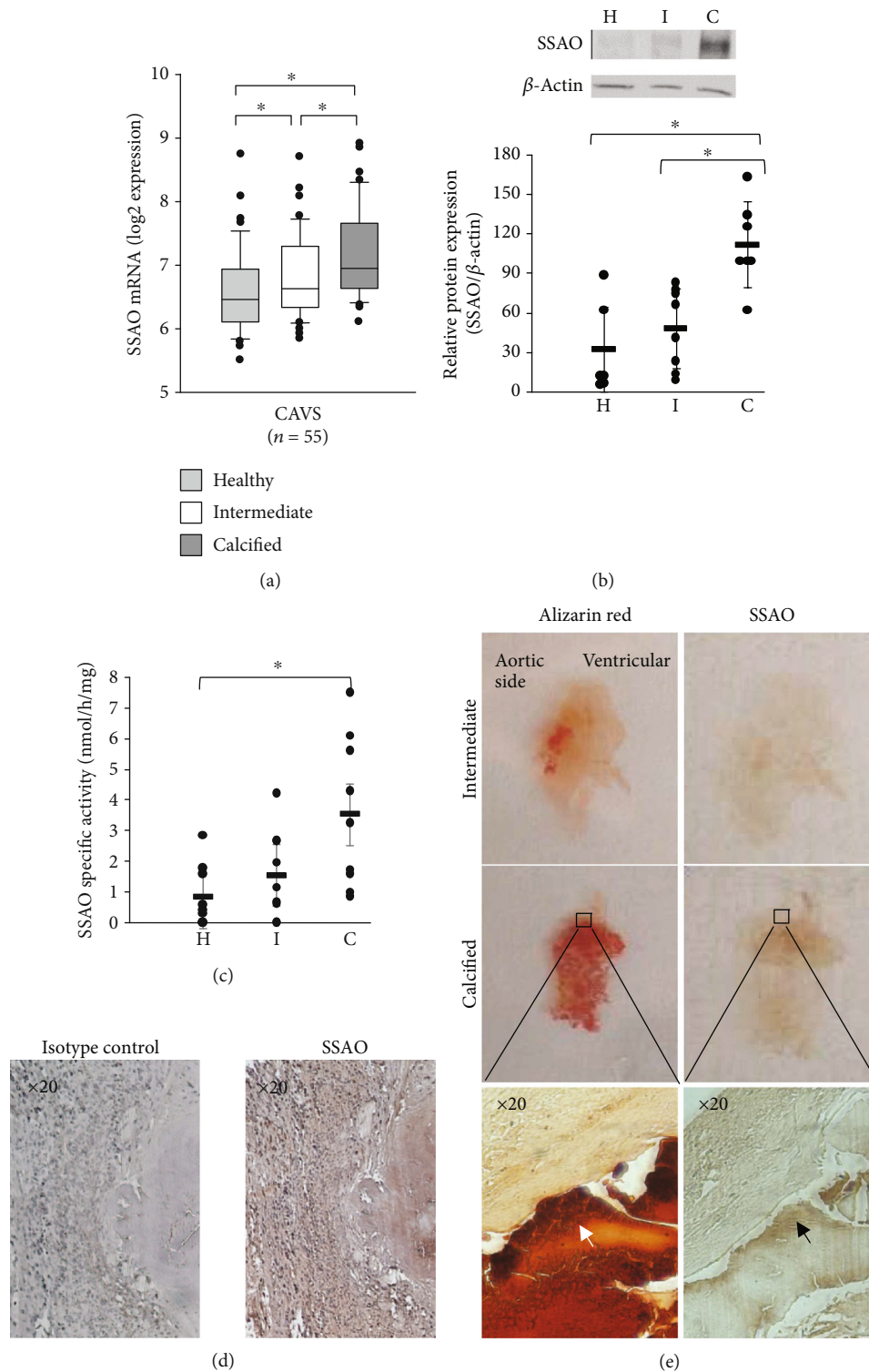


FIGURE 1: Expression and activity of SSAO are increased in calcified areas of human aortic valves. (a) SSAO mRNA expression in 55 human aortic valves derived from patients with CAVS was significantly increased in intermediate (I) and calcified (C) areas compared to healthy (H) valve tissue. (b) SSAO protein expression analysed by Western blot and quantified for $n = 5 - 7$ samples in each group. (c) Specific SSAO activity ($n = 9$) significantly increased in calcified (C) valve tissue. Data are presented as the mean \pm SD. * $P < 0.05$ versus healthy valves. (d) Immunohistochemical stainings of SSAO in human aortic valves compared with isotype control (representative of $n = 4$). (e) Histological alizarin red (left panels) and SSAO immunohistochemical stainings (right panels) in an intermediate and in a highly calcified aortic valve showing high expression of SSAO in the proximity of calcified zones. The four upper panels present one entire cusp of an aortic valve and the lower panels show micrographs with a 20x magnification.

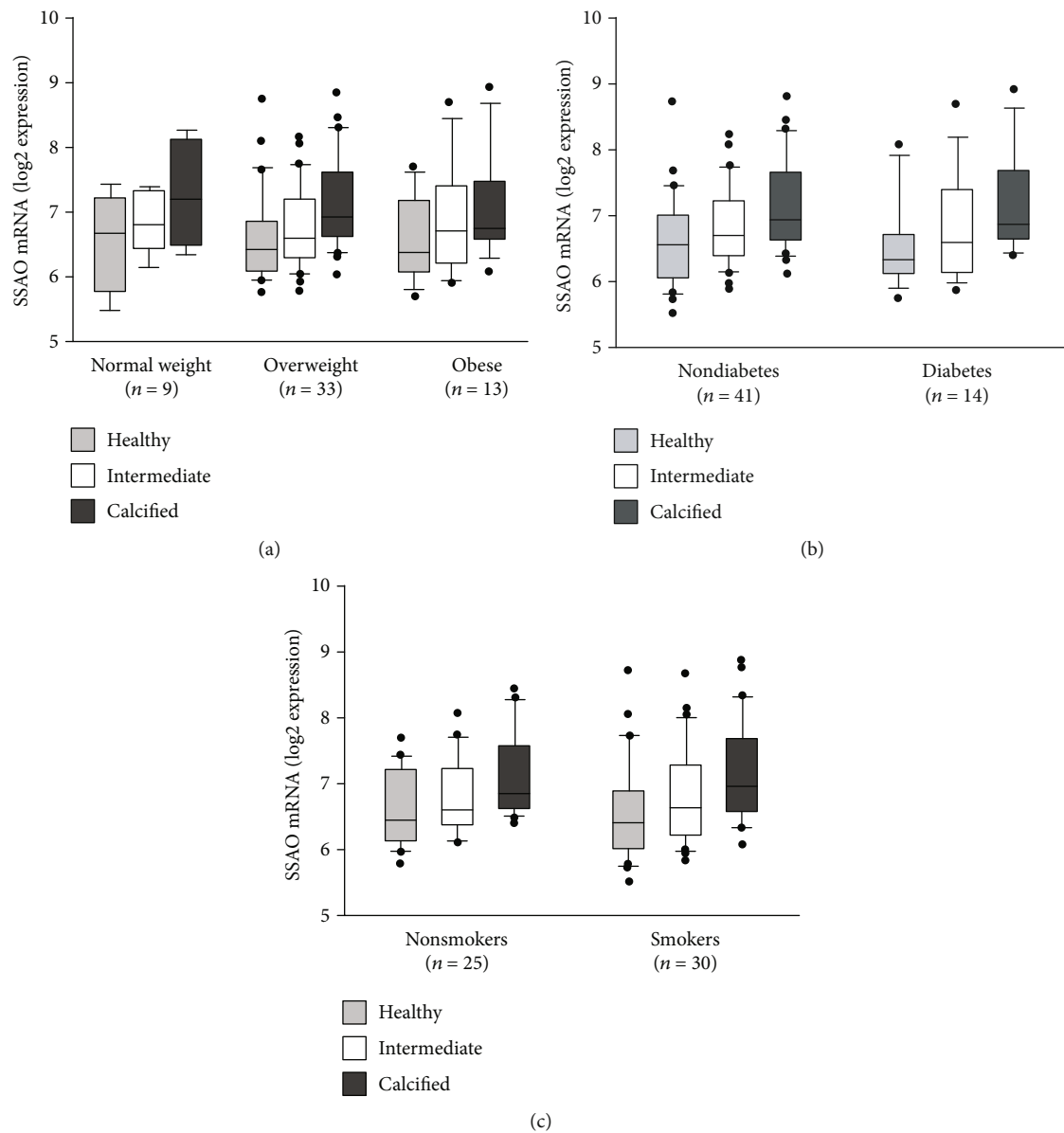


FIGURE 2: SSAO expression after stratification according to oxidative stress-associated risk factors for CAVS. SSAO mRNA expression levels in healthy, intermediate, and calcified aortic valve tissue. (a) Stratification according to body mass index (BMI): normal weight (BMI < 25), overweight (BMI: 25–30), and obese (BMI > 30). (b) Stratification according to the prevalence of type 2 diabetes mellitus. (c) Stratification according to smoking (nonsmokers versus current and former smokers). While the significant changes were retained for the type of tissue (healthy, intermediate, and calcified aortic valve tissue), no significant differences were detected between the different strata (two-way ANOVA).

3.3. SSAO Expression in Relation to Pathways of Oxidative Stress. Correlation analysis of SSAO mRNA expression with other pathways associated with oxidative stress was performed in $n = 64$ human aortic valves with different degrees of calcification derived from patients with CAVS ($n = 55$) and aortic valve regurgitation ($n = 9$). Although the univariate analyses indicated significant correlations for SSAO with soluble serine hydroxymethyltransferase 1 (SHMT1) as well as with superoxide dismutases 2 and 3 (SOD2 and 3) in healthy tissue, none of these correlations were statistically significant after correction for multiple comparisons (Table 1, top row). However, correlations for SSAO with

cytochrome b-245, alpha polypeptide (CYBA), and SOD3 achieved the Bonferroni-corrected statistical significance threshold ($P < 0.007$) in intermediate tissue (Table 1, middle row). Those correlations were, however, not statistically significant in calcified tissue. In contrast, SSAO significantly correlated with poly(ADP-ribose) polymerase 1 (PARP1) in calcified tissue (Table 1, bottom row).

3.4. Effect of SSAO Inhibition on VIC Calcification In Vitro. Primary cultures of VIC isolated from aortic valves from $n = 6$ CAVS patients expressed SSAO mRNA after 48 h of culture in the absence ($\Delta Ct_{\text{control}} = 15.9 \pm 1.45$) and presence

TABLE 1: Spearman correlations (Rho) for SSAO mRNA with mRNA levels of poly(ADP-ribose) polymerase 1 (PARP1), soluble serine hydroxymethyltransferase 1 (SHMT1), NADPH oxidase 4 (NOX4), cytochrome b-245, alpha polypeptide (CYBA), and superoxide dismutases (SOD) 1-3 in healthy, intermediate, and calcified tissue from human aortic valves. Bonferroni-corrected significance threshold is 0.007.

Healthy	PARP1	SHMT1	NOX4	CYBA	SOD1	SOD2	SOD3
Rho	0.045	0.32	-0.059	0.052	-0.11	0.28	0.33
P	0.722	0.011	0.642	0.682	0.399	0.027	0.0075
N	64	64	64	64	64	64	64
Intermediate	PARP1	SHMT1	NOX4	CYBA	SOD1	SOD2	SOD3
Rho	0.26	0.27	0.20	0.41	0.042	0.26	0.34
P	0.036	0.031	0.12	0.00096	0.74	0.043	0.0064
N	64	64	64	64	64	64	64
Calcified	PARP1	SHMT1	NOX4	CYBA	SOD1	SOD2	SOD3
Rho	0.37	-0.17	-0.075	0.21	-0.21	0.055	-0.11
P	0.0031	0.18	0.56	0.099	0.093	0.67	0.38
N	64	64	64	64	64	64	64

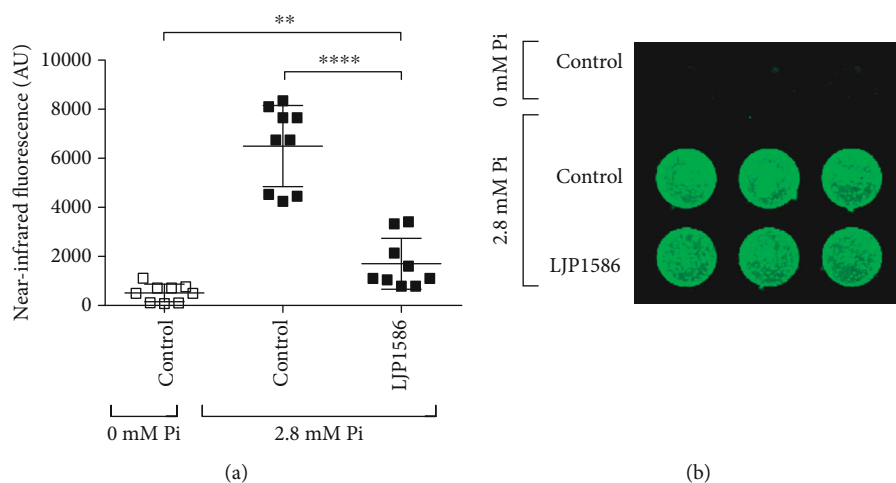


FIGURE 3: SSAO inhibition decreases calcification of human aortic valve interstitial cells. Valvular interstitial cells from aortic valves derived from $n = 9$ patients were cultured in the absence and presence of 2.8 mM inorganic phosphate (Pi). (a) The SSAO inhibitor LJP1586 ($1 \mu\text{M}$) significantly inhibited calcification, measured as near-infrared fluorescence and quantified using Image Studio software. $**P < 0.005$; $****P < 0.0001$. (b) Valvular interstitial cells from one patient are exemplarily shown.

($\Delta\text{Ct}_{\text{osteogenic}} = 16.3 \pm 1.34$) of a high concentration of phosphate (2.8 mM) in the growth medium. Furthermore, SSAO activity was detected in VIC cultured under both conditions, and VIC SSAO activity was inhibited by 70% by the specific SSAO inhibitor LJP1586 ($1 \mu\text{M}$). When VIC isolated from $n = 9$ CAVS patients were cultured under high phosphate conditions, calcification was significantly decreased by LJP1586 ($1 \mu\text{M}$; Figure 3).

4. Discussion

This is the first report showing a gradual and significant increase in SSAO mRNA, protein, and activity in human aortic valves, which were divided into healthy, intermediate, and calcified tissue. The SSAO upregulation with valve calcification was independent of the cardiovascular and CAVS risk factors: obe-

sity, diabetes, and smoking. Furthermore, a significant correlation of SSAO expression with pathways of oxidative stress was also revealed, with, in particular, a significant correlation with PARP1 in calcified tissue. Finally, we demonstrate that inhibition of SSAO activity decreased VIC calcification *in vitro*. Taken together, these results indicate a link between SSAO, oxidative stress, and aortic valve calcification and point to SSAO inhibition as a putative therapeutic approach to be explored for the prevention of valve calcification and CAVS progression.

A gradual upregulation of SSAO with the progression of aortic valve calcification is supported by the observational data on valvular mRNA expression in the present study. This was confirmed for protein expression by Western blot, which exhibited a similar pattern with significantly higher levels in calcified parts. Also, immunohistochemical analysis supported a localization of SSAO expression in proximity to

calcified regions of the aortic valve tissue. The latter findings confirm previous results that have detected SSAO being upregulated in calcified stenotic aortic valves [6]. Moreover, our results extend the observation to show also increased SSAO activity in calcified valve tissue. We show that SSAO is present and functional in healthy areas of CAVS valves. The mean specific SSAO activity was approximately 800 pmol/h/mg, which is around 3 to 4 times higher compared with cartilage from human femoral knee joints [9]. Furthermore, we show that calcified parts of human aortic valves exhibited a 5.7 times higher SSAO activity compared to healthy parts of the same valves, supporting that SSAO mRNA and activity increase as the CAVS disease progresses. Indeed, a strong increase in SSAO expression and activity has also been described in other disease states, such as osteoarthritis human knee joints [9].

When expressed and active in a tissue, SSAO generates H_2O_2 and hence contributes to the local oxidative stress. SSAO is also increased in several disease states associated with an increased systemic oxidative stress. Interestingly, obesity [11, 14, 22], diabetes [12, 15], and smoking [16, 23] are all examples of cardiovascular risk factors associated with both increased SSAO expression and an increased risk of incident CAVS. In the present study, we did, however, not detect any significant changes in the pattern of valvular SSAO mRNA expression after stratification according to BMI, prevalent diabetes, or smoking status, suggesting that the observed upregulation of SSAO mRNA with calcification was not affected by systemic states of increased oxidative stress.

SSAO is also related to other pathways of oxidative stress [24–26]. In the present study, we show that the correlations of SSAO with oxidative stress pathways vary at different disease stages. Whereas no significant correlations were revealed in healthy valve tissue, we identify CYBA and SOD3 mRNA levels as being significantly correlated with SSAO mRNA in intermediate stages of valve calcification. CYBA, also known as p22phox, is an essential component of superoxide generating NADPH oxidase (Nox) complex and is increased in osteoblasts around calcifying foci [27]. The lack of correlation for SSAO with Nox4 in the present study supports a differential regulation of Nox subunits in calcification processes [27]. Surprisingly, SSAO was significantly associated with SOD3 in intermediate but not calcified valve tissue, which may represent a defense mechanism. SOD3 and catalase are downregulated with aortic valve calcification and in CAVS [28]. Indeed, SOD3 and catalase adenoviral transfection to VIC reestablishes an impaired DNA damage response and reduces early markers of VIC activation [28]. SOD3 dismutation hence requires concomitant catalase to degrade H_2O_2 for a full antioxidative effect. Inhibiting additional H_2O_2 generation by SSAO may potentially serve to limit oxidative stress in CAVS. Importantly, SSAO exhibited a significant correlation only with PARP1 in calcified valve tissue. PARP1 is a nuclear enzyme activated by DNA strand breakage and oxidative stress. Interestingly, PARP1 correlates with disease severity in CAVS and is induced by proinflammatory stimulation of human VIC [29]. PARP1 may directly participate in soft tissue calcification by means of releasing extracellular poly(ADP-ribose) in response to oxidative and/or DNA damage [30].

The addition of H_2O_2 in the Pi-induced calcification model further increased calcium deposition *in vitro*, and VIC derived from calcified valves were more susceptible to oxidative stress compared with VIC from healthy valves [3]. Oxidative stress also induces the expression of Runx2, a transcriptional factor of osteoblasts [27], expressed by VIC under osteogenic conditions [31]. To determine the mechanisms behind the observed associations of SSAO expression with valve calcification, we finally show SSAO mRNA expression and activity in VIC and that inhibition of SSAO by LJP1586 decreased calcification of VIC *in vitro*. These findings are in line with studies of SSAO expression in chondrocytes, in which the hypertrophic differentiation is delayed by LJP1586, a response that is accompanied by lower expression of calcification markers such as alkaline phosphatase, osteopontin, and MMP9. These findings suggest that inhibiting SSAO in valves may slow down the mineralization process.

Some limitations of the present study must be acknowledged. The observational data on SSAO expression in human aortic valves cannot determine the causal relation of the findings. We can also not rule out that correlation of SSAO with PARP1 and other markers of oxidative stress are not dependent on unknown covariates. Finally, we cannot exclude that the expression of SSAO by other cell types in the aortic valve, such as endothelial cells and dendritic cells [32], may contribute to disease progression.

5. Conclusion

This work provides evidence that, in addition to being a possible disease marker, SSAO could be implicated in the mechanism of valve calcification. This could offer a new therapeutic perspective for CAVS.

Data Availability

The data used to support the findings of this study are included within the article.

Conflicts of Interest

The authors declare that there are no conflicts of interest regarding the publication of this paper.

Acknowledgments

Magnus Bäck is an awardee of a Gutenberg Chair of Excellence from the Région Grand Est and the Eurométropole de Strasbourg. This research was further funded by the AGing Innovation & Research (AGIR) Program on Normal and Pathological Aging in partnership with the University Hospital of Nancy, the University of Lorraine, the Lorraine Region (through the operational program FEDER-FSE Lorraine et Massif des Vosges 2014-2020), and the Urban Community of Nancy. SCP is supported by the Professor Nanna Svartz Foundation. MB is supported by the Swedish Research Council (Grant number 2019-01486), the Swedish Heart-Lung Foundation (grant number 20180571), King Gustaf V and Queen Victoria Freemason Foundation, the Stockholm

County Council (grant number 20170365), and Marianne and Marcus Wallenberg Foundation (grant number 2015.0104). AFC is supported by a donation from Mr. Fredrik Lundberg. We thank Professor Sirpa Jalkanen for the generous gift of LJP1586.

References

- [1] J. D. Miller, Y. Chu, R. M. Brooks, W. E. Richenbacher, R. Pena-Silva, and D. D. Heistad, "Dysregulation of antioxidant mechanisms contributes to increased oxidative stress in calcific aortic valvular stenosis in humans," *Journal of the American College of Cardiology*, vol. 52, no. 10, pp. 843–850, 2008.
- [2] N. M. Rajamannan, "Bicuspid aortic valve disease: the role of oxidative stress in Lrp5 bone formation," *Cardiovascular Pathology*, vol. 20, no. 3, pp. 168–176, 2011.
- [3] Y. Xue, C. S. Hilaire, L. Hortells, J. A. Phillippi, V. Sant, and S. Sant, "Shape-specific nanoceria mitigate oxidative stress-induced calcification in primary human Valvular interstitial cell culture," *Cellular and Molecular Bioengineering*, vol. 10, no. 5, pp. 483–500, 2017.
- [4] Y. Tang, Q. Xu, H. Peng et al., "The role of vascular peroxidase 1 in ox-LDL-induced vascular smooth muscle cell calcification," *Atherosclerosis*, vol. 243, no. 2, pp. 357–363, 2015.
- [5] M. Zhang, L. Liu, F. Zhi et al., "Inactivation of semicarbazide-sensitive amine oxidase induces the phenotypic switch of smooth muscle cells and aggravates the development of atherosclerotic lesions," *Atherosclerosis*, vol. 249, pp. 76–82, 2016.
- [6] T. Anger, F. K. Pohle, L. Kandler et al., "VAP-1, eotaxin3 and MIG as potential atherosclerotic triggers of severe calcified and stenotic human aortic valves: effects of statins," *Experimental and Molecular Pathology*, vol. 83, no. 3, pp. 435–442, 2007.
- [7] H. Altug Cakmak, S. Aslan, M. Erturk et al., "Assessment of the relationship between serum vascular adhesion protein-1 (VAP-1) and severity of calcific aortic valve stenosis," *The Journal of Heart Valve Disease*, vol. 24, no. 6, pp. 699–706, 2015.
- [8] K. El Hadri, M. Moldes, N. Mercier, M. Andreani, J. Pairault, and B. Feve, "Semicarbazide-sensitive amine oxidase in vascular smooth muscle Cells," *Arteriosclerosis, Thrombosis, and Vascular Biology*, vol. 22, no. 1, pp. 89–94, 2002.
- [9] A. Filip, A. Pinzano, A. Bianchi et al., "Expression of the semicarbazide-sensitive amine oxidase in articular cartilage: its role in terminal differentiation of chondrocytes in rat and human," *Osteoarthritis and Cartilage*, vol. 24, no. 7, pp. 1223–1234, 2016.
- [10] N. Mercier, M. Moldes, K. El Hadri, and B. Feve, "Semicarbazide-sensitive amine oxidase activation promotes adipose conversion of 3T3-L1 cells," *The Biochemical Journal*, vol. 358, Part 2, pp. 335–342, 2001.
- [11] H. G. Weiss, J. Klocker, B. Labeck et al., "Plasma amine oxidase: a postulated cardiovascular risk factor in nondiabetic obese patients," *Metabolism*, vol. 52, no. 6, pp. 688–692, 2003.
- [12] F. Boomsma, A. H. van den Meiracker, S. Winkel et al., "Circulating semicarbazide-sensitive amine oxidase is raised both in type I (insulin-dependent), in type II (non-insulin-dependent) diabetes mellitus and even in childhood type I diabetes at first clinical diagnosis," *Diabetologia*, vol. 42, no. 2, pp. 233–237, 1999.
- [13] P. H. Yu, "Increase of formation of methylamine and formaldehyde in vivo after administration of nicotine and the potential cytotoxicity," *Neurochemical Research*, vol. 23, no. 9, pp. 1205–1210, 1998.
- [14] S. C. Larsson, M. Bäck, J. M. B. Rees, A. M. Mason, and S. Burgess, "Body mass index and body composition in relation to 14 cardiovascular conditions in UK Biobank: a Mendelian randomization study," *European Heart Journal*, vol. 41, no. 2, pp. 221–226, 2020.
- [15] S. C. Larsson, A. Wallin, N. Hakansson, O. Stackelberg, M. Bäck, and A. Wolk, "Type 1 and type 2 diabetes mellitus and incidence of seven cardiovascular diseases," *International Journal of Cardiology*, vol. 262, pp. 66–70, 2018.
- [16] S. C. Larsson, A. Wolk, and M. Bäck, "Alcohol consumption, cigarette smoking and incidence of aortic valve stenosis," *Journal of Internal Medicine*, vol. 282, no. 4, pp. 332–339, 2017.
- [17] M. Carracedo, G. Artiach, A. Witasz et al., "The G-protein coupled receptor ChemR23 determines smooth muscle cell phenotypic switching to enhance high phosphate-induced vascular calcification," *Cardiovascular Research*, vol. 115, no. 10, pp. 1557–1566, 2019.
- [18] M. Carracedo, O. Persson, P. Saliba-Gustafsson et al., "Upregulated autophagy in calcific aortic valve stenosis confers protection of valvular interstitial cells," *International Journal of Molecular Sciences*, vol. 20, no. 6, p. 1486, 2019.
- [19] E. Nagy, D. C. Andersson, K. Caidahl et al., "Upregulation of the 5-lipoxygenase pathway in human aortic valves correlates with severity of stenosis and leads to leukotriene-induced effects on valvular myofibroblasts," *Circulation*, vol. 123, no. 12, pp. 1316–1325, 2011.
- [20] T. Matsumoto, T. Furuta, Y. Nimura, and O. Suzuki, "Increased sensitivity of the fluorometric method of Snyder and Hendley for oxidase assays," *Biochemical Pharmacology*, vol. 31, no. 12, pp. 2207–2209, 1982.
- [21] M. Carracedo, A. Witasz, A. R. Qureshi et al., "Chemerin inhibits vascular calcification through ChemR23 and is associated with lower coronary calcium in chronic kidney disease," *Journal of Internal Medicine*, vol. 286, no. 4, pp. 449–457, 2019.
- [22] S. C. Larsson, A. Wolk, N. Hakansson, and M. Bäck, "Overall and abdominal obesity and incident aortic valve stenosis: two prospective cohort studies," *European Heart Journal*, vol. 38, no. 28, pp. 2192–2197, 2017.
- [23] Y. C. Wang, H. Y. Li, J. N. Wei et al., "Serum vascular adhesion protein-1 level is higher in smokers than non-smokers," *Annals of Human Biology*, vol. 40, no. 5, pp. 413–418, 2013.
- [24] F. Boomsma, U. M. Bhaggoo, A. M. B. van der Houwen, and A. H. van den Meiracker, "Plasma semicarbazide-sensitive amine oxidase in human (patho)physiology," *Biochimica et Biophysica Acta*, vol. 1647, no. 1-2, pp. 48–54, 2003.
- [25] P. H. Yu, "Deamination of methylamine and angiopathy; toxicity of formaldehyde, oxidative stress and relevance to protein glycooxidation in diabetes," *Journal of Neural Transmission. Supplementum*, vol. 52, pp. 201–216, 1998.
- [26] P. H. Yu, S. Wright, E. H. Fan, Z. R. Lun, and D. Gubisne-Harberle, "Physiological and pathological implications of semicarbazide-sensitive amine oxidase," *Biochimica et Biophysica Acta*, vol. 1647, no. 1-2, pp. 193–199, 2003.
- [27] M. Liberman, E. Bassi, M. K. Martinatti et al., "Oxidant generation predominates around calcifying foci and enhances progression of aortic valve calcification," *Arteriosclerosis*,

- Thrombosis, and Vascular Biology*, vol. 28, no. 3, pp. 463–470, 2008.
- [28] E. Branchetti, R. Sainger, P. Poggio et al., “Antioxidant enzymes reduce DNA damage and early activation of valvular interstitial cells in aortic valve sclerosis,” *Arteriosclerosis, Thrombosis, and Vascular Biology*, vol. 33, no. 2, pp. e66–e74, 2013.
- [29] E. Nagy, K. Caidahl, A. Franco-Cereceda, and M. Bäck, “Increased transcript level of poly(ADP-ribose) polymerase (PARP-1) in human tricuspid compared with bicuspid aortic valves correlates with the stenosis severity,” *Biochemical and Biophysical Research Communications*, vol. 420, no. 3, pp. 671–675, 2012.
- [30] K. H. Müller, R. Hayward, R. Rajan et al., “Poly(ADP-ribose) links the DNA damage response and biomineralization,” *Cell Reports*, vol. 27, no. 11, pp. 3124–3138.e13, 2019, e3113.
- [31] J. Hjortnaes, K. Shaper, C. Goettsch et al., “Valvular interstitial cells suppress calcification of valvular endothelial cells,” *Atherosclerosis*, vol. 242, no. 1, pp. 251–260, 2015.
- [32] M. Salmi, K. Kalimo, and S. Jalkanen, “Induction and function of vascular adhesion protein-1 at sites of inflammation,” *The Journal of Experimental Medicine*, vol. 178, no. 6, pp. 2255–2260, 1993.

Research Article

LncRNA MALAT1 Suppression Protects Endothelium against oxLDL-Induced Inflammation via Inhibiting Expression of MiR-181b Target Gene TOX

Liuqing Wang,¹ Yinliang Qi,² Yi Wang,³ Haitao Tang,³ Zhenzhen Li,³ Yuan Wang,³ Songtao Tang ⁴ and Huaqing Zhu ³

¹Department of Clinical Laboratory, The Third Clinical School of Heifei of Anhui Medical University, Hefei 230051, China

²General Department of Hyperbaric Oxygen, Hefei Hospital Affiliated to Anhui Medical University, Hefei 230011, China

³Laboratory of Molecular Biology and Department of Biochemistry, Anhui Medical University, Hefei 230032, China

⁴Department of Endocrinology, The First Affiliated Hospital of Anhui Medical University, Hefei 230022, China

Correspondence should be addressed to Songtao Tang; tangst.healthy@163.com and Huaqing Zhu; aydzhq@126.com

Received 16 May 2019; Accepted 31 October 2019; Published 16 December 2019

Guest Editor: Aneta Radziwon-Balicka

Copyright © 2019 Liuqing Wang et al. This is an open access article distributed under the Creative Commons Attribution License, which permits unrestricted use, distribution, and reproduction in any medium, provided the original work is properly cited.

Rare studies have been conducted to investigate the exact interactions between lung adenocarcinoma transcript 1 (MALAT1), thymocyte selection-associated high mobility group box (TOX), and miRNAs in the pathogenesis of atherosclerosis (AS). We aim to investigate the crosstalk between MALAT1 and TOX and evaluate whether the regulatory mechanism was associated with the miRNA network. AS tissues were collected to determine the level of MALAT1 expression in AS patients, together with determination of miR-181b expression. Cultured endothelial cells were utilized to analyze the expressions of MALAT1, miR-181b, and TOX in the presence of oxLDL. Luciferase activity assay was conducted to evaluate the potential target sites of miR-181b on MALAT1 and TOX. In this study, we demonstrated that MALAT1 was upregulated in patients with AS. MALAT1 silencing significantly downregulated the expression of the miR-181b target gene TOX via reversing the effect of miR181b. Importantly, positive modulation of miR181b and inhibition of MALAT1 and TOX significantly attenuated oxLDL-induced endothelial inflammation and oxidative stress. Moreover, the MAPK signal pathways in endothelial cells were also inhibited through regulation of above endogenous RNAs. In summary, MALAT1 suppression protects the endothelium from oxLDL-induced inflammation and oxidative stress in endothelial cells by upregulation of miR-181b and downregulation of TOX.

1. Introduction

Atherosclerosis (AS), induced by plaque formation inside the arteries, is a lethal condition responsible for heart attack and stroke [1, 2]. Currently, AS has been closely related to the pathogenesis of cardiovascular diseases (CVDs), serving as the most common cause for death [3, 4]. Oxidized low-density lipoprotein (oxLDL) has been widely demonstrated to be involved in the development of AS by causing an oxidative chain reaction and inducing endothelial dysfunction. However, its exact mechanism is not well defined.

MicroRNAs (miRNAs), a class of small noncoding single-stranded RNA, have been reported to negatively regulate the gene expression by degradation or posttranscriptional regulation of target sequences. Several miRNAs have been considered to participate in the pathogenesis of AS. For instance, miR-27b is a cholesterol-responsive hepatic miRNA that represses a large number of targets involving in lipid metabolism and lipoprotein remodeling that play important roles in AS [5]. MiR-146a is an important cytokine-responsive miRNA conferring atheroprotective properties in vessel walls [6]. In addition, miR-146a showed

elevation in atherosclerotic plaques of human and mouse [7]. To date, increasing evidence shows that miR-181b plays a critical role in mice and human subjects by serving as an inhibitor of endothelial inflammatory responses through targeting NF- κ B signaling in both acute and chronic CVDs [8]. However, little is known about the exact roles of miR-181b in AS.

Human metastasis-associated lung adenocarcinoma transcript 1 (MALAT1), an 8.7 kb lncRNA on chromosome 11q13, has been demonstrated to be overexpressed in several cancers [9]. However, the roles of MALAT1 in the pathogenesis of CVDs are still not well defined. In a previous study, high expression levels of conserved MALAT1 were reported to involve in the physiological progress of endothelial cells and were related to the CVD-associated complications [10]. These lead us to investigate the roles of MALAT1 in the pathogenesis of AS.

Thymocyte selection-associated high mobility group box (TOX), which was reported to be regulated by lncRNA [11], has been closely related to the immune cell-associated proliferative diseases, such as cancer. However, whether TOX is associated with immune cell-related inflammation and oxidative stress in the progress of AS requires further clarification.

To date, rare studies have been conducted to investigate the exact interaction between MALAT1, TOX, and miRNAs. In this study, we evaluated the crosstalk between MALAT1 and TOX through investigating whether the regulatory mechanism was associated with the miRNA network.

2. Materials and Methods

2.1. Patients. Fifty AS patients and fifty healthy subjects were recruited in this study. The diagnosis was based on a history of chest pain, coronary angiography results, and characteristic ECG changes. The baseline characteristics of the two groups were compared. The peripheral blood sample (10 ml) was collected in an EDTA-containing vacutainer tube from each individual for further analysis.

2.2. Cell Culture. Human umbilical vein endothelial cells (HUVECs) obtained from American Tissue Culture College were cultivated in DMEM medium containing 10% fetal bovine serum (FBS, Gibco), 100 U U/ml streptomycin, and 100 U U/ml penicillin at 37°C in a humidified incubator in 5% CO₂-95% air.

2.3. Cell Transfection. A miR181b mimic (Qiagen) and a modified antagomir (GenePharm) were utilized for the cell transfection in order to induce overexpression and inhibition of miR-181b in cultured cells, respectively. Transfection was conducted using the TransMessenger transfection agent (Qiagen) according to the manufacturer's instructions. A scrambled oligonucleotide (GenePharm) was used as control.

2.4. ROS, TNF- α , and NADPH Determination. ROS production in tissues and cultured cells was detected according to the previous description [12]. Initially, cells were homogenized in reaction buffer. Protein concentration was measured using the BCA method. Proteins were incubated with 20 μ M DCF-DA at 37°C for 3 h. The fluorescence was measured by a

TABLE 1: Basic parameters and characteristics of subjects in different groups.

	Control	AS	P value
N	50	50	ns
Sex (M/F)	31/19	27/23	ns
Age (year)	63.8 \pm 7.3	65.4 \pm 6.4	ns
BMI (kg/m ²)	28.8 \pm 3.0	27.3 \pm 3.2	ns
TC (mmol/l)	4.14 \pm 0.39	6.75 \pm 0.42*	<0.01
HDL-c (mmol/l)	1.45 \pm 0.32	1.48 \pm 0.47	ns
TG (mmol/l)	1.51 \pm 0.45	1.67 \pm 0.72	ns
LDL-c (mmol/l)	2.15 \pm 0.37	4.46 \pm 0.51*	<0.01
Hypertension	24	29	ns
Diabetes	0	0	ns
History of IHD	6	8	ns
Smokers	10	10	ns

Data are expressed as mean \pm SD values. AS: atherosclerosis; BMI: body mass index; TC: total cholesterol; HDL-c: high-density lipoprotein; TG: triglycerides; LDL-c: low-density lipoprotein; IHD: ischemic heart disease.

spectrofluorometer at an excitation of 488 nm and an emission of 525 nm, respectively. TNF- α level in the supernatants of HUVECs was determined using ELISA method [12]. The test was performed at least in triplicate. NADPH oxidase was also detected according to the previous description [12]. Lucigenin-enhanced chemiluminescence was used to evaluate the activity of NADPH oxidase in cell lysates with a multilabel counter (Victor 3 Wallac). In brief, 20 μ g protein, 100 μ mol/l NADPH, and 5 μ mol/l lucigenin were used for the assay. The procedures were conducted in the presence of DPI. Afterwards, the light signal was determined every 5 s. Finally, the NADPH oxidase activity was presented as counts per second (CPS).

2.5. Real-Time PCR. Total RNA was extracted from HUVECs using TRIzol reagent according to the manufacturer's instructions. The first cDNA strand was synthesized using approximately 2 μ g RNA with the TransScript kit (Takara), according to the manufacturer's instructions. Real-time PCR was performed based on the specific primers for MALAT1 (forward primer 5'-TCTGCAGGGACTACAG CAAG-3'; reverse primer 5'-TCACATT GGTGAATCCGT CT-3') and TOX (forward primer 5'-TTCTCTGTG TCAC CCCATGA-3'; reverse primer 5'-TCTGGCATCACAGA AATG GA-3'), using SYBR green. The mRNA level was normalized by GAPDH. The amplification results were calculated as 2^(- $\Delta\Delta$ Ct), according to the previous description [13].

2.6. Western Blotting Analysis. Lysis buffer containing protease and phosphatase inhibitors were utilized to extract the protein from tissues or cells. The protein was electrophoresized on a 10% SDS-PAGE gel, followed by transferring to a nitrocellulose membrane (Bio-Rad, CA, USA). Subsequently, the membrane was treated using 5% nonfat milk and then was incubated with MALAT1, TOX, ERK, and p38

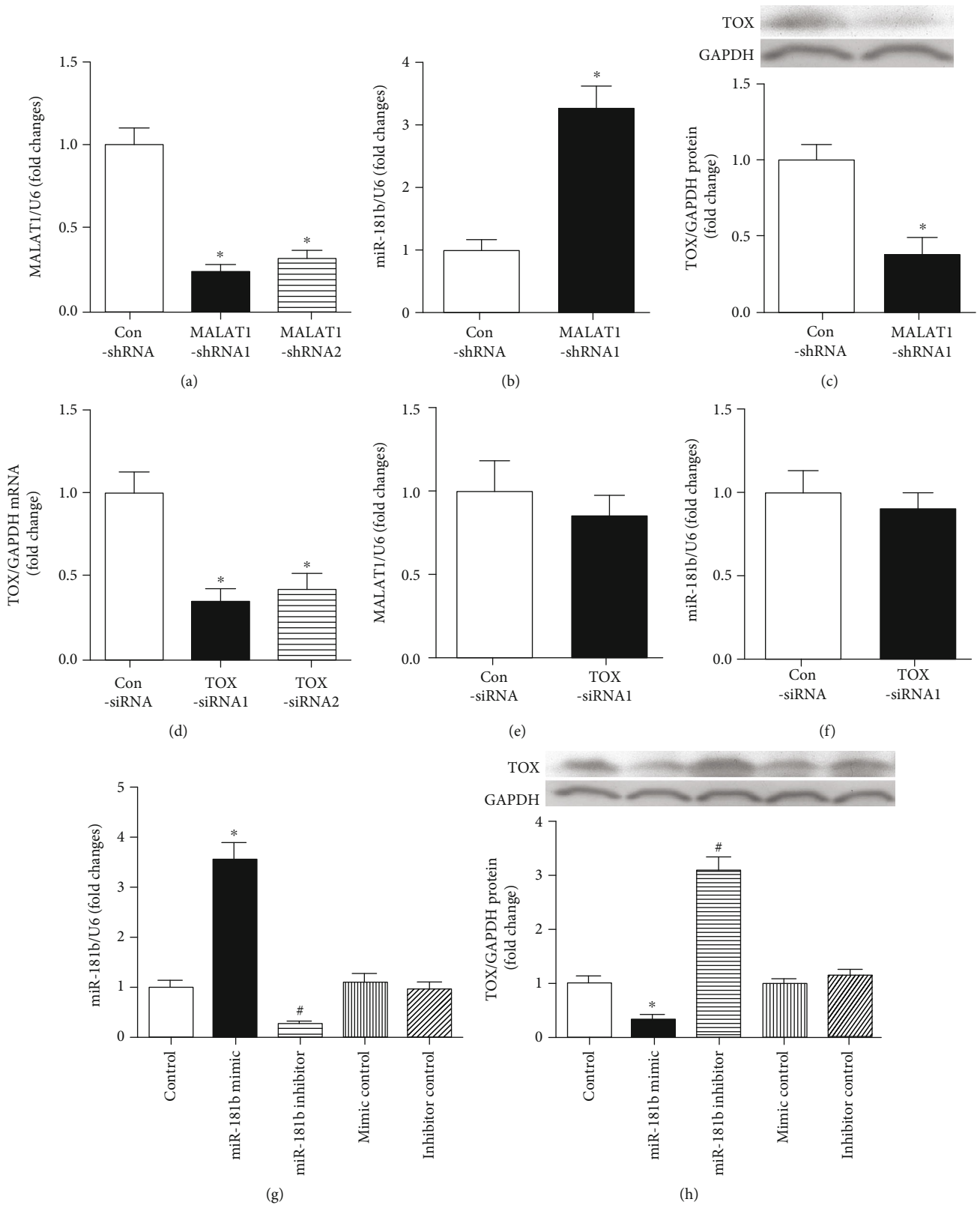


FIGURE 1: Interactions among MALAT1, TOX, and miR-181b. (a) Inhibitory effects of MALAT1-shRNAs on the MALAT1 mRNA expression as determined using RT-PCR. * $P < 0.05$ versus the control group. (b, c) HUVECs were transfected using MALAT1-shRNA1 for 24 h, followed by determining the expression of miR181b and TOX using RT-PCR and Western blot analysis, respectively. * $P < 0.05$ versus the control group. (d) RT-PCR showed TOX mRNA was downregulated after TOX siRNA. * $P < 0.05$ versus the control group. (e, f) Expressions of MALAT1 and miR181b were measured following 24 h of TOX siRNA treatment. (g, h) Alteration of miR-181b and TOX protein levels in cultured HUVECs about 24 h after various transfection treatments. * $P < 0.05$ versus the control group; # $P < 0.05$ versus the control group.

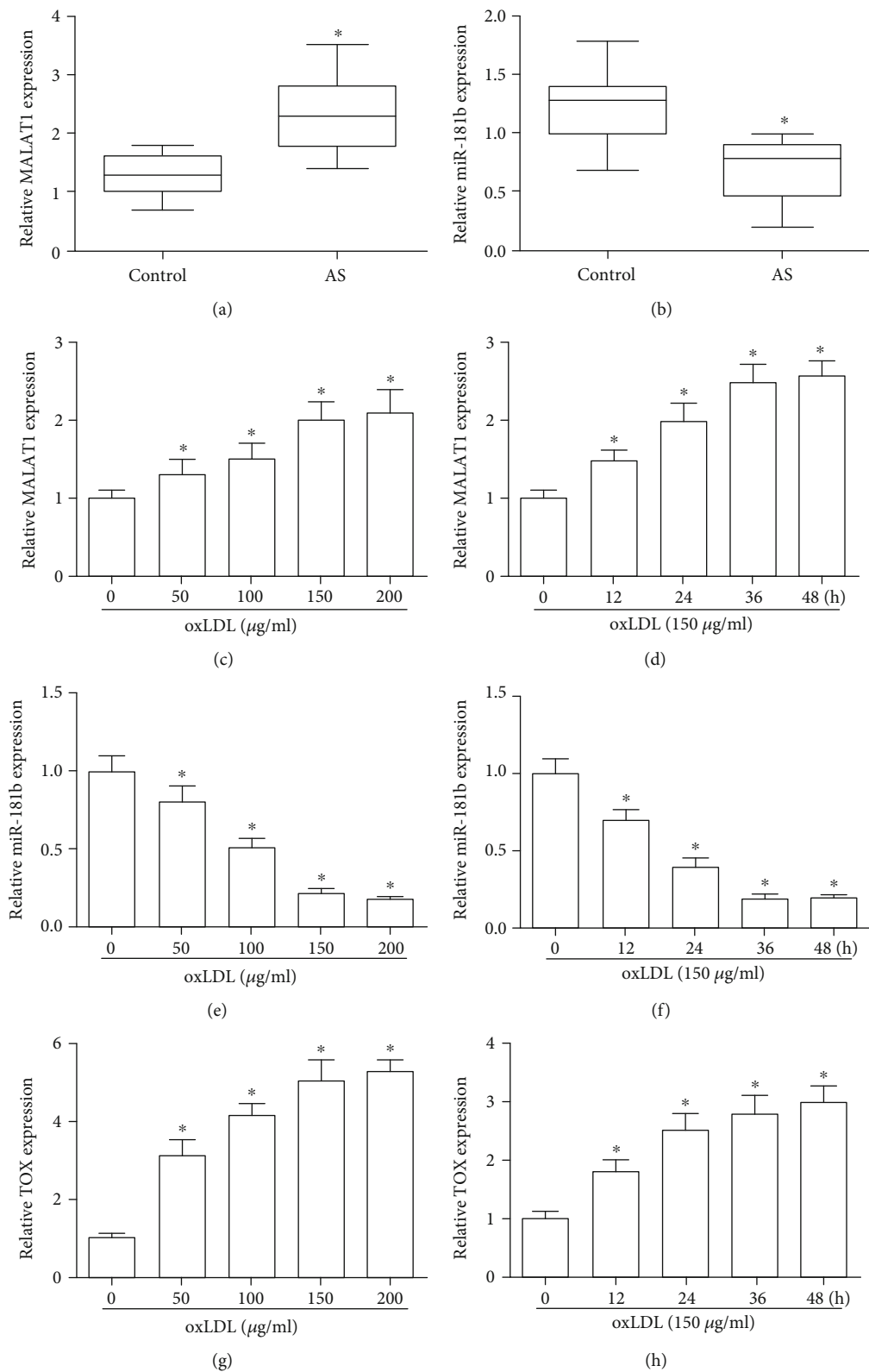


FIGURE 2: MALAT1 and miR-181b expression in AS patients and oxLDL-treated HUVECs. (a, b) Levels of circulating lncRNA MALAT1 and miR-181b in healthy volunteers and AS patients measured by RT-PCR. * $P < 0.05$ versus the control group. (c–h) Relative expression of MALAT1, miR-181b, and TOX about 24 h after treating with various concentrations of oxLDL (0, 50, 100, 150, and 200 $\mu\text{g/ml}$) or treating with oxLDL (150 $\mu\text{g/ml}$) for different times. * $P < 0.05$ versus the control group.

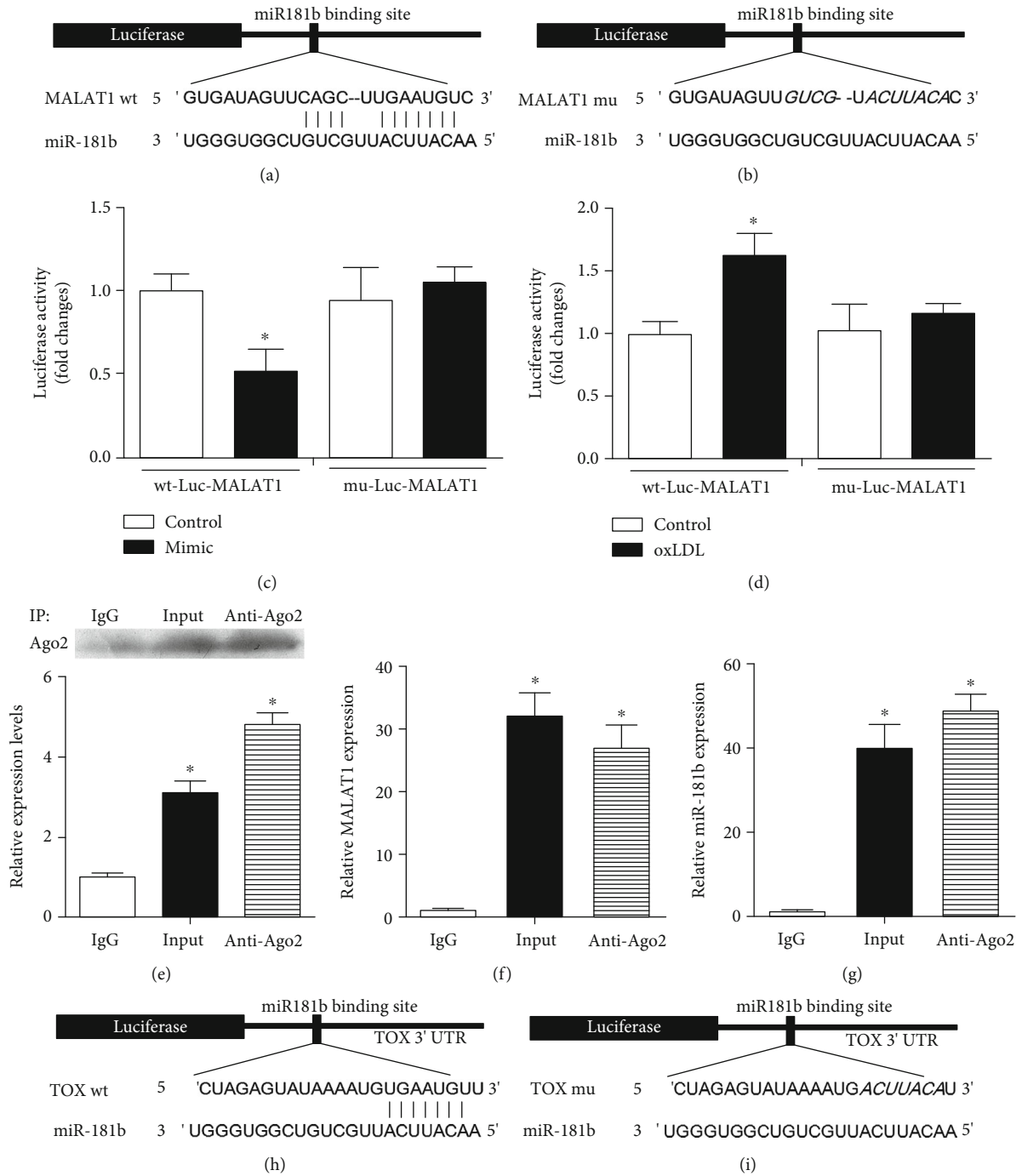


FIGURE 3: Continued.

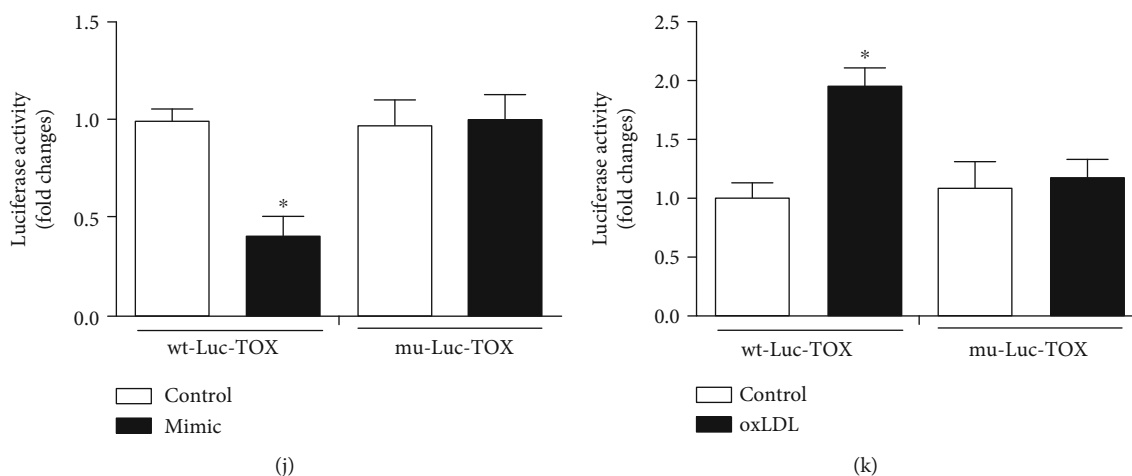


FIGURE 3: Potential binding sites of miR-181b for MALAT1 and TOX. (a, b) The wild-type and mutated miR-181b binding sites in the MALAT1 3'-UTR. (c-g) The miR-181b mimics and the luciferase constructs were cotransfected into cultured HUVECs. Cellular lysates from cultured cells were used for RIP with an Ago2 antibody. The Ago2 protein level was detected by Western blot analysis. The mRNA expression of MALAT1 and miR-181b in the immunoprecipitate was measured by RT-PCR. * $P < 0.05$ versus the control group (c, d). * $P < 0.05$ compared with IgG (e-g). (h, i) The wild-type and mutated miR-181b binding sites in the 3'-UTR of TOX. (j, k) Luciferase activity of the wild-type and mutant Luc TOX groups. * $P < 0.05$ versus the control group.

antibodies overnight at 4°C. Afterwards, the mixture was incubated with the HRP-conjugated secondary antibodies at room temperature for 1 h. The same membrane probed with GAPDH served as a loading control.

2.7. Luciferase Reporter Assay. The luciferase vector (Addgene Inc.) including the 3'-UTR of MALAT1 and TOX containing the miR-181b response elements (wt-Luc-MALAT1 and wt-Luc-TOX) was used for the luciferase reporter assay. Site-directed gene mutation was utilized to construct a mutation in the miR-181b response elements of 3'-UTR of MALAT1 and TOX (mu-Luc-MALAT1 and mu-Luc-TOX). Subsequently, the wild and mutant 3'-UTR were cloned to the firefly luciferase-expressing vector. For the luciferase assay, HUVECs were seeded in 48-cell plates and then transfected using 200 ng plasmid DNA including wild or mutant MALAT1 and TOX, respectively.

2.8. Statistical Analysis. SPSS 18.0 software was used for the data analysis. The data were shown as mean \pm standard deviation (SD). One-way ANOVA and parametric *t*-test were used for the intergroup comparisons. $P < 0.05$ was considered to be significant difference.

3. Results

3.1. Basic Parameters and Characteristics of Subjects in Different Groups. As shown in Table 1, total cholesterol (TC) and low-density lipoprotein (LDL-c) of patients in the AS group were higher than those of controls. Other parameters and characteristics were similar between two groups.

3.2. Relationship among MALAT1, miR-181b, and TOX. Expression of MALAT1 was downregulated significantly after treating with MALAT1-shRNA1 and MALAT1-shRNA2, respectively ($P < 0.05$, Figure 1(a)). In cases of MALAT1

downregulation, the expression of miR-181b showed significant upregulation ($P < 0.05$, Figure 1(b)). Besides, after downregulation of MALAT1, TOX protein expression also showed significant decrease ($P < 0.05$, Figure 1(c)). TOX siRNA1 and TOX siRNA2 transfection could significantly downregulate the expression of TOX, especially the TOX siRNA1 ($P < 0.05$, Figure 1(d)). Then, we determined the expression of MALAT1 and miR-181b in cases of TOX siRNA1, which indicated that there were no significant changes in their expression ($P > 0.05$, Figures 1(e) and 1(f)). On the contrary, expression of TOX showed significant decrease in the presence of miR-181b mimics (Figures 1(g) and 1(h)). This implied that there might be a potential association among MALAT1, miR-181b, and TOX.

3.3. Expression of MALAT1 and miR-181b in AS Patients and oxLDL-Treated Cells. In the blood samples of AS cases, MALAT1 level showed significant increase compared with the normal individuals ($P < 0.05$, Figure 2(a)). Meanwhile, relative miR-181b expression in AS cases showed significant decrease compared with that of the normal individuals ($P < 0.05$, Figure 2(b)). Upon treating with oxLDL with different doses and times, the MALAT1 was significantly upregulated in a dose- and time-dependent manner ($P < 0.05$, Figures 2(c) and 2(d)). In contrast, the expression of miR-181b was significant downregulated in cases of oxLDL in a dose- and time-dependent manner, respectively ($P < 0.05$, Figures 2(e) and 2(f)). After treating with oxLDL with different doses and times, expression of TOX showed significant increase compared with control also in a dose- and time-dependent manner ($P < 0.05$, Figures 2(g) and 2(h)).

3.4. Direct Binding between miR-181b and MALAT1. Luciferase assay indicated that miR-181b mimics induced decrease of luciferase activity of MALAT1. However, a reduced effect was found for the MALAT1 mutant ($P < 0.05$, Figure 3(a)).

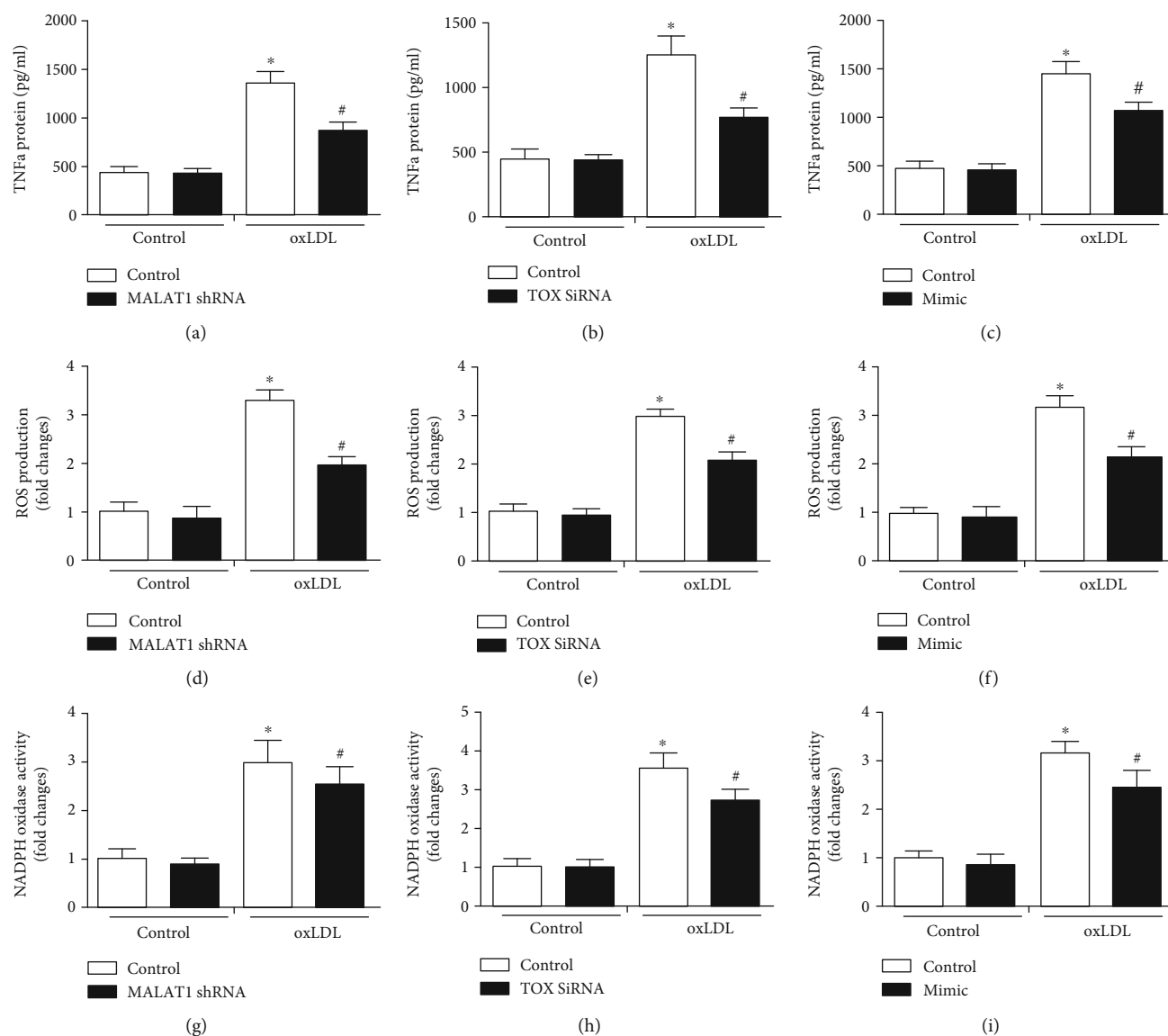


FIGURE 4: Modulation of MALAT1, TOX, and miR-181b regulated the expression of TNF- α , ROS production, and NADPH oxidase activity. (a–c) TNF- α protein expression was determined after treating with MALAT1 shRNA, TOX siRNA, and miR-181b mimic, together with ROS production (d–f) and NADPH oxidase activity (g–i). * $P < 0.05$ versus the control group; # $P < 0.05$ versus the oxLDL control group.

In the MALAT1 mutants, there were no statistical differences between the miR-181b group and control ($P > 0.05$, Figures 3(a) and 3(c)). In wild-type MALAT1, oxLDL induced significant increase of luciferase activity, while such effect was reduced after mutation in certain sites of MALAT1 (Figures 3(b) and 3(d)). In this section, we used Ago2 antibody to precipitate the Ago2 protein from cultured cells (Figure 3(e)). The mRNA expression of both MALAT1 and miR-181b was significantly enriched in the immunoprecipitates (Figures 3(c) and 3(d)). On this basis, we confirmed that there was a direct binding between MALAT1 and miR-181b.

3.5. Direct Binding between miR-181b and TOX. To identify the potential binding sites of miR-181b on TOX, luciferase test was performed, which indicated miR-181b mimics induced

decrease of luciferase activity of TOX. However, a reduced effect was found for the mutant ($P < 0.05$, Figure 3(e)). In TOX mutants, there were no statistical differences between the miR-181b group and control ($P > 0.05$, Figures 3(f) and 3(g)). In wild type, oxLDL induced significant increase of luciferase activity, while such effect was reduced after mutation in certain sites of TOX (Figures 3(h)–3(k)).

3.6. Determination of TNF- α Expression, ROS Production, and NADPH Oxidase Activity in oxLDL-Treated Cells. Compared with control, significant inhibition was noticed in the TNF- α expression, ROS production, and NADPH oxidase activity in MALAT1 shRNA, TOX siRNA, and miR-181b mimic groups in the presence of oxLDL ($P < 0.05$, Figure 4). In addition, miR-181b inhibitor usage reversed the significantly downregulating effects of MALAT1

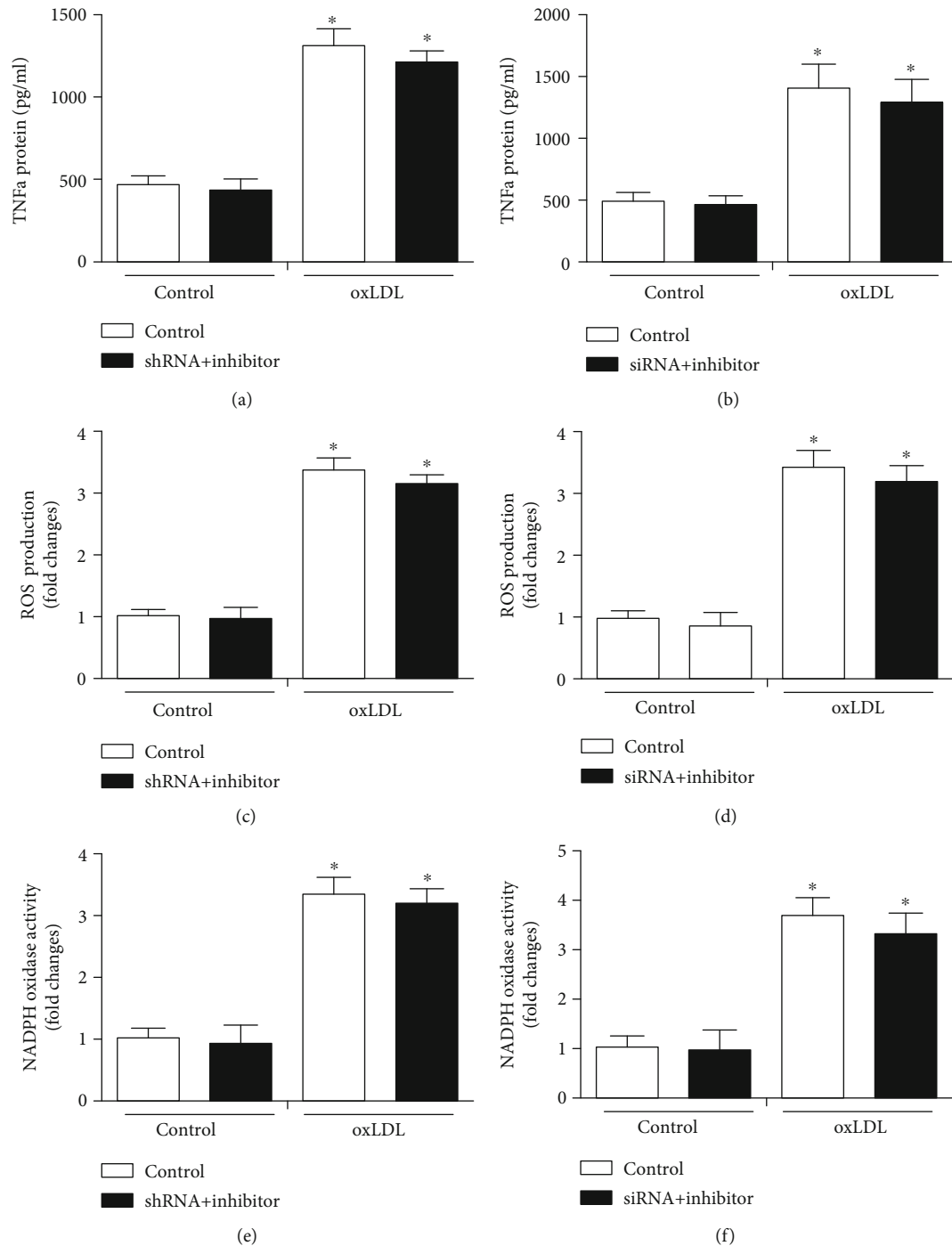


FIGURE 5: MiR-181b inhibitor in combination with MALAT1 shRNA and TOX siRNA regulated the expression of TNF- α , ROS production, and NADPH oxidase activity. (a–f) TNF- α protein expression was determined after treating with MALAT1 shRNA+miR-181b inhibitor and TOX siRNA+miR-181b inhibitor, together with ROS production and NADPH oxidase activity. * $P < 0.05$ versus the control group.

shRNA and TOX siRNA on TNF- α expression, ROS production, and NADPH oxidase activity in the presence of oxLDL ($P < 0.05$, Figure 5).

3.7. Roles of MALAT1/miR181b/TOX in the ERK Signaling Pathway. In this section, we determined the roles of MALAT1/miR181b/TOX in the MAPK signaling pathway.

MALAT1 shRNA could attenuate the expression of pERK and pp38 compared with the control group ($P < 0.05$, Figures 6(a) and 6(b)). However, such phenomenon was offset in the MALAT1 shRNA+miR181b inhibitor group ($P < 0.05$, Figures 6(a) and 6(b)). TOX siRNA could significantly downregulate expression of pERK and pp38 compared with the control group ($P < 0.05$, Figures 6(c) and 6(d)). The

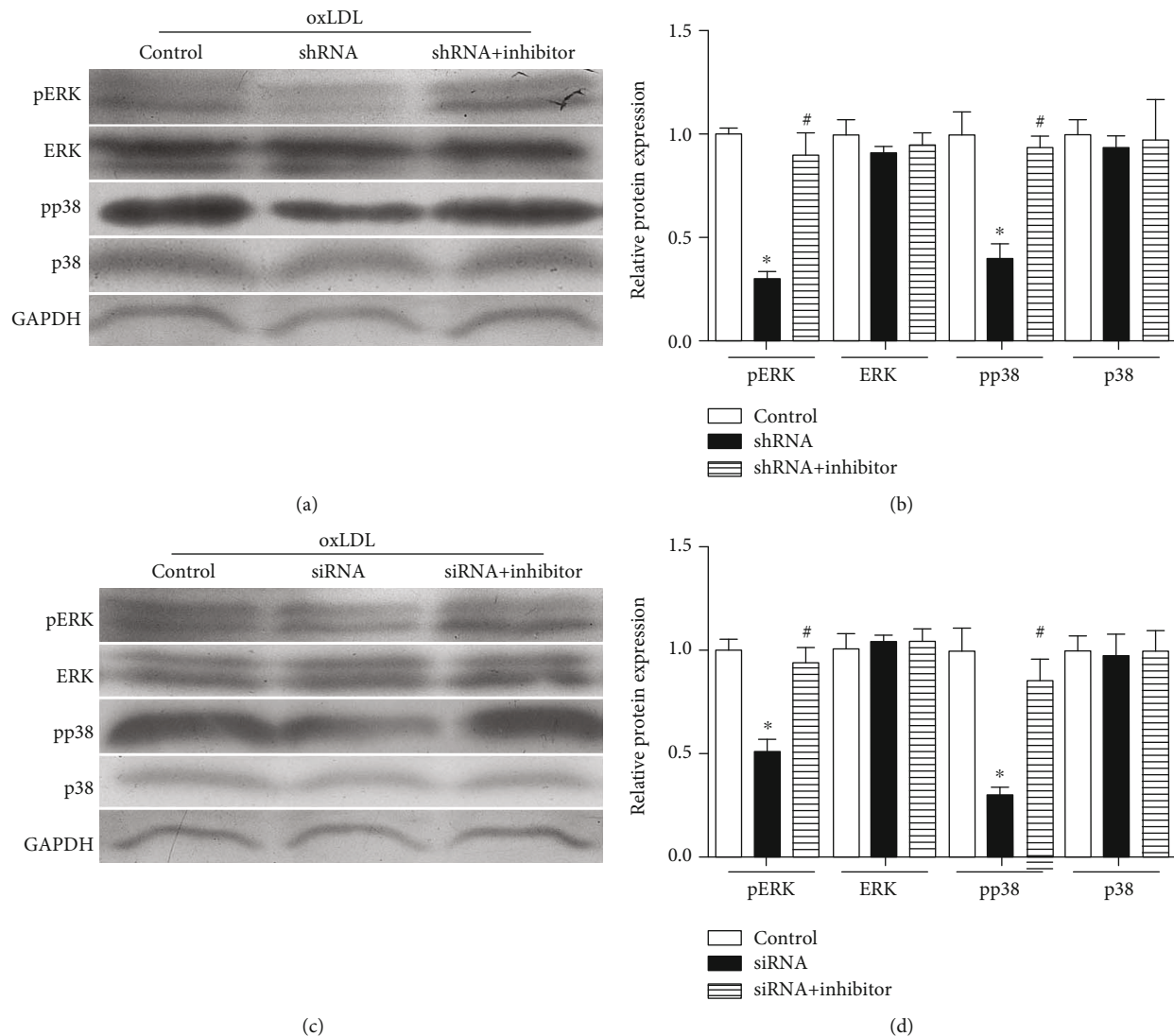


FIGURE 6: The MALAT1/miR-181b/TOX pathway is associated with the MAPK pathway. (a, b) Expression of pERK and pp38 after treating with MALAT1 shRNA and shRNA+inhibitor. * $P < 0.05$ versus the control group. # $P < 0.05$ versus the shRNA group. (c, d) Expression of pERK and pp38 after treating with TOX siRNA and siRNA+inhibitor. * $P < 0.05$ versus the control group; # $P < 0.05$ versus the siRNA group.

decreased expression of pERK and pp38 in response to MALAT1 silencing could also be offset by the TOX siRNA +miR181b inhibitor ($P < 0.05$, Figures 6(c) and 6(d)).

4. Discussion

OxLDL and several inflammatory cytokines have been reported to be related with pathogenesis of AS [14]. According to the previous description, oxLDL deposition in endothelial barrier is also closely involved in AS [15, 16]. These reports lead us to investigate the potential targets of oxLDL, especially the downstream components of oxLDL in the development of AS, together with identification of potential lncRNAs involving in that signaling pathway.

lncRNAs have been reported to involve in regulating expression of several genes. To our best knowledge, most of the lncRNAs-related studies have been focusing on the roles of cancer progression. However, little is known about their

roles in the cardiovascular diseases. In a previous study, lincRNA-p21 played an important role in the pathogenesis and progression of coronary heart disease [17]. Moreover, lncRNA APF was crucial for the regulation of autophagic cell death and myocardial infarction by targeting miR-188-3p [18]. Furthermore, it is important to investigate the crosstalk between lncRNAs and miRNAs, which may deepen our understanding on the mechanisms and pathogenesis of CVDs.

lncRNA MALAT1 is highly expressed in endothelial cells, which is closely implicated in several biological pathways. As an upstream component, MALAT1 is reported to associate with the AS. Several miRNAs including miR-101, miR-217, and miR-9 were correlated with MALAT1 [19, 20]. However, the crosstalk between MALAT1, miRNAs, and downstream targets with respect to oxLDL-induced endothelial dysfunction is still not well defined. As previously described, miRNA-181b was closely related to AS, vascular

inflammation, and oxidative stress. For instance, systemic delivery of microRNA-181b inhibited vascular inflammation and AS in apolipoprotein E-deficient mice [21]. In addition, TOX plays an important role in the signaling pathways leading to CD4⁺ or CD8⁺ single-positive functionally distinct major T cell populations [22, 23], which was closely related to AS. In this study, we determined the roles of the MALAT1/miR-181b/TOX signaling pathway in the setting of AS in cases of oxLDL-induced endothelial dysfunction. In the presence of oxLDL, the expression of MALAT1 and TOX in endothelial cells was significantly upregulated presenting in a dose-dependent manner. In contrast, the expression of miR-181b was significantly downregulated in cases of oxLDL. Furthermore, it has been found that downregulation of MALAT1 could increase miR-181b expression and facilitate miR-181b-mediated TOX inhibition. These implied that there might be a potential link among MALAT1, miR-181b, and TOX. To confirm this, luciferase activity assay was performed to prove that direct bindings were existed between MALAT1 and miR-181b as well as between miR-181b and TOX. In our research, we investigated the link between MALAT1/miR-181b/TOX and inflammatory factors in the pathogenesis of CVD, by investigating TNF- α expression, ROS production, and NADPH oxidase activity. On this basis, we confirmed that regulation of MALAT1, miR-181b, and TOX expressions could modulate the expression of inflammatory factors that may contribute to the pathogenesis of CVD.

The MAPK signaling pathway is reported to play a physiological role in neuronal survival and endothelial cell response to atherosclerosis [24, 25]. A close link should be attached to the ERK and p38 signaling pathways in the proliferation of vascular endothelial cells and smooth muscle cells in the pathogenesis of AS. To our best knowledge, inhibition of pERK and pp38 overexpression contributed to the control of AS development. Our data showed the phosphorylation of ERK and p38 in endothelial cells showed significant decrease when exposed to MALAT1 shRNA and TOX siRNA in the presence of oxLDL. These effects were reversed by miR-181b inhibitor. On this basis, modulation of MALAT1/miR-181b/TOX may trigger downregulation of the MAPK signal pathway, which may attenuate the development of AS.

5. Conclusion

We presented the interactions among MALAT1, TOX, and miR-181b in oxLDL-induced endothelial dysfunction. Suppression of MALAT1 may attenuate inflammation in oxLDL-incubated endothelial cells by upregulating of miR-181b and inhibiting the expression of TOX, which is closely related to the inhibition of the MAPK signaling pathway that attenuated the pathogenesis of AS accordingly.

Data Availability

The data used to support the findings of this study are available from the corresponding authors upon request.

Ethical Approval

The animal experiments were conducted in line with the *Guide for the Care and Use of Laboratory Animals* issued by US National Institutes of Health (No. 85-23, 2011). The study protocols were approved by the Ethics Committee of Anhui Medical University.

Conflicts of Interest

The authors declared they do not have anything to disclose regarding conflict of interest with respect to this manuscript.

Authors' Contributions

ZHQ and TST contributed to the conception and design of the experiments. TST and WY drafted and critically revised the article. WLQ and WY completed the human experiments. TST, QYL, WLQ, and WY completed the cell experiments. LZZ and THT contributed to the analysis. ZHQ and TST gave the final approval and agreed to be accountable for all aspects of work ensuring integrity and accuracy. Liuqing Wang, Yinliang Qi, and Yi Wang contributed equally to this work.

Acknowledgments

This study was supported by the National Natural Science Foundation of China (nos. 81570419, 81270372, and 81900750), Cultivation Project for the National Natural Science Foundation of the First Affiliated Hospital of Anhui Medical University (no. 2558), and Grants for Scientific Research of BSKY (no. XJ201617).

References

- [1] M. S. Rahman and K. Woollard, "Atherosclerosis," *Advances in Experimental Medicine and Biology*, vol. 1003, pp. 121–144, 2017.
- [2] A. D. Gepner, R. Young, J. A. Delaney et al., "Comparison of Carotid Plaque Score and Coronary Artery Calcium Score for Predicting Cardiovascular Disease Events: The Multi-Ethnic Study of Atherosclerosis," *Journal of the American Heart Association*, vol. 6, no. 2, 2017.
- [3] A. O. Oyenuga, D. Couper, K. Matsushita, E. Boerwinkle, and A. R. Folsom, "Association of monocyte myeloperoxidase with incident cardiovascular disease: The Atherosclerosis Risk in Communities Study," *PLoS One*, vol. 13, no. 10, article e0205310, 2018.
- [4] J. Ma and H. Li, "The role of gut microbiota in atherosclerosis and hypertension," *Frontiers in Pharmacology*, vol. 9, p. 1082, 2018.
- [5] B. Laffont and K. J. Rayner, "MicroRNAs in the pathobiology and therapy of atherosclerosis," *The Canadian Journal of Cardiology*, vol. 33, no. 3, pp. 313–324, 2017.
- [6] Z. Jahangir, A. Bakillah, and J. Iqbal, "Regulation of sphingolipid metabolism by microRNAs: a potential approach to alleviate atherosclerosis," *Diseases*, vol. 6, no. 3, p. 82, 2018.
- [7] H. S. Cheng, R. Besla, A. Li et al., "Paradoxical suppression of atherosclerosis in the absence of microRNA-146a," *Circulation Research*, vol. 121, no. 4, pp. 354–367, 2017.

- [8] X. Sun, B. Icli, A. K. Wara et al., "MicroRNA-181b regulates NF- κ B-mediated vascular inflammation," *The Journal of Clinical Investigation*, vol. 122, no. 6, pp. 1973–1990, 2012.
- [9] R. Lin, S. Maeda, C. Liu, M. Karin, and T. S. Edgington, "A large noncoding RNA is a marker for murine hepatocellular carcinomas and a spectrum of human carcinomas," *Oncogene*, vol. 26, no. 6, pp. 851–858, 2007.
- [10] X. Zhang, M. H. Hamblin, and K. J. Yin, "The long noncoding RNA Malat1: its physiological and pathophysiological functions," *RNA Biology*, vol. 14, no. 12, pp. 1705–1714, 2017.
- [11] C. Wu, H. Liu, F. Zhang et al., "Long noncoding RNA expression profile reveals lncRNAs signature associated with extracellular matrix degradation in kashin-beck disease," *Scientific Reports*, vol. 7, no. 1, article 17553, 2017.
- [12] Z. Lu, F. Wang, P. Yu et al., "Inhibition of miR-29b suppresses MAPK signaling pathway through targeting SPRY1 in atherosclerosis," *Vascular Pharmacology*, vol. 102, pp. 29–36, 2018.
- [13] K. J. Livak and T. D. Schmittgen, "Analysis of Relative Gene Expression Data Using Real-Time Quantitative PCR and the 2- $\Delta\Delta$ CT Method," *Methods*, vol. 25, no. 4, pp. 402–408, 2001.
- [14] J. Frostegard, "Autoimmunity, oxidized LDL and cardiovascular disease," *Autoimmunity Reviews*, vol. 1, no. 4, pp. 233–237, 2002.
- [15] S. Kayo, M. Ohsawa, S. Ehara et al., "Oxidized low-density lipoprotein levels circulating in plasma and deposited in the tissues: Comparison between Helicobacter pylori-associated gastritis and acute myocardial infarction," *American Heart Journal*, vol. 148, no. 5, pp. 818–825, 2004.
- [16] S. Mitra, A. Deshmukh, R. Sachdeva, J. Lu, and J. L. Mehta, "Oxidized low-density lipoprotein and atherosclerosis implications in antioxidant therapy," *The American Journal of the Medical Sciences*, vol. 342, no. 2, pp. 135–142, 2011.
- [17] S. S. Tang, J. Cheng, M. Y. Cai et al., "Association of lncRNA-p21 Haplotype with Coronary Artery Disease in a Chinese Han Population," *Disease markers*, vol. 2016, Article ID 9109743, 7 pages, 2016.
- [18] K. Wang, C. Y. Liu, L. Y. Zhou et al., "APF lncRNA regulates autophagy and myocardial infarction by targeting miR-188-3p," *Nature Communications*, vol. 6, no. 1, p. 6779, 2015.
- [19] X. Wang, M. Li, Z. Wang et al., "Silencing of long noncoding RNA MALAT1 by miR-101 and miR-217 inhibits proliferation, migration, and invasion of esophageal squamous cell carcinoma cells," *The Journal of Biological Chemistry*, vol. 290, no. 7, pp. 3925–3935, 2015.
- [20] D. Fang, H. Yang, J. Lin et al., "17 β -estradiol regulates cell proliferation, colony formation, migration, invasion and promotes apoptosis by upregulating miR-9 and thus degrades MALAT-1 in osteosarcoma cell MG-63 in an estrogen receptor-independent manner," *Biochemical and Biophysical Research Communications*, vol. 457, no. 4, pp. 500–506, 2015.
- [21] X. Sun, S. He, A. K. Wara et al., "Systemic Delivery of MicroRNA-181b Inhibits Nuclear Factor- κ B Activation, Vascular Inflammation, and Atherosclerosis in Apolipoprotein E-Deficient Mice," *Circulation Research*, vol. 114, no. 1, pp. 32–40, 2014.
- [22] T. Chen, Q. Li, X. Zhang et al., "TOX expression decreases with progression of colorectal cancers and is associated with CD4 T-cell density and *Fusobacterium nucleatum* infection," *Human Pathology*, vol. 79, pp. 93–101, 2018.
- [23] N. Page, B. Klimek, M. De Roo et al., "Expression of the DNA-binding factor TOX promotes the encephalitogenic potential of microbe-induced autoreactive CD8⁺ T cells," *Immunity*, vol. 48, no. 5, pp. 937–950.e8, 2018.
- [24] F. Jeanneteau and K. Deinhardt, "Fine-tuning MAPK signaling in the brain," *Communicative & Integrative Biology*, vol. 4, no. 3, pp. 281–283, 2011.
- [25] B. A. Rose, T. Force, and Y. Wang, "Mitogen-activated protein kinase signaling in the heart: angels versus demons in a heart-breaking tale," *Physiological Reviews*, vol. 90, no. 4, pp. 1507–1546, 2010.

Research Article

LOX-1, the Common Therapeutic Target in Hypercholesterolemia: A New Perspective of Antiatherosclerotic Action of Aegeline

Abhilasha Singh ^{1,2}, Ashok Kumar Srinivasan,^{1,3} Lakshmi Narasimhan Chakrapani ¹,
and Periandavan Kalaiselvi ¹

¹Department of Medical Biochemistry, Dr. ALM Post Graduate Institute for Basic Medical Sciences, University of Madras, Chennai, India

²Preclinical Stroke Modelling Laboratory, Burke Neurological Institute, Weill Cornell Medicine, White Plains, New York 10605, USA

³Department of HIV, National Institute for Research in Tuberculosis, Chennai, India

Correspondence should be addressed to Periandavan Kalaiselvi; pkalaiselvi2011@gmail.com

Received 16 May 2019; Revised 25 September 2019; Accepted 5 October 2019; Published 30 November 2019

Guest Editor: Aneta Radziwon-Balicka

Copyright © 2019 Abhilasha Singh et al. This is an open access article distributed under the Creative Commons Attribution License, which permits unrestricted use, distribution, and reproduction in any medium, provided the original work is properly cited.

Background. Lectin-like oxidized low-density lipoprotein receptor-1 (LOX-1) is the major receptor for oxidized low-density lipoprotein (Ox-LDL) in the aorta of aged rats. Ox-LDL initiates LOX-1 activation in the endothelium of lipid-accumulating sites of both animal and human subjects of hypercholesterolemia. Targeting LOX-1 may provide a novel diagnostic strategy towards hypercholesterolemia and vascular diseases. **Hypothesis.** This study was planned to address whether aegeline (AG) could bind to LOX-1 with a higher affinity and modulate the uptake of Ox-LDL in hypercholesterolemia. **Study Design.** Thirty-six Wistar rats were divided into six groups. The pathology group rats were fed with high-cholesterol diet (HCD) for 45 days, and the treatment group rats were fed with HCD and aegeline/atorvastatin (AV) for the last 30 days. **In vivo** and **in vitro** experiments were carried out to assay the markers of atherosclerosis like Ox-LDL and LOX-1 levels. Histopathological examination was performed. Oil Red O staining was carried out in the IC-21 cell line. Docking studies were performed. **Results.** AG administration effectively brought down the lipid levels induced by HCD. The lowered levels of Ox-LDL and LOX-1 in AG-administered rats deem it to be a potent antihypercholesterolemic agent. Compared to AV, AG had a pronounced effect in downregulating the expression of lipids evidenced by Oil Red O staining. AG binds with LOX-1 at a higher affinity validated by docking. **Conclusion.** This study validates AG to be an effective stratagem in bringing down the lipid stress induced by HCD and can be deemed as an antihypercholesterolemic agent.

1. Introduction

Atherosclerosis is a pathological condition characterized by lipid infiltration and plaque formation in the arteries. There are numerous risk factors associated with atherosclerosis: aging and age-associated changes in gene expression of the arterial wall have been proposed among the most important risk factors [1]. Age-associated arterial changes may contribute to the pathological events in atherosclerosis like hyperplasia, medial thickening, endothelial dysfunction that augments monocyte/endothelial adherence, enhanced endothelial cell apoptosis, and diminished vascular cell replicative capacity [2]. Hyperlipidaemia and reactive oxygen species formation (ROS) are the other important factors in the initi-

ation and progression of atherosclerosis [3]. Low-density lipoprotein (LDL) cholesterol is an established risk factor for coronary artery disease: in the presence of oxidative stress, these LDL particles get oxidized to form a lipoprotein species that is particularly atherogenic in nature. These oxidized-LDL contributes to the atherosclerotic plaque initiation and progression through a myriad of mechanisms which includes the induction of endothelial cell activation/dysfunction, macrophage-induced foam cell formation, and smooth muscle cell migration and proliferation [4]. The biological effects of Ox-LDL are mediated via a number of molecules such as scavenger receptor SR AI/II, SR B1, CD36, and LOX-1 [5]. Li et al. [6] are the pioneers in identifying that lectin-like oxidized low-density lipoprotein receptor 1

(LOX-1) is the critical molecule that is responsible for Ox-LDL uptake by endothelial cells. LOX-1 is a type II membrane protein comprising of four domains, and the c-terminal end residues and several conserved positively charged residues spanning the lectin domain are essential for Ox-LDL binding. Besides Ox-LDL, LOX-1 can recognize apoptotic/aged cells, activated platelets, and bacteria, implying versatile physiological functions [7]. The major contribution of LOX-1 to the atherogenic events has been confirmed in animal models. LOX-1 knockout mice exhibit reduced intimal thickness and inflammation and increased expression of protective factors [8]. On the contrary, LOX-1-overexpressing mice present an accelerated atherosclerotic lesion formation which is associated with increased inflammation [9]. LOX-1 activation by Ox-LDL causes endothelial changes that are characterized by the activation of nuclear factor- κ B through an increased reactive oxygen species, subsequent induction of adhesion molecules, and endothelial apoptosis [10]. Taken together, these findings support the possible contribution of LOX-1 in the pathogenesis of atherosclerosis, and identification of antagonists for LOX-1 might be a good therapeutic approach to vascular diseases.

Statins (3-hydroxy-3-methylglutaryl coenzyme A reductase inhibitors) are the first-line choice for lowering total and LDL cholesterol levels and they have been proven to reduce the risk of coronary artery disease. Recent data suggest that these compounds, in addition to their lipid-lowering ability, can also reduce the production of reactive oxygen species and increase the resistance of LDL to oxidation [11]. Clinical evidence also suggests that atorvastatin has been found to reduce the risk of cardiovascular disease by decreasing serum total cholesterol and low-density lipoprotein cholesterol in coronary artery diseases [12]. Studies by Biocca et al. [13] suggested the interaction of atorvastatin to LOX-1. Accordingly, atorvastatin has been selected to be the standard drug in the present study. Even though statins are the established treatment for hypercholesterolemia and cardiovascular diseases, they are associated with skeletal muscle, metabolic, neurological, and other possible side effects. This persuades us to look for an alternative therapy with lesser side effects and one that has a phytomedicine base [14]. Aegeline is a purified compound obtained from the leaf extract of the plant "*Aegle marmelos*." The plant has been explored extensively for the presence of bioactive compounds and for its therapeutics. However, aegeline is one among the compounds comparatively less explored for its potential in targeting LOX-1 and this study is among the first studies designed to explore that potential. Aegeline shows a structural similarity to that of beta 3 adrenergic receptor agonists [15] which have been found to have a significant role in lipolysis, which is why the current study was designed to harness this potential of aegeline.

2. Materials and Methods

2.1. Source of Chemicals. Aegeline was procured from Clear-synth Canada. Bovine serum albumin (BSA) and the primers for genes of interest were procured from Sigma-Aldrich,

USA. An iScript cDNA synthesis kit was purchased from Bio-Rad USA, and an enhanced chemiluminescence (ECL) kit was purchased from Millipore Corporation, USA. RPMI (Roswell Park Memorial Institute) 1640 medium with ATCC modification (2 mM L-glutamine, 10 mM HEPES, 1 mM sodium pyruvate, 4500 mg/l glucose, and 1500 mg/l sodium bicarbonate for use in incubators using 5% CO₂ in air), antibiotics, and fetal bovine serum were purchased from Invitrogen (Groningen, The Netherlands). Oil Red O was purchased from HiMedia Laboratories Pvt. Ltd. (India). All other chemicals used were of analytical grade and were obtained from Medox Biotech, India Pvt. Ltd. (Sisco Research Laboratories Pvt. Ltd. (SRL)), Genei Laboratories Pvt. Ltd., and CDH (Central Drug House Pvt. Ltd., Mumbai, India).

2.2. Animals. Male albino rats of wistar strain were obtained from the Central Animal House Facility, University of Madras, Taramani Campus, and experiments were conducted in accordance with guidelines approved by the Institutional Animal Ethical Committee (IAEC No. 01/19/2014). The animals were housed two per cage in large spacious cages under conditions of controlled temperature (25.2°C) with 12/12 h light/dark cycle and were given food and water *ad libitum*.

2.3. Study Design. The animals were divided into the following six groups with six animals in each group:

- (1) Group 1—control (3-month-old) rats fed with normal rat feed for 45 days
- (2) Group 2—aged-control (24-month-old) rats fed with normal rat feed for 45 days
- (3) Group 3—aged rats fed with HCD for 45 days
- (4) Group 4—aged rats fed with HCD for 45 days and supplemented with AG (20 mg/kg of body weight) for the last 30 days [16]
- (5) Group 5—aged rats fed with HCD for 45 days and supplemented with AV (1.5 mg/kg of body weight) for the last 30 days [17]
- (6) Group 6—aged rats fed with a normal diet and administered AG alone for the last 30 days (hypercholesterolemia was induced by HCD comprising normal rat chow supplemented with 4% cholesterol, 1% cholic acid, and 30% coconut oil [16])

At the end of the experimental period, rats were anesthetized with ketamine (22 mg/kg b.wt., i/p) and aorta were excised immediately, immersed in ice-cold physiological saline, and weighed. A 10% tissue homogenate was prepared by using Tris-HCl buffer (0.01 M) pH 7.4 for biochemical assays. The rest of the tissue was stored at -80°C for protein expression studies. Blood samples were collected by cardiac puncture into anticoagulant-containing and anticoagulant-free test tubes. Blood samples were kept at room temperature for 30 min, allowed to clot, and then centrifuged at 3000 rpm for 10 min to collect the serum. Plasma was collected by the centrifugation of the anticoagulated blood. Small sections

from each tissue were kept aside for histological studies. Part of the tissue was fixed in formalin (10% formaldehyde) for immunohistochemical analysis. Paraffin wax sections were prepared with the fixed tissues.

2.4. Lipid and Lipoprotein Profile. Total cholesterol (TC), triglycerides (TG), and high-density lipoproteins (HDL) in serum were assessed using commercial kits that spin react in a semiautomatic analyzer (RX Monza, Randox, UK).

2.4.1. LDL (Low-Density Lipoprotein) and VLDL (Very Low-Density Lipoprotein). LDL cholesterol was calculated according to the Friedwald formula:

$$\text{LDL} = \text{total cholesterol} - (\text{VLDL} + \text{HDL cholesterol}),$$

$$\text{VLDL (very low-density lipoprotein)} = \frac{\text{TG}}{5}. \quad (1)$$

The values of total cholesterol, triglycerides, HDL, VLDL, and LDL are expressed as mg/dl.

2.4.2. Atherogenic Index. AI was calculated as follows:

$$\text{AI} = \log \left(\frac{\text{TG}}{\text{HDL-C}} \right). \quad (2)$$

2.4.3. Free Fatty Acids. Tissue free fatty acids were estimated by the method of Hron and Menahan [18]. Free fatty acid content in tissue is expressed as $\mu\text{E/l}$.

2.5. Histopathological Studies. The histology of aorta was studied using haematoxylin and eosin (H&E) staining. A portion of the aorta tissue was fixed in 10% buffered formalin. The washed tissues were dehydrated in the descending grades of isopropanol and finally cleared in xylene. The tissues were then embedded in molten paraffin wax. Sections were cut at $5\ \mu\text{m}$ thickness and stained with haematoxylin and eosin. The sections were then viewed under a light microscope (Nikon "ECLIPSE E400" microscope, Japan) for histopathological changes.

2.6. Assay of Oxidized LDL by ELISA. The levels of Ox-LDL in serum were measured using ELISA as described by Crowther [19]. The levels are expressed as pg/ml.

2.7. Western Blot Analysis. The tissue homogenate was prepared in 50-100 μl of lysis buffer (with protease inhibitors) and centrifuged, and the supernatant was collected. Total tissue extracts containing 50-100 μg of protein samples were prepared in sodium dodecyl sulphate (SDS) sample buffer (Sigma-Aldrich) and were separated by SDS-electrophoresis on 10%-12% polyacrylamide gels, further transferred to a polyvinylidene difluoride (PVDF) membrane prior to immune detection, and subjected to western blot analysis. The antibodies against LOX-1 (goat anti-rabbit IgG-HRP conjugate, 1:1000) were purchased from Abcam and were used to detect protein levels in the aorta tissues. To verify the uniformity of the protein load and transfer efficiency across the test samples, membranes were reprobated with

beta-actin (Cell Signalling Technology, 1:1000 dilution). Immunoreactive bands were developed by Immobilon Western Chemiluminescent HRP Substrate (Millipore Corporation, Billerica, USA), visualized using an enhanced chemiluminescence system (ChemiDoc, Bio-Rad, USA), and presented in comparison to beta-actin expression.

2.8. Cell Culture. Monolayer cultures of IC-21 cells (NCCS, Pune, India) were cultured in RPMI 1640 with ATCC modification supplemented with 10% heat-inactivated fetal bovine serum (FBS) and antibiotics (mixture 1% penicillin/streptomycin/nystatin). Cells were incubated in T25 tissue culture flasks at 37°C in a humidified atmosphere (5% CO_2 and 95% air environment). Aegeline was dissolved in 0.1% DMSO, and Ox-LDL was suspended in PBS. Aegeline at a concentration of $10\ \mu\text{M}$ (based on a dose-fixation study) was used for the studies. The cells were then divided into five groups for various experiments to be performed (Group 1—IC-21 cells were maintained in RPMI 1640 without any treatment; Group 2—IC-21 cells were exposed to Ox-LDL at a concentration of $100\ \mu\text{g/ml}$ for 24 hours; Group 3—IC-21 cells were treated with aegeline followed by Ox-LDL at a concentration of $100\ \mu\text{g/ml}$ for 24 hours; Group 5—IC-21 cells were treated with atorvastatin ($20\ \mu\text{g}$) [20] followed by Ox-LDL at a concentration of $100\ \mu\text{g/ml}$ [21] for 24 hours; and Group 5—IC-21 cells were treated with aegeline alone.

2.9. Oil Red O Staining. Oil Red O staining was performed as prescribed by Lillie and Ashburn [22]. Cells were plated in 24-well tissue culture plates (Costar) at a density of 1×10^5 cells/ml and upon reaching subconfluence, the macrophages were incubated with Ox-LDL ($100\ \mu\text{g/ml}$) for 24 h, the medium was aspirated, and the cells were rinsed twice with 0.01 M PBS. Cells were fixed with 4% PFA for 10 min and then rinsed in PBS for 3 times. To this, 60% isopropanol was added and incubated for 5 min and rinsed. The working solution of Oil Red O stain was added and set aside for 5 min, then washed with PBS. Haematoxylin was added and allowed to stand for 1 min, and tissues were washed with PBS to remove residual stain. The slides were viewed under phase contrast microscope; lipids appeared red and the nuclei appeared blue.

2.10. In Silico Study. Geometry-optimized molecular structures for aegeline and atorvastatin were obtained using the iGEMDOCK (a generic evolutionary method for molecular docking) automated docking program. iGEMDOCK is a software used for integrated structure-based virtual screening, molecular docking, postscreening analysis, and visualization step. The 3-dimensional (3D) coordinates of four target proteins were selected and obtained from the protein data bank (PDB). The PDB id of LOX-1 (1YPQ) was selected for the in silico study. The 3D structure coordinates of each therapeutic target protein and ligand molecules were implemented through the GEMDOCK-graphical environment interface. Before doing docking analysis, the output path was set. GEMDOCK default parameters included the population size ($n = 200$), generation ($g = 70$), and number of solutions ($s = 10$) to compute the probable ligand-binding mechanism

TABLE 1: Aegeline alters the HCD-induced lipid anomaly in aged hypercholesterolemic rats.

Parameters	Group 1	Group 2	Group 3	Group 4	Group 5	Group 6
TC (mg/dl)	132.10 ± 9.37	207.59 ± 15.65 ^a	284.63 ± 21.34 ^{ab}	215.27 ± 22.61 ^c	220.44 ± 16.29 ^c	181.07 ± 13.39 ^b
VLDL (mg/dl)	19.02 ± 1.42	22.35 ± 1.71 ^a	27.01 ± 2.33 ^{ab}	24.35 ± 21.42 ^c	25.17 ± 2.25 ^c	20.14 ± 1.57 ^b
LDL (mg/dl)	72.71 ± 5.68	152.13 ± 12.37 ^a	235.84 ± 22.43 ^{ab}	161.01 ± 14.46 ^c	167.94 ± 5.58 ^c	122.32 ± 10.98 ^b
HDL (mg/dl)	40.37 ± 3.14	33.11 ± 3.01 ^a	21.79 ± 2.15 ^{ab}	29.91 ± 2.37 ^c	27.33 ± 2.55 ^c	37.27 ± 1.86 ^b
TG (mg/dl)	95.12 ± 7.63	111.75 ± 9.52 ^a	135.22 ± 14.81 ^{ab}	121.73 ± 11.56 ^c	125.88 ± 12.81 ^c	100.81 ± 9.30 ^b
FFA (μE/l)	211.27 ± 15.84	279.81 ± 25.51 ^a	322 ± 33.83 ^{ab}	291.52 ± 29.21 ^c	295.19 ± 23.61 ^c	252.36 ± 24.19 ^b
Atherogenic index	0.37	0.527	0.792	0.608	0.663	0.431

Atherogenic index was calculated according to the following formula: $\log(TG/HDL - C)$. Each value represents mean ± SEM for six rats in each group. Values are statistically significant at the level of $p < 0.05$. ^aGroup 2 compared with Group 1. ^{ab}Group 3 compared with Group 1 and Group 2. ^cGroup 4 compared with Group 3. Group 5 compared with Group 3. Group 6 compared with Group 2. Group 1: young control; Group 2: aged control; Group 3: aged+HCD; Group 4: aged+HCD+aegeline; Group 5: aged+HCD+atorvastatin; Group 6: aged+aegeline.

for each target protein LOX-1. Then the docking run was started using a GEMDOCK scoring function. After docking, the individual binding pose of each ligand was observed and their binding affinity with the target proteins were analyzed. Visual examination of the predicted binding geometries (docking poses) thereby contributes crucially to the further development of a lead compound. In the postdocking screening, the best-binding pose and total energy of each ligand were analyzed. The details of the best-binding pose and total energy values were saved in an output folder. The protein-ligand binding site was analyzed and visualized by using PyMOL.

3.11. Statistical Analysis. Data are presented as mean ± standard error of mean (SEM) of the results obtained from the average of at least three to six independent experiments. Results were analyzed by one-way analysis of variance (ANOVA) using the SPSS software package for Windows (version 20.0; SPSS Inc., Chicago, IL, USA) and p values were determined using the Student-Newman-Keuls and least significant difference post hoc tests. Differences among means were considered statistically significant when the p value was less than 0.05.

3. Results (In Vivo)

3.1. Serum Lipid and Lipoprotein Profile. Table 1 shows the impact of aegeline on the serum lipid profile of experimental groups. Assessment of the serum lipid profile in the present study reveals that there was a significant ($p < 0.05$) increase in the levels of serum total cholesterol (1.37-fold), triglycerides (1.21-fold), LDL (1.55-fold), VLDL (1.22-fold), and free fatty acids (FFA) (1.15-fold) along with a concomitant decrease in HDL (1.57-fold) in HCD-alone-fed aged rats when compared to the aged control rats. Aegeline and atorvastatin supplementation to HCD-fed rats demonstrated a significant decline ($p < 0.05$) in serum total cholesterol, triglycerides, LDL, VLDL, and FFA with a concomitant increase ($p < 0.05$) in HDL, when compared to the HCD-alone-fed group. Moreover, it was observed that aegeline and atorvastatin have almost similar beneficial effects on reducing lipid levels in the serum. The atherogenic index was found to reach

the maximum in the HCD-fed groups as expected, and aegeline and atorvastatin were capable of bringing down the atherogenic index to normal levels.

3.2. Histopathological Studies. The haematoxylin and eosin staining in the aorta sections of rats is shown in Figure 1. The young control group showed normal tissue architecture, such as even thickness and inner and outer elastic plates with no signs of lipid deposition or necrosis. The aged control group had shown deterioration in tissue architecture with a considerable increase in tissue thickness, whereas the HCD-fed group showed a necrotic core in tunica media which could possibly mean lipid deposition and cell vacuolization. The illustration in Figure 2 is a pictorial representation showing the lipid accumulation in the HCD artery. Aegeline treatment to HCD-challenged rats showed no signs of abnormal architecture in the tunica intimal and medial layers. Though there were small signs of cellular vacuolization in atorvastatin-treated rats, there was no increase in thickness of the intimal layer as observed in the microscopic image. The aegeline-alone-treated aorta of aged rats showed no changes in the aortic architecture.

3.3. Assay of Ox-LDL by ELISA. Figure 3 displays the levels of Ox-LDL in the serum of various experimental groups. The assessment of the serum levels of Ox-LDL in HCD-fed rats revealed that there was a significant increase (2.66-fold) when compared to that of aged control rats. On the other hand, supplementation of aegeline/atorvastatin to HCD-fed rats brought down the serum levels of Ox-LDL when compared to HCD-alone-fed rats by 1.52- and 1.72-fold, respectively.

3.4. AG and AV: Effect on the Protein Expression Profile of LOX-1. The levels of scavenger receptor LOX-1 in the aorta of different experimental animals are depicted in Figure 4. LOX-1 levels were increased by 58.73% and 161.30% in aged control and HCD-fed rats when compared to the young rats. Drug treatments significantly brought down the levels comparable to that of the aged control rats with a greater percentage reduction observed with aegeline (31.05%) than atorvastatin (22.70%).

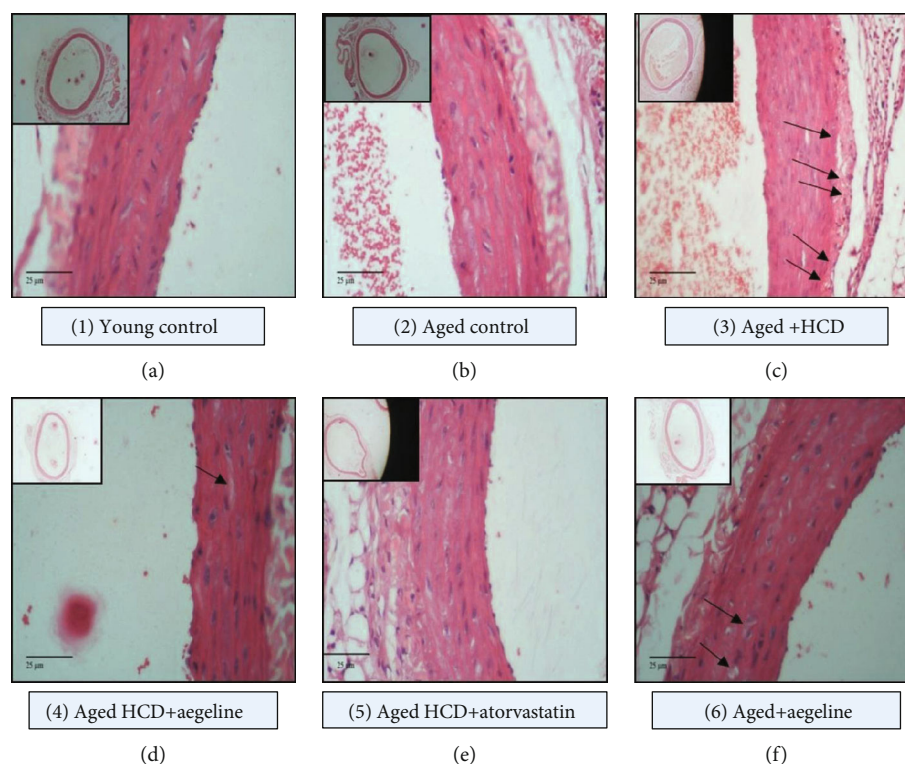


FIGURE 1: Histopathological sections of aorta in various experimental groups fed with HCD and the efficacy of aegeline (20x). Light microscopic analysis of the pathological H&E-stained aorta sections of rats (20x). (a) Young control (Group 1): aorta shows normal tissue architecture such as even thickness and inner and outer elastic plates with no signs of lipid deposition or necrosis. (b) Aged control (Group 2): aorta shows lean deterioration in the tissue architecture with considerable increase in tissue thickness. (c) Aged+HCD (Group 3): aorta shows necrotic core in tunica media which could possibly mean lipid deposition and cell vacuolization. (d) Aged+HCD+aegeline (Group 4): aorta shows no signs of abnormal architecture in the tunica intima and medial layers; however, there is mild cell vacuolization. (e) Aged+HCD+atorvastatin (Group 5): aorta shows lean deterioration in the tissue architecture and cell vacuolization. (f) Aged+aegeline (Group 6): aorta shows thin and smooth vessel wall with even thickness.

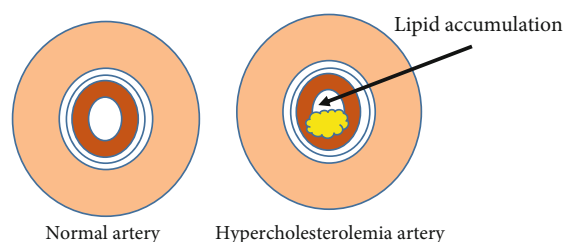


FIGURE 2: The pictorial representation of normal and HCD-challenged artery.

3.5. In Vitro

3.5.1. Oil Red O Staining. Figure 5 represents the Oil Red O staining of IC-21 cells, where Group 1 control cells showed normal nuclear morphology with no signs of lipid staining in the cytoplasm of cells. In cells incubated with Ox-LDL (Group 2), there was an observed red staining in the cytoplasm and around the nucleus, which is a positive sign of foam cell formation. On the other hand, aegeline (Group 3) showed less Oil Red O staining in the cytoplasm. However, atorvastatin treatment showed Oil Red O uptake with lowered significance as compared to aegeline. Aegeline-alone-treated cells showed normal cellular morphology.

3.6. Result of LOX-1 Docking Studies

3.6.1. Results of In Silico Studies. Docking studies have been carried out by taking 1VKX to understand the nature of the interaction of aegeline and atorvastatin with LOX-1. Performing a stable docking procedure in iGEMDOCK by taking LOX-1 as a target with aegeline resulted in the most stable drug receptor complex with a LOX-1-aegeline docking score of -95.28 kcal/mol (Figure 6(a)) and an atorvastatin docking score of -74.04 kcal/mol (Figure 6(b)). The docking of aegeline with oxidized-LDL receptors exhibited a strong interaction, and the results showed that aegeline has extensive interactions with Ile-149, Gln-193, Ala-194, Asp-147, Phe-158, and Try-197 of one subunit and Gln-193, Tyr-197, and Asp-147 of another subunit of a LOX-1 homodimer with a fitness score of -95.3 kcal/mol.

4. Discussion

4.1. Effect of Aegeline on HCD-Induced Lipid Abnormalities. Being overweight or obese is associated with alterations in plasma lipids and a broad spectrum of cardiometabolic disorders, including an increase in plasma low-density lipoprotein cholesterol (LDL-C) and triglyceride (TG) concentrations

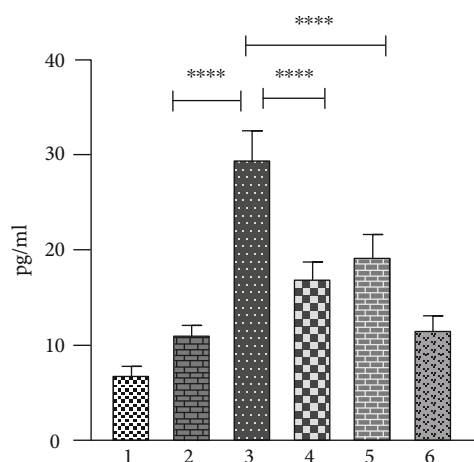


FIGURE 3: Aegeline mitigates the HCD-induced increase in the levels of serum Ox-LDL in aged experimental rats. Each bar represents mean \pm SEM for six rats in each group. Values are statistically significant at the level of $p < 0.05$, where Group 2 is compared with Group 1 and Group 3 is compared with Group 2. Groups 4 and 5 are compared with Group 3, and Group 6 is compared with Group 2. Group 1: young control; Group 2: aged control; Group 3: aged+HCD; Group 4: aged+HCD+aegeline; Group 5: aged+HCD+atorvastatin; Group 6: aged+aegeline.

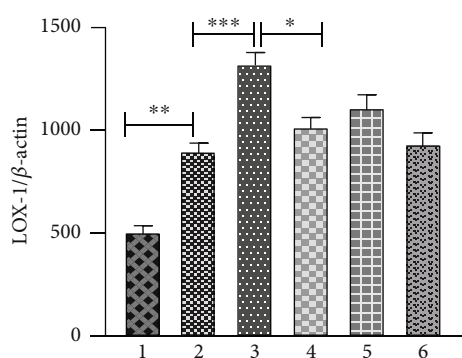
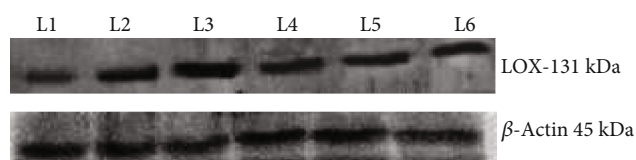


FIGURE 4: Effect of aegeline on the expression of scavenger receptors in the aorta of aged rats fed with HCD. Each bar represents mean \pm SEM for six rats in each group. Values are statistically significant at the level of $p < 0.05$, where Group 2 is compared with Group 1 and Group 3 is compared with Group 2. Groups 4 and 5 are compared with Group 3, and Group 6 is compared with Group 2. Group 1: young control; Group 2: aged control; Group 3: aged+HCD; Group 4: aged+HCD+aegeline; Group 5: aged+HCD+atorvastatin; Group 6: aged+aegeline.

[16, 23]. On analysis of the lipid profile, we found that total cholesterol and LDL cholesterol were significantly high in the aged group when compared to young control rats. Ele-

vated plasma LDL-C levels represent one of the key causal factors for the development of atherosclerosis and subsequent coronary artery disease [4]. In addition, the studies have also found a gradual decline in the fractional clearance of LDL from the circulation with age and reduced expression of hepatic LDLRs with increasing age in some species [16, 24]. In the present study, rats fed with HCD exhibited high levels of LDL, VLDL, triglycerides, total cholesterol, and free fatty acids (FFA) in serum as compared to aged rats fed with a normal diet. Similar alterations in lipid and lipoprotein parameters in rats fed with HCD have been reported in earlier studies [16, 23] and the observed increase in the cholesterol levels in HCD-fed rats may be due to the presence of cholic acid in the diet, which might have been a responsible factor for the increased absorption of cholesterol in the intestine [16]. The supplementation of a high-cholesterol diet also reduced the HDL cholesterol levels, which is in corroboration with the available literature that state that increased levels of atherogenic lipids with a concomitant decrease in HDL is a characteristic feature observed in high-cholesterol-diet-fed rats [16]. The observed increased levels of cholesterol, LDL, and VLDL are also reflected in the atherogenic index calculated in the current study. The hypocholesterolemic activity of atorvastatin, a statin by origin, has been attributed to its multifaceted efficacy in modulating cholesterol metabolism. Moreover, Liu et al. [17] have demonstrated that the hypocholesterolemic activity of atorvastatin is mainly attributed to its ability to inhibit or decrease the production of apoB-containing lipoproteins. Not only aegeline as observed in the current study but even its other derivatives obtained from the *Aegle marmelos* plant have also been shown to have anti-hyperlipidemic activities [15]. The leaf extract of *Aegle marmelos* is shown to exert an antihyperlipidemic potential in HCD rats, where there is altered lipid metabolism [22]. Aegeline has also been shown to possess both anti-inflammatory and antihyperlipidemic activity as observed in our previous study in fatty liver conditions [16]. Hence, both aegeline and atorvastatin decrease the atherogenic risk, thereby affording cardioprotection. Moreover, the efficacy of aegeline in combating hypercholesterolemia is more or less similar to that of atorvastatin.

4.2. Effect of Aegeline on HCD-Induced Atherosclerotic Plaque Progression. In concordance with the above observations on lipid anomalies in HCD-fed rats, the histological findings in this study on the aortic wall demonstrated that there was an increase in the tunica medial thickness most probably due to lipid deposition in the aorta. The thickening of the aortic intima is one of the key features of atherosclerosis and correlated well with the biochemical parameters observed in atherogenic-diet-fed rats. Zhou et al. [25] have also reported that HCD feeding to rats results in a marked thickening of the intima. Carotid intima thickness measurements have been commonly used in observational studies as a marker for atherosclerosis to evaluate its determinants and consequences in various populations [26]. These effects were abrogated with the administration of atorvastatin for 30 days. A study done by Taylor et al. [27] has stated that atorvastatin had a significant impact on the reduction of intima-media

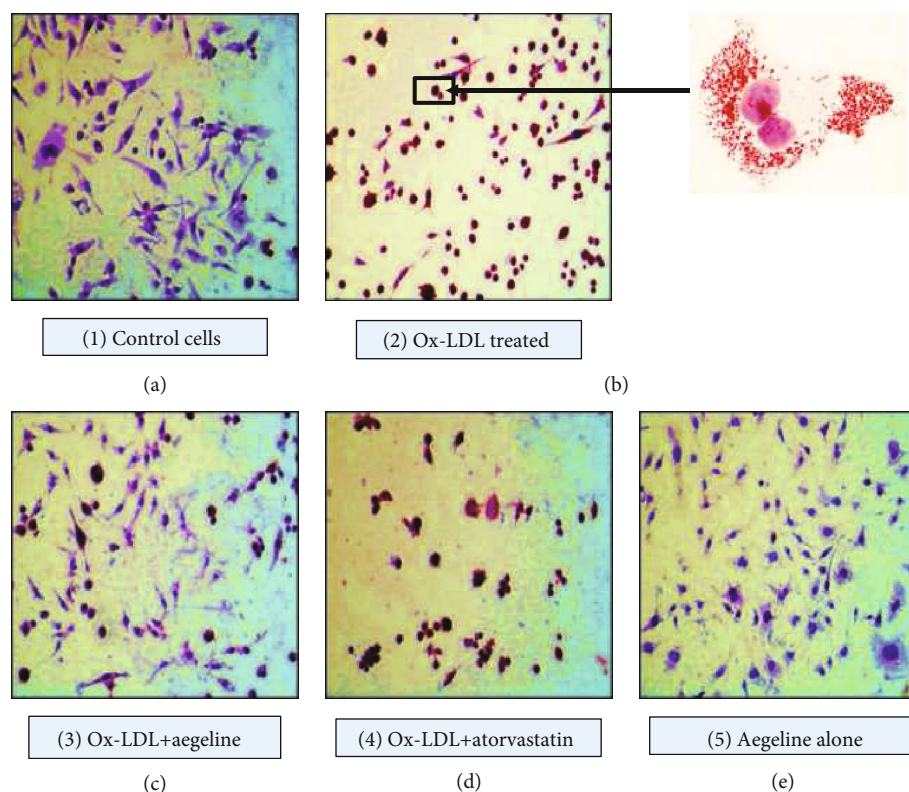


FIGURE 5: Oil Red O lipid staining in IC-21 cells treated with Ox-LDL and the lipid-lowering effect of aegeline.

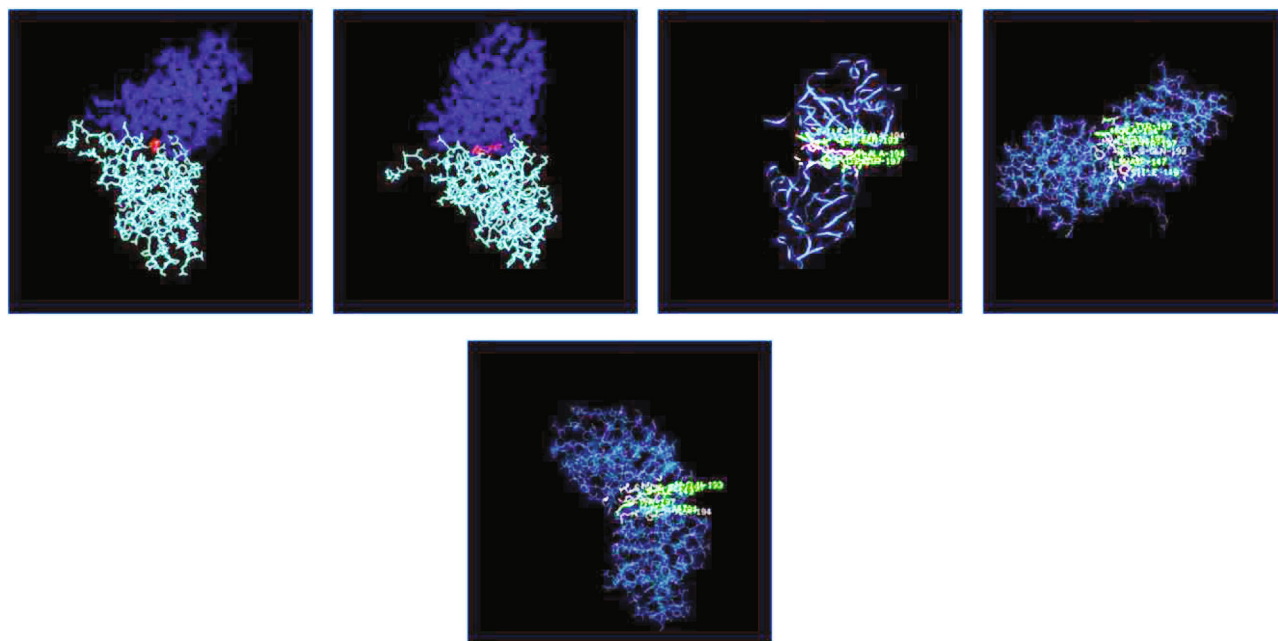
thickness. Another follow-up study has shown that statin drugs including atorvastatin were seen to reduce carotid intima-media thickness along with soft plaque regression [28]. On aegeline supplementation, the intima was found to be near normal.

Both atorvastatin and aegeline have shown anti-inflammatory action [16], and so it might improve endothelial function. An improvement in endothelial function would have resulted in a reduction of intimal thickness.

4.3. Effect of Aegeline on Serum Ox-LDL. When oxidative stress is present, ROS may modify or damage lipids, proteins, and DNA with deleterious consequences for vascular function and structure [29]. LDL is one such lipoprotein more susceptible to oxidative modifications, and several studies performed over the past decade illustrate that the oxidatively modified form of LDL is more accountable than native LDL in the progression of atherogenesis [4]. Our studies also have identified Ox-LDL levels to be high in the serum of HCD-fed rats which is in concurrence with the available literature [5]. According to the classical hypothesis, Ox-LDL accumulates in the atherosclerotic lesions over a prolonged period of time. But recent studies carried out with aged rats show changes in the level of Ox-LDL, and this signifies the dynamics of the Ox-LDL state that it can equilibrate between circulation and tissues [30]. Hence, the increased Ox-LDL levels in the plasma of HCD-fed rats is the true reflection of the pathogenic process that occurs in the rat aorta. Retention of LDL in the vessel wall with subsequent oxidation is also considered to be an important event in the early stages of an athero-

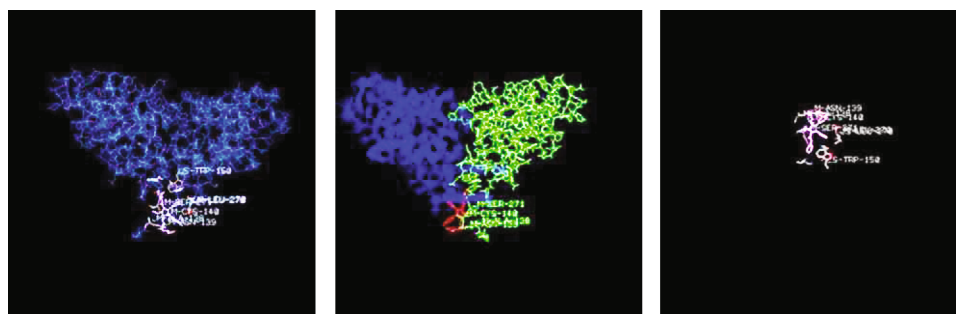
sclerotic lesion playing a key role in endothelial dysfunction and atherogenesis. Oxidized LDL, in fact, activates endothelial cells by inducing the expression of several cell surface adhesion molecules which mediate the rolling and adhesion of blood leukocytes (monocytes and T cells); after adhesion to the endothelium, leukocytes migrate into the intima in response to chemokines. Monocytes then differentiate into macrophages that upregulate both Toll-like receptors (TLRs) and scavenger receptors (SRs) that internalize Ox-LDL, leading to lipid accumulation and foam cell formation [5]. Therefore, increased levels of Ox-LDL might be responsible for initiating the events involved in plaque formation as substantiated by intimal thickness in the HCD-fed animal aortas. Aegeline or atorvastatin supplementation has brought down the serum levels of Ox-LDL in rats challenged with HCD. In vitro studies conducted by Sarkar et al. [31] have identified that structural analogs of aegeline are potent inhibitors of LDL oxidation. However, so far no reports have been stated with reference to the impact of aegeline on serum levels of oxidized LDL. On the other hand, Fuhrman et al. [32] have reported that atorvastatin therapy decreases serum lipid and Ox-LDL levels. It is obvious from our observations that aegeline mitigates cholesterol-mediated ROS to a greater extent by reducing the levels of cholesterol by its anti-hypercholesterolemic effect indirectly, since it was able to reduce the levels of Ox-LDL.

4.4. Effect of Aegeline on Receptors of Ox-LDL. The mechanism of Ox-LDL uptake is widely studied. Early work suggested that the uptake of oxidized LDL occurs via a



Compound	Energy	H-S GLN 193	H-S TYR 197	H-M ASP 147	V-S ILE 149	V-M GLN 193	V-S GLN 193	V-M ALA 194	V-M ASP 147	V-S PHE 158	V-M ALA 194	V-S TYR 197
<input checked="" type="checkbox"/> 1yxk-aegeline-8.pdb	-95.3	<input checked="" type="checkbox"/>	<input checked="" type="checkbox"/>	<input checked="" type="checkbox"/>	<input checked="" type="checkbox"/>	<input checked="" type="checkbox"/>	<input checked="" type="checkbox"/>	<input checked="" type="checkbox"/>	<input checked="" type="checkbox"/>	<input checked="" type="checkbox"/>	<input checked="" type="checkbox"/>	<input checked="" type="checkbox"/>
Compound		Energy			VDW			Hbond		Elec		
<input checked="" type="checkbox"/> 1yxk-aegeline-8.pdb		-95.28			-83.29			-11.99		0		

(a)



Compound	Energy	V-S TRP 150	V-M LEU 270	V-S LEU 270	V-M ALA 138	V-M ASN 139	V-M CYS 140	V-M SER 271	
<input checked="" type="checkbox"/> 1yxk-atorvastatin-0.pdb	-74	<input checked="" type="checkbox"/>	<input checked="" type="checkbox"/>	<input checked="" type="checkbox"/>	<input checked="" type="checkbox"/>	<input checked="" type="checkbox"/>	<input checked="" type="checkbox"/>	<input checked="" type="checkbox"/>	
Compound		Energy			VDW		HBond		Elec
<input checked="" type="checkbox"/> 1yxk-atorvastatin-0.pdb		-74.04			-74.04		0		0

(b)

FIGURE 6: (a) Molecular docking of LOX-1 with aegeline. (b) Molecular docking of LOX-1 with atorvastatin.

scavenger receptor, the lectin-like oxidized low-density lipoprotein receptor-1 (LOX-1) [5]. LOX-1 has been identified first in endothelial cells as the major Ox-LDL receptor; however, also macrophages and smooth muscle cells express LOX-1 together with other scavenger receptors, altogether contributing to the induction of endothelial dysfunction by

several mechanisms [5]. The potential role of LOX-1 in the pathogenesis of atherosclerosis includes endocytosis of Ox-LDL, expression colocalization with atherosclerosis enhanced by risk factors of atherosclerosis. The present study has demonstrated the enhanced manifestation in the levels of LOX-1 in aged and aged HCD rats concomitant with the previous

studies which state that there is upregulated LOX-1 expression in the endothelium of HCD-fed rabbits [33]. Macrophages bind and internalize Ox-LDL through CD36, and thus activated macrophages secrete oxidants, including myeloperoxidase, which oxidizes LDL, and thus enlarges the pool of Ox-LDL [5]. Our studies have shown that both atorvastatin and aegeline are able to reduce the expression of LOX-1 in aged and aged HCD-fed rats.

4.5. Aegeline Augments Foam Cell Formation Induced by Ox-LDL. Macrophage-derived foam cell formation is the early hallmark of atherogenesis. Hence, we wanted to study the effect of aegeline and atorvastatin on foam cell formation in IC-21 macrophage cells. Oil Red O staining of IC-21 cells showed normal nuclear morphology with no signs of lipid staining in the cytoplasm. However, when cells were incubated with Ox-LDL, they showed the positive staining of Oil Red O inside the cytosol due to the uptake of Ox-LDL inside these cells. This is in corroboration with the previous study conducted by Yang et al. [33] stating that incubating macrophage cells with Ox-LDL resulted in extensive lipid accumulation in the cytosol. Aegeline/atorvastatin treatment has greatly reduced lipid accumulation in macrophage cells. These observations explicitly show that aegeline not only reduces Ox-LDL formation but also regulates the uptake of the same. One mechanism by which it can do this is by downregulating the scavenger receptor, for which data from in vivo studies support its downregulation (Figure 4). On the other hand, it might prevent the interaction between LOX-1 and Ox-LDL by binding to LOX-1. Hence, molecular docking studies were carried out using iGEMDOCK to find out if there is any interaction between LOX-1 and aegeline. LOX-1 is a protein that is made up of 273 residues comprising four domains. The first 36 residues form the cytoplasmic tail followed by a single transmembrane domain made up of amino acids from 37 to 58 and an extracellular region containing two domains, the first one comprising residues from 58 to 142 and the second from 143 to 273 which is a C-type lectin-like domain (CTLD) responsible for Ox-LDL recognition. Aegeline specifically has interaction with the CTLD domain. Francone et al. [34] have reported that mutations of certain residues present in the tunnel, particularly Ile-149, impair binding to Ox-LDL, confirming the crucial role of the tunnel in ligand interaction and binding. Furthermore, Biocca et al. [13] have docked atorvastatin with LOX-1 and found that Ile-149 of LOX-1 interacts with statins and Ile-149 is always involved in the stability of contact with these drugs. Point mutations on Ile-149, which point to the empty space in the center of the tunnel, markedly reduce the binding of Ox-LDL and a series of oxidized phospholipids. The “clamp motion” mechanism, which is hypothesized as a mechanism for Ox-LDL catching, is only observed in the absence of ligands and blocked when the CTLD hydrophobic tunnel is filled. Docking results showed that aegeline has extensive interaction with Ile-149, Gln-193, Ala-194, Asp-147, Phe-158, and Try-197 of one subunit and Gln-193, Tyr-197, and Asp-147 of another subunit of the LOX-1 homodimer with a fitness score of -95.3. Aegeline also binds to Ile-149 indicating a stable interaction. Docking atorva-

statin with LOX-1 has docking energy of -74.04 which is slightly lower than that of aegeline with LOX-1, thereby showing more favorable binding than the statin drug. Hence, LOX-1 seems to be an attractive target for the therapy of a number of cardiovascular diseases. In this regard, aegeline has a tremendous potential to inhibit LOX-1 which needs to be further explored.

5. Summary/Conclusion

Aegeline at a concentration of 20 mg/kg body weight is effective in reducing the lipid anomalies in aged hypercholesterolemic rats when compared to atorvastatin by targeting LOX-1 as observed in western blot and docking studies. Aegeline had a pronounced effect in downregulating the expression of lipids evidenced by oxidized-LDL expression and Oil Red O staining. This study validates aegeline as a potent anti-hypercholesterolemic agent.

Abbreviations

CAD:	Coronary artery disease
CTLD:	C-type lectin-like domain
CVD:	Cardiovascular disease
ELISA:	Enzyme-linked immunosorbent assay
HCD:	High-cholesterol diet
HDL:	High-density lipoprotein
H&E:	Haematoxylin and eosin
IC-21:	Infected cell passage number 21
LDL:	Low-density lipoprotein
LOX:	Oxidized low-density lipoprotein receptor
Ox-LDL:	Oxidized low-density lipoprotein
PBS:	Phosphate-buffered saline
RPMI:	Roswell Park Memorial Institute
VLDL:	Very low-density lipoprotein.

Data Availability

The data used to support the findings of this study are included within the article.

Ethical Approval

All experiments were performed in accordance with the guidelines approved by the Institutional Animal Ethical Committee (IAEC No: 01/19/2014).

Conflicts of Interest

The authors declare that they have no potential conflict of interest including any financial and personal relationships with other people or organizations.

Authors' Contributions

Dr. Abhilasha Singh, the first author, designed and executed the experimental work; collected, analyzed, and interpreted the data; and drafted the manuscript. Dr. Ashok Kumar S. assisted with the in vitro experiment and docking studies. Dr. Lakshmi Narasimhan assisted with the in vivo

experiment and Dr. Kalaiselvi Periandavan conceived the idea, provided directions for designing the experiments, and supervised the entire work.

Acknowledgments

The financial assistance to Dr. Abhilasha Singh, Department of Medical Biochemistry, from the UPE-PHASE II and UGC-BSR Fellowship, New Delhi, Government of India, is gratefully acknowledged.

Authors greatly appreciate Dr. Kishore Kumar Narasimhan and Raj Moyal for assisting with formatting the manuscript.

References

- [1] C. Wanner, K. Amann, and T. Shoji, "The heart and vascular system in dialysis," *The Lancet*, vol. 388, no. 10041, pp. 276–284, 2016.
- [2] W. Zhu, B. C. Kim, M. Wang et al., "TGF β 1 reinforces arterial aging in the vascular smooth muscle cell through a long-range regulation of the cytoskeletal stiffness," *Scientific Reports*, vol. 8, no. 1, p. 2668, 2018.
- [3] D. A. Chistiakov, A. N. Orekhov, and Y. V. Bobryshev, "Contribution of neovascularization and intraplaque haemorrhage to atherosclerotic plaque progression and instability," *Acta Physiologica*, vol. 213, no. 3, pp. 539–553, 2015.
- [4] T. Head, S. Daunert, and P. J. Goldschmidt-Clermont, "The aging risk and atherosclerosis: a fresh look at arterial homeostasis," *Frontiers in Genetics*, vol. 8, 2017.
- [5] N. Di Pietro, G. Formoso, and A. Pandolfi, "Physiology and pathophysiology of oxLDL uptake by vascular wall cells in atherosclerosis," *Vascular Pharmacology*, vol. 84, pp. 1–7, 2016.
- [6] C. Li, J. Zhang, H. Wu et al., "Lectin-like oxidized low-density lipoprotein receptor-1 facilitates metastasis of gastric cancer through driving epithelial-mesenchymal transition and PI3K/Akt/GSK3 β activation," *Scientific Reports*, vol. 7, 2017.
- [7] X. Xie, L. Zhang, Y. Lin et al., "Imiquimod induced ApoE-deficient mice might be a composite animal model for the study of psoriasis and dyslipidaemia comorbidity," *Journal of Dermatological Science*, vol. 88, no. 1, pp. 20–28, 2017.
- [8] Z. Ding, S. Liu, X. Wang et al., "Cross-talk between LOX-1 and PCSK9 in vascular tissues," *Cardiovascular Research*, vol. 107, no. 4, pp. 556–567, 2015.
- [9] W. Xie, L. Li, M. Zhang et al., "MicroRNA-27 prevents atherosclerosis by suppressing lipoprotein lipase-induced lipid accumulation and inflammatory response in apolipoprotein E knockout mice," *PLoS One*, vol. 11, no. 6, 2016.
- [10] K. T. Ji, L. Qian, J. L. Nan et al., "Ox-LDL induces dysfunction of endothelial progenitor cells via activation of NF- κ B," *BioMed Research International*, vol. 2015, Article ID 175291, 8 pages, 2015.
- [11] M. Margaritis, F. Sanna, and C. Antoniades, "Statins and oxidative stress in the cardiovascular system," *Current Pharmaceutical Design*, vol. 23, 2017.
- [12] R. K. Wadhera, D. L. Steen, I. Khan, R. P. Giugliano, and J. M. Foody, "A review of low-density lipoprotein cholesterol, treatment strategies, and its impact on cardiovascular disease morbidity and mortality," *Journal of Clinical Lipidology*, vol. 10, no. 3, pp. 472–489, 2016.
- [13] S. Biocca, F. Iacovelli, S. Matarazzo et al., "Molecular mechanism of statin-mediated LOX-1 inhibition," *Cell Cycle*, vol. 14, no. 10, pp. 1583–1595, 2015.
- [14] P. D. Thompson, G. Panza, A. Zaleski, and B. Taylor, "Statin-associated side effects," *Journal of the American College of Cardiology*, vol. 67, no. 20, pp. 2395–2410, 2016.
- [15] S. Rajan, S. Satish, K. Shankar et al., "Aegeline inspired synthesis of novel β 3-AR agonist improves insulin sensitivity *in vitro* and *in vivo* models of insulin resistance," *Metabolism*, vol. 85, pp. 1–3, 2018.
- [16] A. Singh, S. Gowtham, L. N. Chakrapani et al., "Aegeline vs Statin in the treatment of Hypercholesterolemia: A comprehensive study in rat model of liver steatosis," *Functional Foods in Health and Disease*, vol. 8, no. 1, pp. 1–16, 2018.
- [17] M. W. Liu, R. Liu, H. Y. Wu et al., "Atorvastatin has a protective effect in a mouse model of bronchial asthma through regulating tissue transglutaminase and triggering receptor expressed on myeloid cells-1 expression," *Experimental and Therapeutic Medicine*, vol. 14, no. 2, pp. 917–930, 2017.
- [18] W. T. Hron and L. A. Menahan, "A sensitive method for the determination of free fatty acids in plasma," *Journal of Lipid Research*, vol. 22, no. 2, pp. 377–381, 1981.
- [19] J. R. Crowther, *The ELISA Guidebook*, Springer Science & Business Media, 2000.
- [20] H. Xiao, Q. Zhang, Y. Lin, B. S. Reddy, and C. S. Yang, "Combination of atorvastatin and celecoxib synergistically induces cell cycle arrest and apoptosis in colon cancer cells," *International Journal of Cancer*, vol. 122, no. 9, pp. 2115–2124, 2008.
- [21] Y. Chen, M. Chen, Z. Wu, and S. Zhao, "Ox-LDL induces ER stress and promotes the adipokines secretion in 3T3-L1 adipocytes," *PLoS One*, vol. 8, no. 10, 2013.
- [22] R. D. Lillie and L. L. Ashburn, "Supersaturated solutions of fat stains in dilute isopropanol for demonstration of acute fatty degeneration not shown by Herxheimer's technique," *Archives Pathology*, vol. 36, pp. 432–440, 1943.
- [23] A. Singh, L. N. Chakrapani, S. Ashok Kumar et al., "Ethanol extract of *Aegle marmelos* mediates its hypocholesterolemic effect by retarding circulatory oxidized LDL formation via 12/15 lipoxygenase pathway," *European Journal of Biomedical and Pharmaceutical Sciences*, vol. 4, no. 7, pp. 412–423, 2017.
- [24] H. H. Liu and J. J. Li, "Aging and dyslipidemia: a review of potential mechanisms," *Ageing Research Reviews*, vol. 19, pp. 43–52, 2015.
- [25] J. M. Zhou, H. M. Wang, Y. Z. Lv, Z. Z. Wang, and W. Xiao, "Anti-atherosclerotic effect of Longxuetongluo capsule in high cholesterol diet induced atherosclerosis model rats," *Biomedicine & Pharmacotherapy*, vol. 97, pp. 793–801, 2018.
- [26] G. Asghari, P. Dehghan, P. Mirmiran et al., "Insulin metabolism markers are predictors of subclinical atherosclerosis among overweight and obese children and adolescents," *BMC Pediatrics*, vol. 18, no. 1, p. 368, 2018.
- [27] A. J. Taylor, S. M. Kent, P. J. Flaherty, L. C. Coyle, T. T. Markwood, and M. N. Vernalis, "ARBITER: Arterial Biology for the Investigation of the Treatment Effects of Reducing Cholesterol: a randomized trial comparing the effects of atorvastatin and pravastatin on carotid intima medial thickness," *Circulation*, vol. 106, no. 16, pp. 2055–2060, 2002.
- [28] E. De Groot, S. I. Van Leuven, R. Duivenvoorden et al., "Measurement of carotid intima-media thickness to assess progression and regression of atherosclerosis," *Nature Reviews Cardiology*, vol. 5, no. 5, 2008.

- [29] S. Menini, C. Iacobini, C. Ricci, C. B. Fantauzzi, and G. Pugliese, "Protection from diabetes-induced atherosclerosis and renal disease by D-carnosine-octylester: effects of early vs late inhibition of advanced glycation end-products in ApoE-null mice," *Diabetologia*, vol. 58, no. 4, pp. 845–853, 2015.
- [30] C. M. Shih, F. Y. Lin, J. S. Yeh et al., "Dysfunctional high density lipoprotein failed to rescue the function of oxidized low density lipoprotein-treated endothelial progenitor cells: a novel index for the prediction of HDL functionality," *Translational Research*, vol. 205, pp. 17–32, 2019.
- [31] S. Sarkar, R. Sonkar, G. Bhatia, and N. Tadigoppula, "Synthesis of new N-acryl-1-amino-2-phenylethanol and N-acyl-1-amino-3-aryloxypropanols and evaluation of their antihyperlipidemic, LDL-oxidation and antioxidant activity," *European Journal of Medicinal Chemistry*, vol. 80, pp. 135–144, 2014.
- [32] B. Fuhrman, L. Koren, N. Volkova, S. Keidar, T. Hayek, and M. Aviram, "Atorvastatin therapy in hypercholesterolemic patients suppresses cellular uptake of oxidized-LDL by differentiating monocytes," *Atherosclerosis*, vol. 164, no. 1, pp. 179–185, 2002.
- [33] X. Yang, J. Zhang, L. Chen et al., "The role of UNC5b in ox-LDL inhibiting migration of RAW264.7 macrophages and the involvement of CCR7," *Biochemical and Biophysical Research Communications*, vol. 505, no. 3, pp. 637–643, 2018.
- [34] O. L. Francone, M. Tu, L. J. Royer et al., "The hydrophobic tunnel present in LOX-1 is essential for oxidized LDL recognition and binding," *Journal of Lipid Research*, vol. 50, no. 3, pp. 546–555, 2009.

Research Article

Can Lipoic Acid Attenuate Cardiovascular Disturbances Induced by Ethanol and Disulfiram Administration Separately or Jointly in Rats?

Anna Bilska-Wilkosz ¹, Magdalena Kotańska ², Magdalena Górný,¹ Barbara Filipek ², and Małgorzata Iciek¹

¹Chair of Medical Biochemistry, Jagiellonian University, Medical College, 7 Kopernika Street, PL 31-034 Kraków Poland

²Department of Pharmacodynamics, Jagiellonian University, Medical College, 9 Medyczna Street, PL 30-688 Kraków, Poland

Correspondence should be addressed to Anna Bilska-Wilkosz; mbbilska@cyf-kr.edu.pl

Received 17 May 2019; Revised 24 October 2019; Accepted 2 November 2019; Published 22 November 2019

Guest Editor: Aneta Radziwon-Balicka

Copyright © 2019 Anna Bilska-Wilkosz et al. This is an open access article distributed under the Creative Commons Attribution License, which permits unrestricted use, distribution, and reproduction in any medium, provided the original work is properly cited.

The exogenous lipoic acid (LA) is successfully used as a drug in the treatment of many diseases. It is assumed that after administration, LA is transported to the intracellular compartments and reduced to dihydrolipoic acid (DHLA) which is catalyzed by NAD(P)H-dependent enzymes. The purpose of this study was to investigate whether LA can attenuate cardiovascular disturbances induced by ethanol (EtOH) and disulfiram (DSF) administration separately or jointly in rats. For this purpose, we measured systolic and diastolic blood pressure, recorded electrocardiogram (ECG), and estimated mortality of rats. We also studied the activity of aldehyde dehydrogenase (ALDH) in the rat liver. It was shown for the first time that LA partially attenuated the cardiac arrhythmia (extrasystoles and atrioventricular blocks) induced by EtOH and reduced the EtOH-induced mortality of animals, which suggests that LA may have a potential for use in cardiac disturbance in conditions of acute EtOH intoxication. The administration of EtOH, LA, and DSF separately or jointly affected the ALDH activity in the rat liver since a significant decrease in the activity of the enzyme was observed in all treatment groups. The results indicating that LA is an inhibitor of ALDH activity are very surprising.

1. Introduction

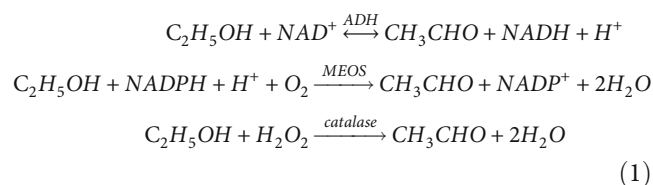
According to the World Health Organization (WHO) in 2016, the alcohol abuse resulted in 3 million deaths (5.3% of all deaths) worldwide and 132.6 million disability-adjusted life years (DALYs), i.e., 5.1% of all DALYs in that year [1]. DALYs are the sum of years of life lost due to premature mortality as well as years of life lost due to time lived in less than full health.

According to the authors of that report, the cardiovascular diseases (CVDs) are the leading cause of mortality globally, causing 17.9 million deaths (31.6% of all deaths) and 413.2 million DALYs (15.9% of all DALYs). Globally in

2016, alcohol caused an estimated net CVD burden of 593 000 deaths (3.3% of all CVD deaths) and 13 million CVD DALYs (3.2% of all CVD DALYs). CVDs were responsible for 19.8% and 9.8% of all alcohol-attributable deaths and DALYs lost, respectively [1].

Metabolism of ethanol (EtOH) in the human body occurs mainly in the liver. EtOH can be oxidized to acetaldehyde by three routes: (1) in the presence of NAD in the reversible reaction catalyzed by alcohol dehydrogenase (ADH; E.C 1.1.1.1), (2) in the presence of NADPH and molecular oxygen (O₂) in the reaction catalyzed by microsomal ethanol oxidizing system (MEOS), and (3) in the presence of hydrogen peroxide (H₂O₂) in the reaction catalyzed by catalase

(EC 1.11.1.6). ADH is the main enzyme in EtOH metabolism. This enzyme oxidizes 92–96% of the ingested alcohol [2].



The second step of EtOH metabolism is catalyzed by aldehyde dehydrogenase (ALDH; E.C 1.2.1.3). This enzyme converts acetaldehyde to acetic acid which can be involved in a number of metabolic processes within the organism.



Disulfiram (tetraethylthiuram disulfide, antabuse, or DSF) is a well-known inhibitor of ALDH. By inhibiting ALDH activity, DSF causes EtOH intolerance due to poisoning with acetaldehyde, the concentration of which is high after EtOH consumption. It means that EtOH intake during DSF treatment results in the accumulation of acetaldehyde, which is associated with a risk of severe often life-threatening cardiovascular disturbances, including cardiac arrhythmia, drop in blood pressure, circulatory collapse, and death. These unpleasant and potentially life-threatening symptoms are known as DSF-EtOH reaction (DER). Of course, it is known that intoxication by excessive EtOH consumption alone (without DSF) can also cause death due to hypotonia and cardiovascular failure [3].

Therefore, it appears that it is justified to search for drugs capable of attenuating toxicity of EtOH alone and preventing or halting the progression of the DER/DSF-like reactions. We wished to examine whether lipoic acid (LA, 5-[(3R)-dithiolan-3-yl]pentanoic acid) would be able to attenuate cardiovascular disturbances induced by EtOH and/or DSF. Why LA? There are reports that LA is able to reduce myocardial injury and preserve cardiac function during ischemia-reperfusion injury [4, 5]. Many studies on animal models have also confirmed that LA can prevent progressive remodeling and even improve cardiac function [6]. Dudek et al. have indicated that LA protects the heart against myocardial post ischemia-reperfusion arrhythmias via K_{ATP} channel activation in isolated rat hearts [7]. The experimental study of Sokołowska et al. has proven a beneficial effect of LA on cyanate toxicity in the rat heart [8]. Skibska et al. in their excellent review indicated that although LA is used in various diseases, it can be particularly effective in cardiovascular diseases, including ischemic heart disease, hypertension, and heart failure [9].

Thus, in this study, we hypothesized for the first time that LA treatment can attenuate cardiovascular disturbances induced by EtOH and DSF administration separately or jointly in rats. For this purpose, systolic and diastolic blood pressure were measured, electrocardiogram (ECG) was recorded, and mortality of rats was estimated. Moreover, the activity of ALDH in the rat liver was studied.

2. Materials and Methods

2.1. Reagents. In this study, the formulation Thiogamma was used, which contains LA as the pharmacologically active substance. Thiogamma was obtained from Hexal®AG, (Holzkirchen, Germany). Thiopental sodium was obtained from HEFA-Freon Arzneimittel (Germany). Heparin sodium was obtained from Polfa S.A. (Poland). Disulfiram, EDTA, Folin-Ciocalteu reagent, 4-methylpyrazole, NAD, propionaldehyde, and rotenone were provided by Sigma-Aldrich Chemical Company (Poznań, Poland). All other reagents were of analytical grade and were obtained from Polish Chemical Reagent Company (POCh, Gliwice, Poland).

2.2. Animals and In Vivo Treatment. All procedures were performed according to the Animal Use and Care Committee Guidelines and were approved by the Ethics Committee of the Jagiellonian University, Kraków, Poland (registration number 106/2009 and ZI/UJ/403/2007). The experiments were carried out on male Wistar rats (180–200 g). Animals were housed in plastic cages in a room at a constant temperature of $20 \pm 2^\circ\text{C}$ with a natural light-dark cycle. They had free access to standard pellet diet and water. The tested compounds were administered at doses calculated per kg body weight (bw). EtOH was given by a gavage, and LA and DSF by intraperitoneal (IP) injection. The control group was injected IP with 0.6 ml of saline (0.9% NaCl).

2.3. Blood Pressure. The rats were anesthetized by IP injection of thiopental (70 mg/kg). The left carotid artery was cannulated with polyethylene tubing filled with heparin solution in saline to facilitate pressure measurements using a Datamax apparatus (Columbus Instruments, Ohio). The animals were assigned to eight groups of 6 animals each. Blood pressure was measured as follows:

- (i) Group received 0.9% NaCl: measurement lasted 30 min
- (ii) EtOH group: measurement was conducted before EtOH administration (2.5 g/kg) and was continued for 30 min thereafter
- (iii) Group I (LA group): measurement was conducted before LA administration (100 mg/kg) and was continued for 60 min thereafter
- (iv) Group II (DSF group): measurement was conducted before DSF (100 mg/kg) administration and was continued for 60 min thereafter
- (v) Group III (DSF+LA group): measurement was conducted before LA (100 mg/kg) and DSF (100 mg/kg) administration and was continued for 60 min thereafter
- (vi) Group IV (LA+EtOH group): measurement was conducted before LA administration (100 mg/kg) and was continued for 30 min thereafter. In the 30th min, EtOH (2.5 g/kg) was administered and the measurement was continued for the next 30 min

- (vii) Group V (DSF+EtOH group): measurement was conducted before DSF (100 mg/kg) administration and was continued for 30 min thereafter. In the 30th min, EtOH (2.5 g/kg) was administered and the measurement was continued for the next 30 min
- (viii) Group VI (LA+DSF+EtOH group): measurement was conducted before LA (100 mg/kg) and DSF (100 mg/kg) administration and was continued 30 min thereafter. In the 30th min, EtOH (2.5 g/kg) was administered and the measurement was continued for the next 30 min

Subsequently, animals were sacrificed. The livers were removed, washed in 0.9% NaCl, placed in liquid nitrogen, and stored at -80°C until biochemical tests were performed.

2.4. Electrocardiogram Recording (ECG). The rats were anesthetized by IP injection of thiopental at a dose of 70 mg/kg. The ECG was recorded with three needle electrodes placed on the skin on the right and left chest and the left foot. Electrocardiographic investigations were carried out using Multi-card 30 apparatus, standard lead II, and paper speed of 50 mm/s. The ECG was standardized before each tracing to achieve appropriate sensitivity (2 mV pulse produces 20 mm height) and chart speed (50 mm/s). The animals were assigned to seven groups of 6 animals. ECG evaluated such parameters as extrasystole, bradycardia, atrioventricular blocks, and mortality. For each group, the percentage of animals, in which the disturbance occurred, was calculated.

- (i) Group A (EtOH): the ECG recording started in the 1st min and ended in the 30th min after EtOH administration (2.5 g/kg)
- (ii) Group B (LA+EtOH): the ECG recording started in the 1st min after LA administration (100 mg/kg) and was conducted for the next 30 min. In the 30th min, EtOH (2.5 g/kg) was administered; the ECG recording ended in the 60th min after LA administration (30 min after EtOH administration)
- (iii) Group C (LA): the ECG recording started in the 1st min and ended in the 60th min after LA administration (100 mg/kg)
- (iv) Group D (DSF): the ECG recording started in the 1st min and ended in the 60th min after DSF administration (100 mg/kg)
- (v) Group E (LA+DSF group): the ECG recording started in the 1st min and ended in 60th min after LA (100 mg/kg) and DSF (100 mg/kg) administration
- (vi) Group F (LA+DSF+EtOH group): the ECG recording started in the 1st min after LA (100 mg/kg) and DSF (100 mg/kg) administration and was conducted for the next 30 min. In the 30th min, EtOH (2.5 g/kg) was administered. The recording of ECG ended in the 60th min after LA and DSF administration (30 min after EtOH administration)

- (vii) Group G (DSF+EtOH group): the ECG recording started in the 1st min after DSF (100 mg/kg) administration and was conducted for the next 30 min. In the 30th min, EtOH (2.5 g/kg) was administered. The ECG recording ended in the 60th min after DSF administration (30 min after EtOH administration)

2.5. Determination of ALDH Activity in the Rat Liver Homogenate. The assay mixture contained liver homogenate, sodium phosphate buffer (pH 8.2), NAD, EDTA, 4-methylpyrazole, and rotenone. The reaction was initiated by the addition of propionaldehyde as a substrate. 4-Methylpyrazole was added to inhibit alcohol dehydrogenase, and rotenone to inhibit mitochondrial NADH oxidase. The blank sample without the homogenate or the substrate was run simultaneously. The activity of ALDH was calculated by using the molar extinction coefficient of NADH of $6.22 \text{ mM}^{-1} \text{ cm}^{-1}$ at 340 nm with the use of a modified protocol published earlier [10, 11]. Enzyme-specific activity was expressed as $\text{nmol NADH min}^{-1} \text{ mg}^{-1} \text{ protein}$. The protein content was determined by the method which is based on the reaction of peptide bonds and aromatic amino acid residues with Folin-Ciocalteu reagent (a mixture of phosphotungstic and phosphomolybdic acids) in alkaline environment in the presence of copper (II) ions. Protein bound with copper ions reduces the above acids to respective oxides. Absorbance was measured at 500 nm [12].

2.6. Statistics. All statistical calculations were carried out with the use of GraphPad Prism 6.0 computer program.

The results obtained from measurements of blood pressure are presented as the mean \pm SEM of animals in each group. The statistical calculations were performed using a two-way ANOVA Multiple Comparison and post hoc Tukey test.

The results obtained from measurements of ALDH activity in rat liver homogenates are presented as the mean \pm SD for each group of animals. The statistical calculations were performed using a one-way ANOVA and post hoc Tukey test.

For all data, the values of $p < 0.05$ were considered to be statistically significant.

3. Results

3.1. The Effect of Ethanol Administration on Systolic and Diastolic Blood Pressure in Rats. The blood pressure in rats, which received 0.9% NaCl was 130.67/105.33 mmHg at $t = 0$ measurement. The blood pressure was 105.33/103.67 mmHg measured at 30 minutes ($t = 30$) after administration of salt (Figure 1).

EtOH administration caused a statistically significant decrease only in diastolic blood pressure at 30 minutes of measurement compared to the pressure measured before the administration of EtOH, i.e., at $t = 0$ (Figure 1). Blood pressure measured before EtOH administration ($t = 0$) was 122.67/99.33 mmHg, while measured at 30 min ($t = 30$) amounted to 102.33/69.33 mmHg (Figure 1).

3.2. The Effect of Lipoic Acid on the Systolic and Diastolic Blood Pressure in Rats. Systolic blood pressure measured

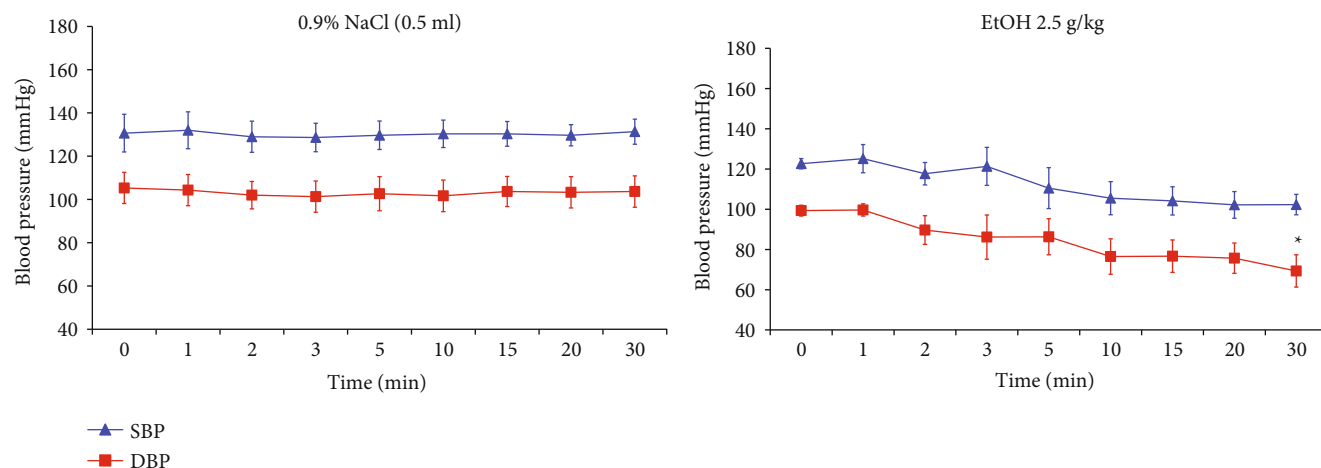


FIGURE 1: The effect of 0.9% NaCl or EtOH on the systolic and diastolic blood pressure (SBP and DBP, respectively) in rats measured for 30 min. Each group comprised 6 animals ($n = 6$). Data are shown as the mean \pm SEM. Significant vs. the blood pressure measured before the administration of EtOH, i.e., at $t = 0$; * $p < 0.05$.

before administration of LA ($t = 0$) was 132.5 mmHg, while measured 60 minutes after administration of LA was 115.33 mmHg. Statistically significant changes in systolic blood pressure were observed from 30 minutes after administration of LA. This means that LA lowers systolic blood pressure in rats. However, the effect of LA on the diastolic blood pressure was not observed (Figure 2(a)).

3.3. The Effect of Disulfiram on the Systolic and Diastolic Blood Pressure in Rats. DSF administration statistically significantly decreased systolic and diastolic blood pressure in rats. Blood pressure measured before DSF treatment ($t = 0$) was 127.67/89.5 mmHg while determined at 60 minutes ($t = 60$) was 105/72 mmHg. Statistically significant changes in systolic and diastolic blood pressure were observed from 40th to 50th minute, respectively, after administration of DSF. This means that DSF lowers blood pressure in rats (Figure 2(b)).

3.4. The Effect of Combined Lipoic Acid and Disulfiram Treatment on the Systolic and Diastolic Blood Pressure in Rats. The combined LA and DSF treatment statistically significantly reduced systolic and diastolic blood pressure in rats. Blood pressure before joint administration of LA and DSF ($t = 0$) was 123.6/95.33 mmHg, while recorded at 60 minutes ($t = 60$) was 104.67/63.33 mmHg (Figure 2(c)). Statistically significant changes in diastolic and systolic blood pressure were observed from 10th to 15th minute, respectively, after administration of LA and DSF.

This means that the combined administration of LA and DSF lowers blood pressure in rats (Figure 2(c)).

3.5. The Effect of Combined Lipoic Acid and Ethanol Treatment on the Systolic and Diastolic Blood Pressure in Rats. The combined LA and EtOH treatment statistically significantly reduced systolic and diastolic blood pressure in rats. Blood pressure before administration of EtOH was 118.33/93.67 mmHg, while measured 30 minutes after

administration of EtOH was 111.5/81.5 mmHg. However, the pressure measured at $t = 0$ minutes, i.e., before any compounds were administered, was 132.5/103.67 mmHg (Figure 2(d)).

Blood pressure values measured in the EtOH group, LA group, and LA+EtOH group at the endpoint of the experiment were 102.33/69.33, 115.33/89.67, and 111.5/81.5, respectively.

This means that in the presence of LA, the decrease in blood pressure is smaller than in the group of rats receiving only EtOH.

3.6. The Effect of Combined Disulfiram and Ethanol Treatment on the Systolic and Diastolic Blood Pressure in Rats. The combined DSF and EtOH treatment statistically significantly reduced systolic and diastolic blood pressure in rats. Blood pressure before administration of EtOH was 110.33/84.67 mmHg, while measured 30 minutes after administration of EtOH was 82.33/54.87 mmHg. However, the pressure measured at $t = 0$ minutes, i.e., before any compounds were administered, was 119.17/91.5 mmHg (Figure 2(e)).

Blood pressure values measured in the EtOH group, DSF group, and DSF+EtOH group at the endpoint of the experiment were 102.33/69.33, 105/72, and 82.33/54.87 mmHg, respectively.

This means that in the presence of DSF, the decrease in blood pressure is bigger than in the group of rats receiving only EtOH.

3.7. The Effect of Combined Lipoic Acid, Disulfiram, and Ethanol Treatment on the Systolic and Diastolic Blood Pressure in Rats. Blood pressure before administration of EtOH was 101.33/72 mmHg, while measured 30 minutes after administration of EtOH was 100.87/67.67 mmHg. However, the pressure measured at $t = 0$ minutes, i.e., before LA and DSF were administered, was 121.67/98.33 mmHg (Figure 2(f)).

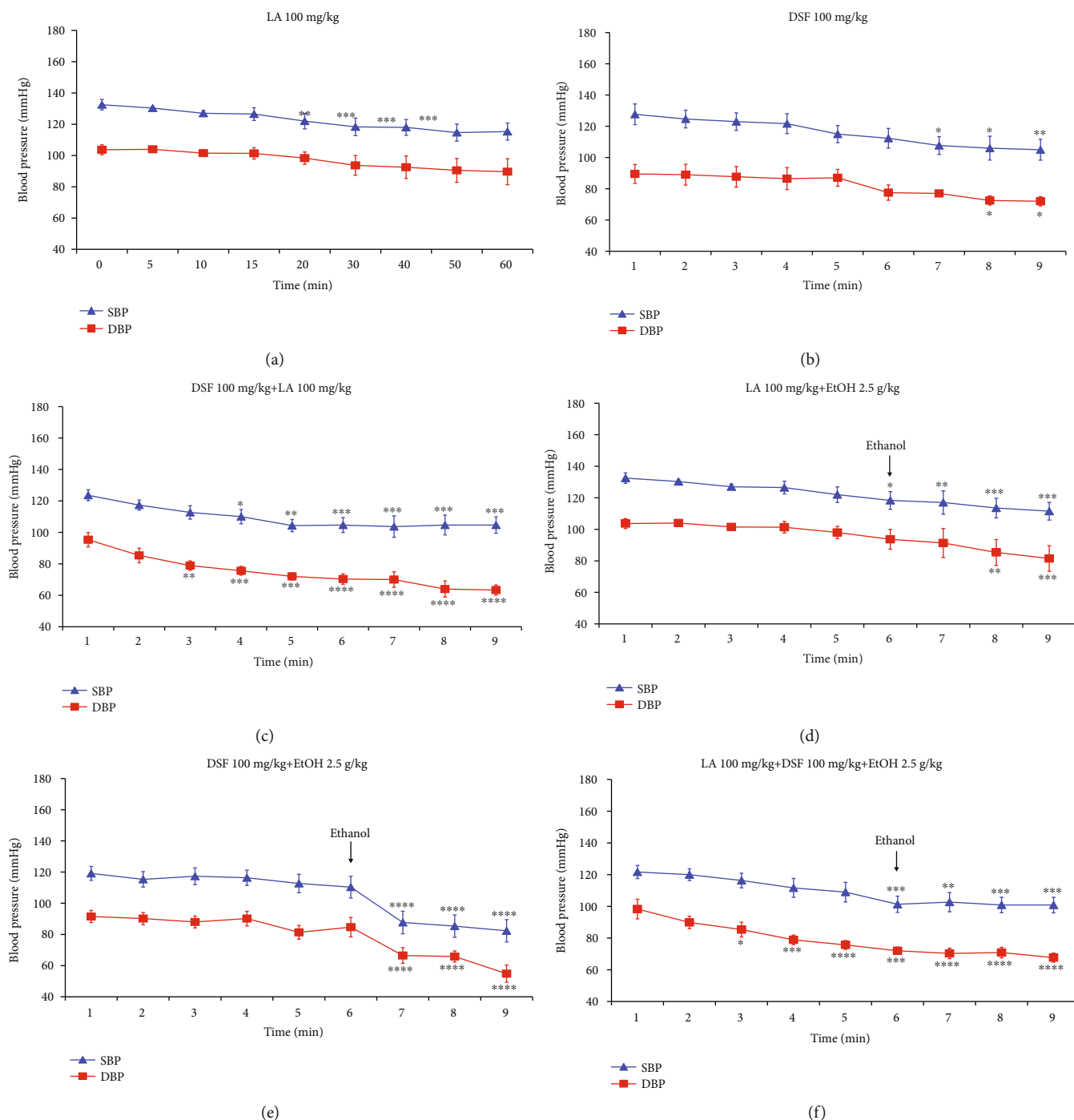


FIGURE 2: The effect of LA, DSF, and various combinations of these chemical compounds with EtOH on the systolic and diastolic blood pressure (SBP and DBP, respectively) in rats. Each group comprised 6 animals ($n = 6$). Data are shown as the mean \pm SEM. Significant vs. the blood pressure measured at $t = 0$ minutes, i.e., before the administration of any drugs. * $p < 0.05$; *** $p < 0.001$.

Blood pressure values measured in the EtOH group, LA group, DSF group, LA+DSF group, LA+EtOH group, DSF+EtOH group, and LA+DSF+EtOH at the endpoint of the experiment were 102.33/69.33, 115.33/89.67, 105/72, 104.67/63.33, 111.5/81.5, 82.33/54.87, and 100.87/67.67 mmHg, respectively.

This means that the greatest reduction in blood pressure occurs in the group of rats receiving DSF and EtOH (82.33/54.87 mmHg). However, in the group of animals,

which apart from DSF and EtOH also received LA, the decrease in blood pressure was significantly smaller (100.87/67.67 mmHg).

Figure 3 shows changes in systolic (a) and diastolic (b) blood pressure in all groups of rats which received EtOH. Taken together, a statistically significant decrease in systolic and diastolic blood pressure vs. group receiving only 0.9% NaCl (control group) presented in Figure 1 was observed in 3 groups: EtOH group, DSF+EtOH group,

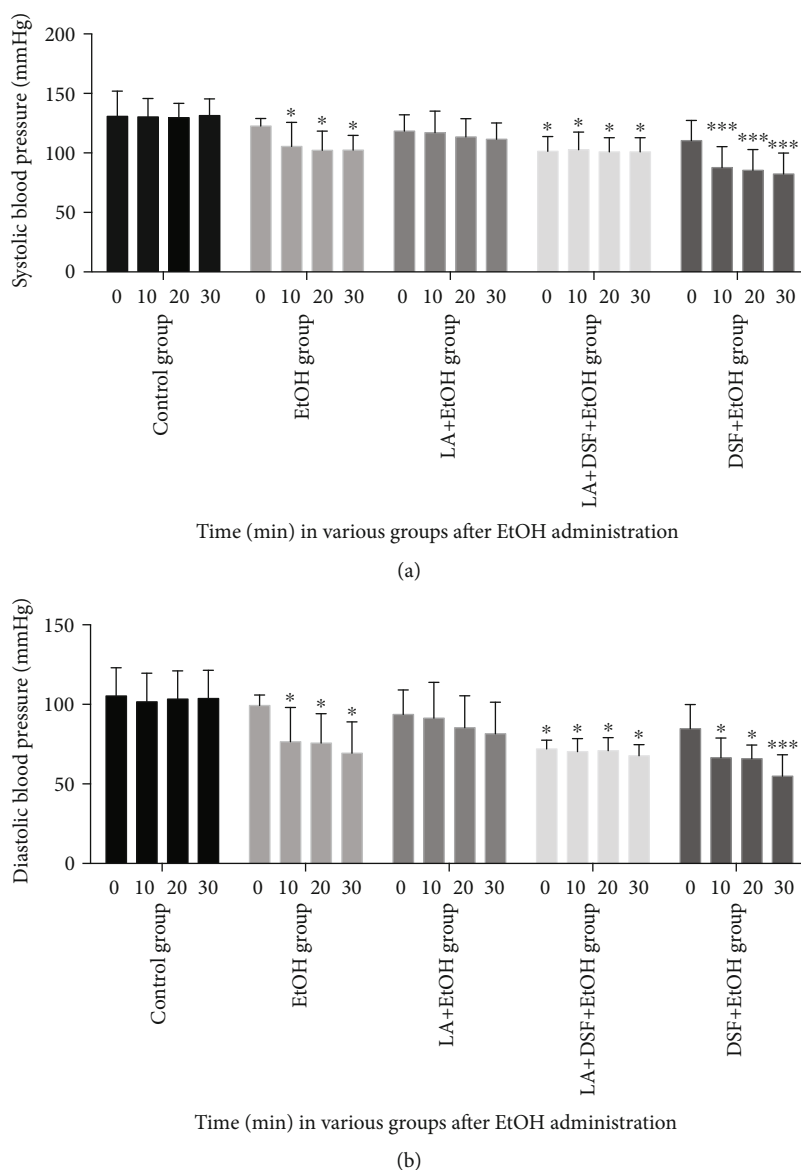


FIGURE 3: The changes in systolic (a) and diastolic (b) blood pressure in all groups of rats which received EtOH. Each group comprised 6 animals ($n = 6$). Data are shown as the mean \pm SEM. Significant vs. group receiving 0.9% NaCl (control group); * $p < 0.05$; *** $p < 0.001$.

and LA+DSF+EtOH group. The greatest drop in blood pressure vs. group receiving 0.9% NaCl (control group) was noted in EtOH-treated rats which were given DSF 30 min before EtOH.

3.8. The Effect of Various Combinations of Ethanol, Lipoic Acid, and Disulfiram on the Heart Rhythm Disturbances in Rats and on the Activity of Aldehyde Dehydrogenase in the Rat Liver. The obtained results are shown in Tables 1 and 2.

Bradycardia was seen in all groups of rats; however, in EtOH-treated group (group A) and in the group treated with EtOH 30 min after LA and DSF administration (group F), bradycardia affected 100% of animals. In the remaining groups, 83.5% of rats exhibited bradycardia. It is noteworthy that bradycardia occurred also in 83.5% of animals receiving LA alone (group C). Moreover, in rats treated first with LA

and 30 min later with EtOH (group B), bradycardia was seen also in 83.5% of animals, which could suggest a protective action of LA (Table 1).

Extrasystoles were observed in 50% of rats in the EtOH-treated group (group A) and in 33.3% of rats in the group treated with EtOH 30 min after LA administration (group B). It indicates that prior LA administration reduced the number of animals in which extrasystoles were observed (Table 1).

Atrioventricular blocks were observed in 16.7% of rats receiving EtOH (group A) and in 16.7% of rats treated with EtOH 30 min after LA (group B). In this case, LA administration did not decrease the number of rats with this disturbance (Table 1).

Deaths of animals were observed in four groups. In the EtOH-treated group (group A), four animals died (66.7%),

TABLE 1: The effect of various combinations of ethanol (EtOH), lipoic acid (LA), and disulfiram (DSF) on the heart rhythm disturbances and mortality in rats.

Disorders	EtOH Group A	LA+EtOH Group B	LA Group C	DSF Group D	DSF+LA Group E	DSF+LA+EtOH Group F	DSF+EtOH Group G
Extrasystoles	3 min (50%)	30 min (33.3%)	None	None	None	None	None
Bradycardia	5 min (100%)	40 min (83.5%)	60 min (83.5%)	20 min (83.5%)	25 min (83.5%)	30 min (100%)	40 min (83.5%)
Atrioventricular blocks (min/%)	3/16.7 5/16.7 30/16.7	30/16.7	None	None	None	None	None
Death (min/%)	5/16.7 10/50	40/16.7	None	None	None	40/33.3 50/33.3	40/66.7

Each group comprised 6 animals ($n = 6$). Data are presented as a percentage of animals with the heart rhythm disturbances and mortality in rats.

TABLE 2: The effect of various combinations of ethanol (EtOH), lipoic acid (LA), and disulfiram (DSF) on the aldehyde dehydrogenase activity in the rat liver.

Treatment	Activity of ALDH in the rat liver (IU/min/mg protein)
Group receiving NaCl	38.41 ± 5.00
EtOH group	^{aaa,bbb} 18.075 ± 4.05 ^c
LA (group I)	^{aaa,b} 11.3 ± 4.44 ^d
DSF (group II)	^{aaa} 6.43 ± 1.37 ^{ddd}
LA+DSF (group III)	^{aaa,ccc} 6.75 ± 1.42 ^{ddd}
LA+EtOH (group IV)	^{aaa} 8.10 ± 2.66 ^{ddd}
DSF+EtOH (group V)	^{aaa} 6.56 ± 1.04 ^{ddd}
LA+DSF+EtOH (group VI)	^{aaa,ccc} 4.09 ± 2.00 ^{ddd}

Data are shown as the mean ± standard deviation (SD) of 6 animals per group ($n = 6$); ^{aaa} $p < 0.001$ vs. group receiving 0.9% NaCl; ^b $p < 0.05$ and ^{bbb} $p < 0.001$ vs. DSF group; ^c $p < 0.05$ and ^{ccc} $p < 0.001$ vs. LA group, ^d $p < 0.05$ and ^{ddd} $p < 0.001$ vs. EtOH group.

one at 5 min and three at 10 min after EtOH administration. In the LA+EtOH group (group B), one animal died (16.7%) 10 min after EtOH administration (at 40 min of the experiment, EtOH was administered 30 min after LA treatment). In the DSF+LA+EtOH group (group F), four animals died (66.7%), two 10 min after EtOH administration (at 40 min of the experiment) and two 20 min after EtOH administration (at 50 min of the experiment, EtOH was administered 30 min after LA and DSF treatment). In the DSF+EtOH group (group G), four animals died (66.7%) 10 min after EtOH administration (at 40 min of the experiment, EtOH was administered 30 min after DSF).

Taken together, the results presented in Table 1 demonstrated bradycardia in all tested animals (groups A-G), while extrasystoles and atrioventricular blocks were observed only in the group treated with EtOH alone (group A) and in EtOH-treated rats which were given LA 30 min before EtOH (group B). Deaths of animals were observed in all EtOH-treated groups, but the fewest animals died (one animal, which corresponds to 16.7%) in the group of animals which was treated with LA 30 min prior to EtOH administration (group B: LA+EtOH group).

The results presented in Table 2 indicated that the administration of EtOH, LA, and DSF separately or jointly affected the ALDH activity in the rat liver. A significant decrease in the activity of the enzyme vs. group receiving 0.9% NaCl was observed in the all treatment groups.

4. Discussion

The obtained results indicated that the greatest blood pressure drop was observed in the group administered EtOH after DSF treatment (Figures 2(e) and 3). It is commonly known that DSF has been used for over 70 years as an alcohol-averse agent in the treatment of alcoholism. By inhibiting ALDH activity, DSF causes EtOH intolerance due to poisoning with acetaldehyde. It causes a spectrum of undesirable symptoms collectively called DSF-EtOH reaction (DER). Prancheva et al. described a case of a 53-year-old man in whom DER manifested as severe hypotension (blood pressure was 35/20 mmHg) accompanied by ischemic stroke [13].

The present data demonstrated also that in this experiment, a number of animals died in all EtOH-treated groups, but the fewest animals died (one animal, which corresponds to 16.7%) in the LA+EtOH group. The question arises why, despite the relatively low dose of EtOH, 66.7% of the animals died in the group that only received EtOH. It is assumed that blood alcohol levels (BACs) exceeding 500 mg% can result in death in humans as a result of paralysis of respiratory centers in the brain stem. On the other hand, there are known cases when alcohol produced death in humans at the values of BAC ranging from under 200 mg% to over 600 mg% [14, 15]. Why some people survive high BAC and others do not is an open question. In our opinion, it is similar in animals. Jones proposed to consider that when examining deaths due to acute ethanol poisoning, among all other factors, lady luck should not be forgotten [15].

The present data demonstrated also that mortality in the group treated with DSF and then with EtOH (DSF+EtOH) was 66.7% (and was the same as in the group administered LA and DSF before EtOH (LA+DSF+EtOH)). Development of cardiovascular collapse in patients with DER has been described by many authors. Ho et al. reported a patient with DER in whom initial volume resuscitation and dopamine infusion failed to restore the BP and blood pressure returned

to normal range only after noradrenaline administration [16]. A similar case was described by Milne and Parke [17]. The present results indicate that LA can partially attenuate arrhythmia (extrasystoles and atrioventricular blocks) induced by EtOH. Many literature data confirm that LA exerts powerful protective effects in numerous cardiovascular diseases [7, 18, 19].

The obtained results demonstrated also that all DSF-treated groups of animals showed the reduced ALDH activity in the liver which is obvious (Table 2). In addition, we observed that EtOH given alone also inhibited ALDH activity (Table 2). Despite the counter-intuitive nature of this discovery, the result is consistent with some results obtained by other authors [20–22]. On the other hand, the results indicating that LA is an inhibitor of ALDH activity turned out to be very surprising (Table 2), the more so that our previous observations *in vitro* indicated that the presence of LA or DHLA had no effect on the activity of yeast ALDH. Those observations demonstrated also that DHLA but not LA could protect ALDH against DSF-induced blockade, while neither LA nor DHLA were able to restore the ALDH activity when it already had been inhibited by DSF [23]. However, it should be noted that it is increasingly more frequently underlined that biological effects of LA obtained *in vitro* often differ from those observed *in vivo* which was largely unnoticed until recently [24, 25]. Some authors highlighted that LA could participate, like glutathione (GSH), in S-thiolation of proteins and this process is perceived to be a molecular “switch” decisive for intracellular redox status of thiols able to control cellular metabolic pathways [25]. In the case of GSH, the formation of a mixed disulfide (G-S-S-Protein) usually leads to inhibition of the biological activity of the protein [26].

The mammalian ALDH is a redox-sensitive protein, and the cysteine sulfhydryl group in its active site plays an essential role in its activity. Therefore, it is possible that ALDH forms a mixed disulfide with LA (LA-S-S-ALDH) which leads to a decrease in its activity. However, the problem of S-thiolation involving LA is still not well understood and there is virtually no literature data while those that can be found are based more on suppositions and deductions, and not on hard scientific evidence. Therefore, it seems that this direction of research is worthy of attention.

Taken together, the present results indicated that LA in rats can attenuate cardiovascular disorders induced by the administration of EtOH. In our opinion, it was caused by the ability of LA to ameliorate the reductive stress which occurs as a result of metabolic processes related to EtOH. The reductive stress is a counterpart of oxidative stress and is defined as an abnormal increase in reducing equivalents. EtOH produces reductive stress since its metabolism results in overproduction of NADH. A decrease in the NAD⁺/NADH ratio causes a decline in the activity of oxidoreductases (reductive stress), resulting in an altered metabolic situation that might be the first insult leading towards several pathologies [27]. NADH excess has many metabolic consequences, of which suppression of the Krebs cycle (tricarboxylic acid cycle (TCA cycle)) and the mitochondrial respiratory chain seem the most important. It is known that

the TCA cycle together with the associated electron transport systems plays a key role in energy production. Inhibition of both TCA cycle and respiratory chain hinders energy generation from any compound, including EtOH. Thus, EtOH insidiously “deceives” the body because NADH accumulation and TCA cycle inhibition are signals of intracellular energy abundance, whereas actually the body faces a significant energy deficit. Furthermore, the elevated NADH levels suppress synthesis of UDP-glucuronic acid (UDPGA) compounds that must be attached to various xenobiotics (drugs, poisons, dietary supplements, etc.) before they can be excreted from the body.

Some researchers have observed that many degenerative diseases are associated with a hypoxic state that results in an increased NADH/NAD⁺ ratio [28, 29]. Many authors also showed that reductive stress played an important role in the development of cardiomyopathy in mice [30, 31]. In addition, overproduction of reducing equivalents imparted pleiotropic effects on gene expression, mitochondrial dysfunction [32], and protein quality control [33] in cardiomyopathy in mice.

It should be remembered that exogenous LA after administration is reduced to DHLA by NAD(P)H-dependent enzymes which in a simplified form can be expressed as



As a result of this reaction, NADH is oxidized to NAD, and thus the NAD⁺/NADH ratio increases. Hence, it is a plausible proposal that LA partially attenuated the toxicity of EtOH by decreasing the reductive stress level. It is worth noting that this is the first time when the novel hypothesis was presented that LA, which is normally considered to be an antioxidant, is also required for protection against reductive stress.

In conclusion, this study for the first time demonstrated that LA could partially attenuate the cardiac arrhythmia (extrasystoles and atrioventricular blocks) induced by EtOH and reduced the EtOH-induced mortality of animals, which supports a potential of LA for use in acute EtOH-intoxication and suggests that further experiments are necessary to elucidate the mechanism of action of LA as an antidote to EtOH poisoning.

Data Availability

No data were used to support this study.

Conflicts of Interest

The authors have declared no conflict of interest.

Acknowledgments

This work was supported by statutory funds of the Faculty of Medicine and Faculty of Pharmacy, Jagiellonian University Medical College, Kraków, Poland.

References

- [1] World Health Organization, *Global Status Report on Alcohol and Health 2018*, World Health Organization, Geneva, 2018, Licence: CC BY-NC-SA 3.0 IGO.
- [2] T. Zima, "Alcohol abuse," *The Journal of International Federation of Clinical Chemistry and Laboratory Medicine*, vol. 29, no. 4, pp. 285–289, 2018.
- [3] A. M. A. Ghani, E. Faiz, A. Nielsen, and R. Bilberg, "What is the cause of death, when alcohol dependent persons die prematurely?," *Drug and Alcohol Dependence*, vol. 97, pp. 120–126, 2019.
- [4] X. Wang, Y. Yu, L. Ji, X. Liang, T. Zhang, and C. X. Hai, "Alpha-lipoic acid protects against myocardial ischemia/reperfusion injury via multiple target effects," *Food and Chemical Toxicology*, vol. 49, no. 11, pp. 2750–2757, 2011.
- [5] K. Schönheit, L. Gille, and H. Nohl, "Effect of α -lipoic acid and dihydrolipoic acid on ischemia/reperfusion injury of the heart and heart mitochondria," *Biochimica et Biophysica Acta (BBA)-Molecular Basis of Disease*, vol. 1271, no. 2–3, pp. 335–342, 1995.
- [6] C.-J. Li, L. Lv, H. Li, and D.-M. Yu, "Cardiac fibrosis and dysfunction in experimental diabetic cardiomyopathy are ameliorated by alpha-lipoic acid," *Cardiovascular Diabetology*, vol. 11, no. 1, article 73, 2012.
- [7] M. Dudek, J. Knutelska, M. Bednarski et al., "Alpha lipoic acid protects the heart against myocardial post ischemia-reperfusion arrhythmias via K_{ATP} channel activation in isolated rat hearts," *Pharmacological Reports*, vol. 66, no. 3, pp. 499–504, 2014.
- [8] M. Sokolowska, M. Kostański, E. Lorenc-Koci, A. Bilska, M. Iciek, and L. Włodek, "The effect of lipoic acid on cyanate toxicity in the rat heart," *Pharmacological Reports*, vol. 66, no. 1, pp. 87–92, 2014.
- [9] B. Skibska and A. Gorąca, "The protective effect of lipoic acid on selected cardiovascular diseases caused by age-related oxidative stress," *Oxidative Medicine and Cellular Longevity*, vol. 2015, Article ID 313021, 11 pages, 2015.
- [10] C. W. Loomis and J. F. Brien, "Inhibition of hepatic aldehyde dehydrogenases in the rat by calcium carbimide (calcium cyanamide)," *Canadian Journal of Physiology and Pharmacology*, vol. 61, no. 9, pp. 1025–1034, 1983.
- [11] S. O. Tottmar, H. Pettersson, and K. H. Kiessling, "The subcellular distribution and properties of aldehyde dehydrogenases in rat liver," *Biochemical Journal*, vol. 135, no. 4, pp. 577–586, 1975.
- [12] O. Lowry, N. J. Rosebrough, A. L. Farr, and R. J. Randal, "Protein measurement with the Folin phenol reagent," *Journal of Biological Chemistry*, vol. 193, no. 1, pp. 265–275, 1951.
- [13] M. Prancheva, S. Krasteva, S. Tufkova, T. Karaivanova, V. Nizamova, and Y. Iliev, "Severe hypotension and ischemic stroke after disulfiram-ethanol reaction," *Folia Medica*, vol. 52, no. 3, pp. 70–73, 2010.
- [14] A. Koski, E. Vuori, and I. Ojanpera, "Relation of postmortem blood alcohol and drug concentrations in fatal poisonings involving amitriptyline, propoxyphene and promazine," *Human and Experimental Toxicology*, vol. 24, no. 8, pp. 389–396, 2005.
- [15] W. Jones, "Alcohol, its analysis in blood and breath for forensic purposes, impairment effects, and acute toxicity," *Wiley Interdisciplinary Reviews: Forensic Science*, vol. 1, no. 6, article e1353, 2019.
- [16] M. P. Ho, C. M. Liu, C. H. Yo, C. C. Lee, and C. L. Chen, "Refractive hypotension in a patient with disulfiram-ethanol reaction," *The American Journal of the Medical Sciences*, vol. 333, no. 1, pp. 53–55, 2007.
- [17] H. J. Milne and T. R. Parke, "Hypotension and ST depression as a result of disulfiram ethanol reaction," *European Journal of Emergency Medicine*, vol. 14, no. 4, pp. 228–229, 2007.
- [18] S. D. Wollin and P. J. Jones, " α -Lipoic acid and cardiovascular disease," *The Journal of Nutrition*, vol. 133, no. 11, pp. 3327–3330, 2003.
- [19] A. M. McNeilly, G. W. Davison, M. H. Murphy et al., "Effect of α -lipoic acid and exercise training on cardiovascular disease risk in obesity with impaired glucose tolerance," *Lipids in Health and Disease*, vol. 10, no. 1, p. 217, 2011.
- [20] S. Tran, M. Nowicki, D. Chatterjee, and R. Gerlai, "Acute and chronic ethanol exposure differentially alters alcohol dehydrogenase and aldehyde dehydrogenase activity in the zebrafish liver," *Progress in Neuro-Psychopharmacology and Biological Psychiatry*, vol. 56, pp. 221–226, 2015.
- [21] Y. Tomita, T. Haseba, M. Kurosu, and T. Watanabe, "Effects of acute ethanol intoxication on aldehyde dehydrogenase in mouse liver," *Arukuru kenkyu to yakubutsu izon= Japanese journal of alcohol studies & drug dependence*, vol. 25, no. 2, pp. 116–128, 1990.
- [22] M. E. Lebsack, E. R. Gordon, and C. S. Lieber, "Effect of chronic ethanol consumption on aldehyde dehydrogenase activity in the baboon," *Biochemical Pharmacology*, vol. 30, no. 16, pp. 2273–2277, 1981.
- [23] A. Bilska-Wilkosz, M. Górny, and M. Iciek, "Inactivation of aldehyde dehydrogenase by disulfiram in the presence and absence of lipoic acid or dihydrolipoic acid: an in vitro study," *Biomolecules*, vol. 9, no. 8, p. 375, 2019.
- [24] A. Bilska-Wilkosz, M. Górny, M. Dudek et al., "Inactivation of aldehyde dehydrogenase by nitroglycerin in the presence and absence of lipoic acid and dihydrolipoic acid. Implications for the problem of differential effects of lipoic acid *in vitro* and *in vivo*," *Acta Poloniae Pharmaceutica*, vol. 73, no. 6, pp. 1531–1538, 2016.
- [25] K. P. Shay, R. F. Moreau, E. J. Smith, and T. M. Hagen, "Is α -lipoic acid a scavenger of reactive oxygen species in vivo? Evidence for its initiation of stress signaling pathways that promote endogenous antioxidant capacity," *IUBMB Life*, vol. 60, no. 6, pp. 362–367, 2008.
- [26] P. Klatt and S. Lamas, "Regulation of protein function by S-glutathiolation in response to oxidative and nitrosative stress," *European Journal of Biochemistry*, vol. 267, no. 16, pp. 4928–4944, 2000.
- [27] J. S. Teodoro, A. P. Rolo, and C. M. Palmeira, "The NAD ratio redox paradox: why does too much reductive power cause oxidative stress?," *Toxicology Mechanisms and Methods*, vol. 23, no. 5, pp. 297–302, 2013.
- [28] Y. Ido, C. Kilo, and J. R. Williamson, "Cytosolic NADH/NAD⁺, free radicals, and vascular dysfunction in early diabetes mellitus," *Diabetologia*, vol. 40, no. 14, pp. S115–S117, 1997.
- [29] B. Lipinski, "Evidence in support of a concept of reductive stress," *British Journal of Nutrition*, vol. 87, no. 1, pp. 93–94, 2002.
- [30] N. S. Rajasekaran, P. Connell, E. S. Christians et al., "Human α B-crystallin mutation causes oxido-reductive stress and protein aggregation cardiomyopathy in mice," *Cell*, vol. 130, no. 3, pp. 427–439, 2007.

- [31] X. Zhang, X. Min, C. Li et al., "Involvement of reductive stress in the cardiomyopathy in transgenic mice with cardiac-specific overexpression of heat shock protein 27," *Hypertension*, vol. 55, no. 6, pp. 1412–1417, 2010.
- [32] A. Maloyan, A. Sanbe, H. Osinska et al., "Mitochondrial dysfunction and apoptosis underlie the pathogenic process in α -B-crystallin desmin-related cardiomyopathy," *Circulation*, vol. 112, no. 22, pp. 3451–3461, 2005.
- [33] B. Bukau, J. Weissman, and A. Horwich, "Molecular chaperones and protein quality control," *Cell*, vol. 125, no. 3, pp. 443–451, 2006.

Research Article

Activation of TGR5 Partially Alleviates High Glucose-Induced Cardiomyocyte Injury by Inhibition of Inflammatory Responses and Oxidative Stress

Li Deng,^{1,2} Xuxin Chen,³ Yi Zhong,¹ Xing Wen,¹ Ying Cai,¹ Jiafu Li ¹, Zhongcai Fan,¹ and Jian Feng ¹

¹Department of Cardiology, The Affiliated Hospital of Southwest Medical University, Luzhou, Sichuan, China

²Department of Rheumatology, The Affiliated Hospital of Southwest Medical University, Luzhou, Sichuan, China

³Department of Pulmonary and Critical Care Medicine, The Sixth Medical Center of Chinese PLA General Hospital, Beijing, China

Correspondence should be addressed to Jian Feng; jerryfeng@swmu.edu.cn

Received 12 April 2019; Accepted 23 October 2019; Published 21 November 2019

Guest Editor: Adrian Doroszko

Copyright © 2019 Li Deng et al. This is an open access article distributed under the Creative Commons Attribution License, which permits unrestricted use, distribution, and reproduction in any medium, provided the original work is properly cited.

High glucose- (HG-) induced cardiomyocyte injury is the leading cause of diabetic cardiomyopathy, which is associated with the induction of inflammatory responses and oxidative stress. TGR5 plays an important role in the regulation of glucose metabolism. However, whether TGR5 has cardioprotective effects against HG-induced cardiomyocyte injury is unknown. Neonatal mouse cardiomyocytes were isolated and incubated in a HG medium. Protein and mRNA expression was detected by western blotting and RT-PCR, respectively. Cell apoptosis was determined by Hoechst 33342 staining and flow cytometry. After treatment of cells with HG, TGR5-selective agonist INT-777 reduced the increase in expression of proinflammatory cytokines and NF- κ B, whereas pretreatment of cells with TGR5 shRNA significantly reduced the inhibitory effects of INT-777. We also found that INT-777 increased the protein expression of Nrf2 and HO-1. In the presence of TGR5 shRNA, the expression of Nrf2 and HO-1 was reduced, indicating that TGR5 may exert an antioxidant effect partially through the Nrf2/HO-1 pathway. Furthermore, INT-777 treatment inhibited HG-induced ROS production and apoptosis that were attenuated in the presence of TGR5 shRNA or ZnPP (HO-1 inhibitor). Activation of TGR5 has cardioprotective effects against HG-induced cardiomyocyte injury and could be a pharmacological target for the treatment of diabetic cardiomyopathy.

1. Introduction

Type 2 diabetes mellitus (T2DM) is a major health concern and burden on economies, which affected 2.8% of the world population in 2000 with morbidity estimated to reach 4.4% by 2030 [1]. T2DM is associated with many cardiovascular diseases. The cardiovascular complications are wide-ranging and due at least in part to chronic elevation of blood glucose levels. Although vascular damage is the most devastating complication of diabetes, hyperglycemia-induced myocardium injury in the absence of coronary artery disease and hypertension, termed as diabetic cardiomyopathy [2–4], has received increasing attention in particular [5, 6]. The cellular and molecular mechanisms underlying hyperglycemia-induced cardiac damage are complicated and multifactorial.

Reactive oxygen species (ROS) elevation, inflammation, and apoptosis, which are caused by high blood glucose, are major precursors and contributors to the development of diabetic cardiomyopathy [7–9]. Such pathological changes induce diastolic function impairments, myocardial fibrosis, and cardiac complications [3, 6, 8, 9].

A member of the G protein-coupled receptor family, G protein-coupled bile acid receptor 1 (GPBAR1; also known as TGR5), has been recently identified as a drug target for diabetes treatment [10–12]. TGR5 is activated by bile acids and mediates the endocrine effects of bile acids on energy balance, inflammation, digestion, and sensation [13]. Bile acids have been reported to increase energy expenditure and prevent the development of obesity and insulin resistance, which are mediated by TGR5 [14]. A previous study

has demonstrated that TGR5 in pancreatic cells regulates insulin secretion to maintain glucose homeostasis [12]. Based on these studies, TGR5 is thought to be a critical receptor for regulation of energy expenditure and a potential therapeutic target of diabetes. However, whether TGR5 activation prevents diabetes-associated cardiomyocyte injury is still unclear.

TGR5 expression has been found in cardiomyocytes and is associated with dysregulation of biliary fibrosis-induced cardiac energetics [15], suggesting that TGR5 plays an important role in cardiovascular homeostasis. Moreover, TGR5 activation reduces cytokine release and diminishes the inflammatory response [13, 16]. TGR5 is also linked to signaling pathways involved in cell survival and apoptosis [17]. Thus, we hypothesized that activation of TGR5 may be beneficial for protection against high glucose- (HG-) induced cardiomyocyte injury. Although a recent study showed that TGR5 activation improves myocardial adaptability to physiological, inotropic, and pressure-induced stress in mice [18], the role of TGR5 in HG-induced cardiomyocyte injury and the related molecular mechanisms are largely unknown.

2. Methods

2.1. Primary Mouse Cardiomyocyte Isolation, Culture, and Treatment. The protocol for the animal experiments was approved by the Experimental Animal Ethics Committee of Southwest Medical University. Animal handling and care were performed in strict compliance with the U.S. National Institutes of Health Guide for the Care and Use of Laboratory Animals (1996 revision). Primary cardiomyocytes were isolated from 20 to 30 neonatal Kunming mouse hearts, following a protocol reported previously [19, 20] with minor modifications. Less than 3-day-old neonatal mice were briefly rinsed in an antiseptic 75% alcohol solution. Mice were anaesthetized with 1% isoflurane and then euthanized by decapitation. Whole hearts were extracted from the mice using curved scissors and quickly transferred into a dish containing phosphate-buffered saline (PBS) without Ca^{2+} and Mg^{2+} . Nonmyocardial tissues, such as lung tissues and large vessels, were removed. Neonatal mouse hearts were washed in PBS without Ca^{2+} and Mg^{2+} to remove blood. The neonatal mouse hearts were then transferred into another dish containing 0.25% trypsin-EDTA and incubated at 4°C overnight. The next day, the trypsin-EDTA solution was removed, and fetal bovine serum (FBS) was added. The hearts were then digested in a collagenase solution containing 0.5–1.0 mg/mL collagenase and 5 mg/mL albumin at 37°C. The digested tissues were dispersed by pipetting for 10 min, and the cell suspension was transferred into sterile centrifuge tubes. Fresh collagenase solution was added to the remaining tissues, and the above process was repeated two to four times until all tissues were digested and all cells were collected. After centrifugation, the harvested cells were resuspended in a 10 mL plating medium (DMEM supplemented with 10% FBS and 1% penicillin-streptomycin), plated in a 10 cm culture dish, and incubated at 37°C with 5% CO_2 for 70 min. Unattached cardiomyocytes were collected from the 10 cm dish, resus-

pended in a fresh medium with 5-bromodeoxyuridine (0.1 mmol/L), and seeded in a 35 mm dish or 24-well culture plate coated with polylysine.

2.2. Gene Silencing by RNAi. TGR5 shRNA adenoviral particles were obtained from Hanbio Biotechnology (Shanghai, China), and Nrf2 shRNA lentiviral particles were obtained from Genechem Corporation (Shanghai, China). Experiments were performed in accordance with the manufacturer's instructions. Cells were infected with TGR5 or Nrf2 shRNA viral particles for 48 h before experiments.

2.3. Immunoblotting. Tissues or cells were washed twice with ice-cold PBS and lysed in lysis buffer (10 mM Tris-HCl, pH 8, 150 mM NaCl, 1% NP-40, 1 mM PMSF, and 10 mg/mL each leupeptin and aprotinin). The lysates (20 μg protein) were separated by 10%–12% SDS-polyacrylamide gel electrophoresis and transferred onto a polyvinylidene fluoride membrane. The membrane was washed with Tris-buffered saline+Tween-20 (TBST), blocked with 5% skim milk powder in TBST for 3 h, and then incubated with the appropriate primary antibody at dilutions recommended by the supplier. Membranes were probed with a rabbit anti-phospho-I κ B α (Ser32) antibody (1:1000, Cell Signaling Technology, MA), mouse anti-NF- κ B p65 (L8F6) antibody (1:1000, Cell Signaling Technology), rabbit anti-Nrf2 (D1Z9C) antibody (1:1000, Cell Signaling Technology), rabbit anti-HO-1 antibody (1:1000, Cell Signaling Technology), or anti-TGR5 antibody (1:500, Santa Cruz Biotechnology, CA). Then, the primary antibodies were detected with goat anti-rabbit or anti-mouse IgG (1:1000, Beyotime, China) conjugated with horseradish peroxidase. Bands were visualized with enhanced chemiluminescence (Pierce, MA). Equal amounts of protein transferred onto the membranes were verified by immunoblotting for GAPDH (1:1000, Cell Signaling Technology) or histone H3 (1:500, Biogot Biotechnology CO, Atlanta, Georgia, USA).

2.4. RNA Extraction and PCR. Total RNA from cells and tissues was extracted by Trizol (Tiangen, Beijing, China) and used to synthesize cDNA that served as the template for amplification of TNF- α , IL-6, and IL-1 β genes. Primers were as follows: TNF- α forward primer, 5'-GGCGGTGCC TATGTCTCA-3' and TNF- α reverse primer, 5'-GGCA GCCTTGTCCCTTGA-3' (363 bp); IL-6 forward primer, 5'-GCCTTCTTGGGACTGAT-3' and IL-6 reverse primer, 5'-CTGGCTTTGTCTTTCTTGT-3' (383 bp); IL-1 β forward primer, 5'-CTCGTGCTGTCCGACCCAT-3' and IL-1 β reverse primer, 5'-CAGGCTTGTGCTCTGCTTGTGA-3' (343 bp). The amplifications were performed using a reverse transcription-polymerase chain reaction (RT-PCR) kit (Tiangen). Mouse GAPDH was used as the endogenous control. The relative expression of target genes was normalized to GAPDH mRNA levels.

2.5. Hoechst 33342 Staining. Apoptotic cells were characterized by nuclear condensation of chromatin and/or nuclear fragmentation using a Hoechst 33342 staining kit (Solarbio, China), according to the manufacturer's instructions. In

brief, after treatments, the cells were fixed with 1 mL staining buffer and then stained with 5 μ L Hoechst 33342 and 5 μ L PI. The cells were incubated at 4°C or in an ice bath for 20–30 min. After incubation, the cells were washed once with PBS and spotted onto slides for microscopy.

2.6. Flow Cytometric Analysis. Apoptosis and intracellular ROS levels were measured by flow cytometry [21]. To analyze ROS production, the cells were incubated with DCFH-DA (10 μ M) at 37°C for 20 min, and then the intracellular ROS level was determined by flow cytometry. For apoptosis analysis, cells were trypsinized, harvested, washed twice with cold PBS, and then centrifuged, followed by removal of the supernatant and resuspension in 1 mL of 1x binding buffer. The cells were gently vortexed, incubated for 10 min at room temperature while protected from light, and then stained with 5 μ L Annexin V-FITC. Then, the cells were stained with 5 μ L of a PI solution at room temperature for 5 min while protected from light. The cells were resuspended with 500 μ L PBS and vortexed gently. Cells were analyzed by flow cytometry within 1 h. FITC and PI fluorescence were excited by a laser source with a wavelength of 494 nm and detected by 520 and 636 nm band-pass filters, respectively.

2.7. Measurement of Cell Viability. Cell viability was determined using the conventional methylthiazolyl tetrazolium (MTT) reduction assay. After treatments, cell viability was measured at various time points. Twenty microliters of MTT (5 mg/mL) was added to each well, followed by incubation for 4 h at 37°C with CO₂. The medium was then removed, and the formazan crystals were solubilized with DMSO. Absorbance was measured at 490 nm on a microplate reader (Bio-Rad, Hercules, CA).

2.8. Statistical Analysis. Data are expressed as the mean \pm SD. All statistical analyses were performed by one-way analysis of variance (ANOVA) for repeated measures, and comparisons among groups were made by one-way ANOVA with the Student-Newman-Keuls test. A value of $P < 0.05$ was considered as significant.

3. Results

3.1. High Glucose Promotes the mRNA Expression of Proinflammatory Cytokines and Activation of NF- κ B Signaling in Mouse Cardiomyocytes. To determine the effects of HG on the inflammatory response in mouse cardiomyocytes, the mRNA expression of proinflammatory cytokines was measured. Cardiomyocytes were exposed to HG for 1, 2, 4, 8, 16, and 24 h. In cells treated with 33 mM HG, the mRNA expression of IL-1 β , IL-6, and TNF- α was increased up to 16, 8, and 4 h, respectively, and decreased thereafter (Figure 1(a)). The NF- κ B signaling pathway was also analyzed. Cardiomyocytes were exposed to HG for 1, 2, 3, 6, 12, and 24 h. HG increased the protein expression of p-I κ B α and NF- κ B in cardiomyocytes. The protein expression of p-I κ B α and NF- κ B was increased up to 6 and 2 h, respectively, and decreased thereafter (Figure 1(b)). These data indicated that HG may induce the inflammatory response through activation of NF- κ B signaling in mouse cardiomyocytes.

3.2. Activation of TGR5 Reduces HG-Induced Increases in the Expression of Proinflammatory Cytokines and NF- κ B in Mouse Cardiomyocytes. To determine the effect of TGR5 on the inflammatory response, cardiomyocytes were infected with TGR5 shRNA adenoviral particles for 24 h or pretreated with 100 μ M SQ22536 (cAMP inhibitor) for 3 h and then treated with 30 μ M INT-777 (selective TGR5 agonist) for 3 h, followed by exposure to HG for 6 h. As shown by western blotting, pretreatment of cardiomyocytes with INT-777 inhibited HG-induced protein expression of p-I κ B α , whereas the inhibitory effect of INT-777 was attenuated by TGR5 shRNA or SQ22536 (Figure 2(a)). Similarly, INT-777 inhibited HG-induced protein expression of NF- κ B, and TGR5 shRNA or SQ22536 reduced the inhibitory effects of INT-777 (Figure 2(a)). Furthermore, INT-777 or JSH-23 (NF- κ B inhibitor) suppressed the HG-induced mRNA expression of IL-1 β , IL-6, and TNF- α . Treatment with TGR5 shRNA or SQ22536 ameliorated the inhibitory effects of INT-777 on the mRNA expression of IL-1 β , IL-6, and TNF- α (Figure 2(b)). These results suggested that the NF- κ B signaling pathway was involved in TGR5-mediated cardioprotection.

3.3. Activation of TGR5 Induces the Nrf2/HO-1 Pathway in Mouse Cardiomyocytes. The Nrf2/HO-1 signaling pathway is an important regulator of oxidative stress. Therefore, we determined whether activation of TGR5 induces the Nrf2/HO-1 axis in cardiomyocytes. TGR5 agonist INT-777 increased the protein expression of Nrf2 and HO-1 in cardiomyocytes up to 2 and 6 h, respectively, which was decreased thereafter (Figures 3(a) and 3(b)). The increase in protein expression of Nrf2 by INT-777 treatment was reduced after pretreatment with TGR5 shRNA or SQ22536 (Figure 3(c)). Next, cells were infected with either control or Nrf2 shRNA. Nrf2 shRNA significantly abated Nrf2 protein expression compared with the control (Figure 3(d)). Similarly, INT-777-induced HO-1 expression was also reduced by TGR5 shRNA, SQ22536, or Nrf2 shRNA (Figure 3(e)). These findings indicated that activation of TGR5 may have antioxidant effects partially mediated by inducing the Nrf2/HO-1 pathway.

3.4. Activation of TGR5 Alleviates HG-Induced Oxidative Stress in Mouse Cardiomyocytes. To examine the benefit of TGR5 against HG insult, oxidative stress and Nrf2/HO-1 axis (an antioxidant response system) were examined in primary neonatal mouse cardiomyocytes. Flow cytometry showed that INT-777 alone at various concentrations did not induce ROS production (Figures 4(a) and 4(b)). However, when cells were treated with HG, the intracellular ROS level was increased. INT-777 significantly reduced the level of ROS in HG-treated cells, whereas the effect of INT-777 was abolished in the presence of TGR5 shRNA or the HO-1 inhibitor ZnPP (Figures 4(c) and 4(d)). Immunoblotting data showed that Nrf2 and HO-1 were increased in HG condition compared with the control group (Figures 4(e) and 4(f)), while INT-777 treatment further increased the expression of Nrf2 and HO-1 significantly compared with the HG group (Figures 4(e) and 4(f)).

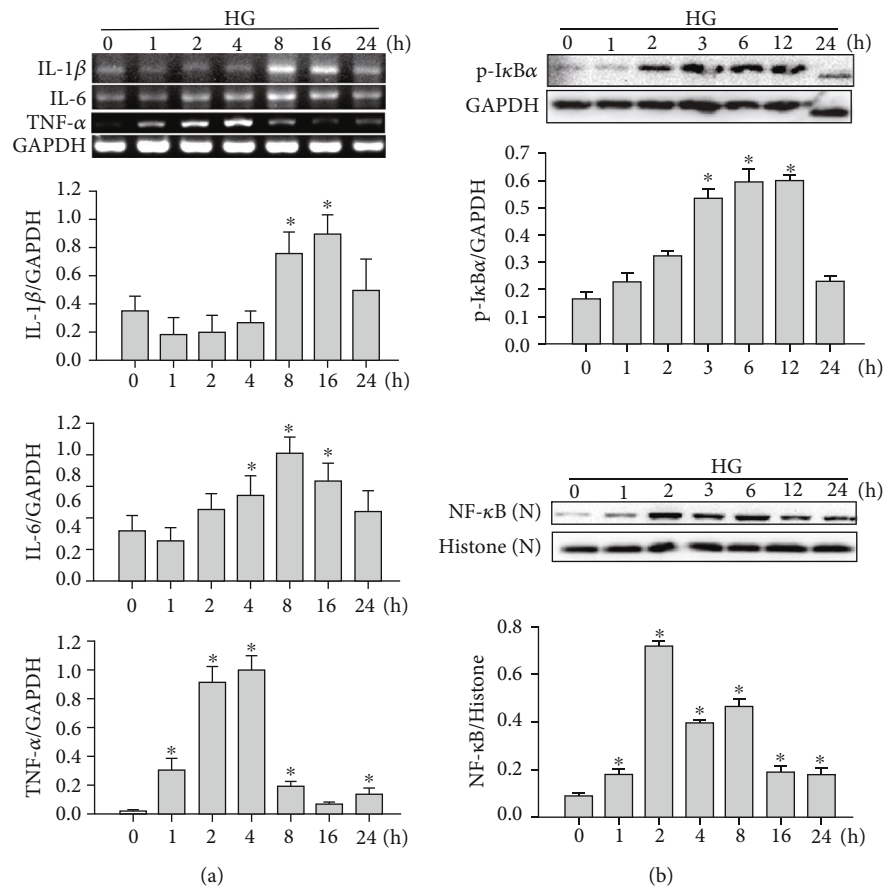


FIGURE 1: HG promotes mRNA expression of proinflammatory cytokines and activation of NF- κ B signaling in mouse cardiomyocytes. (a) HG-induced proinflammatory cytokine expression. Cardiomyocytes were treated with HG (33 mM) for the indicated times. IL-1 β , IL-6, and TNF- α mRNA expression was determined by RT-PCR. (b) HG-induced activation of NF- κ B signaling. Cardiomyocytes were treated with HG (33 mM) for the indicated times. Proteins (20 μ g) from cell lysates or nuclear (N) fractions were subjected to immunoblotting. Data are expressed as the mean \pm SD of three independent experiments. * P < 0.05 vs. 0 h.

3.5. Activation of TGR5 Attenuates HG-Induced Apoptosis in Mouse Cardiomyocytes. To investigate the effect of TGR5 on HG-induced apoptosis, we employed Hoechst 33342 staining and flow cytometry to measure apoptosis after treatment with HG, INT-777, TGR5 shRNA, and ZnPP. As shown in Figure 5(a), HG increased nuclear condensation that was inhibited by INT-777. Pretreatment with TGR5 shRNA or ZnPP mitigated the protective effect of INT-777 against HG-induced nuclear condensation. Similarly, INT-777 reduced HG-induced apoptosis, whereas the protective effect of INT-777 was ameliorated by TGR5 shRNA or ZnPP (Figure 5(b)). Microscopic examination revealed results similar to those of Hoechst 33342 staining and flow cytometry (Figure 5(c)). Furthermore, the effect of TGR5 was analyzed by MTT assays. Cell death was significantly increased under the HG condition. Cardiomyocytes treated with INT-777 showed suppression of cell death induced by HG. Cell death was increased in the presence of TGR5 shRNA or ZnPP (Figure 5(d)). These data support the notion that activation of TGR5 reduces HG-induced apoptosis partially through the Nrf2/HO-1 pathway.

4. Discussion

TGR5 is a G protein-coupled receptor that plays a key role in the physiological activities of bile acid [13]. Previous studies have indicated that TGR5 may be a novel target to regulate glucose metabolism for diabetes therapy. The TGR5 ligand (oleanolic acid) shows significant blood glucose-lowering and weight-losing effects in diabetic animal models induced by STZ [22, 23] and enhances glucose tolerance [10]. TGR5 activation by oleanolic acid induces glucagon-like peptide-1 production and secretion that improve liver and pancreas functions [24, 25]. However, the effects of TGR5 on HG-induced cardiomyocyte damage are unclear. Our data are consistent with the hypothesis that TGR5 activation protects against HG-induced cardiomyocyte damage by suppressing inflammatory cytokines and ROS overproduction and that TGR5 may be a pharmacological target for the treatment of HG-induced disorders.

Myocardial injury involved in T2DM is mainly due to direct metabolic damage of cardiomyocytes by hyperglycemia. Inflammatory responses and oxidative stress are implicated in the mechanism, and inhibiting the inflammatory

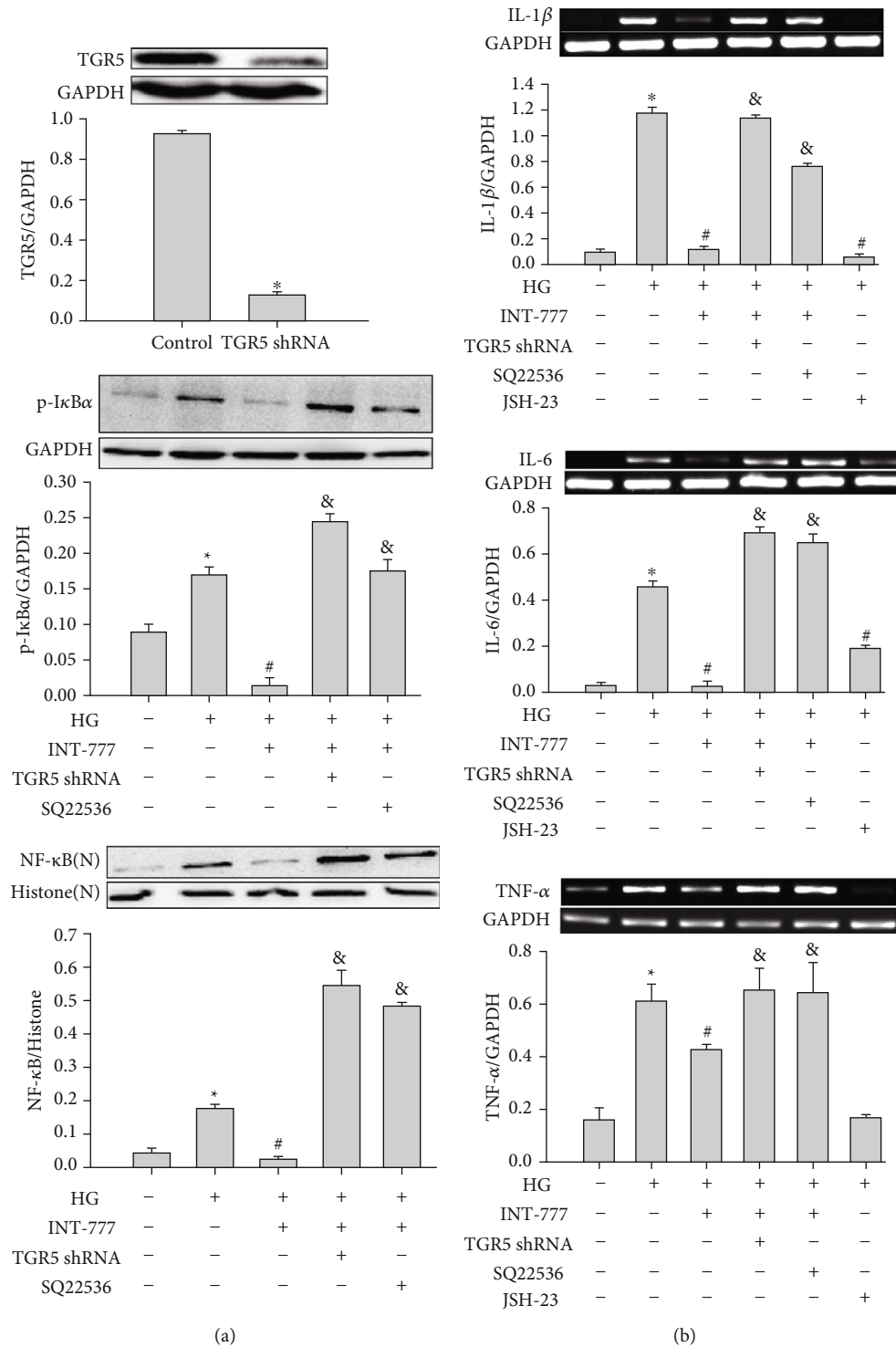


FIGURE 2: Activation of TGR5 reduces the HG-induced increase in the expression of proinflammatory cytokines and NF-κB signaling in mouse cardiomyocytes. (a) Cells were infected with TGR5 shRNA adenoviral particles for 48 h or pretreated with 100 μM SQ22536 (cAMP inhibitor) for 3 h and then treated with 30 μM INT-777 (selective TGR5 agonist) for 3 h, followed by addition of HG to cardiomyocytes for a further 6 h. Proteins (20 μg) from cell lysates or nuclear (N) fractions were subjected to immunoblotting. (b) Cells were infected with TGR5 shRNA adenoviral particles for 48 h or pretreated with 100 μM SQ22536 for 3 h and then treated with 30 μM INT-777 for 3 h or 30 μM JSH-23 (NF-κB inhibitor) for 1 h, followed by exposure to HG for a further 2 h (TNF-α) or 8 h (IL-1β and IL-6). IL-1β, IL-6, and TNF-α mRNA expression was determined by RT-PCR. Data are expressed as the mean ± SD of three independent experiments. *P < 0.05 vs. control; #P < 0.05 vs. HG; &P < 0.05 vs. HG+INT-777.

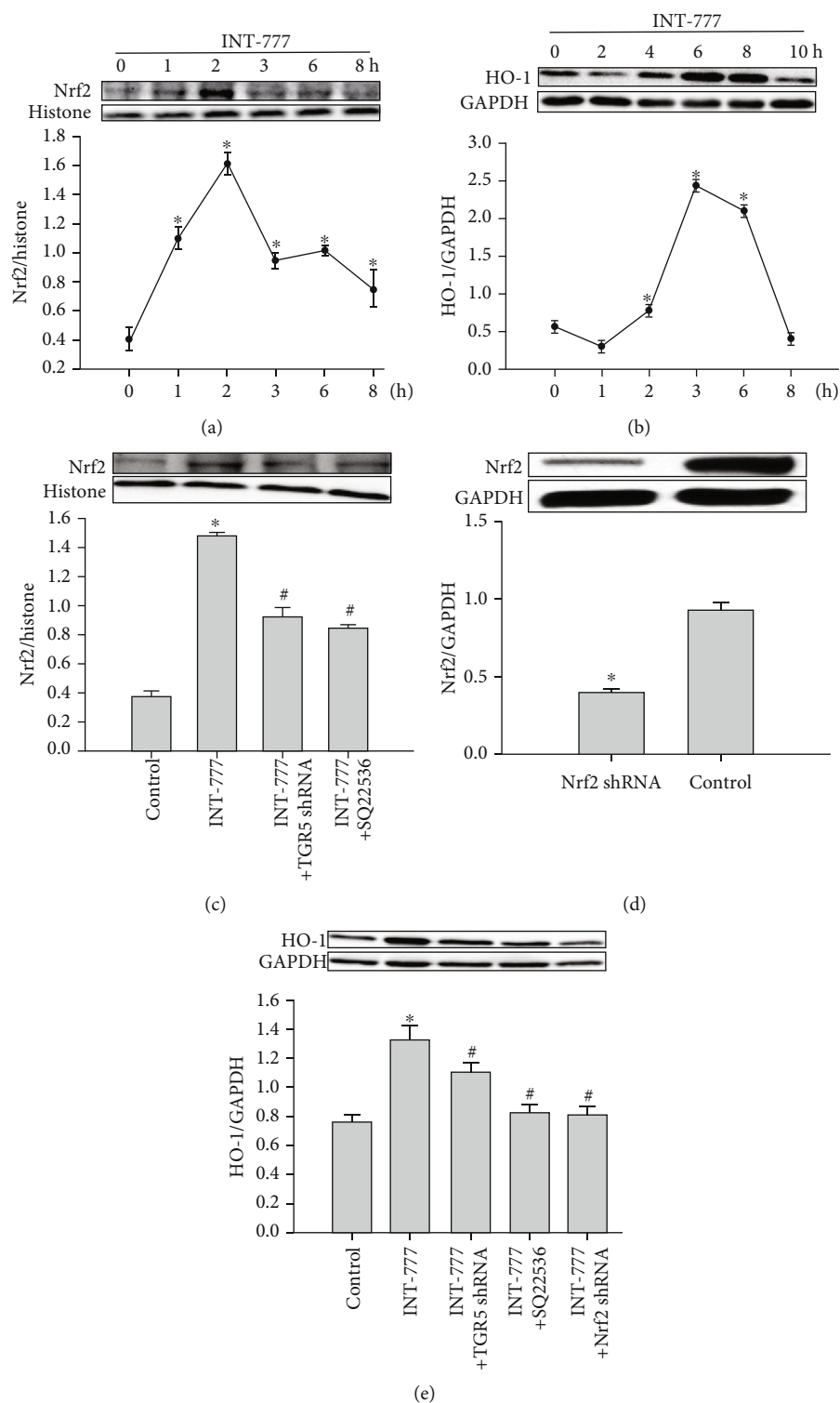


FIGURE 3: Activation of TGR5 induces the Nrf2/HO-1 pathway in mouse cardiomyocytes. (a) Nuclear extracts were prepared from cardiomyocytes treated with INT-777 (30 μ M) at the indicated time points to detect Nrf2 protein by immunoblotting. (b) Cells were treated with 30 μ M INT-777 for the indicated times to detect HO-1 by immunoblotting. (c) Cells were infected with TGR5 shRNA adenoviral particles for 48 h or pretreated with 100 μ M SQ22536 (cAMP Inhibitor) for 3 h and then treated 30 μ M INT-777 for 2 h. Proteins (20 μ g) from nuclear (N) fractions were subjected to immunoblotting. (d) Cells were infected with Nrf2 shRNA lentiviral particles for 48 h. Proteins from cell lysates were subjected to immunoblotting. (e) Cells were infected with TGR5 or Nrf2 shRNA viral particles for 48 h or pretreated with 100 μ M SQ22536 for 3 h and then treated with 30 μ M INT-777 for 6 h. Proteins from cell lysates were subjected to immunoblotting. Data are expressed as the mean \pm SD of three independent experiments. * P < 0.05 vs. 0 h or control; # P < 0.05 vs. HG.

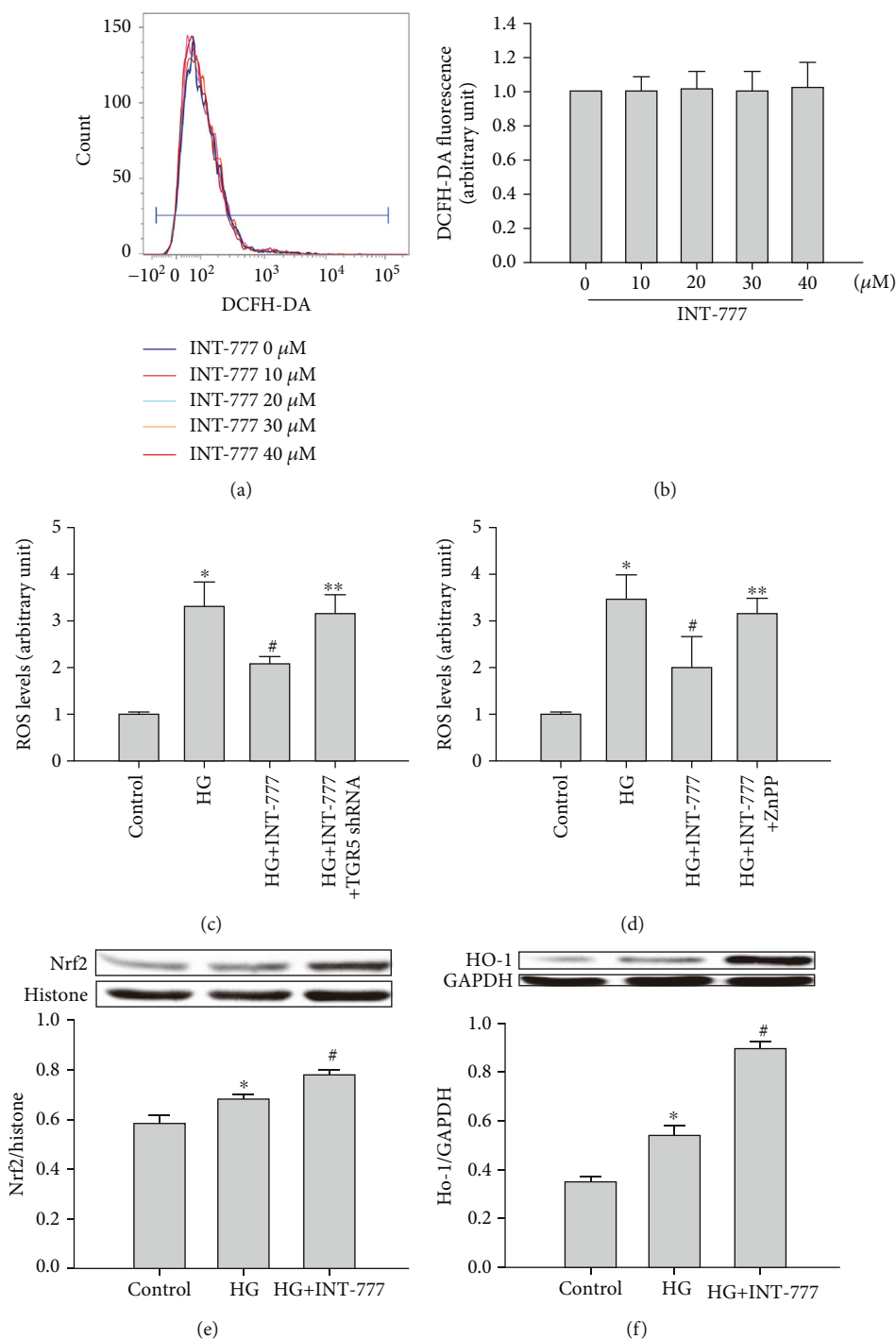


FIGURE 4: Effect of TGR5 activation on HG-induced oxidative stress in mouse cardiomyocytes. (a, b) ROS production was detected by flow cytometry with DCFH-DA staining at 20 min after INT-777 treatment. ROS levels were calculated as fold changes relative to no treatment (0 μM). (c, d) Changes in ROS production were detected by flow cytometry with DCFH-DA staining. Cells were infected with TGR5 shRNA adenoviral particles for 48 h, or cells were pretreated with 10 μM ZnPP for 1 h and then treated with INT-777 for 3 h, followed by addition of HG to cells for a further 12 h. ROS levels were calculated as fold changes relative to the control. (e, f) Immunoblotting for the expression of Nrf2 and HO-1 in cells. Cells were treated with INT-777 for 3 h, followed by addition of HG to cells for a further 12 h. Data are expressed as the mean \pm SD of three independent experiments. * $P < 0.05$ vs. control; # $P < 0.05$ vs. HG; ** $P < 0.05$ vs. HG+INT-777.

response and oxidative stress is useful for diabetic cardiomyopathy. For example, K_{ATP} channel opening protects H9c2 cardiac cells against HG-induced injury by inhibiting ROS and inflammation [26]. Suppressing the inflammatory

response and oxidative stress by kaempferol also attenuates hyperglycemia-induced cardiac damage [27]. Moreover, aza resveratrol-chalcone derivative 6b protects mice against diabetic cardiomyopathy by alleviating inflammation and

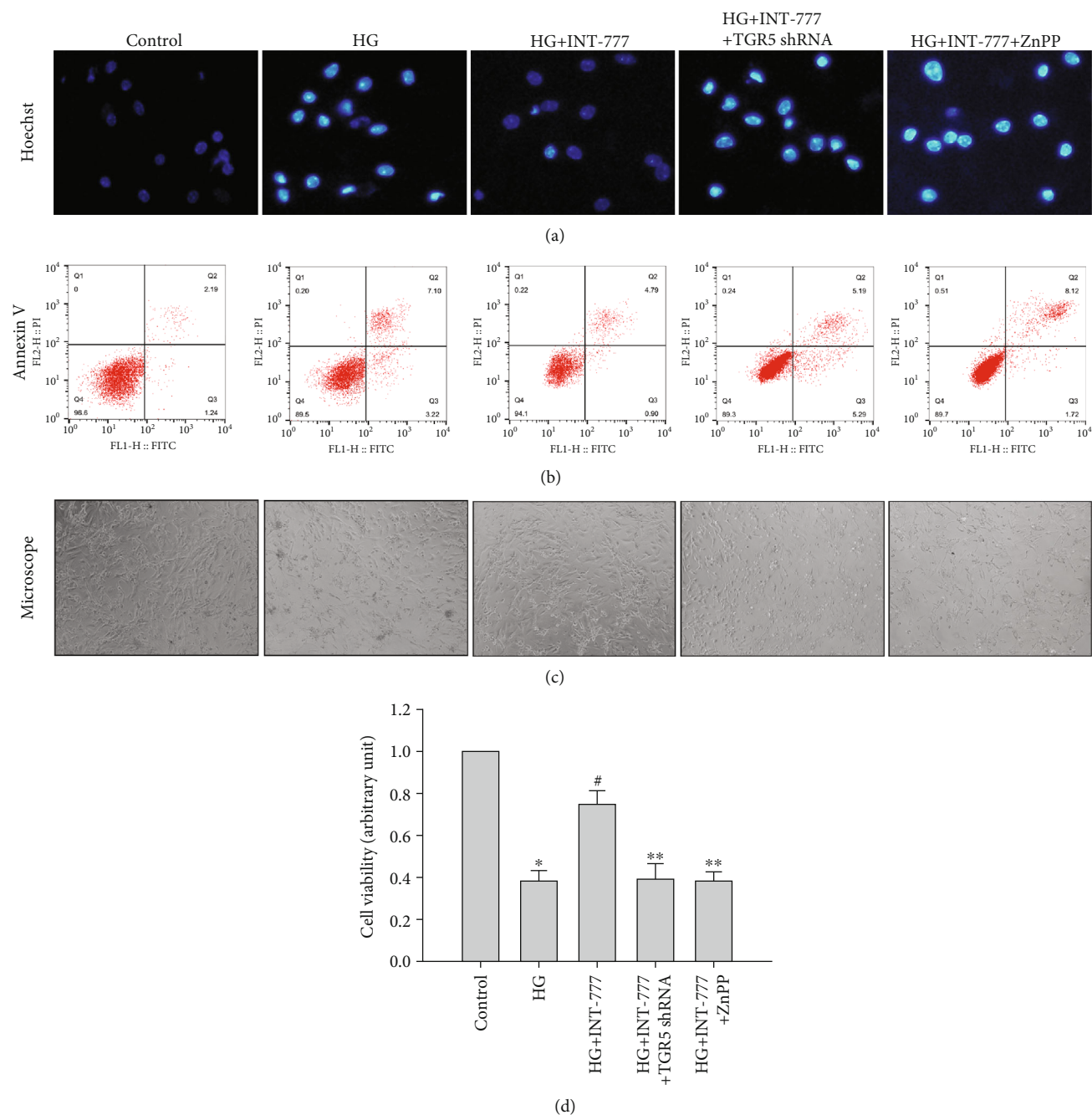


FIGURE 5: Activation of TGR5 attenuates HG-induced apoptosis in mouse cardiomyocytes. (a) Cells were infected with TGR5 shRNA adenoviral particles for 48 h or pretreated with $10 \mu\text{M}$ ZnPP for 1 h and then treated with $30 \mu\text{M}$ INT-777 for 3 h, followed by addition of HG to cardiomyocytes for a further 24 h. Cells with condensed or fragmented nuclei were defined as apoptotic cells. (b) Cells were infected with TGR5 shRNA adenoviral particles for 48 h or pretreated with $10 \mu\text{M}$ ZnPP for 1 h and then treated with $30 \mu\text{M}$ INT-777 for 3 h, followed by addition of HG to cardiomyocytes for a further 24 h. Cells were stained with FITC-labeled Annexin V and PI, and flow cytometry was used to detect apoptotic cells. (c) Microscopy was used to observe the morphology of mouse cardiomyocytes treated as described in (a) and (b). (d) Cell viability was measured by MTT assays. * $P < 0.05$ vs. control; # $P < 0.05$ vs. HG; ** $P < 0.05$ vs. HG+INT-777.

oxidative stress [28]. Therefore, we focused on the effect of TGR5 on the inflammatory response and oxidative stress in cardiomyocytes.

Activation of TGR5 results in the cascade of the adenylyl cyclase/cAMP signaling pathway [13]. The cAMP signaling pathway mediates inhibition of TGR5 binding to NF- κ B and lowers proinflammatory cytokines IL-1 α , IL-1 β , IL-6,

and TNF- α [16, 29]. Because of reports indicating an important role of TGR5 in the regulation of inflammation [13, 16, 17], we considered that TGR5 may protect against HG-induced cardiomyocyte inflammation. NF- κ B has been identified as a key regulator of the inflammatory response, which transcriptionally activates proinflammatory cytokine genes such as IL-1 β , IL-6, and TNF- α [30, 31]. Under

inactivated conditions, NF- κ B is localized in the cytoplasm by its inhibitory molecule ($\text{I}\kappa\text{B}$). Upon stimulation, $\text{I}\kappa\text{B}$ kinase phosphorylates $\text{I}\kappa\text{B}\alpha$. As a result, NF- κ B dissociates from the complex and translocates into the nucleus to regulate target genes [32]. In our study, HG increased the translocation of NF- κ B into the nucleus by increasing the phosphorylation of $\text{I}\kappa\text{B}\alpha$. Moreover, treatment of cardiomyocytes with JSH-23 (an NF- κ B inhibitor) greatly suppressed the HG-induced mRNA expression of proinflammatory cytokines, including IL-1 β , IL-6, and TNF- α , suggesting involvement of the NF- κ B pathway in HG-induced expression of proinflammatory cytokines. Next, we examined whether activation of TGR5 reduced proinflammatory cytokines through NF- κ B pathways. The TGR5-selective ligand INT-777 inhibited the HG-induced phosphorylation of $\text{I}\kappa\text{B}\alpha$ and nuclear translocation of NF- κ B in cardiomyocytes. The inhibitory effects of INT-777 were significantly attenuated by knockdown of TGR5 or treatment with SQ22536 (a cAMP inhibitor). These results suggested that activation of TGR5 under HG conditions exerts anti-inflammatory effects by suppressing the NF- κ B pathway in cardiomyocytes.

In addition to inflammation, hyperglycemia-induced ROS overproduction contributes to the development of cardiac complications in diabetic patients. As a cytoprotective enzyme, HO-1 has critical antioxidant functions [33]. Nrf2, a transcription factor, regulates HO-1 promoter activity and induces HO-1 expression [34]. It has been reported that the Nrf2/HO-1 pathway is involved in the pathophysiological processes of diabetes and cardiac complications [35–37]. Therefore, we speculated that the Nrf2/HO-1 pathway may be involved in the cytoprotection of TGR5. Our study showed that INT-777 induced Nrf2 nuclear localization and upregulated HO-1 expression. Furthermore, increased HO-1 protein expression induced by INT-777 was inhibited by Nrf2 shRNA. TGR5 shRNA also attenuated Nrf2 nuclear localization and the subsequent upregulation of HO-1 expression. Under HG conditions, treatment with INT-777 also increased the protein expression of Nrf2 and HO-1 in cardiomyocytes. Notably, the increase in HO-1 expression induced by INT-777 was not completely eliminated by TGR5 shRNA in this study. Therefore, we believe that Nrf2/HO-1 signaling may be partially mediated by TGR5, indicating that activation of TGR5 may exert antioxidant effects partially through the Nrf2/HO-1 pathway.

The effect of TGR5 activation on ROS generation remains controversial. Previous studies have shown that TGR5 is essential for bile acid-dependent cholangiocyte proliferation by increasing reactive oxygen species [38], and TGR5 mediates taurodeoxycholic acid-induced H_2O_2 production in human Barrett's and oesophageal adenocarcinoma cells [39]. However, Wang et al. [40] showed that TGR5 activated by INT-777 decreases oxidative stress and increases fatty acid β -oxidation in human podocytes treated with HG. Additionally, INT-777 extenuates pancreatic acinar cell necrosis by inhibiting ROS production and the NLRP3 inflammasome pathway [41]. Moreover, lithocholic acid (a natural agonist of TGR5) does not affect HG-induced elevation of ROS production in H9c2 cells [42]. These inconsistent observations may be due to different agonists,

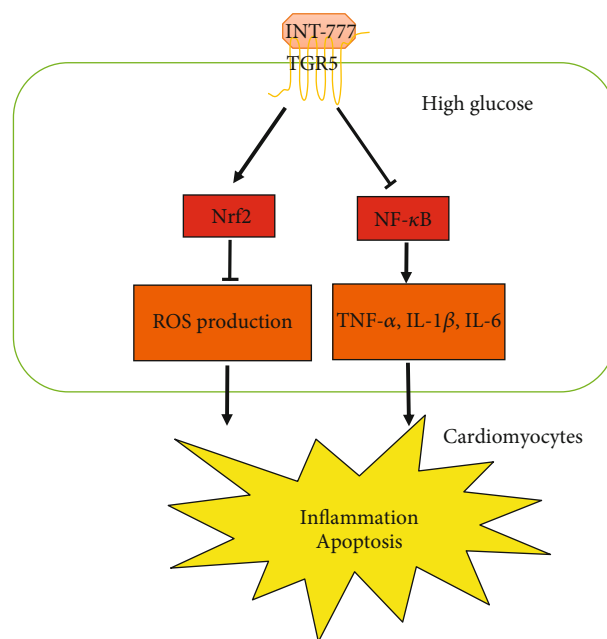


FIGURE 6: Schematic illustration of the preventive effect of TGR5 against HG-induced injury in cardiomyocytes. HG induces ROS production and expression of proinflammatory cytokine, such as IL-1 β , IL-6, and TNF- α , resulting in inflammation and apoptosis. Activation of TGR5 attenuates HG-induced cardiomyocyte injury partially by inhibiting the NF- κ B pathway and activating the Nrf2 pathway.

cell types, and experimental conditions. In the present study, we found that ROS was not induced by treatment with INT-777 at various concentrations, and INT-777 decreased HG-induced ROS production in cardiomyocytes. The antioxidant effect of INT-777 was abrogated by TGR5 shRNA or the HO-1 inhibitor ZnPP. Furthermore, HG-induced cell apoptosis was reduced by INT-777. Treatment of cells with TGR5 shRNA or ZnPP also attenuated the protective effect of INT-777.

In addition to the heart, TGR5 is also expressed in other organs of the body, especially the gallbladder. Previous studies have shown that activation of TGR5 exerts antidiabetic effects but causes gallbladder filling that may induce unwanted toxic effects on the gallbladder [43, 44]. Accordingly, local activation of TGR5 needs to be applied in the future.

5. Conclusions

Activation of TGR5 protected against HG-induced cardiomyocyte injury by suppressing inflammation and apoptosis partially through inhibiting the NF- κ B pathway and activating the Nrf2 pathway (Figure 6). Therefore, TGR5 could be a pharmacological target for the treatment of diabetic cardiomyopathy.

Data Availability

The data used to support the findings of this study are included within the article.

Conflicts of Interest

The authors have no other relevant affiliations or financial involvement with any organization or entity with a financial interest in or financial conflict with the subject matter or materials discussed in the manuscript apart from those disclosed.

Authors' Contributions

Li Deng and Xuxin Chen contributed equally to this paper.

Acknowledgments

We thank Yi Li and Dan Wu (Department of Cardiology, the Affiliated Hospital of Southwest Medical University, Luzhou, Sichuan, China) for technical assistance. We also thank M. Arico from Liwen Bianji, Edanz Group China (<http://www.liwenbianji.cn/ac>), for editing the English text of a draft of this manuscript. This study was supported by the National Natural Science Foundation of China (31300946 and 81300050), the Luzhou Municipal People's Government-Sichuan Medical University Science and Technology Strategic Cooperation (2015LZCYD-S03(7/7)), and the Beijing Natural Science Foundation (7182163).

References

- [1] S. Wild, G. Roglic, A. Green, R. Sicree, and H. King, "Global prevalence of diabetes: estimates for the year 2000 and projections for 2030," *Diabetes Care*, vol. 27, no. 5, pp. 1047–1053, 2004.
- [2] S. Rubler, J. Dlugash, Y. Z. Yuceoglu, T. Kumral, A. W. Branwood, and A. Grishman, "New type of cardiomyopathy associated with diabetic glomerulosclerosis," *The American Journal of Cardiology*, vol. 30, no. 6, pp. 595–602, 1972.
- [3] S. Boudina and E. D. Abel, "Diabetic cardiomyopathy revisited," *Circulation*, vol. 115, no. 25, pp. 3213–3223, 2007.
- [4] M. Letonja and D. Petrovič, "Is diabetic cardiomyopathy a specific entity," *World Journal of Cardiology*, vol. 6, no. 1, pp. 8–13, 2014.
- [5] T. Mazzone, A. Chait, and J. Plutzky, "Cardiovascular disease risk in type 2 diabetes mellitus: insights from mechanistic studies," *The Lancet*, vol. 371, no. 9626, pp. 1800–1809, 2008.
- [6] J. M. Forbes and M. E. Cooper, "Mechanisms of diabetic complications," *Physiological Reviews*, vol. 93, no. 1, pp. 137–188, 2013.
- [7] X. Palomer, L. Salvadó, E. Barroso, and M. Vázquez-Carrera, "An overview of the crosstalk between inflammatory processes and metabolic dysregulation during diabetic cardiomyopathy," *International Journal of Cardiology*, vol. 168, no. 4, pp. 3160–3172, 2013.
- [8] J. D. Schilling and D. L. Mann, "Diabetic cardiomyopathy: bench to bedside," *Heart Failure Clinics*, vol. 8, no. 4, pp. 619–631, 2012.
- [9] D. M. Ansley and B. Wang, "Oxidative stress and myocardial injury in the diabetic heart," *The Journal of Pathology*, vol. 229, no. 2, pp. 232–241, 2013.
- [10] H. Sato, C. Genet, A. Strehle et al., "Anti-hyperglycemic activity of a TGR5 agonist isolated from *Olea europaea*," *Biochemical and Biophysical Research Communications*, vol. 362, no. 4, pp. 793–798, 2007.
- [11] A. K. Jain, J. X. Wen, K. S. Blomenkamp et al., "Oleanolic acid improves gut atrophy induced by parenteral nutrition," *Journal of Parenteral and Enteral Nutrition*, vol. 40, no. 1, pp. 67–72, 2016.
- [12] D. P. Kumar, S. Rajagopal, S. Mahavadi et al., "Activation of transmembrane bile acid receptor TGR5 stimulates insulin secretion in pancreatic β cells," *Biochemical and Biophysical Research Communications*, vol. 427, no. 3, pp. 600–605, 2012.
- [13] Y. Kawamata, R. Fujii, M. Hosoya et al., "A G protein-coupled receptor responsive to bile acids," *The Journal of Biological Chemistry*, vol. 278, no. 11, pp. 9435–9440, 2003.
- [14] M. Watanabe, S. M. Houten, C. Matakaki et al., "Bile acids induce energy expenditure by promoting intracellular thyroid hormone activation," *Nature*, vol. 439, no. 7075, pp. 484–489, 2006.
- [15] M. S. Desai, Z. Shabier, M. Taylor et al., "Hypertrophic cardiomyopathy and dysregulation of cardiac energetics in a mouse model of biliary fibrosis," *Hepatology*, vol. 51, no. 6, pp. 2097–2107, 2010.
- [16] T. W. Pols, M. Nomura, T. Harach et al., "TGR5 activation inhibits atherosclerosis by reducing macrophage inflammation and lipid loading," *Cell Metabolism*, vol. 14, no. 6, pp. 747–757, 2011.
- [17] V. Stepanov, K. Stankov, and M. Mikov, "The bile acid membrane receptor TGR5: a novel pharmacological target in metabolic, inflammatory and neoplastic disorders," *Journal of Receptor and Signal Transduction Research*, vol. 33, no. 4, pp. 213–223, 2013.
- [18] Z. Eblimit, S. Thevananther, S. J. Karpen et al., "TGR5 activation induces cytoprotective changes in the heart and improves myocardial adaptability to physiologic, inotropic, and pressure-induced stress in mice," *Cardiovascular Therapeutics*, vol. 36, no. 5, article e12462, 2018.
- [19] E. Ehler, T. Moore-Morris, and S. Lange, "Isolation and culture of neonatal mouse cardiomyocytes," *Journal of Visualized Experiments*, no. 79, 2013.
- [20] W. E. Louch, K. A. Sheehan, and B. M. Wolska, "Methods in cardiomyocyte isolation, culture, and gene transfer," *Journal of Molecular and Cellular Cardiology*, vol. 51, no. 3, pp. 288–298, 2011.
- [21] W. Y. Wu, Y. D. Li, Y. K. Cui et al., "The natural flavone aca-cetin confers cardiomyocyte protection against hypoxia/reoxygenation injury via AMPK-mediated activation of Nrf2 signaling pathway," *Frontiers in Pharmacology*, vol. 9, p. 497, 2018.
- [22] C. L. de Melo, M. G. Queiroz, S. G. Fonseca et al., "Oleanolic acid, a natural triterpenoid improves blood glucose tolerance in normal mice and ameliorates visceral obesity in mice fed a high-fat diet," *Chemico-Biological Interactions*, vol. 185, no. 1, pp. 59–65, 2010.
- [23] P. S. Ngubane, B. Masola, and C. T. Musabayane, "The effects of Syzygium aromaticum-derived oleanolic acid on glycogenic enzymes in streptozotocin-induced diabetic rats," *Renal Failure*, vol. 33, no. 4, pp. 434–439, 2011.
- [24] S. Katsuma, A. Hirasawa, and G. Tsujimoto, "Bile acids promote glucagon-like peptide-1 secretion through TGR5 in a murine enteroendocrine cell line STC-1," *Biochemical and Biophysical Research Communications*, vol. 329, no. 1, pp. 386–390, 2005.

- [25] C. Thomas, A. Gioiello, L. Noriega et al., "TGR5-mediated bile acid sensing controls glucose homeostasis," *Cell Metabolism*, vol. 10, no. 3, pp. 167–177, 2009.
- [26] W. Liang, M. Chen, D. Zheng et al., "The opening of ATP-sensitive K⁺ channels protects H9c2 cardiac cells against the high glucose-induced injury and inflammation by inhibiting the ROS-TLR4-necroptosis pathway," *Cellular Physiology and Biochemistry*, vol. 41, no. 3, pp. 1020–1034, 2017.
- [27] X. Chen, J. Qian, L. Wang et al., "Kaempferol attenuates hyperglycemia-induced cardiac injuries by inhibiting inflammatory responses and oxidative stress," *Endocrine*, vol. 60, no. 1, pp. 83–94, 2018.
- [28] S. You, J. Qian, C. Sun et al., "An Aza resveratrol–chalcone derivative 6b protects mice against diabetic cardiomyopathy by alleviating inflammation and oxidative stress," *Journal of Cellular and Molecular Medicine*, vol. 22, no. 3, pp. 1931–1943, 2018.
- [29] Y. D. Wang, W. D. Chen, D. Yu, B. M. Forman, and W. Huang, "The G-protein-coupled bile acid receptor, Gpbar1 (TGR5), negatively regulates hepatic inflammatory response through antagonizing nuclear factor κ light-chain enhancer of activated B cells (NF- κ B) in mice," *Hepatology*, vol. 54, no. 4, pp. 1421–1432, 2011.
- [30] M. Ghosh, V. Aguirre, K. Wai, H. Felfly, W. D. Dietrich, and D. D. Pearce, "The interplay between cyclic AMP, MAPK, and NF- κ B pathways in response to proinflammatory signals in microglia," *BioMed Research International*, vol. 2015, Article ID 308461, 18 pages, 2015.
- [31] A. U. Ahmed, B. R. Williams, and G. E. Hannigan, "Transcriptional activation of inflammatory genes: mechanistic insight into selectivity and diversity," *Biomolecules*, vol. 5, no. 4, pp. 3087–3111, 2015.
- [32] M. Bartekova, J. Radosinska, M. Jelemensky, and N. S. Dhalla, "Role of cytokines and inflammation in heart function during health and disease," *Heart Failure Reviews*, vol. 23, no. 5, pp. 733–758, 2018.
- [33] M. A. Perrella and S. F. Yet, "Role of heme oxygenase-1 in cardiovascular function," *Current Pharmaceutical Design*, vol. 9, no. 30, pp. 2479–2487, 2003.
- [34] A. Loboda, E. Rojczyk-Golebiewska, B. Bednarczyk-Cwynar, Z. Lucjusz, A. Jozkowicz, and J. Dulak, "Targeting nrf2-mediated gene transcription by triterpenoids and their derivatives," *Biomolecules & Therapeutics*, vol. 20, no. 6, pp. 499–505, 2012.
- [35] H. Li, W. Yao, M. G. Irwin et al., "Adiponectin ameliorates hyperglycemia-induced cardiac hypertrophy and dysfunction by concomitantly activating Nrf2 and Brg1," *Free Radical Biology & Medicine*, vol. 84, pp. 311–321, 2015.
- [36] Y. Tan, T. Ichikawa, J. Li et al., "Diabetic downregulation of Nrf2 activity via ERK contributes to oxidative stress-induced insulin resistance in cardiac cells in vitro and in vivo," *Diabetes*, vol. 60, no. 2, pp. 625–633, 2011.
- [37] H. H. Liao, J. X. Zhu, H. Feng et al., "Myricetin possesses potential protective effects on diabetic cardiomyopathy through inhibiting I κ B α /NF κ B and enhancing Nrf2/HO-1," *Oxidative Medicine and Cellular Longevity*, vol. 2017, Article ID 8370593, 14 pages, 2017.
- [38] M. Reich, K. Deutschmann, A. Sommerfeld et al., "TGR5 is essential for bile acid-dependent cholangiocyte proliferation in vivo and in vitro," *Gut*, vol. 65, no. 3, pp. 487–501, 2016.
- [39] J. Hong, J. Behar, J. Wands et al., "Role of a novel bile acid receptor TGR5 in the development of oesophageal adenocarcinoma," *Gut*, vol. 59, no. 2, pp. 170–180, 2010.
- [40] X. X. Wang, M. H. Edelstein, U. Gafter et al., "G protein-coupled bile acid receptor TGR5 activation inhibits kidney disease in obesity and diabetes," *Journal of the American Society of Nephrology*, vol. 27, no. 5, pp. 1362–1378, 2016.
- [41] B. Li, N. Yang, C. Li et al., "INT-777, a bile acid receptor agonist, attenuates pancreatic acinar cells necrosis in a mouse model of acute pancreatitis," *Biochemical and Biophysical Research Communications*, vol. 503, no. 1, pp. 38–44, 2018.
- [42] K. C. Cheng, W. T. Chang, F. Y. Kuo, Z. C. Chen, Y. Li, and J. T. Cheng, "TGR5 activation ameliorates hyperglycemia-induced cardiac hypertrophy in H9c2 cells," *Scientific reports*, vol. 9, no. 1, article 3633, 2019.
- [43] D. A. Briere, X. Ruan, C. C. Cheng et al., "Novel small molecule agonist of TGR5 possesses anti-diabetic effects but causes gallbladder filling in mice," *PLoS one*, vol. 10, no. 8, article e0136873, 2015.
- [44] T. Li, S. R. Holmstrom, S. Kir et al., "The G protein-coupled bile acid receptor, TGR5, stimulates gallbladder filling," *Molecular Endocrinology*, vol. 25, no. 6, pp. 1066–1071, 2011.

Research Article

Cardiovascular Risk Factors and Haematological Indexes of Inflammation in Paralympic Athletes with Different Motor Impairments

Marco Bernardi ^{1,2}, Anna Lucia Fedullo,³ Barbara Di Giacinto,⁴ Maria Rosaria Squeo,⁴ Paola Aiello,^{1,5} Donatella Dante,¹ Silvio Romano ⁶, Ludovico Magaudda,⁷ Ilaria Peluso ⁵, Maura Palmery ¹ and Antonio Spataro⁴

¹Department of Physiology and Pharmacology “V. Erspamer”, Sapienza University of Rome, Italy

²Comitato Italiano Paralimpico, Rome, Italy

³Federazione Italiana Pallacanestro In Carrozzina (FIPIC), Rome, Italy

⁴Institute of Sport Medicine and Science, Sport e Salute, Rome, Italy

⁵Research Centre for Food and Nutrition, Council for Agricultural Research and Economics (CREA-AN), Rome, Italy

⁶Department of Life, Health and Environmental Sciences, University of L'Aquila, Italy

⁷Sport Medicine Unit AOU “G. Martino”, BIOMORF Department University of Messina, Italy

Correspondence should be addressed to Marco Bernardi; marco.bernardi@uniroma1.it and Ilaria Peluso; i.peluso@tiscali.it

Received 12 July 2019; Accepted 30 October 2019; Published 18 November 2019

Guest Editor: Aneta Radziwon-Balicka

Copyright © 2019 Marco Bernardi et al. This is an open access article distributed under the Creative Commons Attribution License, which permits unrestricted use, distribution, and reproduction in any medium, provided the original work is properly cited.

Haematological indexes of both inflammation and platelet activation have been suggested as predictive markers of cardiovascular disease (CVD), which has high prevalence in Paralympic athletes (PA). Different mechanisms could play a role in increasing CVD risk in PA with spinal cord injury (PA-SCI), lower limb amputation (PA-LLA), or upper limb impairment (PA-ULI). We compared, in 4 groups of PA competing in power, intermittent (mixed metabolism), and endurance sports, Framingham Risk Score (FRS), metabolic syndrome criteria (MetS-C), inflammation (INFLA) Score, 5 haematological indexes of platelet activation (mean platelet volume (MPV), platelet distribution width (PDW), and the ratios between MPV and platelet (MPVPR), between MPV and lymphocyte (MPVLR), and between PDW and lymphocyte (PDWLR)) and the endogenous antioxidants uric acid (UA) and bilirubin (BR). A retrospective chart review of PA from preparticipation examinations' records (London 2012 and Sochi 2014 Paralympics) was performed. We included 25 PA-SCI (13 with high and 12 with low lesion, PA-SCI-H and PA-SCI-L), 15 PA-LLA, and 10 PA-ULI. FRS and INFLA Score did not differ among groups, but PA-SCI-H had lower HDL, compared to PA-SCI-L and PA-ULI. PA-LLA had more MetS diagnostic criteria with significant higher glucose levels than other groups. PA-SCI-H had significantly lower lymphocytes' count compared to PA-LLA and higher MPV, PDW, MPVPR, MPVLR, and PDWLR. SCI-H had lower BR, haemoglobin, haematocrit, proteins, and creatinine. No interaction was found between the 3 kinds of sitting sports and the 2 groups of health conditions (PA-SCI and PA-LLA). In conclusion, PA-LLA had a higher cardiometabolic risk, whereas PA-SCI-H had a higher platelet-derived cardiovascular risk. Further larger studies are needed to investigate the relationship between indexes of inflammation/oxidation and dietary habit, body composition, and physical fitness/performance in PA with motor impairments.

1. Introduction

The common activities of daily life, carried out by individuals with spinal cord injury (SCI) or lower limb amputation (LLA), forced by their impairment to be sedentary, determine

a vicious circle that perpetuates and increases sarcopenia, fat mass and osteoporosis [1], oxidative stress [2], chronic systemic inflammation [3], reduction of cardiovascular efficiency [4], dyslipidemia, insulin resistance, and atherosclerotic cardiovascular disease (CVD) risk [5]. Only physical exercise

and sport are effective weapons to counter this debilitating cycle in these individuals [6], to reduce the CVD risk [1–3]. Despite the beneficial effect of exercise, high prevalence of CVD risk factors was found in Paralympic athletes with SCI (PA-SCI) and with other disorders [7]. Multiple lines of evidence have revealed common mechanisms behind cardiovascular and inflammatory diseases and clarified the metabolic and cardiovascular pathways involved in rheumatoid arthritis (RA) [8]. In particular, CVD comorbidities depend on several pathogenic mechanisms, and even if atherosclerosis is the most frequently involved, further mechanisms include microvascular dysfunction, arrhythmias, cardiac autonomic deregulation, inflammation, and immunologic abnormalities, as well as the effects of pharmacological treatments [8]. Cardiovascular autonomic nervous system dysfunction, typical in individuals with SCI, is commonly observed in RA, and it has been suggested that lowering the inflammation may represent the most effective intervention to reduce arrhythmic risk in these patients [9]. The authors suggested that these considerations could be more generally applicable to all the diseases characterized by chronic systemic inflammation [9]. Increased sympathetic activity is associated with higher mean platelet volume (MPV), with mechanisms involving peripheral activation [10]. Individuals with SCI had more extensive basal, exercise-induced [11], and oxidized-low density lipoprotein-mediated platelet activation and higher levels of lipid peroxides [12] than people without SCI. In a randomized controlled trial, a 12-week arm-cranking exercise program reduced oxidative damage and increased oxygen uptake peak in sedentary adults with SCI [2]. Regarding the antioxidant defence system, it was found that both total antioxidant status and erythrocyte glutathione peroxidase activity were significantly increased at the end of the training program, whereas plasmatic levels of lipid (malondialdehyde) and protein (carbonyl groups) oxidation markers were significantly reduced [2].

Although biomarkers of oxidative stress are relevant in the evaluation of the disease status, there is a lack of consensus concerning the validation, standardization, and reproducibility of methods for the measurement of reactive oxygen species (ROS) in leukocytes and platelets, markers based on ROS-induced modifications of lipids, DNA, and proteins, enzymatic players of redox status, and nonenzymatic antioxidant capacity of human body fluids [13]. In particular, bilirubin (BR) and/or uric acid (UA) could produce interferences in the measurement of markers of oxidative stress [13].

In a report regarding two rowers with physical impairment, qualified for the Paralympic Games in Rio 2016, high levels of BR before an exercise protocol (progressive test on a rowing ergometer until exhaustion) and during recovery (17 hours after completion of the test) were observed compared to postexercise (5 minutes postexercise), and similar trends were also observed in UA concentrations [14]. On the other hand, in individuals with chronic SCI, hyperuricemia is associated with hyperinsulinemia, elevated body mass index (BMI), and abnormal lipoprotein metabolism, but not with age or duration of injury [15]. Data from a meta-analysis reported positive relationships between UA and both

nonalcoholic fatty liver disease and metabolic syndrome (MetS) [16]. In a recent retrospective chart review [17], conducted on veterans with SCI, cardiometabolic risk scores, including the most widely used CVD risk prediction Framingham Risk Score (FRS), as well as the MetS classification, may lead to different interpretations of a true risk and can account for inconsistencies between research and clinical practice. Individuals with SCI can experience blood pressure fluctuations due to neurological changes, potentially limiting the validity and/or reliability of tools used in able people in the SCI population. On the other hand, haematological indexes of inflammation/platelet activation, including platelet count (P) [18, 19], markers of platelet activation (mean platelet volume (MPV) and platelet distribution width (PDW)) [20–22], neutrophil-to-lymphocyte ratio (NLR), lymphocyte-to-monocyte ratio (LMR), platelet-to-lymphocyte ratio, mean platelet volume (MPV), and platelet distribution width (PDW) to platelet (MPVPR and PDWPR) and to lymphocyte (MPVLR and PDWLR) ratios [23, 24], have all been suggested as predictive markers of CVD risk [9, 20, 22, 25, 26], and granulocyte-to-lymphocyte ratio (GLR) has been included in the inflammation (INFLA) Score [19].

In this study, we aimed to compare the FRS, MetS criteria, INFLA Score, other haematological indexes of inflammation/platelet activation, and clinical markers (including the endogenous antioxidants UA and BR) in PA-SCI, PA-LLA, and PA with upper limb impairment (PA-ULI).

2. Methods

2.1. Selection Process of Retrospective Chart Review. We conducted a retrospective chart review of PA screened for Paralympic eligibility [27] before the Games of London 2012 and Sochi 2014. The preparticipation examinations' records, including general medical examination, instrumental, and urine and blood laboratory tests, were screened, and PA were selected based on the following criteria.

The inclusion criteria were PA-SCI, PA-LLA or PA-ULI, as well as availability of results for FRS, MetS criteria, and INFLA Score evaluations. The exclusion criteria were other health conditions (spina bifida, poliomyelitis, cerebral palsy, and other neuromuscular and/or skeletal disorders), visual impairments, and the use of anticoagulants and antiplatelet drugs. It should be stressed that platelets' indexes, among the primary outcomes of the study, could be affected (in particular) by antiplatelet drugs. Specifically, two PA were in treatment with acetylsalicylic acid and were excluded from the study, whereas none was in treatment with anticoagulants. On the other hand, the use of drugs for diabetes, hypertension, and dyslipidaemia was not considered exclusion criteria, being the use of these drugs included in the criteria for metabolic syndrome proposed by the National Cholesterol Education Program—Third Adult Treatment Panel (NCEP-ATP III).

Other characteristics of subjects, including type of impairment, sport, diseases, and use of drugs and supplements, as well as clinically relevant parameters (endogenous antioxidants, markers of anaemia, etc.), were recorded. From that, women, who can have monthly physiological variation

in markers of anaemia, were also excluded. Applying the above criteria, 50 athletes were selected 25 PA-SCI, 15 PA-LLA, and 10 PA-ULI.

According to the autonomic dysfunction reported in individuals with SCI and the adrenal gland innervation [28, 29], PA-SCI were divided in two groups: 13 with high (from cervical (C)8/thoracic(T)1, incomplete, to T9, PA-SCI-H) and 12 with low (from T10 to lumbar (L)5, PA-SCI-L) lesion.

Included PA 19 practice endurance sports (3 PA-SCI-H, 6 PA-SCI-L, 2 PA-LLA, and 8 PA-ULI), 10 power sports (4 PA-SCI-H, 4 PA-LLA, and 2 PA-ULI), and 20 mixed sports (aerobic/anaerobic) (5 PA-SCI-H, 6 PA-SCI-L, and 9 PA-LLA).

2.2. Data Extraction and Analysis. The Framingham Score was calculated according to literature [30, 31]. MetS was evaluated by the NCEP-ATP III criteria: triglycerides (TG) \geq 150 mg/dL or use of lipid-lowering drugs, systolic blood pressure (SBP) \geq 130 mmHg, diastolic DBP \geq 85 mmHg or use of antihypertensive agents, glucose \geq 100 mg/dL or use of medications for diabetes, and in men high-density lipoprotein cholesterol (HDL) $<$ 40 mg/dL and waist circumference $>$ 102 cm [32]. Cholesterol/HDL and low-density lipoprotein cholesterol (LDL)/HDL ratios were also calculated [33].

INFLA Score, including C reactive protein (CRP), white blood cell (WBC), P, and GLR, was calculated as previously described [19]. Haematological indexes of inflammation and of platelet activation were calculated, including NLR, LMR, PLR, MPVPR, PDWPR, MPVLR, and PDWLR [23, 24, 26].

Other parameters were evaluated, including UA, BR, fibrinogen, proteins, creatine phosphokinase (CPK), iron, red blood cells (RBC), haemoglobin (Hb), haematocrit (HCT), mean corpuscular volume (MCV), mean cell haemoglobin (MCH), mean cell haemoglobin concentration (MCHC), the platelet/MCH ratio (PMCHR) [34], that had high values when iron-deficient anemia (IDA) was accompanied by vitamin B12 deficiency, and the serum UA to creatinine (Cr) ratio (UA/Cr), associated with a higher risk of MetS [35].

2.3. Statistical Analysis. Results that passed the normality test (Shapiro-Wilk) or Equal Variance Test were analyzed by analysis of variance (ANOVA), others by Kruskal-Wallis One Way Analysis of Variance on Ranks.

Two-way Analysis of Variance was conducted to evaluate the interaction between sport (endurance, power, and mixed) and impairment on data from PA-SCI (overall) and PA-LLA. PA-ULI were excluded from this analysis due to the absence of PA practicing mixed sports. The significance of the differences between groups was evaluated using the Student-Newman-Keuls or Dunn's (normality test Shapiro-Wilk and Equal Variance Test failed) methods. Spearman correlation was performed between variables (all PA, $n = 50$).

3. Results

3.1. Cardiovascular Risk. The Framingham Score did not differ among groups, but PA-SCI-H had lower HDL, compared

to PA-SCI-L and PA-ULI (Table 1). Two-way ANOVA revealed that there is not a statistically significant interaction between sports and health conditions (PA-SCI and PA-LLA) (HDL $p = 0.830$).

No differences were found in CHOL, LDL, and ratios (CHOL/HDL and LDL/HDL). These ratios were correlated with both FRS (CHOL/HDL: coefficient = 0.607, $p < 0.001$, LDL/HDL: coefficient = 0.638, $p < 0.001$) and MetS ATP III (CHOL/HDL: coefficient = 0.496, $p < 0.001$, LDL/HDL: coefficient = 0.607, $p < 0.001$).

Although only 6 athletes (12%, 6/50) fulfilled the 3 criteria needed for MetS diagnosis (1 PA-SCI-H, 1 PA-SCI-L, and 4 PA-LLA), PA-LLA subjects had more criteria compared to other groups (PA-SCI-H: 1 PA with 3 criteria: W, HDL, and TG, 1 PA with 2 criteria: GLU and HDL, 5 PA with 1 criterion: 1 W, 1 BP, and 3 GLU, 6 PA no criteria; PA-SCI-L: 1 PA with 3 criteria: SBP/DBP, GLU, and TG, 1 PA with 2 criteria: GLU and BP, 3 PA with high BP only, 1 PA with low HDL only; 6 PA no criteria; PA-LLA: 1 PA with 4 criteria: BP, GLU, HDL, and TG, 3 PA with 3 criteria: 3 BP, GLU, and TG; 1 GLU, HDL, and TG, 4 PA with 2 criteria: 4 BP and GLU, 1 GLU and HDL, 5 PA with GLU only, 1 PA no criteria; PA-ULI: 7 PA with 1 criterion: 1 BP and 6 GLU, 3 PA no criteria) and GLU levels were higher in PA-LLA compared to PA-SCI (Table 1). Two-way ANOVA revealed that there is not a statistically significant interaction between sports and health conditions (PA-SCI and PA-LLA) (MetS ATP III $p = 0.810$; GLU $p = 0.440$).

3.2. Inflammation and Thrombotic Risk. Although means of INFLA Score, including CRP, WBC, P, and GLR, were all below 0, the value was lower in PA-ULI compared to PA-LLA (Table 2), but it did not reach a statistical significance.

PA-SCI-H had significantly lower L count compared to PA-LLA and higher MPV, PDW, and/or related platelet-activation indexes compared to other groups (Table 2). On the other hand, PA-LLA had higher M count (Table 2). The latter was correlated with CHOL/HDL (coefficient: 0.294, $p < 0.05$), TG (coefficient: 0.399, $p < 0.01$), GLU (coefficient: 0.367, $p < 0.01$), MetS (coefficient: 0.337, $p < 0.05$), N (coefficient: 0.570, $p < 0.001$), and INFLA Score (coefficient: 0.554, $p < 0.001$). Two-way ANOVA revealed that there is not a statistically significant interaction between sports and health conditions (PA-SCI and PA-LLA) for all variables (L: $p = 0.840$; M: $p = 0.287$; MPV: $p = 0.116$; PDW: $p = 0.189$; MPVPR: $p = 0.141$; MPVLR: $p = 0.766$; PDWLR: $p = 0.702$).

3.3. Endogenous Antioxidants, Other Clinical Parameters, and Relationship with Platelet-Activation Indexes. Among endogenous antioxidants, only BR was higher in PA-ULI compared to PA-SCI-H (Table 3), but UA/Cr was higher in PA-SCI-H and PA-SCI-L compared to PA-ULI, due to the lower levels of Cr in PA-SCI (Table 3). Moreover, compared to other groups, PA-SCI-H had lower Hb (vs. PA-LLA and PA-ULI), HCT% (vs. PA-LLA and PA-SCI-L), and proteins (vs. PA-LLA and PA-ULI) (Table 3). Two-way ANOVA

TABLE 1: Framingham Score and MetS criteria (NCEP-ATP III).

	PA-SCI-H (<i>n</i> = 13)	PA-SCI-L (<i>n</i> = 12)	PA-LLA (<i>n</i> = 15)	PA-ULI (<i>n</i> = 10)
Framingham score	2.3 ± 1.9	1.9 ± 1.8	3.8 ± 1.2	2.7 ± 1.2
Age (years) (sex (all men))	40.1 ± 2.0	36.6 ± 3.1	39.2 ± 1.3	37.9 ± 2.5
Smokers	2/13	1/12	4/15	1/10
CHOL (mg/dL)	178 (139-201)	207 (162-229)	209 (188-235)	200 (192-210)
HDL (mg/dL) (NCEP-ATP III: <40)	47.8 ± 2.4	63.0 ± 3.9 vs. SCI-H <i>p</i> < 0.05	54.1 ± 4.0	64.0 ± 3.7 vs. SCI-H <i>p</i> < 0.05
SBP (mmHg) (NCEP-ATP III: ≥130)	120 (110-122)	122 (120-130)	120 (110-130)	120 (117-121)
Met-S criteria (NCEP-ATP III) not included in the Framingham Score				
DBP (mmHg) (NCEP-ATP III: ≥ 85)	75 (70-80)	80 (72-85)	80 (60-85)	72 (67-80)
W (cm) (NCEP-ATP III: >102)	82 (76-98)	80 (77-90)	89 (80-97)	82 (73-87)
GLU (mg/dL) (NCEP-ATP III: ≥100)	94.9 ± 2.0 vs. LLA <i>p</i> < 0.001	96.8 ± 1.9 vs. LLA <i>p</i> < 0.001	106.9 ± 1.2	100.4 ± 1.7 vs. LLA > <i>p</i> < 0.05
TG (mg/dL) (NCEP-ATP III: ≥150)	87 (79-115)	59 (43-103)	97 (65-160)	64 (56-93)
Met-S (NCEP-ATP III)	0.5 (0.0-1.0) vs. LLA <i>p</i> < 0.05	0.5 (0.0-1.8) vs. LLA <i>p</i> < 0.05	2.0 (1.0-3.0)	1.0 (0.0-1.0)
LDL (mg/dL)	110 ± 11	124 ± 15	134 ± 9	123 ± 5
LDL/HDL	2.4 (1.5-3.2)	1.8 (1.2-2.6)	2.2 (1.8-3.8)	2.1 (1.7-2.2)
CHOL/HDL	3.7 (2.8-4.6)	3.0 (2.4-3.9)	3.4 (3.0-5.7)	3.3 (2.9-3.4)

MetS: metabolic syndrome; NCEP-ATP III: National Cholesterol Education Program—Third Adult Treatment Panel; CHOL: cholesterol; HDL: high-density lipoproteins; SBP: systolic blood pressure; DBP: diastolic blood pressure; W: waist circumference; GLU: glucose; TG: triglycerides. Data are expressed as mean and SEM (normality test (Shapiro-Wilk) passed; One Way Analysis of Variance, followed by All Pairwise Multiple Comparison Procedures (Student-Newman-Keuls Method)) or median and interquartile range (25%-75%) (normality test (Shapiro-Wilk) failed; Kruskal-Wallis One Way Analysis of Variance on Ranks, followed by All Pairwise Multiple Comparison Procedures (Dunn's Method)).

TABLE 2: INFLA Score, WBC-related, and P-related parameters.

	PA-SCI-H (<i>n</i> = 13)	PA-SCI-L (<i>n</i> = 12)	PA-LLA (<i>n</i> = 15)	PA-U LI (<i>n</i> = 10)
INFLA score	-3.3 ± 1.6	-3.6 ± 1.8	-1.3 ± 1.8	-4.6 ± 2.3
CRP (mg/L)	1.5 (0.5-4.8)	0.9 (0.4-2.9)	0.8 (0.5-1.5)	0.5 (0.2-5.0)
WBC (10 ³ /microL)	5.2 ± 0.3	5.4 ± 0.4	6.4 ± 0.4	5.8 ± 0.4
P (10 ³ /microL)	213.4 ± 10.9	247.2 ± 13.5	237.5 ± 13.6	220.0 ± 19.3
GLR	1.9 (1.5-2.8)	1.4 (1.2-1.9)	1.7 (1.5-1.9)	1.6 (1.1-2.0)
NLR	1.7 (1.4-2.7)	1.3 (1.1-1.9)	1.6 (1.3-1.8)	1.5 (1.1-1.9)
N (10 ³ /microL)	2.9 ± 0.2	2.8 ± 0.2	3.6 ± 0.3	3.1 ± 0.3
L (10 ³ /microL)	1.6 ± 0.1	1.9 ± 0.2	2.2 ± 0.1 vs. SCI-H <i>p</i> < 0.05	2.0 ± 0.1
M (10 ³ /microL)	0.47 ± 0.03 vs. LLA <i>p</i> < 0.05	0.42 ± 0.03 vs. LLA <i>p</i> < 0.05	0.59 ± 0.04	0.43 ± 0.05 vs. LLA <i>p</i> < 0.05
G (10 ³ /microL)	3.1 ± 0.2	3.0 ± 0.2	3.9 ± 0.3	3.3 ± 0.3
LMR	2.9 (2.5-5.4)	4.8 (3.9-5.4)	4.2 (3.1-4.3)	5.0 (4.1-6.2)
PLR	131 (100-185)	127 (114-143)	99 (97-132)	100 (96-132)
MPV (fL)	10.1 (10-10.6)	8.8 (8.7-9.5) vs. SCI-H <i>p</i> < 0.001	9.4 (8.9-9.7) vs. SCI-H <i>p</i> < 0.05	9.9 (9.6-10.1)
MPVPR (fL/10 ³ /microL)	0.05 (0.04-0.06)	0.03 (0.03-0.04) vs. SCI-H <i>p</i> < 0.01	0.04 (0.03-0.05)	0.04 (0.04-0.05)
MPVLR (fL/10 ³ /microL)	6.6 (5.4-8.0)	5.1 (3.7-5.6)	4.6 (3.6-5.2) vs. SCI-H <i>p</i> < 0.01	5.0 (4.4-5.5)
PDW (fL)	12.0 (11.2-14.0)	10.6 (10.0-12.1) vs. SCI-H <i>p</i> < 0.05	11.2 (10.4-12.4)	12.1 (11.4-12.7)
PDWPR (fL/10 ³ /microL)	0.06 (0.05-0.08)	0.04 (0.04-0.05)	0.04 (0.04-0.06)	0.05 (0.05-0.06)
PDWLR (fL/10 ³ /microL)	8.2 (6.6-9.7)	5.8 (4.4-6.7) vs. SCI-H <i>p</i> < 0.01	5.3 (4.2-6.2) vs. SCI-H <i>p</i> < 0.01	5.8 (5.5-7.1)
Fibrinogen (mg/dL)	247 (227-303)	260 (240 ± 41.4)	240 (228-270)	261 (220-299)

INFLA Score includes C reactive protein (CRP), white blood cell (WBC) and platelet (Pt) counts and granulocyte-to-lymphocyte ratio (GLR), neutrophil-to-lymphocyte ratio (NLR), neutrophil (N), lymphocyte (L), monocyte (M), granulocyte (G), lymphocyte-to-monocyte ratio (LMR), platelet-to-lymphocyte ratio (PLR), mean platelet volume to platelet (MPVPR), mean platelet volume to lymphocyte (MPVLR), platelet distribution width (PDW), platelet distribution width to platelet (PDWPR), and platelet distribution width to lymphocyte (PDWLR). Data are expressed as mean and SEM (normality test (Shapiro-Wilk) passed; One Way Analysis of Variance, followed by All Pairwise Multiple Comparison Procedures (Student-Newman-Keuls Method)) or median and interquartile range (25%-75%) (normality test (Shapiro-Wilk) failed; Kruskal-Wallis One Way Analysis of Variance on Ranks, followed by All Pairwise Multiple Comparison Procedures (Dunn's Method)).

TABLE 3: Endogenous antioxidants and other clinically relevant markers.

	PA-SCI-H (<i>n</i> = 13)	PA-SCI-L (<i>n</i> = 12)	PA-LLA (<i>n</i> = 15)	PA-ULI (<i>n</i> = 10)
UA (mg/dL)	5.6 (5.1-6.5)	6.0 (5.1-6.6)	5.8 (5.3-6.2)	5.4 (4.2-6.2)
UA/Cr	7.3 (6.5-8.2) vs. ULI <i>p</i> < 0.05	7.8 (5.7-9.1) vs. ULI <i>p</i> < 0.05	5.9 (5.8-6.8)	5.6 (4.4-5.7)
BR (mg/dL)	0.4 (0.3-0.6)	0.5 (0.5-0.7)	0.6 (0.5-0.8)	0.9 (0.6-1.4) vs. SCI-H <i>p</i> < 0.01
RBC (10 ⁶ /microL)	4.7 ± 0.1	5.0 ± 0.1	5.0 ± 0.1	5.0 ± 0.1
Hb (g/dL)	13.6 ± 1.3	14.4 ± 0.2	14.9 ± 0.2 vs. SCI-H <i>p</i> < 0.01	14.7 ± 0.3 vs. SCI-H <i>p</i> < 0.01
HCT (%)	40.5 ± 0.8	43.0 ± 0.6 vs. SCI-H <i>p</i> < 0.05	44.2 ± 0.6 vs. SCI-H <i>p</i> < 0.01	43.1 ± 0.9
MCV (fL)	86.6 ± 1.3	85.9 ± 1.2	89.1 ± 1.3	86.6 ± 1.2
MCH (pg)	29.2 (28.4-30.5)	28.6 (27.5-30.0)	29.9 (29.3-31.4)	29.4 (28.9-29.9)
PMCHR	7.4 ± 0.5	8.5 ± 0.5	7.9 ± 0.5	7.5 ± 0.7
MCHC (g/dL)	33.7 ± 0.2	33.4 ± 0.2	33.8 ± 0.2	34.0 ± 0.2
Iron (mcg/dL)	82.7 ± 10.0	84.2 ± 8.7	106.1 ± 7.7	98.0 ± 15.0
Urea (mg/dL)	34.3 ± 2.6	41.0 ± 2.2	36.4 ± 3.1	38.9 ± 1.7
Cr (mg/dL)	0.75 ± 0.03 vs. ULI <i>p</i> < 0.001 vs. LLA <i>p</i> < 0.001	0.80 ± 0.04 vs ULI <i>p</i> < 0.01 vs. LLA <i>p</i> < 0.01	0.96 ± 0.03	1.02 ± 0.04
Proteins (g/dL)	7.0 ± 0.1	7.3 ± 0.1	7.4 ± 0.1 vs. SCI-H <i>p</i> < 0.05	7.4 ± 0.1 vs SCI-H <i>p</i> < 0.05
CPK (U/L)	161 (98-218)	197 (148-296)	142 (109-185)	152 (139-331)

UA: uric acid, BR: bilirubin, CR: creatinine, RBC: red blood cells, Hb: haemoglobin, HCT: haematocrit, MCV: mean corpuscular volume, MCH: mean cell haemoglobin, MCHPR: MCH/platelet ratio, MCHC: mean cell haemoglobin concentration, CPK: creatine phosphokinase. Data are expressed as mean and SEM (normality test (Shapiro-Wilk) passed; One Way Analysis of Variance, followed by All Pairwise Multiple Comparison Procedures (Student-Newman-Keuls Method) or median and interquartile range (25%-75%) (normality test (Shapiro-Wilk) failed; Kruskal-Wallis One Way Analysis of Variance on, followed by All Pairwise Multiple Comparison Procedures (Dunn's Method)).

revealed that there is not a statistically significant interaction between sports and health conditions (PA-SCI and PA-LLA) for variables (BR: $p = 0.276$; UA/Cr: $p = 0.556$; Cr: $p = 0.751$; Hb: $p = 0.943$; HCT: $p = 0.984$; proteins: $p = 0.525$).

Direct and inverse correlations were observed for Cr with proteins (coefficient: 0.284, $p < 0.05$), Hb (coefficient: 0.378, $p < 0.01$), iron (coefficient: 0.453, $p < 0.01$), L (coefficient: 0.415, $p < 0.01$), LMR (coefficient: 0.292, $p < 0.05$), MPVLR (coefficient: -0.351, $p < 0.05$), PDWLR (coefficient: -0.314, $p < 0.05$), and PLR (coefficient: -479, $p < 0.001$), the latter being correlated with UA/Cr (coefficient: 0.284, $p < 0.05$) and inversely related to PDW (coefficient: -0.348, $p < 0.05$) and iron (coefficient: 0.337, $p < 0.05$).

Interesting, platelet-activation indexes were inversely correlated with proteins (MPVLR coefficient: -0.349, $p < 0.05$; MPVPR coefficient: -0.323, $p < 0.05$; PDWLR coefficient: -0.299, $p < 0.05$), Cr (MPVLR coefficient: -0.351, $p < 0.05$; PDWLR coefficient: -0.314, $p < 0.05$), Hb (MPVLR coefficient: -0.528, $p < 0.001$; PDWLR coefficient: -0.509, $p < 0.001$), HCT (MPVLR coefficient: -0.459, $p < 0.001$; PDWLR coefficient: -0.459, $p < 0.001$), RBC (MPVLR coefficient: -0.405, $p < 0.01$; PDWLR -0.441, $p < 0.01$), PMCHR (MPVLR coefficient: -0.404, $p < 0.01$; MPVPR coefficient: -0.913, $p < 0.001$; PDWLR coefficient: -0.482, $p < 0.001$; PDWPR coefficient: -0.888, $p < 0.001$), GLU (MPVLR coefficient: -0.384, $p < 0.05$; MPVPR coefficient: -0.338*, $p < 0.05$; PDWLR coefficient: -0.405, $p < 0.01$; PDWPR coefficient: -0.336, $p < 0.05$), MetS ATP III (MPVLR coefficient: -0.312, $p < 0.05$; MPVPR coefficient: -0.310, $p < 0.05$; PDWLR coefficient: -0.334, $p < 0.05$; PDW/P coefficient: -0.308, $p < 0.05$), and INFLA Score (MPVPR coefficient: -0.484, $p < 0.001$; PDWPR coefficient: -0.440, $p < 0.001$). On the other hand, INFLA Score was correlated with MetS (coefficient: 0.281, $p < 0.05$) and the latter was correlated with FRS (coefficient: 0.423, $p < 0.01$).

4. Discussion

Evidence-based screening tools designed specifically for PA to identify and classify those at CVD risk currently do not exist. In the present study, FRS did not differ among groups, whereas PA-LLA had more criteria needed for MetS diagnosis and higher GLU levels compared to both PA-SCI and PA-ULI. The complexity of identifying MetS in the population with SCI has been previously discussed, and this warrants caution in applying standard definitions of MetS to patients with SCI [17, 36]. It has been reported that variables, such as age, smoking, FRS, diabetes mellitus, CHOL, LDL, TG, and CRP, were not significantly associated with extent of coronary disease (CHD) [37]. CRP is a nonspecific marker of inflammation [38], produced predominantly in hepatocytes in response to several cytokines [39]. Although in the last decade the role of CRP level as predictor of CV events, adding prognostic information supported by the FRS, has been investigated, the improvement in CHD/CVD risk stratification or reclassification from addition of CRP to FRS was small and inconsistent [38–42]. Despite testing for CRP level is used in clinical practice, due to the fact that the test is widely available, the US Preventive Services Task

Force (USPSTF) recommendation on using nontraditional risk factors in CHD risk assessment concluded that the current evidence is insufficient to assess the balance of benefits and harms of using the CRP level in risk assessment for CVD in asymptomatic adults to prevent CVD events [43]. Among the factors that constrain the predictive performance of CRP in CHD are the absence of a threshold value (general populations versus CHD patients) and the fact that CRP is not only associated with BP, CHOL, age, and gender but also with diabetes, smoking, left ventricular hypertrophy, and atrial fibrillation, all of which already contribute to the FRS [40]. Moreover, CRP levels might vary as part of the acute phase response, this limitation might bias the risk estimates toward the null and lead to an underestimation of risk [44]. Interleukin- (IL-) 6, one of the most potent drivers of CRP production, is released from activated leukocytes in response to infection or trauma and from vascular smooth muscle cells in response to atherosclerosis [39], but CRP is also released by both skeletal muscle and adipose tissue [45]. From that, body composition, sport-related energy expenditure, and physical fitness/performance parameters [46–48] could be confounding factors in the evaluation of inflammation by CRP measurement. In particular, arm-cranking exercise improved the plasma levels of inflammatory cytokines and adipokines in sedentary adults with SCI [3].

It is well known that a healthy lifestyle, including physical activity and Mediterranean diet, is essential in reducing CVD risk [41, 49]. However, in the European adolescents included in the HELENA study, despite diet has been suggested as a moderator in the association of sedentary behaviors with inflammatory biomarkers [50], the Mediterranean diet score and some healthy food subgroups were positively associated with IL-6 (pulses), alanine aminotransferase (ALT) (vegetables), and CRP (vegetables) [51]. In addition, despite monomeric CRP, stimulated by platelet activation, has prothrombotic and inflammatory properties, definitive evidence for CRP as a causative factor in atherothrombosis is lacking [39].

Probably due to all the above-mentioned confounding factors and due to the fact that the CVD risk within population subgroups may be quite different from the mean risk observed in a population [38, 43], we did not find significant differences in CRP and INFLA Score among PA-SCI-H, PA-SCI-L, PA-LLA, and PA-ULI, but INFLA Score was correlated with MetS ATP III. The latter was correlated with FRS. On the other hand, PA-SCI-H had significantly lower L count compared to PA-LLA and higher MPV, PDW, and/or related platelet-activation indexes, and inverse correlations were found for INFLA Score and MetS ATP III and platelet-activation indexes (MPVPR, MPVLR, and PDWLR).

Moreover, PA-SCI-H and/or PA-SCI-L had lower Hb (vs. PA-LLA and PA-ULI), HCT% (vs. PA-LLA and PA-SCI-L), proteins (vs. PA-LLA and PA-ULI), and creatinine (Cr) (vs. PA-LLA and PA-ULI). Inverse correlations were found for these markers, as well as BR, and platelet-activation indexes.

Although the recommendations regarding antiplatelet therapy (low-dose aspirin) in asymptomatic individuals with a moderate FRS risk are controversial [41, 43], it is known

that individuals with SCI suffered a significantly higher risk of deep vein thrombosis than able people and that this risk is associated with plasma macrophage migration inhibitor [52], a regulator of innate immunity [53].

It has been reported that RBC, HGB, and HCT were negatively significantly associated with platelet aggregation, suggesting an effect of RBC-derived NO on P aggregability [54]. NO, produced in RBC membrane and cytoplasm by endothelial-type nitric oxide synthase (eNOS), inhibited platelet aggregation [54]. On the other hand, it has been reported that low concentrations of plasma amino acids, including L-arginine, the precursor for NO synthesis, in malnourished patients enhanced the occurrence of thrombotic events [55, 56]. Moreover, athletes with SCI can be at risk of low energy availability from proteins (based on the recommendation for athletes: 1.2–2.0 g of protein/kg of body weight) and of micronutrients' deficiency (in particular iron, vitamin B12, and vitamin D) [57]. In our study, no differences were found in PMCHR (marker of IDA associated with cobalamin deficiency) and mean values did not reach the cut-off value of >12.00 [35]. On the other hand, it has been reported that vitamin D deficiency may be associated with increased MPV [58], whereas malnutrition, lower values of albumin, creatinine, protein intake, and haemoglobin were associated with a higher P count [59]. In our study MPV was higher in PA-SCI-H, despite no differences in P were observed. However, it has been reported that the P of SCI group subjects did not differ significantly from those of control subjects, but platelet aggregability was higher in SCI compared to controls [11]. Besides, SCI had high platelet activation [11] and ROS-mediated damage [12]. However, in both wheelchair athletes and nonathletes, comparing to the control group, low levels of lipid oxidation (TBARS: thiobarbituric acid reactive substances) and high levels of fibrinogen have been previously reported, whereas no significant differences were found between wheelchair athletes and nonathletes in both markers [60]. Accordingly, we did not observe differences among group in fibrinogen, and within endogenous antioxidants, only BR was lower in PA-SCI-H and PA-SCI-L versus PA-ULI.

5. Conclusion

In this work, for the first time, we compared the FRS, the MetS criteria, the INFLA Score, and other haematological indexes of inflammation/platelet activation and clinical markers in PA-SCI-H, PA-SCI-L, PA-LLA, and PA-ULI. Despite PA-LLA had more cardiometabolic risk factors, assessed by MetS ATP III criteria, and higher GLU levels, no differences were found in FRS, INFLA Score, and CRP. PA-LLA had higher M count that was correlated with CHOL/HDL ratio, TG, GLU, MetS, and INFLA Score. On the other hand, PA-SCI-H had significantly lower L count compared to LLA and higher MPV, PDW, and/or related platelet-activation indexes (MPVPR, MPVLR, and PDWLR). Therefore, PA-LLA had a higher cardiometabolic risk, whereas PA-SCI, previously resulted a population in which the common markers of CVD risk and/or oxidative stress are not applicable [17, 36, 60], had a higher platelet-derived

cardiovascular risk, probably associated with malnutrition in SCI-H. There are some limitations of our study that should be noted, including gender selection (findings may not be generalizable to women), PA-SCI subdivision and groups unbalanced for sport activity (endurance, mixed, and power) [46, 27]. Besides, inherent limitations of retrospective medical record reviews must be acknowledged, including a lack of data that could have added valuable insight such as dietary habit [41, 49]. Although further larger studies are needed to investigate the relationship among haematological indexes of inflammation and dietary habit, body composition, and physical fitness/performance [6, 61] in athletes with motor impairment, platelet-activation indexes could be among the indicators of CVD risk in SCI Paralympics.

Data Availability

The data used to support the findings of this study are restricted by the Ethics Committee in order to protect patient privacy. Data are available from Marco Bernardi and Antonio Spataro for researchers who meet the criteria for access to confidential data.

Ethical Approval

Approval for the study was obtained from the Review Board of the Institute. All procedures of the study complied with the Declaration of Helsinki as revised in 2000.

Consent

Written informed consent was waived for all athletes undergoing the standard clinical pursuant the Italian law (number 76/2008) and the institute policy.

Conflicts of Interest

The authors declare that there is no conflict of interests regarding the publication of this paper.

Authors' Contributions

Marco Bernardi and Ilaria Peluso designed the research; Anna Lucia Fedullo, Barbara di Giacinto, Maria Rosaria Squeo, Paola Aiello, and Donatella Dante collected the data; Marco Bernardi, Anna Lucia Fedullo, and Ilaria Peluso analyzed the data; Marco Bernardi, Ilaria Peluso, Silvio Romano, and Ludovico Magaudda wrote the paper. Antonio Spataro and Maura Palmery critically reviewed the paper. Marco Bernardi and Antonio Spataro supervised the whole project.

Acknowledgments

The authors would like to thank the Paralympic athletes who willingly participated in this study. The study was funded by the Italian Paralympic Committee.

References

- [1] P. L. Jacobs and M. S. Nash, "Exercise recommendations for individuals with spinal cord injury," *Sports Medicine*, vol. 34, no. 11, pp. 727–751, 2004.
- [2] F. J. Ordonez, M. A. Rosety, A. Camacho et al., "Arm-anking exercise reduced oxidative damage in adults with chronic spinal cord injury," *Archives of Physical Medicine and Rehabilitation*, vol. 94, no. 12, pp. 2336–2341, 2013.
- [3] M. Rosety-Rodriguez, A. Camacho, I. Rosety et al., "Low-grade systemic inflammation and leptin levels were improved by arm cranking exercise in adults with chronic spinal cord injury," *Archives of Physical Medicine and Rehabilitation*, vol. 95, no. 2, pp. 297–302, 2014.
- [4] N. Webborn and P. Van de Vliet, "Paralympic medicine," *The Lancet*, vol. 380, no. 9836, pp. 65–71, 2012.
- [5] W. A. Bauman and A. M. Spungen, "Coronary heart disease in individuals with spinal cord injury: assessment of risk factors," *Spinal Cord*, vol. 46, no. 7, pp. 466–476, 2008.
- [6] V. Palmieri, A. Spataro, and M. Bernardi, "Cardiovascular eligibility in specific conditions: the Paralympic athlete," *Medicina dello Sport*, vol. 63, no. 1, pp. 95–101, 2010.
- [7] J. A. Filho, X. M. Salvetti, M. T. de Mello, A. C. da Silva, and B. L. Filho, "Coronary risk in a cohort of Paralympic athletes," *British Journal of Sports Medicine*, vol. 40, no. 11, pp. 918–922, 2006.
- [8] S. Romano, E. Salustri, P. Ruscitti, F. Carubbi, M. Penco, and R. Giacomelli, "Cardiovascular and metabolic comorbidities in rheumatoid arthritis," *Current Rheumatology Reports*, vol. 20, no. 12, p. 81, 2018.
- [9] P. E. Lazzerini, P. L. Capecchi, and F. Laghi-Pasini, "Systemic inflammation and arrhythmic risk: lessons from rheumatoid arthritis," *European Heart Journal*, vol. 38, no. 22, pp. 1717–1727, 2017.
- [10] H. K. Kabul, M. Celik, U. Ç. Yuksel et al., "Increased sympathetic activation in patients with vasovagal syncope is associated with higher mean platelet volume levels," *European Review for Medical and Pharmacological Sciences*, vol. 18, no. 2, pp. 235–241, 2014.
- [11] J. S. Wang, C. F. Yang, and M. K. Wong, "Effect of strenuous arm crank exercise on platelet function in patients with spinal cord injury," *Archives of Physical Medicine and Rehabilitation*, vol. 83, no. 2, pp. 210–216, 2002.
- [12] J. S. Wang, C. F. Yang, M. K. Wong, S. E. Chow, and J. K. Chen, "Effect of strenuous arm exercise on oxidized-LDL-potentiated platelet activation in individuals with spinal cord injury," *Thrombosis and Haemostasis*, vol. 84, no. 1, pp. 118–123, 2000.
- [13] I. Marrocco, F. Altieri, and I. Peluso, "Measurement and clinical significance of biomarkers of oxidative stress in humans," *Oxidative Medicine and Cellular Longevity*, vol. 2017, Article ID 6501046, 32 pages, 2017.
- [14] R. Nowak, R. Buryta, K. Krupecki et al., "The impact of the progressive efficiency test on a rowing ergometer on white blood cells distribution and clinical chemistry changes in Paralympic rowers during the preparatory stage before the Paralympic games in Rio, 2016 - a case report," *Journal of Human Kinetics*, vol. 60, pp. 255–263, 2017.
- [15] Y. G. Zhong, E. Levy, and W. A. Bauman, "The relationships among serum uric acid, plasma insulin, and serum lipoprotein levels in subjects with spinal cord injury," *Hormone and Metabolic Research*, vol. 27, no. 6, pp. 283–286, 1995.
- [16] Z. Liu, S. Que, L. Zhou, and S. Zheng, "Dose-response Relationship of Serum Uric Acid with Metabolic Syndrome and Non-alcoholic Fatty Liver Disease Incidence: A Meta-analysis of Prospective Studies," *Scientific Reports*, vol. 5, no. 1, article 14325, 2015.
- [17] A. M. Yahiro, B. C. Wingo, S. Kunwor, J. Parton, and A. C. Ellis, "Classification of obesity, cardiometabolic risk, and metabolic syndrome in adults with spinal cord injury," *The Journal of Spinal Cord Medicine*, pp. 1–12, 2019.
- [18] B. Izzi, M. Bonaccio, G. de Gaetano, and C. Cerletti, "Learning by counting blood platelets in population studies: survey and perspective a long way after Bizzozero," *Journal of Thrombosis and Haemostasis*, vol. 16, no. 9, pp. 1711–1721, 2018.
- [19] G. Pounis, M. Bonaccio, A. di Castelnuovo et al., "Polyphenol intake is associated with low-grade inflammation, using a novel data analysis from the Moli-sani study," *Thrombosis and Haemostasis*, vol. 115, no. 2, pp. 344–352, 2016.
- [20] F. Peng, Z. Li, C. Yi et al., "Platelet index levels and cardiovascular mortality in incident peritoneal dialysis patients: a cohort study," *Platelets*, vol. 28, no. 6, pp. 576–584, 2017.
- [21] S. Y. Cho, H. J. Lee, and T. S. Park, "Mean platelet volume in patients with increased γ -glutamyl transferase," *Platelets*, vol. 26, no. 3, pp. 283–284, 2015.
- [22] M. A. Vatankulu, O. Sonmez, G. Ertas et al., "A new parameter predicting chronic total occlusion of coronary arteries: platelet distribution width," *Angiology*, vol. 65, no. 1, pp. 60–64, 2014.
- [23] T. Osadnik, K. Bujak, K. Osadnik et al., "Novel inflammatory biomarkers may reflect subclinical inflammation in young healthy adults with obesity," *Endokrynologia Polska*, vol. 70, no. 2, pp. 135–142, 2019.
- [24] I. Korzonek-Szlacheta, A. Danikiewicz, J. Szkodziński et al., "Relationship between plasma pentraxin 3 concentration and platelet indices in patients with stable coronary artery disease," *Angiology*, vol. 69, no. 3, pp. 264–269, 2018.
- [25] İ. Taşoğlu, D. Sert, N. Colak, A. Uzun, M. Songur, and A. Ecevit, "Neutrophil-lymphocyte ratio and the platelet-lymphocyte ratio predict the limb survival in critical limb ischemia," *Clinical and Applied Thrombosis/Hemostasis*, vol. 20, no. 6, pp. 645–650, 2014.
- [26] T. R. Batista, R. C. d. Figueiredo, and D. R. A. Rios, "Platelets volume indexes and cardiovascular risk factors," *Revista da Associação Médica Brasileira*, vol. 64, no. 6, pp. 554–559, 2018.
- [27] A. Pelliccia, F. M. Quattrini, M. R. Squeo et al., "Cardiovascular diseases in Paralympic athletes," *British Journal of Sports Medicine*, vol. 50, no. 17, pp. 1075–1080, 2016.
- [28] A. M. Williams, C. M. Gee, C. Voss, and C. R. West, "Cardiac consequences of spinal cord injury: systematic review and meta-analysis," *Heart*, vol. 105, no. 3, pp. 217–225, 2019.
- [29] D. Theisen, "Cardiovascular determinants of exercise capacity in the Paralympic athlete with spinal cord injury," *Experimental Physiology*, vol. 97, no. 3, pp. 319–324, 2012.
- [30] P. W. F. Wilson, R. B. D'Agostino, D. Levy, A. M. Belanger, H. Silbershatz, and W. B. Kannel, "Prediction of coronary heart disease using risk factor categories," *Circulation*, vol. 97, no. 18, pp. 1837–1847, 1998.
- [31] F. Score <http://www.siditalia.it/clinica/formule-e-calcolatori/score-di-framingham>.
- [32] S. M. Grundy, J. I. Cleeman, S. R. Daniels et al., "Diagnosis and management of the metabolic syndrome: an American Heart Association/National Heart, Lung, and Blood Institute

- scientific statement," *Circulation*, vol. 112, no. 17, pp. 2735–2752, 2005.
- [33] I. M. J. R. Artha, A. Bhargah, N. K. Dharmawan et al., "High level of individual lipid profile and lipid ratio as a predictive marker of poor glycemic control in type-2 diabetes mellitus," *Vascular Health and Risk Management*, vol. 15, pp. 149–157, 2019.
- [34] C. Beyan, K. Kaptan, E. Beyan, and M. Turan, "The platelet count/mean corpuscular hemoglobin ratio distinguishes combined iron and vitamin B12 deficiency from uncomplicated iron deficiency," *International Journal of Hematology*, vol. 81, no. 4, pp. 301–303, 2005.
- [35] K. Moriyama, "The association between the serum uric acid to creatinine ratio and metabolic syndrome, liver function, and alcohol intake in healthy Japanese subjects," *Metabolic Syndrome and Related Disorders*, vol. 17, no. 7, pp. 380–387, 2019.
- [36] H. M. M. Herath, N. P. Weerasinghe, T. P. Weeraratna, and A. Amarathunga, "A comparison of the prevalence of the metabolic syndrome among Sri Lankan patients with type 2 diabetes mellitus using WHO, NCEP-ATP III, and IDF definitions," *International Journal of Chronic Diseases*, vol. 2018, Article ID 7813537, 8 pages, 2018.
- [37] A. B. A. Bampi, C. E. Rochitte, D. Favarato, P. A. Lemos, and P. L. d. Luz, "Comparison of non-invasive methods for the detection of coronary atherosclerosis," *Clinics*, vol. 64, no. 7, pp. 675–682, 2009.
- [38] J. T. Wilkins and D. M. Lloyd-Jones, "USPSTF recommendations for assessment of cardiovascular risk with nontraditional risk factors: finding the right tests for the right patients," *JAMA*, vol. 320, no. 3, pp. 242–244, 2018.
- [39] O. Yousuf, B. D. Mohanty, S. S. Martin et al., "High-sensitivity C-reactive protein and cardiovascular disease: a resolute belief or an elusive link?," *Journal of the American College of Cardiology*, vol. 62, no. 5, pp. 397–408, 2013.
- [40] T. Shah, J. P. Casas, J. A. Cooper et al., "Critical appraisal of CRP measurement for the prediction of coronary heart disease events: new data and systematic review of 31 prospective cohorts," *International Journal of Epidemiology*, vol. 38, no. 1, pp. 217–231, 2009.
- [41] V.-K. Ton, S. S. Martin, R. S. Blumenthal, and M. J. Blaha, "Comparing the new European cardiovascular disease prevention guideline with prior American Heart Association guidelines: an editorial review," *Clinical Cardiology*, vol. 36, no. 5, pp. E1–E6, 2013.
- [42] J. S. Lin, C. V. Evans, E. Johnson, N. Redmond, E. L. Coppola, and N. Smith, "Nontraditional risk factors in cardiovascular disease risk assessment: updated evidence report and systematic review for the US Preventive Services Task Force," *JAMA*, vol. 320, no. 3, pp. 281–297, 2018.
- [43] US Preventive Services Task Force, S. J. Curry, A. H. Krist et al., "Risk assessment for cardiovascular disease with nontraditional risk factors," *JAMA*, vol. 320, no. 3, pp. 272–280, 2018.
- [44] P. M. Ridker and J. D. Silvertown, "Inflammation, C-reactive protein, and atherothrombosis," *Journal of Periodontology*, vol. 79, Supplement 8, pp. 1544–1551, 2008.
- [45] F. Li, Y. Li, Y. Duan, C.-A. A. Hu, Y. Tang, and Y. Yin, "Myokines and adipokines: involvement in the crosstalk between skeletal muscle and adipose tissue," *Cytokine & Growth Factor Reviews*, vol. 33, pp. 73–82, 2017.
- [46] M. Bernardi, S. Carucci, F. Faiola et al., "Physical fitness evaluation of Paralympic winter sports sitting athletes," *Clinical Journal of Sport Medicine*, vol. 22, no. 1, pp. 26–30, 2012.
- [47] M. Bernardi, E. Guerra, B. di Giacinto, A. di Cesare, V. Castellano, and Y. Bhambhani, "Field evaluation of Paralympic athletes in selected sports: implications for training," *Medicine and Science in Sports and Exercise*, vol. 42, no. 6, pp. 1200–1208, 2010.
- [48] M. Bernardi, F. M. Quattrini, A. Rodio et al., "Physiological characteristics of America's cup sailors," *Journal of Sports Sciences*, vol. 25, no. 10, pp. 1141–1152, 2007.
- [49] M. Ciccotti, A. Raguzzini, T. Sciarra et al., "Nutraceutical-based integrative medicine: adopting a Mediterranean diet pyramid for attaining healthy ageing in veterans with disabilities," *Current Pharmaceutical Design*, vol. 24, no. 35, pp. 4186–4196, 2018.
- [50] A. B. Arouca, A. M. Santaliesra-Pasías, L. A. Moreno et al., "Diet as a moderator in the association of sedentary behaviors with inflammatory biomarkers among adolescents in the HELENA study," *European Journal of Nutrition*, vol. 58, no. 5, pp. 2051–2065, 2019.
- [51] A. Arouca, N. Michels, L. A. Moreno et al., "Associations between a Mediterranean diet pattern and inflammatory biomarkers in European adolescents," *European Journal of Nutrition*, vol. 57, no. 5, pp. 1747–1760, 2018.
- [52] D. M. Wu, Z. H. Zheng, S. Wang et al., "Association between plasma macrophage migration inhibitor factor and deep vein thrombosis in patients with spinal cord injuries," *Aging*, vol. 11, no. 8, pp. 2447–2456, 2019.
- [53] T. Calandra and T. Roger, "Macrophage migration inhibitory factor: a regulator of innate immunity," *Nature Reviews Immunology*, vol. 3, no. 10, pp. 791–800, 2003.
- [54] K. Karolczak, B. Soltysik, T. Kostka, P. J. Witas, and C. Watala, "Platelet and red blood cell counts, as well as the concentrations of uric acid, but not homocysteinaemia or oxidative stress, Contribute Mostly to Platelet Reactivity in Older Adults," *Oxidative Medicine and Cellular Longevity*, vol. 2019, Article ID 9467562, 16 pages, 2019.
- [55] T. M. Brunini, A. C. Mendes-Ribeiro, J. C. Ellory, and G. E. Mann, "Platelet nitric oxide synthesis in uremia and malnutrition: a role for L-arginine supplementation in vascular protection?," *Cardiovascular Research*, vol. 73, no. 2, pp. 359–367, 2007.
- [56] C. D. da Silva, T. M. Brunini, P. F. Reis et al., "Effects of nutritional status on the L-arginine-nitric oxide pathway in platelets from hemodialysis patients," *Kidney International*, vol. 68, no. 5, pp. 2173–2179, 2005.
- [57] K. Figel, K. Pritchett, R. Pritchett, and E. Broad, "Energy and nutrient issues in athletes with spinal cord injury: are they at risk for low energy availability?," *Nutrients*, vol. 10, no. 8, p. 1078, 2018.
- [58] M. Cumhuri Cure, E. Cure, S. Yuce, T. Yazici, I. Karakoyun, and H. Efe, "Mean platelet volume and vitamin D level," *Annals of Laboratory Medicine*, vol. 34, no. 2, pp. 98–103, 2014.
- [59] M. Z. Molnar, E. Streja, C. P. Kovesdy et al., "High platelet count as a link between renal cachexia and cardiovascular mortality in end-stage renal disease patients," *The American Journal of Clinical Nutrition*, vol. 94, no. 3, pp. 945–954, 2011.

- [60] E. J. Garbeloti, R. C. Paiva, C. B. Restini, M. T. Durand, C. E. Miranda, and V. E. Teixeira, "Biochemical biomarkers are not dependent on physical exercise in patients with spinal cord injury," *BBA Clinical*, vol. 6, pp. 5–11, 2016.
- [61] E. Bernardi, S. A. Delussu, F. M. Quattrini, A. Rodio, and M. Bernardi, "Energy balance and dietary habitus of America's cup sailors," *Journal of Sports Sciences*, vol. 25, no. 10, pp. 1161–1168, 2007.

Research Article

5 α ,6 α -Epoxyphytosterols and 5 α ,6 α -Epoxycholesterol Increase Oxidative Stress in Rats on Low-Cholesterol Diet

Tomasz Wielkoszyński ¹, Jolanta Zalejska-Fiolka ², Joanna K. Strzelczyk ³,
Aleksander J. Owczarek ⁴, Armand Cholewka ⁵, Aneta Krawczyk ⁶, and Agata Stanek ⁷

¹Higher School of Strategic Planning in Dąbrowa Górnicza, Kościelna 6 St., 41-300 Dąbrowa Górnicza, Poland

²Medical University of Silesia, School of Medicine with the Division of Dentistry in Zabrze, Department of Biochemistry, Jordana 19 St., 41-808 Zabrze, Poland

³Medical University of Silesia, School of Medicine with the Division of Dentistry in Zabrze, Department of Medical and Molecular Biology, Jordana 19 St., 41-808 Zabrze, Poland

⁴Medical University of Silesia, School of Pharmacy with the Division of Laboratory Medicine, Department of Statistics, Department of Instrumental Analysis, Ostrogórska 30 St, Sosnowiec 41-209, Poland

⁵University of Silesia, Department of Medical Physics, Chelkowski Institute of Physics, Uniwersytecka 4 St., 40-007 Katowice, Poland

⁶Medical Center and Lab, Aleja Marszałka Piłsudskiego 10, 41-300 Dąbrowa Górnicza, Poland

⁷Medical University of Silesia, School of Medicine with the Division of Dentistry in Zabrze, Department of Internal Medicine, Angiology and Physical Medicine, Batorego 15 St., 41-902 Bytom, Poland

Correspondence should be addressed to Agata Stanek; astanek@tlen.pl

Received 10 June 2019; Accepted 16 September 2019; Published 15 November 2019

Guest Editor: Adrian Doroszko

Copyright © 2019 Tomasz Wielkoszyński et al. This is an open access article distributed under the Creative Commons Attribution License, which permits unrestricted use, distribution, and reproduction in any medium, provided the original work is properly cited.

Objective. Cholesterol oxidation products have an established proatherogenic and cytotoxic effect. An increased exposure to these substances may be associated with the development of atherosclerosis and cancers. Relatively little, though, is known about the effect of phytosterol oxidation products, although phytosterols are present in commonly available and industrial food products. Thus, the aim of the research was to assess the effect of 5 α ,6 α -epoxyphytosterols, which are important phytosterol oxidation products, on redox state in rats. **Material and Methods.** The animals were divided into 3 groups and exposed to nutritional sterols by receiving feed containing 5 α ,6 α -epoxyphytosterols (ES group) and 5 α ,6 α -epoxycholesterol (Ech group) or sterol-free feed (C group). The levels of malondialdehyde (MDA), conjugated dienes (CD), and ferric reducing antioxidant potential (FRAP) were assayed in the plasma; anti-7-ketocholesterol antibodies and activity of paraoxonase-1 (PON1) were determined in serum, whereas the activity of catalase (CAT), glutathione reductase (GR), glutathione peroxidase (GPx), S-glutathione transferase (GST), and superoxide dismutase (SOD) were assayed in RBCs. **Results.** During the experiment, the levels of lipid peroxidation products increased, such as CD and anti-7-ketocholesterol antibodies. At the same time, the plasma levels of FRAP and serum activity of PON1 decreased alongside the reduced activity of GPx, GR, and SOD in RBCs. There was no effect of the studied compounds on the plasma MDA levels or on the activity of CAT and GST in RBCs. **Conclusions.** Both 5 α ,6 α -epoxyphytosterols and 5 α ,6 α -epoxycholesterols similarly dysregulate the redox state in experimental animal model and may significantly impact atherogenesis.

1. Introduction

Cholesterol is the most common animal sterol. It is present in every cell, as a plasma membrane component, and in the extracellular space, as a plasma lipoprotein component. Its

wide bioavailability and chemical structure (monounsaturated alcohol) make cholesterol prone to oxidation, which leads to oxysterol formation [1]. Apart from endogenous production, oxysterols can also be sourced from nutrition, in particular, from cholesterol-rich foods after

long-term thermal processing, gamma irradiation, or long-term storage [2].

Recently, food products containing phytosterols and phytostanols have been widely promoted. Animal experimental studies and epidemiological studies demonstrated their positive effect on lipoprotein status by, e.g., inhibiting intestinal absorption of exogenous cholesterol. Population studies show that increased intake of phytosterols and phytostanols leads to a significant decrease in total cholesterol and LDL cholesterol levels, as well as favourably affects HDL cholesterol and triacylglycerol levels [3, 4].

However, the health effects of oxidated phytosterols' intake have not been widely studied yet, although they are present in abundance in widely available and popular sterol- and stanol-containing margarines or can form during thermal processing of food products. The available literature lacks a full report on a study involving sterol administration to experimental animals which assessed sterol effect on oxidative stress. Thus, the aim of the research was to assess the effect of 5 α ,6 α -epoxyphytosterols and 5 α ,6 α -epoxycholesterol on oxidative stress markers in experimental animals.

2. Material and Methods

2.1. Animals. The protocol was approved by the Bioethical Committee for Animal Experimentation of the Medical University of Silesia in Katowice, Poland (approval no. 27/2007, dated April 17th, 2007). All animals received humane care in compliance with the 8th edition of the *Guide for the Care and Use of Laboratory Animals* published by the National Institute of Health [5].

Male Wistar rats, with the body weight of 130-180 g at baseline, were sourced from the Centre for Experimental Medicine, Medical University of Silesia in Katowice. During the experiment, the rats were kept on wood shaving bedding in standard single rodent cages, at the temperature of 20-25°C, with artificial lighting (a 12 h/12 h day/night cycle). The feed was administered once a day, and tap water was available *ad libitum*. Prior to the commencement of the experiment, the animals were kept in the conditions described above for an acclimation period of 2 weeks to ensure reproducible results. The rats were divided into 3 groups (15 animals each), to receive the following:

- (i) Feed containing 5 α ,6 α -epoxyphytosterols acetate at 100 mg per 1 kg of feed (ES group)
- (ii) Feed containing 5 α ,6 α -epoxycholesterol acetate at 100 mg per 1 kg of feed (ECh group)
- (iii) Oxysterol-free feed (controls, C group)

Daily estimated sterol dose was 10 mg per 1 kg of animal body weight (assuming the feed intake is equal to 10% of the animal body weight). Labofeed B (Wytwórnia Pasz, Kcynia, Poland), a standard laboratory maintenance feed for rodents, was used during the study. The feed was administered for 90 days. The animals were weighted before and after the experiment. After 3 months, the rats were anaesthetised with the mixture of ketamine (50

mg/kg), droperidol (1 mg/kg), and fentanyl (0.1 mg/kg) administered i.m. and euthanised by cardiac exsanguination and cervical dislocation.

2.2. Synthesis of 5 α ,6 α -Epoxycholesterol and 5 α ,6 α -Epoxyphytosterols Acetate. The 5 α ,6 α -epoxycholesterol acetate and 5 α ,6 α -epoxyphytosterols acetate were synthesized, respectively, from cholesterol and sitosterol (Sigma-Aldrich, USA) by acetylation and subsequent oxidation with *m*-chloroperoxybenzoic acid (Sigma-Aldrich, USA) as described by McCarthy et al. [6]. Next, the oxidation mixture was purified by column chromatography on silica gel using chloroform-acetone (4:1, v/v) as a mobile phase. Fractions containing pure ester were controlled by TLC technique (silica gel plates, solvent as above), pooled, and dried under vacuum.

According to information from the manufacturer, "sitosterol" contained about 90% β -sitosterol and ca. 10% other phytosterols and phytostanols. Thus, its oxidation products are named as 5 α ,6 α -epoxyphytosterols.

2.3. Blood Sample Collection. Blood samples were collected to tubes containing ethylenediaminetetraacetic acid (Sarstedt, S-Monovette with 1.6 mg/mL EDTA-K3) and into tubes with a clot activator (Sarstedt, S-Monovette). The blood samples were centrifuged (10 min, 900 g 4°C) and then the plasma and serum were immediately separated and stored at the temperature of -70°C, until biochemical analyses were performed. The red blood cells (RBCs) retained from the removal of EDTA plasma underwent a triple wash with cooled PBS and were lysed after the last wash in 10 mM Tris-HCl buffer pH 7.4 to obtain 10% lysates which were frozen for further analyses [7-9].

The levels of free radical damage markers, i.e., malondialdehyde (MDA), conjugated dienes (CD), and ferric reducing antioxidant power (FRAP) were assayed in EDTA plasma. Anti-7-ketocholesterol antibodies and paraoxonase-1 (PON1) activity were assayed in serum. The activity of catalase (CAT), glutathione reductase (GR), glutathione peroxidase (GPx), S-glutathione transferase (GST), and superoxide dismutase (SOD) were assayed in lysed RBCs.

2.4. Biochemical Analyses

2.4.1. Oxidative Stress Analyses

(1) Determination of Lipid Peroxidation Products and Antibodies against 7-Ketocholesterol. Plasma MDA levels were determined as thiobarbituric acid reactive substances (TBARS) by spectrofluorimetric method after its derivatization with thiobarbituric acid as described by Wasowicz et al. [10] and expressed in μ mol/L. The inter- and intra-assay coefficients of variation (CV) were 3.5% and 5.3%, respectively.

Plasma conjugated diene (CD) levels were determined by second derivative ultraviolet spectrophotometry as described by Corongiu et al. [11] and expressed in μ mol/L. The inter- and intra-assay coefficients of variation (CV) were 6.2% and 8.9%, respectively.

Concentration of anti-7-ketocholesterol antibodies in serum was determined by ELISA method with the use of 7-

ketocholesterol-bovine serum albumin conjugate as previously described [12]. The results were expressed as AU/mL (arbitrary units per mL). The inter- and intra-assay coefficients of variation (CV) were 8.4% and 10.2%, respectively.

(2) *Determination of Nonenzymatic Antioxidant Status.* The total antioxidant capacity of plasma was measured as the ferric reducing ability of plasma (FRAP) according to Benzie and Strain [13] and calibrated using Trolox and expressed in $\mu\text{mol/L}$. The inter- and intra-assay coefficients of variation (CV) were 1.1% and 3.8%, respectively.

(3) *Determination of Activity of Antioxidant Enzymes.* Antioxidant enzyme activity was assayed in lysed RBCs obtained using 10 mM Tris-HCl buffer pH 7.2. Haemoglobin levels in lysed RBCs were estimated by Drabkin's method.

Catalase (CAT; E.C.1.11.1.6.) activity was determined in erythrocytes with the hydrogen peroxide-methanol method at 25°C developed by Johansson and Borg [14]. The method is based on the reaction of catalase with methanol in the presence of an optimal concentration of hydrogen peroxide. The obtained formaldehyde is measured spectrophotometrically at 550 nm after derivatization with Purpald as a chromogen. The enzymatic activity of catalase was expressed in kU/gHb. The inter- and intra-assay coefficients of variation (CV) were 6.8% and 9.7%, respectively.

The activity of erythrocytes glutathione reductase (GR; E.C.1.6.4.2) was determined by kinetic spectrophotometric method at 37°C using Biotech (USA) kits as per manufacturer's instructions [15, 16]. The results were expressed as International Units per a gram of haemoglobin [IU/hHb]. The inter- and intra-assay coefficients of variation (CV) were 4.2% and 6.1%, respectively.

The activity of erythrocyte glutathione peroxidase (GPx; E.C.1.11.1.9.) was determined by Paglia and Valentine's kinetic method [17] at 37°C, with t-butyl peroxide as a substrate and expressed as micromoles of NADPH oxidized per minute and normalized to one gram of haemoglobin [IU/gHb]. The inter- and intra-assay coefficients of variation (CV) were 1.8% and 3.5%, respectively.

The activity of glutathione S-transferase (GST) in RBCs was determined by kinetic spectrophotometric method [18] at 37°C using the Cayman Chemical (USA) kits. The results were expressed as International Units per a gram of haemoglobin [IU/hHb]. The inter- and intra-assay coefficients of variation (CV) were 2.7% and 3.9%, respectively.

The erythrocyte superoxide dismutase (SOD; E.C.1.15.1.1) activity was assayed using the Oyanagui method [19]. The enzymatic activity was expressed in nitrite unit (NU) in each mg of haemoglobin (Hb) [mg/Hb]. In this method, one nitrite unit (1 NU) means a 50% inhibition of nitrite ion production by SOD. The inter- and intra-assay coefficients of variation (CV) were 2.8% and 6.3%, respectively.

Paraoxonase-1 (PON-1) serum activity was assayed using the kinetic method with paraoxon (*o,o*-diethyl-*o*-(*p*-nitrophenyl)-phosphate; Sigma-Aldrich, USA) as a substrate at 37°C [20]. For cholinesterase inactivation, physostigmine salicylate (eserine) was added to serum samples ten minutes

prior to the assay. One unit (1 IU) of PON-1 is the amount of enzyme sufficient to decompose 1 micromole of substrate per minute under testing conditions [IU/L]. Inter- and intra-assay coefficients (CV) of variation were 2.6% and 4.4%, respectively.

2.5. *Statistical Analyses.* Statistical analysis was performed using STATISTICA 30 PL (Tibco Inc., Palo Alto, CA, USA) and StataSE 12.0 (StataCorp LP, TX, USA) and R software (CRAN). The *p* value below 0.05 was considered statistically significant. All tests were two-tailed. Imputations were not done for missing data. Nominal and ordinal data were expressed as percentages, while interval data were expressed as mean value \pm standard deviation if normally distributed or as median/interquartile range if the distribution was skewed or nonnormal. Distribution of variables was evaluated by the Shapiro-Wilk test, and homogeneity of variances was assessed using the Levene test. The comparisons were made using one-way parametric ANOVA with Tukey post hoc test.

The number of animals in each group was imposed by restrictions of the Bioethical Committee for Animal Experimentation of the Medical University of Silesia in Katowice. Nevertheless, to ensure the reliability of our results, the power analysis of the test was performed. The test power level, typically used in biomedical research, was assumed as not less than 80%.

3. Results

Among the markers of free radical damage, changes in their plasma concentration were only demonstrated for conjugated dienes. Their level significantly increased in the ECh group ($p < 0.05$ vs controls). Additionally, the level of anti-7-ketocholesterol antibodies increased significantly in both groups exposed to oxysterols. Whereas there were no significant differences in the levels of MDA between the study groups, there was an increasing trend demonstrated in both groups exposed to oxysterols. Plasma FRAP level was significantly lower in groups exposed to oxysterols (ES and ECh groups) as compared to controls.

In terms of antioxidant enzyme activity in RBCs, significant differences in the activity of GPx, GR, and SOD were demonstrated between the study groups, with no differences in the activity of CAT and GST. There was a significant decrease in GPx, GR, and SOD activity in RBCs demonstrated in ES and ECh groups as compared to controls, with no difference between the ES and ECh groups. The serum activity of paraoxonase-1 (PON-1) significantly decreased during the experimental exposure to oxysterols in low-cholesterol diet. The lowest PON-1 activity was demonstrated in the ECh group, with a slightly smallest reduction shown in the ES group.

Changes to oxidative stress parameters are shown in Table 1 and Figures 1–7.

4. Discussion

There is ample evidence to support oxidative stress induction by oxidized cholesterol derivatives. However, there are only

TABLE 1: Oxidative stress markers (mean value \pm standard deviation (SD)) (MDA: malondialdehyde levels, anti-7-ketoCh- anti-ketocholesterol antibody levels; FRAP: total antioxidant capacity of plasma levels; CAT: activity of catalase; GPx: activity of glutathione peroxidase; GR: activity of glutathione reductase; SOD: activity of superoxide dismutase; GST: activity of glutathione S-transferase; PON-1: activity of paraoxonase-1) in plasma (p), serum (s), and erythrocytes (e) of rats fed with 5 α ,6 α -epoxycholesterol (ECh group) and 5 α ,6 α -epoxyphyosterols (ES group) vs controls (C).

	ECh group	ES group	C group	<i>p</i>
MDA (p) [μ mol/L]	3.40 \pm 1.0	3.0 \pm 0.55	2.7 \pm 0.41	0.0545
Conjugated dienes (p) [μ mol/L]	76.7 \pm 15.9	70.0 \pm 16.2	55.0 \pm 13.1	<0.01
Anti-7-ketoCh (s) [AU/mL]	202.2 \pm 122.3	164.9 \pm 75.0	92.1 \pm 41.0	<0.01
FRAP (p) [μ mol/L]	214.7 \pm 38.8	220.6 \pm 22.1	248.8 \pm 26.8	<0.01
CAT(e) [kIU/g Hb]	194.5 \pm 18.6	187.9 \pm 22.0	194.4 \pm 19.3	0.600
GPx (e) [IU/g Hb]	155.0 \pm 15.5	154.5 \pm 14.0	171.3 \pm 16.0	<0.01
GR (e) [IU/g Hb]	0.78 \pm 0.16	0.78 \pm 0.15	0.99 \pm 0.12	<0.001
SOD (e) [NU/g Hb]	180.3 \pm 14.8	187.0 \pm 17.1	209.7 \pm 24.5	<0.001
GST (e) [IU/g Hb]	0.22 \pm 0.04	0.22 \pm 0.03	0.24 \pm 0.05	0.509
PON-1 (s) [IU/L]	286.1 \pm 29.6	294.5 \pm 27.8	332.5 \pm 20.0	<0.001

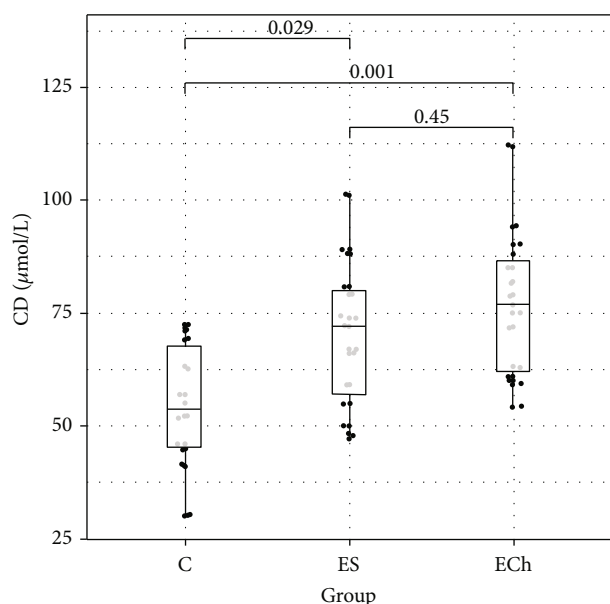


FIGURE 1: Conjugated diene (CD) levels (mean value \pm standard deviation (SD)) in the plasma of rats exposed to 5 α ,6 α -epoxycholesterol (ECh group) and 5 α ,6 α -epoxyphyosterols (ES group) vs controls (C).

single reports to discuss this effect of oxysterols. Until now, the only published evidence of peroxidative effect of oxysterols was the study by Tomoyori et al. [21], who demonstrated an increase of plasma F2- α isoprostane levels in mice fed with a mixture of oxidized phytosterols, despite a simultaneous absence of their atherogenic effect. Much more is known about the harmful effect of oxidized cholesterol derivatives. Most authors agree that cytotoxic effect of oxysterols (such as induction of apoptosis) is primarily due to upregulated production of reactive oxygen species in cells exposed to oxysterols [22, 23]. The exposure of U937 cells or macrophages to 7-hydroxycholesterol led to increased apoptosis associated with the depletion of intracel-

lular reduced glutathione [24, 25]. The exposure of U937 cells to 7-ketocholesterol or 7 α -hydroxycholesterol also upregulated the cellular production of superoxide radical anion and downregulated nitric oxide biosynthesis [26–28], whereas the exposure to 5 α -6 α -epoxycholesterol did not have that effect [29]. It also seems that simultaneous exposure to the mixture of oxysterols has a stronger effect than the exposure to any individual oxysterol [22].

In our study, the concentration of conjugated dienes as early lipid peroxidation products increased significantly in rats exposed to oxysterols (both oxysterols and cholesterol derivatives). It may indicate the intensified production of free radicals in animals exposed to the tested compounds. The conjugated diene assay may offer specificity at least comparable to the one of thiobarbituric acid reactive substance assay (TBARS), which is confirmed by a significantly higher concentration of conjugated dienes in plasma samples of animals exposed to 5 α ,6 α -epoxycholesterol than in controls, with no significant differences in the concentration of MDA determined as TBARS, demonstrated in our study.

The available data show that anti-7-ketocholesterol antibody determination may be the means to indirectly monitor the severity of oxidative stress [12, 30]. The immunogenic potential of oxidized cholesterol derivatives results, for instance, from the formation of aldehyde adducts, generated during oxidation of cholesterol esters, 9-oxonanylcholesterol, and 5-oxovalerylcholesterol, to proteins, especially apolipoprotein B [30]. It has also been shown that 7-ketocholesteryl 9-carboxinonate (oxLig-1) is a specific ligand for α 2-glycoprotein-1. As a result, it binds specifically oxidized LDL, containing oxidized cholesterol derivatives, which is the link between autoimmune response to phospholipids (α 2-GP-1) and atherogenesis [31]. Given that ketocholesterol is one of the major oxysterols, our analysis of anti-7-ketocholesterol antibody levels in a rat model provided very interesting data. We demonstrated a significant increase in the concentration of these antibodies in both groups exposed to oxysterols as compared to the controls.

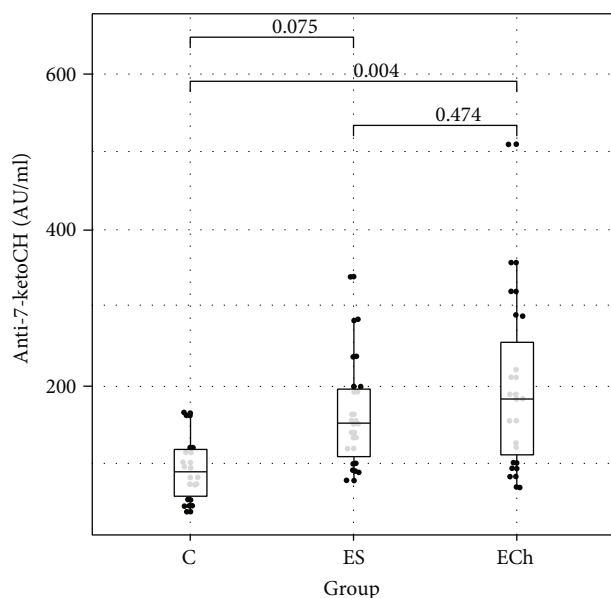


FIGURE 2: Anti-7-ketocholesterol (anti-7-ketoCH) antibody levels (mean value \pm standard deviation (SD)) in the serum of rats exposed to 5 α ,6 α -epoxycholesterol (ECh group) and 5 α ,6 α -epoxyphytosterols (ES group) vs controls (C).

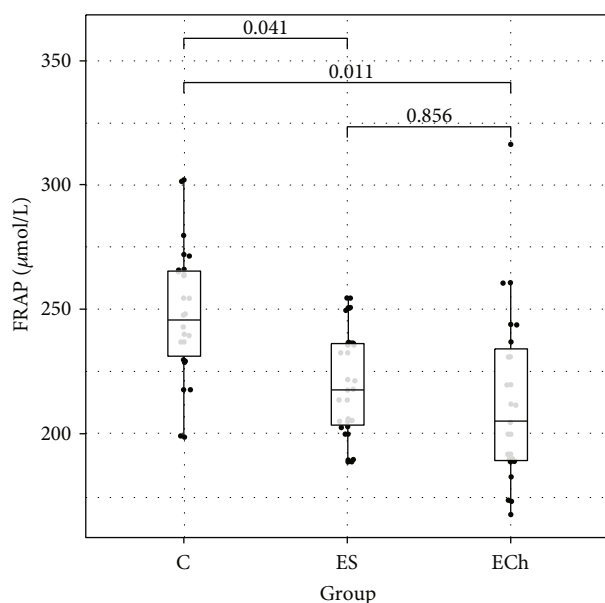


FIGURE 3: Ferric reducing antioxidant power (FRAP) levels (mean value \pm standard deviation (SD)) in the plasma of rats exposed to 5 α ,6 α -epoxycholesterol (ECh group) and 5 α ,6 α -epoxyphytosterols (ES group) vs controls (C).

Since animals in any of the groups were not directly exposed to 7-ketocholesterol, the increase in the concentration of these antibodies could be solely attributable to the increase in endogenous 7-ketocholesterol formation and resultant increased immune exposure to this sterol.

The analysis of changes in the FRAP demonstrated its significant decrease in the ES and ECh groups as compared

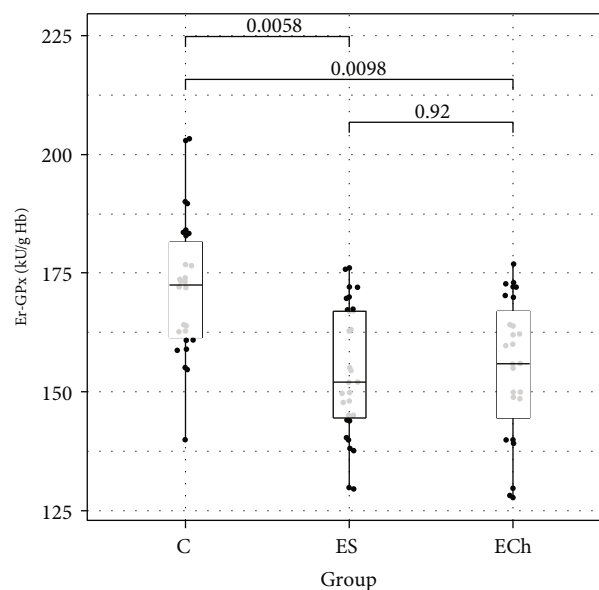


FIGURE 4: Activity of erythrocytes glutathione peroxidase (GPx) (mean value \pm standard deviation (SD)) of rats exposed to 5 α ,6 α -epoxycholesterol (ECh group) and 5 α ,6 α -epoxyphytosterols (ES group) vs controls (C).

to controls. The effect of oxysterols on antioxidant activity assessed using FRAP assay, or levels of individual nonenzymatic antioxidants included in the FRAP assay, has not yet been described in any published work. Similarly, there are relatively few studies to assess the effect of oxysterols on the activity of antioxidant enzymes. Since it has been postulated that toxicity and proapoptotic effect of oxysterols are associated with an increased formation of reactive oxygen species, the majority of available papers report *in vitro* studies (mainly in cell cultures), and only a few document antioxidant enzyme changes in animals following the *in vivo* exposure to oxysterols. In rats exposed to hydrogen peroxide as an oxidative stress inductor, an increased production of oxysterols (25-hydroxy-, 7 α -hydroxy- and 7-ketocholesterol), elevated MDA levels, and decreased plasma activity of CAT and SOD were observed [32]. However, it is difficult to conclude that the observed changes in enzymatic activity were directly triggered by oxidized cholesterol derivatives. Studies assessing the effect of oxysterols generated in a free radical-mediated process in ovarian cells showed intensified lipid peroxidation (determined as a part of TBARS) alongside increased activity of SOD and CAT [33].

In our study, the analysis of changes in the activity of superoxide dismutase in RBCs during rat exposure to 5,6-epoxysterols indicated the depletion of antioxidant defense mechanisms, which was manifested by a decrease in the activity of superoxide dismutase in ECh and ES groups. Whereas there were no significant changes in CAT activity in RBCs, the activity of GPx and GR in RBCs decreased significantly during the experimental exposure of rats to oxysterols, which was demonstrated in both ECh and ES groups in our study. We did not demonstrate significant changes to GST in RBCs.

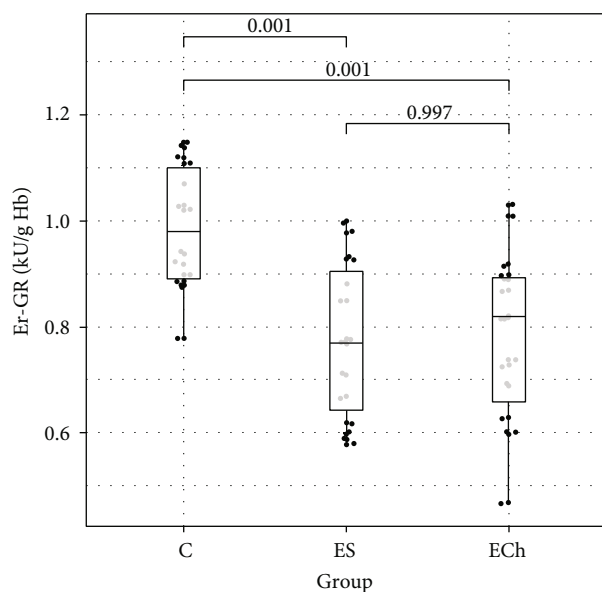


FIGURE 5: Activity of erythrocytes glutathione reductase (GR) (mean value \pm standard deviation (SD)) of rats exposed to $5\alpha,6\alpha$ -epoxycholesterol (ECh group) and $5\alpha,6\alpha$ -epoxyphytosterols (ES group) vs controls (C).

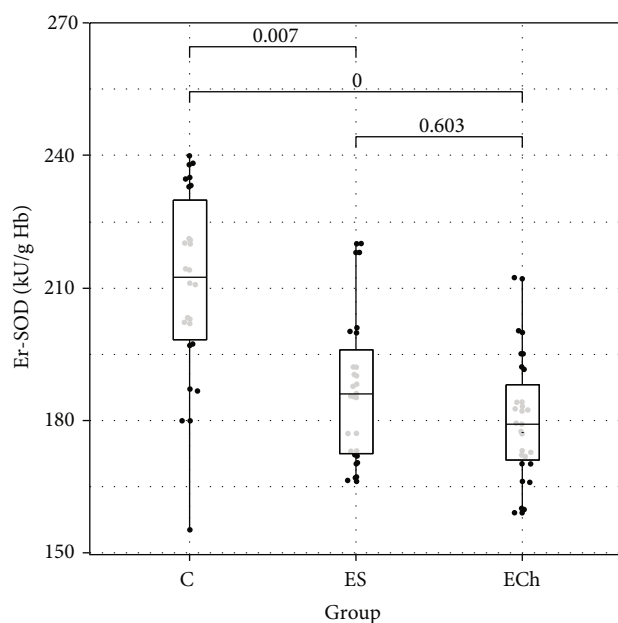


FIGURE 6: Activity of erythrocytes superoxide dismutase (SOD) (mean value \pm standard deviation (SD)) of rats exposed to $5\alpha,6\alpha$ -epoxycholesterol (ECh group) and $5\alpha,6\alpha$ -epoxyphytosterols (ES group) vs controls (C).

A decrease was also demonstrated in serum paraoxonase-1 activity in groups exposed to $5\alpha,6\alpha$ -epoxycholesterol, and phytosterols $5\alpha,6\alpha$ -epoxides derivatives in this study, which may be explained by their direct effect on PON-1 biosynthesis or on oxidative stress, and may be associated with an increased formation of endogenous lipid hydro-

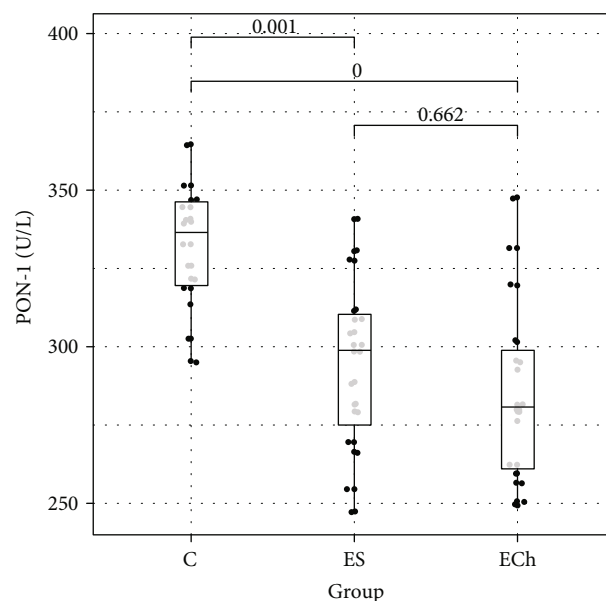


FIGURE 7: Paraoxonase-1 (PON-1) activity (mean value \pm standard deviation (SD)) in the serum of rats exposed to $5\alpha,6\alpha$ -epoxycholesterol (ECh group) and $5\alpha,6\alpha$ -epoxyphytosterols (ES group) vs controls (C).

peroxides. The involvement of immune mechanisms contributing to effective elimination of PON-1 from circulation cannot be ruled out, either. Hedrick et al. demonstrated decreased serum PON-1 activity and concentration CL57BL/6 mice on atherogenic diet during the first 7 days of the experiment, whereas its respective mRNA expression in the liver remained unaffected. The finding was explained as associated with the accelerated HDL elimination from the plasma [34]. Other studies pointed to the effect of high-lipid diet on PON-1 activity. It is likely that similar mechanisms were involved, as a test meal containing thermally processed fats caused a reduction in PON-1 activity in clinically healthy volunteers, while the intake of nonoxidized fat caused an increase in the enzymatic activity of PON-1 in plasma [35].

Therefore, a reduced activity of PON-1 manifested in rodents in response to oxyphytosterols and oxycholesterols seems an important determinant of their proatherogenic profile in laboratory animals.

The limitations of the current study include a small sample size and the inability to monitor the dynamics of changes in the studied parameters, as the redox state undergoes dynamic changes throughout the exposure to the studied compounds. Similarly, it seems warranted to study the effect of other derivatives of phytosterols and cholesterol than epoxysterols in animal models. It would also be beneficial to assess the effect of those compounds on redox state in an animal model consuming atherogenic, high-cholesterol feed. What is novel about this study, though, is that it evaluates the effect of oxyphytosterols on the redox state and its associated mechanisms, as the available research mainly focuses on the effect of oxidized cholesterol derivatives on antioxidant mechanisms.

5. Conclusions

5 α ,6 α -Epoxyphytosterols and 5 α ,6 α -epoxycholesterol similarly impair the redox state in rats by increasing the production of free oxygen radicals and free radical-mediated lipid modification, as well as by affecting the mechanisms of non-enzymatic antioxidant defense and the activity of antioxidant enzymes.

Data Availability

All data is included in the table and figures within the article.

Conflicts of Interest

The authors declare that there are no conflicts of interest regarding the publication of this paper.

Acknowledgments

This work was supported by the grants from the Medical University of Silesia (KNW-2-156/09, KNW-1-053/N/7/Z and KNW-1-109/K/8/Z).





References

- [1] T. Wielkoszyński, J. Zalejska-Fiolka, J. K. Strzelczyk et al., "Oxysterols increase inflammation, lipid marker levels and reflect accelerated endothelial dysfunction in experimental animals," *Mediators of Inflammation*, vol. 2018, Article ID 2784701, 9 pages, 2018.
- [2] D. Innosa, A. Ianni, F. Palazzo et al., "High temperature and heating effect on the oxidative stability of dietary cholesterol in different real food systems arising from eggs," *European Food Research and Technology*, vol. 245, no. 7, pp. 1533–1538, 2019.
- [3] H. Gylling and P. Simonen, "Phytosterols, Phytostanols, and Lipoprotein Metabolism," *Nutrients*, vol. 7, no. 9, pp. 7965–7977, 2015.
- [4] J. Köhler, D. Teupser, A. Elsässer, and O. Weingärtner, "Plant sterol enriched functional food and atherosclerosis," *British Journal of Pharmacology*, vol. 174, no. 11, pp. 1281–1289, 2017.
- [5] Guide for the Care and Use of Laboratory Animals, *National Research Council (US) Committee for the Update of the Guide for the Care and Use of Laboratory Animals*, National Academies Press, Washington, DC, USA, 8th edition, 2011, <https://www.ncbi.nlm.nih.gov/books/NBK54050/>.
- [6] F. O. McCarthy, J. Chopra, A. Ford et al., "Synthesis, isolation and characterisation of β -sitosterol and β -sitosterol oxide derivatives," *Organic & Biomolecular Chemistry*, vol. 3, no. 16, pp. 3059–3065, 2005.
- [7] A. Stanek, A. Cholewka, T. Wielkoszyński, E. Romuk, K. Sieroń, and A. Sieroń, "Increased levels of oxidative stress markers, soluble CD40 ligand, and carotid intima-media thickness reflect acceleration of atherosclerosis in male patients with ankylosing spondylitis in active phase and without the classical cardiovascular risk factors," *Oxidative Medicine and Cellular Longevity*, vol. 2017, Article ID 9712536, 8 pages, 2017.
- [8] A. Stanek, A. Cholewka, T. Wielkoszyński, E. Romuk, and A. Sieroń, "Whole-body cryotherapy decreases the levels of inflammatory, oxidative stress, and atherosclerosis plaque markers in male patients with active-phase ankylosing spondylitis in the absence of classical cardiovascular risk factors," *Mediators of Inflammation*, vol. 2018, Article ID 8592532, 11 pages, 2018.
- [9] A. Stanek, K. Sieroń-Stoltny, E. Romuk et al., "Whole-body cryostimulation as an effective method of reducing oxidative stress in healthy men," *Advances in Clinical and Experimental Medicine*, vol. 25, no. 6, pp. 1281–1291, 2016.
- [10] W. Wasowicz, J. Neve, and A. Peretz, "Optimized steps in fluorometric determination of thiobarbituric acid-reactive substances in serum: importance of extraction pH and influence of sample preservation and storage," *Clinical Chemistry*, vol. 39, no. 12, pp. 2522–2526, 1993.
- [11] F. P. Corongiu, S. Banni, and M. A. Dessi, "Conjugated dienes detected in tissue lipid extracts by second derivative spectrophotometry," *Free Radical Biology & Medicine*, vol. 7, no. 2, pp. 183–186, 1989.
- [12] T. Wielkoszyński, M. Szewczyk, M. Zembala, and M. Szumska, "Concentration of anti-7-ketocholesterol antibodies in patient sera after heart transplantation," *Transplantation Proceedings*, vol. 41, no. 8, pp. 3206–3208, 2009.
- [13] I. F. F. Benzie and J. J. Strain, "The Ferric Reducing Ability of Plasma (FRAP) as a Measure of "Antioxidant Power": The FRAP Assay," *Analytical Biochemistry*, vol. 239, no. 1, pp. 70–76, 1996.
- [14] L. H. Johansson and L. A. H. Borg, "A spectrophotometric method for determination of catalase activity in small tissue samples," *Analytical Biochemistry*, vol. 174, no. 1, pp. 331–336, 1988.
- [15] A. Meister and M. E. Anderson, "Glutathione," *Annual Review of Biochemistry*, vol. 52, no. 1, pp. 711–760, 1983.
- [16] C. R. Wheeler, J. A. Salzman, N. M. Elsayed, S. T. Omaye, and D. W. Korte Jr., "Automated assays for superoxide dismutase, catalase, glutathione peroxidase, and glutathione reductase activity," *Analytical Biochemistry*, vol. 184, no. 2, pp. 193–199, 1990.
- [17] D. Paglia and W. Valentine, "Studies on the quantitative and qualitative characterization of erythrocyte glutathione peroxidase," *Journal of Laboratory and Clinical Medicine*, vol. 70, no. 1, pp. 158–169, 1967.
- [18] W. H. Habig and W. B. Jakoby, "[51] Assays for differentiation of glutathione S-Transferases," *Methods in Enzymology*, vol. 77, pp. 398–405, 1981.
- [19] Y. Oyanagui, "Reevaluation of assay methods and establishment of kit for superoxide dismutase activity," *Analytical Biochemistry*, vol. 142, no. 2, pp. 290–296, 1984.
- [20] M. I. Mackness, D. Harty, D. Bhatnagar et al., "Serum paraoxonase activity in familial hypercholesterolaemia and insulin-dependent diabetes mellitus," *Atherosclerosis*, vol. 86, no. 2-3, pp. 193–199, 1991.
- [21] H. Tomoyori, Y. Kawata, T. Higuchi et al., "Phytosterol oxidation products are absorbed in the intestinal lymphatics in rats but do not accelerate atherosclerosis in apolipoprotein E-deficient mice," *The Journal of Nutrition*, vol. 134, no. 7, pp. 1690–1696, 2004.
- [22] L. Ryan, "Oxidised products of cholesterol: their role in apoptosis," *Current Nutrition & Food Science*, vol. 1, no. 1, pp. 41–51, 2005.
- [23] A. Vejux, L. Malvitte, and G. Lizard, "Side effects of oxysterols: cytotoxicity, oxidation, inflammation, and phospholipidosis,"

- Brazilian Journal of Medical and Biological Research*, vol. 41, no. 7, pp. 545–556, 2008.
- [24] G. Lizard, C. Miguet, G. Bessède et al., “Impairment with various antioxidants of the loss of mitochondrial transmembrane potential and of the cytosolic release of cytochrome *c* occurring during 7-ketocholesterol-induced apoptosis,” *Free Radical Biology & Medicine*, vol. 28, no. 5, pp. 743–753, 2000.
- [25] Y. C. O’Callaghan, J. A. Woods, and N. M. O’Brien, “Characteristics of 7 β -hydroxycholesterol-induced cell death in a human monocytic blood cell line, U937, and a human hepatoma cell line, HepG2,” *Toxicology in Vitro*, vol. 16, no. 3, pp. 245–251, 2002.
- [26] F. Biasi, G. Leonarduzzi, B. Vizio et al., “Oxysterol mixtures prevent proapoptotic effects of 7-ketocholesterol in macrophages: implications for proatherogenic gene modulation,” *The FASEB Journal*, vol. 18, no. 6, pp. 693–695, 2004.
- [27] G. Leonarduzzi, F. Biasi, E. Chiarpotto, and G. Poli, “Trojan horse-like behavior of a biologically representative mixture of oxysterols,” *Molecular Aspects of Medicine*, vol. 25, no. 1-2, pp. 155–167, 2004.
- [28] A. Stanek, A. Gadowska-Cicha, K. Gawron et al., “Role of nitric oxide in physiology and pathology of the gastrointestinal tract,” *Mini-Reviews in Medicinal Chemistry*, vol. 8, no. 14, pp. 1549–1560, 2008.
- [29] M. Rosenblat and M. Aviram, “Oxysterol-induced activation of macrophage NADPH-oxidase enhances cell-mediated oxidation of LDL in the atherosclerotic apolipoprotein E deficient mouse: inhibitory role for vitamin E,” *Atherosclerosis*, vol. 160, no. 1, pp. 69–80, 2002.
- [30] Y. Kawai, A. Saito, N. Shibata et al., “Covalent binding of oxidized cholesteryl esters to Protein,” *Journal of Biological Chemistry*, vol. 278, no. 23, pp. 21040–21049, 2003.
- [31] Q. Liu, K. Kobayashi, J. Furukawa et al., “ ω -carboxyl variants of 7-ketocholesteryl esters are ligands for β_2 -glycoprotein I and mediate antibody-dependent uptake of oxidized LDL by macrophages,” *Journal of Lipid Research*, vol. 43, no. 9, pp. 1486–1495, 2002.
- [32] A. M. El-Dakak, M. H. M. Ahmed, and S. A. Ismail, “Effect of some natural antioxidants on ox sterol formed endogenously in hypercholesterolemia rats,” *Egyptian Journal of Biomedical Science*, vol. 28, pp. 1–18, 2008.
- [33] M. C. Hall, “The effect of oxysterols, individually and as a representative mixture from food, on in vitro cultured bovine ovarian granulosa cells,” *Molecular and Cellular Biochemistry*, vol. 292, no. 1-2, pp. 1–11, 2006.
- [34] C. C. Hedrick, K. Hassan, G. P. Hough et al., “Short-term feeding of atherogenic diet to mice results in reduction of HDL and paraoxonase that may be mediated by an immune mechanism,” *Arteriosclerosis, Thrombosis and Vascular Biology*, vol. 20, no. 8, pp. 1946–1952, 2000.
- [35] W. H. F. Sutherland, R. J. Walker, S. A. de Jong, A. M. van Rij, V. Phillips, and H. L. Walker, “Reduced Postprandial serum paraoxonase activity after a meal rich in used cooking fat,” *Arteriosclerosis, Thrombosis and Vascular Biology*, vol. 19, no. 5, pp. 1340–1347, 1999.

Research Article

Early Oxidative Stress Response in Patients with Severe Aortic Stenosis Undergoing Transcatheter and Surgical Aortic Valve Replacement: A Transatlantic Study

Michael Mahmoudi,¹ Juan Guillermo Gormaz,² Marcia Erazo ,³ Michael Howard,² Cristian Baeza,³ Martin Feelisch,¹ Nick Curzen,¹ Bartosz Olechowski ,¹ Bernadette Fernandez,¹ Magdalena Minnion,¹ Monika Mikus-Lelinska,¹ Mia Meiss,¹ Laurie Lau,¹ Nicolas Valls,³ Abraham I. J. Gajardo ,³ Amy Rivotta,² Rodrigo Carrasco,^{2,3} Gabriel Cavada,^{2,3} Maria Jesus Vergara,³ and Gabriel Maluenda ,^{2,3}

¹Faculty of Medicine, University of Southampton, UK

²Faculty of Medicine, Universidad del Desarrollo, Clinica Alemana, Santiago, Chile

³Faculty of Medicine, University of Chile, San Borja Arriaran Hospital, Santiago, Chile

Correspondence should be addressed to Gabriel Maluenda; gabrielmaluenda@gmail.com

Received 11 July 2019; Revised 20 August 2019; Accepted 17 September 2019; Published 13 November 2019

Guest Editor: Adrian Doroszko

Copyright © 2019 Michael Mahmoudi et al. This is an open access article distributed under the Creative Commons Attribution License, which permits unrestricted use, distribution, and reproduction in any medium, provided the original work is properly cited.

Myocardial ischemia/reperfusion-related oxidative stress as a result of cardiopulmonary bypass is thought to contribute to the adverse clinical outcomes following surgical aortic valve replacement (SAVR). Although the acute response following this procedure has been well characterized, much less is known about the nature and extent of oxidative stress induced by the transcatheter aortic valve replacement (TAVR) procedure. We therefore sought to examine and directly compare the oxidative stress response in patients undergoing TAVR and SAVR. A total of 60 patients were prospectively enrolled in this exploratory study, 38 patients undergoing TAVR and 22 patients SAVR. Reduced and oxidized glutathione (GSH, GSSG) in red blood cells as well as the ferric-reducing ability of plasma (FRAP) and plasma concentrations of 8-isoprostanes were measured at baseline (S1), during early reperfusion (S2), and 6-8 hours (S3) following aortic valve replacement (AVR). TAVR and SAVR were successful in all patients. Patients undergoing TAVR were older (79.3 ± 9.5 vs. 74.2 ± 4.1 years; $P < 0.01$) and had a higher mean STS risk score (6.6 ± 4.8 vs. 3.2 ± 3.0 ; $P < 0.001$) than patients undergoing SAVR. At baseline, FRAP and 8-isoprostane plasma concentrations were similar between the two groups, but erythrocytic GSH concentrations were significantly lower in the TAVR group. After AVR, FRAP was markedly higher in the TAVR group, whereas 8-isoprostane concentrations were significantly elevated in the SAVR group. In conclusion, TAVR appears not to cause acute oxidative stress and may even improve the antioxidant capacity in the extracellular compartment.

1. Introduction

Myocardial ischemia/reperfusion injury (MRI) related to cardiopulmonary bypass has been linked to adverse clinical outcomes following cardiac surgery [1–4]. Changes in reactive oxygen species (ROS) following surgical aortic valve replacement (SAVR) have been well documented in the literature

[3]. Furthermore, preoperative ROS biomarkers such as malondialdehyde, a reactive breakdown product of lipid oxidation, have been shown to be predictors of adverse outcomes at 30-day and 1-year follow-up [5]. In contrast to SAVR, transcatheter aortic valve replacement (TAVR) is associated with shorter duration of myocardial ischemia and hypotension and may be associated with a lower degree of MRI. Apart

from a single study using a new electrochemical technique to assess redox status in serum [6], which suggests that TAVR may be associated with lower oxidative stress as compared to SAVR, pertinent additional information is sparse [7]. However, the regulation of redox status in the intracellular compartment differs considerably from that in the extracellular space [8], and physiological processes are not governed by simple electrochemical potentials [9, 10]. Moreover, “oxidative stress” is an open concept with many contributing factors, the significance of which have not been established. The aim of the present study was to describe the early oxidative stress response in the blood of patients undergoing TAVR and compare them with a group of patients undergoing SAVR by applying established biochemical readouts of cellular and extracellular redox status.

2. Methods

2.1. Study Design. This was a prospective, observational, exploratory study designed to compare two series of patients with severe symptomatic aortic stenosis (AS) undergoing either TAVR ($n = 38$) or SAVR ($n = 22$). The study was conducted at the San Borja Arriaran Cardiovascular Center (Santiago, Chile), Clinica Alemana (Santiago, Chile), and the University Hospital Southampton NHS Foundation Trust (Southampton, UK). All patients gave written informed consent, and the study was conducted under Ethics Committee Board approval (Central Metropolitan Health Service Ethical Committee, Santiago, Chile, Project ID: 378/14; RES Committee North West Liverpool East, UK, IRAS Project ID: 206946). The study is registered at ClinicalTrials.gov (NCT02841917).

2.2. Eligibility Criteria for TAVR. Severe AS was defined by transthoracic echocardiography as aortic valve area $< 1 \text{ cm}^2$ or index valve area $< 0.8 \text{ cm}^2/\text{m}^2$ in the presence of mean aortic gradient $> 40 \text{ mmHg}$ or peak velocity $> 4 \text{ m/s}$. The local Heart Team assessed each candidate with severe AS according to the clinical background and imaging. Consideration was given in each case to the estimated surgical risk, including such features as severe comorbidities, advanced age, frailty, or thoracic anatomy unfavorable for SAVR. Society of Thoracic Surgeons (STS) score $> 8\%$ for mortality defined patients at a high risk for SAVR. There were no age restrictions for TAVR. Access site, either transfemoral or transapical, was determined according to the Heart Team recommendation.

2.3. Eligibility Criteria for SAVR. Patients with severe symptomatic AS undergoing SAVR served as the control group. These patients fulfilled the same echocardiographic criteria as patients undergoing TAVR but were considered to be at a lower surgical risk by the Heart Team. There were no age restrictions for SAVR.

2.4. Baseline Evaluation. The following studies were performed prior to the Heart Team evaluation: (1) complete blood count, coagulation tests, serum biochemistry, and liver function tests; (2) transthoracic echocardiogram; (3) coronary angiography, and (4) CT angiographic assessment of

the ascending aorta, the thoracic aorta, and the aorto-iliofemoral tree.

2.5. Oxidative Stress Measurements. Peripheral venous blood was collected, using EDTA, heparin, and serum vacutainers, prior to the patients being transferred to the operating theatre for their procedure (S1), within 10 minutes of completion of SAVR/TAVR (S2) and 6-8 hours post SAVR/TAVR (S3). Samples were immediately subjected to centrifugation for separation into plasma, serum, and red blood cells and stored at -80°C . Samples were analyzed for (1) antioxidant potential in the extracellular compartment using the “ferric-reducing ability of plasma” (FRAP) [11], (2) intracellular redox status by measurement of reduced (GSH) and oxidized glutathione (GSSG) in red blood cells [12], and (3) lipid oxidation by measurement of plasma concentrations of 8-isoprostane (8-epi-prostaglandin- $\text{F}_{2\alpha}$) using a commercial assay kit (Cayman Chemical).

2.6. Statistical Analysis. Continuous variables are expressed as the mean \pm SD. Categorical variables are expressed as frequencies and percentages. Baseline characteristics and post-procedural differences were compared using the chi-square independence test for categorical variables and the Student *t*-test for continuous variables. Intratime values per group were compared through regression analysis adjusted by the STS score. Intragroup changes in oxidative stress biomarkers were analyzed in terms of the slope of the trend. A mixed model was applied to evaluate the potential effects of red blood cell transfusion and procedural time variables, including “procedural time,” “fluoroscopic time,” “rapid-pacing time,” and “cardiopulmonary by-pass time,” on ROS following AVR. Statistical significance was assumed at $P < 0.05$. Statistical analyses were performed using Stata version 15® (StataCorp LLC, Texas, USA).

3. Results

The baseline clinical characteristics are summarized in Table 1. As compared to the SAVR group, female gender, older age, diabetes mellitus, smoking history, previous myocardial infarction, coronary artery disease, chronic renal impairment, and history of atrial fibrillation were more common in the TAVR group. The TAVR group had a higher risk profile than the SAVR group (mean STS score 6.6 ± 4.8 vs. 3.2 ± 3.0 ; $P < 0.001$; mean Log Euroscore 2 12.7 ± 8.8 vs. 5.1 ± 7.9 ; $P < 0.001$).

Baseline echocardiographic findings are summarized in Table 2. All patients underwent successful TAVR and SAVR. Procedural details are described in Table 3. One patient developed cardiac tamponade during TAVR due to pacing wire-induced right ventricular perforation, which was treated with pericardiocentesis.

Absolute values and changes in oxidative stress biomarkers are summarized in Table 4 and Figures 1–5. At baseline, the TAVR group had significantly lower GSH concentrations, similar concentrations of GSSG, and similar GSH/GSSG ratios. Intragroup changes showed a significant drop in GSH concentration following SAVR, whereas no

TABLE 1: Baseline clinical characteristics.

	TAVR (<i>n</i> = 38)	SAVR (<i>n</i> = 22)	<i>P</i> value
Age, years ± SD	79.3 ± 9.5	74.2 ± 4.1	0.02
Female, <i>n</i> (%)	25 (65.8)	9 (40.9)	0.06
Caucasian, <i>n</i> (%)	17 (44.7)	8 (36.4)	0.47
BMI, kg/m ² ± SD	27.6 ± 5.9	28.2 ± 3.8	0.67
Hypertension, <i>n</i> (%)	30 (78.9)	17 (77.3)	0.88
Type-2 diabetes, <i>n</i> (%)	15 (39.5)	3 (13.6)	0.03
Previous smoking, <i>n</i> (%)	17 (44.7)	3 (13.6)	0.01
Hypercholesterolemia, <i>n</i> (%)	16 (42.1)	8 (36.4)	0.66
Previous myocardial infarction, <i>n</i> (%)	11 (28.9)	0	0.01
Coronary artery disease	17 (44.7)	4 (9.1)	0.04
1-vessel CAD	4	4	
2-vessel CAD	7	0	
3-vessel CAD	6	0	
Previous PCI, <i>n</i> (%)	6 (15.8)	2 (9.1)	0.46
Previous CABG, <i>n</i> (%)	11 (28.9)	0	0.01
Previous CVA/TIA, <i>n</i> (%)	3 (7.9)	3 (13.6)	0.47
Peripheral vascular disease, <i>n</i> (%)	5 (13.2)	4 (18.2)	0.61
Chronic lung disease, <i>n</i> (%)	9 (23.7)	2 (9.1)	0.16
Chronic renal insufficiency	22 (57.9)	7 (31.8)	0.05
History of atrial fibrillation, <i>n</i> (%)	14 (36.8)	3 (13.6)	0.05
eGFR (mL/min)	59.8 ± 28.5	71.2 ± 019.2	0.10
Hemoglobin (g/dL)	12.0 ± 2.9	12.7 ± 1.6	0.26
STS risk score, ±SD	6.6 ± 4.8	3.2 ± 3.0	<0.01
Logistic Euroscore 2, ±SD	12.7 ± 8.8	5.1 ± 7.9	<0.01

BMI = body mass index; CAD = coronary artery disease; CABG = coronary artery bypass grafting; CVA = cerebrovascular accident; CHF = congestive heart failure; eGFR = estimated glomerular filtration rate; PCI = percutaneous coronary intervention; SD = standard deviation; STS = Society of Thoracic Surgeons; TAVR = transcatheter aortic valve replacement; TIA = transient ischemic attack.

TABLE 2: Baseline echocardiographic characteristics.

	TAVR (<i>n</i> = 38)	SAVR (<i>n</i> = 22)	<i>P</i> value
LV end-diastolic dimension, mm ± SD	48.3 ± 8.9	45.3 ± 5.8	0.25
LV end-systolic dimension, mm ± SD	33.5 ± 10.7	28.6 ± 7.9	0.14
LV ejection fraction, % ± SD	54.3 ± 18.0	61.2 ± 8.2	0.11
Aortic valve area, cm ² ± SD	0.6 ± 0.2	0.7 ± 0.3	0.30
Peak aortic velocity, m/s ± SD	4.4 ± 1.2	5.1 ± 1.1	0.16
Mean aortic valve gradient, mmHg ± SD	44.5 ± 15.9	51.8 ± 20	0.15
Pulmonary artery pressure, mmHg ± SD	46.6 ± 14.1	42.9 ± 17	0.55
Moderate to severe aortic regurgitation, <i>n</i> (%)	6 (15.8)	1 (4.5)	0.19
Moderate to severe mitral regurgitation, <i>n</i> (%)	8 (21.1)	2 (9.1)	0.23
Moderate to severe tricuspid regurgitation, <i>n</i> (%)	8 (21.1)	1 (4.5)	0.08

LV = left ventricle; SAVR = surgical aortic valve replacement; SD = standard deviation; TAVR = transcatheter aortic valve replacement.

significant changes in concentrations of GSSG or GSH/GSSG ratio occurred in the two groups (Figures 1–3). Following AVR, the concentrations of GSH and GSSG and the GSH/GSSG ratio were similar in the two groups. Baseline FRAP and 8-isoprostane concentrations were similar

between the two groups. FRAP levels showed a significant intragroup increase following TAVR (Figure 4), whereas 8-isoprostane concentrations showed a significant intragroup increase following SAVR (Figure 5). FRAP was significantly higher in the TAVR group at the S2 interval, whilst 8-

TABLE 3: Procedural characteristics.

	TAVR (<i>n</i> = 38)	SAVR (<i>n</i> = 22)	<i>P</i> value
<i>Access site</i>			
Transfemoral, <i>n</i> (%)	28 (73.7)		
Transapical, <i>n</i> (%)	10 (26.3)		
Sternotomy, <i>n</i> (%)		100	
<i>Valve type</i>			
Sapien XT, <i>n</i> (%)	21 (79.4)		
Sapien 3, <i>n</i> (%)	11 (38.2)		
Evolut-R, <i>n</i> (%)	6 (47.1)		
Surgical bioprosthesis, <i>n</i> (%)		22 (100)	
Mean size, mm ± SD	25.4 ± 2.5	24.1 ± 2.2	0.07
Procedural time, min ± SD	99 ± 42	184 ± 43	<0.01
Fluoroscopy time, min ± SD	17.6 ± 7.9	—	
Cardiopulmonary bypass time, min ± SD	—	74.5 ± 31.6	
Aortic clamp time, min ± SD	—	61.0 ± 31.3	
General anaesthesia, <i>n</i> (%)	33 (86.8)	22 (100)	0.14
Conscious sedation, <i>n</i> (%)	5	0	

SAVR = surgical aortic valve replacement; SD = standard deviation; TAVR = transcatheter aortic valve replacement.

isoprostane concentrations were significantly higher in the SAVR group at the S3 interval. No statistically significant associations were observed between changes in erythrocytic glutathione status and circulating 8-isoprostane concentrations (data not shown).

The effect of red blood cell transfusion and procedural time variables following AVR was explored using a mixed model that included the treatment option and duration of the procedures adjusted by the STS score. Changes in ROS did not correlate with red blood cell transfusion and procedural time variables.

In-hospital and 3-month outcomes are summarized in Tables 5 and 6. There was no in-hospital death. Two patients (3.33%) developed ischemic stroke after the procedure, one in each group. VARC-2 defined major bleeding occurred in one patient undergoing TAVR and 2 patients undergoing SAVR. Patients undergoing SAVR received more transfusions, had longer ICU and overall hospital stay, and developed postprocedural atrial fibrillation more frequently than those treated with TAVR. The rate of myocardial infarction and acute renal failure was similar among the two groups. At 3-month follow-up, two patients had died in the TAVR group: one due to congestive heart failure and the second due to severe liver failure.

4. Discussion

The present study demonstrates that TAVR does not induce an acute oxidative stress response; this finding may be of particular significance for aged and frail patients at a high risk for periprocedural complications. Our data confirm and extend earlier findings using an electrochemical method [6] and are consistent with previous literature regarding the oxidative stress response in patients undergoing SAVR.

Oxidative stress was originally defined as an imbalance between ROS generation and antioxidant defense; over the years, the concept evolved further to reflect the complexity of the underlying regulatory processes and molecules involved and provide an explanation for the aberrations in redox regulation typically associated with pathophysiology [13, 14]. Under normal physiological conditions, ROS serve as integral components of cellular signaling pathways [14, 15]. A balanced redox state is established as a consequence of chemical and enzymatic interactions between the major ROS producing systems (NADPH oxidase, xanthine oxidase, nitric oxide synthase, myeloperoxidase, and lipoxygenases) and the major antioxidant systems (catalase, superoxide dismutase, glutathione peroxidase, and glutathione S transferases as well as α -tocopherol, ascorbic acid, reduced glutathione, and protein thiols) [14, 15]. Excess production or reduced degradation of ROS by the antioxidant defense systems imposes an oxidative burden upon the cellular environment leading to modification of various biomolecules and functional defects. In MRI, xanthine oxidase catalyzes the formation of uric acid with the coproduction of superoxide; superoxide release results in the recruitment and activation of neutrophils and their adherence to endothelial cells, which stimulates the formation of xanthine oxidase in the endothelium with further superoxide production [16]. Oxidation of DNA and proteins is accompanied by membrane damage initiated by lipid peroxidation, alterations in membrane permeability, modification of protein structures, and functional changes [17].

Patients with severe AS have been reported to have imbalances between endogenous oxidant and antioxidant characteristic of oxidative stress. This in turn has been linked to the pathogenesis of aortic valve degeneration [3, 18, 19]. One of the main advantages of TAVR is the relatively short ischemic time, which could mitigate MRI. We find that

TABLE 4: Changes in oxidative stress-related biomarkers according to transcatheter or surgical aortic valve replacement.

Measured parameter mean \pm SD	TAVR ($n = 38$)	SAVR ($n = 22$)	Adjusted P value
GSH S1	3.15 \pm 0.79	3.57 \pm 0.87	0.018
GSH S2	3.10 \pm 0.90	2.87 \pm 0.98	0.931
GSH S3 (nmol/mg protein)	3.23 \pm 0.74	2.85 \pm 0.77	0.498
Slope for trend	0.022	-0.330	
P value	0.698	<0.001	
GSSG S1	0.27 \pm 0.18	0.29 \pm 0.11	0.942
GSSG S2	0.30 \pm 0.32	0.39 \pm 0.32	0.650
GSSG S3 (nmol/mg protein)	0.26 \pm 0.15	0.30 \pm 0.13	0.475
Slope for trend	-0.005	0.003	
P value	0.842	0.804	
GSH/GSSG S1	16.5 \pm 9.1	13.9 \pm 5.1	0.568
GSH/GSSG S2	15.4 \pm 9.3	10.9 \pm 7.7	0.380
GSH/GSSG S3	20.5 \pm 27.4	11.8 \pm 6.5	0.237
Slope for trend	1.860	-0.880	
P value	0.319	0.199	
FRAP S1	339.1 \pm 90.9	329.8 \pm 74.1	0.410
FRAP S2	359.6 \pm 94.3	314.8 \pm 68.6	0.017
FRAP S3 (μ mol/L)	357.0 \pm 119.8	327.1 \pm 113.5	0.212
Slope for trend	12.6	-0.22	
P value	0.027	0.983	
8-Isop S1	40.6 \pm 18.3	41.0 \pm 16.1	0.553
8-Isop S2	41.0 \pm 22.1	41.8 \pm 22.3	0.635
8-Isop S3 (pg/mL)	40.1 \pm 21.8	52.0 \pm 26.1	0.046
Slope for trend	-2.56	46.5	
P value	0.86	0.028	

GSH = reduced glutathione; GSSG = oxidized glutathione; FRAP = ferric-reducing ability of plasma; S = sample; SAVR = surgical aortic valve replacement; SD = standard deviation; TAVR = transcatheter aortic valve replacement; 8-Isop = 8-isoprostane.

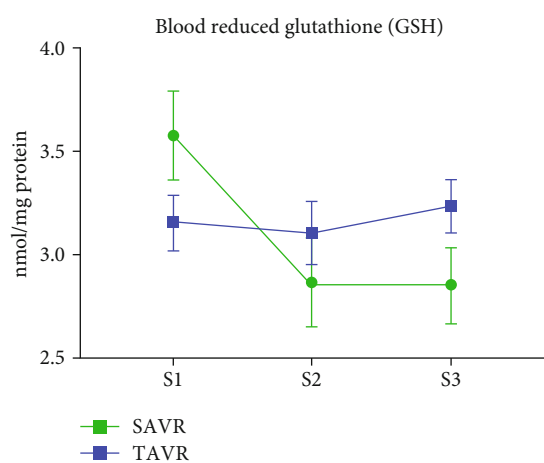


FIGURE 1: Blood reduced glutathione following aortic valve replacement. The reduced glutathione levels in red blood cells dropped significantly following SAVR whereas no change was observed after TAVR. Abbreviations: S1: sample 1; S2: sample 2; S3: sample 3.

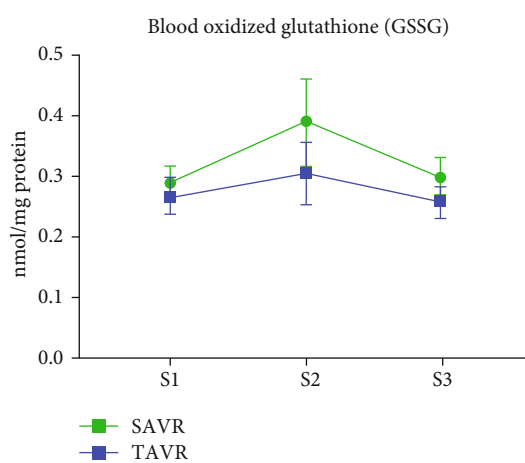


FIGURE 2: Blood oxidized glutathione following aortic valve replacement. Changes in oxidized glutathione concentrations in red blood cells were similar among patients undergoing SAVR or TAVR. Abbreviations: S1: sample 1; S2: sample 2; S3: sample 3.

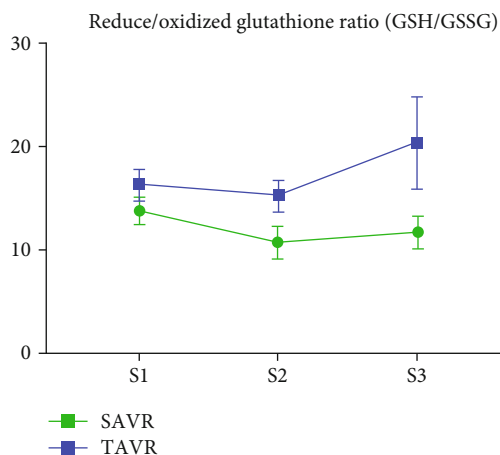


FIGURE 3: Ratio of blood reduced over oxidized glutathione following aortic valve replacement. Changes in reduced/oxidized glutathione ratio in red blood cells were similar among patients undergoing SAVR or TAVR. Abbreviations: S1: sample 1; S2: sample 2; S3: sample 3.

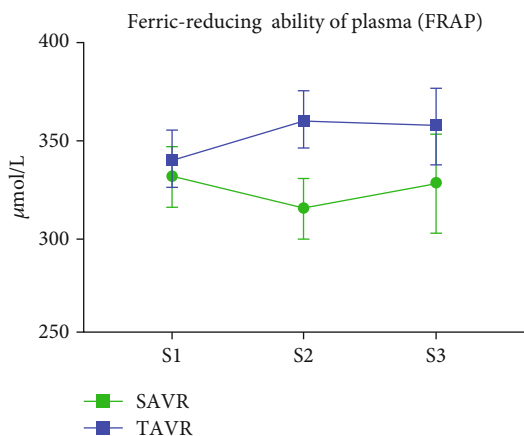


FIGURE 4: Ferric-reducing ability of plasma following aortic valve replacement. The ferric-reducing antioxidant power of the plasma increased significantly following TAVR whereas no change was observed after SAVR. Abbreviations: S1: sample 1; S2: sample 2; S3: sample 3.

intracellular glutathione concentrations are significantly lower in patients undergoing TAVR, which may reflect a compromised capacity to cope with oxidative stress. Given that this observation remained significant after adjustment for the STS risk score, it would suggest that other confounders such as the patients' nutritional status and age may be important contributing factors.

We find an absence of an early oxidative stress response in patients undergoing TAVR as evidenced by changes in the concentration of 8-isoprostanes, a specific and reliable indicator of lipid oxidation. Unexpectedly, TAVR patients also presented with a significant and consistent increase in FRAP. This assay is independent of the availability of sulfhydryl groups, therefore complementary to the glutathione measurements in red blood cells, and often associated with low-molecular-weight antioxidants such as plasma uric acid.

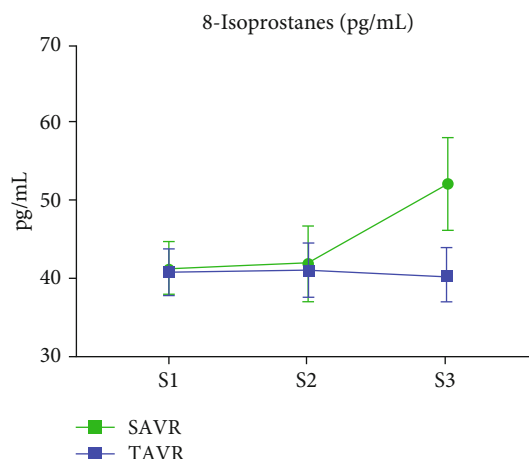


FIGURE 5: Plasmatic concentrations of 8-isoprostanes following aortic valve replacement. The 8-isoprostane levels in plasma increased significantly following SAVR whereas no change was observed after TAVR. Abbreviations: S1: sample 1; S2: sample 2; S3: sample 3.

The increase in FRAP we observed may be related in part to the less invasive nature of TAVR, its lower ischemic time, and therefore a lesser MRI burden. Alternatively, the relatively rapid hemodynamic improvement following AVR may lead to enhanced shear stress-induced release of endothelial nitric oxide, which in addition to its role as an endogenous vasodilator has potent antioxidant properties [20, 21], possibly leading to an antioxidant-sparing effect. It may also indicate that the oxidative imbalance observed in patients with severe AS is amenable to correction by a minimally invasive and rapid restoration of normal physiology following relief of aortic obstruction.

Red blood cell storage has been linked to ROS generation and antioxidant consumption [22, 23]. It has been proposed that free radical-mediated damage may initiate and further exacerbate iron release during RBC storage further enhancing free radical-mediated cellular damage. In this study, we could not demonstrate any correlation between red blood cell transfusion and changes in oxidative stress biomarkers.

5. Study Limitations

Due to the nonrandomized nature of this observational study, the SAVR and TAVR groups were different with differing risk scores. Given the relatively small sample size, we did neither test for possible associations between any of the oxidative stress readouts with clinical outcomes nor perform any subgroup analyses. Rather, the aim in our study was to describe the temporal changes in ROS/oxidative stress in patients undergoing TAVR by using patients undergoing SAVR as a reference arm.

6. Conclusion

As compared to patients undergoing SAVR, patients undergoing TAVR did not show significant changes in biomarkers

TABLE 5: In-hospital clinical outcomes.

	TAVR (<i>n</i> = 38)	SAVR (<i>n</i> = 22)	<i>P</i> value
Death, <i>n</i> (%)	0	0	0.99
Cerebrovascular accident, <i>n</i> (%)	1 (2.6)	1 (4.5)	0.69
Myocardial infarction, <i>n</i> (%)	0	0	0.99
Major bleeding, <i>n</i> (%)	1 (2.6)	2 (9.1)	0.27
Periprocedural transfusions, <i>n</i> (%)	1 (2.6)	8 (36.4)	<0.01
Red blood cell transfusion, units ± SD	0.1 ± 0.3	0.6 ± 1.7	0.06
New atrial fibrillation, <i>n</i> (%)	3 (7.9)	6 (27.3)	0.04
Permanent pacemaker, <i>n</i> (%)	2 (5.3)	2 (9.1)	0.57
Acute renal failure, <i>n</i> (%)	3 (7.9)	3 (9.1)	0.87
Stay at intensive care unit, hours ± SD	64 ± 65	128 ± 130	0.01
Length of admission, days ± SD	4.9 ± 2.6	8.4 ± 4.6	<0.01

SAVR = surgical aortic valve replacement; SD = standard deviation; TAVR = transcatheter aortic valve replacement.

TABLE 6: Clinical outcomes at 90-day follow-up.

	TAVR (<i>n</i> = 38)	SAVR (<i>n</i> = 22)	<i>P</i> value
Death, <i>n</i> (%)	2 (5.3)	0	0.27
Readmission, <i>n</i> (%)	3 (7.9)	1 (4.5)	0.62
Cerebrovascular accident, <i>n</i> (%)	1 (2.6)	1 (4.5)	0.68
Myocardial infarction, <i>n</i> (%)	0	0	0.99

SAVR = surgical aortic valve replacement; TAVR = transcatheter aortic valve replacement.

of oxidative stress despite having greater comorbidities and impaired baseline antioxidant defenses. TAVR was associated with an improvement in the antioxidant capacity of plasma. Larger studies would be required to determine if these potentially beneficial alterations are associated with clinical outcomes in patients undergoing TAVR.

Abbreviations

AS: Aortic stenosis
 FRAP: Ferric-reducing ability of plasma
 GSH: Reduced glutathione
 GSSH: Oxidized glutathione
 MRI: Myocardial ischemia and reperfusion injury
 ROS: Reactive oxygen species
 SAVR: Surgical aortic valve replacement
 STS: Society of Thoracic Surgeons
 TAVR: Transcatheter aortic valve replacement.

Data Availability

The data used to support the findings of this study are available from the corresponding author upon request.

Conflicts of Interest

Gabriel Maluenda is a TAVR proctor for Edwards Lifesciences.

Acknowledgments

This study was funded by the “National Funding for Scientific & Technological Development” FONDECYT, Study ID #11140383, Government of Chile, Santiago, Chile.

References

- [1] D. J. Hausenloy and D. M. Yellon, “The evolving story of “conditioning” to protect against acute myocardial ischaemia-reperfusion injury,” *Heart*, vol. 93, no. 6, pp. 649–651, 2007.
- [2] S. Scolletta, F. Carlucci, B. Biagioli et al., “Nt-proBNP changes, oxidative stress, and energy status of hypertrophic myocardium following ischemia/reperfusion injury,” *Biomedicine & Pharmacotherapy*, vol. 61, pp. 160–166, 2007.
- [3] V. Cavalca, E. Tremoli, B. Porro et al., “Oxidative stress and nitric oxide pathway in adult patients who are candidates for cardiac surgery: patterns and differences,” *Interactive Cardiovascular and Thoracic Surgery*, vol. 17, no. 6, pp. 923–930, 2013.
- [4] R. Rodrigo, P. Korantzopoulos, M. Cereceda et al., “A randomized controlled trial to prevent post-operative atrial fibrillation by antioxidant reinforcement,” *Journal of the American College of Cardiology*, vol. 62, no. 16, pp. 1457–1465, 2013.
- [5] J. Parenica, P. Nemeč, J. Tomandl et al., “Prognostic utility of biomarkers in predicting of one-year outcomes in patients with aortic stenosis treated with transcatheter or surgical aortic valve implantation,” *PLoS One*, vol. 7, no. 12, article e48851, 2012.
- [6] K. Heldmaier, C. Stoppe, A. Goetzenich et al., “Oxidation-reduction potential in patients undergoing transcatheter or

- surgical aortic valve replacement,” *BioMed Research International*, vol. 2018, Article ID 8469383, 10 pages, 2018.
- [7] B. Marchandot, M. Kibler, A. L. Charles et al., “Does transcatheter aortic valve replacement modulate the kinetic of superoxide anion generation?,” *Antioxidants & Redox Signaling*, vol. 31, no. 5, pp. 420–426, 2019.
- [8] M. M. Cortese-Krott, A. Koning, G. G. C. Kuhnle et al., “The reactive species interactome: evolutionary emergence, biological significance, and opportunities for redox metabolomics and personalized medicine,” *Antioxidants & Redox Signaling*, vol. 27, no. 10, pp. 684–712, 2017.
- [9] L. Flohé, “The fairytale of the GSSG/GSH redox potential,” *Biochimica et Biophysica Acta (BBA) - General Subjects*, vol. 1830, no. 5, pp. 3139–3142, 2013.
- [10] J. Santolini, S. A. Wootton, A. A. Jackson, and M. Feelisch, “The redox architecture of physiological function,” *Current Opinion in Physiology*, vol. 9, pp. 34–47, 2019.
- [11] I. F. Benzie and J. J. Strain, “The ferric reducing ability of plasma (FRAP) as a measure of “antioxidant power”: the FRAP assay,” *Analytical Biochemistry*, vol. 239, no. 1, pp. 70–76, 1996.
- [12] P. J. Hissin and R. Hilf, “A fluorometric method for determination of oxidized and reduced glutathione in tissues,” *Analytical Biochemistry*, vol. 74, no. 1, pp. 214–226, 1976.
- [13] I. Juranek and S. Bezek, “Controversy of free radical hypothesis: reactive oxygen species – cause or consequence of tissue injury?,” *General Physiology and Biophysics*, vol. 24, no. 3, pp. 263–278, 2005.
- [14] H. Sies, C. Berndt, and D. P. Jones, “Oxidative stress,” *Annual Review of Biochemistry*, vol. 86, pp. 715–748, 2017.
- [15] P. D. Ray, B. Huang, and Y. Tsuji, “Reactive oxygen species (ROS) homeostasis and redox regulation in cellular signaling,” *Cellular Signalling*, vol. 24, no. 5, pp. 981–990, 2012.
- [16] D. N. Granger, “Role of xanthine oxidase and granulocytes in ischemia-reperfusion injury,” *American Journal of Physiology-Heart and Circulatory Physiology*, vol. 255, pp. H1269–H1275, 1988.
- [17] N. R. Webster and J. F. Nunn, “Molecular structure of free radicals and their importance in biological reactions,” *British Journal of Anaesthesia*, vol. 60, no. 1, pp. 98–108, 1988.
- [18] J. D. Miller, Y. Chu, R. M. Brooks, W. E. Richenbacher, R. Peña-Silva, and D. D. Heistad, “Dysregulation of antioxidant mechanisms contributes to increased oxidative stress in calcific aortic valvular stenosis in humans,” *Journal of the American College of Cardiology*, vol. 52, no. 10, pp. 843–850, 2008.
- [19] E. J. Farrar, G. D. Huntley, and J. Butcher, “Endothelial-derived oxidative stress drives myofibroblastic activation and calcification of the aortic valve,” *PLoS One*, vol. 10, no. 4, article e0123257, 2015.
- [20] D. A. Wink, K. M. Miranda, M. G. Espey et al., “Mechanisms of the antioxidant effects of nitric oxide,” *Antioxidants & Redox Signaling*, vol. 3, no. 2, pp. 203–213, 2001.
- [21] R. Erkens, T. Suvorava, T. R. Sutton et al., “Nrf2 deficiency unmasks the significance of nitric oxide synthase activity for cardioprotection,” *Oxidative Medicine and Cellular Longevity*, vol. 2018, Article ID 8309698, 15 pages, 2018.
- [22] D. Orlov and K. Karkouti, “The pathophysiology and consequences of red blood cell storage,” *Anaesthesia*, vol. 70, p. 29–e12, 2015.
- [23] K. Collard, D. White, and A. Copplestone, “The influence of storage age on iron status, oxidative stress and antioxidant protection in paediatric packed cell units,” *Blood Transfusion*, vol. 12, no. 2, pp. 210–219, 2014.

Research Article

miR-200a Attenuated Doxorubicin-Induced Cardiotoxicity through Upregulation of Nrf2 in Mice

Xiaoping Hu,¹ Huagang Liu,² Zhiwei Wang ¹, Zhipeng Hu,¹ and Luocheng Li¹

¹Department of Cardiovascular Surgery, Renmin Hospital of Wuhan University, Wuhan, Hubei 430060, China

²Department of Vascular Surgery, Renmin Hospital of Wuhan University, Wuhan, Hubei 430060, China

Correspondence should be addressed to Zhiwei Wang; wangzhiwei@whu.edu.cn

Received 12 May 2019; Revised 7 August 2019; Accepted 31 August 2019; Published 3 November 2019

Guest Editor: Aneta Radziwon-Balicka

Copyright © 2019 Xiaoping Hu et al. This is an open access article distributed under the Creative Commons Attribution License, which permits unrestricted use, distribution, and reproduction in any medium, provided the original work is properly cited.

Nuclear factor (erythroid-derived 2)-like 2 (Nrf2) was closely involved in doxorubicin- (DOX-) induced cardiotoxicity. MicroRNA-200a (miR-200a) could target Keap1 mRNA and promote degradation of Keap1 mRNA, resulting in Nrf2 activation. However, the role of miR-200a in DOX-related cardiotoxicity remained unclear. Our study is aimed at investigating the effect of miR-200a on DOX-induced cardiotoxicity in mice. For cardioprotective expression, male mice received an injection of an adeno-associated virus 9 (AAV9) system carrying miR-200a or miR-scramble. Four weeks later, mice received a single intraperitoneal injection of DOX at 15 mg/kg. In our study, we found that miR-200a mRNA was the only microRNA that was significantly decreased in DOX-treated mice and H9c2 cells. miR-200a supplementation blocked whole-body wasting and heart atrophy caused by acute DOX injection, decreased the levels of cardiac troponin I and the N-terminal pro-brain natriuretic peptide, and improved cardiac and adult cardiomyocyte contractile function. Moreover, miR-200a reduced oxidative stress and cardiac apoptosis without affecting matrix metalloproteinase and inflammatory factors in mice with acute DOX injection. miR-200a also attenuated DOX-induced oxidative injury and cell loss in vitro. As expected, we found that miR-200a activated Nrf2 and Nrf2 deficiency abolished the protection provided by miR-200a supplementation in mice. miR-200a also provided cardiac benefits in a chronic model of DOX-induced cardiotoxicity. In conclusion, miR-200a protected against DOX-induced cardiotoxicity via activation of the Nrf2 signaling pathway. Our data suggest that miR-200a may represent a new cardioprotective strategy against DOX-induced cardiotoxicity.

1. Introduction

Doxorubicin (DOX), a quinone-containing anthracycline, has been widely used for the treatment of both solid and hematologic malignancies [1]. Its therapeutic use is limited by its dose-dependent cardiotoxicity, resulting in cardiomyocyte loss, mitochondrial dysfunction, myofibrillar degeneration, and congestive heart failure with poor prognosis [2]. The pathogenesis of DOX-induced cardiotoxicity is complex, but a solid body of evidence indicates that oxidative stress is closely involved [3].

There were a higher level of mitochondria and relatively lower levels of antioxidant enzymes in the heart samples, making the heart more sensitive to DOX-related injury [4]. It has been reported that oxidative stress and subsequent lipid peroxidation could be detected in the hearts within three

hours after DOX treatment [5]. Accumulation of reactive oxygen species (ROS) resulted in structural changes of biological macromolecules and death of cardiomyocytes [6]. Therefore, the search for an effective and safe antagonist of oxidative stress would be of great significance for the treatment of DOX-related cardiac toxicity.

Nuclear factor (erythroid-derived 2)-like 2 (Nrf2), a basic leucine zipper transcription factor, is essential for detoxification gene regulation in mammals [7]. Under physiological conditions, Nrf2 is bound in the cytosol by Kelch-like ECH associating protein 1 (Keap1), which is a scaffold protein for the ubiquitination and degradation of Nrf2 [8]. In response to oxidative stress, Nrf2 is released from Keap1 and translocates to the nucleus to regulate the expression of antioxidant and detoxification gene [9]. Nrf2 was decreased in DOX-treated hearts, and restoration of Nrf2 could

mitigate DOX-induced cardiotoxicity [10], suggesting targeting Nrf2 as a therapeutic strategy for the treatment of DOX-induced cardiotoxicity.

MicroRNAs (miRNAs or miRs) are highly conserved single-stranded noncoding RNAs that can posttranslationally modify mRNA [11]. Dysregulation of miRNAs has been implicated in many diseases including doxorubicin-induced cardiotoxicity [12]. The miR-200 family has been highlighted for its action in the maintenance of the epithelial phenotype [13]. A recent study indicated that miR-200a acted as a tumor suppressor by targeting FOXA1 in glioma [14]. miR-200a attenuated myocardial necroptosis via targeting RING finger protein 11 [15]. Moreover, miR-200a resulted in Nrf2 activation by targeting Keap1 mRNA and promoting degradation of Keap1 mRNA in diabetic nephropathy [16]. We hypothesized that overexpression of miR-200a in mice could attenuate DOX-induced cardiotoxicity. To investigate this possibility, we overexpressed miR-200a using an adeno-associated virus 9 (AAV9) system in DOX-treated mice. We examined the effect of miR-200a overexpression on DOX-induced oxidative injury and cell apoptosis in mice.

2. Methods

2.1. Animals. Protocols involving the use of animals were approved by the Institutional Animal Care and Use Committees in Renmin Hospital of Wuhan University. C57BL/6J male mice were also purchased from the Jackson Laboratory and housed in Renmin Hospital of Wuhan University with free access to food and water. An AAV9 system carrying miR-200a or miR-scramble was generated by Hanbio Technology (Shanghai, China). For cardiotropic expression, male mice (age: 8-10 weeks; 25-30 g) received 1×10^{11} viral genome of AAV9-miR-200a or AAV9-miR-scramble by tail vein injection according to a previous study [17]. Four weeks later, male C57BL/6J mice received a single intraperitoneal injection of DOX-HCl (Adriamycin, Sigma-Aldrich, St. Louis, MO, USA) at 15 mg/kg to mimic acute DOX exposure according to a previous study [18]. Control mice were treated with the same volume of normal saline (NS), which was used to dissolve DOX. The animals were observed and weighed daily. Echocardiography was performed at 5 days after DOX injection, and animals were sacrificed thereafter. Knockdown of cardiac Nrf2 was carried out in the acute DOX regime experiment using adenoviral vectors carrying Nrf2 small hairpin RNAs (shRNAs) or scrambled shRNA, which was generated by Hanbio (Shanghai, China). To knock down Nrf2, mice were given an intramyocardial injection of 2×10^9 viral genome particles in 1 location of the left ventricle according to a previous study [19]. One week after adenoviral injection, these mice were subjected to DOX injection to mimic acute DOX exposure. To mimic chronic DOX exposure, the mice in the DOX and DOX+miR-200a groups ($n = 10$ for each group) were injected intraperitoneally with DOX (5 mg/kg every week, the total cumulative dose is 20 mg/kg) for 4 times; the control mice received saline. After 2 weeks post the

last injection, cardiac functions in the mice with chronic DOX injection were examined and the animals were then sacrificed. To observe the effect of miR-200a on the survival rate in mice with chronic DOX exposure, the mice ($n = 15$ for each group) were injected intraperitoneally with DOX (5 mg/kg every week, the total cumulative dose is 20 mg/kg) or saline for 4 times. After the first injection of DOX, these mice were observed daily for 6 weeks.

2.2. Echocardiography and Hemodynamic Analysis. Mice were exposed to mild anaesthesia with 1.5% isoflurane. Echocardiography was performed on six mice per group with the Vevo 2100 ultrasound, which was connected to an ultrasound system (SSD-5500; Aloka, Tokyo, Japan). Left ventricle end-diastolic and end-systolic diameters were measured.

To detect hemodynamic parameters, a microtip pressure-volume catheter (SPR-839; Millar Instruments, USA) was inserted through an apical stab into the ventricle to measure cardiac function. Hemodynamic measurements were analyzed using IOX software (EMKAtech).

2.3. Western Blotting. Proteins were extracted from frozen heart tissues and subjected to sodium dodecyl sulfate-polyacrylamide gel electrophoresis [20, 21]. After that, the proteins were transferred to PVDF membranes (Merck Millipore, Massachusetts, USA). Membranes were then blocked in nonfat milk for 2 hours and incubated overnight at 4°C with primary antibodies against Nrf2 (Abcam, Cambridge, MA, UK, ab62352, 1:1000), heme oxygenase 1 (HO-1, Abcam, ab13248, 1:1000), GAPDH (Abcam, ab181602, 1:1000), Bax (Abcam, ab32503, 1:1000), and Bad (Abcam, ab32445, 1:1000). After that, the membrane was reacted with the secondary antibodies for 1 h at room temperature, was stained with an enhanced chemiluminescence reagent, and was visualized using the BIO-RAD ChemiDoc Touch Imaging System (BIO-RAD, Hercules, CA, USA). GAPDH was used as the internal control.

2.4. RNA Extraction and Real-Time RT-PCR. Total RNA extraction was performed using a TRIzol reagent (Invitrogen Corp., CA). DNase-treated total RNA (2 μ g) was reverse transcribed using SuperScript II reverse transcriptase (Invitrogen Corp.). Gene expression analysis was carried out using the Fast SYBR Green master mix (Applied Biosystems) and the QuantStudio 12k Flex real-time PCR system (ThermoFisher, Ecublens, Switzerland). Results were normalized to GAPDH mRNA as an internal control. The miRNA level was determined using a Bulge-Loop miRNA qRT-PCR Starter Kit (Ribobio Technology, Guangzhou, China). U6 was used as the internal control of miRNA.

2.5. Adult Cardiomyocyte Isolation and Mechanics Detection. Hearts were collected and mounted onto a temperature-controlled Langendorff system. Hearts were digested with a Ca^{2+} -free Krebs-Henseleit bicarbonate buffer containing Liberase Blendzymes (0.1 mg/ml) for 30 min at 37°C, which was obtained from Roche Diagnostics (Indianapolis, IN). Adult cardiomyocytes with rod-shaped and clear edges were used in our detection within 6 h of isolation. An IonOptix™ soft-

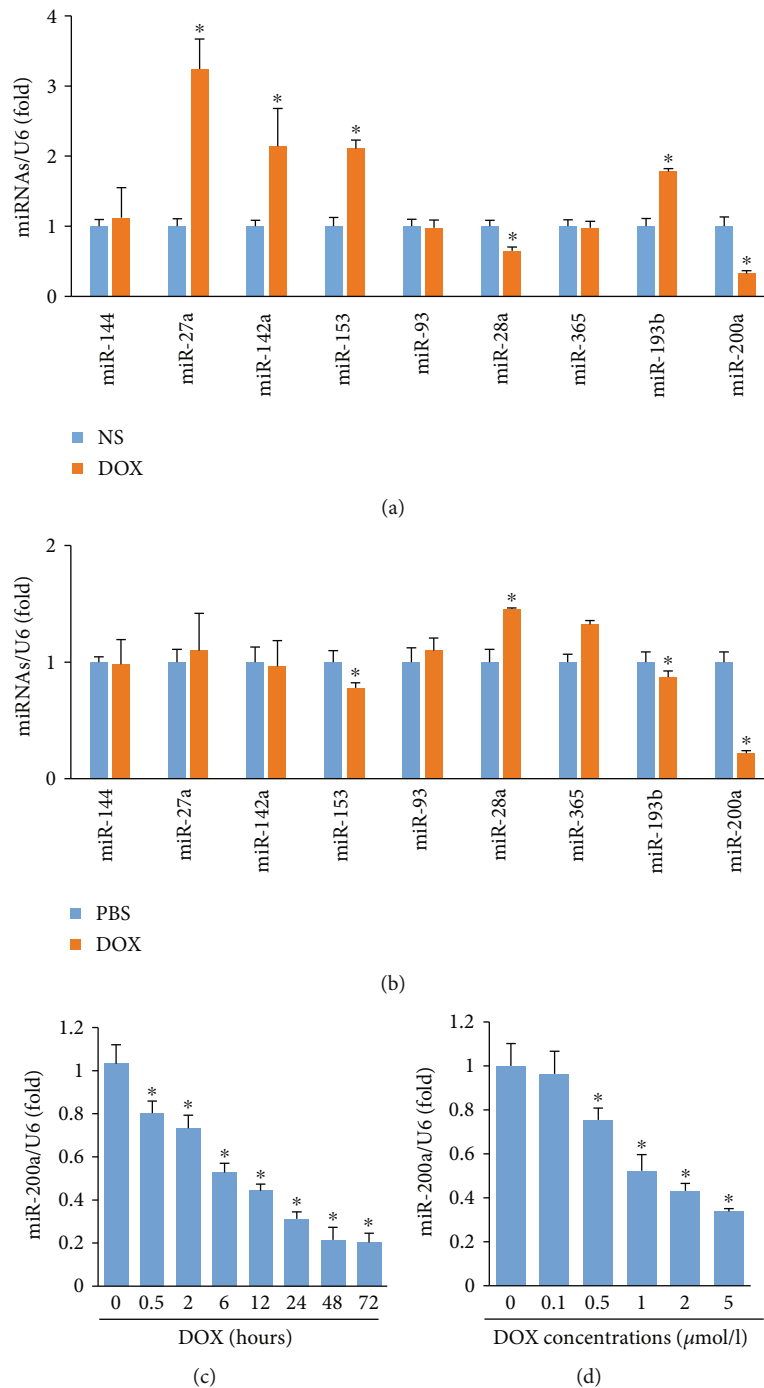


FIGURE 1: miR-200a was decreased in DOX-induced cardiac injury: (a) the levels of miRNAs in the hearts ($n = 6$); (b) the levels of miRNAs in the H9c2 cells ($n = 6$); (c, d) the levels of miR-200a in the H9c2 cells ($n = 6$). * $P < 0.05$ compared with the group with saline or PBS.

edge system (IonOptix, Milton, MA) was used to detect mechanical properties according to a previous study [22]. Cell shortening and relengthening, as reflected by peak shortening (PS) and maximal velocities of shortening/relengthening ($\pm dL/dt$), were assessed.

2.6. Glutathione, Malondialdehyde, and 4-Hydroxynonenal Detection. The fresh heart tissues were homogenized in ice-cold sodium phosphate buffer, and the supernatant fraction was collected for the detection of the levels of

glutathione (GSH) and oxidized GSH (GSSG), malondialdehyde (MDA), and 4-hydroxynonenal (4-HNE). The kit for MDA detection was obtained from Nanjing Jiancheng Bioengineering Institute (Nanjing, China). A 4-HNE assay kit was provided by Abcam. The quantitative measurement of MDA and 4-HNE in heart homogenate was performed according to the manufacturer's instructions. GSH and GSSG were determined by a GSH and GSSG assay kit from Beyotime Biotechnology (Beijing, China) using the 2-vinyl pyridine spectrophotometric method.

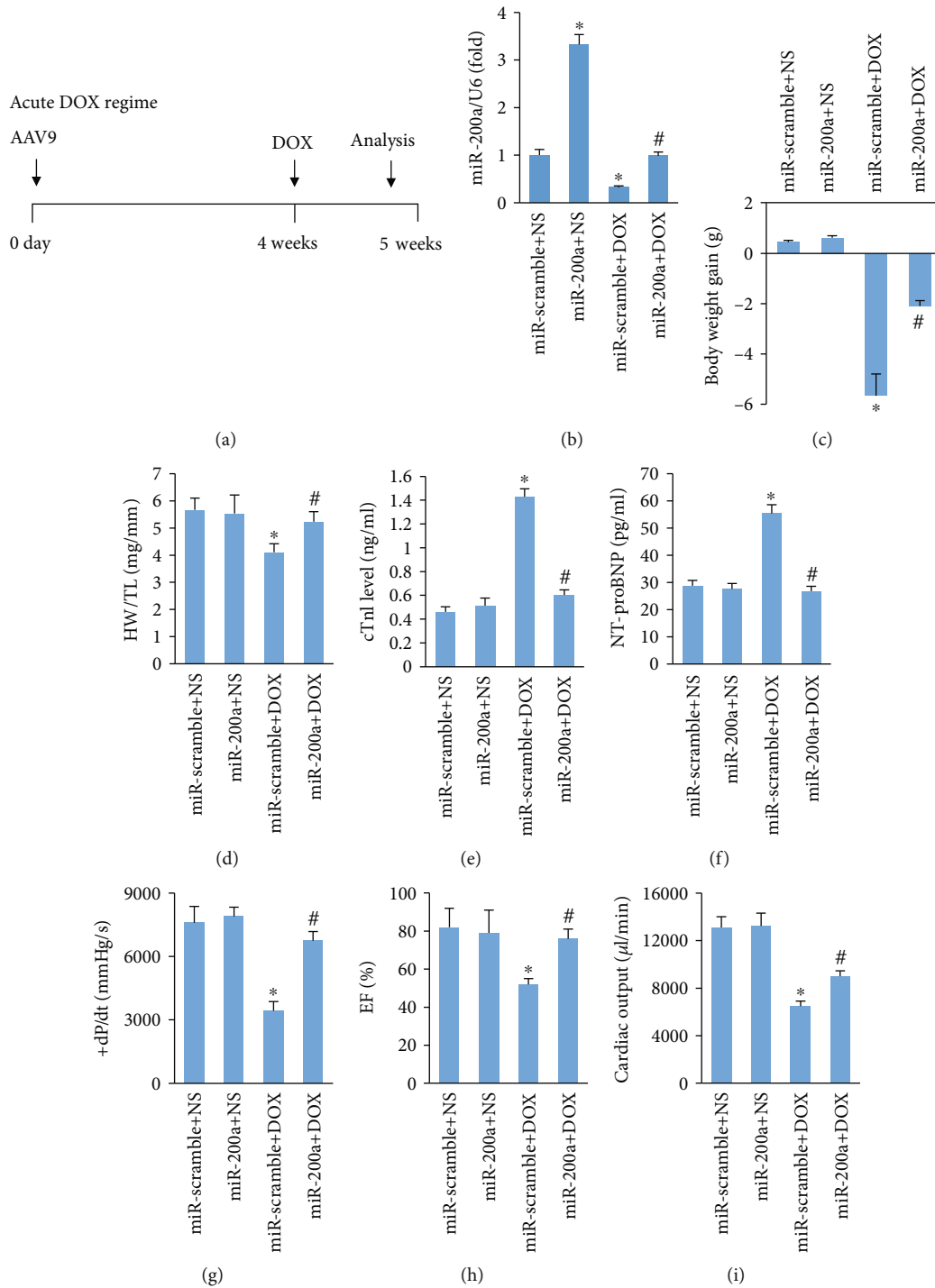


FIGURE 2: miR-200a overexpression improved cardiac function in mice: (a) schedule of the acute DOX regime experiment; (b) the levels of miR-200a in the hearts ($n = 6$); (c) the alteration in body weight ($n = 12$); (d) alterations in the ratio of heart weight to tibial length ($n = 12$); (e, f) the level of cTnl and NT-proBNP ($n = 6$), (g, h) the alteration in +dP/dt and EF in mice ($n = 10$); (i) cardiac output in the mice ($n = 10$). * $P < 0.05$ compared with the group with saline. # $P < 0.05$ compared with mice after DOX injection.

2.7. Measurement of Cardiac Injury Markers. To detect plasma cardiac troponin I (cTnl) and the N-terminal probrain natriuretic peptide (NT-proBNP) levels, blood samples were collected from mice at 3 days after DOX injection. The NT-proBNP detection kit was provided by MyBioSource (CA, USA). The cTnl assay kit was obtained

from Life Diagnostics, Inc. (West Chester, PA). NT-proBNP and cTnl were detected to reflect the acute cardiac injury according to standard procedures.

2.8. TUNEL Staining. Detection of apoptosis in the hearts was performed by a terminal deoxynucleotidyl transferase-

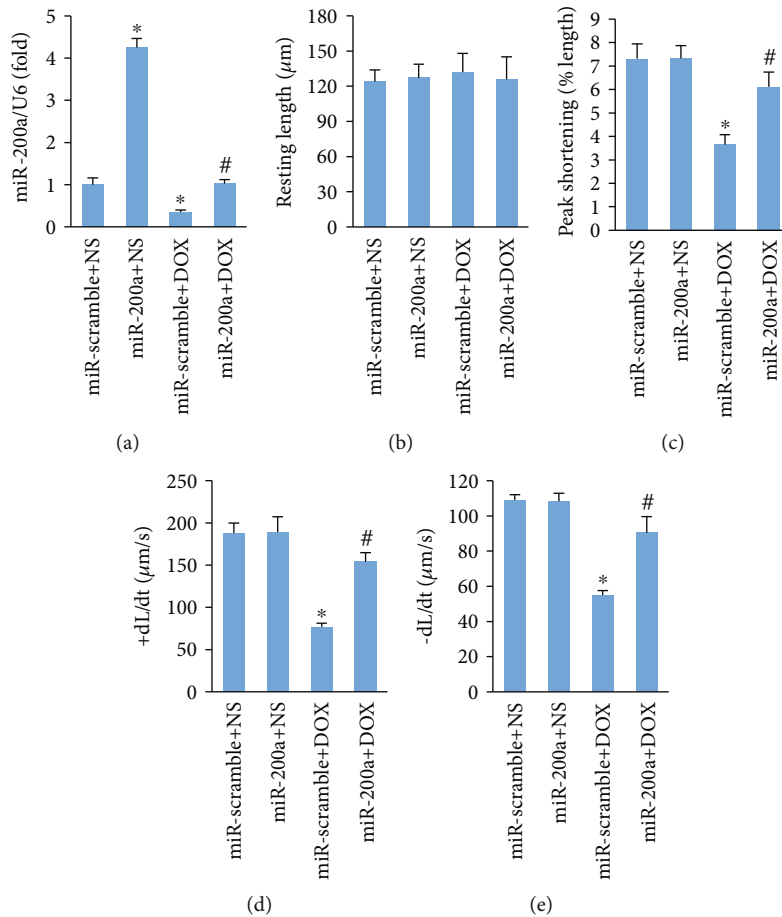


FIGURE 3: miR-200a improved adult cardiomyocyte contractile properties: (a) the levels of miR-200a; (b) resting cell length; (c) peak shortening; (d, e) maximal velocity of shortening (+dL/dt) and maximal velocity of relengthening (-dL/dt). * $P < 0.05$ compared with the group with saline. # $P < 0.05$ compared with mice after DOX injection. $n = 50$ cells from 4 mice per group.

mediated nick-end labelling (TUNEL) assay according to the instruction provided with the kit (Roche Diagnostics, Indianapolis). The nucleus was labelled with DAPI.

2.9. Cell Culture. H9c2 cells were cultured in DMEM (high glucose, Gibco) supplemented with 10% fetal bovine serum (FBS) and 1% penicillin and streptomycin. The H9c2 cells were pretreated with micrON miR-200a (50 nmol/l, Ribobio Technology) or micrON mimic negative control for 48 hours and then incubated with DOX at 5 $\mu\text{g}/\text{ml}$ or the same volume of PBS for 24 h. At the endpoint of experiments, cells were harvested for further detection.

The commercial rat Nrf2 siRNA and control siRNA were purchased from Santa Cruz Biotechnology (Santa Cruz, CA, USA). We used three siRNAs to deplete Nrf2 expression. The one that resulted in the most significant downregulation of endogenous Nrf2 expression as confirmed by PCR and western was used for further experiments. The H9c2 cells were seeded on 6-well plates at 1×10^5 cells/well for 48 hours. After 60-70% confluence, the cells were transfected with control siRNA or siNrf2 (100 pmol/l) using Lipofectamine 2000 (Invitrogen Corp.). Cells were harvested after 48-hour transfection for further experiments.

2.10. DCF-DA Staining. Dihydrodichlorofluorescein diacetate (DCF-DA) staining was applied to measure the generation of ROS. H9c2 cells were reacted with DCF-DA (10 $\mu\text{mol}/\text{l}$) for 30 min at 37°C in the dark. After washing 5 times with PBS, the cells were observed using a confocal microscope.

2.11. Statistical Analysis. Data were presented as means \pm standard deviation. We used the unpaired t -test to compare significance between two groups. One-way ANOVA followed by the Tukey post hoc test was used to compare the difference between more than two groups. P values < 0.05 were considered to be statistically significant.

3. Result

3.1. miR-200a Was Decreased in Hearts of DOX-Treated Mice. We first determined miRNAs that target Nrf2 in the mice with DOX injection. All the miRNAs that were reported to regulate the level of Nrf2 were detected [23], including miR-144, miR-27a, miR-142a, miR-153, miR-93, miR-28a, miR-365, miR-193b, and miR-200a. miR-27a, miR-142a, miR-153, and miR-193b expressions increased, while miR-28a and miR-200a expressions decreased in the hearts after DOX treatment (Figure 1(a)). Next, H9c2 cells were treated

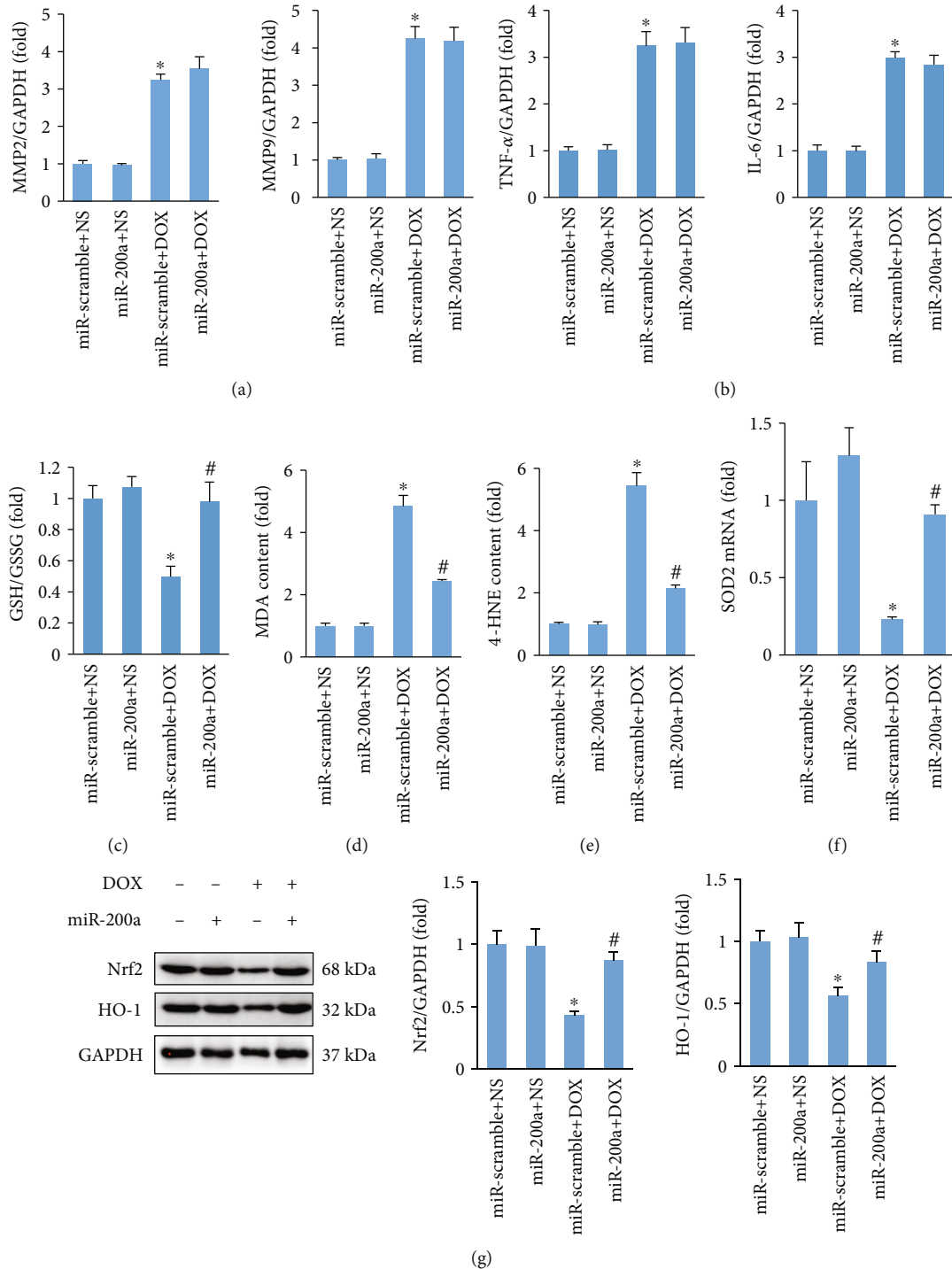


FIGURE 4: miR-200a reduced oxidative stress in DOX-treated mice: (a) the level of MMP2 and MMP9 in the hearts ($n = 6$); (b) the level of TNF- α and IL-6 in the hearts ($n = 6$); (c, d) the levels of GSH and cardiac MDA in the hearts ($n = 6$); (e) the level of 4-HNE in the hearts ($n = 6$); (f) the level of SOD2 mRNA in the hearts ($n = 6$); (g) protein expression of Nrf2 and HO-1 ($n = 6$). * $P < 0.05$ compared with the group with saline. # $P < 0.05$ compared with mice after DOX injection.

with DOX, and miRNAs that regulate the level of Nrf2 were also detected. miR-28a and miR-365 expressions increased, while miR-153 and miR-200a expressions decreased in the DOX-treated H9c2 cells (Figure 1(b)). Therefore, we concluded that miR-200a may be involved in DOX-induced car-

diac injury. Further study revealed that miR-200a was significantly decreased in a time-dependent manner and dose-dependent manner (Figures 1(c) and 1(d)). These data suggested that miR-200a might play a key role in the DOX-induced cardiotoxicity.

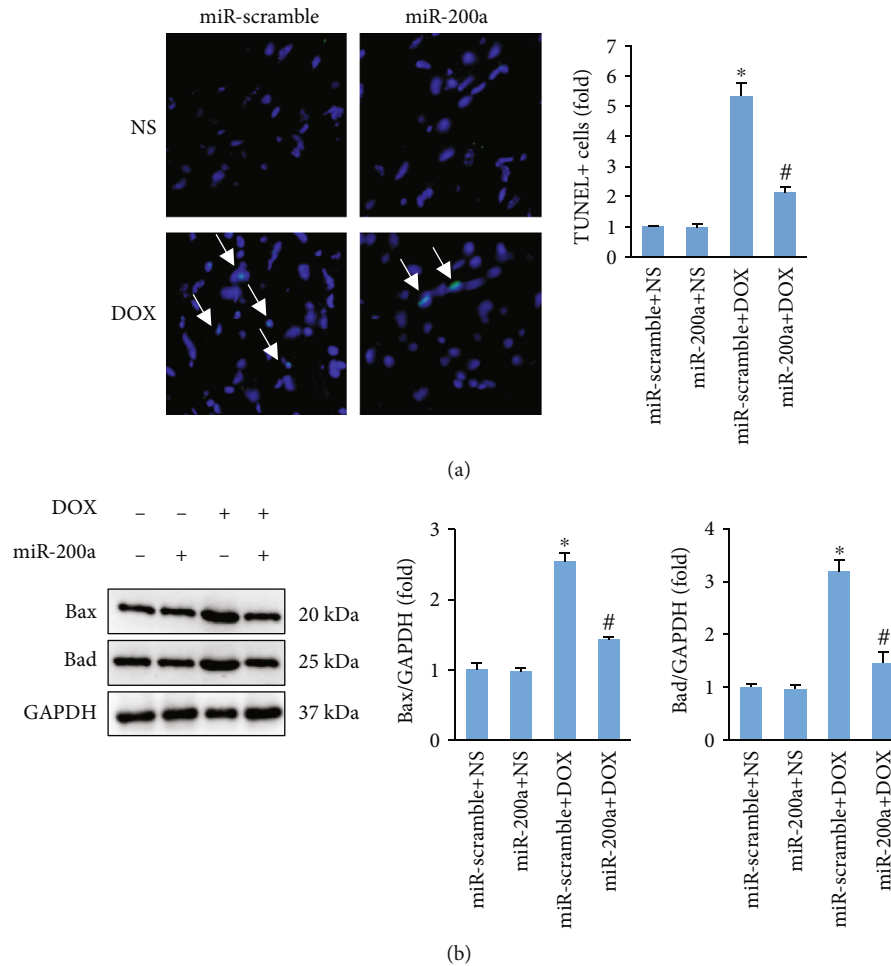


FIGURE 5: miR-200a suppressed cardiac apoptosis in DOX-treated mice. (a) TUNEL staining ($n = 6$). (b) Western analysis indicated the expression of Bax and Bad in the hearts ($n = 6$). * $P < 0.05$ compared with the group with saline. # $P < 0.05$ compared with mice after DOX injection.

3.2. miR-200a Overexpression Protected against DOX-Induced Acute Cardiac Injury. We first established an acute model of DOX-induced cardiotoxicity. In this experiment, mice were first infected with AAV9-miR-200a or AAV9-miR-scramble for 4 weeks and were subjected to DOX or saline (Figure 2(a)). Reduced miR-200a expression in the hearts of DOX-treated mice was almost restored to the normal level (Figure 2(b)). The animals were then followed up for five days before sacrifice. miR-200a overexpression blunted the decrease of body weight in DOX-treated mice (Figure 2(c)). The ratio of heart weight to tibial length was significantly decreased in DOX-treated mice, and this pathological alteration was blocked (Figure 2(d)). A single injection of DOX (15 mg/kg) induced the elevation of cTnI and NT-proBNP level, which was prevented by miR-200a overexpression (Figures 2(e) and 2(f)). Administration of DOX caused worsening of left ventricle systolic function, as reflected by maximum first derivative of ventricular pressure with respect to time (+dP/dt), ejection fraction (EF), and cardiac output, but mice with miR-200a overexpression preserved +dP/dt, EF, and cardiac output compared with mice with miR-scramble after DOX treatment (Figures 2(g)–2(i)).

3.3. miR-200a Overexpression Reduced Adult Cardiomyocyte Contractile Dysfunction after DOX Treatment. Subsequently, we determined the effect of miR-200a overexpression on contractile function of single adult cardiomyocyte which was isolated from mice with acute DOX injection. As expected, reduced miR-200a expression in the adult cardiomyocytes isolated from DOX-treated mice was restored to the normal level (Figure 3(a)). miR-200a has no significant effect on resting cell length between four groups (Figure 3(b)). Adult cardiomyocytes in the mice with DOX treatment showed a reduced peak shortening and maximal velocity of shortening/relengthening (\pm dL/dt). After miR-200a overexpression, these pathological alterations were largely blocked (Figures 3(c)–3(e)).

3.4. miR-200a Overexpression Attenuated DOX-Induced Oxidative Stress in Mice. Matrix metalloproteinase (MMP) activation is a key event in DOX-induced acute cardiotoxicity [24]. Therefore, we first detected the alteration in the mRNA level of MMP2 and MMP9 and found that miR-200a did not prevent the elevation of MMP2 and MMP9 expressions in DOX-treated mice (Figure 4(a)). Next, we detected the levels of inflammatory factors in DOX-treated hearts and found

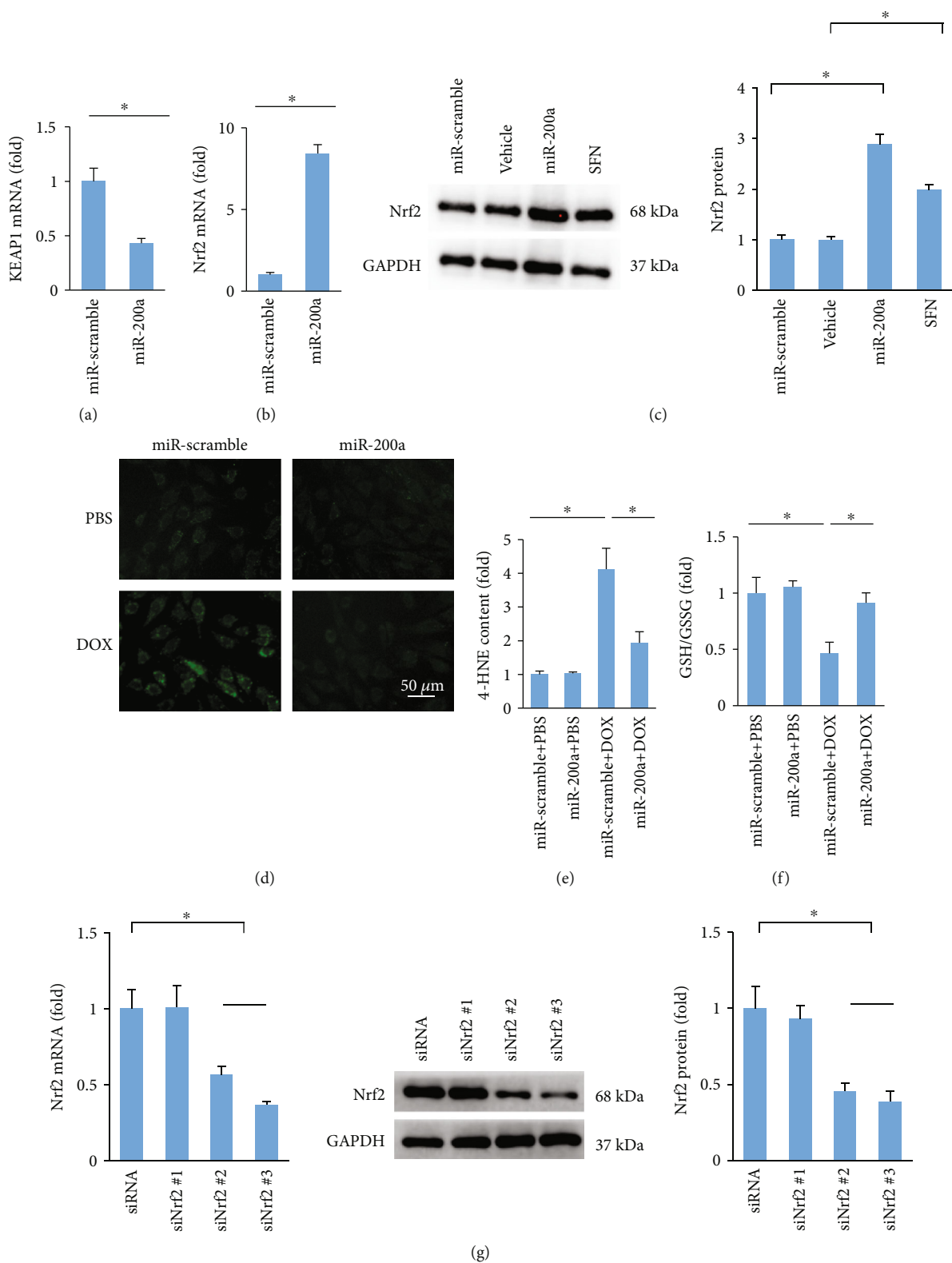


FIGURE 6: Continued.

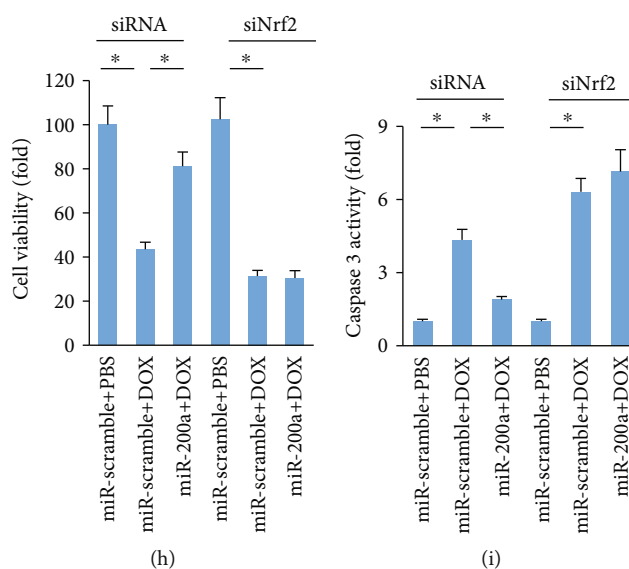


FIGURE 6: miR-200a provided cardioprotection via activating the Nrf2 signaling pathway: (a, b) the level of Keap1 and Nrf2 in the H9c2 cells ($n = 6$); (c) the protein expression of Nrf2 ($n = 6$); (d) DCF-DA staining; (e, f) the levels of 4-HNE and GSH in the cells ($n = 6$); (g) the level of Nrf2 in the cells ($n = 6$); (h) cell viability ($n = 6$); (i) caspase 3 activity ($n = 6$). * $P < 0.05$.

that there was no difference in the levels of inflammatory factors between miR-scramble+DOX and miR-200a+DOX groups (Figure 4(b)). Acute DOX injection decreased the ratio of GSH and GSSG, and this downregulation was blocked by miR-200a (Figure 4(c)). Acute DOX injection induced abnormal accumulation of 4-HNE and MDA, and these accumulations of 4-HNE and MDA were inhibited by miR-200a overexpression (Figures 4(d) and 4(e)). Further detection found that miR-200a restored the mRNA of SOD2 in DOX-treated mice (Figure 4(f)). Western blot analysis demonstrated that Nrf2 and its downstream target were markedly decreased in the DOX-treated group, and miR-200a almost restored Nrf2 and HO-1 protein expression to the normal levels (Figure 4(g)).

3.5. miR-200a Inhibited DOX-Induced Myocardial Apoptosis in Mice with Acute DOX Injection. Expectedly, the number of TUNEL-positive cells was markedly increased in heart sections of mice with acute DOX compared to that in mice with saline only (Figure 5(a)). Interestingly, DOX-induced TUNEL-positive cells were attenuated by miR-200a (Figure 5(a)). Subsequent detection of Bax and Bad expressions in the hearts revealed that miR-200a attenuated the levels of Bax and Bad in mice (Figure 5(b)).

3.6. Nrf2 Deficiency Antagonized the Protective Effects against DOX-Related Injury in H9c2 Cells. It has been reported that Keap1 interacted with Nrf2 and retained Nrf2 in the cytoplasm [8]. miR-200a destabilized Keap1 and resulted in a reduction in Keap1 protein level [16]. Thus, we measured Keap1 mRNA levels and found that Keap1 mRNA level was significantly decreased in miR-200a-infected cells (Figure 6(a)). Further analysis showed that miR-200a caused an increase in Nrf2 mRNA expression (Figure 6(b)). Consistent with this finding, we found that miR-200a overexpression also significantly increased Nrf2 protein expression (Figure 6(c)). We also confirmed that

sulforaphane, a well-studied natural product, could increase Nrf2 protein expression (Figure 6(c)). Next, we compared the generation of ROS, as labelled by DCF-DA in DOX- and DOX+miR-200a-treated H9c2 cells. The data in our study showed that miR-200a could significantly block DOX-induced formation of ROS in H9c2 cells (Figure 6(d)). The increased 4-HNE content in cells with DOX treatment was also inhibited after miR-200a administration (Figure 6(e)). miR-200a also restored GSH/GSSG to the normal level in DOX-treated cells (Figure 6(f)). Next, we verified the hypothesis that the protection provided by miR-200a was mediated by Nrf2. We used three siRNAs to deplete Nrf2 expression. The one (siNrf2 #3) that resulted in the most significant downregulation of endogenous Nrf2 expression as confirmed by PCR and western was used for further experiments (Figure 6(g)). We found that miR-200a significantly improved cell viability and decreased caspase 3 activity in DOX-treated cells, and these protections were completely blocked after Nrf2 deficiency (Figure 6(h) and 6(i)).

3.7. The Protective Effects of miR-200a against DOX-Induced Acute Cardiotoxicity Were Reversed by the Deficiency of Nrf2 in Mice. To determine whether miR-200a exerted its protection via activation of Nrf2 in mice, we used three shRNAs to deplete Nrf2 expression in the hearts. The one (shNrf2 #3) that resulted in the most significant downregulation of endogenous Nrf2 expression as confirmed by PCR and western was intramyocardially injected (Figures 7(a) and 7(b)). One week after adenoviral injection, these mice were subjected to DOX injection to mimic acute DOX exposure. As indicated in our study, miR-200a lost its protection in cardiac injury, as reflected by EF, NT-proBNP, MDA content, and caspase 3 activity, in mice (Figures 7(c)–7(f)).

3.8. miR-200a Also Provided Cardiac Benefit in a Chronic Model of DOX-Induced Cardiotoxicity. To mimic chronic

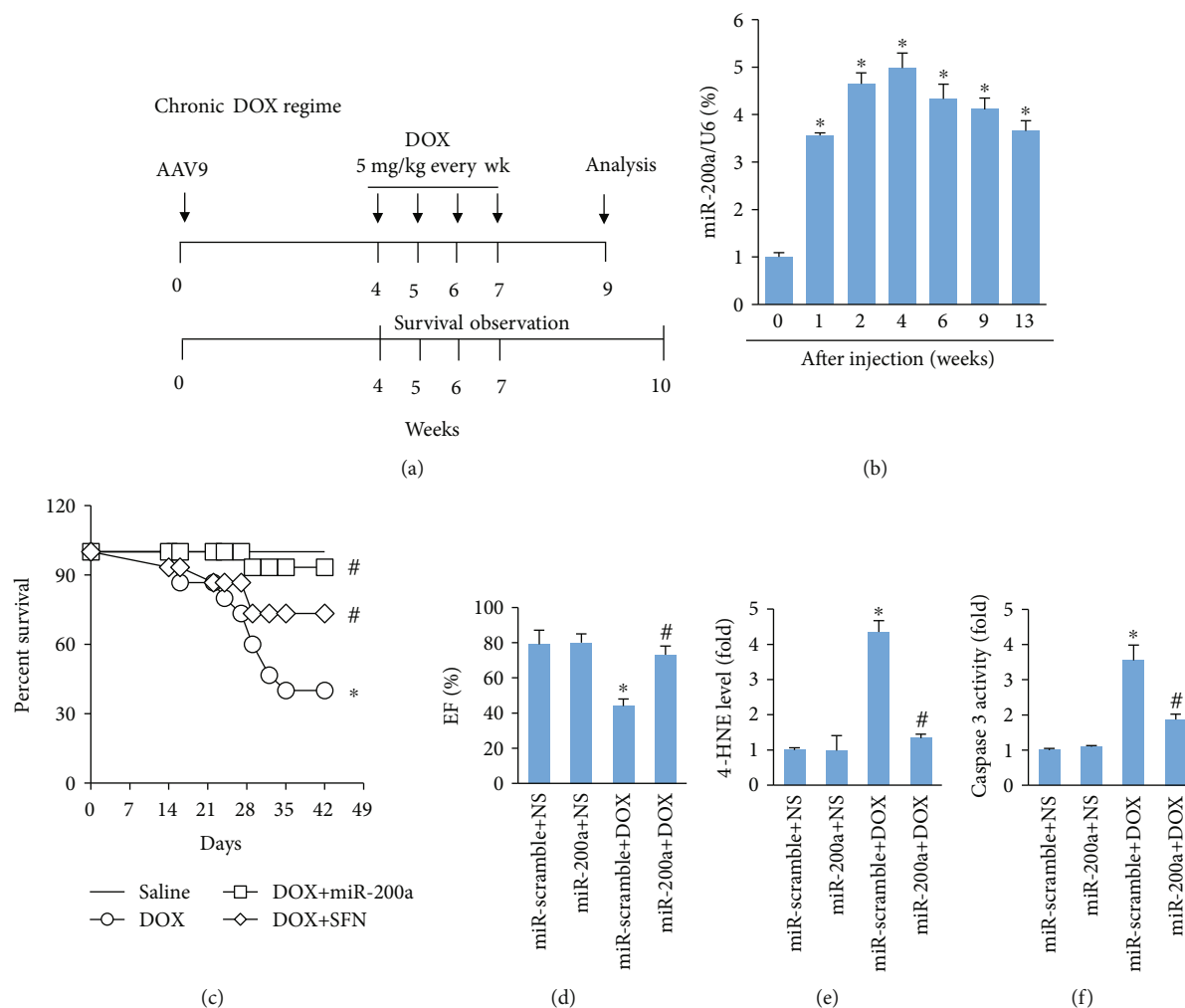


FIGURE 8: miR-200a protected the hearts from DOX-induced chronic cardiotoxicity: (a) schedule of the acute DOX regime experiment; (b) the level of miR-200a in the hearts ($n = 6$); (c) survival rate in the groups ($n = 15$); (d) EF in the four groups ($n = 10$); (e) the level of 4-HNE in the hearts ($n = 6$); (f) caspase 3 activity ($n = 6$). * $P < 0.05$ compared with the group with saline. # $P < 0.05$ compared with mice after DOX injection.

200a also protected the hearts from DOX-induced chronic damage. These findings positively suggest that miR-200a overexpression strategies may be helpful for promoting cardiomyocyte survival in DOX-treated mice.

Recently, accumulating evidence supported the notion that miR-200a was closely involved in cardiovascular diseases [13, 23]. Yang et al. reported that miR-200a-5p promoted cardiomyocyte hypertrophy via inhibiting the expression of stress-related selenoproteins to alter glucose transport [26]. miR-200a-5p was identified to be upregulated under Se-deficient stimulation, and miR-200a-5p deficiency attenuated myocardial necroptosis induced by Se deficiency [15]. Inconsistent with the study, we found that miR-200a could provide protection against DOX-induced cardiac injury, as reflected by the body weight gain and the levels of NT-proBNP and cTnI. miR-200a supplementation also improved cardiac function in mice. We postulate that subtle differences in the animal strain and disease model might lead to discordant observations.

MMP2 and MMP9 mRNAs were significantly increased in the ventricles of mice at 2 days after DOX treatment [24].

Consistent with this finding, we also confirmed that MMP2 and MMP9 were increased in the mouse hearts after treatment with DOX. However, there was no difference between DOX+miR-scramble and DOX+miR-200a groups in the mRNA levels of MMP2 and MMP9, implying that miR-200a exerting its function was not mediated by the alteration in MMP content. Inflammation also played a key role in the pathogenesis of DOX-related cardiac injury [27]; therefore, we detected alteration in the mRNA levels of inflammatory factors. The data in our study suggested that miR-200a cannot affect the cardiac inflammation in the DOX-treated mice.

It has been reported that scavenging ROS protects against DOX-induced cardiac apoptosis [28]. Cardiac-specific overexpression of metallothionein protected against DOX-related cardiac dysfunction [29]. Here, we found that 4-HNE and MDA productions were enhanced in the DOX heart and were reduced by miR-200a overexpression. In addition, we have also found that miR-200a preserved the reduced GSH level induced by DOX but also elevated to a level comparable to that of normal control mice. Further detection found that miR-200a also largely attenuated

DOX-induced cell apoptosis in hearts and in H9c2 cells. As expected, we found that miR-200a could activate Nrf2 and miR-200a lost its protection against oxidative stress and cell viability after Nrf2 deficiency, suggesting that the protection of miR-200a was dependent on the activation of Nrf2.

Several natural products have been evaluated for their ability to attenuate DOX-induced cardiotoxicity but with little success [30, 31]. Low bioavailability and low scavenging efficacy toward oxidants were the main reasons [32]. In our study, we compare the ability of sulforaphane and miR-200a to activate Nrf2 in vitro and in vivo and found that the two both largely activate Nrf2. Moreover, miR-200a had a better effect on the survival rate in chronic cardiotoxicity. In addition, several lines of evidence demonstrated that miR-200a was a tumor suppressor [33, 34], suggesting that miR-200a treatment might not compromise the oncological efficacy of DOX.

In conclusion, our results suggest that miR-200a protects DOX-induced acute toxicity by activating Nrf2 to attenuate oxidative stress and apoptotic cell death, prevents DOX-induced cardiomyopathy, and ameliorates cardiac dysfunction. The present findings suggest that miR-200a supplementation may represent a new cardioprotective strategy against DOX-induced cardiotoxicity.

Data Availability

The data that support the findings of this study are available from the corresponding author upon reasonable request.

Conflicts of Interest

The authors declare that they have no conflicts of interest.

Authors' Contributions

Xiaoping Hu and Huagang Liu are joint first authors.

Acknowledgments

This work was supported by grants from the National Natural Science Foundation of China (No. 80700289).

References

- [1] Y. Octavia, C. G. Tocchetti, K. L. Gabrielson, S. Janssens, H. J. Crijns, and A. L. Moens, "Doxorubicin-induced cardiomyopathy: from molecular mechanisms to therapeutic strategies," *Journal of Molecular and Cellular Cardiology*, vol. 52, no. 6, pp. 1213–1225, 2012.
- [2] T. Eschenhagen, T. Force, M. S. Ewer et al., "Cardiovascular side effects of cancer therapies: a position statement from the Heart Failure Association of the European Society of Cardiology," *European Journal of Heart Failure*, vol. 13, no. 1, pp. 1–10, 2011.
- [3] A. Ghigo, M. Li, and E. Hirsch, "New signal transduction paradigms in anthracycline-induced cardiotoxicity," *Biochimica et Biophysica Acta*, vol. 1863, no. 7, pp. 1916–1925, 2016.
- [4] A. V. Maksimenko and A. V. Vavaev, "Antioxidant enzymes as potential targets in cardioprotection and treatment of cardiovascular diseases. Enzyme antioxidants: the next stage of pharmacological counterwork to the oxidative stress," *Heart International*, vol. 7, no. 1, p. hi.2012.e3, 2012.
- [5] L. Chaiswing, M. P. Cole, D. K. St Clair, W. Ittarat, L. I. Szweda, and T. D. Oberley, "Oxidative damage precedes nitrate damage in Adriamycin-induced cardiac mitochondrial injury," *Toxicologic Pathology*, vol. 32, no. 5, pp. 536–547, 2004.
- [6] T. Simunek, M. Sterba, O. Popelova, M. Adamcova, R. Hrdina, and V. Gersl, "Anthracycline-induced cardiotoxicity: overview of studies examining the roles of oxidative stress and free cellular iron," *Pharmacological Reports*, vol. 61, no. 1, pp. 154–171, 2009.
- [7] S. Zhou, W. Sun, Z. Zhang, and Y. Zheng, "The role of Nrf2-mediated pathway in cardiac remodeling and heart failure," *Oxidative Medicine and Cellular Longevity*, vol. 2014, 16 pages, 2014.
- [8] D. D. Zhang, "Mechanistic studies of the Nrf2-Keap1 signaling pathway," *Drug Metabolism Reviews*, vol. 38, no. 4, pp. 769–789, 2008.
- [9] J. W. Kaspar, S. K. Niture, and A. K. Jaiswal, "Nrf2:Keap1 signaling in oxidative stress," *Free Radical Biology & Medicine*, vol. 47, no. 9, pp. 1304–1309, 2009.
- [10] P. Singh, R. Sharma, K. McElhanon et al., "Sulforaphane protects the heart from doxorubicin-induced toxicity," *Free Radical Biology & Medicine*, vol. 86, pp. 90–101, 2015.
- [11] M. Murri and H. el Azzouzi, "MicroRNAs as regulators of mitochondrial dysfunction and obesity," *American Journal of Physiology. Heart and Circulatory Physiology*, vol. 315, no. 2, pp. H291–H302, 2018.
- [12] S. Greco, G. Zaccagnini, C. Voellenkle, and F. Martelli, "MicroRNAs in ischaemic cardiovascular diseases," *European Heart Journal Supplements: Journal of the European Society of Cardiology*, vol. 18, suppl E, pp. E31–E36, 2016.
- [13] G. Eades, Y. Yao, M. Yang, Y. Zhang, S. Chumsri, and Q. Zhou, "miR-200a regulates SIRT1 expression and epithelial to mesenchymal transition (EMT)-like transformation in mammary epithelial cells," *The Journal of Biological Chemistry*, vol. 286, no. 29, pp. 25992–26002, 2011.
- [14] H. Jordan, "The uses of health cures. Goals of health resort therapy," *Fortschritte der Medizin*, vol. 106, no. 22, pp. 457–459, 1988.
- [15] T. Yang, C. Cao, J. Yang et al., "miR-200a-5p regulates myocardial necroptosis induced by Se deficiency via targeting RNF11," *Redox Biology*, vol. 15, pp. 159–169, 2018.
- [16] H. Wu, L. Kong, Y. Tan et al., "C66 ameliorates diabetic nephropathy in mice by both upregulating NRF2 function via increase in miR-200a and inhibiting miR-21," *Diabetologia*, vol. 59, no. 7, pp. 1558–1568, 2016.
- [17] L. Benard, J. G. Oh, M. Cacheux et al., "Cardiac Stim1 silencing impairs adaptive hypertrophy and promotes heart failure through inactivation of mTORC2/Akt signaling," *Circulation*, vol. 133, no. 15, pp. 1458–1471, 2016, discussion 1471.
- [18] R. Hullin, M. Metrich, A. Sarre et al., "Diverging effects of enalapril or eplerenone in primary prevention against doxorubicin-induced cardiotoxicity," *Cardiovascular Research*, vol. 114, no. 2, pp. 272–281, 2018.
- [19] Z. G. Ma, Y. P. Yuan, S. C. Xu et al., "CTRP3 attenuates cardiac dysfunction, inflammation, oxidative stress and cell death in diabetic cardiomyopathy in rats," *Diabetologia*, vol. 60, no. 6, pp. 1126–1137, 2017.

- [20] Z. G. Ma, J. Dai, Y. P. Yuan et al., "T-bet deficiency attenuates cardiac remodelling in rats," *Basic Research in Cardiology*, vol. 113, no. 3, 2018.
- [21] Z. G. Ma, Y. P. Yuan, X. Zhang et al., "C1q-tumour necrosis factor-related protein-3 exacerbates cardiac hypertrophy in mice," *Cardiovascular Research*, vol. 115, no. 6, pp. 1067–1077, 2019.
- [22] T. A. Doser, S. Turdi, D. P. Thomas, P. N. Epstein, S. Y. Li, and J. Ren, "Transgenic overexpression of aldehyde dehydrogenase-2 rescues chronic alcohol intake-induced myocardial hypertrophy and contractile dysfunction," *Circulation*, vol. 119, no. 14, pp. 1941–1949, 2009.
- [23] Y. Liu, L. N. Li, S. Guo et al., "Melatonin improves cardiac function in a mouse model of heart failure with preserved ejection fraction," *Redox Biology*, vol. 18, pp. 211–221, 2018.
- [24] K. Kizaki, R. Ito, M. Okada et al., "Enhanced gene expression of myocardial matrix metalloproteinases 2 and 9 after acute treatment with doxorubicin in mice," *Pharmacological Research*, vol. 53, no. 4, pp. 341–346, 2006.
- [25] J. Herrmann, A. Lerman, N. P. Sandhu, H. R. Villarraga, S. L. Mulvagh, and M. Kohli, "Evaluation and management of patients with heart disease and cancer: cardio-oncology," *Mayo Clinic Proceedings*, vol. 89, no. 9, pp. 1287–1306, 2014.
- [26] T. Yang, T. Liu, C. Cao, and S. Xu, "miR-200a-5p augments cardiomyocyte hypertrophy induced by glucose metabolism disorder via the regulation of selenoproteins," *Journal of Cellular Physiology*, vol. 234, no. 4, pp. 4095–4103, 2019.
- [27] Y. P. Yuan, Z. G. Ma, X. Zhang et al., "CTRP3 protected against doxorubicin-induced cardiac dysfunction, inflammation and cell death via activation of Sirt1," *Journal of Molecular and Cellular Cardiology*, vol. 114, pp. 38–47, 2018.
- [28] S. Kotamraju, E. A. Konorev, J. Joseph, and B. Kalyanaraman, "Doxorubicin-induced apoptosis in endothelial cells and cardiomyocytes is ameliorated by nitron spin traps and ebselen. Role of reactive oxygen and nitrogen species," *Journal of Biological Chemistry*, vol. 275, no. 43, pp. 33585–33592, 2000.
- [29] Y. J. Kang, Y. Chen, A. Yu, M. Voss-McCowan, and P. N. Epstein, "Overexpression of metallothionein in the heart of transgenic mice suppresses doxorubicin cardiotoxicity," *The Journal of Clinical Investigation*, vol. 100, no. 6, pp. 1501–1506, 1997.
- [30] L. Xi, S. G. Zhu, A. Das et al., "Dietary inorganic nitrate alleviates doxorubicin cardiotoxicity: mechanisms and implications," *Nitric Oxide*, vol. 26, no. 4, pp. 274–284, 2012.
- [31] G. C. Pereira, A. M. Silva, C. V. Diogo, F. S. Carvalho, P. Monteiro, and P. J. Oliveira, "Drug-induced Cardiac Mitochondrial Toxicity and Protection: From Doxorubicin to Carvedilol," *Current Pharmaceutical Design*, vol. 17, no. 20, pp. 2113–2129, 2011.
- [32] H. J. Forman, K. J. A. Davies, and F. Ursini, "How do nutritional antioxidants really work: nucleophilic tone and para-hormesis versus free radical scavenging in vivo," *Free Radical Biology & Medicine*, vol. 66, pp. 24–35, 2014.
- [33] C. Liu, W. Hu, L. L. Li et al., "Roles of miR-200 family members in lung cancer: more than tumor suppressors," *Future Oncology*, vol. 14, no. 27, pp. 2875–2886, 2018.
- [34] X. Chen, K. Liu, P. Yang et al., "microRNA-200a functions as a tumor suppressor by targeting FOXA1 in glioma," *Experimental and Therapeutic Medicine*, vol. 17, pp. 221–229, 2018.

Research Article

Sitagliptin-Dependent Differences in the Intensity of Oxidative Stress in Rat Livers Subjected to Ischemia and Reperfusion

Małgorzata Trocha,¹ Małgorzata Krzystek-Korpacka ,² Anna Merwid-Ląd,¹ Beata Nowak,¹ Małgorzata Pieśniewska,¹ Piotr Dziegiel,^{3,4} Agnieszka Gomułkiewicz,³ Przemysław Kowalski,⁵ Dorota Diakowska ,⁶ Adam Szeląg,¹ and Tomasz Sozański ¹

¹Department of Pharmacology, Wrocław Medical University, Jana Mikulicza-Radeckiego 2, 50-345 Wrocław, Poland

²Department of Medical Biochemistry, Wrocław Medical University, Chałubińskiego 10, 50-368 Wrocław, Poland

³Department of Human Morphology and Embryology, Division of Histology and Embryology, Wrocław Medical University, Chałubińskiego 6a, 50-368 Wrocław, Poland

⁴Department of Physiotherapy, University School of Physical Education, I.J. Paderewskiego 35, 51-612 Wrocław, Poland

⁵Department of Pathomorphology and Oncological Cytology, Wrocław Medical University, Borowska 213, 50-556 Wrocław, Poland

⁶Division of Nervous System Diseases, Department of Clinical Nursing, Faculty of Health Sciences of Wrocław Medical University, K. Bartla 5, 51-618 Wrocław, Poland

Correspondence should be addressed to Tomasz Sozański; tsoz@wp.pl

Received 30 March 2019; Revised 22 July 2019; Accepted 21 September 2019; Published 31 October 2019

Guest Editor: Aneta Radziwon-Balicka

Copyright © 2019 Małgorzata Trocha et al. This is an open access article distributed under the Creative Commons Attribution License, which permits unrestricted use, distribution, and reproduction in any medium, provided the original work is properly cited.

Purpose. Ischemia/reperfusion (IR) is the main cause of liver damage after transplantation. We evaluated the effect of sitagliptin (STG) on oxidative stress parameters in the rat liver under IR. **Methods.** Rats were treated with STG (5 mg/kg) (S and SIR) or saline solution (C and CIR). Livers from CIR and SIR were subjected to ischemia (60 min) and reperfusion (24 h). During reperfusion, aminotransferases (ALT and AST) were determined in blood samples. Thiobarbituric acid reactive substances (TBARS), superoxide dismutase (SOD), catalase (CAT), paraoxonase-1 (PON1), glutathione peroxidase (GPx), and the mRNA expression of SOD1 were determined in liver homogenates after reperfusion. Different regions of livers were also histologically evaluated. **Results.** The PON1 activity was higher, and the TBARS level was lower in SIR than in CIR. There was an inverse relationship between TBARS and PON1 levels in the whole cohort. The GPx activity was lower in ischemic than in nonischemic groups regardless of the STG treatment. In SIR, the SOD1 activity was higher compared to that in CIR. In S, the expression of SOD1 mRNA was the highest of all examined groups and positively correlated with the SOD1 activity in the whole animal cohort. During IR aminotransferases, the activity in the drug-treated group was lower in all examined points of time. In drug-treated groups, the percentage of steatosis was higher than that in nontreated groups regardless of IR. **Conclusions.** The protective effect of STG on the rat liver, especially its antioxidant properties, was revealed under IR conditions.

1. Introduction

Ischemia/reperfusion (IR) is the main cause of liver injury that occurs during such procedure as transplantation or hepatectomy [1]. Initially, this damage is caused by ischemia, but further, it is aggravated by reperfusion. Among the many phenomena occurring in the IR, there is an excessive production of free radicals and the development

of oxidative stress [2, 3]. Lipid peroxidation is one of the manifestations of oxidative imbalance accompanying rapid tissue reoxygenation and responsible for detrimental effects of IR. The process is initiated by the attack of reactive oxygen species (ROS) on double bonds of membrane phospholipids, glycolipids, and cholesterol. Malondialdehyde among others, are end products of lipid peroxidation. Lipid peroxidation, if not counteracted by antioxidants,

leads to the deterioration of cellular membranes, loss of cell integrity, and cell death [4].

Superoxide dismutases (SODs) are antioxidant enzymes that convert superoxide radicals to oxygen and hydrogen peroxide [2]. There are three isoforms of SOD in mammals: SOD1, SOD2, and SOD3. SOD1, the major cytoplasmic isoenzyme which activity depends on the presence of the Cu and Zn, is expressed highly in selected tissues, mainly in the liver [5]. Hydrogen peroxide is reduced by selenium-containing enzyme—glutathione peroxidase (GPx) to water. Additionally, it is converted to water and molecular oxygen by catalase (CAT)—antioxidant enzyme located mainly in peroxisomes [6]. GPx is the most tightly associated with lipid peroxidation. In addition to preventing hydroxyl radical from forming, GPx is also responsible for two-electron reduction of hydroperoxides, primary products of lipid peroxidation, averting their one-electron reduction that facilitates propagation phase of the process [4]. Paraoxonase-1 (PON1) is a liver-synthesized esterase and lactonase characterized by broad substrate specificity. Best known is the enzyme form residing on HDL and involved in the protection of lipoproteins against lipid peroxidation. Apart from circulation, PON1 is present mainly in the liver where it participates in the inactivation of oxidative by-products, generated during biotransformation of xenobiotics in the microsomes [7]. Intracellular form of PON1 was also shown to involve in the stabilization of lipid membranes and the enhancement of their integrity under oxidative stress conditions [8]. Thiobarbituric acid reactive substances (TBARS) are the final lipid peroxidation product. The accumulation of malondialdehyde (MDA) occurs already in the ischemic phase and ROS-generating reperfusion exacerbating lipid peroxidation [9]. Due to inhibition of oxidative phosphorylation [10], ischemia accelerates processes, such as glycolysis and ketogenesis, which yield methylglyoxal as a by-product. Methylglyoxal is a glycoside factor initiating lipid peroxidation, leading to the formation of MDA [11]. Moreover, MDA can be synthesized enzymatically from thromboxane A₂ [4], the synthesis of which is upregulated during ischemia [12].

Because extensive damage of the liver subjected to IR depends, among others, on the intensity of oxidative stress, the search for such substances that would enhance the antioxidant defense is justified. Sitagliptin (STG) belongs to a group of oral hypoglycemic drugs that, through inhibition of the dipeptidyl peptidase-4 (DPP-4) activity, prolong the half-life and thus action of incretins—glucose-dependent insulinotropic polypeptide (GIP) and glucagon-like peptide-1 (GLP-1) [13, 14]. STG is approved in more than 130 countries worldwide in monotherapy or in combination with other hypoglycemic drugs for the treatment of patients with type 2 diabetes. STG is generally well tolerated, with gently or moderately intensified adverse events [15]. The choice of STG could be based on the additional properties of this drug, such as antioxidative action, that have been reported in some works [16, 17].

The aim of this work was to evaluate the potential antioxidative and hepatoprotective properties of STG administered chronically to rats prior to liver IR procedure.

2. Materials and Methods

2.1. Animals. The study was carried out on Wistar male rats at the age of 2–3 months. Animals were housed in individual chambers in standard conditions (a 12:12 h light-dark cycle, humidity 45–60%, continuous ventilation, and the temperature maintained at 21–23°C).

2.1.1. Ethical Approval and Informed Consent. All procedures performed in the study were in accordance with the ethical standards of the institutional and/or national research committee. All applicable international, national, and/or institutional guidelines for the care and use of animals were followed. The experiment protocol was approved by the 1st Local Ethics Committee on the Animal Research of the Institute of Immunology and Experimental Therapy Polish Academy of Sciences in Wrocław (# 80/2012 of December 5, 2012).

2.2. Chemicals. Sitagliptin (Januvia, tabl. 100 mg; MSD, Poland), heparin (Heparinum WZF, amp. 25000 U/5 ml; Polfa Warszawa, Poland), ketamine hydrochloride (Bioketan, Vetoquinol Biowet, Poland), medetomidine hydrochloride (Domitor, amp. 1 mg/ml, Orion Pharma, Finland), butorphanol tartrate (Morphasol, amp. 4 mg/ml, aniMedica GmbH, Germany), 0.9% sodium chloride solution (Polpharma S.A., Poland), and Ringer's solution (Polfa Lublin S.A., Poland) were used in the study.

2.3. Experimental Design. Following adaptation period, rats were divided randomly into 4 groups. In group C ($n = 9$) and CIR ($n = 9$), animals were not treated with STG. In group S ($n = 8$) and SIR ($n = 10$), animals received STG (5 mg/kg p.o.) once a day for 2 weeks prior to the surgical procedure. Livers from groups SIR and CIR were subjected to the IR procedure. To determine the initial activity of ALT and AST, blood samples were obtained from the tail vein after the STG treatment.

2.4. IR Procedure. After intramuscular injection of medetomidine hydrochloride (0.1 mg/kg), ketamine hydrochloride (7 mg/kg), and butorphanol tartrate (2 mg/kg), animals were subjected to midline laparotomy. In groups CIR and SIR, branches of the hepatic artery and portal vein were occluded with a microvascular clip, which caused 70% of the liver (median and left lateral lobes) to be ischemic. Rats were given heparin (200 U/kg) to prevent blood coagulation. The clip was removed after 60 min of ischemia to allow reperfusion for 24 h. At 2, 6, and 24 h of reperfusion, samples of blood were collected to determine the activity of aminotransferases. Once the experiment was terminated, livers were weighted and ischemic lobes were isolated. A part of the liver lobes was placed in the RNAlater RNA Stabilization Reagent (Qiagen, Germany) and used for real-time PCR. Remaining ischemic liver tissue was homogenized, and supernatant was collected.

In S and C groups, rats underwent the same anesthesia and surgical procedure as in the ischemic groups (CIR and SIR), but after midline laparotomy, the branches of the portal vein and hepatic artery were not occluded. Blood samples

were obtained at the same time points as in the case of ischemic groups. After 24 hours of reperfusion, the same lobes of livers were isolated as in ischemic groups. All surgical procedures with or without I/R were blindly performed by the same experienced team of researchers.

2.5. The Homogenization of Isolated Fragments of the Liver. Liver tissue fragments (400-500 mg) were homogenized 1:2 (*w/v*) in Tris-EDTA buffer pH 7.2 (10 mM Tris, 1 mM EDTA, 1 mM MgCl₂, and 150 mM KCl) with 1% deoxycholate, 1 mM PMSF, and 1% Triton X-100, using ceramic lysing matrix beads and the FastPrep-24™ homogenizer (MP Biomedicals, LCC, CA, USA). Homogenates were centrifuged (14,000 × g, 10 min, 4°C), and supernatants were collected, aliquoted, and stored at -80°C. Prior to analyses, homogenate samples were diluted with Tris-EDTA buffer or respective assay buffers with optimal dilution factors established for each assay by serial dilutions.

2.6. Oxidative Stress Parameters and Biochemical Analyses. The concentrations of thiobarbituric acid reactive substances (TBARS) were determined with the thiobarbituric acid spectrophotometric assay [18] with the addition of butylated hydroxytoluene (Fluka, Switzerland). The activities of copper-zinc superoxide dismutase (SOD1) and GPx were measured using Superoxide Dismutase Assay Kits and Glutathione Peroxidase Assay Kits (Cayman Chemical, MI, USA), according to the manufacturer's instructions and expressed as units (U/g for SOD) or kilounits (kU/g for GPx) per gram of liver tissue. The CAT activity was measured according to the procedure described by Bartosz [19], in which the decrease in absorbance at 240 nm, caused by decomposition of hydrogen peroxide (H₂O₂), was assessed for one minute. One unit of an enzyme activity is defined as one millimole of degraded H₂O₂ per minute. The enzyme activity was expressed as kilounits per gram (kU/g) of liver tissue.

The PON1 activity was determined spectrophotometrically by measuring the rates of phenyl acetate (Sigma-Aldrich, St. Louis, MO) hydrolysis, according to the Arylesterase/Paraoxonase Assay Kit protocol (ZeptoMetrix Co., Buffalo, NY). The enzyme activity was expressed in kilounits per gram (kU/g) of liver tissue. One unit (U) of the enzyme activity was defined as one mmol of released phenol per 1 liter per minute in 25°C. The enzyme activity towards phenyl acetate (PON1 arylesterase activity) is considered as a surrogate for the enzyme concentration [20]. All measurements were conducted at least in duplicates, and technical replicates were averaged.

Serum activities of aminotransferases (ALT and AST) and protein concentration in homogenates were assayed using a commercial enzymatic method in a certified laboratory.

2.7. RNA Isolation and Reverse Transcription. Total RNA was isolated from the studied tissue samples with RNeasy Mini Kit (Qiagen, Hilden, Germany) according to the manufacturer's protocol. To eliminate genomic DNA contamination, on-column DNase digestion was performed using RNase-

Free DNase Set (Qiagen, Hilden, Germany). Quantity and purity of RNA samples were assessed by measuring the absorbance at 260 and 280 nm with NanoDrop1000 Spectrophotometer (Thermo Fisher Scientific, Wilmington, DE, USA). First-strand cDNA was synthesized using the High Capacity cDNA Reverse Transcription Kit (Applied Biosystems, Carlsbad, CA, USA).

2.8. Real-Time PCR. The mRNA expression of SOD1 was determined by real-time PCR with 7900HT Fast Real-Time PCR System and TaqMan Gene Expression Master Mix (Applied Biosystems, Carlsbad, CA, USA). Beta-2 microglobulin (B2M) was used as reference gene. For the reactions, the following sets of primers and TaqMan probes were used: Rn00566938_m1 for SOD1 and Rn00560865_m1 for B2M (Applied Biosystems, Carlsbad, CA, USA). All reactions were performed in triplicates in standardized thermal cycling conditions, including polymerase activation at 50°C for 2 min, denaturation at 94°C for 10 min, and 40 cycles of denaturation at 94°C for 15 s followed by annealing and synthesis at 60°C for 1 min. The relative amount of SOD1 at the mRNA level (RQ) was calculated by the 2^{-ΔΔCt} method.

2.9. Histological Examination. Different regions of the isolated lobes of livers from ischemic and nonischemic groups were fixed in 10% formalin and embedded in paraffin. Sections of 4.5 μm were made and stained with hematoxylin-eosin. Then, they were histologically evaluated under a light microscope for the severity of ischemic necrosis, degree of steatosis as percentage of the microscopic field (small cytoplasmic vacuoles containing lipids or single fat droplets displacing the nuclei of hepatocytes), neutrophil infiltration, and destruction of hepatic architecture.

3. Statistical Analysis

Data distribution and homogeneity of variances were tested using Kolmogorov-Smirnov and Levene tests, respectively. Normally distributed data (SOD1 activity and expression, CAT, and aminotransferases) were expressed as means ± SD and analyzed using one-way ANOVA with Bonferroni correction for multiple testing, followed by post hoc test. Nonnormally distributed data (TBARS, PON1, and GPx) were expressed as medians with interquartile range and analyzed using Kruskal-Wallis *H* test with the Conover post hoc analysis. Statistical analysis of the effect of the drug and time of reperfusion on the aminotransferase activity was performed using repeated measures ANOVA. Correlation analysis was conducted using Spearman (ρ) or Pearson (r) correlation tests, depending on the data distribution. All tests were two-tailed, and hypotheses were considered positively verified if $p < 0.05$. The analyses were performed using MedCalc Statistical Software version 17.4.4 (MedCalc Software bvba, Ostend, Belgium; <https://www.medcalc.org>; 2017) and Statistica (13.1).

4. Results

4.1. Aminotransferases. After 2 weeks of the STG administration, before surgical procedure, the activity of ALT in rats

from treated groups (S+SIR) was significantly lower compared to nontreated groups (C+CIR) ($p < 0.05$). At 2 h of reperfusion, the significant increase in the ALT activity was noticed regardless of STG administration (CIR vs. C, $p < 0.01$ and SIR vs. S, $p < 0.05$). Values of ALT in the STG-treated ischemic group were insignificantly lower than in the nontreated group. Differences between AST activities were also significant between nonischemic and ischemic nontreated groups (CIR vs. C, $p < 0.01$). After 6 h of reperfusion, the activity of ALT was statistically higher in the nontreated ischemic group compared to the nonischemic group (CIR vs. C, $p < 0.01$). In STG-treated groups, this difference was close to the significance threshold (SIR vs. S, $p = 0.06$). After 24 h of reperfusion, the activity of aminotransferases was the highest in the ischemic nontreated group (CIR vs. C, $p < 0.01$ for AST and $p < 0.05$ for ALT). The increase in the aminotransferase activity in STG-treated groups was not significant. Hence, therein, in the case of ALT, that difference was close to the significance threshold (SIR vs. CIR, $p = 0.05$), and in the case of AST, that difference was significant (SIR vs. CIR, $p < 0.01$) (Figures 1(a) and 1(b)).

4.2. Parameters of Oxidative Stress. The differences in TBARS were noticed in nontreated groups. The concentration of TBARS was significantly greater in IR-exposed livers compared to nonischemic group (CIR vs. C, $p < 0.05$). In drug-treated groups, the concentration of TBARS was lower in the ischemic group compared to S (SIR vs. S, $p < 0.05$). Hence, in the STG-treated ischemic group, the level of this parameter was significantly lower compared to the nontreated ischemic group (SIR vs. CIR, $p < 0.01$) (Figure 2(a)).

The activity of PON1 was significantly lower in the nontreated ischemic group than in the nonischemic group (CIR vs. C, $p < 0.05$). Significant difference was also noticed between nontreated and drug-treated nonischemic groups (C vs. S, $p < 0.05$). In IR-exposed groups, the activity of PON1 was statistically higher in STG-treated groups compared to nontreated one (CIR vs. SIR, $p < 0.05$) (Figure 2(b)). There was an inverse relationship between TBARS accumulation and PON1 activity in whole cohort ($\rho = -0.42$, $p = 0.011$). The association was stronger in IR animals (CIR and SIR) ($\rho = -0.64$, $p = 0.003$).

In IR-exposed groups, the activity of GPx was significantly lower than in nonischemic groups regardless of STG treatment (CIR vs. C, $p < 0.05$; SIR vs. S, $p < 0.01$) (Figure 2(c)). No significant differences in the activity of CAT between experimental groups were noticed. Ischemic-dependent statistically insignificant decrease in the activity of CAT was visible only in nontreated groups (Figure 2(d)).

Ischemic-dependent decrease in the activity of SOD1 in groups nontreated with STG was close to the significance threshold (CIR vs. C, $p = 0.07$). In drug-treated groups, the SOD1 activity was similar regardless of IR. Hence, in the IR conditions in the drug-treated group, the SOD1 activity was significantly higher compared to that in the nontreated group (SIR vs. CIR, $p < 0.05$) (Figure 2(e)).

4.3. SOD1 mRNA Expression. In the nonischemic group treated with STG, the expression of SOD1 mRNA significantly increased and was the highest of all examined groups (S vs. C and SIR, $p < 0.05$, and S vs. CIR, $p < 0.01$) (Figure 2(f)).

SOD1 expression positively but moderately correlated with the SOD1 activity in the whole animal cohort ($r = 0.41$, $p = 0.015$). However, this association resulted from a tight relationship between parameters in nontreated animals and was nonexistent in STG-treated ones (Figure 3). Comparison of correlation coefficients between C and CIR groups showed them to be similarly high ($r = 0.72$, $p = 0.027$ and $r = 0.73$, $p = 0.025$, respectively).

4.4. Histological Findings. No significant differences in the hepatic structure were seen in both ischemic and nonischemic groups of rats. Livers from those groups featured normal architecture, and only slight degree of necrosis and neutrophil infiltration was seen in ischemic groups regardless of the STG treatment. In drug-treated groups, the percentage of steatosis was statistically higher than that in nontreated groups. Described differences were visible in both ischemic and nonischemic groups (CIR vs. SIR, $p < 0.05$, and C vs. S, $p < 0.01$) (Figure 4).

5. Discussion

A body of evidence has gathered concerning protective effect of new drugs on hepatic cells during IR, providing rationale for new therapeutic strategies. Among others, glucose-lowering activity of incretins, and hence indirectly of STG, translates into reduced oxidative stress, condition fueled by hyperglycemia [21]. Moreover, STG has been found to be an efficient scavenger of reactive oxygen species (ROS), directly reducing superoxide generation in various organs [22], but the STG effect on oxidative balance in the liver remains unknown. Our work was carried out to understand the effect of STG on the oxidative stress parameters in the liver under IR conditions.

IR resulted in decreased activities of all enzymes examined in our work, but the difference was significant solely in the case of GPx. There is still no consensus regarding IR effect on the SOD1 activity. While some of the authors have shown it to be decreased [23–25], others have found it to be elevated [26] or, as in the case of IR in mice's kidneys, showed the response to be depended on sex [27]. Therefore, to verify SOD1 status, we examined also SOD1 gene expression. Corroborating its reduced activity, relative SOD1 expression was insignificantly decreased by ca 10% upon IR conditions. Interestingly, SOD1 and GPx activities were affected by IR to the same extent (ca 18%), which corresponds well with 20% drop in glutathione level, an electron donor in the reactions catalyzed by GPx, reported recently by Weng et al. [23].

STG has been shown to increase the SOD, CAT, and GPx activities in kidneys [16], organs with the highest DPP-4 activity [21]. However, this effect was observed only in rats with diabetes. In the kidneys of healthy animals, the SOD activity decreased slightly, the CAT activity increased slightly, and the GPx activity remained unchanged [28].

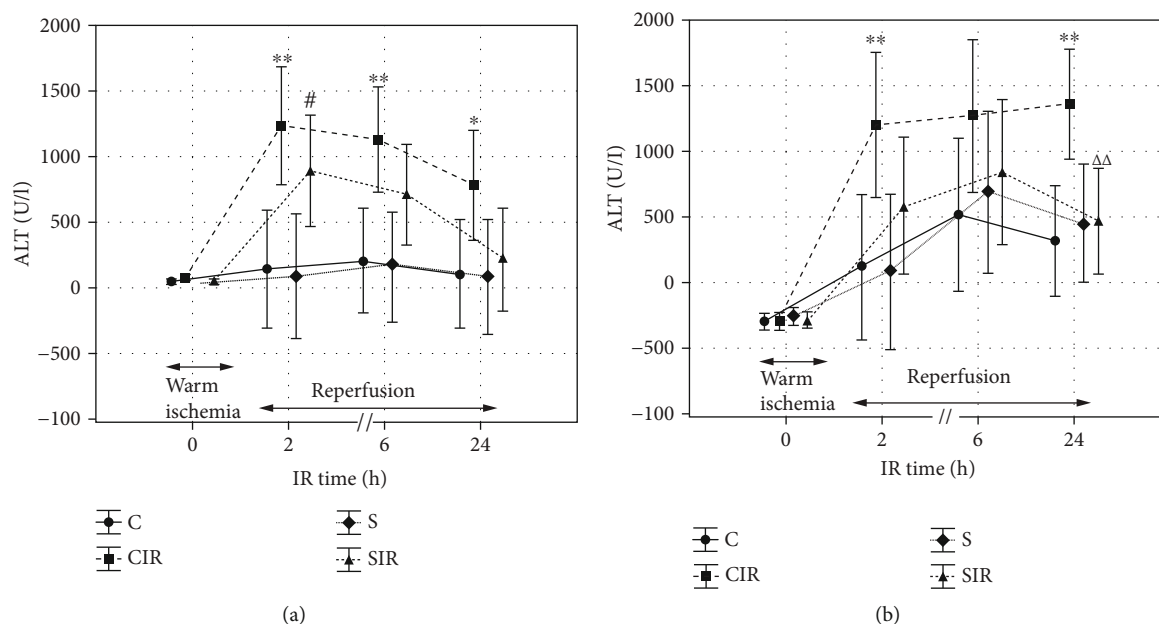


FIGURE 1: Influence of IR and STG treatment on activity of ALT (a) and AST (b). Values are presented as the mean + SD. Group C, nontreated and nonsubjected to IR; group CIR, nontreated and subjected to IR; group S, STG-treated and nonsubjected to IR; group SIR, STG-treated and subjected to IR. Specific comparisons: * $p < 0.05$ and ** $p < 0.01$ (compared to C), # $p < 0.05$ (compared to S), and $\Delta\Delta p < 0.01$ (compared to CIR).

These observations may imply that beneficial effects of drug are displayed solely in the presence of an additional factor increasing the oxidative stress. IR is another condition, in which STG treatment has been associated with improved antioxidant status both at systemic level [29] and locally in myocardium [24], kidney [28], and hippocampus [30]. In our work, carried out on rat livers, the protective effect of STG was visible only under IR conditions. In the ischemic liver, the CAT and SOD1 activities decreased insignificantly in untreated groups but remained unchanged in the STG group. Therefore, in the case of SOD1, significant differences were observed between treated and untreated groups.

Interestingly, SOD1 expression in our STG-treated nonischemic livers was significantly upregulated, which, however, did not translate into increased enzyme activity. The discrepancy between drug effect on enzyme gene expression and activity could also be found in the case of GPx in kidneys: its mRNA expression decreased [31] but enzymatic activity increased [16]. One must keep in mind that many factors may affect translation and thus up- or downregulate expression on protein level as compared to mRNA copy numbers or, in the case of the enzymes, also modulate their activity. Indeed, antioxidant enzymes are sensitive to oxidative damage themselves. Moderate oxidative imbalance stimulates expression of antioxidant enzymes through activation of *Nrf2*, but it may also diminish their activity by causing oxidative modifications, e.g., oxidation of cysteine thiols. However, the correlation analysis of SOD1 expression and activity showed them to be tightly and positively correlated with nontreated animals, but it was completely abolished in STG-treated animals. Taken together, results showed that STG differently affected SOD1 at transcriptional and enzyme

activity levels and was responsible for the disruption of the association between both parameters.

Nrf2 is a key transcription factor responsible for induction of antioxidant enzymes synthesis. It was recently demonstrated that STG downregulated the expression of *Nrf2* in rat kidneys, with concomitant upregulation of its inhibitor—Keep1. These findings imply that, at least in kidneys, antioxidant action of STG is associated rather with direct reduction of intracellular ROS or with increased stability of GLP-1. Since we observed upregulation of SOD1 expression in the liver, it would be of interest to investigate the drug effect on hepatic *Nrf2* [31].

A reduction of hepatic PON1 activity during lipid peroxidation and liver damage was an early occurring phenomenon, what was shown in animal models [32]. Accordingly, a drop in the PON1 activity has accompanied also hepatic IR injury [33, 34]. Corroborating these observations, we found PON1 to be significantly decreased in the ischemic nontreated group. In line with the beneficial effect on the oxidative balance attributed to STG during IR [25, 28, 30], the enzyme activity in the ischemic drug-treated group was restored and significant differences were observed between treated and untreated groups. However, the PON1 activity was diminished in drug-treated animals not subjected to IR. These results seem to imply that STG *per se* might have a negative impact on the enzyme. A positive correlation between the PON1 activity and insulin resistance was shown [35, 36]. The high glucose concentration was shown to induce activation of specific protein (SP)-1 [37, 38], a transcription factor activating the PON1 promoter in cultured hepatocytes [37]. STG increasing the sensitivity of tissues to insulin may negatively affect the

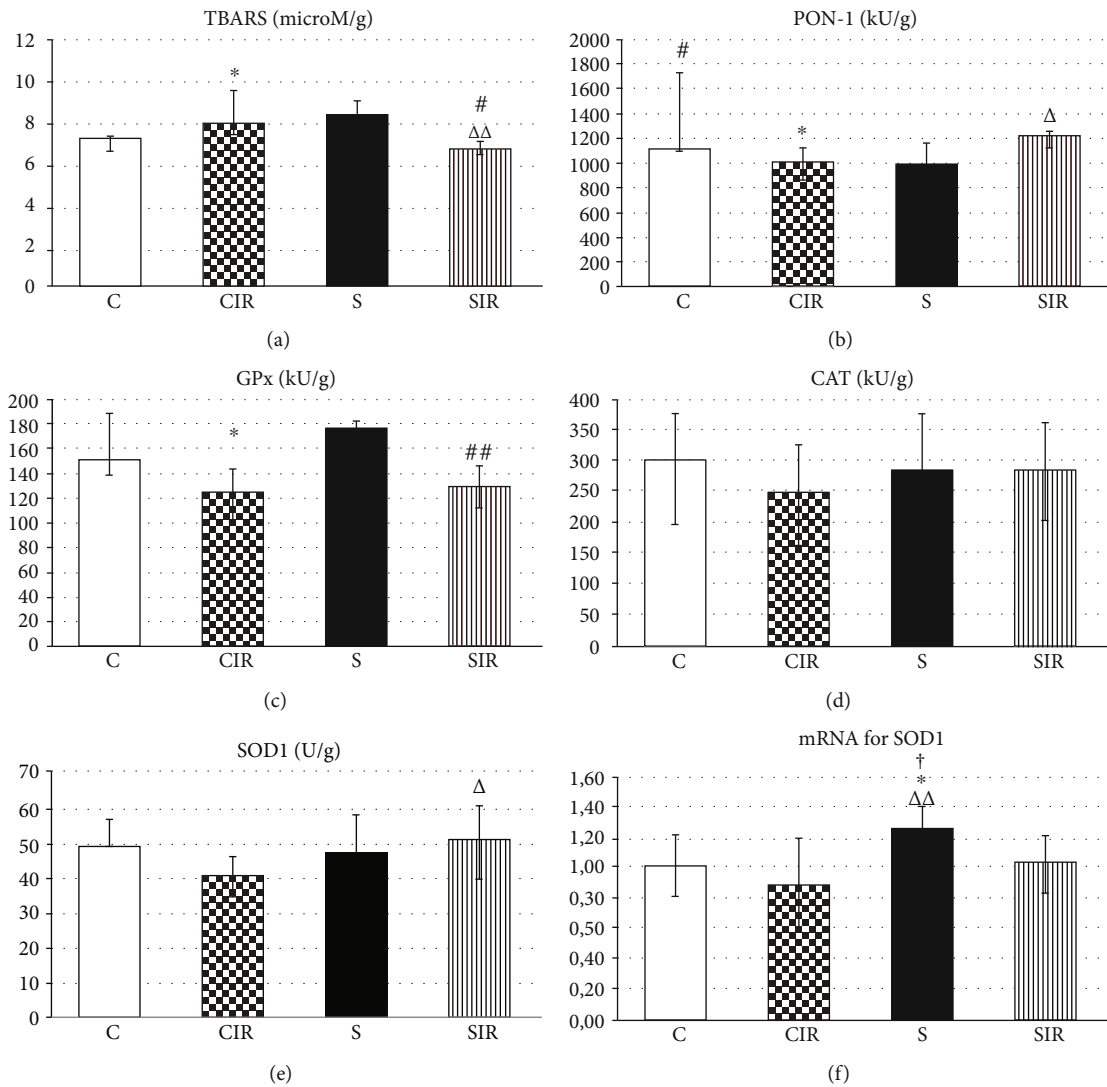


FIGURE 2: Influence of IR and STG treatment on TBARS (a), PON-1 (b), GPx (c), CAT (d), SOD1 (e), and mRNA for SOD1 (f) levels. Values are presented as the mean + SD. Group C, nontreated and nonsubjected to IR; group CIR, nontreated and subjected to IR; group S, STG-treated and nonsubjected to IR; group SIR, STG-treated and subjected to IR. Specific comparisons: * $p < 0.05$ (compared to C), # $p < 0.05$ and ## $p < 0.01$ (compared to S), Δ $p < 0.05$ and ΔΔ $p < 0.01$ (compared to CIR), and † $p < 0.05$ (compared to SIR).

expression of PON1 in the liver. However, functional studies are needed to determine the exact effect of STG on the enzyme.

Simultaneously with the decreased activity of PON1 in untreated ischemic livers, a significant increase in TBARS concentration was observed. Our findings corroborate earlier reports on increased accumulation of lipid peroxidation products in response to IR injury in the liver [9, 26, 39–42]. STG has been reported to possess antioxidant properties manifested, among others, by its capability to limit lipid peroxidation [22]. Under IR conditions, the effect of STG lowering MDA accumulation has previously been observed in the brain [30], kidney [28], and heart [25]. We showed that MDA formation was reduced after STG treatment also in livers subjected to IR. However, without pathology such as IR or diabetes, STG seems to have an opposite effect and increase the accumulation of TBARS, what was also noticed by other authors [29, 43].

While unexpected, this finding is consistent with the diminishing effect of the drug on PON1 and a close negative correlation between liver PON1 activity and accumulation of TBARS observed in our study as well. Therefore, considering the role of PON1 in protection against lipid peroxidation [7, 8], enhanced lipid peroxidation in STG-treated animals might directly result from drug-induced inhibition of PON1. Surprisingly, in studies evaluating beneficial effects of various drugs on IR injury, a control drug-treated group has frequently been missing, also in the case of STG [25, 30].

The histological evaluation of liver specimens showed no significant differences in IR-dependent liver structure. Only slight degree of necrosis and neutrophil infiltration was observed in ischemic groups. To monitor the liver dysfunction, which intensifies with the duration of IR, we determine the activity of aminotransferases—enzymes released from damaged hepatocytes [44, 45]. As in our previous works [46–48], we have also demonstrated in this work that the

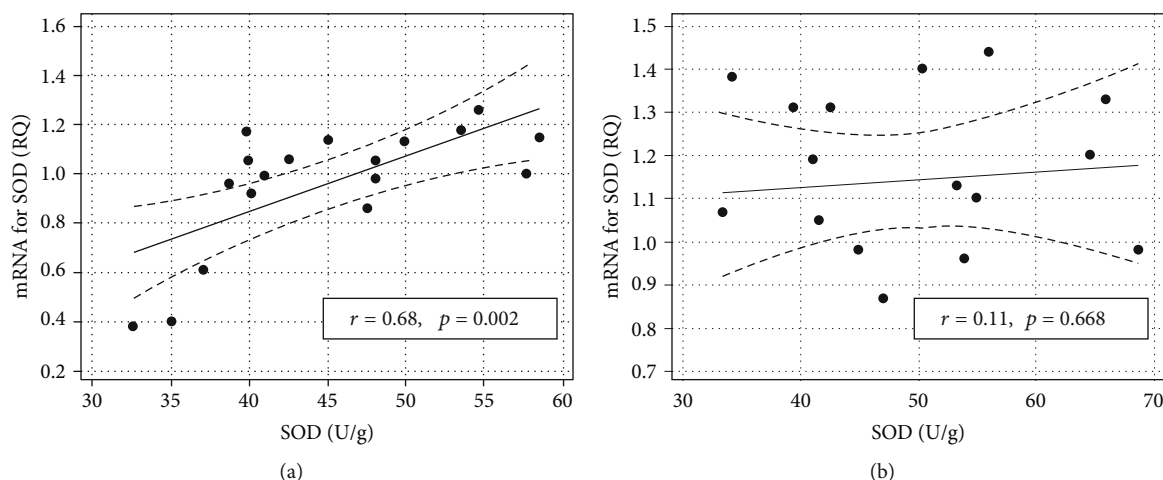


FIGURE 3: Comparison of correlation between SOD1 expression and activity in control (nontreated) (a) and STG-treated (b) animals. Data presented as regression line with 95% confidence interval (dashed lines).

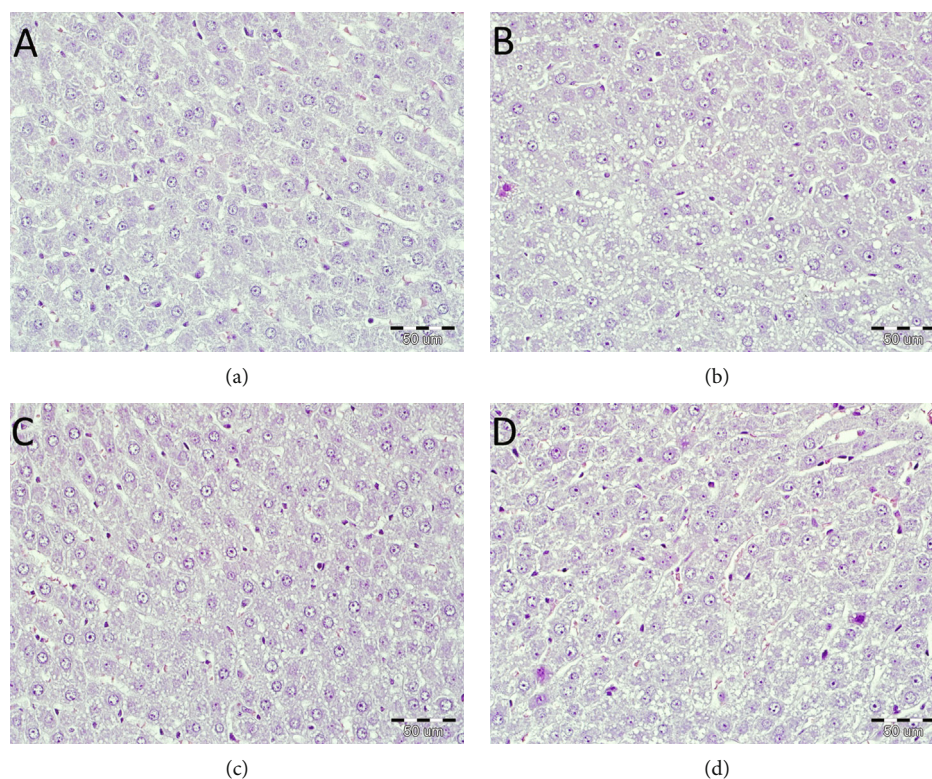


FIGURE 4: Histopathological examination of liver tissue. Histological examination (stained with hematoxylin-eosin, magnification $\times 400$, bar $50 \mu\text{m}$) from group C, rats nontreated and nonsubjected to IR (a); group CIR, rats nontreated and subjected to IR (b); group S, rats treated with STG and not subjected to IR (c); and from group SIR, rats treated with STG and subjected to IR (d). No significant differences in the hepatic structure were seen in both ischemic and nonischemic groups of rats. In drug-treated groups, the percentage of steatosis was statistically higher than that in nontreated groups (CIR vs. SIR, $p < 0.05$, and C vs. S, $p < 0.01$).

aminotransferase activity was significantly increased, most pronounced in the nontreated ischemic group. Therefore, despite a minimal histological abnormality, we may suspect a low-degree liver injury evoked by IR.

The STG is minimally metabolized in the liver, and over 80% is excreted with the urine in unaltered form [49]. Therefore, this medicine has a safe and beneficial

pharmacokinetics even in patients with liver damage. The STG safety profile assessed in many studies is rather good, and the risk of liver damage does not increase. In clinical trials, the use of STG alone or in combination with other oral antidiabetic agents did not cause alterations in AST or ALT [50, 51]. There are only a few cases of serious liver damage after STG treatment [52, 53]. In our work, the

effect of STG therapy on liver damage probably depends on the initial conditions. The higher steatosis rates observed in STG-treated groups suggested detrimental effects of the drug itself during chronic treatment. On the other hand, the aminotransferase activity before and during IR in the drug-treated group was lower at all time points, and in the 24-hour reperfusion, the difference was significant. Such results, however, indicate a protective effect of STG, which is more visible in harmful conditions, such as IR in our case.

6. Conclusions

Summing up, the action of STG strongly depends on additional factors increasing the oxidative stress, such as IR. In the nonischemic group, the effect of STG on oxidative parameters was invisible or even negative. However, under IR, the action of this drug is beneficial. Also, despite the small degree of steatosis, the aminotransferase activity analysis does not suggest any hepatotoxic action of STG. Contrarily, even a slight protective effect of this drug was seen, especially in IR conditions.

Although significant results have been obtained in this work, the limitations of this study should be considered. In our work, we observed the effect of STG only on the parameters of oxidative stress in the rat liver subjected to IR. It will be important in further studies to also examine other markers of liver injury during IR, especially the ones associated with inflammation and apoptosis. To better explain the STG's mechanism of protective action, we also plan to explore a grip point of this drug. Furthermore, we are now aware, that by extending the duration of administration and using higher STG doses, a more pronounced effect of this drug may be achieved. And finally, the limitations of a partial liver ischemia model used in this work need to be considered. During the induced ischemia of the middle and left lateral lobe, there is an increased blood flow in the rest of the liver, which can affect liver function and regeneration. Exchange of oxygen from perfused to ischemic part of the liver may affect the values of oxidative stress parameters obtained in this experiment.

Abbreviations

ALT:	Aminotransferase alanine
AST:	Aminotransferase aspartate
CAT:	Catalase
DPP-4:	Dipeptidyl peptidase-4
GIP:	Glucose-dependent insulinotropic polypeptide
GLP-1:	Glucagon-like peptide-1
GPx:	Glutathione peroxidase
H ₂ O ₂ :	Hydrogen peroxide
IR:	Ischemia/reperfusion
MDA:	Malondialdehyde
PON1:	Paraoxonase-1
ROS:	Reactive oxygen species
SOD:	Superoxide dismutase
STG:	Sitagliptin
TBARS:	Thiobarbituric acid reactive substances.

Data Availability

The laboratory data used to support the findings of this study are available from the corresponding author upon request.

Conflicts of Interest

The authors declare that there is no conflict of interest.

Authors' Contributions

Małgorzata Trocha conceived and designed the study, conducted the experiment, participated in the acquisition of laboratory data, analyzed and interpreted the data, drafted the article, and finally approved and guaranteed the manuscript. Małgorzata Krzystek-Korpacka assayed the redox parameters and PON1 in liver homogenates and drafted the manuscript part of the Materials and Methods section concerning determination of redox parameters and PON1. Anna Merwid-Ląd conducted the experiment and revised the manuscript to be submitted. Beata Nowak analyzed and interpreted the data and revised the manuscript to be submitted. Małgorzata Pieśniewska conducted the experiment on animals. Piotr Dzięgiel assayed the SOD1 mRNA expressions, contributed to the writing of the manuscript, and revised the manuscript to be submitted. Agnieszka Gomułkiewicz assayed the SOD1 mRNA expressions, drafted the manuscript part of the Materials and Methods section concerning SOD1 mRNA expressions, and revised the manuscript to be submitted. Przemysław Kowalski carried out the histopathological evaluations. Dorota Diakowska collected the laboratory data and revised the manuscript to be submitted. Adam Szeląg analyzed and interpreted the data, contributed to the writing of the manuscript, and revised the manuscript to be submitted. Tomasz Sozański conceived and designed the study, analyzed and interpreted the data, contributed to the writing of the manuscript, and revised the manuscript to be submitted. All authors read and approved the manuscript.

Acknowledgments

The study was financially supported by the statutory means of Wrocław Medical University (ST-555).

References

- [1] A. Cobreros, L. Sainz, B. Lasheras, and E. Cenarruzabeitia, "Hepatotoxicity of ethanol: protective effect of calcium channel blockers in isolated hepatocytes," *Liver*, vol. 17, no. 2, pp. 76–82, 1997.
- [2] C. Fan, R. M. Zwacka, and J. F. Engelhardt, "Therapeutic approaches for ischemia/reperfusion injury in the liver," *Journal of Molecular Medicine*, vol. 77, no. 8, pp. 577–592, 1999.
- [3] A. Stanek, A. Gadowska-Cicha, K. Gawron et al., "Role of nitric oxide in physiology and pathology of the gastrointestinal tract," *Mini Reviews in Medicinal Chemistry*, vol. 8, no. 14, pp. 1549–1560, 2008.
- [4] A. Ayala, M. F. Muñoz, and S. Argüelles, "Lipid peroxidation: production, metabolism, and signaling mechanisms of

- malondialdehyde and 4-hydroxy-2-nonenal,” *Oxidative Medicine and Cellular Longevity*, vol. 2014, Article ID 360438, 31 pages, 2014.
- [5] Y. Fukai and M. Ushio-Fukai, “Superoxide dismutases: role in redox signaling, vascular function, and diseases,” *Antioxidants & Redox Signaling*, vol. 15, no. 6, pp. 1583–1606, 2011.
- [6] S. Wassmann, K. Wassmann, and G. Nickenig, “Modulation of oxidant and antioxidant enzyme expression and function in vascular cells,” *Hypertension*, vol. 44, no. 4, pp. 381–386, 2004.
- [7] J. Camps, J. Marsillach, and J. Joven, “Measurement of serum paraoxonase-1 activity in the evaluation of liver function,” *World Journal of Gastroenterology*, vol. 15, no. 16, pp. 1929–1933, 2009.
- [8] D. A. Chistiakov, A. A. Melnichenko, A. N. Orekhov, and Y. V. Bobryshev, “Paraoxonase and atherosclerosis-related cardiovascular diseases,” *Biochimie*, vol. 132, pp. 19–27, 2017.
- [9] S. M. Lee, M. J. Park, T. S. Cho, and M. G. Clemens, “Hepatic injury and lipid peroxidation during ischemia and reperfusion,” *Shock*, vol. 13, no. 4, pp. 279–284, 2000.
- [10] F. Z. Meerson, V. E. Kagan, Y. P. Kozlov, L. M. Belkina, and Y. V. Arkhipenko, “The role of lipid peroxidation in pathogenesis of ischemic damage and the antioxidant protection of the heart,” *Basic Research in Cardiology*, vol. 77, no. 5, pp. 465–485, 1982.
- [11] N. Murata-Kamiya and H. Kamiya, “Methylglyoxal, an endogenous aldehyde, crosslinks DNA polymerase and the substrate DNA,” *Nucleic Acids Research*, vol. 29, no. 16, pp. 3433–3438, 2001.
- [12] A. Yan, T. Zhang, X. Yang et al., “Thromboxane A2 receptor antagonist SQ29548 reduces ischemic stroke-induced microglia/macrophages activation and enrichment and ameliorates brain injury,” *Scientific Reports*, vol. 6, article 35885, 2016.
- [13] J. E. Campbell and D. J. Drucker, “Pharmacology, physiology, and mechanisms of incretin hormone action,” *Cell Metabolism*, vol. 17, no. 6, pp. 819–837, 2013.
- [14] C. F. Deacon, “Dipeptidyl peptidase 4 inhibition with sitagliptin: a new therapy for type 2 diabetes,” *Expert Opinion on Investigational Drugs*, vol. 16, no. 4, pp. 533–545, 2007.
- [15] L. J. Scott, “Sitagliptin: a review in type 2 diabetes,” *Drugs*, vol. 77, no. 2, pp. 209–224, 2017.
- [16] J. Vaghasiya, N. Sheth, Y. Bhalodia, and R. Manek, “Sitagliptin protects renal ischemia reperfusion induced renal damage in diabetes,” *Regulatory Peptides*, vol. 166, no. 1-3, pp. 48–54, 2011.
- [17] Y. T. Chen, T. H. Tsai, C. C. Yang et al., “Exendin-4 and sitagliptin protect kidney from ischemia-reperfusion injury through suppressing oxidative stress and inflammatory reaction,” *Journal of Translational Medicine*, vol. 11, no. 1, pp. 1–19, 2013.
- [18] C. A. Rice-Evans, A. T. Diplock, and M. C. R. Symons, *Techniques in free radical research*, Elsevier Science Publishers BV, Amsterdam, 1991.
- [19] G. Bartosz, *Druga twarz tlenu. Wolne rodniki w przyrodzie. (The other face of oxygen. Free radicals in the environment)*, Wydawnictwo Naukowe PWN, Warszawa, 2nd edition, 2004.
- [20] L. G. Costa, A. Vitalone, T. B. Cole, and C. E. Furlong, “Modulation of paraoxonase (PON1) activity,” *Biochemical Pharmacology*, vol. 69, no. 4, pp. 541–550, 2005.
- [21] C. Mega, E. Teixeira-de-Lemos, R. Fernandes, and F. Reis, “Renoprotective effects of the dipeptidyl peptidase-4 inhibitor sitagliptin: a review in type 2 diabetes,” *Journal Diabetes Research*, vol. 2017, article 5164292, 14 pages, 2017.
- [22] L. Liu, J. Liu, X. Y. Tian et al., “Uncoupling protein-2 mediates DPP-4 inhibitor-induced restoration of endothelial function in hypertension through reducing oxidative stress,” *Antioxidants & Redox Signaling*, vol. 21, no. 11, pp. 1571–1581, 2014.
- [23] J. Weng, W. Li, X. Jia, and W. An, “Alleviation of ischemia-reperfusion injury in liver steatosis by augmenting of liver regeneration is attributed to antioxidation and preservation of mitochondria,” *Transplantation*, vol. 101, no. 10, pp. 2340–2348, 2017.
- [24] Z. Chen, T. Ding, and C.-G. Ma, “Dexmedetomidine (DEX) protects against hepatic ischemia/reperfusion (I/R) injury by suppressing inflammation and oxidative stress in NLRC5 deficient mice,” *Biochemical and Biophysical Research Communications*, vol. 493, no. 2, pp. 1143–1150, 2017.
- [25] G. Chang, P. Zhang, L. Ye et al., “Protective effects of sitagliptin on myocardial injury and cardiac function in an ischemia/reperfusion rat model,” *European Journal of Pharmacology*, vol. 718, no. 1-3, pp. 105–113, 2013.
- [26] M. Arslan, F. Metin Çomu, A. Küçük, L. Oztürk, and F. Yaylak, “Dexmedetomidine protects against lipid peroxidation and erythrocyte deformability alterations in experimental hepatic ischemia reperfusion injury,” *Libyan Journal of Medicine*, vol. 7, no. 1, article 18185, 2012.
- [27] M. P. Schneider, J. C. Sullivan, P. F. Wach et al., “Protective role of extracellular superoxide dismutase in renal ischemia/reperfusion injury,” *Kidney International*, vol. 78, no. 4, pp. 374–381, 2010.
- [28] A. Nuransoy, A. Beytur, A. Polat, E. Samdanci, M. Sagir, and H. Parlakpınar, “Protective effect of sitagliptin against renal ischemia reperfusion injury in rats,” *Renal Failure*, vol. 37, no. 4, pp. 687–693, 2015.
- [29] S. Karabulut, Z. M. Coskun, and S. Bolkent, “Immunohistochemical, apoptotic and biochemical changes by dipeptidyl peptidase-4 inhibitor-sitagliptin in type-2 diabetic rats,” *Pharmacological Reports*, vol. 67, no. 5, pp. 846–853, 2015.
- [30] A. E. El-Sahar, M. M. Safar, H. F. Zaki, A. S. Attia, and A. A. Ain-Shoka, “Sitagliptin attenuates transient cerebral ischemia/reperfusion injury in diabetic rats: implication of the oxidative-inflammatory-apoptotic pathway,” *Life Sciences*, vol. 126, pp. 81–86, 2015.
- [31] E. Civantos, E. Bosch, E. Ramirez et al., “Sitagliptin ameliorates oxidative stress in experimental diabetic nephropathy by diminishing the miR-200a/Keap-1/Nrf2 antioxidant pathway,” *Diabetes, Metabolic Syndrome and Obesity: Targets and Therapy*, vol. 10, pp. 207–222, 2017.
- [32] N. Ferre, J. Camps, M. Cabre, A. Paul, and J. Joven, “Hepatic paraoxonase activity alterations and free radical production in rats with experimental cirrhosis,” *Metabolism*, vol. 50, no. 9, pp. 997–1000, 2001.
- [33] H. Kandis, S. Karapolat, U. Yildirim, A. Saritas, S. Gezer, and R. Memisogullari, “Effects of *Urtica dioica* on hepatic ischemia-reperfusion injury in rats,” *Clinics*, vol. 65, no. 12, pp. 1357–1361, 2010.
- [34] A. Tüfek, O. Tokgöz, I. Aliosmanoglu et al., “The protective effects of dexmedetomidine on the liver and remote organs against hepatic ischemia reperfusion injury in rats,” *International Journal of Surgery*, vol. 11, no. 1, pp. 96–100, 2013.

- [35] M. Bednarska-Makaruk, A. Graban, W. Lipczyńska-Łojkowska et al., "Positive correlation of paraoxonase 1 (PON1) activity with serum insulin level and HOMA-IR in dementia. A possible advantageous role of PON1 in dementia development," *Journal of the Neurological Sciences*, vol. 324, pp. 172–175, 2013.
- [36] A. Yamada, T. Shoji, H. Tahara, M. Emolo, and Y. Nishizawa, "Effect of insulin resistance on serum paraoxonase activity in a nondiabetic population," *Metabolism Clinical and Experimental*, vol. 50, no. 7, pp. 805–811, 2001.
- [37] Y. Ikeda, T. Suehiro, K. Ariei, Y. Kumon, and K. Hashimoto, "High glucose induces transactivation of the human paraoxonase 1 gene in hepatocytes," *Metabolism*, vol. 57, no. 12, pp. 1725–1732, 2008.
- [38] K. Beishline and J. Azizkhan-Clifford, "Sp1 and the 'hallmarks of cancer'," *The FEBS Journal*, vol. 282, no. 2, pp. 224–258, 2015.
- [39] D. Giakoustidis, N. Kontos, S. Iliadis et al., "Severe total hepatic ischemia and reperfusion: relationship between very high alpha-tocopherol uptake and lipid peroxidation," *Free Radical Research*, vol. 35, no. 2, pp. 103–109, 2001.
- [40] N. Yun, J. W. Kang, and S. M. Lee, "Protective effects of chlorogenic acid against ischemia/reperfusion injury in rat liver: molecular evidence of its antioxidant and anti-inflammatory properties," *The Journal of Nutritional Biochemistry*, vol. 23, no. 10, pp. 1249–1255, 2012.
- [41] J. Kim, H. Y. Kim, and S. M. Lee, "Protective effects of geniposide and genipin against hepatic ischemia/reperfusion injury in mice," *Biomolecules & Therapeutics*, vol. 21, no. 2, pp. 132–137, 2013.
- [42] E. Tak, G. C. Park, S. H. Kim et al., "Epigallocatechin-3-gallate protects against hepatic ischaemia-reperfusion injury by reducing oxidative stress and apoptotic cell death," *The Journal of International Medical Research*, vol. 44, no. 6, pp. 1248–1262, 2016.
- [43] Z. M. Coskun, M. Koyuturk, S. Karabulut, and S. Bolkent, "CB-1R and GLP-1R gene expressions and oxidative stress in the liver of diabetic rats treated with sitagliptin," *Pharmacological Reports*, vol. 69, no. 4, pp. 822–829, 2017.
- [44] E. E. Montalvo-Javé, M. A. García-Puig, T. Escalante-Tattersfield, J. Peña-Sánchez, H. Vázquez-Meza, and J. A. Ortega-Salgado, "Biochemical analysis and lipid peroxidation in liver ischemic preconditioning," *Cirugía y Cirujanos*, vol. 79, no. 2, pp. 132–140, 2011.
- [45] C. Wu, P. Wang, J. Rao et al., "Triptolide alleviates hepatic ischemia/reperfusion injury by attenuating oxidative stress and inhibiting NF- κ B activity in mice," *The Journal of Surgical Research*, vol. 166, no. 2, pp. e205–e213, 2011.
- [46] M. Trocha, A. Merwid-Łąd, E. Chlebda, M. Pieśniewska, T. Sozański, and A. Szeląg, "Effect of simvastatin treatment on rat livers subjected to ischemia/reperfusion," *Pharmacological Reports*, vol. 62, no. 4, pp. 757–762, 2010.
- [47] M. Trocha, A. Merwid-Łąd, E. Chlebda et al., "Influence of ezetimibe on selected parameters of oxidative stress in rat liver subjected to ischemia/reperfusion," *Archives of Medical Science*, vol. 10, no. 4, pp. 817–824, 2014.
- [48] M. Trocha, A. Merwid-Łąd, M. Pieśniewska et al., "Age-related differences in function and structure of rat livers subjected to ischemia/reperfusion," *Archives of Medical Science*, vol. 14, no. 2, pp. 388–395, 2018.
- [49] D. J. Drucker and M. A. Nauck, "The incretin system: glucagon-like peptide-1 receptor agonists and dipeptidyl peptidase-4 inhibitors in type 2 diabetes," *The Lancet*, vol. 368, no. 9548, pp. 1696–1705, 2006.
- [50] I. Raz, M. Hanefel, L. Xu, C. Caria, D. Williams-Herman, and H. Khatami, "Efficacy and safety of the dipeptidyl peptidase-4 inhibitor sitagliptin as monotherapy in patients with type 2 diabetes mellitus," *Diabetologia*, vol. 49, no. 11, pp. 2564–2571, 2006.
- [51] M. A. Nauck, G. Meininger, D. Sheng, L. Terranella, and P. P. Stein, "Efficacy and safety of the dipeptidyl peptidase-4 inhibitor, sitagliptin, compared with the sulfonylurea, glipizide, in patients with type 2 diabetes inadequately controlled on metformin alone: a randomized, double-blind, non-inferiority trial," *Diabetes, Obesity and Metabolism*, vol. 9, no. 2, pp. 194–205, 2007.
- [52] M. Toyoda-Akui, H. Yokomori, F. Kaneko et al., "A case of drug-induced hepatic injury associated with sitagliptin," *Internal Medicine*, vol. 50, no. 9, pp. 1015–1020, 2011.
- [53] B. N. Gross, L. B. Cross, J. Foard, and Y. Wood, "Elevated hepatic enzymes potentially associated with sitagliptin," *The Annals of Pharmacotherapy*, vol. 44, no. 2, pp. 394–395, 2010.

Research Article

Malondialdehyde and Uric Acid as Predictors of Adverse Outcome in Patients with Chronic Heart Failure

Ewa Romuk ¹, Celina Wojciechowska ², Wojciech Jacheć ²,
Aleksandra Zemła-Woszek ¹, Alina Momot ³, Marta Buczkowska ⁴,
and Piotr Rozentryt ^{4,5}

¹Department of Biochemistry, School of Medicine with the Division of Dentistry, Medical University of Silesia, Jordana 19 Street, 41-808 Zabrze, Poland

²Second Department of Cardiology, School of Medicine with the Division of Dentistry, Medical University of Silesia, M. C. Skłodowskiej 10 Street, 41-800 Zabrze, Poland

³Institute of Computer Science, Silesian University of Technology, 44-100 Gliwice, Poland

⁴Department of Toxicology and Health Protection, School of Public Health, Medical University of Silesia, 41-902 Bytom, Poland

⁵3rd Department of Cardiology, SMDZ in Zabrze, Medical University of Silesia, Silesian Centre for Heart Disease, 41-800 Zabrze, Poland

Correspondence should be addressed to Ewa Romuk; eromuk@gmail.com

Received 12 July 2019; Accepted 24 August 2019; Published 9 October 2019

Guest Editor: Adrian Doroszko

Copyright © 2019 Ewa Romuk et al. This is an open access article distributed under the Creative Commons Attribution License, which permits unrestricted use, distribution, and reproduction in any medium, provided the original work is properly cited.

In chronic heart failure (HF), some parameters of oxidative stress are correlated with disease severity. The aim of this study was to evaluate the importance of oxidative stress biomarkers in prognostic risk stratification (death and combined endpoint: heart transplantation or death). In 774 patients, aged 48–59 years, with chronic HF with reduced ejection fraction (median: 24.0 (20–29)%), parameters such as total antioxidant capacity, total oxidant status, oxidative stress index, and concentration of uric acid (UA), bilirubin, protein sulfhydryl groups (PSH), and malondialdehyde (MDA) were measured. The parameters were assessed as predictive biomarkers of mortality and combined endpoint in a 1-year follow-up. The multivariate Cox regression analysis was adjusted for other important clinical and laboratory prognostic markers. Among all the oxidative stress markers examined in multivariate analysis, only MDA and UA were found to be independent predictors of death and combined endpoint. Higher serum MDA concentration increased the risk of death by 103.0% (HR = 2.103; 95% CI (1.330–3.325)) and of combined endpoint occurrence by 100% (HR = 2.000; 95% CI (1.366–2.928)) per $\mu\text{mol/L}$. Baseline levels of MDA in the 4th quartile were associated with an increased risk of death with a relative risk (RR) of 3.64 (95% CI (1.917 to 6.926), $p < 0.001$) and RR of 2.71 (95% CI (1.551 to 4.739), $p < 0.001$) for the occurrence of combined endpoint as compared to levels of MDA in the 1st quartile. Higher serum UA concentration increased the risk of death by 2.1% (HR = 1.021; 95% CI (1.005–1.038), $p < 0.001$) and increased combined endpoint occurrence by 1.4% (HR = 1.014; 95% CI (1.005–1.028), $p < 0.001$), for every 10 $\mu\text{mol/L}$. Baseline levels of UA in the 4th quartile were associated with an increased risk for death with a RR of 3.21 (95% CI (1.734 to 5.931)) and RR of 2.73 (95% CI (1.560 to 4.766)) for the occurrence of combined endpoint as compared to the levels of UA in the 1st quartile. In patients with chronic HF, increased MDA and UA concentrations were independently related to poor prognosis in a 1-year follow-up.

1. Introduction

Despite advances in diagnosis and therapy, prognosis in patients with heart failure (HF) is still poor. The prevalence of chronic HF with reduced ejection fraction is increasing,

and 1-year mortality is still growing [1]. Evaluation of mortality risk may be a crucial component that can help in choosing patients for invasive treatment (LVAD, HT) [2]. Many parameters are useful in predicting prognosis in patients with chronic HF. Some parameters like natriuretic

peptides, age, sex, etiology, NYHA class, left ventricle ejection fraction, and diabetes markedly influence the prognosis of HF [3]. Different biological processes like oxidative stress, inflammation, neurohormonal activation, vascular remodeling, and renal impairment are crucial for the development of the disease [4, 5].

Numerous biomarkers can be a reflection of various pathophysiological pathways [5]. Beyond the well-known N-terminal brain propeptide (NT-proBNP), simple biochemical parameters like sodium, creatinine, or hemoglobin can reflect systemic abnormalities in HF. Several studies have found a correlation between different parameters of oxidative stress and HF severity [6–8]. During oxidative stress, excessive production of reactive oxygen species exceeds the possibility of antioxidant protection. However, their role in the pathogenesis of HF remains unclear [9].

There is still a need to search for a new, easily measured biomarker that can help us understand the HF pathophysiology [5]. Oxidative stress markers, namely, lipid and protein oxidation products, uric acid (UA), and bilirubin, play a multifold role in redox balance during HF, and assessment of these parameters may offer an advantage as compared to other well-known clinical HF markers.

Some studies show serum UA as a poor marker for the prognosis of HF [10, 11]. Impaired oxidative metabolism in HF can be a result of increased xanthine oxidase activity which generates superoxide free radicals proportional to UA synthesis [12–14].

Considering that HF is a state of chronic deterioration of oxidative mechanisms due to enhanced oxidative stress, we assessed if UA, total antioxidant capacity (TAC), total oxidant status (TOS), products of lipid peroxidation (MDA), and protein sulfhydryl groups (PSH), when added to known risk factors, are associated with adverse outcome in patients with stable chronic HF in a 1-year follow-up.

2. Study Group and Methods

2.1. Patients. In our study, we analyzed the data collected in Prospective Registry of Heart Failure (PR-HF), undertaken since 2003, and Studies Investigating Co-morbidities Aggravating Heart Failure (SICA-HF) described elsewhere [15]. For a prospective cohort study, consecutive patients with primarily chronic systolic HF (LVEF \leq 40%) were recruited from the patients referred to our Inpatient Clinic as potential candidates for heart transplantation. The primary inclusion criterion was a clinical diagnosis of HF according to published contemporary ESC criteria. Patients received optimal medical pharmacotherapy for at least 3 months before inclusion. Participants were excluded if they had a noncardiac condition resulting in an expected mortality of less than 12 months as judged by the treating physician or had a history of alcohol abuse or known antioxidant supplementation or if they were unable or unwilling to provide informed consent. Study criteria were fulfilled in 1216 PR-HF or SICA-HF. The data of 774 participants (aged 48–59 years) who had completed clinical laboratory assessment were included into final analysis.

2.2. Endpoints of the Study. Endpoints of the study were death and combined endpoint (death or urgent heart transplantation).

2.3. Consent of the Patient and the Opinion of the Bioethical Commission. All participants provided written informed consent, and the protocol was approved by the participating institution.

2.4. Clinical Assessments. At the time of study entry, detailed clinical data were obtained using a standardized questionnaire. Ischemic cardiomyopathy was recognized according to the definition proposed by Felker et al. [16], based on patients who have undergone coronary angiography within six months before inclusion. History of smoking was defined as current or previous use of tobacco products. Comorbidities such as hypertension, hypercholesterolemia, or diabetes mellitus were recognized based on clinical history, current medication, or actual measurements of respective variables. Body mass and height were measured on a day of inclusion visit and body mass indices (BMI) were calculated. The NYHA classification and cardiopulmonary exercise testing CPX were used to assess functional capacity [17]. Two-dimensional transthoracic echocardiography was performed in all patients, and echocardiographic images were acquired in standard views as recommended by the American Society of Echocardiography Committee [18]. Follow-up events including all-cause mortality and cardiac transplantation were prospectively ascertained every 6 months via direct or phone contact with patients or their family members by a dedicated research personnel. In some cases, the exact data of death were obtained from the national identification number database. All participants provided written informed consent, and the protocol was approved by the participating institution.

2.5. Biochemical Methods. Venous blood samples obtained at enrollment were processed, separated by centrifugation at 1500 g for 10 minutes, frozen at -70°C , and partially stored at -70°C until time of assay. UA, bilirubin, lipid parameters, blood hemoglobin, and serum iron, sodium, creatinine, glucose, and albumin concentrations were measured by colorimetric method (Roche, Cobas 6000 e 501). NT-proBNP was measured by chemiluminescence method (Roche, Cobas 6000 e 501). Spectrophotometric method by Erel was used to determine total oxidant status (TOS). In this method, the reaction proceeds in an acidic environment and consists of measuring the color intensity of complex of Fe^{3+} ions and Xylenol orange [19]. TOS is expressed in mmol/L.

TAC was measured by colorimetric methods given by Erel, based on 2,2'-azino-bis(3-ethylbenzothiazoline-6-sulfonate) (ABTS+) reaction [20]. In this method, reduced ABTS, a colorless molecule, is oxidized to blue-green ABTS⁺. After mixing the colored ABTS⁺ with any substance that can be oxidized, it is reduced to its original colorless reduced form and the reacted substance is oxidized. TAC is expressed in mmol/L.

Oxidative stress index (OSI) is expressed as ratio of TOS to TAC. The OSI was calculated according to the following

formula: $OSI = [(TOS, \text{mmol/L}) / (TAC, \text{mmol/L})]$ [21]. The concentration of sulfhydryl groups (PSH) in serum was determined by the Koster method using 5,5'-dithiobis (2-nitrobenzoic acid) or DTNB. After reduction by the sulfhydryl group-containing compounds, DTNB gives a yellow-colored anionic 5-thio-2-nitrobenzoic acid [21]. The absorbance was measured with a Shimadzu 1700 UV-VIS spectrophotometer at a wavelength of 412 nm [22]. PSH concentration is expressed in $\mu\text{mol/g}$ protein.

Malondialdehyde (MDA) was measured by Ohkawa's method. The method is based on the reaction of lipid peroxides with thiobarbituric acid with spectrofluorimetric detection. The excitation wavelength was 515 nm, and emission wavelength was 552 nm. MDA concentration was calculated from the standard curve, prepared for 1,1,3,3-tetraethoxypropane, and expressed in $\mu\text{mol/L}$ [23].

2.6. Statistical Analysis. The study subjects were divided into groups, for the purpose of the analysis, depending on outcome: A—patients who survived without endpoints, B—patients who died, and C—patients who achieved combined endpoint. Distribution of all continuous variables was evaluated by the Shapiro-Wilk test. The continuous data were presented as median with the first and fourth quartiles (because of abnormal distribution of the data) and were compared using *U* Mann-Whitney test. Categorical data are presented as absolute numbers and percentage and were compared using the chi-square test with Yates correction.

Further estimations of risk were performed using Cox proportional-hazards model. All demographic, clinical, echocardiography, laboratory variables, and medication data were included in a univariate Cox analysis, but only variables with a value of $p \leq 0.05$ in univariate analysis were included in the multivariate model. The results of the Cox analysis were reported as relative risks with corresponding 95% confidence intervals (CI). Cumulative survival curves were constructed as time to the endpoint by the Kaplan-Meier method, the survival of the groups of patients separated from the quartiles of MDA and UA concentrations was assessed, and the differences were tested for significance by the log-rank test. Differences in the number of achieved endpoints in particular subgroups were also assessed by the Kruskal-Wallis ANOVA test.

Results were considered statistically significant if $p < 0.05$. Lack of statistical significance was indicated by NS (nonsignificant).

Statistical analysis was performed using STATISTICA 13.1 PL (StatSoft, Poland, Cracow).

3. Results

3.1. Baseline Characteristics of Study Population and Subgroups in Relation to Endpoint. Over a follow-up of one year, there were 106 deaths (group B) and 135 patients reached combined endpoint; there were 29 urgent heart transplantations and 106 deaths (group C). Baseline clinical characteristics for patients enrolled in the study are shown in Table 1 and on Figure 1. The median age was 54 (48-59)

years, and 664 patients (85.79%) were male. In general, ischemic HF was more common than nonischemic (61.89% vs. 38.11%) and more frequent in patients who died. The population was classified by the treating cardiologist as having symptomatic systolic HF NYHA class I-II ($n = 339$; 43.8%) and NYHA class III-IV ($n = 435$; 56.2%). The left ventricle was more enlarged in groups B and C with median of ejection fraction in all patients as 24.0% (20.0-29.0). Patients who reached endpoints were more likely to be older (only group B), with lower BMI, longer disease duration, more advanced NYHA class, and lower value of maximum oxygen consumption in cardiopulmonary exercise testing. Diabetes as a comorbid condition was more frequent, and ICD presence was rare. The percentage of use of ACE, loop diuretics, thiazides, statins, and digitalis between groups without endpoint and groups B and C was different while that of beta blockers, angiotensin-2 receptor blockers, mineralocorticoid receptor antagonist, fibrates, and xanthine oxidase inhibitors was similar. In both groups with adverse outcomes, decreased glomerular filtration, sodium and HDL cholesterol concentrations, and significantly increased NT-proBNP concentration were observed. Among the oxidative stress parameters evaluated in our study, UA, bilirubin, and MDA were higher in the groups with unfavorable prognosis. However, TAC, TOS, and OSI were similar for all the groups while PSH was lower in group B.

3.2. Association between Redox Parameters and Risk of All-Cause Death

3.2.1. Uni- and Multivariate Cox Regression Analyses. Demographic and clinical parameters, basic laboratory parameters, comorbidities, pharmacotherapy, and oxidative stress-related markers assessed as risk factors for all-cause death in 1-year follow-up in uni- and multivariate Cox regression analyses are presented in Table 2.

In univariate Cox regression analysis, higher levels of TAC (HR = 3.263 per mmol/L; $p = 0.017$), UA (HR = 1.036 per 10 $\mu\text{mol/L}$; $p < 0.001$), bilirubin (HR = 1.031 per $\mu\text{mol/L}$; $p < 0.001$), and MDA (HR = 1.967 per $\mu\text{mol/L}$; $p < 0.001$) and lower levels of PSH (HR = 0.853 per $\mu\text{mol/g}$ protein, $p = 0.026$) were associated with the risk of death. In order to evaluate these oxidative stress parameters in the context of all available clinical information, a final multivariate model was generated that included all significant clinical, laboratory, and treatment predictors. Multivariate analysis revealed that oxidative stress-related risk factors of death were UA (increase of risk (IoR) by 2.1% per 10 $\mu\text{mol/L}$) and higher serum MDA concentration (IoR by 110.3% per mmol/L). Moreover, in a multivariate analysis, independent risk factors were lower MVO₂ (IoR by 11.1% per mL/min/kg B.M.), lower LVEF (IoR by 6.27% by every 1%p), lower sodium (IoR by 6.95% per mmol/L), and higher level of NT-proBNP (IoR by 0.9% per 100 pg/mL). Multivariate analysis showed that the following factors are associated with a better prognosis: use of ACE inhibitors (reduction of risk (RoR) by 55.7%) and presence of ICD (RoR by 90.1%).

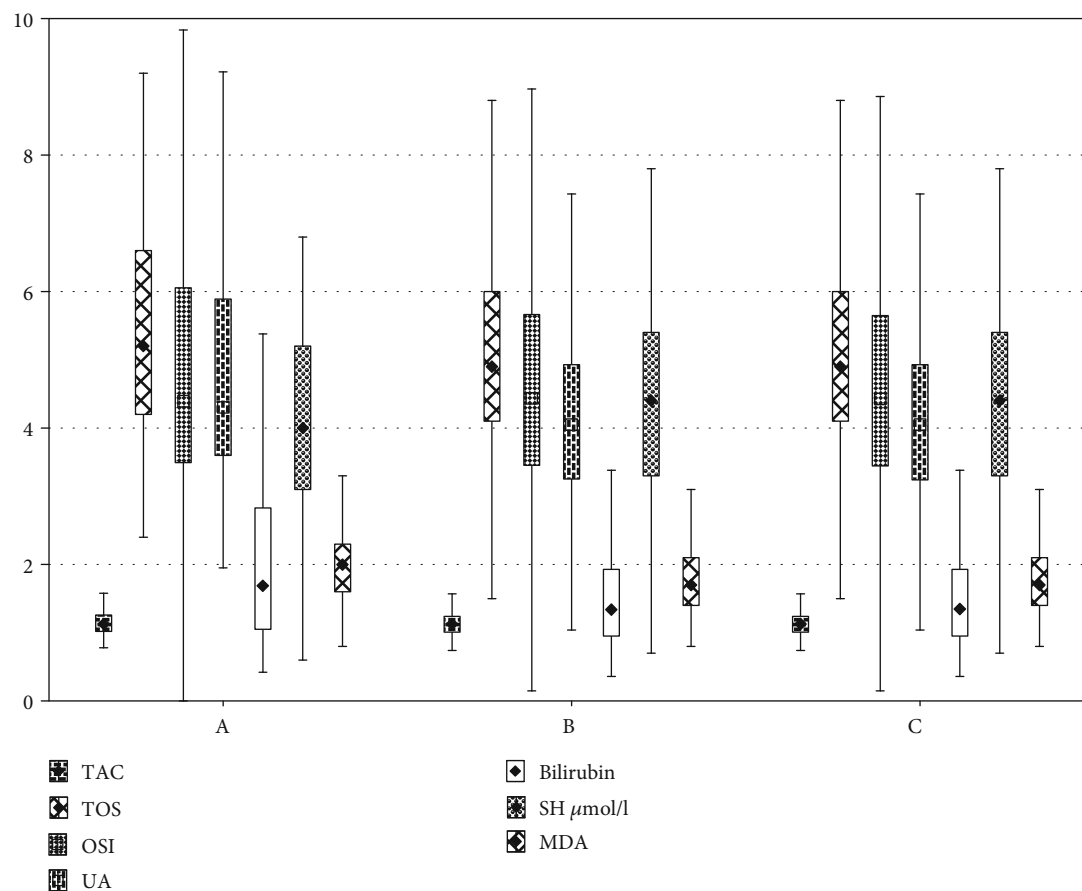
TABLE 1: Baseline characteristic of examined group and comparison of subgroups separated on the basis of prognosis.

	All groups N = 774	Survivors N = 639 A	Death N = 106 B	<i>p</i> B vs. A	Death or OHT N = 135 C	<i>p</i> C vs. A
General characteristics						
Male <i>n</i> (%)	664 (85.79)	549 (85.78)	93 (87.74)	0.726	115 (85.19)	0.932
Age (years)	54.00 48.00-59.00	54.00 48.00-59.00	56.00 50.00-61.00	0.019	55.00 50.00-60.00	0.191
BMI (kg/m ²)	26.24 23.49-29.10	26.40 23.81-29.39	25.13 21.78-28.89	0.035	24.77 21.78-28.44	0.002
Duration of symptoms before inclusion (months)	33.85 13.43-69.43	33.17 12.93-65.40	51.05 18.90-81.00	0.002	44.80 15.60-79.93	0.013
NYHA class	3.00 2.00-3.00	2.00 2.00-3.00	3.00 3.00-4.00	0.000	3.00 3.00-3.00	0.000
Maximum measured VO ₂ (mL/min/kg B.M.)	15.00 12.20-18.45	15.50 12.90-19.10	12.05 9.60-14.20	0.000	12.35 9.70-14.20	0.000
LVEDD (mm)	69.00 64.00-76.00	69.00 63.00-76.00	70.00 65.00-77.00	0.201	72.00 65.00-77.00	0.046
LVEDV (mL)	225.0 170.0-285.0	218.0 163.0-278.0	250.0 198.0-319.50	0.002	250.0 200.0-320.0	0.000
LVEF (1%)	24.00 20.00-29.00	25.00 20.00-30.00	20.00 17.00-25.00	0.000	20.00 17.00-25.00	0.000
Basic biochemistry						
Hemoglobin (g/100 mL)	14.02 13.05-14.99	14.02 13.05-14.99	13.94 12.73-14.99	0.428	14.02 12.89-15.15	0.788
Sodium (mmol/L)	136.00 134.00-139.00	137.00 134.00-139.00	135.00 131.0-137.0	0.000	135.00 132.0-138.0	0.000
Iron concentration (μmol/L)	17.20 12.00-22.20	17.50 12.30-22.50	15.90 11.07-20.90	0.071	15.11 10.80-20.90	0.004
Creatinine clearance (mL/min)	95.09 69.76-119.38	98.89 73.53-121.70	75.66 59.83-100.12	0.000	79.84 59.83-104.23	0.000
Serum protein (g/L)	71.00 67.00-75.00	71.00 67.00-75.00	72.00 67.00-77.00	0.105	72.00 67.00-77.00	0.207
Albumin (g/L)	42.00 39.00-44.00	42.00 39.00-44.00	41.00 38.00-44.00	0.131	40.00 38.00-44.00	0.011
Fasting glucose (mmol/L)	5.50 5.00-6.30	5.50 5.00-6.30	5.60 5.00-6.90	0.305	5.60 5.00-6.70	0.643

TABLE 1: Continued.

	All groups N = 774	Survivors N = 639 A	Death N = 106 B	Death or OHT N = 135 C	P C vs. A
Total cholesterol (mmol/L)	4.29	4.30	4.27	4.25	0.431
	3.65-5.21	3.65-5.21	3.57-5.25	3.57-5.19	
Triglycerides (mmol/L)	1.21	1.24	1.12	1.13	0.122
	0.89-1.73	0.90-1.77	0.84-1.58	0.86-1.60	
Cholesterol HDL (mmol/L)	1.15	1.16	1.09	1.10	0.018
	0.94-1.41	0.96-1.42	0.83-1.37	0.83-1.37	
Cholesterol LDL (mmol/L)	2.44	2.43	2.51	2.50	0.578
	1.90-3.16	1.89-3.11	1.92-3.27	1.90-3.26	
NT-proBNP (pg/mL)/100	13.91	12.24	29.64	30.63	0.000
	6.39-31.81	5.56-25.66	16.20-52.04	15.53-52.65	
Comorbidities					
Ischemic heart disease n (%)	479 (61.89)	391 (61.00)	74 (70.00)	88 (65.00)	0.085
Diabetes n (%)	218 (28.17)	169 (26.41)	39 (36.79)	49 (36.30)	0.027
Arterial hypertension n (%)	423 (54.65)	357 (55.78)	55 (51.89)	66 (48.89)	0.361
Permanent atrial fibrillation n (%)	183 (23.64)	146 (22.81)	33 (31.13)	37 (27.41)	0.307
ICD presence n (%)	215 (27.78)	209 (32.66)	4 (3.77)	6 (4.44)	0.000
Smoker n (%)	265 (34.24)	224 (35.00)	33 (31.13)	41 (30.37)	0.346
Pharmacotherapy					
Beta-blockers n (%)	759 (98.06)	629 (98.28)	102 (96.23)	130 (96.30)	0.196
ACE inhibitors (yes/no)	666 (86.05)	564 (88.13)	77 (72.64)	102 (75.56)	0.000
ARB (yes/no)	82 (10.59)	69 (10.78)	8 (7.55)	13 (9.63)	0.762
Loop diuretics (yes/no)	679 (87.73)	549 (85.78)	103 (97.17)	130 (96.30)	0.001
Thiazide diuretics (yes/no)	99 (12.79)	69 (10.78)	25 (23.58)	30 (22.22)	0.000
MRA (yes/no)	713 (92.12)	589 (92.03)	96 (90.57)	124 (91.85)	0.961
Statins (yes/no)	506 (65.37)	428 (66.88)	58 (54.72)	78 (57.78)	0.052
Fibrates (yes/no)	28 (3.62)	25 (3.91)	2 (1.89)	3 (2.22)	0.483
Digitalis (yes/no)	352 (45.48)	280 (43.75)	55 (51.89)	72 (53.33)	0.000
XO inhibitors (yes/no)	285 (36.82)	229 (35.78)	41 (38.68)	56 (41.48)	0.164

BMI: body mass index; NYHA: New York Heart Association functional class; VO₂: rate of oxygen consumption; VO₂ max: maximum rate of oxygen consumption; VCO₂: rate of carbon dioxide output; LVEDD: left ventricle end-diastolic diameter; LVEDV: left ventricle end-diastolic volume; LVEF: left ventricle ejection fraction; NT-proBNP: N-terminal pro-B-type natriuretic peptide; CM: cardiomyopathy; ICD: implantable cardioverter defibrillator; ACE inhibitor: angiotensin-converting enzyme inhibitor; ARB: angiotensin-2 receptor blockers; MRA: mineralocorticoid receptor antagonists; XO: xanthine oxidase; NS: nonsignificant.



	All group N = 774	Survivors N = 639 A	Death N = 106 B	<i>p</i> B vs A	Death or OHT N = 135 C	<i>p</i> C vs A
TAC (mmol/L)	1.13 (1.02-1.24)	1.13 (1.01-1.24)	1.15 (1.02-1.28)	0.073	1.13 (1.02-1.26)	0.209
TOS (mmol/L)	4.90 (4.10-6.10)	4.90 (4.10-6.00)	5.15 (4.20-6.60)	0.146	5.20 (4.20-6.60)	0.114
OSI (TOS/TAC)	4.42 (3.45-5.70)	4.43 (3.44-5.65)	4.22 (3.32-6.04)	0.830	4.40 (3.49-6.06)	0.541
Uric acid ($\mu\text{mol/L}$)/100	4.09 (3.31-5.05)	4.05 (3.24-4.93)	4.46 (3.63-6.16)	0.000	4.30 (3.60-5.89)	0.000
Bilirubin ($\mu\text{mol/L}$)/10	1.38 (0.98-2.05)	1.35 (0.95-1.93)	1.81 (1.15-2.83)	0.000	1.69 (1.05-2.83)	0.000
PSH ($\mu\text{mol/g}$ of protein)	4.30 (3.30-5.40)	4.40 (3.30-5.40)	4.00 (3.00-5.10)	0.038	4.00 (3.10-5.20)	0.088
MDA ($\mu\text{mol/L}$)	1.77 (1.39-2.15)	1.72 (1.37-2.11)	1.96 (1.63-2.34)	0.000	1.956 (1.63-2.34)	0.000

FIGURE 1: Oxidative stress parameters in examined subgroups depending on prognosis. TAC: total antioxidant capacity; TOS: total oxidant status; OSI: oxidative stress index; MDA: malondialdehyde; PSH: sulfhydryl groups; NS: nonsignificant.

TABLE 2: Clinical and laboratory parameters as risk factors of death of patients with CHF in one-year follow-up. Uni- and multivariate Cox regression analyses.

	Univariate Cox regression analysis			Multivariate Cox regression analysis		
	HR	95% CI	<i>p</i>	HR	95% CI	<i>p</i>
General characteristics						
Male (yes/no)	0.993	0.575-1.715	0.981			
Age (1 year)	1.021	1.001-1.041	0.035	1.012	0.984-1.040	0.406
BMI (1 kg/m ²)	0.957	0.915-1.001	0.053			
Duration of symptoms (1 month)	1.005	1.001-1.008	0.006	1.001	0.996-1.006	0.700
NYHA class (by 1)	3.080	2.334-4.065	0.000	1.023	0.659-1.587	0.921
VO ₂ max. (1 mL/min/kg B.M.)	1.208	1.144-1.247	0.000	1.111	1.035-1.192	0.004
LVEDD (1 mm)	1.009	0.989-1.029	0.400			
LVEDV (1 mL)	1.003	1.001-1.006	0.004			
Lower LVEF (%)	1.078	1.026-1.111	0.000	1.063	1.017-1.110	0.006
Basic biochemistry						
Hemoglobin ↓ (1 g/100 mL)	1.042	0.927-1.171	0.491			
Sodium ↓ (1 mmol/L)	1.122	1.078-1.168	0.000	1.070	1.012-1.131	0.018
Iron concentration ↓ (1 μmol/L)	1.019	0.994-1.045	0.129			
Creatinine clearance ↓ (1 mL/min)	1.014	1.008-1.020	0.000	1.002	0.993-1.010	0.735
Serum protein (1 g/L)	1.028	0.997-1.060	0.074			
Albumin ↓ (1 g/L)	1.056	1.008-1.105	0.021	1.018	0.953-1.088	0.592
Fasting glucose (1 mmol/L)	1.082	0.988-1.185	0.090			
Total cholesterol (1 mmol/L)	0.959	0.817-1.126	0.609			
Triglycerides (1 mmol/L)	0.831	0.643-1.073	0.156			
Cholesterol HDL (1 mmol/L)	0.608	0.368-1.005	0.053			
Cholesterol LDL (1 mmol/L)	1.079	0.895-1.301	0.425			
NT-proBNP (100 pg/mL)	1.017	1.013-1.021	0.000	1.009	1.000-1.017	0.042
Comorbidities						
Ischemic CM (yes/no)	1.279	0.853-1.919	0.233			
Diabetes (yes/no)	1.531	1.031-2.272	0.035	1.065	0.643-1.764	0.806
Arterial hypertension (yes/no)	0.863	0.590-1.264	0.450			
Atrial fibrillation (yes/no)	1.488	0.986-2.245	0.058			
ICD presence (yes/no)	0.090	0.033-0.244	0.000	0.099	0.031-0.319	0.000
Smoker (yes/no)	0.835	0.554-1.260	0.391			
Pharmacotherapy						
Beta-blockers (yes/no)	0.434	0.160-1.178	0.101			
ACE inhibitors (yes/no)	0.375	0.245-0.575	0.000	0.443	0.257-0.764	0.003
ARB (yes/no)	0.874	0.455-1.675	0.684			
Loop diuretics (yes/no)	5.308	1.684-16.726	0.004	1.759	0.403-7.677	0.452
Thiazide diuretics (yes/no)	2.367	1.512-3.707	0.000	1.757	0.956-3.226	0.069
MRA (yes/no)	0.852	0.445-1.633	0.630			
Statins (yes/no)	0.616	0.420-0.902	0.013	1.082	0.648-1.807	0.763
Fibrates (yes/no)	0.496	0.122-2.010	0.326			
Digitalis (yes/no)	1.370	0.936-2.005	0.105			
XO inhibitors (yes/no)	0.991	0.930-1.056	0.781			
Oxidative stress markers						
TAC (1 mmol/L)	3.263	1.237-8.607	0.017	0.618	0.150-2.546	0.505
TOS (1 mmol/L)	1.052	0.990-1.118	0.102			

TABLE 2: Continued.

	Univariate Cox regression analysis			Multivariate Cox regression analysis		
	HR	95% CI	<i>p</i>	HR	95% CI	<i>p</i>
OSI (TOS/TAC)	1.018	0.964-1.075	0.516			
Uric acid (10 $\mu\text{mol/L}$)	1.036	1.024-1.048	0.000	1.021	1.005-1.038	0.012
Bilirubin (1 $\mu\text{mol/L}$)	1.031	1.020-1.043	0.000	0.991	0.971-1.010	0.339
PSH (1 $\mu\text{mol/g}$ of protein)	0.853	0.741-0.982	0.026	1.097	0.919-1.310	0.306
MDA (1 $\mu\text{mol/L}$)	1.967	1.410-2.742	0.000	2.103	1.330-3.325	0.001

BMI: body mass index; NYHA: New York Heart Association functional class; VO_2 max.: maximum rate of oxygen consumption; LVEDD: left ventricle end-diastolic diameter; LVEDV: left ventricle end-diastolic volume; LVEF: left ventricle ejection fraction; NT-proBNP: N-terminal pro-B-type natriuretic peptide; CHF: chronic heart failure; ICD: implantable cardioverter defibrillator; ACE inhibitor: angiotensin-converting enzyme inhibitor; ARB: angiotensin-2 receptor blockers; MRA: mineralocorticoid receptor antagonists; XO: xanthine oxidase; TAC: total antioxidant capacity; TOS: total oxidant status; OSI: oxidative stress index; MDA: malondialdehyde; PSH: sulfhydryl groups; NS: nonsignificant.

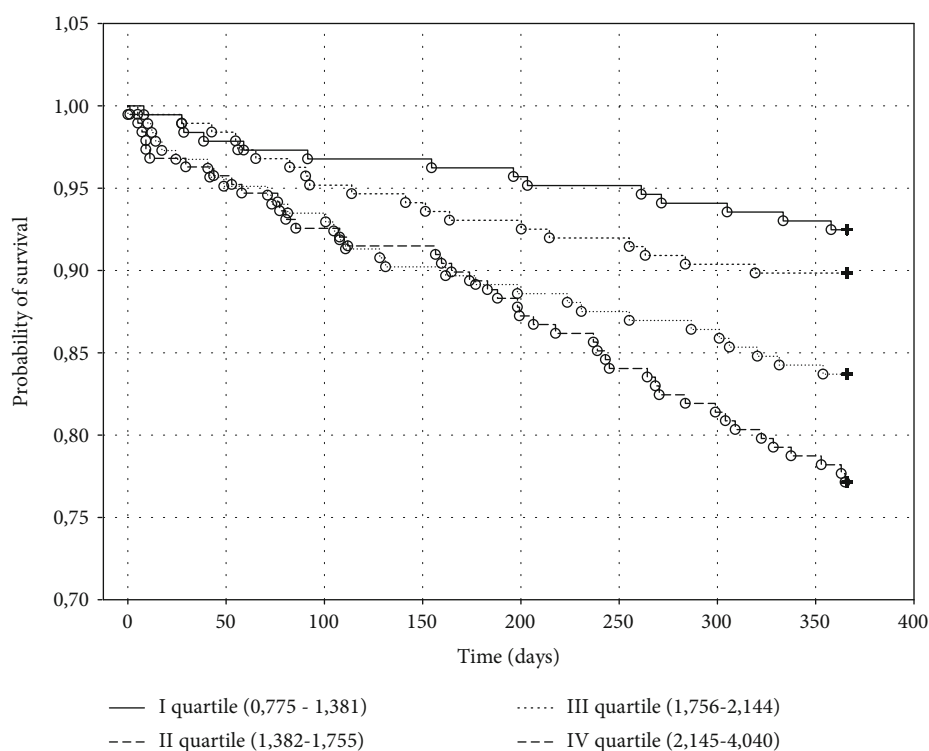


FIGURE 2: The Kaplan-Meier probability of survival in heart failure patients depending on malondialdehyde concentration in one-year follow-up. Significant coefficient for the whole model: $p < 0.001$.

3.2.2. Kaplan-Meier Survival Analysis. The Kaplan-Meier death curves for biomarker quartiles of MDA and UA are shown, respectively, in Figures 2 and 3.

There were 14 (7.35%) deaths in the first quartile, 19 (10.16%) deaths in the second quartile, 30 (16.30%) deaths in the third quartile, and 43 (22.87%) deaths in the fourth quartile of MDA ($p < 0.001$), whereas there were 16 (8.47%) deaths in the first quartile, 25 (13.44%) deaths in the second quartile, 22 (12.09%) deaths in the third quartile, and 43 (22.87%) deaths in the fourth quartile of UA ($p < 0.001$).

Baseline levels of MDA in the upper quartile were associated with the risk of death with a RR of 3.64 (95% CI (1.917 to 6.926)) compared to levels of MDA in the bottom quartile.

Baseline levels of UA in the upper quartile were associated with the risk of death with a RR of 3.21 (95% CI (1.734 to 5.931)) compared to levels of UA in the bottom quartile.

3.3. Association between Redox Parameters and Risk of Combined Endpoint

3.3.1. Uni- and Multivariate Cox Regression Analyses. Risk factors of death or HT in one-year follow-up in univariate and multivariate Cox regression analyses are shown in Table 3. In univariate Cox regression analysis, the following markers reflecting oxidative stress were the risk factors of death or HT: higher concentration of UA (HR = 1.029 per

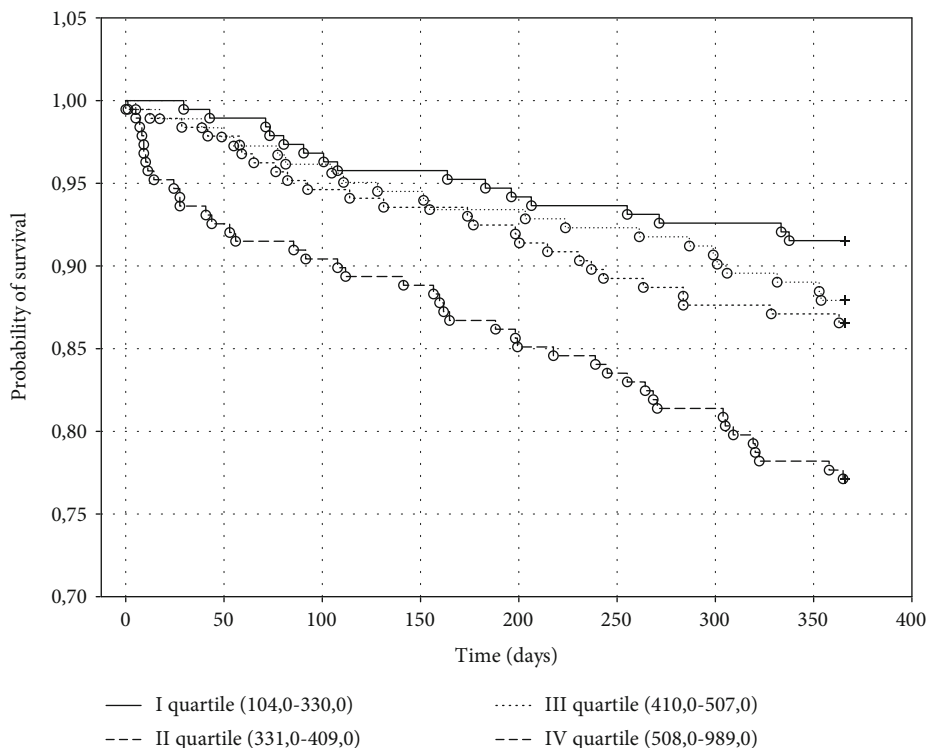


FIGURE 3: The Kaplan-Meier probability of survival in heart failure patients depending on serum uric acid concentration in one-year follow-up. Significant coefficient for the whole model: $p < 0.001$.

10 $\mu\text{mol/L}$; $p < 0.001$), bilirubin (HR = 1.029 per $\mu\text{mol/L}$; $p < 0.001$), and MDA (HR = 2.037 per $\mu\text{mol/L}$; $p < 0.001$). Multivariate analysis showed that only two parameters reflecting oxidative stress were independent predictors of combined endpoint, UA (IoR by 1.40% per 10 $\mu\text{mol/L}$) and higher serum MDA concentration (IoR by 100% per mmol/L). Moreover, in a multivariate analysis, independent risk factors were lower MVO_2 (IoR by 9.41% per mL/min/kg B.M.), lower LVEF (IoR by 7.35% by every 1%p), lower sodium (IoR by 5.37% per mmol/L), and higher level of NT-proBNP (IoR by 0.7% per 100 pg/mL). Multivariate analysis showed that the following factors are associated with a better prognosis: use of ACE inhibitors (RoR by 43.2%) and presence of ICD (RoR by 82.1%).

3.3.2. Kaplan-Meier Survival Analysis. The Kaplan-Meier combined endpoint curves for biomarker quartiles of MDA and UA are shown, respectively, in Figures 4 and 5.

There were 21 (10.88%) deaths or HT in the first quartile, 25 (12.95%) in the second quartile, 41 (21.03%) in the third quartile, and 48 (24.87%) deaths in the fourth quartile of MDA ($p < 0.001$), whereas there were 21 (10.82%) deaths or HT in the first quartile, 34 (17.44%) in the second quartile, 32 (16.679%) in the third quartile, and 48 (24.87%) deaths or HT in the fourth quartile of UA ($p < 0.001$).

Baseline levels of MDA in the 4th quartile were associated with the risk of occurrence of combined endpoint with a RR of 2.71 (95% CI (1.551 to 4.739)) as compared to levels of MDA in the 1st quartile.

Baseline levels of UA in the 4th quartile were associated with the risk of occurrence of combined endpoint with a RR of 2.73 (95% CI (1.560 to 4.766)) as compared to levels of UA in the 1st quartile.

4. Discussion

To the best of our knowledge, this is one of the few large prospective studies assessing the effect of oxidative stress parameters including MDA, TAC, TOS, PSH, UA, and bilirubin on prognosis in patients with HF. Increased UA, bilirubin, and MDA were associated with death or OHT in 1-year follow-up. Additionally, higher TAC and lower PSH were risk factors of death. It is worth emphasizing that MDA and UA remained predictors of death and a combined endpoint after considering known demographic, clinical, and biochemical prognostic factors in the analysis.

These data provide a comprehensive evaluation of the prevalence and prognostic importance of redox balance abnormalities in chronic HF due to reduced left ventricular systolic function. Prior studies investigating redox balance abnormalities in HF patients were relatively smaller and evaluated highly selected populations. In several of them, oxidative stress parameter levels were shown to have a significant correlation with hemodynamic measurements, natriuretic serum peptides, and other prognostic parameters of HF [24–26].

There was an inverse relation between the severity of the disease (as measured by the left ventricular ejection fraction, LVEF) and MDA levels, supporting the hypothesis that free

TABLE 3: Clinical and laboratory parameters as risk factors of death or OHT of patients with CHF in one-year follow-up. Uni- and multivariate Cox regression analyses.

	Univariate Cox regression analysis			Multivariate Cox regression analysis		
	HR	95% CI	<i>p</i>	HR	95% CI	<i>p</i>
General characteristics						
Male (yes/no)	1.003	0.617-1.629	0.992			
Age (1 year)	1.009	0.993-1.026	0.272			
BMI (1 kg/m ²)	0.946	0.909-0.984	0.006	0.976	0.924-1.030	0.377
Duration of symptoms (1 month)	1.004	1.001-1.007	0.019	1.001	0.997-1.005	0.683
NYHA class (by 1)	2.815	2.201-3.601	0.000	1.122	0.764-1.648	0.556
VO ₂ max. (1 mL/min/kg B.M.)	1.192	1.138-1.248	0.000	1.094	1.032-1.161	0.003
LVEDD (1 mm)	1.014	0.996-1.032	0.139			
LVEDV (1 mL)	1.004	1.002-1.005	0.000			
Lower LVEF (1%)	1.087	1.057-1.119	0.000	1.075	1.025-1.117	0.000
Basic biochemistry						
Hemoglobin ↓ (1 g/100 mL)	1.006	0.907-1.115	0.913			
Sodium ↓ (1 mmol/L)	1.099	1.058-1.142	0.000	1.054	1.003-1.106	0.037
Iron concentration ↓ (1 μmol/L)	1.028	1.004-1.050	0.021	1.020	0.990-1.052	0.184
Creatinine clearance ↓ (1 mL/min)	1.013	1.007-1.018	0.000	1.000	0.992-1.007	0.912
Serum protein ↓ (1 g/L)	0.980	0.954-1.007	0.152			
Albumin ↓ (1 g/L)	1.067	1.025-1.111	0.002	1.011	0.923-1.072	0.707
Fasting glucose (1 mmol/L)	1.068	0.983-1.160	0.123			
Total cholesterol (1 mmol/L)	0.965	0.838-1.112	0.624			
Triglycerides (1 mmol/L)	0.855	0.687-1.065	0.163			
Cholesterol HDL (1 mmol/L)	0.594	0.379-0.932	0.023	1.140	0.705-1.843	0.594
Cholesterol LDL (1 mmol/L)	1.079	0.915-1.273	0.365			
NT-proBNP (100 pg/mL)	1.016	1.013-1.020	0.000	1.007	1.000-1.015	0.038
Comorbidities						
Ischemic CM (yes/no)	1.179	0.828-1.681	0.360			
Diabetes (yes/no)	1.490	1.049-2.116	0.026	1.170	0.750-1.825	0.489
Arterial hypertension (yes/no)	0.796	0.568-1.115	0.184			
Atrial fibrillation (yes/no)	1.265	0.867-1.847	0.223			
ICD presence (yes/no)	0.127	0.059-0.271	0.000	0.179	0.082-0.391	0.000
Smoker (yes/no)	0.803	0.557-1.160	0.242			
Pharmacotherapy						
Beta-blockers (yes/no)	0.541	0.200-1.464	0.227			
ACE inhibitors (yes/no)	0.447	0.301-0.665	0.000	0.568	0.345-0.935	0.026
ARB (yes/no)	0.899	0.508-1.593	0.715			
Loop diuretics (yes/no)	4.984	1.843-13.477	0.002	1.832	0.552-6.079	0.323
Thiazide diuretics (yes/no)	2.179	1.452-3.270	0.000	1.579	0.909-2.744	0.105
MRA (yes/no)	1.079	0.567-2.053	0.817			
Statins (yes/no)	0.710	0.504-1.000	0.051			
Fibrates (yes/no)	0.578	0.184-1.814	0.347			
Digitalis (yes/no)	1.469	1.047-2.061	0.026	0.828	0.541-1.266	0.383
XO inhibitors (yes/no)	0.993	0.955-1.034	0.746			
Oxidative stress markers						
TAC (1 mmol/L)	2.405	0.993-5.824	0.052			
TOS (1 mmol/L)	1.044	0.986-1.104	0.139			
OSI (TOS/TAC)	1.016	0.966-1.068	0.537			

TABLE 3: Continued.

	Univariate Cox regression analysis			Multivariate Cox regression analysis		
	HR	95% CI	<i>p</i>	HR	95% CI	<i>p</i>
Uric acid (10 $\mu\text{mol/L}$)	1.029	1.018-1.040	0.000	1.014	1.001-1.028	0.042
Bilirubin (1 $\mu\text{mol/L}$)	1.029	1.018-1.039	0.000	0.995	0.977-1.013	0.580
PSH (1 $\mu\text{mol/g}$ of protein)	0.891	0.786-1.011	0.073			
MDA (1 $\mu\text{mol/L}$)	2.037	1.517-2.735	0.000	2.000	1.366-2.928	0.000

BMI: body mass index; NYHA: New York Heart Association functional class; VO_2 max.: maximum rate of oxygen consumption; LVEDD: left ventricle end-diastolic diameter; LVEDV: left ventricle end-diastolic volume; LVEF: left ventricle ejection fraction; NT-proBNP: N-terminal pro-B-type natriuretic peptide; CHF: chronic heart failure; ICD: implantable cardioverter defibrillator; ACE inhibitor: angiotensin-converting enzyme inhibitor; ARB: angiotensin-2 receptor blockers; MRA: mineralocorticoid receptor antagonists; XO: xanthine oxidase; TAC: total antioxidant capacity; TOS: total oxidant status; OSI: oxidative stress index; MDA: malondialdehyde; PSH: sulfhydryl groups; NS: nonsignificant.

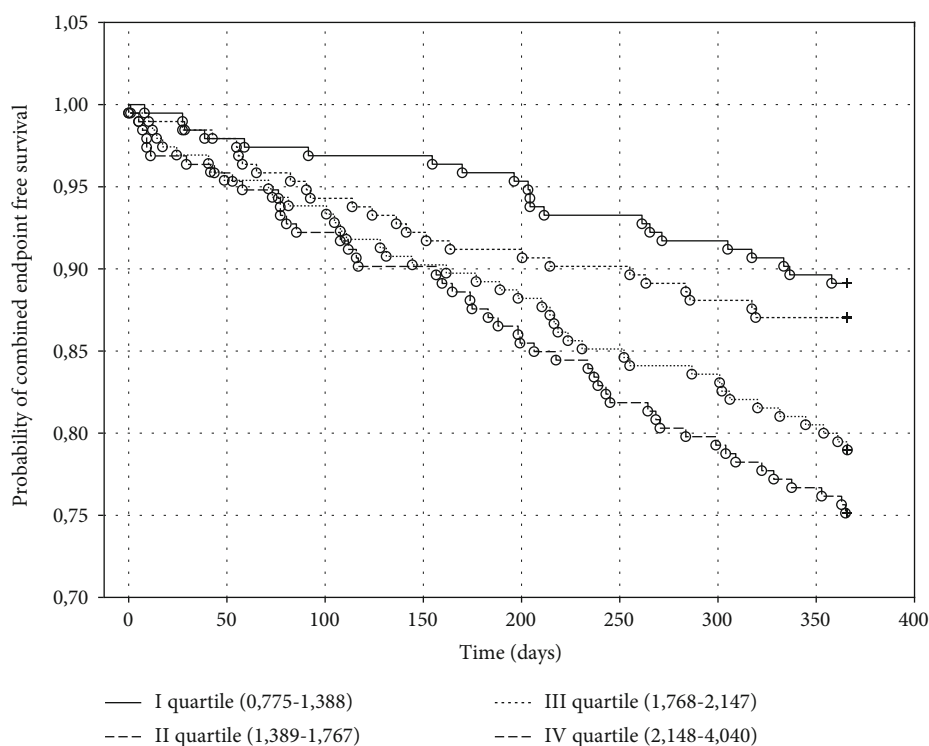


FIGURE 4: The Kaplan-Meier probability of combined endpoint-free survival in heart failure patients depending on serum malondialdehyde concentration in one-year follow-up. Significant coefficient for the whole model: $p < 0.001$.

radical production is indeed involved in HF and may be linked to its severity [27].

Our results are consistent with those of a study by Radovanovic et al., in which it was reported that high plasma MDA concentration ($>8 \mu\text{mol/L}$) was a significant independent predictor of mortality in 120 patients with chronic HF in median 13-month follow-up. The patients with MDA above cut-off had eight times higher mortality risk. Protein thiol groups were decreased only in patients with NYHA class IV and were not predictors of death. In our study, PSH concentration was lower in groups of patients who died and was a risk factor in univariate analysis; however, it showed no prognostic significance in multivariate model [28].

Similar predictive significance of MDA levels was also found in other oxidative diseases, such as chronic renal failure [29] and coronary artery disease [30].

The high plasma level of MDA was shown to be a strong independent predictor of cardiovascular disease and mortality in patients on hemodialysis [31].

The most representative subanalysis of the predictive value of MDA in 634 patients from the Prospective Randomized Evaluation of the Vascular Effects of Norvasc Trial showed that MDA is an independent risk factor for a cardiovascular event. Patients with MDA concentration in the highest quartile had a RR of 3.3 for major vascular events (myocardial infarction—fatal, nonfatal, stroke), RR of 4.1 for nonfatal vascular events (unstable angina), and RR of 3.8 for major vascular procedures (percutaneous interventions, coronary artery bypass grafting) as compared to the lowest quartile. In a multivariate analysis, the prognostic value was independent of the other inflammatory biomarkers (IL-6, CRP) and classical risk factors of atherosclerosis [30].

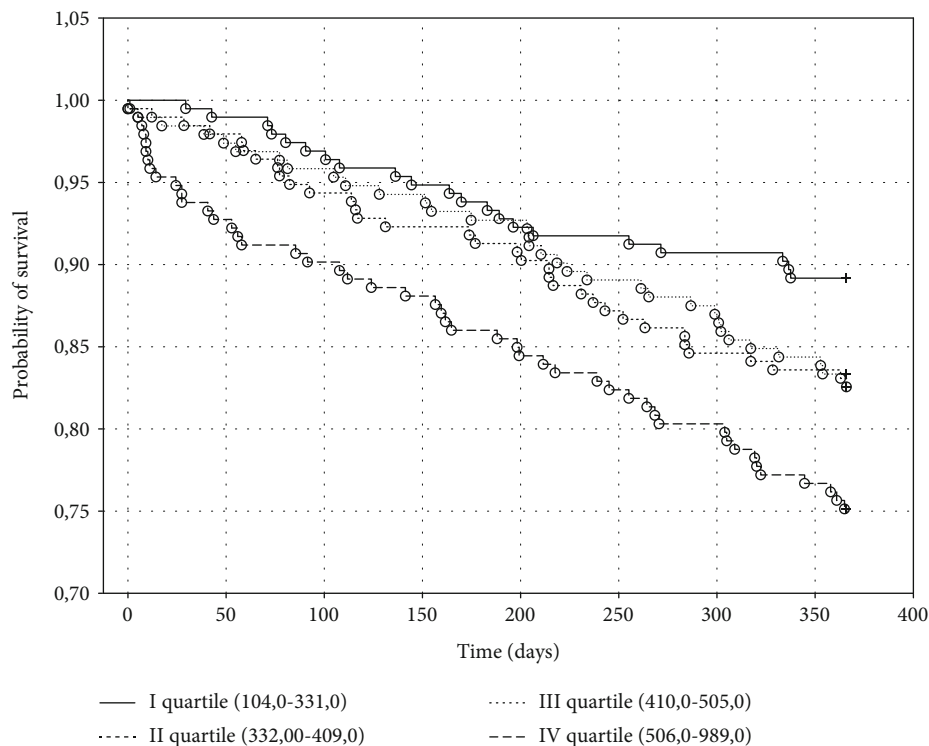


FIGURE 5: The Kaplan-Meier probability of combined endpoint-free survival in heart failure patients depending on uric acid concentration in one-year follow-up. Significant coefficient for the whole model: $p < 0.01$.

In the present study, patients with MDA levels in the highest quartile had a RR of 3.64 for death and a RR of 2.71 for combined endpoint as compared to the lowest quartile, and MDA was shown to be a strong independent predictor of adverse outcome in HF patients. MDA remained a strong poor prognosis biomarker even after adjustment for other important clinical and laboratory prognostic markers.

Similarly, elevated level of UA was an independent risk factor of death or urgent heart transplantation in 1-year follow-up. Participants with a UA level in the upper quartile had a RR of 3.21 for all-cause death and a RR of 2.73 for combined endpoint as compared to the lowest quartile. Results of UA testing as a predictor of death due to cardiovascular causes and all-cause death in different patient populations are not consistent. In the large epidemiological studies, the adjustment of UA to cardiovascular disease risk factors did not confirm the prognostic value of UA [32]. However, Ioachimescu et al. showed that an increase in serum UA by 1 mg% was associated with 39% increase in the risk of death in univariate Cox regression analysis and 26% increase in the risk of death in multivariate model (after adjusting for age, sex, alcohol consumption, smoking status, body mass index, blood pressure, history of cardiovascular disease, estimated glomerular filtration rate, levels of cholesterol fractions, plasma glucose levels, and other cardiovascular risk factors) in the cohort of patients with high risk of cardiovascular disease [33].

Similarly, in heart failure population, elevated serum UA levels were independently associated with an increased risk of

adverse clinical outcomes, both in patients with acute HF [34, 35] and in those with chronic HF [36].

The role of UA as a prognostic factor was confirmed in a study by Iliesiu et al. UA was the most powerful predictor of survival for patients with severe HF (NYHA classes III and IV), with a RR of 7.4 for death in patients with elevated UA (>9.5 mg/dL). Additionally, UA and MDA concentrations were higher in HF patients with lower EF and increased LV filling pressures, and a strong positive correlation between concentrations of MDA and UA was detected [37].

Similarly, the analysis by Wu et al. demonstrated that elevated serum UA levels are an independent predictor of mortality in patients with severe systolic HF [38]. Jankowska et al. documented that hyperuricemia was an independent predictor of death in 18-month follow-up in patients with mild and moderate HF (NYHA I-III) [39]. In a study by Anker et al., it was shown that high serum UA levels were a strong, independent marker of impaired prognosis in patients with moderate to severe HF in derivation and validation group. UA concentration ≥ 565 $\mu\text{mol/L}$ was a valid prognostic marker and useful for metabolic, hemodynamic, and functional staging in chronic HF [10].

Hyperuricemia in HF may be due to the upregulation of xanthine oxidase (XO), a key enzyme in the generation of oxygen free radicals and can reflect an impairment of oxidative metabolism [6]. Significant factors that may also increase the UA concentration in HF are reduced glomerular filtration rate and diuretic use. However, in the present study as well as other previous studies, a significant effect of hyperuricemia

on outcomes was observed even after the adjustment for risk factors including renal dysfunction and treatment with thiazide and loop diuretics [40, 41]. Although the question of whether UA is a marker of oxidative stress or a causal factor in the pathogenesis of HF remains unresolved, UA has the potential to serve as an important risk biomarker in heart failure patients. Gotsman et al. demonstrated that increased mortality in patients with UA in upper quartiles (>7.7 mg/dL) and treatment with allopurinol was associated with improved survival [42]. However, in a study by Wu et al., the adjusted risk of death associated with allopurinol use was similar to or slightly worse than the adjusted risk associated with the highest quartile UA among patients without treatment with allopurinol [38]. Givertz et al. showed that xanthine oxidase inhibition in the patients with elevated UA levels and reduced ejection fraction was not effective in improving quality of life, exercise capacity, clinical status, or left ventricular ejection fraction at 24-week follow-up [43]. The results obtained confirm the prognostic properties of UA in HF patients; however, like the study by Givertz et al., we did not show a protective effect of allopurinol therapy.

Serum bilirubin has more recently been described as an independent indicator of right ventricular dysfunction [44]. Allen et al. showed that elevated total bilirubin was the predictor of adverse outcome of cardiovascular death or HF hospitalization and all-cause mortality even after adjustment for other clinical prognostic variables [45]. In a small study by Charniot et al., the authors observed decreased TAC in acute HF patients and suggest that it may be responsible for arrhythmias and complications of AHF [46].

In our study, bilirubin and TAC had strong predictive power in univariate analysis. However, when incorporated into other well-established HF markers, there was no influence of bilirubin and TAC on adverse outcome in HF patients.

5. Conclusion

Our study, conducted on a large group of patients, had sufficient numbers of events to investigate a wide range of prognostically important clinical and laboratory variables, especially oxidative markers. Other authors had often assessed the effect of a single oxidative stress marker on the survival of HF patients. We have evaluated a wide range of oxidative stress markers and their impact on mortality and morbidity in HF patients. Finally, malondialdehyde and UA were strongly associated with worse prognosis in this group of patients, even after adjusting for a wide array of other predictors, even well-known NT-proBNP. Proposed biomarkers may be useful in terms of 1-year all-cause mortality. MDA and especially UA tests are widely available, noninvasive laboratory tests. In the light of the results obtained in this study, it seems that validation of elevated MDA and UA levels as independent predictors of outcome has a potentially significant value for risk stratification of chronic HF patients. However, the clinical usefulness of the above findings requires confirmation in subsequent studies.

Data Availability

The original data is available after contact with the corresponding author.

Conflicts of Interest

The authors declare that there is no conflict of interests regarding the publication of this paper.

Acknowledgments

This work was funded by the Medical University of Silesia grant no. KNW-1/096/K/8/0, Poland.

References

- [1] M. G. Crespo-Leiro, S. D. Anker, A. P. Maggioni et al., "European Society of Cardiology Heart Failure Long-Term Registry (ESC-HF-LT): 1-year follow-up outcomes and differences across regions," *European Journal of Heart Failure*, vol. 18, no. 6, pp. 613–625, 2016.
- [2] W. C. Levy, D. Mozaffarian, D. T. Linker et al., "The Seattle Heart Failure Model: prediction of survival in heart failure," *Circulation*, vol. 113, no. 11, pp. 1424–1433, 2006.
- [3] R. Pfister, H. Diedrichs, A. Schiedermaier et al., "Prognostic impact of NT-proBNP and renal function in comparison to contemporary multi-marker risk scores in heart failure patients," *European Journal of Heart Failure*, vol. 10, no. 3, pp. 315–320, 2008.
- [4] A. M. Richards, "What we may expect from biomarkers in heart failure," *Heart Failure Clinics*, vol. 5, no. 4, pp. 463–470, 2009.
- [5] B. Ky, B. French, W. C. Levy et al., "Multiple biomarkers for risk prediction in chronic heart failure," *Circulation: Heart Failure*, vol. 5, no. 2, pp. 183–190, 2012.
- [6] F. Leyva, S. D. Anker, I. F. Godsland et al., "Uric acid in chronic heart failure: a marker of chronic inflammation," *European Heart Journal*, vol. 19, no. 12, pp. 1814–1822, 1998.
- [7] R. B. D'Agostino Sr., R. S. Vasan, M. J. Pencina et al., "General cardiovascular risk profile for use in primary care: the Framingham Heart Study," *Circulation*, vol. 117, no. 6, pp. 743–753, 2018.
- [8] R. S. Velagaleti, P. Gona, M. G. Larson et al., "Multimarker approach for the prediction of heart failure incidence in the community," *Circulation*, vol. 122, no. 17, pp. 1700–1706, 2010.
- [9] C. Bergamini, M. Cicoira, A. Rossi, and C. Vassanelli, "Oxidative stress and hyperuricaemia: pathophysiology, clinical relevance, and therapeutic implications in chronic heart failure," *European Journal of Heart Failure*, vol. 11, no. 5, pp. 444–452, 2009.
- [10] S. D. Anker, W. Doehner, M. Rauchhaus et al., "Uric acid and survival in chronic heart failure: validation and application in metabolic, functional, and hemodynamic staging," *Circulation*, vol. 107, no. 15, pp. 1991–1997, 2003.
- [11] M. M. Kittleson, M. E. St John, V. Bead et al., "Increased levels of uric acid predict haemodynamic compromise in patients with heart failure independently of B-type natriuretic peptide levels," *Heart*, vol. 93, no. 3, pp. 365–367, 2007.

- [12] L. S. Terada, D. M. Guidot, J. A. Leff et al., "Hypoxia injures endothelial cells by increasing endogenous xanthine oxidase activity," *Proceedings of the National Academy of Sciences of the United States of America*, vol. 89, no. 8, pp. 3362–3366, 1992.
- [13] G. Lazzarino, P. Raatikainen, M. Nuutinen et al., "Myocardial release of malondialdehyde and purine compounds during coronary bypass surgery," *Circulation*, vol. 90, no. 1, pp. 291–297, 1994.
- [14] F. Leyva, S. Anker, J. W. Swan et al., "Serum uric acid as an index of impaired oxidative metabolism in chronic heart failure," *European Heart Journal*, vol. 18, no. 5, pp. 858–865, 1997.
- [15] "Studies Investigating Co-morbidities Aggravating Heart Failure (SICA-HF)," 2016, <https://clinicaltrials.gov/>.
- [16] G. M. Felker, L. K. Shaw, and C. M. O'Connor, "A standardized definition of ischemic cardiomyopathy for use in clinical research," *Journal of the American College of Cardiology*, vol. 39, no. 2, pp. 210–218, 2002.
- [17] The Criteria Committee of the New York Heart Association, *Nomenclature and Criteria for Diagnosis of Diseases of the Heart and Blood Vessels*, Little Brown, Boston, MA, USA, 1964.
- [18] R. M. Lang, M. Bierig, R. B. Devereux et al., "Recommendations for chamber quantification: a report from the American Society of Echocardiography's Guidelines and Standards Committee and the Chamber Quantification Writing Group, developed in conjunction with the European Association of Echocardiography, a branch of the European Society of Cardiology," *Journal of the American Society of Echocardiography*, vol. 18, no. 12, pp. 1440–1463, 2005.
- [19] O. Erel, "A new automated colorimetric method for measuring total oxidant status," *Clinical Biochemistry*, vol. 38, no. 12, pp. 1103–1111, 2005.
- [20] O. Erel, "A novel automated method to measure total antioxidant response against potent free radical reactions," *Clinical Biochemistry*, vol. 37, no. 2, pp. 112–119, 2004.
- [21] A. Acar, M. Ugur Cevik, O. Evliyaoglu et al., "Evaluation of serum oxidant/antioxidant balance in multiple sclerosis," *Acta Neurologica Belgica*, vol. 112, no. 3, pp. 275–280, 2012.
- [22] J. F. Koster, P. Biemond, and A. J. Swaak, "Intracellular and extracellular sulphhydryl levels in rheumatoid arthritis," *Annals of the Rheumatic Diseases*, vol. 45, no. 1, pp. 44–46, 1986.
- [23] H. Ohkawa, N. Ohishi, and K. Yagi, "Assay for lipid peroxides in animal tissues by thiobarbituric acid reaction," *Analytical Biochemistry*, vol. 95, no. 2, pp. 351–358, 1979.
- [24] O. Amir, H. Paz, O. Rogowski et al., "Serum oxidative stress level correlates with clinical parameters in chronic systolic heart failure patients," *Clinical Cardiology*, vol. 32, no. 4, pp. 199–203, 2009.
- [25] J. Hokamaki, H. Kawano, M. Yoshimura et al., "Urinary biopyrrins levels are elevated in relation to severity of heart failure," *Journal of the American College of Cardiology*, vol. 43, no. 10, pp. 1880–1885, 2004.
- [26] C. Wojciechowska, E. Romuk, A. Tomasik et al., "Oxidative stress markers and C-reactive protein are related to severity of heart failure in patients with dilated cardiomyopathy," *Mediators of Inflammation*, vol. 2014, Article ID 147040, 10 pages, 2014.
- [27] C. R. Díaz-Vélez, S. García-Castiñeiras, E. Mendoza-Ramos, and E. Hernández-López, "Increased malondialdehyde in peripheral blood of patients with congestive heart failure," *American Heart Journal*, vol. 131, no. 1, pp. 146–152, 1996.
- [28] S. Radovanovic, A. Savic-Radojevic, M. Pljesa-Ercegovac et al., "Markers of oxidative damage and antioxidant enzyme activities as predictors of morbidity and mortality in patients with chronic heart failure," *Journal of Cardiac Failure*, vol. 18, no. 6, pp. 493–501, 2012.
- [29] M. Boaz, Z. Matas, A. Biro et al., "Serum malondialdehyde and prevalent cardiovascular disease in hemodialysis," *Kidney International*, vol. 56, no. 3, pp. 1078–1083, 1999.
- [30] M. F. Walter, R. F. Jacob, B. Jeffers et al., "Serum levels of thiobarbituric acid reactive substances predict cardiovascular events in patients with stable coronary artery disease: a longitudinal analysis of the PREVENT study," *Journal of the American College of Cardiology*, vol. 44, no. 10, pp. 1996–2002, 2004.
- [31] B. Scott, A. Deman, P. Peeters et al., "Cardiac troponin T and malondialdehyde modified plasma lipids in haemodialysis patients," *Nephrology Dialysis Transplantation*, vol. 18, no. 4, pp. 737–742, 2003.
- [32] B. F. Culleton, M. G. Larson, W. B. Kannel, and D. Levy, "Serum uric acid and risk for cardiovascular disease and death: the Framingham Heart Study," *Annals of Internal Medicine*, vol. 131, no. 1, pp. 7–13, 1999.
- [33] A. G. Ioachimescu, D. M. Brennan, B. M. Hoar, S. L. Hazen, and B. J. Hoogwerf, "Serum uric acid is an independent predictor of all-cause mortality in patients at high risk of cardiovascular disease: a preventive cardiology information system (PreCIS) database cohort study," *Arthritis & Rheumatism*, vol. 58, no. 2, pp. 623–630, 2008.
- [34] J. A. Borovac, D. Glavas, J. Bozic, and K. Novak, "Predicting the 1-year all-cause mortality after hospitalization for an acute heart failure event: a real-world derivation cohort for the development of the S2PLiT-UG score," *Heart, Lung and Circulation*, pp. 1–9, 2019.
- [35] A. Palazzuoli, G. Ruocco, M. Pellegrini et al., "Prognostic significance of hyperuricemia in patients with acute heart failure," *The American Journal of Cardiology*, vol. 117, no. 10, pp. 1616–1621, 2016.
- [36] A. Mantovani, G. Targher, P. L. Temporelli et al., "Prognostic impact of elevated serum uric acid levels on long-term outcomes in patients with chronic heart failure: a post-hoc analysis of the GISSI-HF (Gruppo Italiano per lo Studio della Sopravvivenza nella Insufficienza Cardiaca-Heart Failure) trial," *Metabolism*, vol. 83, pp. 205–215, 2018.
- [37] A. Iliesiu, A. Campeanu, D. Marta, I. Parvu, and G. Gheorghe, "Uric acid, oxidative stress and inflammation in chronic heart failure with reduced ejection fraction," *Revista Romana de Medicina de Laborator*, vol. 23, no. 4, pp. 397–406, 2015.
- [38] A. H. Wu, J. K. Ghali, G. W. Neuberg, C. M. O'Connor, P. E. Carson, and W. C. Levy, "Uric acid level and allopurinol use as risk markers of mortality and morbidity in systolic heart failure," *American Heart Journal*, vol. 160, no. 5, pp. 928–933, 2010.
- [39] E. A. Jankowska, B. Ponikowska, J. Majda et al., "Hyperuricaemia predicts poor outcome in patients with mild to moderate chronic heart failure," *International Journal of Cardiology*, vol. 115, no. 2, pp. 151–155, 2007.
- [40] S. Hamaguchi, T. Furumoto, M. Tsuchihashi-Makaya et al., "Hyperuricemia predicts adverse outcomes in patients with heart failure," *International Journal of Cardiology*, vol. 151, no. 2, pp. 143–147, 2011.

- [41] W. Doehner, M. Rauchhaus, V. G. Florea et al., "Uric acid in cachectic and noncachectic patients with chronic heart failure: relationship to leg vascular resistance," *American Heart Journal*, vol. 141, no. 5, pp. 792–799, 2001.
- [42] I. Gotsman, A. Keren, C. Lotan, and D. R. Zwas, "Changes in uric acid levels and allopurinol use in chronic heart failure: association with improved survival," *Journal of Cardiac Failure*, vol. 18, no. 9, pp. 694–701, 2012.
- [43] M. M. Givertz, K. J. Anstrom, M. M. Redfield et al., "Effects of xanthine oxidase inhibition in hyperuricemic heart failure patients: the xanthine oxidase inhibition for hyperuricemic heart failure patients (EXACT-HF) study," *Circulation*, vol. 131, no. 20, pp. 1763–1771, 2015.
- [44] S. Yusuf, M. A. Pfeffer, K. Swedberg et al., "Effects of candesartan in patients with chronic heart failure and preserved left-ventricular ejection fraction: the CHARM-Preserved Trial," *The Lancet*, vol. 362, no. 9386, pp. 777–781, 2003.
- [45] L. A. Allen, G. M. Felker, S. Pocock et al., "Liver function abnormalities and outcome in patients with chronic heart failure: data from the Candesartan in Heart Failure: Assessment of Reduction in Mortality and Morbidity (CHARM) program," *European Journal of Heart Failure*, vol. 11, no. 2, pp. 170–177, 2009.
- [46] J. C. Charniot, N. Vignat, J. P. Albertini et al., "Oxidative stress in patients with acute heart failure," *Rejuvenation Research*, vol. 11, no. 2, pp. 393–398, 2008.

Research Article

Stimulation of Na⁺/K⁺-ATPase with an Antibody against Its 4th Extracellular Region Attenuates Angiotensin II-Induced H9c2 Cardiomyocyte Hypertrophy via an AMPK/SIRT3/PPAR γ Signaling Pathway

Siping Xiong,¹ Hai-Jian Sun ¹, Lei Cao,¹ Mengyuan Zhu,¹ Teng teng Liu,¹ Zhiyuan Wu,¹ and Jin-Song Bian ^{1,2}

¹Department of Pharmacology, Yong Loo Lin School of Medicine, National University of Singapore, Singapore 117597

²National University of Singapore (Suzhou) Research Institute, Suzhou, China

Correspondence should be addressed to Jin-Song Bian; phcbjs@nus.edu.sg

Received 9 March 2019; Revised 9 July 2019; Accepted 2 August 2019; Published 15 September 2019

Guest Editor: Aneta Radziwon-Balicka

Copyright © 2019 Siping Xiong et al. This is an open access article distributed under the Creative Commons Attribution License, which permits unrestricted use, distribution, and reproduction in any medium, provided the original work is properly cited.

Activation of the renin-angiotensin system (RAS) contributes to the pathogenesis of cardiovascular diseases. Sodium potassium ATPase (NKA) expression and activity are often regulated by angiotensin II (Ang II). This study is aimed at investigating whether DR-Ab, an antibody against 4th extracellular region of NKA, can protect Ang II-induced cardiomyocyte hypertrophy. Our results showed that Ang II treatment significantly reduced NKA activity and membrane expression. Pretreatment with DR-Ab preserved cell size in Ang II-induced cardiomyopathy by stabilizing the plasma membrane expression of NKA and restoring its activity. DR-Ab reduced intracellular ROS generation through inhibition of NADPH oxidase activity and protection of mitochondrial functions in Ang II-treated H9c2 cardiomyocytes. Pharmacological manipulation and Western blotting analysis demonstrated the cardioprotective effects were mediated by the activation of the AMPK/Sirt-3/PPAR γ signaling pathway. Taken together, our results suggest that dysfunction of NKA is an important mechanism for Ang II-induced cardiomyopathy and DR-Ab may be a novel and promising therapeutic approach to treat cardiomyocyte hypertrophy.

1. Introduction

Cardiovascular disorders are one of the most common diseases in adults and the leading cause of death worldwide [1]. Pathological activation of renin-angiotensin system (RAS) is a key factor in several cardiovascular diseases [2]. Angiotensin (Ang) II, a critical component of RAS, presents in both systemic circulation and local organs such as the brain, blood vessel, kidney, and heart [2, 3]. Multiple studies reported that increased Ang II leads to hypertension and also directly promotes cardiomyocyte death, hypertrophy, and remodeling [2]. They have proved that Ang II is involved in cardiomyocyte damage [4–6]. Unscrambling the underline mechanisms of Ang II may supply a new therapeutic target for the prevention and treatment of these diseases.

In most mammalian cells, sodium potassium ATPase (NKA) is an energy-transducing ion pump across the plasma membrane [7]. In the past decade, NKA has also been proved to be an ion-pumping-independent receptor function that confers a ligand-like effect of cardiotonic steroids (CTS) on protein/lipid kinases, intracellular Ca²⁺ oscillation, and ROS production [8, 9]. However, drugs targeted at NKA are mainly CTS which was used to treat chronic heart failure, a kind of cardiovascular diseases. These chemical drugs also often cause severe toxic effects, such as cardiac arrhythmias and atrioventricular block, gastrointestinal disorders, nervous system disorders, anorexia, blurred vision, nausea, and vomiting [10]. In recent years, we and other groups have demonstrated that antibody targeted at DR region (897DVEDSYGQQWTYEQR911, amino acid sequence

number showed as in rat), the 4th extracellular domain of α -subunit of NKA, can activate NKA's function [10, 11]. Our previous studies have already proved that DR-Ab produces cardioprotection and protects isoproterenol-induced mouse cardiac injury [10, 12]. Therefore, this antibody was a kind of ideal tool to study the NKA function in relative studies.

Recently, extensive studies have demonstrated that Ang II has a close relationship with NKA. Rasmussen's group reported that Ang II induced NKA inhibition in cardiac myocytes via PKC-dependent activation of NADPH oxidase [13]. Massey et al. also reported that Ang II-dependent phosphorylation of the rat kidney NKA at specific sites can regulate how the NKA releases bound cardiac glycoside [14]. Moreover, Ang II inhibits the NKA activity accompanied with the involvement of an increase in NADPH oxidase-derived $O_2^{\cdot-}$ [15]. Thus, the present study was designed to study the effects of DR-Ab in Ang II-induced cardiac myocyte damage and its underlying mechanism.

2. Material and Methods

2.1. Chemicals and Reagents. Antibodies against p22^{phox}, p47^{phox}, Na⁺/K⁺-ATPase alpha 1 (NKA α 1), PPAR- γ , Sirt-3, β -actin, GAPDH, β -tubulin, and the horseradish peroxidase-conjugated secondary antibodies were purchased from Santa Cruz Biotechnology Inc. (Santa Cruz, CA, USA). Antibodies against phosphorylated and total AMPK were purchased from Cell Signaling Technology (Beverly, MA, USA). The specific primers were synthesized by Integrated DNA Technologies Pte. Ltd. (Singapore). Antibody against α -actinin was obtained from Abcam (Cambridge, MA, USA). Mitochondrial membrane potential assay kit with JC-1 and the kits for measurement of ATP were purchased from Beyotime Institute of Biotechnology (Shanghai, China). Dihydroethidium (DHE) and 2',7'-dichlorofluorescein diacetate (DCFH-DA) were purchased from Sigma-Aldrich (St. Louis, MO, USA). MitoSOXTM was purchased from Invitrogen (Carlsbad, CA, USA). AMPK inhibitor compound C, a selective Sirt3 inhibitor 3-TYP, and PPAR γ antagonists GW9662 were obtained from Cayman Chemical Company (Ann Arbor, MI, USA). DR-Ab was generated and identified in our lab as previously described [12, 16].

2.2. Cell Culture. Embryonic rat heart-derived cells (H9c2, passage 15) preserved by our lab were cultured in high-glucose Dulbecco's modified Eagle's medium (4.5 g/l glucose) supplemented with 10% fetal bovine serum (FBS) and 1% antibiotics (penicillin-streptomycin, Gibco) in humidified air containing 5% CO₂ at 37°C.

Primary neonatal mouse cardiomyocytes: the cardiomyocytes were isolated from 1- to 3-day-old C57BL/6 neonatal mice as described previously [17–19]. In short, the hearts were placed into ice-cold Hanks' balanced saline solution (HBSS; Life Technologies). After removal of atrial and aortic appendages, the cardiomyocytes were collected by using 0.2 mg/ml collagenase type II (Worthington Biochemical, Lakewood, NJ) and 0.6 mg/ml pancreatin (Sigma, MAK030, St. Louis, MO) at common cellular incubator. The supernatant-containing suspended cells were cultured in

minimum essential medium with 10% fetal bovine serum for 2 h to remove nonmyocytes. Then, the culture medium was changed to minimum essential medium containing 10% FBS with 1% antibiotics after seeding for 48 h. Cardiomyocytes were seeded 3 days prior to use.

All primary cell culture protocols were performed strictly according to the principles and guidance of Institutional Animals Care and Use Committee at the National University of Singapore.

2.3. Intracellular and Mitochondrial ROS Measurement. After fixing collected H9c2 cells, they were incubated with DHE (10 μ M) and DCFH-DA (10 μ M) in a dark and humidified incubator at 37°C for 30 min as previously described [20] and changed the solution to phosphate-buffered saline (PBS) and observed on microscope immediately.

Mitochondrial ROS production was measured with a fluorogenic dye named MitoSOX Red (Invitrogen, Darmstadt, Germany). Cells were loaded with 1 μ M MitoSOX Red for 30 min at 37°C protecting from light and washed cells with PBS and then observed on microscope (DMi 8; Leica, Microsystems, Germany).

The fluorescence signals were captured and analyzed with the Image-Pro Plus 6.0 (Version 6.0, Media Cybernetics, Bethesda, MD, USA) in same parameters.

2.4. Western Blotting Analysis. After washing twice with PBS, the cells were lysed with ice-cold lysis buffer. The cell lysate was centrifuged at 10,000 g for 10 min at 4°C. Equal amount of proteins was electrophoresed, transferred, blotted, and then incubated with required primary antibodies at 4°C overnight. After washing with TBST buffer three times, the membranes were incubated with appropriate secondary horseradish peroxidase- (HRP-) conjugated antibodies. Then, membranes were detected using an ECL Advanced Western Blot Detection Kit (Millipore Darmstadt, Germany). The integrated optical density was quantified with the Image-Pro Plus 6.0 software.

2.5. Measurement of Mitochondrial Membrane Potential. Mitochondrial membrane potential was detected with 5,5',6,6'-tetrachloro-1,1',3,3'-tetraethylbenzimidazolcarbocyanine iodide (JC-1) (Beyotime Institute of Biotechnology, Shanghai, China). The H9c2 cells were stained with JC-1 and observed with a fluorescence microscope (DMi 8; Leica, Microsystems, Germany).

2.6. Real-Time PCR. Total RNA extraction was performed with TRIzol (Life Technologies, USA) according to the manufacturer's instructions, and then RevertAid First-Strand cDNA Synthesis Kit (Thermo Scientific, USA) was used for reverse transcription. Following, GoTaq[®] quantitative PCR (qPCR) Master Mix (Promega, USA) was used for quantitative PCR with indicated primers on a VIIA(TM) 7 System (Applied Biosystems). Data were analyzed by normalization against GAPDH. The primers used are indicated as in Table 1.

2.7. Plasma Membrane Extraction. EZ-Link NHS-SS-biotin (Pierce Chemical Co., USA) was used to label surface protein

TABLE 1

Gene (rat)	Primer sequences (5'-3')
GAPDH	Forward: AGGAGTAAGAAACCTGGAC
	Reverse: CTGGGATGGAATTGTGAG
ANF	Forward: CCGTATACAGTGCGGTGTCC
	Reverse: CAGAGAGGGAGCTAAGTGCC
BNP	Forward: AGCTGCTTTGGGCAGAAGAT
	Reverse: AAAACAACCTCAGCCCCTCA
β -MHC	Forward: GACAACGCCTATCAGTACATG
	Reverse: TGGCAGCAATAACAGCAAAA
ND1	Forward: AAGCGGCTCCTTCTCCCTACAAAT
	Reverse: GAAGGGAGCTCGATTTGTTTCTGC
Cytb	Forward: GCAGCTTAACATTCCGCCAATCA
	Reverse: TGTTCTACTGGTTGGCCTCCGATT
mt-co1	Forward: AAGGTTTGGTCTGGCCTTA
	Reverse: GGCAAGGCGTCTTGAGCTAT
CPT-1 β	Forward: TCAAGGTTTGGCTCTATGAGGGCT
	Reverse: TCCAGGGACATCTTGTCTTGCCA
CPT-2	Forward: TCCTGCATACCAGCAGATGAACCA
	Reverse: TATGCAATGCCAAAGCCATCAGGG
LCAD	Forward: AATGGGAGAAAGCCGGAGAAGTGA
	Reverse: GATGCCGCCATGTTTCTCTGCAAT
MCAD	Forward: CTGCTCGCAGAAATGGCGATGAAA
	Reverse: CAAAGGCCTTCGCAATAGAGGCAA
Gene (mouse)	Primer sequences (5'-3')
β -Actin	Forward: CCGTGAAGATGACCCAGA
	Reverse: CTGGGATGGAATTGTGAG
ANP	Forward: ACCTGCTAGACCACCTGGAG
	Reverse: CCTTGGCTGTTATCTTCGGTACCGG
BNP	Forward: GAGGTCACCTATCCTCTGG
	Reverse: GCCATTTCCCTCCGACTTTTCTC
β -MHC	Forward: CCGAGTCCCAGGTCAACAA
	Reverse: CTTCACGGGCACCCCTTGGGA

for 1 h. Cells were washed with PBS containing 100 mM glycine and then lysed in lysis buffer. After protein quantitative, equal proteins (150–300 μ g) were added to Streptavidin (Pierce Chemical Co.) beads at 4°C overnight. Next day, beads were washed thoroughly, resuspended in 30 μ l loading buffer, and analyzed using Western blots.

2.8. Isolation of Endosomes. The preparation of endosomes was fractionated on a floatation gradient. In brief, the treated cells were washed by cold PBS and homogenization buffer (250 mM sucrose and 3 mM imidazole, pH 7.4). After centrifuging for 10 min at 2000 \times g in 4°C, the supernatant was adjusted to 40.6% sucrose, followed by incubation of 35% sucrose supplemented with 3 mM imidazole and 0.5 mM EDTA and homogenization buffer. The samples were centrifuged at 210,000 \times g for 1.5 h; the endosomes were then obtained at the homogenization buffer–35% sucrose interface. The endosome fraction was identified by immunoblots for Rab 7 as previously described [12, 21].

2.9. Measurement of NKA Activity. NKA activity was determined according to previous study [22, 23]. H9c2 cells were homogenized in buffer A containing 20 mM HEPES, 250 mM sucrose, 2 mM EDTA, 1 mM MgCl₂, pH 7.4, and then centrifuged at 20,000 g for 30 min. Consequently, resuspended the pellet in buffer A again and quantified the protein. One 50 μ l aliquot of homogenate was mixed with 50 μ l of reaction buffer 1 (200 mM Tris-HCl, 30 mM MgCl₂, 200 mM NaCl, 60 mM KCl, 10 mM EGTA, pH 7.5). Another 50 μ l aliquot was mixed with reaction buffer 2 (buffer 1 +1 mM ouabain). To prevent protein degradation, 100 μ g/ml PMSF, 2 μ g/ml aprotinin, and 2 μ g/ml pepstatin A were added in. After 1 mM of ATP was added, the mixtures were incubated for 10 min at 37°C and then stopped by adding 10 μ l of 100% (w/v) trichloroacetic acid. After incubating them on ice for 1 h, they were centrifuged at 20,000 g for 30 min. The supernatant without phosphate was assayed with the Phosphate Colorimetric Kit (Sigma, MAK030, St. Louis, MO) at 650 nm.

2.10. Immunofluorescence Staining. Immunofluorescent staining was performed as described previously [24]. The collected H9c2 cardiomyocytes or primary neonatal mouse cardiomyocytes were fixed in freshly made -20°C ethanol at room temperature for 10 min and then permeabilized with 0.1% Triton X-100. After blocking with 5% BSA at room temperature for 1 h, the cells were incubated with the mouse anti-NKA antibody or mouse anti- α -actinin overnight at 4°C. Next, the cells were washed with PBS three times, and then incubated with goat anti-mouse cross-adsorbed secondary antibody, Alexa Fluor 488 (Invitrogen, Carlsbad, CA, USA) for 1 h at room temperature, and the nucleus was stained with DAPI. Goat anti-mouse IgG (H+L) cross-adsorbed secondary antibody, Alexa Fluor 488 (Invitrogen, Carlsbad, CA, USA). The images were captured with a fluorescence microscope (Leica DMi8, Leica, Wetzlar, Germany).

2.11. Statistical Analysis. Data were expressed as mean \pm SD. One-way or two-way ANOVA followed by the post hoc Bonferroni test was used for multiple comparisons. A value of $p < 0.05$ was considered statistically significant.

3. Results

3.1. DR-Ab Improves Ang II-Induced Cardiomyocyte Hypertrophy through Preservation of NKA Activity. The immunofluorescence staining of α -actin was performed to reveal the H9c2 cardiomyocyte morphology (Figure 1(a)) and primary cultured neonatal mouse cardiomyocytes (Figure S1A). It was found that Ang II (100 nM, 48 h) treatment significantly increased the cell size of cardiomyocytes, and this effect was attenuated by pretreatment with DR-Ab (2 μ M, 30 min) (Figure 1(b) and Figure S1B). We also examined the mRNA expression of various hypertrophic biomarkers like atrial natriuretic peptide (ANP), brain natriuretic peptide (BNP), and beta-myosin heavy chain (β -MHC). Similar to what we observed in myocyte morphology, pretreatment with DR-Ab significantly attenuated Ang II-stimulated the above three hypertrophic biomarkers (Figure 1(c) and Figures S1C–S1E).

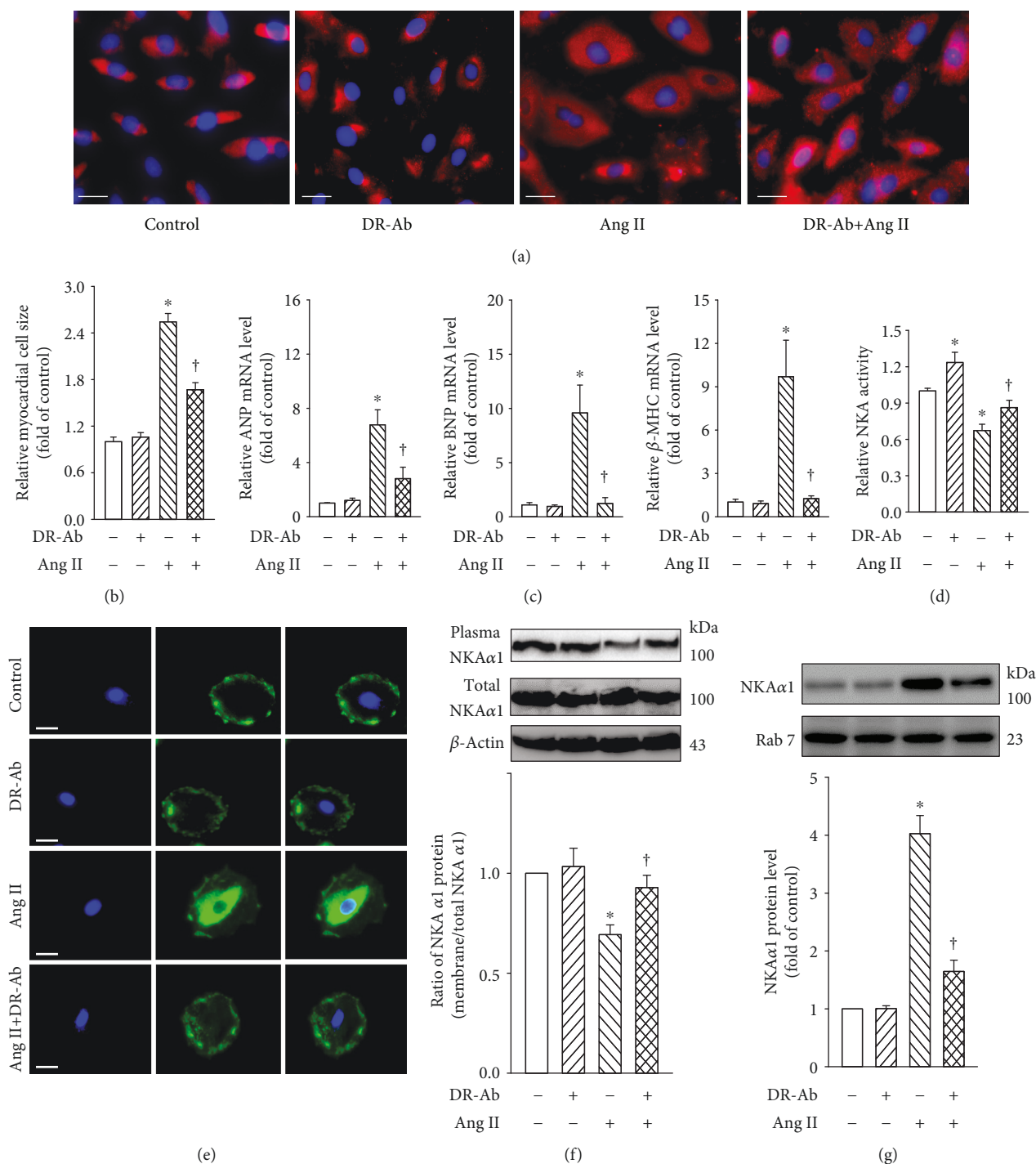


FIGURE 1: Effects of DR-Ab on Ang II-induced H9c2 cardiomyocyte hypertrophy. DR-Ab (2 μ M) was given 30 min before treatment with Ang II (100 nM) for 48 h. (a, b) Representative immunofluorescence staining (a) and group data (b) showing that DR-Ab reversed enlarged cell size caused by Ang II. Red: α -actinin. Blue: DAPI. Scale bar, 25 μ m. *n* = 6. (c) qRT-PCR analysis showing the mRNA levels of ANP, BNP, and β -MHC. *n* = 4. (d–g) DR-Ab reversed Ang II-induced loss of plasma membrane NKA α 1 (e, f), increase of endosome NKA α 1 (g), and downregulation of NKA activity (d). *n* = 4–6. Scale bar, 30 μ m. Blue: DAPI. Green: NKA α 1 staining. **p* < 0.05 versus control group, †*p* < 0.05 versus Ang II alone group.

To study the underlying mechanisms, we first determined the effect of DR-Ab on NKA activity. As shown in Figure 1(d), DR-Ab attenuated Ang II-impaired NKA activity in the H9c2 cardiomyocytes (Figure 1(d)). We further

examined the plasma membrane and total expression of NKA with Western blots and immunostaining. As shown in Figures 1(e)–1(g), treatment with Ang II reduced plasma membrane NKA expression (Figures 1(e) and 1(f) and S1F)

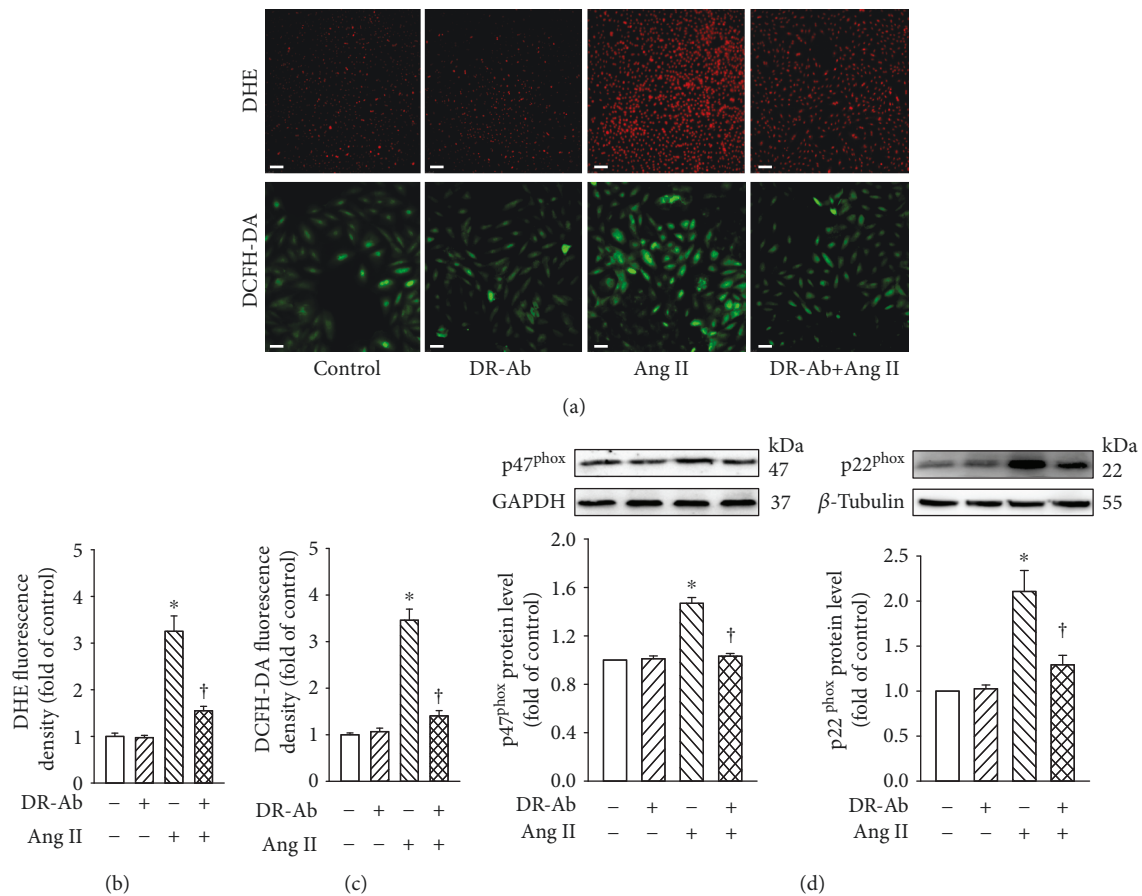


FIGURE 2: Effects of DR-Ab on Ang II-induced intracellular ROS generation in H9c2 cells. DR-Ab (2 μM) was given 30 min before treatment with Ang II (100 nM) for 48 h. (a–c) Representative immunofluorescence image (a) and group data (b, c) showing that DR-Ab decreased ROS generation caused by Ang II. Red: DHE staining (a, upper). Scale bar, 100 μm . Green: DCFH-DA staining (a, lower). Scale bar, 50 μm . $n = 6$. (d) Effect of DR-Ab on the protein level of two subunits of NADPH oxidase: p22^{phox} and p47^{phox}. $n = 4-6$. * $p < 0.05$ versus control group, † $p < 0.05$ versus Ang II alone group.

and increased endosome NKA expression (Figures 1(g) and S1G), but had minor effect on its total protein expression. Pretreatment with DR-Ab reversed the effect of Ang II on plasma and endosome NKA expression. Taken together, our experiments indicated that DR-Ab inhibits plasma membrane NKA endocytosis. Our data imply that membrane NKA expression and activity are important in regulation of cell size when RAS is upregulated.

3.2. DR-Ab Alleviates Ang II-Induced Intracellular ROS Generation in H9c2 Cells. Oxidative stress plays an important role in Ang II-induced cardiomyopathy [2]. We first detected whether DR-Ab can affect Ang II-induced intracellular ROS production by using both DHE and DCFH-DA staining kits. As shown in Figures 2(a)–2(c), Ang II (100 nM, 48 h) significantly increased the generation of superoxide, hydroxyl, peroxyl, and other ROS. Pretreatment with DR-Ab (2 μM , 30 min), which itself had no obvious effect, significantly reduced Ang II-induced intracellular ROS generation (Figures 2(a)–2(c)).

To examine the involvement of NADPH oxidase, we detected the protein expression of two subunits of NADPH oxidase (NOX2): p22^{phox} and p47^{phox}. Western blotting

analysis showed that treatment with Ang II upregulated the protein expression of these two proteins and this effect was attenuated by pretreatment with DR-Ab in both H9c2 and neonatal mouse cardiomyocytes (Figures 2(d) and S1). Our data suggest that DR-Ab may inhibit NADPH oxidase activity in pathological situations.

3.3. DR-Ab Prevents Ang II-Induced Mitochondrial ROS and Energy Metabolic Dysfunction. We further studied mitochondrial ROS generation with MitoSOX™ Red staining. As shown in Figures 3(a) and 3(b), Ang II significantly increased mitochondrial ROS generation in the mitochondria, and this effect was reversed by pretreatment with DR-Ab. The mitochondrial permeability transition, an important step in the induction of cellular apoptosis, was also determined using the unique fluorescent cationic dye, JC-1. It was found that Ang II induced loss of red JC-1 aggregate fluorescence, and only green monomer fluorescence was detected in the cytoplasm of these cells (Figure 3(c)). This effect was also reversed by DR-Ab treatment.

We continued to study the mRNA levels of mitochondrial DNA-encoded genes including ND-1, cyt-b, and mt-co1. Real-time PCR analysis showed that pretreatment

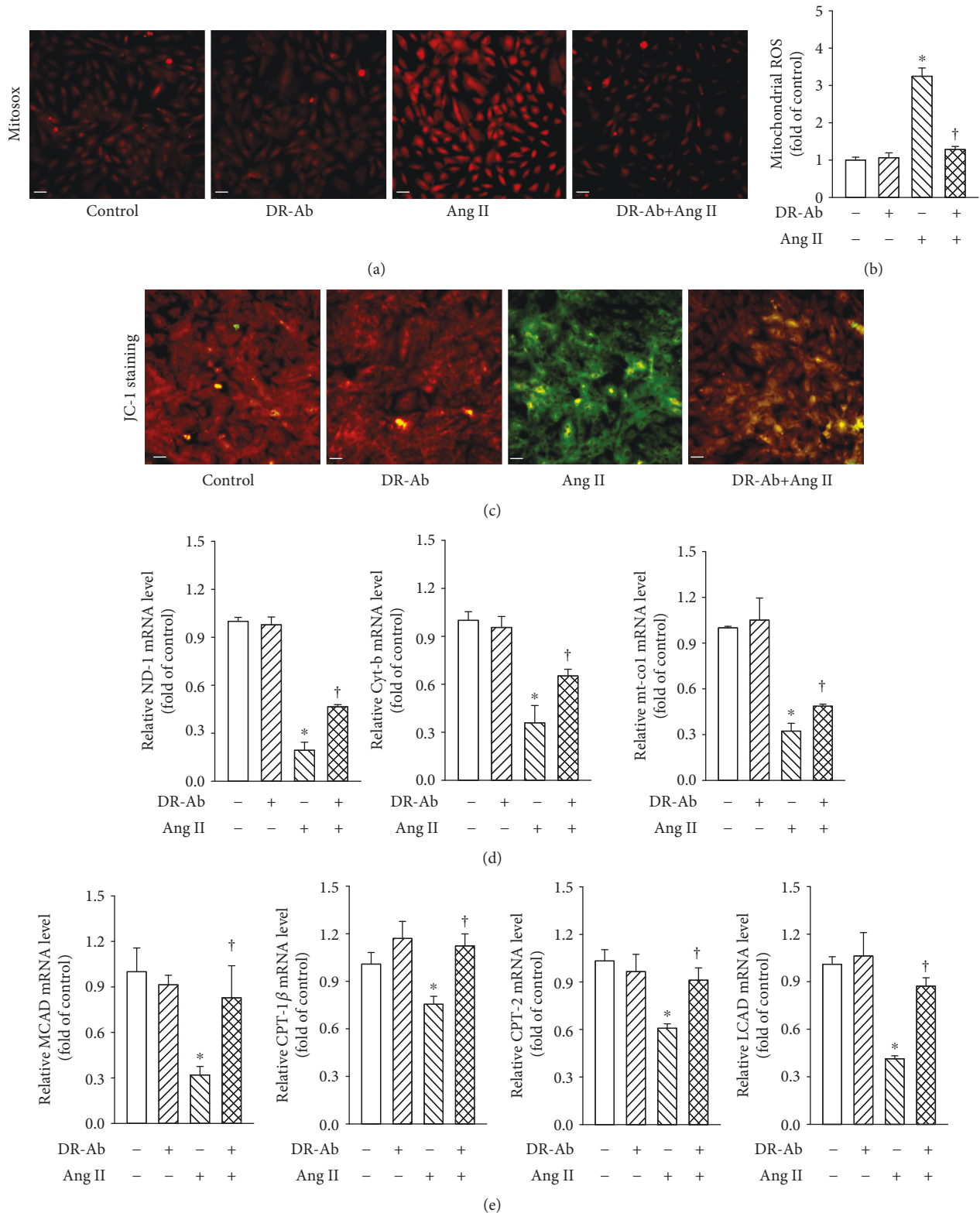
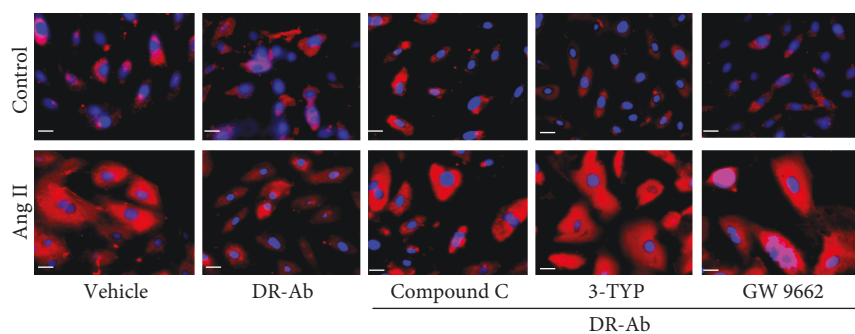
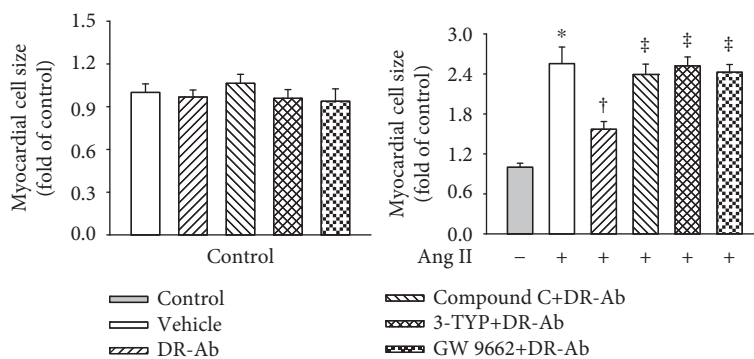


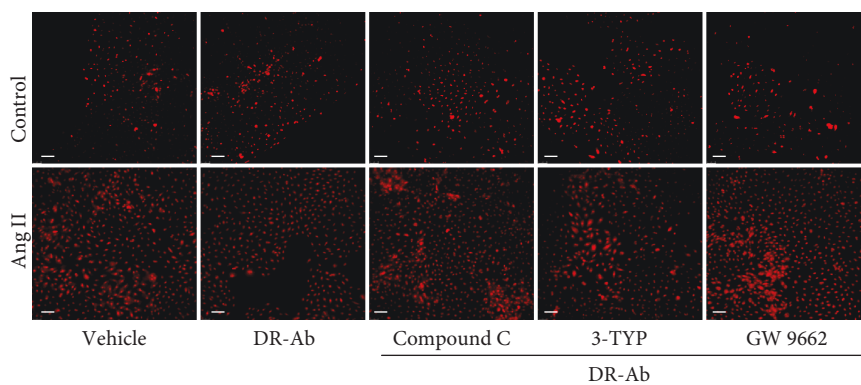
FIGURE 3: Effect of DR-Ab on Ang II-induced mitochondrial ROS (mit-ROS) generation and energy metabolic dysfunction. (a, b) Representative image (a) and group data (b) showing that DR-Ab decreased Ang II-induced mit-ROS generation. Red: Mit-ROS. Scale bar, 50 μm . $n = 4-6$. (c) Representative JC-1 staining showing that DR-Ab reversed mitochondrial membrane potential loss caused by Ang II. Red: aggregate. Green: monomer. Scale bar, 50 μm . (d) qRT-PCR analysis showing that DR-Ab increased the mRNA expression of mitochondrial encoded genes (ND-1, Cyt-b, and mt-co1) in Ang II-treated cells. $n = 4$. (e) qRT-PCR analysis showing the effect of DR-Ab on the mRNA expression of fatty acid oxidation related genes (CPT-1 β , CPT-2, LCAD, and MCAD). $n = 4$. * $p < 0.05$ versus control group, $\dagger p < 0.05$ versus Ang II alone group.



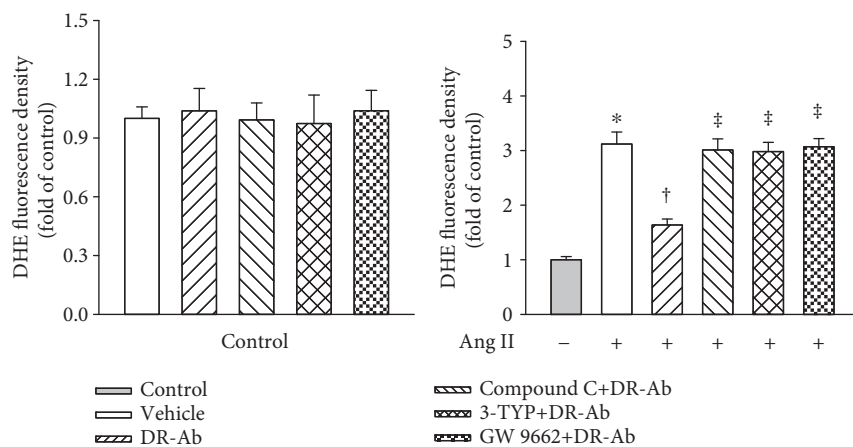
(a)



(b)



(c)



(d)

FIGURE 4: Continued.

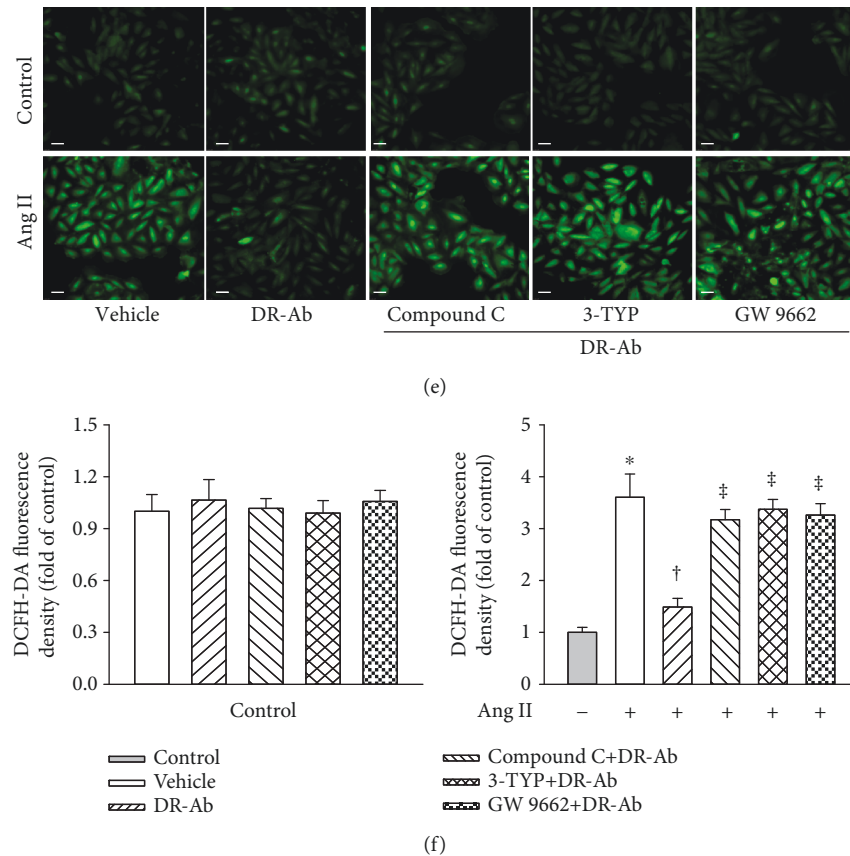


FIGURE 4: Effect of DR-Ab on myocyte hypertrophy and intracellular ROS generation in Ang II-treated H9c2 in the presence and absence of compound C (40 μ M, a selective AMPK inhibitor), 3-TYP (50 μ M, a selective Sirt3 inhibitor), or GW9662 (10 μ M, a PPAR γ antagonist). Cells were treated with these inhibitors for 30 min before DR-Ab (2 μ M, 30 min) and Ang II (100 nM, 48 h). (a, b) Representative immunofluorescence staining (a) and group data (b) showing that blockade of AMPK, Sirt3, or PPAR γ abolished the effect of DR-Ab on cell size. Red: α -actinin. Blue: DAPI. Scale bar, 25 μ m. $n = 4-6$. (c-f) Representative image (c, e) and group data (d, f) showing that blockade of AMPK, Sirt3, or PPAR γ promoted the intracellular ROS which were decreased by DR-Ab in Ang II-induced cells. (c) Red: DHE relative fluorescence density. Scale bar, 100 μ m. $n = 4-6$. (e) Green: DCFH-DA staining. Scale bar, 50 μ m. * $p < 0.05$ versus control, [†] $p < 0.05$ versus Ang II alone group, [‡] $p < 0.05$ versus Ang II+DR-Ab group.

with DR-Ab significantly attenuated Ang II-suppressed expression of these genes (Figure 3(d)). Our data imply that DR-Ab recovered impaired mitochondrial function induced by Ang-II.

Fatty acid oxidation (FAO) is one of the pivotal mechanisms involved in the development of cardiomyopathy [25]. We also studied whether DR-Ab can affect fatty acid metabolism in Ang-II-induced H9C2 cardiomyocyte damage. As shown in Figure 3(e), Ang II-significantly reduced the mRNA expression of FAO-related genes including CPT-1 β , CPT-2, long-chain acyl-CoA dehydrogenase (LCAD), and medium-chain acyl-CoA dehydrogenase (MCAD), and these effects were reversed by pretreatment with DR-Ab. These data suggest that DR-Ab may improve Ang II-induced impaired fatty acid oxidation.

3.4. DR-Ab Protects H9c2 Cardiomyocytes against Ang II-Induced Hypertrophy via Activation of AMPK/Sirt-3/PPAR γ Signaling Pathway. It is well known that the AMPK/Sirt-3/PPAR γ signaling pathway participates in Ang II-induced cardiomyocyte hypertrophy [26–34]. In this study,

we also tested the involvement of this pathway in the effect of DR-Ab. We first repeated the effects of DR-Ab on cell morphology (Figures 4(a) and 4(b)), intracellular (Figures 4(c)–4(f)) and mitochondrial ROS (Figures 5(a) and 5(b)) generation, mitochondrial membrane potential loss (Figure 5(c)), and mitochondrial function-related gene level (Figures 5(d)–5(h)) in the presence and absence of compound C, an AMPK inhibitor, 3-TYP, a selective Sirt3 inhibitor, and GW9662, a PPAR γ antagonist. As shown in Figures 4 and 5, all these inhibitors abolished the protective effects of DR-Ab. Our data suggest that the AMPK/Sirt-3/PPAR γ signaling pathway mediates the cardioprotective effects of DR-Ab.

To further confirm the involvement of this signaling pathway, we observed the effect of DR-Ab on AMPK phosphorylation (P-AMPK). A time-course study showed that DR-Ab obviously increased P-AMPK level and the strongest effect was observed when cells were treated with DR-Ab for 30 min (Figure 6(a)). For this reason, DR-Ab reversed Ang II-suppressed P-AMPK (Figure 6(b)). To study the signaling cascade, compound C, an AMPK inhibitor, was used. As

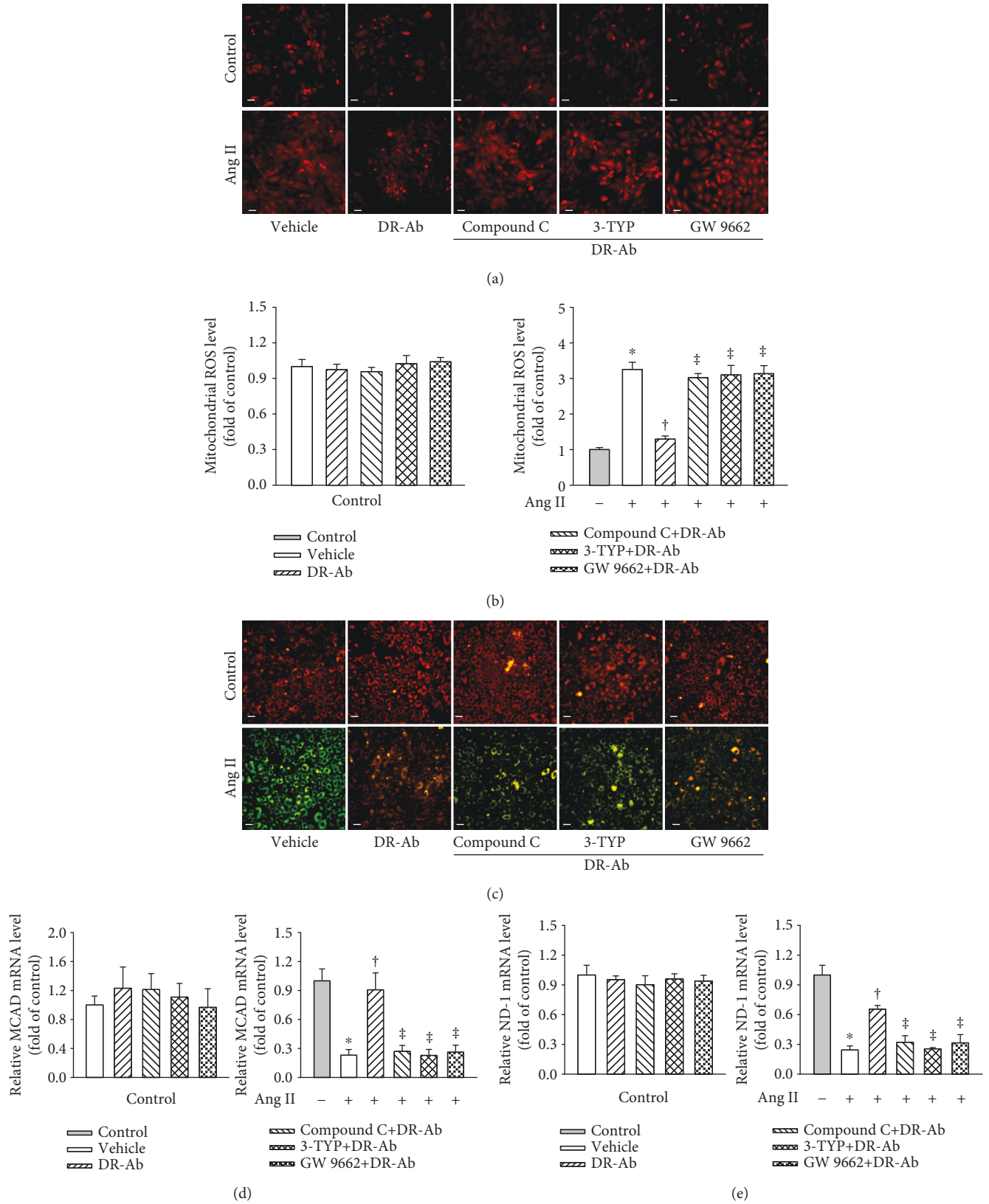


FIGURE 5: Continued.

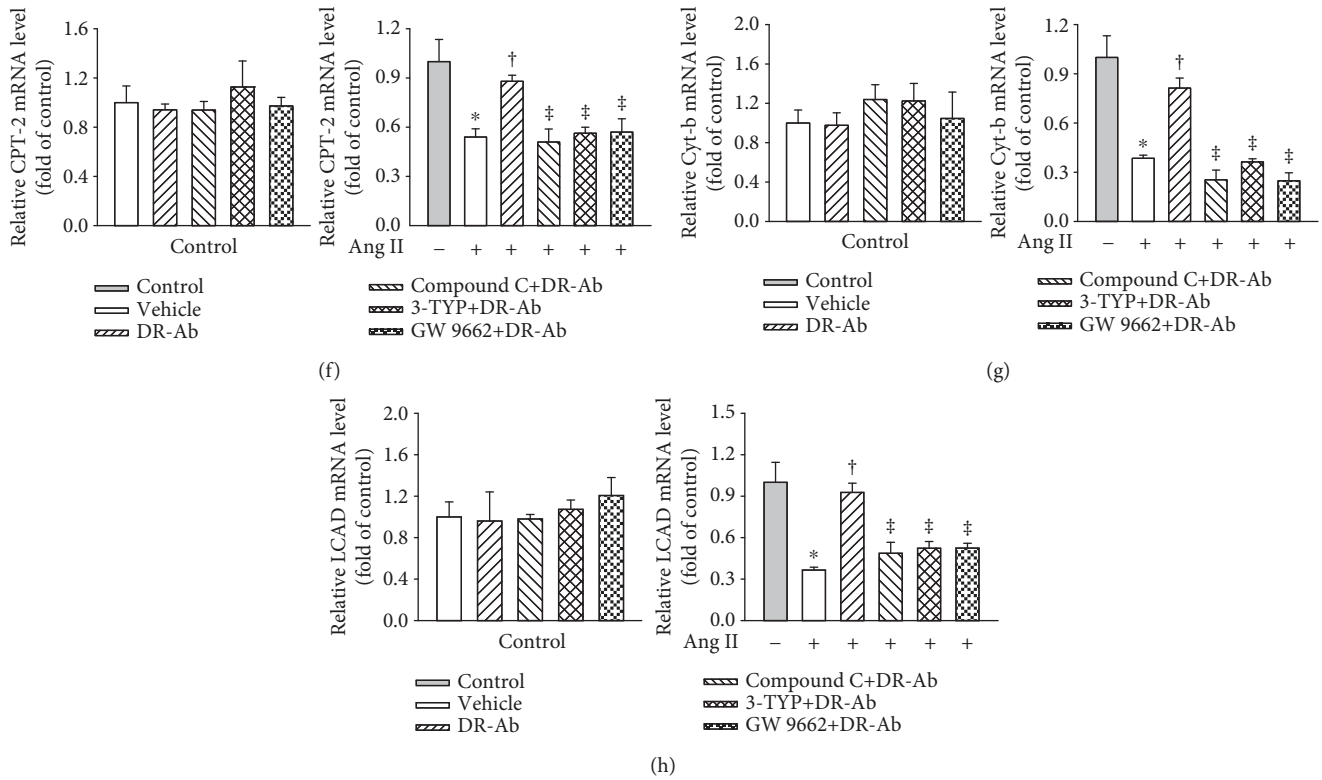


FIGURE 5: Effects of DR-Ab on mit-ROS production and energy metabolic dysfunction in Ang II-treated cells in the presence and absence of inhibitors of AMPK, Sirt3, or PPAR γ . (a, b) Representative image (a) and statistic data (b) showing that blockade of AMPK, Sirt3, or PPAR γ with their inhibitors abolished the protective effect of DR-Ab on mit-ROS production. Red: mit-ROS. Scale bar, 50 μ m. $n = 4-6$. (c) JC-1 staining showing that blockade of AMPK, Sirt3, or PPAR γ reversed the effect of DR-Ab on mitochondrial membrane potential. Red: aggregate. Green: monomer. Scale bar, 50 μ m. (d-h) qRT-PCR analysis showing that blockade of AMPK, Sirt3, or PPAR γ abolished the effects of DR-Ab on the mRNA expression of ND-1, Cyt-b, CPT-2, LCAD, and MCAD. $n = 4-6$. * $p < 0.05$ versus control, † $p < 0.05$ versus Ang II alone group, ‡ $p < 0.05$ versus Ang II+DR-Ab group.

shown in Figures 6(f) and 6(g), compound C abolished the effect of DR-Ab on both Sirt-3 and PPAR γ . Moreover, Ang II treatment significantly reduced the protein levels of PPAR γ and Sirt-3 (Figures 6(c) and 6(d)). These effects were significantly attenuated by incubation with DR-Ab. Interestingly, treatment with 3-TYP, a selective Sirt3 inhibitor, reversed the effect of DR-Ab on PPAR γ protein expression (Figure 6(e)). Taken together, DR-Ab protects H9c2 cardiomyocytes against Ang II-induced hypertrophy may via activate the AMPK/Sirt-3/PPAR γ signaling pathway.

4. Discussion

Ang II, a key component of renin-angiotensin system (RAS), is crucial in cardiovascular physiology and pathology [35]. The increased circulating Ang II level and activated RAS are closely associated with cardiovascular diseases such as cardiac hypertrophy [36] and heart failure [37]. Therefore, Ang II is widely used to mimic the pathology of clinical cardiac hypertrophy. An important function of NKA is to regulate cell volume [38, 39]. Recently, NKA expression and activity were also found to be closely regulated by Ang II [14, 40-42]. For instance, Ang II can inhibit NKA activity via induction of NADPH oxidase-derived O $_2^{*-15}$. Molkenin's group also reported that overexpression of

NKA successfully protects the heart against pathological cardiac hypertrophy and remodeling [43]. We previously reported that DR-Ab protects the heart against oxidative and ischemic injury [10, 12]. In this study, we demonstrated for the first time that DR-Ab prevented Ang II-induced myocyte hypertrophy through observing myocyte size, cell morphology, ROS generation, and mitochondrial functions.

We first investigated whether Ang II can regulate NKA expression and function in this study. It was found that Ang II treatment significantly reduced both plasma expression and activity of NKA. To study whether Ang II-induced pathology is caused by impairment of NKA, we pretreated the cells with DR-Ab which stimulates NKA activity. As expected, DR-Ab improved cardiomyocytes hypertrophy induced by Ang II. The enlarged cell size induced by Ang II was recovered to nearly normal cell after treatment with DR-Ab. Our results suggest that DR-Ab protect cells against Ang II-induced cells injury through preservation of membrane NKA activity, which helps to maintain resting potential, ion transport, and regulates cellular volume.

Oxidative stress plays an important role in Ang II-induced cardiomyopathy [44]. Recent studies have revealed that NKA is one of the target proteins of ROS [45, 46]. Moreover, it was found that NADPH oxidase is crucial for the inhibited NKA activity in cardiac myocytes

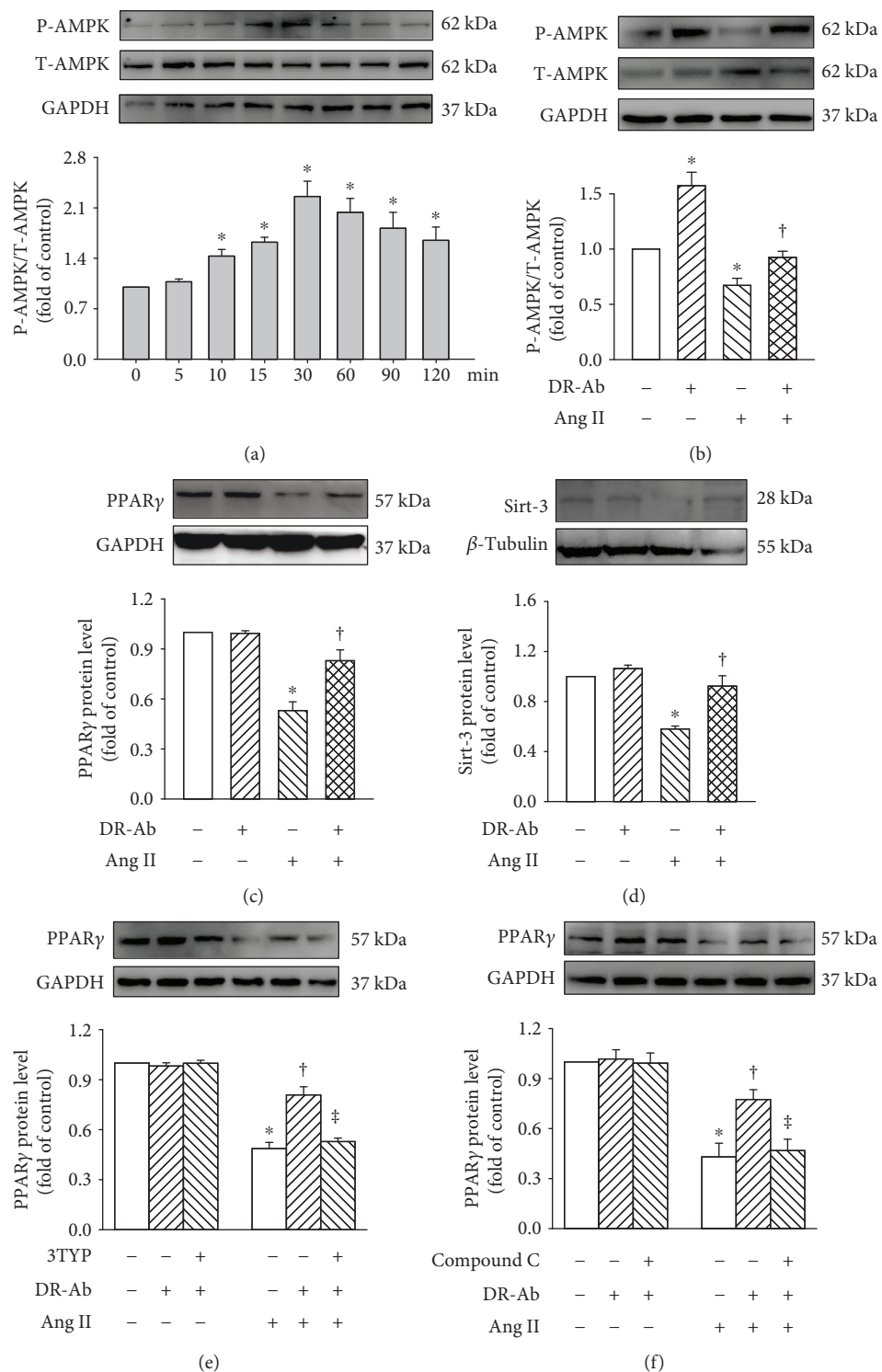


FIGURE 6: Continued.

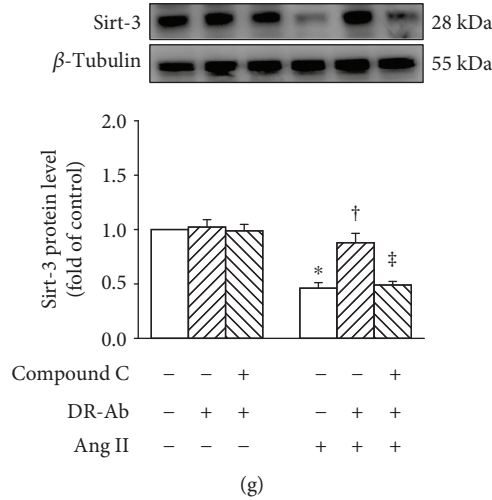


FIGURE 6: Western blotting analysis showing that DR-Ab stimulated AMPK/Sirt-3/PPAR γ signaling pathway. (a) Time-course study showing the effect of DR-Ab on AMPK phosphorylation. (b–d) DR-Ab reversed the effect of Ang II on p-AMPK (b), PPAR γ (c), & Sirt-3 (d). $n = 4-6$. (e) 3-TYP eliminated DR-Ab effect on the PPAR γ level in Ang II-treated cells. $n = 4$. (f, g) Compound C abolished the effect of DR-Ab on the protein expression of PPAR γ (f) and Sirt-3 (g) in Ang II-treated cells. $n = 4-6$. * $p < 0.05$ versus control group, † $p < 0.05$ versus Ang II alone group, ‡ $p < 0.05$ versus Ang II+ DR-Ab.

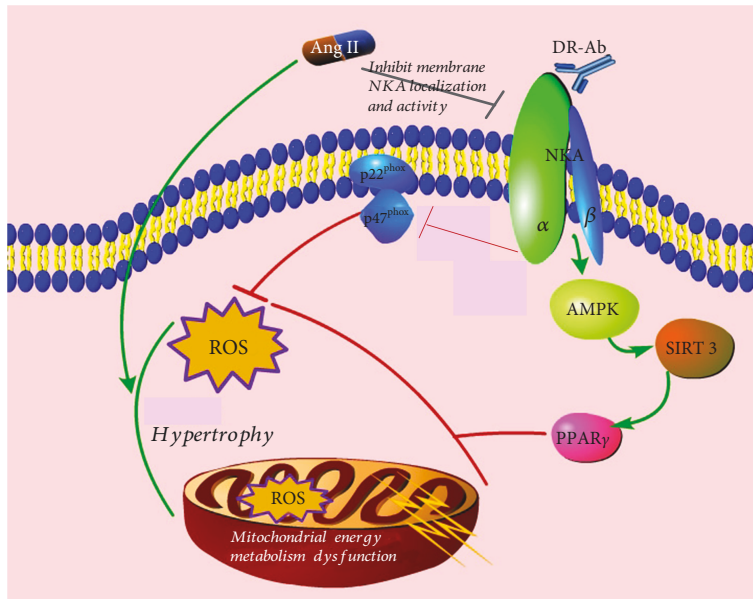


FIGURE 7: Schematic illustration showing the mechanisms for the protective effects of DR-Ab. DR-Ab protects against Ang II-induced cell injury by stabilization of membrane NKA and stimulation of its activity. This helps to maintain the normal intracellular ion homeostasis, thus reserves the cell size. DR-Ab inhibits NADPH oxidase activity by downregulation of p22^{phox} and p47^{phox} expression. Meanwhile, DR-Ab inhibits mitochondrial ROS generation and preserves mitochondrial function through stimulation of the AMPK/Sirt-3/PPAR γ signaling pathway.

treated with Ang II [13]. For the above reasons, we first examined whether DR-Ab can protect cardiomyocytes through inhibition of NADPH oxidase. We found that DR-Ab markedly attenuated Ang II-induced intracellular ROS generation through inhibition of NADPH oxidase. This effect was achieved by inhibition of the upregulated protein expression of p22^{phox} and p47^{phox} caused by Ang II.

Mitochondrial dysfunction also produces high levels of ROS. Multiple experiments were therefore performed to test the mitochondrial functions. We found that Ang II treatment largely increased mitochondrial ROS production and decreased mitochondrial membrane potential. This is consistent with previous studies [47]. We further studied its effects on mitochondrial DNAs, which encode proteins for

the electron transport chain and then produce the majority of cellular energy [48, 49]. Our results showed that Ang II notably decreased the mRNA levels of ND-1, cyt-b, and mt-co1. Metabolic derangement is a signature in pathological cardiac hypertrophy [50]. Ang II also significantly inhibited the mRNA levels of CPT-1 β , CPT-2, LCAD, and MCAD, all of which are important in mitochondrial oxidative phosphorylation and fatty acid metabolism. Interestingly, all the above effects caused by Ang II were significantly reversed by the pretreatment with DR-Ab.

DR-Ab is an antibody targeted at the 4th extracellular domain of α -subunit of NKA. It remains unclear why and how DR-Ab protects mitochondrial functions by binding to NKA. As NKA also serve as a signaling protein [28], we studied the signaling mechanisms underlying the protective effect of DR-Ab. Previous studies revealed that Ang II-induced cardiac hypertrophy is mediated by AMPK- [29–31, 51, 52], Sirt3- [32–34], and PPAR γ - [26–28] dependent mechanisms. Therefore, there is a close relationship between NKA and AMPK [53–56]. On the one hand, activation of AMPK has been reported to regulate the activity and cell surface abundance of NKA [57]. On the other hand, ouabain blocks the carbachol-induced phosphorylation and activation of AMPK [58]; thus, activation of NKA also stimulates AMPK activity [59]. For this reason, we studied the effect of DR-Ab on AMPK activity and found that DR-Ab promoted AMPK phosphorylation. Activation of AMPK has been shown to stimulate Sirt-3 [60–62], and then activated Sirt-3 affects PPAR γ [32] which has been proved in participating in Ang II-induced myocyte hypertrophy [26–28]. In our study, we confirmed the involvement of the Sirt-3/PPAR γ pathway with pharmacological manipulation. Western blotting analysis also confirmed that activation of Sirt-3/PPAR γ is secondary to that of AMPK. Our data suggest that the AMPK/Sirt-3/PPAR γ signaling pathway mediates the protective effects of DR-Ab against Ang II-induced H9c2 cardiomyocyte damage.

In summary, as shown in Figure 7, we found for the first time that DR-Ab prevents Ang II-induced H9c2 cardiomyocyte hypertrophy. This protective effect is mediated by activation of the AMPK/Sirt-3/PPAR γ signaling pathway and stabilization of membrane NKA expression. Our results suggest a novel mechanism and therapeutic strategy in the treatment of cardiac hypertrophy and associated oxidative injury.

Data Availability

The derived data used to support the findings of this study are included within the article. The raw data used to support the findings of this study are available from the corresponding author upon request.

Conflicts of Interest

The authors declare that they have no conflict of interest.

Authors' Contributions

This work was designed by Jin-Song Bian, Hai-Jian Sun, and Siping Xiong. The cells were cultured by Mengyuan Zhu and Zhiyuan Wu. Most experiments were performed by Hai-Jian Sun, Siping Xiong, Lei Cao, and Tengting Liu. Zhiyuan Wu and Mengyuan Zhu performed the statistical analysis. Siping Xiong and Hai-Jian Sun wrote the manuscript. Jin-Song Bian were consultants for the study and helped with manuscript editing. Siping Xiong and Hai-Jian Sun contributed equally to this work.

Acknowledgments

This work was supported by research grants from the Singapore National Medical Research Council (NMRC/CIRG/1432/2015 and NMRC/1274/2010) and the National Nature Science Foundation of China (NSFC 81872865).

Supplementary Materials

Figure S1: Effects of DR-Ab on Ang II-induced hypertrophy in the neonatal mouse cardiomyocytes. DR-Ab (2 μ M) was given 30 min before treatment with Ang II (100 nM) for 48 h. (A-B) Representative immunofluorescence staining (A) and group data (B) showing that DR-Ab reversed enlarged cell size caused by Ang II. Green: NKA α 1. Blue: DAPI. Scale bar, 30 μ m. $n = 6$. (C-E) qRT-PCR analysis showing the mRNA levels of ANP, BNP, and β -MHC. $n = 4$. (F-G) DR-Ab reversed Ang II-induced loss of plasma membrane NKA α 1 (A&F) and increase of endosome NKA α 1 (G). $n = 4-6$. (H-I) Effect of DR-Ab on the protein level of two subunits of NADPH oxidase: p22^{phox} and p47^{phox}. $n = 4-6$. * $p < 0.05$ versus control group, † $p < 0.05$ versus Ang II alone group. (*Supplementary Materials*)

References

- [1] M. Naghavi, A. A. Abajobir, C. Abbafati et al., "Global, regional, and national age-sex specific mortality for 264 causes of death, 1980-2016: a systematic analysis for the Global Burden of Disease Study 2016," *The Lancet*, vol. 390, no. 10100, pp. 1151–1210, 2017.
- [2] Y. Xin, Y. Bai, X. Jiang et al., "Sulforaphane prevents angiotensin II-induced cardiomyopathy by activation of Nrf2 via stimulating the Akt/GSK-3 β /Fyn pathway," *Redox Biology*, vol. 15, pp. 405–417, 2018.
- [3] M. Packer and J. J. V. McMurray, "Importance of endogenous compensatory vasoactive peptides in broadening the effects of inhibitors of the renin-angiotensin system for the treatment of heart failure," *Lancet*, vol. 389, no. 10081, pp. 1831–1840, 2017.
- [4] I. Herichova and K. Szantooova, "Renin-angiotensin system: upgrade of recent knowledge and perspectives," *Endocrine Regulations*, vol. 47, no. 1, pp. 39–52, 2013.
- [5] X. S. Ren, Y. Tong, L. Ling et al., "NLRP3 gene deletion attenuates angiotensin II-induced phenotypic transformation of vascular smooth muscle cells and vascular remodeling," *Cellular Physiology and Biochemistry*, vol. 44, no. 6, pp. 2269–2280, 2018.

- [6] H. J. Sun, P. Li, W. W. Chen, X. Q. Xiong, and Y. Han, "Angiotensin II and angiotensin-(1-7) in paraventricular nucleus modulate cardiac sympathetic afferent reflex in renovascular hypertensive rats," *PLoS One*, vol. 7, no. 12, article e25557, 2012.
- [7] J. B. Lingrel and T. Kuntzweiler, "Na⁺,K⁽⁺⁾-ATPase," *The Journal of Biological Chemistry*, vol. 269, no. 31, pp. 19659–19662, 1994.
- [8] J. Liu, J. Tian, M. Haas, J. I. Shapiro, A. Askari, and Z. Xie, "Ouabain interaction with cardiac Na⁺/K⁺-ATPase initiates signal cascades independent of changes in intracellular Na⁺ and Ca²⁺ concentrations," *The Journal of Biological Chemistry*, vol. 275, pp. 27838–27844, 2000.
- [9] X. Cui and Z. Xie, "Protein interaction and Na/K-ATPase-mediated signal transduction," *Molecules*, vol. 22, no. 6, p. 990, 2017.
- [10] J. Zheng, X. Koh, F. Hua, G. Li, J. W. Larrick, and J. S. Bian, "Cardioprotection induced by Na⁺/K⁺-ATPase activation involves extracellular signal-regulated kinase 1/2 and phosphoinositide 3-kinase/Akt pathway," *Cardiovascular Research*, vol. 89, no. 1, pp. 51–59, 2011.
- [11] K. Y. Xu, E. Takimoto, and N. S. Fedarko, "Activation of (Na⁺ + K⁺)-ATPase induces positive inotropy in intact mouse heart *in vivo*," *Biochemical and Biophysical Research Communications*, vol. 349, no. 2, pp. 582–587, 2006.
- [12] F. Hua, Z. Wu, X. Yan et al., "DR region of Na⁺/K⁺-ATPase is a new target to protect heart against oxidative injury," *Scientific Reports*, vol. 8, no. 1, article 13100, 2018.
- [13] C. N. White, G. A. Figtree, C. C. Liu et al., "Angiotensin II inhibits the Na⁺-K⁺ pump via PKC-dependent activation of NADPH oxidase," *American Journal of Physiology-Cell Physiology*, vol. 296, no. 4, pp. C693–C700, 2009.
- [14] K. J. Massey, Q. Li, N. F. Rossi, R. R. Mattingly, and D. R. Yingst, "Angiotensin II-dependent phosphorylation at Ser¹¹/Ser¹⁸ and Ser⁹³⁸ shifts the E₂ conformations of rat kidney Na⁺/K⁺-ATPase," *The Biochemical Journal*, vol. 443, no. 1, pp. 249–258, 2012.
- [15] S. M. Rahaman, K. Dey, T. Chakraborti, and S. Chakraborti, "Angiotensin II inhibits Na⁺/K⁺ATPase activity in pulmonary artery smooth muscle cells via glutathionylation and with the involvement of a 15.6 kDa inhibitor protein," *Indian Journal of Biochemistry & Biophysics*, vol. 52, pp. 119–124, 2015.
- [16] S. Xiong, X. Yang, X. Yan et al., "Immunization with Na⁺/K⁺ATPase DR peptide prevents bone loss in an ovariectomized rat osteoporosis model," *Biochemical Pharmacology*, vol. 156, pp. 281–290, 2018.
- [17] K. Iwatsubo, S. Minamisawa, T. Tsunematsu et al., "Direct inhibition of type 5 adenylyl cyclase prevents myocardial apoptosis without functional deterioration," *The Journal of Biological Chemistry*, vol. 279, no. 39, pp. 40938–40945, 2004.
- [18] J. Zhang, H. Xiao, J. Shen, N. Wang, and Y. Zhang, "Different roles of β -arrestin and the PKA pathway in mitochondrial ROS production induced by acute β -adrenergic receptor stimulation in neonatal mouse cardiomyocytes," *Biochemical and Biophysical Research Communications*, vol. 489, no. 4, pp. 393–398, 2017.
- [19] K. K. Durham, K. M. Chathely, K. C. Mak et al., "HDL protects against doxorubicin-induced cardiotoxicity in a scavenger receptor class B type 1-, PI3K-, and Akt-dependent manner," *American Journal of Physiology-Heart and Circulatory Physiology*, vol. 314, no. 1, pp. H31–H44, 2018.
- [20] Q. B. Lu, M. Y. Wan, P. Y. Wang et al., "Chicoric acid prevents PDGF-BB-induced VSMC dedifferentiation, proliferation and migration by suppressing ROS/NF κ B/mTOR/P70S6K signaling cascade," *Redox Biology*, vol. 14, pp. 656–668, 2018.
- [21] X. Yan, M. Xun, X. Dou, L. Wu, Y. Han, and J. Zheng, "Regulation of Na⁺-K⁺-ATPase effected high glucose-induced myocardial cell injury through c-Src dependent NADPH oxidase/ROS pathway," *Experimental Cell Research*, vol. 357, no. 2, pp. 243–251, 2017.
- [22] L. Ritter, D. Kleemann, F. H. Hickmann et al., "Disturbance of energy and redox homeostasis and reduction of Na⁺, K⁺-ATPase activity provoked by *in vivo* intracerebral administration of ethylmalonic acid to young rats," *Biochimica et Biophysica Acta (BBA) - Molecular Basis of Disease*, vol. 1852, no. 5, pp. 759–767, 2015.
- [23] Z. Li, S. Li, L. Hu et al., "Mechanisms underlying action of Xinmailong injection, a traditional Chinese medicine in cardiac function improvement," *African Journal of Traditional, Complementary, and Alternative Medicines*, vol. 14, no. 2, pp. 241–252, 2017.
- [24] H. J. Sun, D. Chen, P. Y. Wang et al., "Salusin- β is involved in diabetes mellitus-induced endothelial dysfunction via degradation of peroxisome proliferator-activated receptor gamma," *Oxidative Medicine and Cellular Longevity*, vol. 2017, Article ID 6905217, 14 pages, 2017.
- [25] Y. Sun, Y. Li, C. Liu et al., "The role of angiotensin-like protein 4 in phenylephrine-induced cardiomyocyte hypertrophy," *Bioscience Reports*, vol. 39, no. 7, 2019.
- [26] L. Yan, J. D. Zhang, B. Wang et al., "Quercetin inhibits left ventricular hypertrophy in spontaneously hypertensive rats and inhibits angiotensin II-induced H9C2 cells hypertrophy by enhancing PPAR- γ expression and suppressing AP-1 activity," *PLoS One*, vol. 8, no. 9, article e72548, 2013.
- [27] W. Pang, N. Li, D. Ai, X. L. Niu, Y. F. Guan, and Y. Zhu, "Activation of peroxisome proliferator-activated receptor- γ down-regulates soluble epoxide hydrolase in cardiomyocytes," *Clinical and Experimental Pharmacology and Physiology*, vol. 38, no. 6, pp. 358–364, 2011.
- [28] Y. Yu, B. J. Xue, S. G. Wei et al., "Activation of central PPAR- γ attenuates angiotensin II-induced hypertension," *Hypertension*, vol. 66, no. 2, pp. 403–411, 2015.
- [29] T. Jansen, S. Kröller-Schön, T. Schönfelder et al., " α 1AMPK deletion in myelomonocytic cells induces a pro-inflammatory phenotype and enhances angiotensin II-induced vascular dysfunction," *Cardiovascular Research*, vol. 114, no. 14, pp. 1883–1893, 2018.
- [30] Q. Duan, P. Song, Y. Ding, and M. H. Zou, "Activation of AMP-activated protein kinase by metformin ablates angiotensin II-induced endoplasmic reticulum stress and hypertension in mice *in vivo*," *British Journal of Pharmacology*, vol. 174, no. 13, pp. 2140–2151, 2017.
- [31] S. Mía, T. Castor, K. Musculus, J. Voelkl, I. Alesutan, and F. Lang, "Role of AMP-activated protein kinase α 1 in angiotensin-II-induced renal Tg β -activated kinase 1 activation," *Biochemical and Biophysical Research Communications*, vol. 476, no. 4, pp. 267–272, 2016.
- [32] X. Guo, F. Yan, X. Shan et al., "SIRT3 inhibits Ang II-induced transdifferentiation of cardiac fibroblasts through β -catenin/PPAR- γ signaling," *Life Sciences*, vol. 186, pp. 111–117, 2017.
- [33] G. Meng, J. Liu, S. Liu et al., "Hydrogen sulfide pretreatment improves mitochondrial function in myocardial hypertrophy

- via a SIRT3-dependent manner,” *British Journal of Pharmacology*, vol. 175, no. 8, pp. 1126–1145, 2018.
- [34] L. Guo, A. Yin, Q. Zhang, T. Zhong, S. T. O’Rourke, and C. Sun, “Angiotensin-(1-7) attenuates angiotensin II-induced cardiac hypertrophy via a Sirt3-dependent mechanism,” *American Journal of Physiology-Heart and Circulatory Physiology*, vol. 312, no. 5, pp. H980–H991, 2017.
- [35] J. P. van Kats, D. Methot, P. Paradis, D. W. Silversides, and T. L. Reudelhuber, “Use of a biological peptide pump to study chronic peptide hormone action in transgenic mice: Direct and indirect effects of angiotensin II on the heart,” *The Journal of Biological Chemistry*, vol. 276, no. 47, pp. 44012–44017, 2001.
- [36] J. Sadoshima, Y. Xu, H. S. Slayter, and S. Izumo, “Autocrine release of angiotensin II mediates stretch-induced hypertrophy of cardiac myocytes in vitro,” *Cell*, vol. 75, no. 5, pp. 977–984, 1993.
- [37] G. G. N. Serneri, M. Boddi, I. Cecioni et al., “Cardiac angiotensin II formation in the clinical course of heart failure and its relationship with left ventricular function,” *Circulation Research*, vol. 88, no. 9, pp. 961–968, 2001.
- [38] M. A. Russo, E. Morgante, A. Russo, G. D. Rossum, and M. Tafani, “Ouabain-induced cytoplasmic vesicles and their role in cell volume maintenance,” *BioMed Research International*, vol. 2015, Article ID 487256, 13 pages, 2015.
- [39] K. Dijkstra, J. Hofmeijer, S. A. van Gils, and M. J. A. M. van Putten, “A biophysical model for cytotoxic cell swelling,” *The Journal of Neuroscience*, vol. 36, no. 47, pp. 11881–11890, 2016.
- [40] K. J. Massey, Q. Li, N. F. Rossi, S. M. Keezer, R. R. Mattingly, and D. R. Yingt, “Phosphorylation of rat kidney Na-K pump at Ser938 is required for rapid angiotensin II-dependent stimulation of activity and trafficking in proximal tubule cells,” *American Journal of Physiology-Cell Physiology*, vol. 310, no. 3, pp. C227–C232, 2016.
- [41] A. Gonzalez-Vicente and J. L. Garvin, “Angiotensin II-induced hypertension increases plasma membrane Na pump activity by enhancing Na entry in rat thick ascending limbs,” *American Journal of Physiology-Renal Physiology*, vol. 305, no. 9, pp. F1306–F1314, 2013.
- [42] M. M. Naderi, S. B. Boroujeni, A. Sarvari et al., “The effect of angiotensin on the quality of *in vitro* produced (IVP) sheep embryos and expression of Na⁺/K⁺/ATPase,” *Avicenna Journal of Medical Biotechnology*, vol. 8, pp. 9–15, 2016.
- [43] R. N. Correll, P. Eder, A. R. Burr et al., “Overexpression of the Na⁺/K⁺ ATPase α 2 but not α 1 isoform attenuates pathological cardiac hypertrophy and remodeling,” *Circulation Research*, vol. 114, no. 2, pp. 249–256, 2014.
- [44] G. Zhou, X. Li, D. W. Hein et al., “Metallothionein suppresses angiotensin II-induced nicotinamide adenine dinucleotide phosphate oxidase activation, nitrosative stress, apoptosis, and pathological remodeling in the diabetic heart,” *Journal of the American College of Cardiology*, vol. 52, no. 8, pp. 655–666, 2008.
- [45] A. P. Comellas, L. A. Dada, E. Lecuona et al., “Hypoxia-mediated degradation of Na,K-ATPase via mitochondrial reactive oxygen species and the ubiquitin-conjugating system,” *Circulation Research*, vol. 98, no. 10, pp. 1314–1322, 2006.
- [46] I. Y. Petrushanko, S. Yakushev, V. A. Mitkevich et al., “S-Glutathionylation of the Na,K-ATPase catalytic α subunit is a determinant of the enzyme redox sensitivity,” *The Journal of Biological Chemistry*, vol. 287, no. 38, pp. 32195–32205, 2012.
- [47] W. Xiong, J. Hua, Z. Liu et al., “PTEN induced putative kinase 1 (PINK1) alleviates angiotensin II-induced cardiac injury by ameliorating mitochondrial dysfunction,” *International Journal of Cardiology*, vol. 266, pp. 198–205, 2018.
- [48] K. Srirattana and J. C. St John, “Transmission of dysfunctional mitochondrial DNA and its implications for mammalian reproduction,” in *Cellular and Molecular Basis of Mitochondrial Inheritance*, vol. 231, Advances in Anatomy, Embryology, and Cell Biology, P. Sutovsky, Ed., pp. 75–103, Springer, 2019.
- [49] D. Gao, B. Zhu, H. Sun, and X. Wang, “Mitochondrial DNA methylation and related disease,” *Advances in Experimental Medicine and Biology*, vol. 1038, pp. 117–132, 2017.
- [50] Y. S. Choi, A. B. M. de Mattos, D. Shao et al., “Preservation of myocardial fatty acid oxidation prevents diastolic dysfunction in mice subjected to angiotensin II infusion,” *Journal of Molecular and Cellular Cardiology*, vol. 100, pp. 64–71, 2016.
- [51] C. Beauloye, L. Bertrand, S. Horman, and L. Hue, “AMPK activation, a preventive therapeutic target in the transition from cardiac injury to heart failure,” *Cardiovascular Research*, vol. 90, no. 2, pp. 224–233, 2011.
- [52] B. J. Stuck, M. Lenski, M. Bohm, and U. Laufs, “Metabolic switch and hypertrophy of cardiomyocytes following treatment with angiotensin II are prevented by AMP-activated protein kinase,” *The Journal of Biological Chemistry*, vol. 283, no. 47, pp. 32562–32569, 2008.
- [53] Q. Yuan, Q. Y. Zhou, D. Liu et al., “Advanced glycation end-products impair Na⁺/K⁺-ATPase activity in diabetic cardiomyopathy: role of the adenosine monophosphate-activated protein kinase/sirtuin 1 pathway,” *Clinical and Experimental Pharmacology and Physiology*, vol. 41, no. 2, pp. 127–133, 2014.
- [54] M. S. Ingwersen, M. Kristensen, H. Pilegaard, J. F. P. Wojtaszewski, E. A. Richter, and C. Juel, “Na,K-ATPase activity in mouse muscle is regulated by AMPK and PGC-1 α ,” *The Journal of Membrane Biology*, vol. 242, no. 1, pp. 1–10, 2011.
- [55] B. Benziene, M. Björnholm, L. Lantier, B. Violet, J. R. Zierath, and A. V. Chibalin, “AMP-activated protein kinase activator A-769662 is an inhibitor of the Na⁺-K⁺-ATPase,” *American Journal of Physiology-Cell Physiology*, vol. 297, no. 6, pp. C1554–C1566, 2009.
- [56] I. Vadász, L. A. Dada, A. Briva et al., “AMP-activated protein kinase regulates CO₂-induced alveolar epithelial dysfunction in rats and human cells by promoting Na,K-ATPase endocytosis,” *The Journal of Clinical Investigation*, vol. 118, pp. 752–762, 2008.
- [57] B. Benziene, M. Björnholm, S. Pirkmajer et al., “Activation of AMP-activated protein kinase stimulates Na⁺,K⁺-ATPase activity in skeletal muscle cells,” *The Journal of Biological Chemistry*, vol. 287, no. 28, pp. 23451–23463, 2012.
- [58] S. P. Soltoff and L. Hedden, “Regulation of ERK1/2 by ouabain and Na-K-ATPase-dependent energy utilization and AMPK activation in parotid acinar cells,” *American Journal of Physiology-Cell Physiology*, vol. 295, no. 3, pp. C590–C599, 2008.
- [59] R. Mukhopadhyay, R. Venkatadri, J. Katsnelson, and R. Arav-Boger, “Digitoxin suppresses human cytomegalovirus replication via Na⁺, K⁺/ATPase α 1 subunit-dependent AMP-activated protein kinase and autophagy activation,” *Journal of Virology*, vol. 92, no. 6, 2018.

- [60] J. Gao, S. Liu, F. Xu et al., "Trilobatin protects against oxidative injury in neuronal PC12 cells through regulating mitochondrial ROS homeostasis mediated by AMPK/Nrf2/Sirt3 signaling pathway," *Frontiers in Molecular Neuroscience*, vol. 11, p. 267, 2018.
- [61] L. Y. Chen, Y. Wang, R. Terkeltaub, and R. Liu-Bryan, "Activation of AMPK-SIRT3 signaling is chondroprotective by preserving mitochondrial DNA integrity and function," *Osteoarthritis and Cartilage*, vol. 26, no. 11, pp. 1539–1550, 2018.
- [62] X. L. Zhao and C. Z. Yu, "Vosaroxin induces mitochondrial dysfunction and apoptosis in cervical cancer HeLa cells: involvement of AMPK/Sirt3/HIF-1 pathway," *Chemico-Biological Interactions*, vol. 290, pp. 57–63, 2018.

Research Article

Decreased Lipid Profile and Oxidative Stress in Healthy Subjects Who Underwent Whole-Body Cryotherapy in Closed Cryochamber with Subsequent Kinesiotherapy

Agata Stanek ¹, Ewa Romuk ², Tomasz Wielkoszyński ³, Stanisław Bartuś ⁴,
Grzegorz Cieślak ¹ and Armand Cholewka ⁵

¹Department of Internal Medicine, Angiology and Physical Medicine, School of Medicine with the Division of Dentistry in Zabrze, Medical University of Silesia, Batorego St. 15, 41-902 Bytom, Poland

²Department of Biochemistry, School of Medicine with the Division of Dentistry in Zabrze, Medical University of Silesia, Jordana 19 St., 41-808 Zabrze, Poland

³Higher School of Strategic Planning in Dąbrowa Górnicza, Kościelna 6 St., 41-300 Dąbrowa Górnicza, Poland

⁴Second Department of Cardiology, Institute of Cardiology, Jagiellonian University Medical College, 17 Kopernika St., 31-501 Krakow, Poland

⁵Department of Medical Physics, Chelkowski Institute of Physics, University of Silesia, 4 Uniwersytecka St., 40-007 Katowice, Poland

Correspondence should be addressed to Agata Stanek; astanek@tlen.pl

Received 27 February 2019; Accepted 18 July 2019; Published 14 August 2019

Guest Editor: Adrian Doroszko

Copyright © 2019 Agata Stanek et al. This is an open access article distributed under the Creative Commons Attribution License, which permits unrestricted use, distribution, and reproduction in any medium, provided the original work is properly cited.

Objective. The aim of the study was to estimate the impact of whole-body cryotherapy (WBC) and subsequent kinesiotherapy on oxidative stress and lipid profile when performed in a closed cryochamber on healthy subjects. **Material and Methods.** The effect of ten WBC procedures lasting 3 minutes a day followed by a 60-minute session kinesiotherapy on oxidative stress and lipid profile in healthy subjects (WBC group, $n = 16$) was investigated. The WBC group was compared to the kinesiotherapy only (KT; $n = 16$) group. The routine parameters of oxidative stress (antioxidant enzymatic and nonenzymatic antioxidant status, lipid peroxidation products, total oxidative status (TOS), and oxidative stress index (OSI)) and lipid profile were estimated one day before the beginning and one day after the completion of the research program. **Results.** After treatment, in the WBC group, a significant decrease of oxidative stress markers (TOS and OSI) and a significant increase of total antioxidant capacity were observed. The activity of plasma SOD-Mn and erythrocyte total SOD increased significantly in the WBC group. In the KT group, the erythrocyte activity of total SOD, CAT, and GR decreased significantly after the treatment. The levels of T-Chol and LDL-Chol decreased significantly after treatment in both groups, but the observed decrease of these lipid parameters in the WBC group was higher in comparison to the KT group. The level of TG decreased significantly after treatment in the WBC group only. **Conclusion.** WBC performed in a closed cryochamber followed by kinesiotherapy improves lipid profile and decreases oxidative stress in healthy subjects.

1. Introduction

Whole-body cryotherapy (WBC) is the therapeutic exposure of the total human body to extreme cold temperatures (below -100°C) for a short time (maximum up to 120-180 seconds) [1, 2]. Immediately after each cryotherapy procedure, subjects usually perform an appropriate set of kine-

siotherapy exercises in order to increase and consolidate the beneficial effects of cryogenic temperature treatment [2].

The action of cryogenic temperatures causes several favorable physiological reactions such as an analgesic [1–3], anti-inflammatory [4–6], and the promotion of a circulatory effect [1, 2]. Cryogenic temperatures applied to the whole body also improve mood [7] and have a beneficial influence

TABLE 1: Demographic characteristics of the research subjects.

Characteristic	WBC group (<i>n</i> = 16)	Kinesiotherapy group (<i>n</i> = 16)	<i>P</i> value
Age, years, mean (SD)	45.75 ± 2.08	46.06 ± 1.44	0.459
Sex (M/F)	16/0	16/0	—
BMI, kg/m ² , mean (SD)	23.83 ± 4.5	24.26 ± 6.8	0.957
Smoking (yes/no)	0/16	0/16	—

SD: standard deviation; BMI: body mass index.

on the endocrine system [8, 9]. Additionally, the latest studies show that WBC may improve memory deficits [10], prooxidant-antioxidant balance [11, 12], lipid profile [13], and skin appearance [14, 15].

Until now, WBC has been used mainly in sports medicine [16, 17] and in the treatment of locomotor system diseases [18, 19]. Currently, WBC is used more and more frequently as a wellness method in healthy subjects, to help maintain good health [2, 20], but the mechanisms of WBC action are not fully known.

The effect of WBC treatment may depend on the type of cryochamber in which procedures are performed, the temperature and number of procedures, and whether WBC procedures are connected with a subsequent session of kinesiotherapy [21, 22]. In the available literature, there has been only one study [13], which estimated the influence of WBC on lipid profile parameters in healthy subjects, but WBC procedures were not connected with a subsequent session of kinesiotherapy, and the authors only estimated lipid profile parameters. Similarly, there have been a few studies, which showed a beneficial influence of WBC procedures on the prooxidant-antioxidant balance in healthy subjects, but they were performed in different circumstances (type of cryochamber, temperature, without subsequent sessions of kinesiotherapy), and very often, the authors only estimated the level of selected parameters of prooxidant-antioxidant balance. However, evaluation of oxidative stress severity must be comprised of the determination of oxidative stress markers as well as the activity of enzymatic and nonenzymatic antioxidant systems simultaneously [23, 24]. This is because disruption of the prooxidative-antioxidative balance may be caused by increased reactive oxygen species (ROS) production, impaired ROS elimination, or the combined effect of both processes [25].

In light of the above findings, the aim of this research was to assess the influence of WBC, performed in a closed cryochamber (Wroclawski type) with a subsequent session of kinesiotherapy, on oxidative stress and lipid profile simultaneously in healthy subjects. The scheme of whole-body cryotherapy procedures and estimation of oxidative stress parameters were similar to the methods used in our manuscript published earlier [21].

2. Materials and Methods

2.1. Subjects. The research protocol was approved by the Bioethical Committee of the Medical University of Silesia in Katowice (permission no. NN-6501-93/I/07), Poland.

All analyzed subjects gave written consent for inclusion in the research. All investigations were conducted according to the Declaration of Helsinki principles (1964).

The research engaged 32 healthy nonsmoking male subjects who were divided randomly by a physician into two groups with an allocation ratio of 1:1:16 healthy subjects exposed to whole-body cryotherapy procedures with subsequent kinesiotherapy (WBC group, mean age 46.63 ± 1.5 years) and 16 healthy subjects exposed only to kinesiotherapy procedures (KT group, mean age 45.94 ± 1.24 years), with no significant difference in mean age and body mass index (BMI) between them.

All subjects were healthy volunteers who qualified for a routine complex treatment called cryorehabilitation including WBC (treated as an assisting component) with subsequent kinesiotherapy or kinesiotherapy procedures only, in order to promote and increase wellness. The subjects were not previously exposed to WBC.

Prior to the research, a resting electrocardiogram was performed in all the subjects and each subject was examined by a physician to exclude any coexisting diseases as well as any contraindications for WBC procedures. Before each session of WBC, the blood pressure was measured for each subject [2]. All the subjects were asked to avoid alcohol, any immunomodulators, immunostimulators, hormones, vitamins, minerals, or other substances with antioxidant properties and drugs for 4 weeks before and during the research. The diet of the subjects was not modified, although they were asked to abstain from the consumption of caffeine 12 hours prior to laboratory analyses. They also maintained the same mode of physical activity during the research. The demographic characteristics of the healthy subjects are shown in Table 1.

2.2. Scheme of Whole-Body Cryotherapy and Kinesiotherapy Procedures. The healthy subjects, depending on the group, were exposed either to a cycle of WBC procedures lasting 3 minutes a day with a subsequent 60-minute session of kinesiotherapy or to a 60-minute session of kinesiotherapy only for 10 consecutive days at the same time in the morning, excluding the weekend.

The WBC procedures were performed in a closed cryochamber (Wroclawski type) cooled by liquid nitrogen (produced by Creator, Poland). The cryochamber consisted of an antechamber with the temperature -60°C and a proper chamber, where the temperature reached -120°C. The subjects were let into the chamber in groups of four. Each entry to the cryochamber was preceded by a 30-second adaptation

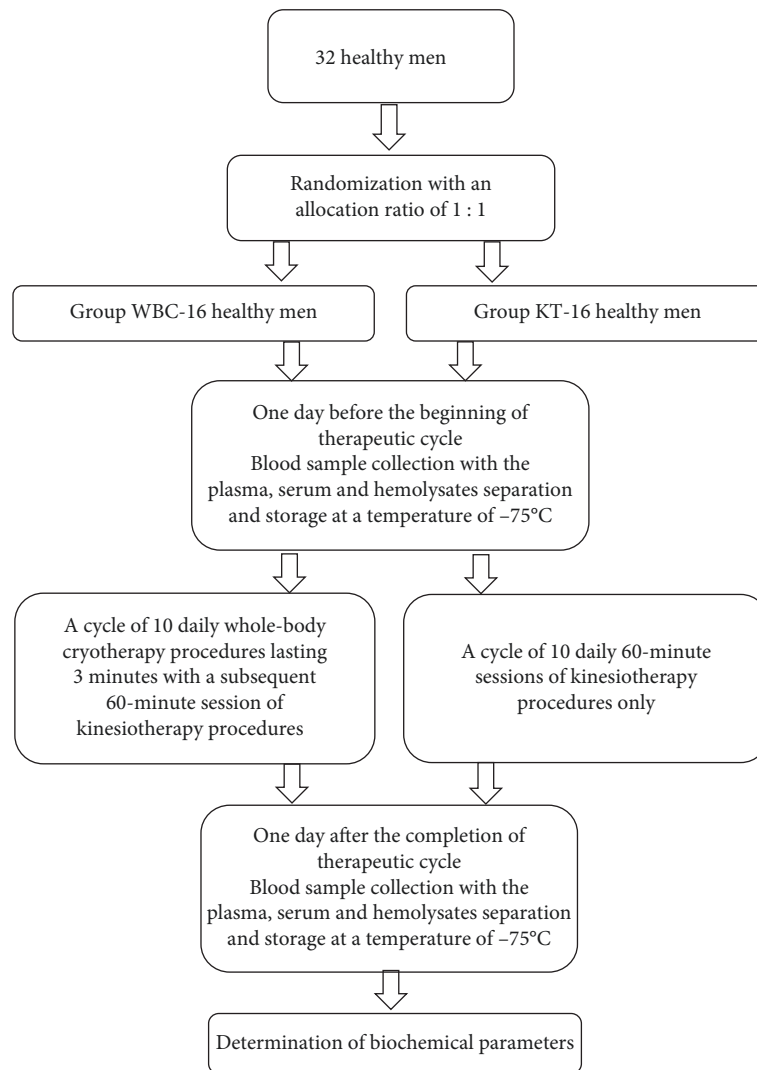


FIGURE 1: A scheme of the study protocol.

period in the antechamber. After adaptation to cryogenic temperatures in the antechamber, the subjects entered the proper chamber for 3 minutes. During the WBC procedure, all the subjects wore swimsuits, cotton socks, gloves, wooden shoes, and also dust masks to protect their mouths and noses and ear-protectors to cover their ears. The subjects were not allowed to wear jewelry, glasses, and contact lenses. Each subject was given information concerning the rules of behaviour in the cryochamber: the need for slow, shallow breathing and no touching each other while moving about (slow walking in circles) [20, 21, 26].

Directly after leaving the cryogenic chamber, the subjects underwent kinesiotherapy lasting for one hour. The program of kinesiotherapy was the same for all the subjects in both groups. The program of kinesiotherapy consisted of exercises on stationary bikes lasting 20 minutes (5 min.: 3.5 Rate of Perceived Exertion (RPE), 4 min.: 5 RPE, 2 min.: 7 RPE, 4 min.: 5 RPE, and 5 min.: 3.5 RPE), treadmill (20 minutes walking at 4.0 mph), and whole body stretching exercises lasting for 20 minutes. All the exercises were carried out under the supervision of physiotherapists [20]. All the sub-

jects completed the research program, and no complications or side effects related to the WBC procedures were observed.

A scheme of the study protocol is presented in Figure 1.

2.3. Blood Sample Collection. Two blood samples of all the subjects were collected in the morning before the first meal: one on the day before the beginning of the procedure and the other on the day after completing the research program. Samples of whole blood (5 ml) were collected from the basilic vein into tubes containing ethylenediaminetetraacetic acid tripotassium salt (Sarstedt, S-Monovette with 1.6 mg/ml EDTA-K₃) and into tubes with a clot activator (Sarstedt, S-Monovette). The blood samples were centrifuged (10 min., 900 g 4°C), and then, the plasma and serum were immediately separated and stored at a temperature of -75°C, until biochemical analyses could be performed. The red blood cells retained from the removal of EDTA-plasma were rinsed with an isotonic salt solution, and then, 10% of the hemolysates were prepared for further analyses. Hemoglobin concentration in the hemolysates was determined by the standard cyanmethemoglobin method. The inter- and

intra-assay coefficients of variations (CV) were 1.1% and 2.4%, respectively.

2.4. Biochemical Analysis

2.4.1. Determination of Lipid Profile Parameters. Total, HDL, and LDL cholesterol (T-Chol, HDL-Chol, LDL-Chol) and triglyceride (TG) concentrations in serum were estimated using routine techniques (Cobas Integra 400 plus analyzer, Roche Diagnostics, Mannheim, Germany). The concentrations were expressed in mg/dl. The inter- and intra-assay coefficients of variations (CV) were, respectively, 2.8% and 5.4% for T-Chol, 3.2% and 5.4% for HDL-Chol, 2.6% and 6.5% for LDL-Chol, and 2.5% and 7.6% for TG.

2.4.2. Oxidative Stress Analysis

(1) Determination of Lipid Peroxidation Products, Total Oxidative Status, and Oxidative Stress Index. The intensity of plasma and the erythrocyte lipid peroxidation was measured spectrofluorimetrically as thiobarbituric acid-reactive substances (TBARS) according to Ohkawa et al. [27]. The TBARS concentrations were expressed as malondialdehyde (MDA) equivalents in $\mu\text{mol/l}$ in plasma or nmol/gHb in erythrocytes. The inter- and intra-assay coefficients of variations (CV) were 2.1% and 8.3%, respectively.

The total oxidant status (TOS) in serum was determined with the method described by Erel [28] and expressed in $\mu\text{mol/l}$. The inter- and intra-assay coefficients of variations (CV) were 2.2% and 6.4%, respectively.

The oxidative stress index (OSI), an indicator of the degree of oxidative stress, was expressed as the ratio of total oxidant status (TOS) to total antioxidant capacity (FRAP) in arbitrary units [29].

(2) Determination of Activity of Antioxidant Enzymes. The activity of superoxide dismutase (SOD, E.C.1.15.1.1) in plasma and erythrocytes was measured by the Oyanagui method [30]. Enzymatic activity was expressed in nitrite unit (NU) in each mg of hemoglobin (Hb) or ml of blood plasma. One nitrite unit (1 NU) means a 50% inhibition of nitrite ion production by SOD in this method. SOD isoenzymes (SOD-Mn and SOD-ZnCu) were measured using potassium cyanide as the inhibitor of the SOD-ZnCu isoenzyme. The inter- and intra-assay coefficients of variations (CV) were 2.8% and 5.4%, respectively.

The erythrocyte catalase (CAT, E.C.1.11.1.6.) activity was assayed by the Aebi [31] kinetic method. It was expressed in IU/mgHb. The inter- and intra-assay coefficients of variations (CV) were 2.6% and 6.1%, respectively.

The activity of glutathione peroxidase (GPx, E.C.1.11.1.9.) in erythrocytes was determined by Paglia and Valentine's kinetic method [32], with t-butyl peroxide as a substrate and expressed as micromoles of NADPH oxidized per minute and normalized to one gram of hemoglobin (IU/gHb). The inter- and intra-assay coefficients of variations (CV) were 3.4% and 7.5%, respectively.

The erythrocyte glutathione reductase (GR, E.C.1.6.4.2) activity was determined by Richterich's kinetic method [33], expressed as micromoles of NADPH utilized per minute and normalized to one gram of hemoglobin (IU/gHb). The inter- and intra-assay coefficients of variations (CV) were 2.1% and 5.8%, respectively.

(3) Determination of Nonenzymatic Antioxidant Status. The total antioxidant capacity of plasma was assayed as the ferric reducing ability of plasma (FRAP) according to Benzie and Strain [34] and calibrated using Trolox. It was expressed in $\mu\text{mol/l}$. The inter- and intra-assay coefficients of variations (CV) were 1.1% and 3.8%, respectively.

The concentration of protein sulfhydryl (PSH) was determined in serum by Koster's method [35], using dithionitrobenzoic acid (DTNB) and expressed in $\mu\text{mol/l}$. The inter- and intra-assay coefficients of variations (CV) were 2.6% and 5.4%, respectively.

The concentration of uric acid (UA) in serum was measured by a uricase-peroxidase method [36] on the Cobas Integra 400 plus analyzer and expressed as mg/dl. The inter- and intra-assay coefficients of variations (CV) were 1.4% and 4.4%, respectively.

2.5. Statistical Analysis. For statistical analysis, the statistical package of Statistica 10 Pl software was used. For each parameter, the indicators of descriptive statistics were determined (mean value and standard deviation (SD)). The normality of the data distribution was checked using the Shapiro-Wilk test, while the homogeneity of the variance was checked by applying Levene's test. In order to compare differences between groups, either an independent sample Student *t* test was used or, alternatively, the Mann-Whitney *U* test. In the case of dependent samples, the Student *t* test was used or alternatively the Wilcoxon test. Differences at the significance level of $P < 0.05$ were considered as statistically significant.

3. Results

3.1. Lipid Profile Parameters. Levels of T-Chol and LDL-Chol decreased significantly after the treatment in both groups, but the observed decrease of these lipid parameters in the WBC group was higher in comparison to the KT group. In turn, in the WBC group, the level of TG decreased significantly after the completion of the treatment in comparison to the KT group. The level of HDL-Chol did not change significantly in both groups (Figures 2–5).

3.2. Lipid Peroxidation Products, Total Oxidative Status, and Oxidative Stress Index. The subjects in the WBC group who underwent a ten-day long cycle of WBC procedures with subsequent kinesiotherapy had, after the completion of the treatment, a statistically significant decrease in plasma MDA, serum TOS, and value of OSI in comparison to initial values. The differences of these parameters prior to posttreatment values (Δ) in the WBC group were significantly higher in comparison to the KT group. The levels of MDA in

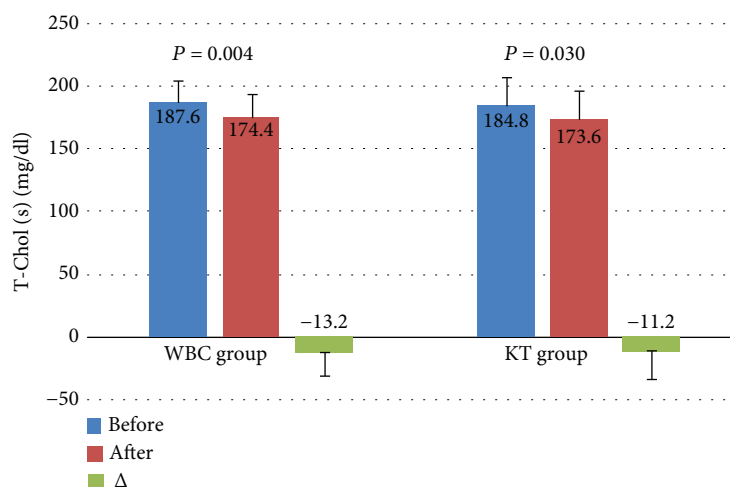


FIGURE 2: Levels of total cholesterol (T-Chol) (mean value \pm standard deviation (SD)) in healthy subjects before and after the completion of a cycle of ten whole-body cryotherapy procedures with subsequent kinesiotherapy (WBC group) or a cycle of ten kinesiotherapy procedures only (KT group), with statistical analyses. (s): serum; Δ : difference prior to posttreatment.

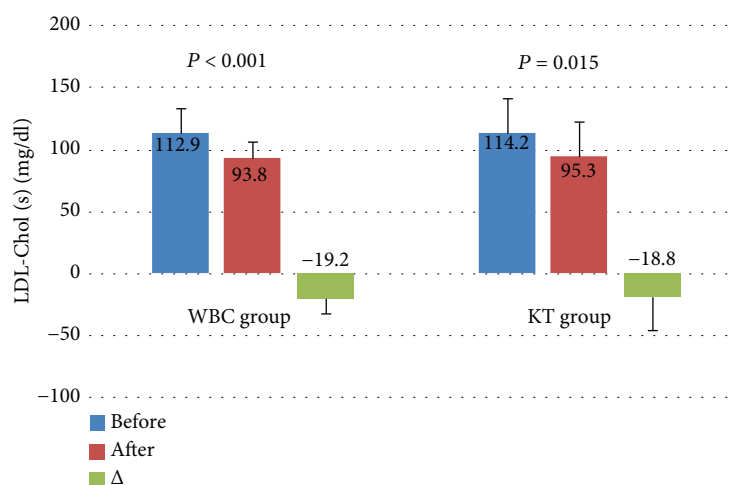


FIGURE 3: Levels of LDL cholesterol (LDL-Chol) (mean value \pm standard deviation (SD)) in healthy subjects before and after the completion of a cycle of ten whole-body cryotherapy procedures with subsequent kinesiotherapy (WBC group) or a cycle of ten kinesiotherapy procedures only (KT group), with statistical analyses. (s): serum; Δ : difference prior to posttreatment.

erythrocyte did not change significantly in the WBC group. In the KT group of subjects who underwent a cycle of only kinesiotherapy, without previous cryotherapy procedures, no significant changes in the levels of plasma and erythrocyte MDA or serum TOS or OSI were observed after the completion of the treatment, in comparison to the initial values before the beginning of the kinesiotherapy cycle (Table 2).

3.3. Antioxidant Enzymes. The subjects in the WBC group had, after the completion of the treatment, a statistically significant increase in the plasma activity of SOD-Mn and erythrocyte total SOD.

However, the activity of plasma total SOD, SOD-CuZn, and erythrocyte activity of CAT, GPx, and GR did not change significantly in the WBC group after the treatment. In the KT group, the erythrocyte activity of total SOD, CAT, and GR, in

contrast to the WBC group, decreased significantly after the treatment. Additionally, the difference prior to posttreatment values (Δ) of erythrocyte total SOD activity in the WBC group was significantly higher as compared to the KT group. Similarly, as in the WBC group, the activity of plasma total SOD, SOD-CuZn, and erythrocyte GPx did not change significantly in the KT group after the treatment.

Additionally, in the KT group, the activity of plasma SOD-Mn and SOD-CuZn did not change significantly after the treatment in comparison to the WBC group (Table 3).

3.4. Nonenzymatic Antioxidant Status. In the WBC group of subjects who underwent a ten-day long cycle of WBC procedures with subsequent kinesiotherapy, FRAP values increased significantly after the treatment. After the completion of the treatment, FRAP values were significantly higher

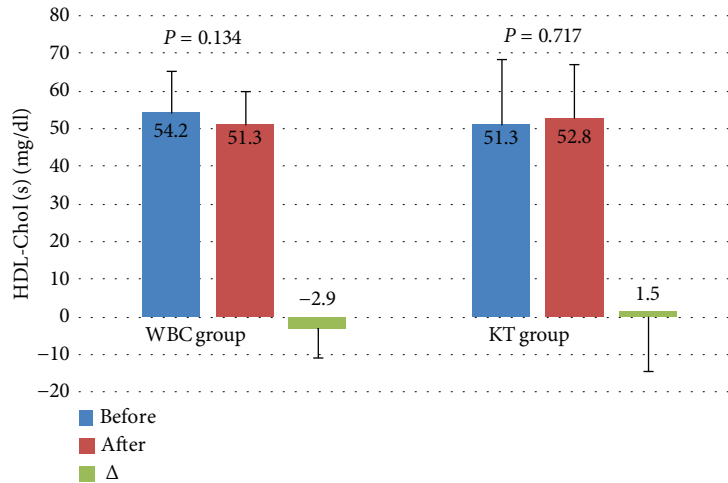


FIGURE 4: Levels of HDL cholesterol (HDL-Chol) (mean value \pm standard deviation (SD)) in healthy subjects before and after the completion of a cycle of ten whole-body cryotherapy procedures with subsequent kinesiotherapy (WBC group) or a cycle of ten kinesiotherapy procedures only (KT group), with statistical analyses. (s): serum; Δ : difference prior to posttreatment.

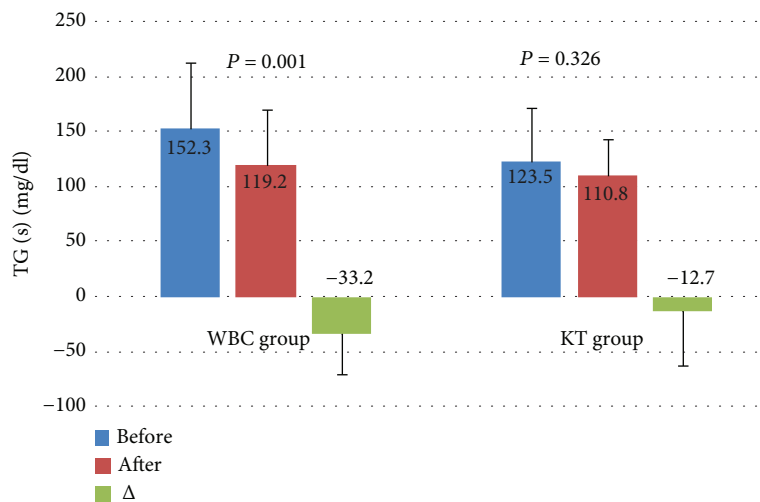


FIGURE 5: Levels of triglycerides (TG) (mean value \pm standard deviation (SD)) in healthy subjects before and after the completion of a cycle of ten whole-body cryotherapy procedures with subsequent kinesiotherapy (WBC group) or a cycle of ten kinesiotherapy procedures only (KT group), with statistical analyses. (s): serum; Δ : difference prior to posttreatment.

in the WBC group when compared to the KT group. Similarly, the difference of this parameter prior to posttreatment values (Δ) in the WBC group was significantly higher in comparison to the KT group. The level of PSH and UA in the WBC group of subjects did not change significantly after the treatment. However, FRP values as well as PSH and UA concentration did not change significantly in the KT group of patients who underwent a cycle of kinesiotherapy only, without previous cryotherapy procedures (Table 4).

4. Discussion

Only a few papers have estimated the impact of WBC on lipid profile parameters. In experimental model animals (rats) who were exposed to WBC for 5 or 10 days, HDL and LDL cholesterol fraction decreased and total cholesterol levels in

animals subjected to -60°C sessions for 10 days remained unchanged [37]. However, in the available literature so far, there has been only one paper on the effect of WBC on lipid profile in healthy subjects. Lubkowska et al. [13] reported reducing T-Ch, LDL-Ch, and TG levels and increasing HDL-Ch level after 20 sessions of WBC in healthy men, but after 10 sessions of WBC only, the LDL-Ch level decreased together with an observed HDL-Ch level increase in healthy men (cryogenic temperature -130°C , liquid nitrogen, without kinesiotherapy procedures). In another paper by these authors [38], in obese subjects without diet modification, a significant decrease in the level of LDL-Ch and TG was observed with a slight increase in the HDL-Ch level after WBC treatment (temperature -120°C , 2-3 minutes, the type of cryochamber not given), including two cryotherapy treatments of 20 daily sessions in the second and the last month of

TABLE 2: Levels of lipid peroxidation parameters, total oxidative status (TOS), and oxidative stress index (OSI) (mean value \pm standard deviation (SD)) in healthy subjects before and after the completion of a cycle of ten whole-body cryotherapy procedures with subsequent kinesiotherapy (WBC group) or a cycle of ten kinesiotherapy procedures only (KT group), with statistical analyses.

Parameters		WBC group	KT group	P
MDA (p) ($\mu\text{mol/l}$)	Before	2.08 \pm 0.47	2.30 \pm 0.52	0.227
	After	1.63 \pm 0.35	2.39 \pm 0.52	<0.001
	P^*	0.013	0.569	
	Δ	-0.45 \pm 0.61	0.09 \pm 0.70	0.027
MDA (e) (nmol/gHb)	Before	0.13 \pm 0.01	0.17 \pm 0.03	<0.001
	After	0.13 \pm 0.01	0.17 \pm 0.05	0.010
	P^*	0.234	0.999	
	Δ	0.00 \pm 0.01	0.00 \pm 0.05	0.799
TOS (s) ($\mu\text{mol/l}$)	Before	20.69 \pm 4.99	10.12 \pm 3.28	<0.001
	After	15.88 \pm 3.77	11.97 \pm 6.71	0.053
	P^*	0.006	0.485	
	Δ	-4.81 \pm 5.51	1.85 \pm 7.80	0.010
OSI (p/s) (arbitrary unit)	Before	19.51 \pm 7.75	6.84 \pm 3.03	<0.001
	After	9.65 \pm 3.18	10.79 \pm 9.02	0.637
	P^*	<0.001	0.196	
	Δ	-9.87 \pm 7.50	3.96 \pm 8.73	<0.001

P : statistical significance of differences between both groups of patients; P^* : statistical significance of differences between values before and after treatment in particular groups of patients. (p): plasma; (s): serum; (e): erythrocyte lysates; Δ : difference prior to posttreatment.

intervention. In our study, we observed a significant decrease in T-Chol, LDL-Ch, and TG levels after a ten-day long cycle of WBC procedures with subsequent kinesiotherapy in healthy subjects. The HDL-Ch level did not change significantly in the present study in the WBC group after the completion of the treatment.

So far, there have not been many reports on the impact of WBC procedures performed in different cryochambers on the prooxidant-antioxidant balance in healthy subjects.

In their study, Dugue et al. [39] observed a significant increase in the value of total peroxy radical-trapping antioxidant capacity of plasma (TRAP) 2 minutes after cold stress in the first 4 weeks of their study. Thirty-five minutes after application of WBC, the values of TRAP did not vary from baseline values. But after 4 weeks, no changes in TRAP values after the WBC were noticed and no long-term changes in basal TRAP values were observed (temperature: -110°C , time: 2 minutes, coolant liquid nitrogen, 3 times per week for 12 weeks, without subsequent kinesiotherapy).

In the study of Lubkowska et al. [40], healthy men were exposed to a single WBC session (temperature: -130°C , time: 3 minutes, closed cryochamber, liquid nitrogen coolant) without subsequent kinesiotherapy. A significant increase in GPx and GR activities, with a simultaneous decrease in CAT and glutathione S-transferase activities, was observed.

TABLE 3: Activities of antioxidant enzymes (mean value \pm standard deviation (SD)) in healthy subjects before and after the completion of a cycle of ten whole-body cryotherapy procedures with subsequent kinesiotherapy (WBC group) or a cycle of ten kinesiotherapy procedures only (KT group), with statistical analyses.

Parameters		WBC group	KT group	P
Total SOD (p) (NU/ml)	Before	9.43 \pm 2.77	11.2 \pm 1.93	0.050
	After	9.40 \pm 3.07	11.6 \pm 3.26	0.062
	P^*	0.818	0.679	
	Δ	-0.03 \pm 4.74	0.40 \pm 3.82	0.775
SOD-Mn (p) (NU/ml)	Before	3.96 \pm 2.01	4.50 \pm 1.41	0.387
	After	5.19 \pm 2.05	5.16 \pm 2.19	0.964
	P^*	0.030	0.179	
	Δ	1.23 \pm 1.96	0.65 \pm 2.00	0.419
SOD-CuZn (p) (NU/ml)	Before	6.77 \pm 2.70	6.72 \pm 1.96	0.957
	After	4.84 \pm 2.05	6.60 \pm 2.92	0.060
	P^*	0.063	0.918	
	Δ	-1.93 \pm 4.05	-0.12 \pm 3.05	0.166
Total SOD (e) (NU/mgHb)	Before	83.0 \pm 9.82	114.0 \pm 20.8	<0.001
	After	102.0 \pm 13.1	98.5 \pm 17.4	0.493
	P^*	0.001	0.002	
	Δ	19.3 \pm 13.9	-15.3 \pm 12.7	<0.001
CAT (e) (IU/mgHb)	Before	104.0 \pm 15.0	128.0 \pm 11.2	0.352
	After	112.0 \pm 11.2	111.0 \pm 15.6	0.242
	P^*	0.179	0.049	
	Δ	34.4 \pm 87.0	39.9 \pm 80.0	0.853
GPx (e) (IU/gHb)	Before	23.1 \pm 3.86	23.8 \pm 7.20	0.752
	After	22.0 \pm 4.57	21.2 \pm 3.71	0.606
	P^*	0.121	0.179	
	Δ	-1.17 \pm 3.31	-2.59 \pm 7.99	0.519
GR (e) (IU/gHb)	Before	1.17 \pm 0.37	1.49 \pm 0.53	0.056
	After	0.99 \pm 0.48	1.14 \pm 0.61	0.450
	P^*	0.134	0.010	
	Δ	-0.18 \pm 0.43	-0.35 \pm 0.44	0.267

P : statistical significance of differences between both groups of patients; P^* : statistical significance of differences between values before and after treatment in particular groups of subjects. (p): plasma; (e): erythrocyte lysates; Δ : difference prior to posttreatment.

A significant increase in the concentration of glutathione, uric acid, albumins, and extraerythrocyte hemoglobin was also observed in the serum of the subjects. The level of TOS did not change after WBC procedure. The authors concluded that a single stimulation with cryogenic temperatures results in oxidative stress in a healthy body, but the level of this stress is not very high.

However, Mila-Kierzenkowska et al. [41] showed that even a single application of cryotherapy prior to exercise may have a beneficial impact on the antioxidant system of the body and alleviates signs of exercise-induced oxidative

TABLE 4: Levels of nonenzymatic antioxidants (mean value \pm standard deviation (SD)) in healthy subjects before and after the completion of a cycle of ten whole-body cryotherapy procedures with subsequent kinesiotherapy (WBC group) or a cycle of ten kinesiotherapy procedures only (KT group), with statistical analyses.

Parameters		WBC group	KT group	P
FRAP ($\mu\text{mol/l}$)	Before	646.1 \pm 146.0	639.4 \pm 83.8	0.876
	After	727.1 \pm 114.4	609.9 \pm 90.4	0.003
	P*	<0.001	0.088	
	Δ	81.0 \pm 59.6	-29.5 \pm 78.9	<0.001
PSH (s) ($\mu\text{mol/l}$)	Before	613.2 \pm 323.1	481.4 \pm 126.8	0.145
	After	588.6 \pm 312.7	451.4 \pm 137.0	0.123
	P*	0.438	0.087	
	Δ	-24.6 \pm 170.1	-30.1 \pm 163.2	0.926
UA (s) (mg/dl)	Before	5.33 \pm 1.50	5.61 \pm 0.86	0.513
	After	5.47 \pm 1.26	5.31 \pm 1.24	0.720
	P*	0.352	0.198	
	Δ	0.15 \pm 0.85	-0.30 \pm 0.88	0.154

P: statistical significance of differences between both groups of patients; P*: statistical significance of differences between values before and after treatment in particular groups of patients. (p): plasma; (s): serum; Δ : difference prior to posttreatment.

stress (a single session of WBC, temperature: -130°C , time: 1-2 min., cryochamber with cold retention, liquid air coolant).

In addition, Miller et al. [42] also observed an increase in total antioxidant status and the level of UA as a result of a series of short-term whole-body cryotherapy (10 WBC sessions, temperature: -130°C , time: 3 minutes, without subsequent kinesiotherapy) in healthy subjects.

In our research, the WBC group who underwent a ten-day long cycle of WBC procedures with subsequent kinesiotherapy had, after the completion of the treatment, a significant decrease in plasma MDA, serum TOS, and value of OSI. This is in comparison to initial values and the KT group of subjects who underwent a cycle of kinesiotherapy only, without previous cryotherapy procedures. Additionally, the subjects in the WBC group had, after the completion of the treatment, a significant increase in the plasma activity of SOD-Mn, FRAP values, and erythrocyte total SOD in comparison to the KT group. So, a ten-day long cycle of WBC procedures performed in a closed cryochamber cooled by liquid nitrogen at the temperature of -120°C with subsequent kinesiotherapy significantly decreased oxidative stress in healthy subjects.

The observed differences in the results of various researches may be related to the type of cryochamber being used and the coolant medium, in addition to the time and temperature of exposure to WBC as well as sex and body mass of subjects. Therefore, further studies are necessary [43].

4.1. Novelty of the Presented Research. In this research, for the first time, we assessed the influence of WBC, performed in a

closed cryochamber (Wroclawski type) with a subsequent session of kinesiotherapy, on oxidative stress and lipid profile parameters, which were estimated simultaneously in healthy subjects.

There have been a few studies [41, 42], which showed a beneficial influence of WBC procedures on the prooxidant-antioxidant balance in healthy subjects, but they were performed in different circumstances (type of cryochamber, temperature, without subsequent sessions of kinesiotherapy), and very often, the authors only estimated the level of selected parameters of prooxidant-antioxidant balance. In the presented study, we estimated oxidative stress assessing the parameters of enzymatic and nonenzymatic antioxidant system as well as parameters of lipid peroxidation, total oxidant status, and oxidative stress index.

Similarly, in the available literature, there has been only one study [13], which estimated the influence of WBC on lipid profile parameters in healthy subjects, but WBC procedures were not connected with a subsequent session of kinesiotherapy, and the authors only estimated lipid profile parameters.

The obtained results in this presented study are similar to our previous research, in which a beneficial impact of ten WBC procedures performed in a cryochamber with cold retention followed by kinesiotherapy (temperature: -120°C , time: 3 min, liquid air coolant) on oxidative stress was observed in healthy subjects [20]. We also observed a similar influence of WBC procedures performed in closed cryochamber [21] as well as in cryochamber with cold retention [44] on oxidative stress in patients with ankylosing spondylitis. Additionally, we observed in patients with ankylosing spondylitis a significant decrease in T-Ch, LDL-Ch, and TG levels after the completion of ten daily procedures of WBC treatment (cryochamber with cold retention cooled by synthetic liquid air, temperature: -120°C) followed by kinesiotherapy [44].

To sum up, for the first time, in our studies, we showed that WBC performed in closed cryochamber and in cryochamber with cold retention has similar effect on oxidative stress and lipid profile. It also seems that it does not depend on the state of health. The obtained results give very important information about indications for the use of WBC by physicians and physiotherapists.

5. General Conclusion

Whole-body cryotherapy procedures performed in a closed cryochamber (Wroclawski type) followed by kinesiotherapy decrease lipid profile as well as oxidative stress in healthy subjects. Whole-body cryotherapy may be a beneficial wellness method.

Data Availability

The data used to support the findings of this study are included within the article.

Conflicts of Interest

The authors declare that there are no conflicts of interests regarding the publication of this paper.

Acknowledgments

This work was supported by grants from the Medical University of Silesia (KNW-1-010/K/8/K and KNW-1-002/K/9/K).

References

- [1] R. Bouzigon, F. Grappe, G. Ravier, and B. Dugue, “Whole- and partial body cryostimulation/cryotherapy: current technologies and practical applications,” *Journal of Thermal Biology*, vol. 61, pp. 67–81, 2016.
- [2] A. Sieroń, G. Cieslar, and A. Stanek, Eds., *Cryotherapy: theoretical bases, biological effects, clinical applications*, Alfa-Medica Press, Bielsko-Biala, 2010.
- [3] A. Stanek, A. Cholewka, G. Cieslar, I. Rosmus-Kuczia, Z. Drzazga, and A. Sieroń, “The assessment of the analgesic action of whole-body cryotherapy in patients with ankylosing spondylitis,” *Fizjoterapia Polska*, vol. 1, no. 4, pp. 49–55, 2011.
- [4] G. Banfi, G. Melegati, A. Barassi et al., “Effects of whole-body cryotherapy on serum mediators of inflammation and serum muscle enzymes in athletes,” *Journal of Thermal Biology*, vol. 34, no. 2, pp. 55–59, 2009.
- [5] H. Pournot, F. Bieuzen, J. Louis et al., “Time-course of changes in inflammatory response after whole-body cryotherapy multi exposures following severe exercise,” *PLoS One*, vol. 6, no. 7, article e22748, 2011.
- [6] A. Stanek, G. Cieslar, K. Strzelczyk et al., “Influence of cryogenic temperatures on inflammatory markers in patients with ankylosing spondylitis and healthy volunteers,” *Polish Journal of Environmental Study*, vol. 19, no. 1, pp. 167–175, 2010.
- [7] J. Rymaszewska, D. Ramsey, and S. Chładzińska-Kiejna, “Whole-body cryotherapy as adjunct treatment of depressive and anxiety disorders,” *Archivum Immunologiae et Therapiae Experimentalis*, vol. 56, no. 1, pp. 63–68, 2008.
- [8] I. Korzonek-Szlacheta, T. Wielkoszyński, A. Stanek, E. Świętochowska, J. Karpe, and A. Sieroń, “Influence of whole-body cryotherapy on the levels of some hormones in professional footballers,” *Endokrynologia Polska*, vol. 58, no. 1, pp. 27–33, 2007.
- [9] J. Leppäluoto, T. Westerlund, P. Huttunen et al., “Effects of long-term whole-body cold exposures on plasma concentrations of ACTH, beta-endorphin, cortisol, catecholamines and cytokines in healthy females,” *Scandinavian Journal of Clinical and Laboratory Investigation*, vol. 68, no. 2, pp. 145–153, 2008.
- [10] J. Rymaszewska, K. M. Urbańska, D. Szcześniak, B. Stańczykiewicz, E. Trypka, and A. Zabłocka, “The improvement of memory deficits after whole-body cryotherapy – the first report,” *CryoLetters*, vol. 39, no. 3, pp. 190–195, 2018.
- [11] P. Sutkowy, B. Augustyńska, A. Woźniak, and A. Rakowski, “Physical exercise combined with whole-body cryotherapy in evaluating the level of lipid peroxidation products and other oxidant stress indicators in kayakers,” *Oxidative Medicine and Cellular Longevity*, vol. 2014, Article ID 402631, 7 pages, 2014.
- [12] A. Wozniak, B. Wozniak, G. Drewa, and C. Mila-Kierzenkowska, “The effect of whole-body cryostimulation on the prooxidant–antioxidant balance in blood of elite kayakers after training,” *European Journal of Applied Physiology*, vol. 101, no. 5, pp. 533–537, 2007.
- [13] A. Lubkowska, G. Banfi, B. Dołęgoska, G. V. M. d’Eril, J. Łuczak, and A. Barassi, “Changes in lipid profile in response to three different protocols of whole-body cryostimulation treatments,” *Cryobiology*, vol. 61, no. 1, pp. 22–26, 2010.
- [14] M. O’Connor, J. V. Wang, and N. Saedi, “Whole- and partial-body cryotherapy in aesthetic dermatology: evaluating a trendy treatment,” *Journal of Cosmetic Dermatology*, 2018.
- [15] A. Skrzek, A. Ciszek, D. Nowicka, and A. Dębiec-Bąk, “Evaluation of changes in selected skin parameters under the influence of extremely low temperature,” *Cryobiology*, vol. 86, pp. 19–24, 2019.
- [16] G. Lombardi, E. Ziemann, and G. Banfi, “Whole-body cryotherapy in athletes: from therapy to stimulation. An updated review of the literature,” *Frontiers in Physiology*, vol. 8, no. 258, p. 16, 2017.
- [17] C. Rose, K. M. Edwards, J. Siegler, K. Graham, and C. Caillaud, “Whole-body cryotherapy as a recovery technique after exercise: a review of the literature,” *International Journal of Sports Medicine*, vol. 38, no. 14, pp. 1049–1060, 2017.
- [18] X. Guillot, N. Tordi, L. Mourrot et al., “Cryotherapy in inflammatory rheumatic diseases: a systematic review,” *Expert Review of Clinical Immunology*, vol. 10, no. 2, pp. 281–294, 2014.
- [19] J. Rivera, M. J. Tercero, J. S. Salas, J. H. Gimeno, and J. S. Alejo, “The effect of cryotherapy on fibromyalgia: a randomised clinical trial carried out in a cryosauna cabin,” *Rheumatology International*, vol. 38, no. 12, pp. 2243–2250, 2018.
- [20] A. Stanek, K. Sieroń-Stoltny, E. Romuk et al., “Whole-body cryostimulation as an effective method of reducing oxidative stress in healthy men,” *Advances in Clinical and Experimental Medicine*, vol. 25, no. 6, pp. 1281–1291, 2016.
- [21] A. Stanek, A. Cholewka, T. Wielkoszyński, E. Romuk, and A. Sieroń, “Decreased oxidative stress in male patients with active phase ankylosing spondylitis who underwent whole-body cryotherapy in closed cryochamber,” *Oxidative Medicine and Cellular Longevity*, vol. 2018, Article ID 7365490, 9 pages, 2018.
- [22] A. Lubkowska, B. Dolegowska, and Z. Szygula, “Whole-body cryostimulation - potential beneficial treatment for improving antioxidant capacity in healthy men - significance of the number of sessions,” *PLoS One*, vol. 7, no. 10, article e46352, 2012.
- [23] A. Stanek, A. Cholewka, T. Wielkoszyński, E. Romuk, K. Sieroń, and A. Sieroń, “Increased levels of oxidative stress markers, soluble CD40 ligand and carotid intima-media thickness reflect acceleration of atherosclerosis in male patients with ankylosing spondylitis in active phase and without the classical cardiovascular risk factors,” *Oxidative Medicine and Cellular Longevity*, vol. 2017, Article ID 9712536, 8 pages, 2017.
- [24] J. Budziosz, A. Stanek, A. Sieroń, J. Witkoś, A. Cholewka, and K. Sieroń, “Effects of low-frequency electromagnetic field on oxidative stress in selected structures of the central nervous system,” *Oxidative Medicine and Cellular Longevity*, vol. 2018, Article ID 1427412, 8 pages, 2018.
- [25] A. Rahal, A. Kumar, V. Singh et al., “Oxidative stress, prooxidants, and antioxidants: the interplay,” *BioMed Research International*, vol. 2014, Article ID 761264, 19 pages, 2014.
- [26] A. Stanek, A. Cholewka, J. Gadula, Z. Drzazga, A. Sieron, and K. Sieron-Stoltny, “Can whole-body cryotherapy with

- subsequent kinesiotherapy procedures in closed type cryogenic chamber improve BASDAI, BASFI, and some spine mobility parameters and decrease pain intensity in patients with ankylosing spondylitis?," *BioMed Research International*, vol. 2015, Article ID 404259, 11 pages, 2015.
- [27] H. Ohkawa, N. Ohishi, and K. Yagi, "Assay for lipid peroxides in animal tissues by thiobarbituric acid reaction," *Analytical Biochemistry*, vol. 95, no. 2, pp. 351–358, 1979.
- [28] O. Erel, "A new automated colorimetric method for measuring total oxidant status," *Clinical Biochemistry*, vol. 38, no. 12, pp. 1103–1111, 2005.
- [29] M. Harma, M. Harma, and O. Erel, "Increased oxidative stress in patients with hydatidiform mole," *Swiss Medical Weekly*, vol. 133, no. 41–42, pp. 563–566, 2003.
- [30] Y. Oyanagui, "Reevaluation of assay methods and establishment of kit for superoxide dismutase activity," *Analytical Biochemistry*, vol. 142, no. 2, pp. 290–296, 1984.
- [31] H. Aebi, "[13] Catalase *in vitro*," *Methods in Enzymology*, vol. 105, pp. 121–126, 1984.
- [32] D. Paglia and W. Valentine, "Studies on the quantitative and qualitative characterization of erythrocyte glutathione peroxidase," *Journal of Laboratory and Clinical Medicine*, vol. 70, no. 1, pp. 158–169, 1967.
- [33] R. Richterich, *Clinical Chemistry: Theory and Practice*, Academic Press, New York, NY, USA, 1969.
- [34] I. F. F. Benzie and J. J. Strain, "The ferric reducing ability of plasma (FRAP) as a measure of "antioxidant power": the FRAP assay," *Analytical Biochemistry*, vol. 239, no. 1, pp. 70–76, 1996.
- [35] J. F. Koster, P. Biemond, and A. J. Swaak, "Intracellular and extracellular sulphhydryl levels in rheumatoid arthritis," *Annals of the Rheumatic Diseases*, vol. 45, no. 1, pp. 44–46, 1986.
- [36] Y. Zhao, X. Yang, W. Lu, H. Liao, and F. Liao, "Uricase based methods for determination of uric acid in serum," *Microchimica Acta*, vol. 164, no. 1–2, pp. 1–6, 2009.
- [37] B. Skrzep-Poloczek, E. Romuk, and E. Birkner, "The effect of whole-body cryotherapy on lipids parameters in experimental rat model," *Balneologia Polska*, vol. 44, no. 1–4, pp. 7–13, 2002.
- [38] A. Lubkowska, W. Dudzińska, I. Bryczkowska, and B. Dołęgowska, "Body composition, lipid profile, adipokine concentration, and antioxidant capacity changes during interventions to treat overweight with exercise programme and whole-body cryostimulation," *Oxidative Medicine and Cellular Longevity*, vol. 2015, Article ID 803197, 13 pages, 2015.
- [39] B. Dugué, J. Smolander, T. Westerlund et al., "Acute and long-term effects of winter swimming and whole-body cryotherapy on plasma antioxidative capacity in healthy women," *Scandinavian Journal of Clinical and Laboratory Investigation*, vol. 65, no. 5, pp. 395–402, 2005.
- [40] A. Lubkowska, M. Chudecka, A. Klimek, Z. Szygula, and B. Fraczek, "Acute effect of a single whole-body cryostimulation on prooxidant-antioxidant balance in blood of healthy, young men," *Journal of Thermal Biology*, vol. 33, no. 8, pp. 464–467, 2008.
- [41] C. Mila-Kierzenkowska, A. Jurecka, A. Woźniak, M. Szpinda, B. Augustyńska, and B. Woźniak, "The effect of submaximal exercise preceded by single whole-body cryotherapy on the markers of oxidative stress and inflammation in blood of volleyball players," *Oxidative Medicine and Cellular Longevity*, vol. 2013, Article ID 409567, 10 pages, 2013.
- [42] E. Miller, Ł. Markiewicz, J. Saluk, and I. Majsterek, "Effect of short-term cryostimulation on antioxidative status and its clinical applications in humans," *European Journal of Applied Physiology*, vol. 112, no. 5, pp. 1645–1652, 2012.
- [43] G. Polidori, S. Cuttelli, L. Hammond et al., "Should whole body cryotherapy sessions be differentiated between women and men? A preliminary study on the role of the body thermal resistance," *Medical Hypotheses*, vol. 120, pp. 60–64, 2018.
- [44] A. Stanek, A. Cholewka, T. Wielkoszyński, E. Romuk, and A. Sieroń, "Whole-body cryotherapy decreases the levels of inflammatory, oxidative stress, and atherosclerosis plaque markers in male patients with active-phase ankylosing spondylitis in the absence of classical cardiovascular risk factors," *Mediators of Inflammation*, vol. 2018, Article ID 8592532, 11 pages, 2018.

Research Article

Metabolites of the Nitric Oxide (NO) Pathway Are Altered and Indicative of Reduced NO and Arginine Bioavailability in Patients with Cardiometabolic Diseases Complicated with Chronic Wounds of Lower Extremities: Targeted Metabolomics Approach (LC-MS/MS)

Małgorzata Krzystek-Korpacka ¹, Jerzy Wiśniewski¹, Mariusz G. Fleszar ^{1,2},
Iwona Bednarz-Misa ¹, Agnieszka Bronowicka-Szydełko¹, Małgorzata Gacka,³
Leszek Masłowski,⁴ Krzysztof Kędzior,¹ Wojciech Witkiewicz,^{5,6} and Andrzej Gamian¹

¹Department of Medical Biochemistry, Wrocław Medical University, Wrocław 50-368, Poland

²PORT Polski Ośrodek Rozwoju Technologii sp, ZOO, Wrocław 54-066, Poland

³Department of Angiology, Hypertension and Diabetes, Wrocław Medical University, Wrocław 50-556, Poland

⁴Department of Angiology, Regional Specialist Hospital, Wrocław 51-124, Poland

⁵Department of Vascular Surgery, Regional Specialist Hospital, Wrocław 51-124, Poland

⁶Research and Development Centre, Regional Specialist Hospital, Wrocław 51-124, Poland

Correspondence should be addressed to Małgorzata Krzystek-Korpacka; malgorzata.krzystek-korpacka@umed.wroc.pl

Received 3 May 2019; Accepted 26 June 2019; Published 14 July 2019

Guest Editor: Aneta Radziwon-Balicka

Copyright © 2019 Małgorzata Krzystek-Korpacka et al. This is an open access article distributed under the Creative Commons Attribution License, which permits unrestricted use, distribution, and reproduction in any medium, provided the original work is properly cited.

Objective. The status of metabolites of the nitric oxide (NO) pathway in patients with chronic wounds in the course of cardiometabolic diseases is largely unknown. Yet arginine supplementation and citrulline supplementation as novel therapeutic modalities aimed at increasing NO are tested. **Material and Methods.** Targeted metabolomics approach (LC-MS/MS) was applied to determine the concentrations of L-arginine, L-citrulline, asymmetric and symmetric dimethylarginines (ADMA and SDMA), and arginine/ADMA and arginine/SDMA ratios as surrogate markers of NO and arginine availability in ulnar and femoral veins, representing systemic and local levels of metabolites, in patients with chronic wounds in the course of cardiometabolic diseases ($n = 59$) as compared to patients without chronic wounds but with similar cardiometabolic burden ($n = 55$) and healthy individuals ($n = 88$). **Results.** Patients with chronic wounds had significantly lower systemic L-citrulline and higher ADMA and SDMA concentrations and lower L-arginine/ADMA and L-arginine/SDMA as compared to healthy controls. The presence of chronic wounds in patients with cardiometabolic diseases was associated with decreased L-arginine but with increased L-citrulline, ADMA, and SDMA concentrations and decreased L-arginine/ADMA and L-arginine/SDMA. Serum obtained from the ulnar and femoral veins of patients with chronic wounds differed by L-arginine concentrations and L-arginine/SDMA ratio, both lower in the femoral vein. Wound etiology affected L-citrulline and SDMA concentrations, lower and higher, respectively, in patients with venous stasis, and the L-arginine/SDMA ratio—lower in venous stasis. The wound type affected L-arginine/ADMA and citrulline—lower in patients with ulcerations or gangrene. IL-6 was an independent predictor of L-arginine/ADMA, VEGF-A of ADMA, G-CSF of L-arginine/SDMA, and GM-CSF of L-citrulline and SDMA. **Conclusion.** Chronic wounds in the course of cardiometabolic diseases are associated with reduced NO and arginine availability due to ADMA and SDMA accumulation rather than arginine deficiency, not supporting its supplementation. Wound character seems to affect NO bioavailability and wound etiology—arginine bioavailability. Arginine concentration and its availability are more markedly reduced at the local level than the systemic level.

1. Introduction

Sufficient synthesis and bioavailability of nitric oxide (NO)—a free radical and a key vasodilator—are crucial for proper functioning of the vascular endothelium. Consequently, NO deficiency is a prerequisite for and a hallmark of endothelial dysfunction, a pathology preceding the development of cardiovascular diseases (CVD) [1]. CVD and their main risk factors, such as obesity, hypertension, and type 2 diabetes mellitus (T2DM), are, in turn, among key factors negatively affecting proper wound healing [2]. Nonhealing wounds constitute a serious problem for affected people and a growing burden for public health care [3]. Currently, they affect 4.5 million people in the United States alone [4] but the incidence of chronic wounds is likely to increase along with estimated rise in the incidence of CVD, obesity, and T2DM [5–8]. The overall prevalence of peripheral artery disease (PAD) in Europe is estimated to be 5.3% but differs by country [9]. The disturbed blood flow and blood vessel damage accompanying CVD and specifically PAD may result in ulcerations or gangrene located in the lower extremities [9–11]. NO-releasing wound dressings as well as diet supplementation with L-arginine, a NO substrate, are currently being evaluated as novel modalities in the treatment of chronic wounds [12, 13].

Successful healing requires spacial and temporal cooperation of a myriad of players, mediating three key phases of the process: inflammatory, proliferative, and remodelling [5]. Nonhealing wounds are believed to be locked in the inflammatory phase [14]. While most mediators are proteins, other molecules, such as NO, are recently gaining attention as potentially relevant for all phases of the healing [15–19]. The importance of NO has been demonstrated by the delayed healing of animals with genetically impaired NO synthesis [20, 21]. Moreover, it has been shown that NO therapy is effective in healing ischemic [22] and diabetic ulcers [23] in experimental animals by inducing reepithelization, angiogenesis, and collagen synthesis.

NO is synthesized by nitric oxide synthases (NOS) from L-arginine, and L-citrulline is the other reaction product. There are three isoforms of the enzyme: constitutively expressed endothelial (eNOS; NOS1) and neuronal (nNOS; NOS3) isoforms and the inducible isoform (iNOS; NOS2) [24]. The activity of NOS enzymes is regulated by methylated derivatives of arginine, of which asymmetric dimethylarginine (ADMA) is believed to be a strong and symmetric dimethylarginine (SDMA) a weak enzyme inhibitor. Both ADMA and SDMA compete with L-arginine for its transporters, and therefore, their accumulation decreases NO production by diminishing L-arginine availability for the NOS enzymes. The ADMA and SDMA pool is regulated at the level of their synthesis, conducted by the protein arginine methyltransferases (PRMTs), and degradation. While ADMA is mostly catabolized to L-citrulline and dimethylamine (DMA), by dimethylarginine dimethylaminohydrolases (DDAHs), SDMA is preferentially excreted with urine. L-Citrulline may be used in the arginine-citrulline cycle to satisfy the body demand for L-arginine [24].

The gaseous nature, high diffusion capacity, and short half-life make NO the ideal signalling molecule but cause its quantification to be a challenge. Therefore, relatively more stable products of NO oxidation, nitrites and nitrates, are measured instead of NO. Nitrate has even been proposed as a “wound healing biomarker and surrogate end point” for treatment of diabetic foot ulcers [18]. Another approach for the assessment of NO and its bioavailability is the evaluation of intermediates in the NO synthesis pathway and inhibitors of NOS enzymes. Of those, the measurement of L-arginine and/or ADMA is the most popular.

Despite the relevance of NO for wound healing, the status of its pathway metabolites and surrogate markers is largely unknown. Recently, an elevation in serum ADMA [25] has been reported in patients with chronic wounds while our own preliminary research showed a decrease in serum L-arginine [26]. However, there seem to be a paucity of data on SDMA and citrulline or regarding the possible association between NO metabolites and wound etiology and the type or their interplay with inflammatory and immune mediators. Therefore, this study was designed to simultaneously evaluate a wider panel of L-arginine/NO pathway metabolites using targeted metabolomics approach and a novel assay recently developed by our group [27]. We measured L-arginine, L-citrulline (referred to hereafter simply as arginine and citrulline), ADMA, and SDMA to determine their status and clinical relevance in patients with chronic wounds of various etiologies and types, at systemic and local levels.

2. Materials and Methods

2.1. Ethical Approval. The study protocol was approved by the Medical Ethics Committees of Wroclaw Medical University (#KB-384/2012) from April 12, 2012, and the study was conducted in accordance with the Helsinki Declaration of 1975, as revised in 1983, and an informed consent has been obtained from all patients.

2.2. Patients. The study population consisted of 202 individuals: 114 patients with cardiovascular diseases and/or diabetes, of whom 59 had chronic wounds of lower extremities, and 88 healthy individuals. Patients were recruited from among patients of the Dept. of Angiology of the Regional Specialist Hospital and the Dept. of Angiology, Hypertension and Diabetes of the Wroclaw Medical University. Concerning patients with nonhealing wounds, only those with wounds in the course of vascular disease and diabetes were included while others, with wounds due to autoimmune diseases, malignancy, infections, or drugs, were not enrolled. Wound etiology was determined by the evaluation of wound characteristics (location and an appearance of the wound, its borders and those of the surrounding skin, pain, and the presence of bleeding on manipulation) in addition to the patient's history and clinical assessment, which was based on the ankle-brachial pressure index, ultrasound, angiography, and computer tomography. The wound etiology was as follows: venous stasis ($n = 25$), ischemic (arterial) ($n = 17$), and neurotrophic ($n = 17$). Patients' wounds were mechanically cleaned of necrotic tissue and excess wound exudate,

photographs were taken, and wound material was collected for bacteriological examination. Subsequently, wounds were washed with antiseptic octenidine dihydrochloride and dressed using a sterile gauze. None of the patients used arginine supplements.

The control group consisted of healthy volunteers recruited from hospital staff and blood donors from Lower Silesian Center of Blood Donation and Therapy, Wrocław, Poland (recruited on the basis of standard eligibility criteria for blood donation with an age > 50 yrs. and an insignificant medical history as additional inclusion criteria for the current study). Table 1 presents detailed characteristics of the study population, and the categorization into examined groups is depicted in Figure 1.

In a subgroup of patients ($n = 7$), blood was sampled from the ulnar and femoral veins in order to compare systemic metabolite concentrations with those more local and closer to the wound.

2.3. Analytical Methods. Blood (7.5 mL), after an overnight fasting, was drawn into serum separator tubes from ulnar veins and, additionally, from femoral veins. Blood was clotted for 30 min and subsequently centrifuged (15 min, 10°C, 720×g). Collected serum was aliquoted and kept frozen at -80° until examination.

2.3.1. Materials. LC-MS-grade acetonitrile, water, and methanol were purchased from Merck Millipore (Warsaw, Poland). L-Arginine, SDMA, ADMA, L-citrulline, sodium tetraborate, benzoyl chloride (BCl), and HPLC-grade formic acid (FA) were obtained from Sigma-Aldrich (Poznan, Poland). Isotope-labeled asymmetric dimethylarginine (2,3,3,4,4,5,5-D7-ADMA, 98%) and L-arginine:HCl (D7-arginine, 98%) were acquired from Cambridge Isotope Laboratories (MA, USA). Leucine-enkephalin was purchased from Waters (Warsaw, Poland).

2.3.2. Quantitative Analysis of Metabolites Involved in NO Synthesis. Serum concentrations of metabolites involved in NO synthesis were measured by stable isotope dilution liquid chromatography tandem mass spectrometry using a Xevo G2 quadrupole-TOF instrument (Waters, Milford, MA, USA) as described in detail by Fleszar et al. [27]. Briefly, aliquots of 100 μ L of sera or the calibration sample, 10 μ L of internal standard solution in water (100 μ M D7-arginine and 20 μ M D7-ADMA), and 50 μ L of borate buffer (0.025 M Na₂B₄O₇·10H₂O, 1.77 mM NaOH, pH = 9.2) were transferred into polypropylene microtubes and vortexed (1 min, 1100 rpm, 25°C). Then, 400 μ L of acetonitrile and 10 μ L of 10% BCl in acetonitrile were added and vortexed (5 min, 1100 rpm, 25°C). After derivatization, samples were centrifuged (7 min, 4°C, 15000 × g) and 100 μ L of supernatants was transferred into a chromatographic glass vial with 300 μ L of water for LC-MS analysis.

2.3.3. LC-ESI-MS Analysis. The LC analysis was carried out on a nanoACQUITY UPLC System equipped with an ACQUITY HSS T3 column (50 × 1.0 mm, 1.75 μ m) with a 0.22 μ m membrane inline filter (Waters). The total run time of the method was 10 min with a flow rate of 80 μ L/min.

Mobile phase A consisted of 0.1% FA in water, while mobile phase B consisted of 0.1% FA in methanol. For ADMA and SDMA isomer separation, the following gradient was applied: 11% B for 0–1 min, 11%–13% B for 1–2 min, 13%–60% B for 2–5 min, 60%–90% B for 5–5.5 min, 90% B for 5.5–6 min, and 90%–11% B for 6–6.05 min. The sample injection volume was 2 μ L.

Mass spectra for the compounds were acquired in a Xevo G2 Q-TOF mass spectrometer (Waters) in positive ion mode electrospray ionization (ESI). The MS operating conditions were as follows: capillary voltage, 3000 V; cone voltage, 40 V; source temperature, 120°C; cone gas flow, 85 L/hour; desolvation temperature, 350°C; and desolvation gas flow, 800 L/hour. Data acquisition was carried on MassLynx Software (Waters) using the following ions: 279.1457 m/z , 286.1897 m/z , 307.1770 m/z , 314.2076 m/z , and 280.1136 m/z for L-arginine, D7-arginine, ADMA and SDMA, D7-ADMA, and L-citrulline, respectively.

As previously described [27], the method is characterized by intra- and interassay coefficients of variation of 1.6% and 3.3% for arginine, 3.2% and 3.1% for citrulline, 7.5% and 9.4% for ADMA, and 6.4% and 7.1% for SDMA determination.

2.4. Statistical Analysis. Data were tested for normality of distribution using the Kolmogorov-Smirnoff test and for homogeneity of variances using Levene's test and presented as means or medians with 95% confidence interval (CI) around them. Between-group differences in means or medians were tested using a *t*-test for independent samples with Welch correction if appropriate or with the Mann-Whitney *U* test (two-group comparisons) and with a one-way ANOVA with the Tukey-Kramer post hoc test or with the Kruskal-Wallis *H* test with the Conover post hoc test (multigroup comparisons). Log-transformation was used if necessary to obtain normality of distribution and/or homogeneity of variances. Additionally, a *t*-test for paired samples was used to analyze differences in metabolite concentrations between femoral and ulnar veins. Frequency analysis was conducted using the chi-squared test. Univariate correlations were examined using Pearson tests. Multivariate linear regression was conducted to discern the independent predictor of NO-associated metabolites. Regression models were built with a stepwise method using the following criteria: enter variable if $p < 0.05$ and remove variable if $p > 0.1$. All calculated probabilities were two-tailed, and p values ≤ 0.05 were considered statistically significant. The analyses were performed using MedCalc Statistical Software version 18.11.6 (MedCalc Software bvba, Ostend, Belgium; <https://www.medcalc.org>; 2019).

3. Results

Both patients' cohorts were well matched with respect to sex distribution, age, and concentrations of biochemical indices, indicative of similar disease burden. There were, however, significant differences in HDL cholesterol and CRP lower and higher, respectively, in patients with chronic wounds (Table 1). There were no sex-related differences in any

TABLE 1: Characteristics of the study population.

Parameter	Healthy controls	Patients with cardiometabolic diseases		p value
		Without chronic wounds	With chronic wounds	
Number of patients	88	55	59	—
Age (yrs.), median (range)	63 (50-73)	64 (49-81)	65 (40-87)	0.086 ^K
Sex (F/M), n	33/55	29/26	22/37	0.145 ^{χ²}
FG (mg/dL), mean (95% CI)	—	159.5 (149-179)	147.2 (105-189)	0.591 ^W
HbA1C (%), mean (95% CI)	—	7.73 (7.2-8.2)	7.98 (7-8.9)	0.620 ^t
CHOL (mg/dL), median (95% CI)	—	168 (163-177)	164 (147-175)	0.162 ^M
HDL (mg/dL), median (95% CI)	—	44.5 (40-49)	35 (32-44)	0.008 ^M
LDL (mg/dL), mean (95% CI)	—	101 (91-112)	89.8 (81-99)	0.104 ^W
TG (mg/dL), mean (95% CI)	—	148.4 (129-171)	126.7 (108-148)	0.156 ^t
Creatinine (mg/dL), mean (95% CI)	—	0.98 (0.92-1.04)	0.89 (0.78-1.02)	0.191 ^W
HGB (g/dL), mean (95% CI)	—	13.5 (13-13.9)	12.9 (12.4-13.8)	0.084 ^t
CRP (mg/L), mean (95% CI)	—	1.7 (1.3-2.3)	19.6 (13.5-28.5)	<0.0001 ^t

yrs.: years; F/M: female-to-male ratio; SD: standard deviation; n: number of patients; FG: fasting glucose; HbA1C: glycated hemoglobin; CHOL: total cholesterol; HDL: high-density lipoprotein cholesterol; LDL: low-density lipoprotein cholesterol; TG: triglycerides; HGB: hemoglobin; CRP: C-reactive protein; ^KKruskal-Wallis *H* test; ^WWelch test; ^{χ²}chi-squared test; ^t*t*-test for independent samples; ^MMann-Whitney *U* test.

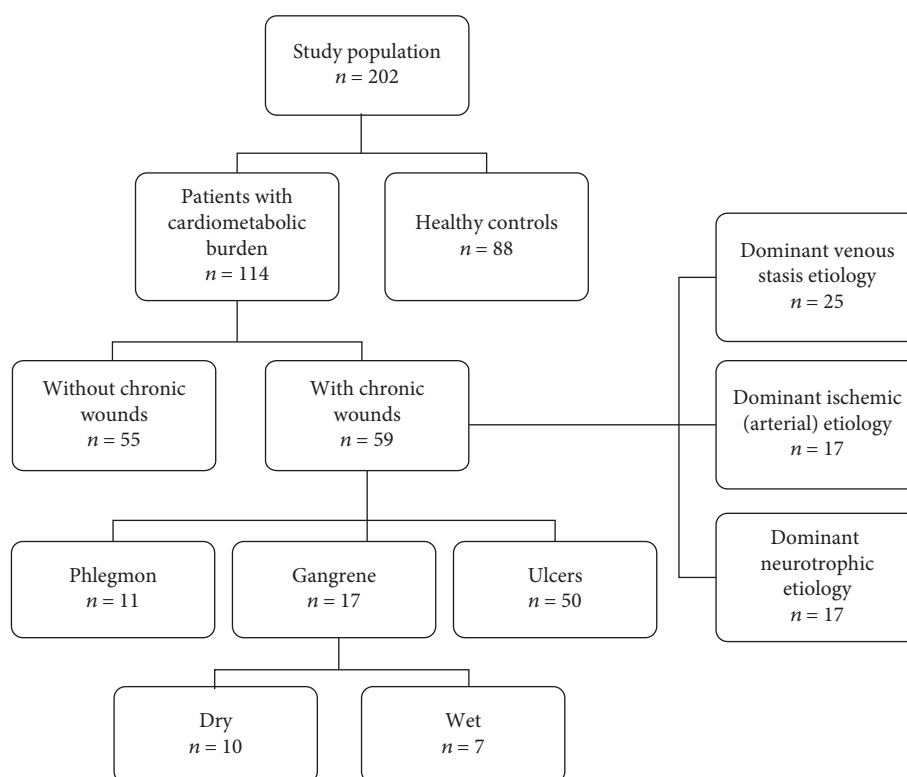


FIGURE 1: Diagram showing the categorization of study population into groups.

intermediate in the arginine/NO pathway among patients with chronic wounds or healthy controls. However, in a group of patients with cardiometabolic diseases without wounds, males had higher citrulline, ADMA, and SDMA concentrations and lower Arg/ADMA and Arg/SDMA ratios (for details, see Suppl. Tab. 1).

3.1. Intermediates in the Arginine/NO Pathway in Patients with Cardiometabolic Diseases with and without Chronic Wounds. As compared to healthy individuals, patients with cardiometabolic diseases without chronic wounds had significantly higher arginine (Figure 2(a)) but lower citrulline (Figure 2(b)) concentrations and comparable ADMA and

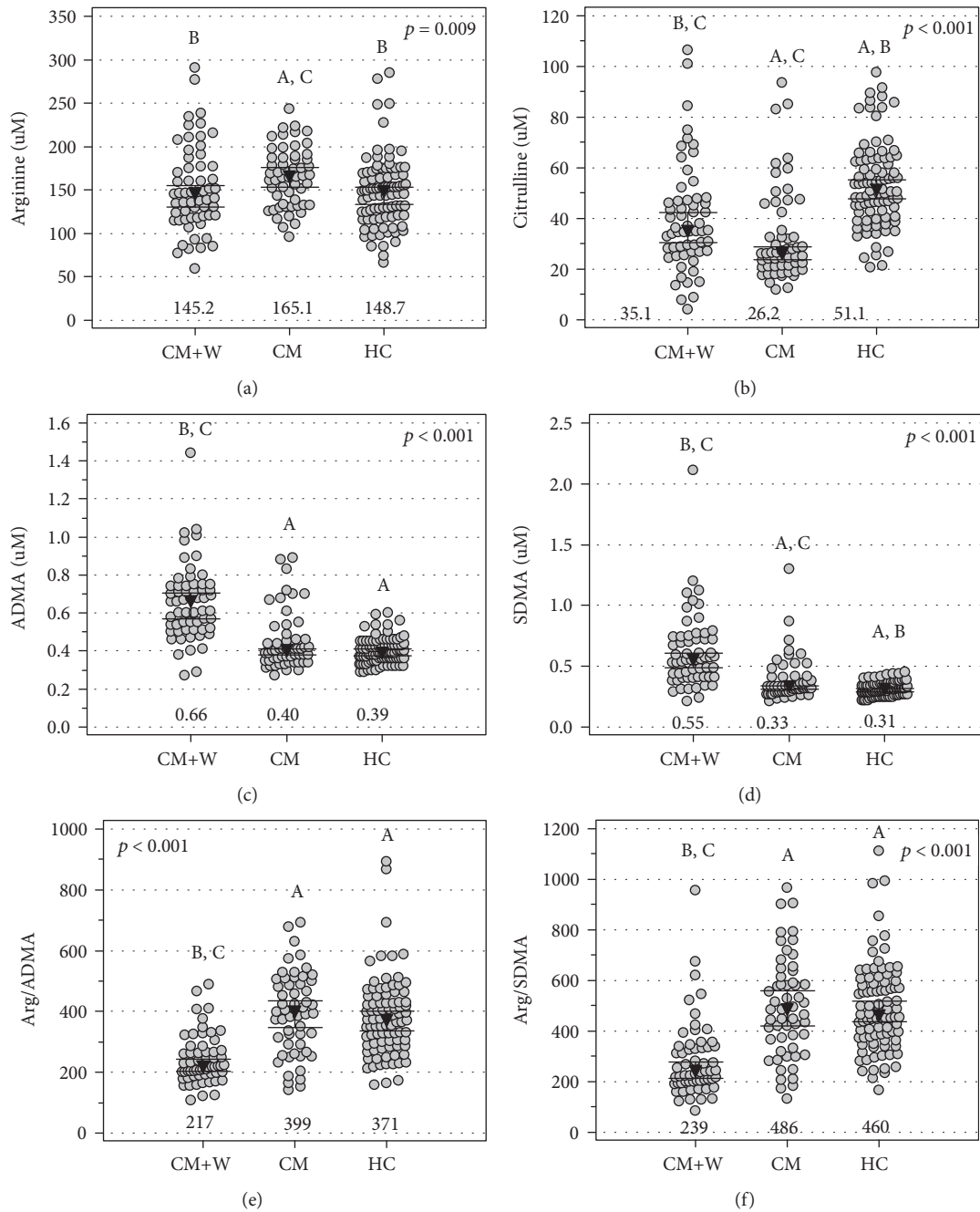


FIGURE 2: Intermediates in the arginine/NO pathway in chronic wounds: (a) arginine, (b) citrulline, (c) ADMA, (d) SDMA, (e) arginine-to-ADMA ratio (Arg/ADMA), and (f) arginine-to-SDMA ratio (Arg/SDMA). Data are presented as medians with 95% confidence intervals and analyzed using the Kruskal-Wallis H test. CM+W: patients with cardiometabolic diseases and chronic wounds; CM: patients with cardiometabolic diseases without chronic wounds; HC: healthy controls. Numbers below the dot plots represent the mean value within a group. Letters above the dot plots indicate groups from which a given group mean differs significantly: A: significantly different from CM +V; B: significantly different from CM; C: significantly different from HC.

SDMA concentrations (Figures 2(c) and 2(d)) and Arg/ADMA and Arg/SDMA ratios (Figures 2(e) and 2(f)). As compared to healthy individuals, patients with cardiometabolic diseases with chronic wounds had significantly lower citrulline (Figure 2(b)) and higher ADMA and SDMA concentrations (Figures 2(c) and 2(d)) and lower Arg/ADMA and Arg/SDMA ratios (Figures 2(e) and 2(f)). The presence of chronic wounds in patients with cardiometabolic diseases was associated with

decreased arginine (Figure 2(a)) but with increased citrulline (Figure 2(b)), ADMA, and SDMA concentrations (Figures 2(c) and 2(d)) and decreased Arg/ADMA and Arg/SDMA ratios (Figures 2(e) and 2(f)).

3.2. Impact of Wound Etiology on Intermediates in the Arginine/NO Pathway. Arginine (Figure 3(a)) and ADMA (Figure 3(c)) did not differ with respect to wound etiology,

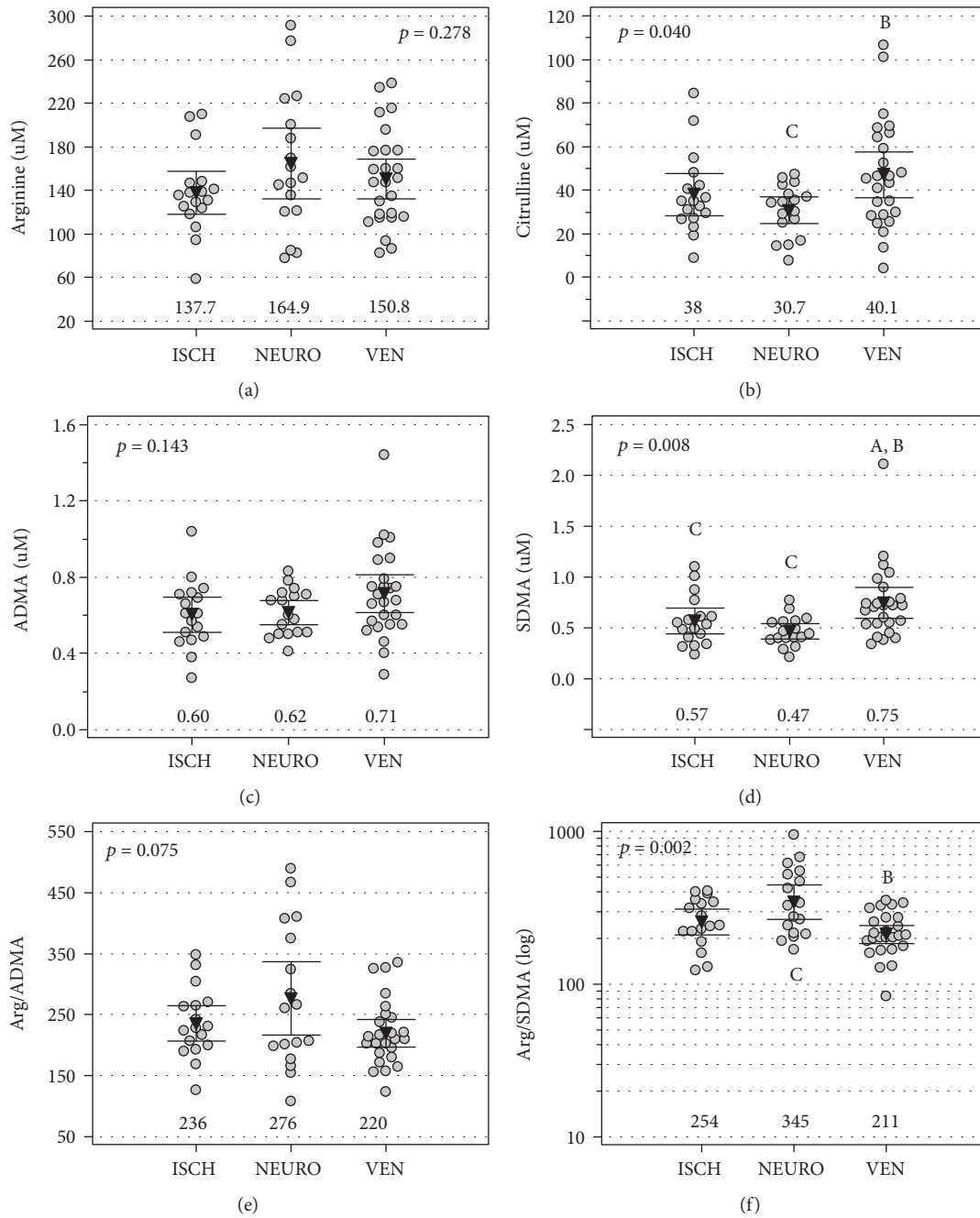


FIGURE 3: Wound etiology and intermediates in the arginine/NO pathway: (a) arginine, (b) citrulline, (c) ADMA, (d) SDMA, (e) arginine-to-ADMA ratio (Arg/ADMA), and (f) arginine-to-SDMA ratio (Arg/SDMA). Data are presented as means with 95% confidence intervals and analyzed using one-way ANOVA. ISCH: ischemic etiology; NEURO: neurotrophic etiology; VEN: venous stasis etiology. Numbers below the dot plots represent the mean value within a group. Letters above/below the dot plots indicate groups from which a given group mean differs significantly: A: significantly different from ISCH; B: significantly different from NEURO; C: significantly different from VEN.

but citrulline concentrations (Figure 2(b)) were significantly higher in patients with venous stasis wounds than in those with neurotrophic wounds. SDMA concentrations (Figure 3(d)) were significantly higher in patients with venous stasis wounds as compared to both neurotrophic and ischemic wounds. The Arg/SDMA ratio (Figure 2(e)) was significantly lower in patients with venous stasis wounds as compared to neurotrophic wounds, and the Arg/ADMA ratio displayed a similar tendency (Figure 3(f)).

3.3. Intermediates in the Arginine/NO Pathway and Wound Characteristics. The concentrations of intermediates of the arginine/NO pathway were compared between patients with and without gangrene and between two of its types (dry and wet) as well as between patients with and without phlegmon or with and without ulceration.

Concerning gangrene, only citrulline concentrations differed significantly and were lower in patients with gangrene (Figure 4(a)). There were no differences in other

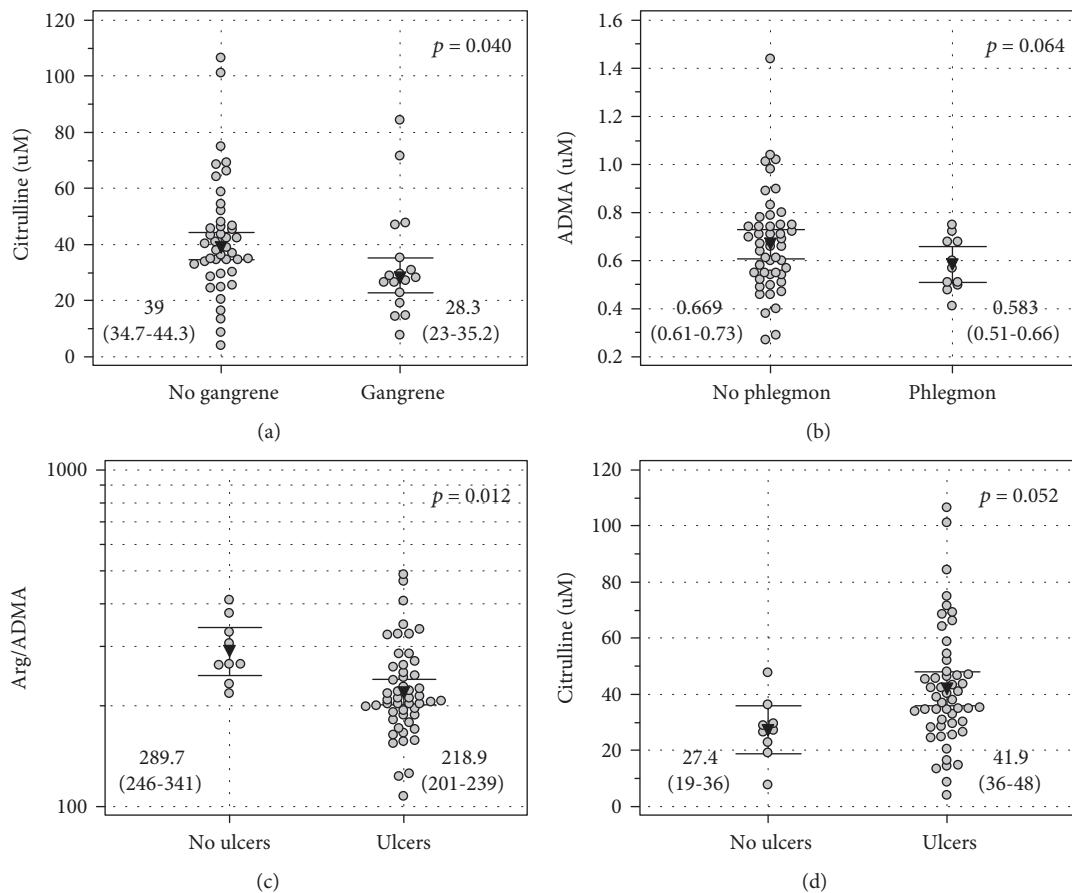


FIGURE 4: Wound type and intermediates in the arginine/NO pathway: (a) citrulline and gangrene, (b) ADMA and phlegmon, (c) Arg/ADMA and ulceration, and (d) citrulline and ulceration. Data are presented as (a) medians or means with 95% confidence intervals and analyzed using (a) the Mann-Whitney U test or t -test for independent samples.

intermediates in the arginine/NO pathway with respect to the presence or absence of gangrene ($p = 0.443$ for arginine, $p = 0.327$ for ADMA, $p = 0.775$ for SDMA, $p = 0.159$ for Arg/ADMA, and $p = 0.547$ for Arg/SDMA) (for details, see Suppl. Fig. 1). Also, the intermediates did not differ with respect to the gangrene type ($p = 0.905$ for arginine, $p = 0.508$ for citrulline, $p = 0.990$ for ADMA, $p = 0.810$ for SDMA, $p = 0.859$ for Arg/ADMA, and $p = 0.940$ for Arg/SDMA) (for details, see Suppl. Fig. 2).

Concerning phlegmon, there were no differences as well ($p = 0.599$ for arginine, $p = 0.183$ for citrulline, $p = 0.134$ for SDMA, $p = 0.208$ for Arg/ADMA, and $p = 0.231$ for Arg/SDMA) (for details, see Suppl. Fig. 3), although ADMA tended to be lower in patients with phlegmon (Figure 4(b)).

Concerning ulceration, ADMA ($p = 0.118$) only tended to be higher in patients with ulcers and arginine ($p = 0.291$) tended to be lower (for details, see Suppl. Fig. 4) but their ratio (Arg/ADMA) was significantly lower in patients with ulceration as compared to those without (Figure 4(c)). Citrulline tended to be elevated in patients with ulceration (Figure 4(d); $41.9 \mu\text{M}$ (35.9-47.9) vs. $27.4 \mu\text{M}$ (18.8-35.9), $p = 0.052$), and SDMA ($p = 0.351$) and Arg/SDMA ($p = 0.101$) did not show significant differences (for details, see Suppl. Fig. 4).

3.4. Intermediates in the Arginine/NO Pathway and Blood Source. For a subgroup of seven patients, blood was sampled from both the ulnar and femoral veins. The comparison of metabolite concentrations with respect to blood source did not show statistically significant differences for ADMA ($p = 0.852$), SDMA ($p = 0.554$), Arg/ADMA ($p = 0.198$), and citrulline ($p = 0.954$) (for details, see Suppl. Fig. 5). However, concentrations of arginine (Figure 5(a)) as well as Arg/SDMA (Figure 5(b)) were significantly lower in blood sampled from the femoral vein than the ulnar vein.

3.5. Correlation Pattern between Intermediates in the Arginine/NO Pathway and Cytokines, Chemokines, and Growth Factors. The correlation patterns between intermediates in the arginine/NO pathway and key cytokines, chemokines, and growth factors implicated in the pathogenesis of wound healing have been examined (Table 2). There was no significant correlation between arginine and any of evaluated mediators. Citrulline correlated negatively with G-CSF, GM-CSF, IL-4, and IL-8. Of these, GM-CSF was an independent predictor of citrulline concentrations, explaining 15% in its variability ($r_{\text{partial}} = -0.39$, $p = 0.013$; $R^2 = 0.155$). ADMA correlated negatively with GM-CSF, TNF α , and VEGF-A. Of these, VEGF-A was an independent predictor of ADMA

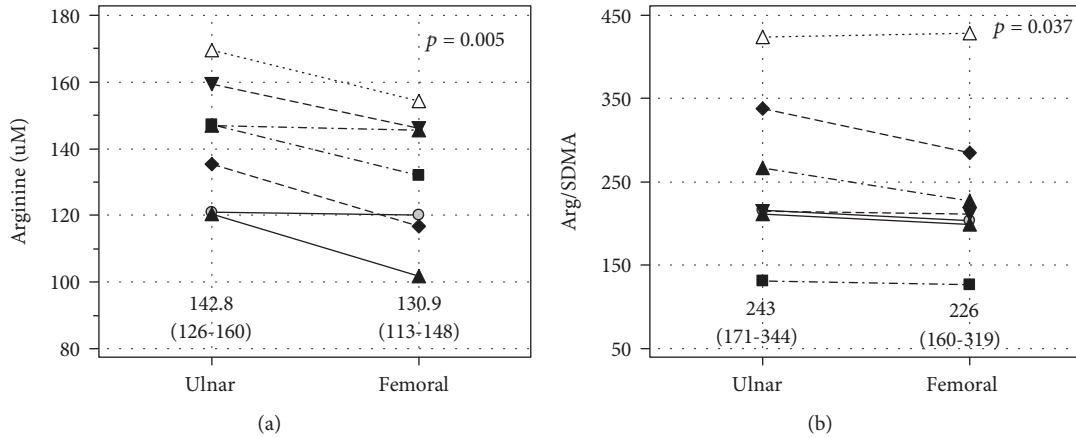


FIGURE 5: Difference in (a) arginine concentrations and (b) arginine-to-SDMA ratio between the ulnar and femoral veins. Data are presented as means with 95% confidence intervals and analyzed using a *t*-test for paired samples.

TABLE 2: Correlation pattern between intermediates in the arginine/NO pathway and cytokines, chemokines, and growth factors.

Cytokine	Arg	Cit	ADMA	SDMA (log)	Arg/ADMA	Arg/SDMA
FGF2	0.13	-0.29	-0.17	-0.28	0.21	0.27
G-CSF	0.12	-0.35*	-0.27	-0.37*	0.42 [‡]	0.41 [‡]
GM-CSF (log)	0.06	-0.39*	-0.36*	-0.42 [‡]	0.39*	0.36*
IL-1 β	0.10	-0.27	-0.27	-0.36*	0.38*	0.35*
IL-4	0.17	-0.32*	-0.21	-0.34*	0.32*	0.36*
IL-6 (log)	0.08	-0.30	-0.39*	-0.23	0.52 [†]	0.27
IL-8	-0.06	-0.36*	-0.30	-0.34*	0.28	0.23
MCP1 (log)	-0.07	-0.24	-0.10	-0.25	0.10	0.20
MIP-1 α	0.07	-0.07	-0.16	-0.20	0.23	0.22
PDGF (log)	0.25	-0.21	-0.10	-0.17	0.27	0.28
TNF α (log)	0.14	-0.31	-0.32*	-0.38*	0.46 [‡]	0.40*
VEGF-A (log)	-0.07	-0.28	-0.37*	-0.28	0.32*	0.14

* $p \leq 0.05$, [‡] $p < 0.01$, and [†] $p < 0.001$. Data were analyzed using the Pearson test and reported as correlation coefficients *r*.

concentrations, explaining 13% in its variability ($r_{\text{partial}} = -0.37$, $p = 0.022$; $R^2 = 0.134$). SDMA correlated negatively with G-CSF, GM-CSF, IL-1 β , IL-4, IL-8, and TNF α . Of these, GM-CSF was an independent predictor of SDMA concentrations, explaining 17% in its variability ($r_{\text{partial}} = -0.42$, $p = 0.008$; $R^2 = 0.174$). Arg/ADMA correlated with G-CSF, GM-CSF, IL-1 β , IL-4, IL-6, VEGF-A, and TNF α , of which IL-6 was an independent predictor, explaining 28% of variability in its value ($r_{\text{partial}} = 0.52$, $p < 0.001$; $R^2 = 0.275$). Arg/SDMA correlated with G-CSF, GM-CSF, IL-1 β , IL-4, and TNF α , of which G-CSF was an independent predictor of the Arg/SDMA ratio, explaining 17% in its variability ($r_{\text{partial}} = 0.41$, $p = 0.010$; $R^2 = 0.167$).

3.6. Interplay between Intermediates in the Arginine/NO Pathway. The pattern of interrelationships of intermediates in the arginine/NO pathway in patients with cardiometabolic diseases with and without chronic wounds has been examined. Arginine did not correlate with any other metabolite in patients with cardiometabolic diseases without chronic

wounds but became directly correlated with the ADMA and SDMA levels in patients with chronic wounds. Citrulline was positively correlated with ADMA and SDMA in both patient groups, but the associations were weaker in patients with chronic wounds. ADMA correlated positively with SDMA, and the association was weaker in patients with chronic wounds (Table 3).

4. Discussion

Detrimental effects of diminished NO bioavailability on cardiovascular health and wound healing are well documented and have led to an outburst of novel treatment strategies aiming at its increase. Intuitively, an elevation in arginine, a direct substrate for NOS enzymes, ought to increase NO availability. Indeed, in addition to wound dressings containing NO precursors [12], the effect of arginine supplementation on a diet has been found beneficial for facilitating the healing of pressure ulcers [13]. However, our results do not confirm that systemic arginine is diminished in patients with chronic wounds to warrant its supplementation. Rather

TABLE 3: Correlation pattern between intermediates in the arginine/NO pathway in patients with cardiometabolic diseases with and without chronic wounds.

Metabolite	Arginine	Citrulline	ADMA	SDMA (log)	Arg/ADMA	Arg/SDMA
Arginine	—	<i>-0.14</i>	<i>-0.15</i>	<i>0.23</i>	—	—
Citrulline	0.20	—	<i>0.81[†]</i>	<i>0.85[†]</i>	<i>-0.62[†]</i>	<i>-0.63[†]</i>
ADMA	0.45 [†]	0.69 [†]	—	<i>0.84[†]</i>	—	—
SDMA (log)	0.28*	0.63 [†]	0.68 [†]	—	—	—
Arg/ADMA	—	-0.35 [‡]	—	—	—	—
Arg/SDMA	—	-0.36 [‡]	—	—	—	—

The right side of the table (in italics) presents correlations in patients without wounds; the left side (in a straight script) presents correlations in patients with chronic wounds. * $p < 0.05$, [‡] $p < 0.01$, and [†] $p < 0.001$. Data were analyzed using the Pearson test and reported as correlation coefficients r .

unexpectedly, they were increased in patients with cardiometabolic burden but without chronic wounds. This observation, however, agrees well with previously reported increased risk for CVD in patients with elevated arginine, independent from traditional risk factors [28]. Still, we also demonstrated that arginine concentrations in the blood from the femoral vein, draining the wounded leg, are significantly lower implying that arginine might indeed be depleted locally. Moreover, also the Arg/SDMA ratio was markedly reduced in the femoral vein than in the ulnar vein, indicative of more severe local arginine depletion.

Nonetheless, it has been suggested that an elevation in systemic or local arginine may not directly translate into increased NO concentrations, a phenomenon explained by impaired arginine availability for NO synthesis by NOS enzymes. At least several mechanisms are in operation, that is, concomitant upregulation of NOS inhibitors, NOS uncoupling due to oxidative stress and tetrahydrobiopterin deficiency, and arginine utilization by an upregulated arginase [29]. Indeed, corroborating the first mechanism, we showed that patients with chronic wounds had increased both ADMA and SDMA concentrations as compared to healthy individuals and patients with cardiometabolic diseases without chronic wounds. Elevated ADMA increases cardiovascular risk [30] and is associated with every disease within the CVD spectrum as well as with CVD risk factors [31]. Mechanistically, ADMA interferes with NO synthesis by inhibiting NOS enzymes and by reducing arginine availability by competing for its membrane transporters. Additionally, it impairs NO signalling by inhibiting eNOS phosphorylation [32]. Also, El-Mesallamy et al. [25] demonstrated that ADMA was elevated in patients with leg ulcers significantly more so than in T2DM patients without neuropathy. SDMA negatively affects arginine availability by inhibiting its membrane transport as well but has not gained as much attention as ADMA as it is only a weak NOS inhibitor. There seems to be a paucity of information on SDMA in chronic wounds in the course of cardiometabolic diseases. In turn, data linking SDMA with a risk of CVD and CVD-caused mortality derived from meta-analyses are contradictory [30, 33]. However, individual studies indicate SDMA elevation to be an independent predictor of CVD-related mortality [34, 35] and to predict renal and cardiovascular outcomes in patients with chronic kidney disease [36]. Furthermore, functional studies have shown SDMA to abolish

anti-inflammatory and antiatherogenic properties of HDL. Consequently, SDMA has been claimed to be a marker of HDL dysfunction [34].

We also observed that due to ADMA and SDMA accumulation, both Arg/ADMA and Arg/SDMA ratios were significantly decreased in patients with chronic wounds, indicating reduced availability of NO and arginine, respectively. Wound character seemed to have an impact on NO bioavailability since the Arg/ADMA ratio was markedly reduced in patients with ulcerations. In turn, wound etiology affected arginine bioavailability as patients with venous stasis had markedly elevated SDMA and decreased Arg/SDMA. The ADMA and SDMA pool is regulated mainly by the rates of their synthesis by type I (ADMA) and type II (SDMA) PRMTs and the rate of their degradation by DDAH enzymes (ADMA) and renal excretion [24]. Impaired renal secretion does not seem to explain the phenomenon of their accumulation in full as cardiometabolic burden, including chronic kidney disease, was similar in patients with and without chronic wounds. There is a paucity of data regarding PRMT and DDAH activity and expression in metabolic disorders and in chronic wounds. However, limited animal studies have linked PRMT overexpression with obesity, nonalcoholic fatty liver disease, and diabetic retinopathy [37, 38] and DDAH downregulation with diabetic retinopathy [38] and impaired vascular homeostasis [39]. PRMT and DDAH might be altered more strongly among patients with chronic wounds than without as they are positively (PRMTs) and negatively (DDAHs) affected by inflammatory mediators [31, 40] and, as we have previously demonstrated, chronic wounds are accompanied by systemic elevation in proinflammatory cytokines [41].

An interesting observation is the difference between SDMA, which was elevated in patients with cardiometabolic burden as compared to controls, and ADMA, which was not. It might result from differences in sensitivity of distinct PRMT enzymes. It has been shown that ADMA-yielding PRMT2 expression is inhibited by high glucose concentration, a common occurrence among our patients, which, in turn, upregulates SDMA synthesis owing to substrate scavenging by type II PRMTs [37].

A direct link between arginine and NO concentrations is further disturbed by NOS uncoupling [29]. The lack of arginine [42], high ADMA concentrations [43], inflammation and oxidative stress [44], and tetrahydrobiopterin deficiency

[45] are considered main culprits of switching enzyme activity from NO synthesis to the production of superoxide anion. As such, the uncoupling of NOS leads not only to the concomitant decrease in NO availability but also to the exacerbation of oxidative stress. Furthermore, NOS enzymes compete for arginine with arginases, the enzymes converting arginine to ornithine. Correspondingly, the upregulated *ARG1* expression has been reported in patients with diabetic foot and venous ulcers [46] as well as in chronic wounds in recessive dystrophic epidermolysis bullosa [47].

Data regarding citrulline association with chronic wounds in the course of cardiometabolic diseases are missing, and those on citrulline in underlying conditions seem to be contradictory. Elevated citrulline has been associated with an increased CVD risk [28] and has a negative impact on arginine bioavailability in obesity and T2DM [48]. However, it is also an effective antioxidant [49], argued to be more effective in restoring cardiometabolic health *via* increasing NO availability than arginine [49]. In addition to improving endothelial function *via* NO-associated mechanisms, citrulline supplementation in patients with vasospastic angina has been shown to reduce the concentrations of oxidized LDL thus alleviating oxidative stress [50]. Citrulline in our study was diminished in patients with cardiometabolic burden as compared to healthy individuals and strongly and positively correlated with NOS inhibitors—ADMA and SDMA. Considering that citrulline is a second reaction product and an effective arginine precursor, these findings seem to confirm reduced rates of NO synthesis among patients with cardiometabolic burden and especially among patients with gangrene. Still, citrulline was less diminished in patients with chronic wounds than those without, particularly in case of wounds of venous stasis etiology. Also, in line with its negative impact on arginine availability, it negatively and strongly correlated with the Arg/SDMA ratio. Debats et al. [51], in turn, found citrulline to be elevated exclusively in patients with infected chronic wounds but not with noninfected or acute wounds.

Inflammatory cytokines are among the initiators of endothelial dysfunction [44] and key players in sustaining inflammation in chronic wounds. Among others, they induce the expression of iNOS [16] but inhibit that of eNOS [52, 53] and contribute to ADMA accumulation [31, 40]. Recently, we have demonstrated that chronic wounds are accompanied by systemic elevation of IL-1 β , IL-4, IL-6, IL-8, FGF-2, MIP-1 α , PDGF-BB, and VEGF-A [41]. Also, markedly elevated CRP and reduced HDL in patients with chronic wounds compared to those with similar cardiometabolic burden are indicative of a higher grade of inflammation in the former. Among our patients, ADMA concentrations were independently and inversely associated with VEGF-A, indicative of the negative impact of ADMA accumulation and resulting diminished NO synthesis on angiogenesis in patients with chronic wounds. We also observed that the higher inflammatory response, indicated by IL-6 concentration, the lower the NO availability, indicated by the reduced Arg/ADMA ratio. We found that GM-CSF was an independent predictor for citrulline and SDMA and G-CSF for Arg/SDMA. G-CSF and GM-CSF are hematopoietic cytokines displaying immu-

nomodulatory and antibiotic-enhancing activities with a proven beneficial effect on wound healing [54–56]. Their concentrations are reduced in patients with chronic wounds [41]. Park et al. [57] demonstrated that G-CSF exerts a protective effect on endothelial cells *via* stimulating eNOS expression and phosphorylation and thus enhancing NO synthesis and signalling. The close relation between G-CSF and Arg/SDMA observed here may indicate an additional mechanism, that is, increased arginine availability.

5. Conclusions

Taken together, our results demonstrate that patients with chronic wounds in the course of cardiometabolic diseases have reduced bioavailability of NO and its substrate, arginine, resulting from ADMA and SDMA accumulation rather than from arginine deficiency. Citrulline, in turn, is decreased in patients with cardiometabolic diseases in general, but the presence of chronic wounds is associated with its elevation, reflecting degree of ADMA, and SDMA accumulation and inversely related to NO and arginine bioavailability. As such, our findings do not support arginine or citrulline supplementation in patients with chronic wounds and rather suggest the need for treatment aiming at decreasing ADMA and SDMA concentrations.

Data Availability

The raw data used to support the findings of this study are available from the corresponding author upon reasonable request.

Conflicts of Interest

The authors declare that there is no conflict of interest regarding the publication of this paper.

Authors' Contributions

Małgorzata Krzystek-Korpacka and Jerzy Wiśniewski contributed equally.

Acknowledgments

The research was supported by statutory funding from Wrocław Medical University (#ST-911).

Supplementary Materials

Supplementary 1. Supplementary Table 1. Effect of sex on intermediates in the arginine/NO pathway among controls and patients with cardiometabolic burden without or with chronic wounds.

Supplementary 2. Supplementary Figure 1. The association of the gangrene presence with intermediates in the arginine/NO pathway.

Supplementary 3. Supplementary Figure 2. The association of the gangrene type with intermediates in the arginine/NO pathway.

Supplementary 4. Supplementary Figure 3. The association of the phlegmon presence with intermediates in the arginine/NO pathway.

Supplementary 5. Supplementary Figure 4. The association of ulcers with intermediates in the arginine/NO pathway.

Supplementary 6. Supplementary Figure 5. Difference in intermediates in the arginine/NO pathway between ulnar and femoral veins.

References

- [1] J. Barthelmes, M. P. Nägele, V. Ludovici, F. Ruschitzka, I. Sudano, and A. J. Flammer, “Endothelial dysfunction in cardiovascular disease and Flammer syndrome-similarities and differences,” *EPMA Journal*, vol. 8, no. 2, pp. 99–109, 2017.
- [2] E. Avishai, K. Yeghiazaryan, and O. Golubnitschaja, “Impaired wound healing: facts and hypotheses for multi-professional considerations in predictive, preventive and personalised medicine,” *EPMA Journal*, vol. 8, no. 1, pp. 23–33, 2017.
- [3] M. Olsson, K. Järbrink, U. Divakar et al., “The humanistic and economic burden of chronic wounds: a systematic review,” *Wound Repair and Regeneration*, vol. 27, no. 1, pp. 114–125, 2019.
- [4] R. E. Jones, D. S. Foster, and M. T. Longaker, “Management of chronic wounds-2018,” *JAMA*, vol. 320, no. 14, pp. 1481–1482, 2018.
- [5] G. Han and R. Ceilley, “Chronic wound healing: a review of current management and treatments,” *Advances in Therapy*, vol. 34, no. 3, pp. 599–610, 2017.
- [6] C. M. Hales, M. D. Carroll, C. D. Fryar, and C. L. Ogden, “Prevalence of obesity among adults and youth: United States, 2015–2016,” *NCHS Data Brief*, no. 288, pp. 1–8, 2017, October 2017, <https://www.cdc.gov/nchs/data/databriefs/db288.pdf>.
- [7] Y. Zheng, S. H. Ley, and F. B. Hu, “Global aetiology and epidemiology of type 2 diabetes mellitus and its complications,” *Nature Reviews Endocrinology*, vol. 14, no. 2, pp. 88–98, 2018.
- [8] T. R. Einarson, A. Acs, C. Ludwig, and U. H. Panton, “Prevalence of cardiovascular disease in type 2 diabetes: a systematic literature review of scientific evidence from across the world in 2007–2017,” *Cardiovascular Diabetology*, vol. 17, no. 1, pp. 83–101, 2018.
- [9] D.-M. Olinic, M. Spinu, M. Olinic et al., “Epidemiology of peripheral artery disease in Europe: VAS Educational Paper,” *International Angiology*, vol. 37, no. 4, pp. 327–334, 2018.
- [10] R. Rayner, K. Carville, J. Keaton, J. Prentice, and N. Santamaria, “Leg ulcers: atypical presentations and associated comorbidities,” *Wound Practice and Research*, vol. 17, pp. 168–185, 2017.
- [11] J. Green, R. Jester, R. McKinley, and A. Pooler, “The impact of chronic venous leg ulcers: a systematic review,” *Journal of Wound Care*, vol. 23, no. 12, pp. 601–612, 2014.
- [12] J. Durão, N. Vale, S. Gomes, P. Gomes, C. C. Barrias, and L. Gales, “Nitric oxide release from antimicrobial peptide hydrogels for wound healing,” *Biomolecules*, vol. 9, no. 1, p. 4, 2019.
- [13] J. C. L. Neyens, E. Cereda, E. P. Meijer, C. Lindholm, and J. M. G. A. Schols, “Arginine-enriched oral nutritional supplementation in the treatment of pressure ulcers: a literature review,” *Wound Medicine*, vol. 16, pp. 46–51, 2017.
- [14] S. Guo and L. A. DiPietro, “Factors affecting wound healing,” *Journal of Dental Research*, vol. 89, no. 3, pp. 219–229, 2010.
- [15] J. D. Luo and A. F. Chen, “Nitric oxide: a newly discovered function on wound healing,” *Acta Pharmacologica Sinica*, vol. 26, no. 3, pp. 259–264, 2005.
- [16] P. Tripathi, P. Tripathi, L. Kashyap, and V. Singh, “The role of nitric oxide in inflammatory reactions,” *FEMS Immunology & Medical Microbiology*, vol. 51, no. 3, pp. 443–452, 2007.
- [17] C. Napoli, G. Paolisso, A. Casamassimi et al., “Effects of nitric oxide on cell proliferation: novel insights,” *Journal of the American College of Cardiology*, vol. 62, no. 2, pp. 89–95, 2013.
- [18] J. V. Boykin Jr., “Wound nitric oxide bioactivity,” *Journal of Wound, Ostomy and Continence Nursing*, vol. 37, no. 1, pp. 25–32, 2010.
- [19] W. T. Weng, C. S. Wu, F. S. Wang et al., “ α -Melanocyte-stimulating hormone attenuates neovascularization by inducing nitric oxide deficiency via MC-Rs/PKA/NF- κ B signaling,” *International Journal of Molecular Sciences*, vol. 19, no. 12, p. 3823, 2018.
- [20] K. Yamasaki, H. D. Edington, C. McClosky et al., “Reversal of impaired wound repair in iNOS-deficient mice by topical adenoviral-mediated iNOS gene transfer,” *Journal of Clinical Investigation*, vol. 101, no. 5, pp. 967–971, 1998.
- [21] P. C. Lee, A. N. Salyapongse, G. A. Bragdon et al., “Impaired wound healing and angiogenesis in eNOS-deficient mice,” *American Journal of Physiology-Heart and Circulatory Physiology*, vol. 277, no. 4, pp. H1600–H1608, 1999.
- [22] M. Jones, J. G. Ganopolsky, A. Labbé et al., “Novel nitric oxide producing probiotic wound healing patch: preparation and in vivo analysis in a New Zealand white rabbit model of ischaemic and infected wounds,” *International Wound Journal*, vol. 9, no. 3, pp. 330–343, 2012.
- [23] K. S. B. Masters, S. J. Leibovich, P. Belem, J. L. West, and L. A. Poole-Warren, “Effects of nitric oxide releasing poly(vinyl alcohol) hydrogel dressings on dermal wound healing in diabetic mice,” *Wound Repair and Regeneration*, vol. 10, no. 5, pp. 286–294, 2002.
- [24] R. Keshet and A. Erez, “Arginine and the metabolic regulation of nitric oxide synthesis in cancer,” *Disease Models & Mechanisms*, vol. 11, no. 8, pp. dmm033332–dmm033341, 2018.
- [25] H. O. El-Mesallamy, N. M. Hamdy, O. A. Ezzat, and A. M. Reda, “Levels of soluble advanced glycation end product-receptors and other soluble serum markers as indicators of diabetic neuropathy in the foot,” *Journal of Investigative Medicine*, vol. 59, no. 8, pp. 1233–1238, 2011.
- [26] J. Wiśniewski, M. G. Fleszar, J. Piechowicz et al., “A novel mass spectrometry-based method for simultaneous determination of asymmetric and symmetric dimethylarginine, l-arginine and l-citrulline optimized for LC-MS-TOF and LC-MS/MS,” *Biomedical Chromatography*, vol. 31, no. 11, article e3994, 2017.
- [27] M. G. Fleszar, J. Wiśniewski, M. Krzystek-Korpacka et al., “Quantitative analysis of L-arginine, dimethylated arginine derivatives, L-citrulline, and dimethylamine in human serum using liquid chromatography-mass spectrometric method,” *Chromatographia*, vol. 81, no. 6, pp. 911–921, 2018.

- [28] M. Magnusson, T. Wang, B. Hedblad et al., "High levels of arginine, citrulline and ADMA are independent predictors of cardiovascular disease," *European Heart Journal*, vol. 34, article P5687, Supplement 1, 2013.
- [29] Y. C. Luiking, G. A. M. Ten Have, R. R. Wolfe, and N. E. P. Deutz, "Arginine de novo and nitric oxide production in disease states," *American Journal of Physiology Endocrinology and Metabolism*, vol. 303, no. 10, pp. E1177–E1189, 2012.
- [30] P. Willeit, D. F. Freitag, J. A. Laukkanen et al., "Asymmetric dimethylarginine and cardiovascular risk: systematic review and meta-analysis of 22 prospective studies," *Journal of the American Heart Association*, vol. 4, no. 6, article e001833, 2015.
- [31] G. Bouras, S. Deftereos, D. Tousoulis et al., "Asymmetric dimethylarginine (ADMA): a promising biomarker for cardiovascular disease?," *Current Topics in Medicinal Chemistry*, vol. 13, no. 2, pp. 180–200, 2013.
- [32] H. Kajimoto, H. Kai, H. Aoki et al., "Inhibition of eNOS phosphorylation mediates endothelial dysfunction in renal failure: new effect of asymmetric dimethylarginine," *Kidney International*, vol. 81, no. 8, pp. 762–768, 2012.
- [33] S. Schlesinger, S. R. Sonntag, W. Lieb, and R. Maas, "Asymmetric and symmetric dimethylarginine as risk markers for total mortality and cardiovascular outcomes: a systematic review and meta-analysis of prospective studies," *PLoS ONE*, vol. 11, no. 11, article e0165811, 2016.
- [34] S. Zewinger, M. E. Kleber, L. Rohrer et al., "Symmetric dimethylarginine, high-density lipoproteins and cardiovascular disease," *European Heart Journal*, vol. 38, no. 20, pp. 1597–1607, 2017.
- [35] P. Jud, F. Hafner, N. Verheyen et al., "Homoarginine/ADMA ratio and homoarginine/SDMA ratio as independent predictors of cardiovascular mortality and cardiovascular events in lower extremity arterial disease," *Scientific Reports*, vol. 8, no. 1, article 14197, 2018.
- [36] I. E. Emrich, A. M. Zawada, J. Martens-Lobenhoffer et al., "Symmetric dimethylarginine (SDMA) outperforms asymmetric dimethylarginine (ADMA) and other methylarginines as predictor of renal and cardiovascular outcome in non-dialysis chronic kidney disease," *Clinical Research in Cardiology*, vol. 107, no. 3, pp. 201–213, 2018.
- [37] R. S. Blanc and S. Richard, "Arginine methylation: the coming of age," *Molecular Cell*, vol. 65, no. 1, pp. 8–24, 2017.
- [38] Y. Chen, X. Xu, M. Sheng, X. Zhang, Q. Gu, and Z. Zheng, "PRMT-1 and DDAHs-induced ADMA upregulation is involved in ROS- and RAS-mediated diabetic retinopathy," *Experimental Eye Research*, vol. 89, no. 6, pp. 1028–1034, 2009.
- [39] J. Leiper, M. Nandi, B. Torondel et al., "Disruption of methylarginine metabolism impairs vascular homeostasis," *Nature Medicine*, vol. 13, no. 2, pp. 198–203, 2007.
- [40] J. H. Kim, B. C. Yoo, W. S. Yang, E. Kim, S. Hong, and J. Y. Cho, "The role of protein arginine methyltransferases in inflammatory responses," *Mediators of Inflammation*, vol. 2016, Article ID 4028353, 11 pages, 2016.
- [41] M. Krzystek-Korpacka, K. Kędzior, L. Masłowski et al., "Impact of chronic wounds of various etiology on systemic profiles of key inflammatory cytokines, chemokines, and growth factors and their interplay," *Advances in Clinical and Experimental Medicine*, vol. 28, no. 10, 2019.
- [42] S. Luo, H. Lei, H. Qin, and Y. Xia, "Molecular mechanisms of endothelial NO synthase uncoupling," *Current Pharmaceutical Design*, vol. 20, no. 22, pp. 3548–3553, 2014.
- [43] C. Xuan, F. J. Chang, X. C. Liu et al., "Endothelial nitric oxide synthase enhancer for protection of endothelial function from asymmetric dimethylarginine-induced injury in human internal thoracic artery," *The Journal of Thoracic and Cardiovascular Surgery*, vol. 144, no. 3, pp. 697–703, 2012.
- [44] S. Karbach, P. Wenzel, A. Waisman, T. Munzel, and A. Daiber, "eNOS uncoupling in cardiovascular diseases—the role of oxidative stress and inflammation," *Current Pharmaceutical Design*, vol. 20, no. 22, pp. 3579–3594, 2014.
- [45] A. Daiber, N. Xia, S. Steven et al., "New therapeutic implications of endothelial nitric oxide synthase (eNOS) function/dysfunction in cardiovascular disease," *International Journal of Molecular Sciences*, vol. 20, no. 1, p. 187, 2019.
- [46] S. A. Abd-El-Aleem, M. W. J. Ferguson, I. Appleton et al., "Expression of nitric oxide synthase isoforms and arginase in normal human skin and chronic venous leg ulcers," *The Journal of Pathology*, vol. 191, no. 4, pp. 434–442, 2000.
- [47] E. B. Jude, A. J. M. Boulton, M. W. J. Ferguson, and I. Appleton, "The role of nitric oxide synthase isoforms and arginase in the pathogenesis of diabetic foot ulcers: possible modulatory effects by transforming growth factor beta 1," *Diabetologia*, vol. 42, no. 6, pp. 748–757, 1999.
- [48] M. Sailer, C. Dahlhoff, P. Giesbertz et al., "Increased plasma citrulline in mice marks diet-induced obesity and may predict the development of the metabolic syndrome," *PLoS ONE*, vol. 8, no. 5, article e63950, 2013.
- [49] T. D. Allerton, D. N. Proctor, J. M. Stephens, T. R. Dugas, G. Spielmann, and B. A. Irving, "L-Citrulline supplementation: impact on cardiometabolic health," *Nutrients*, vol. 10, no. 7, p. 921, 2018.
- [50] M. Morita, M. Sakurada, F. Watanabe et al., "Effects of oral L-citrulline supplementation on lipoprotein oxidation and endothelial dysfunction in humans with vasospastic angina," *Immunology, Endocrine & Metabolic Agents in Medicinal Chemistry*, vol. 13, no. 3, pp. 214–220, 2013.
- [51] I. B. J. G. Debats, D. Booi, N. E. P. Deutz, W. A. Buurman, W. D. Boeckx, and R. R. W. J. van der Hulst, "Infected chronic wounds show different local and systemic arginine conversion compared with acute wounds," *Journal of Surgical Research*, vol. 134, no. 2, pp. 205–214, 2006.
- [52] K. P. Koh, Y. Wang, T. Yi et al., "T cell-mediated vascular dysfunction of human allografts results from IFN- γ dysregulation of NO synthase," *Journal of Clinical Investigation*, vol. 114, no. 6, pp. 846–856, 2004.
- [53] P. F. Lai, F. Mohamed, J. C. Monge, and D. J. Stewart, "Down-regulation of eNOS mRNA expression by TNF α : identification and functional characterization of RNA-protein interactions in the 3' UTR," *Cardiovascular Research*, vol. 59, no. 1, pp. 160–168, 2003.
- [54] F. de Lalla, G. Pellizzer, M. Strazzabosco et al., "Randomized prospective controlled trial of recombinant granulocyte colony-stimulating factor as adjunctive therapy for limb-threatening diabetic foot infection," *Antimicrobial Agents and Chemotherapy*, vol. 45, no. 4, pp. 1094–1098, 2001.
- [55] S. Dogra and R. Sarangal, "Summary of recommendations for leg ulcers," *Indian Dermatology Online Journal*, vol. 5, no. 3, pp. 400–407, 2014.

- [56] S. K. Beidler, C. D. Douillet, D. F. Berndt, B. A. Keagy, P. B. Rich, and W. A. Marston, "Inflammatory cytokine levels in chronic venous insufficiency ulcer tissue before and after compression therapy," *Journal of Vascular Surgery*, vol. 49, no. 4, pp. 1013–1020, 2009.
- [57] K. W. Park, Y. W. Kwon, H. J. Cho et al., "G-CSF exerts dual effects on endothelial cells—opposing actions of direct eNOS induction versus indirect CRP elevation," *Journal of Molecular and Cellular Cardiology*, vol. 45, no. 5, pp. 670–678, 2008.